

anthropogenic forcing during the second half of the 20th century.” The weaker statement in AR5 reflected additional studies with conflicting conclusions on global drought trends (e.g., Sheffield et al. 2012;⁹ Dai 2013¹⁰). Western North America was noted as a region where determining if observed recent droughts were unusual compared to natural variability was particularly difficult. This was due to evidence from paleoclimate proxies of cases of central U.S. droughts during the past 1,000 years that were longer and more intense than historical U.S. droughts.¹¹ Drought is, of course, directly connected to seasonal precipitation totals. Figure 7.1 shows detectable observed recent changes in seasonal precipitation. In fact, the increases in observed summer and fall precipitation are at odds with the projections in Figure 7.5. As a consequence of this increased precipitation, drought statistics over the entire CONUS have declined.^{3, 12} Furthermore, there is no detectable change in meteorological drought at the global scale.⁹ However, a number of individual event attribution studies suggest that if a drought occurs, anthropogenic temperature increases can exacerbate soil moisture deficits (e.g., Seager et al. 2015;¹³ Trenberth et al. 2014¹⁴). Future projections of the anthropogenic contribution to changes in drought risk and severity must be considered in the context of the significant role of natural variability.

8.1.2 Recent Major U.S. Droughts

Meteorological and Agricultural Drought

The United States has suffered a number of very significant droughts of all types since 2011. Each of these droughts was a result of different persistent, large-scale meteorological patterns of mostly natural origins, with varying degrees of attributable human influence. Table 8.1 summarizes available attribution statements for recent extreme U.S. droughts. Statements about meteorological drought are decidedly mixed, revealing the complexities

in interpreting the low tail of the distribution of precipitation. Statements about agricultural drought consistently maintain a human influence if only surface soil moisture measures are considered. The single agricultural drought attribution study at root depth comes to the opposite conclusion.¹⁵ In all cases, these attribution statements are examples of attribution without detection (see Appendix C). The absence of moisture during the 2011 Texas/Oklahoma drought and heat wave was found to be an event whose likelihood was enhanced by the La Niña state of the ocean, but the human interference in the climate system still doubled the chances of reaching such high temperatures.¹⁶ This study illustrates that the effect of human-induced climate change is combined with natural variations and can compound or inhibit the realized severity of any given extreme weather event.

The Great Plains/Midwest drought of 2012 was the most severe summer meteorological drought in the observational record for that region.¹⁷ An unfortunate string of three different patterns of large-scale meteorology from May through August 2012 precluded the normal frequency of summer thunderstorms and was not predicted by the NOAA seasonal forecasts.¹⁷ Little influence of the global sea surface temperature (SST) pattern on meteorological drought frequency has been found in model simulations.¹⁷ No evidence of a human contribution to the 2012 precipitation deficit in the Great Plains and Midwest is found in numerous studies.^{17, 18, 19} However, an alternative view is that the 2012 central U.S. drought can be classified as a “heat wave flash drought”,²⁰ a type of rapidly evolving drought that has decreased in frequency over the past century.³ Also, an increase in the chances of the unusually high temperatures seen in the United States in 2012, partly associated with resultant dry summer soil moisture anomalies, was attributed to the human interference with the



climate system,²¹ indicating the strong feedback between lower soil moisture and higher surface air temperatures during periods of low precipitation. One study found that most, but

not all, of the 2012 surface moisture deficit in the Great Plains was attributable to the precipitation deficit.²² That study also noted that Great Plains root depth and deeper soil mois-

Table 8.1. A list of U.S. droughts for which attribution statements have been made. In the last column, “+” indicates that an attributable human-induced increase in frequency and/or magnitude was found, “-” indicates that an attributable human-induced decrease in frequency and/or magnitude was found, “0” indicates no attributable human contribution was identified. As in Tables 6.2 and 7.1, several of the events were originally examined in the Bulletin of the American Meteorological Society’s (BAMS) State of the Climate Reports and reexamined by Angéilil et al.¹⁸ In these cases, both attribution statements are listed with the original authors first. (Source: M. Wehner)

Authors	Event Year and Duration	Region or State	Type	Attribution Statement
Rupp et al. 2012 ¹³⁰ / Angéilil et al. 2017 ¹⁸	MAMJJA 2011	Texas	Meteorological	+/+
Hoerling et al. 2013 ¹⁶	2012	Texas	Meteorological	+
Rupp et al. 2013 ¹⁹ / Angéilil et al. 2017 ¹⁸	MAMJJA 2012	CO, NE, KS, OK, IA, MO, AR & IL	Meteorological	0/0
Rupp et al. 2013 ¹⁹ / Angéilil et al. 2017 ¹⁸	MAM 2012	CO, NE, KS, OK, IA, MO, AR & IL	Meteorological	0/0
Rupp et al. 2013 ¹⁹ / Angéilil et al. 2017 ¹⁸	JJA 2012	CO, NE, KS, OK, IA, MO, AR & IL	Meteorological	0/+
Hoerling et al. 2014 ¹⁷	MJJA 2012	Great Plains/Midwest	Meteorological	0
Swain et al. 2014 ²⁴ / Angéilil et al. 2017 ¹⁸	ANN 2013	California	Meteorological	+/+
Wang and Schubert 2014 ²⁹ / Angéilil et al. 2017 ¹⁸	JS 2013	California	Meteorological	0/+
Knutson et al. 2014 ¹³¹ / Angéilil et al. 2017 ¹⁸	ANN 2013	California	Meteorological	0/+
Knutson et al. 2014 ¹³¹ / Angéilil et al. 2017 ¹⁸	MAM 2013	U.S. Southern Plains region	Meteorological	0/+
Diffenbaugh et al. 2015 ²⁸	2012–2014	California	Agricultural	+
Seager et al. 2015 ¹³	2012–2014	California	Agricultural	+
Cheng et al. 2016 ¹⁵	2011–2015	California	Agricultural	-
Mote et al. 2016 ³¹	2015	Washington, Oregon, California	Hydrological (snow water equivalent)	+

ture was higher than normal in 2012 despite the surface drying, due to wet conditions in prior years, indicating the long time scales relevant below the surface.²²

The recent California drought, which began in 2011, is unusual in different respects. In this case, the precipitation deficit from 2011 to 2014 was a result of the “ridiculously resilient ridge” of high pressure. This very stable high pressure system steered storms towards the north, away from the highly engineered California water resource system.^{13, 23, 24} A slow-moving high sea surface temperature (SST) anomaly, referred to as “The Blob” — was caused by a persistent ridge that weakened the normal cooling mechanisms for that region of the upper ocean.²⁵ Atmospheric modeling studies showed that the ridge that caused The Blob was favored by a pattern of persistent tropical SST anomalies that were warm in the western equatorial Pacific and simultaneously cool in the far eastern equatorial Pacific.^{23, 26} It was also favored by reduced arctic sea ice and from feedbacks with The Blob’s SST anomalies.²⁷ These studies also suggest that internal variability likely played a prominent role in the persistence of the 2013–2014 ridge off the west coast of North America. Observational records are not long enough and the anomaly was unusual enough that similarly long-lived patterns have not been often seen before. Hence, attribution statements, such as that about an increasing anthropogenic influence on the frequency of geopotential height anomalies similar to 2012–2014 (e.g., Swain et al. 2014²⁴), are without associated detection (Ch. 3: Detection and Attribution). A secondary attribution question concerns the anthropogenic precipitation response in the presence of this SST anomaly. In attribution studies with a prescribed 2013 SST anomaly, a consistent increase in the human influence on the chances of very dry California conditions was found.¹⁸

Anthropogenic climate change did increase the risk of the high temperatures in California in the winters of 2013–2014 and 2014–2015, especially the latter,^{13, 28, 29} further exacerbating the soil moisture deficit and the associated stress on irrigation systems. This raises the question, as yet unanswered, of whether droughts in the western United States are shifting from precipitation control³⁰ to temperature control. There is some evidence to support a relationship between mild winter and/or warm spring temperatures and drought occurrence,³¹ but long-term warming trends in the tropical and North Pacific do not appear to have led to trends toward less precipitation over California.³² An anthropogenic contribution to commonly used measures of agricultural drought, including the Palmer Drought Severity Index (PDSI), was found in California^{28, 33} and is consistent with previous projections of changes in PDSI^{10, 34, 35} and with an attribution study.³⁶ Due to its simplicity, the PDSI has been criticized as being overly sensitive to higher temperatures and thus may exaggerate the human contribution to soil dryness.³⁷ In fact, this study also finds that formulations of potential evaporation used in more complicated hydrologic models are similarly biased, undermining confidence in the magnitude but not the sign of projected surface soil moisture changes in a warmer climate. Seager et al.¹³ analyzed climate model output directly, finding that precipitation minus evaporation in the southwestern United States is projected to experience significant decreases in surface water availability, leading to surface runoff decreases in California, Nevada, Texas, and the Colorado River headwaters even in the near term. However, the criticisms of PDSI also apply to most of the CMIP5 land surface model evapotranspiration formulations. Analysis of soil moisture in the CMIP5 models at deeper levels is complicated by the wide variety in sophistication of their component land models. A pair of studies reveals less



sensitivity at depth-to-surface air temperature increases than at near-surface levels.^{15, 38} Berg et al.³⁹ adjust for the differences in land component model vertical treatments, finding projected change in vertically integrated soil moisture down to 3 meters depth is mixed, with projected decreases in the Southwest and in the south-central United States, but increases over the northern plains. Nonetheless, the warming trend has led to declines in a number of indicators, including Sierra snow water equivalent, that are relevant to hydrological drought.³⁰ Attribution of the California drought and heat wave remains an interesting and controversial research topic.

In summary, there has not yet been a formal identification of a human influence on past changes in United States meteorological drought through the analysis of precipitation trends. Some, but not all, U.S. meteorological drought event attribution studies, largely in the “without detection” class, exhibit a human influence. Attribution of a human influence on past changes in U.S. agricultural drought are limited both by availability of soil moisture observations and a lack of subsurface modeling studies. While a human influence on surface soil moisture trends has been identified with *medium confidence*, its relevance to agriculture may be exaggerated.

Runoff And Hydrological Drought

Several studies focused on the Colorado River basin in the United States that used more sophisticated runoff models driven by the CMIP3 models^{40, 41, 42, 43, 44} showed that annual runoff reductions in a warmer western United States climate occur through a combination of evapotranspiration increases and precipitation decreases, with the overall reduction in river flow exacerbated by human water demands on the basin’s supply. Reduced U.S. snowfall accumulations in much warmer

future climates are virtually certain as frozen precipitation is replaced by rain regardless of the projected changes in total precipitation amounts discussed in Chapter 7: Precipitation Change (Figure 7.6). The profound change in the hydrology of snowmelt-driven flows in the western United States is well documented. Earlier spring runoff⁴⁵ reduced the fraction of precipitation falling as snow⁴⁶ and the snowpack water content at the end of winter,^{47, 48} consistent with warmer temperatures. Formal detection and attribution (Ch. 3: Detection and Attribution) of the observed shift towards earlier snowmelt-driven flows in the western United States reveals that the shift is detectably different from natural variability and attributable to anthropogenic climate change.⁴⁹ Similarly, observed declines in the snow water equivalent in the region have been formally attributed to anthropogenic climate change⁵⁰ as have temperature, river flow, and snowpack.^{41, 51} As a harbinger, the unusually low western U.S. snowpack of 2015 may become the norm.³¹

In the northwestern United States, long-term trends in streamflow have seen declines, with the strongest trends in drought years⁵² that are attributed to a decline in winter precipitation.⁵³ These reductions in precipitation are linked to decreased westerly wind speeds in winter over the region. Furthermore, the trends in westerlies are consistent with CMIP5-projected wind speed changes due to a decreasing meridional temperature and pressure gradients rather than low-frequency climate variability modes. Such precipitation changes have been a primary source of change in hydrological drought in the Northwest over the last 60 years⁵⁴ and are in addition to changes in snowpack properties.

We conclude with *high confidence* that these observed changes in temperature controlled



aspects of western U.S. hydrology are *likely* a consequence of human changes to the climate system.

8.1.3 Projections of Future Droughts

The future changes in seasonal precipitation shown in Chapter 7: Precipitation Change (Figure 7.6) indicate that the southwestern United States may experience chronic future precipitation deficits, particularly in the spring. In much warmer climates, expansion of the tropics and subtropics, traceable to changes in the Hadley circulation, cause shifts in seasonal precipitation that are particularly evident in such arid and semi-arid regions and increase the risk of meteorological drought. However, uncertainty in the magnitude and timing of future southwestern drying is high. We note that the weighted and downscaled projections of Figure 7.6 exhibit significantly less drying and are assessed to be less significant in comparison to natural variations than the original unweighted CMIP5 projections.³⁴

Western U.S. hydrological drought is currently controlled by the frequency and intensity of extreme precipitation events, particularly atmospheric rivers, as these events represent the source of nearly half of the annual water supply and snowpack for the western coastal states.^{55, 56} Climate projections indicate greater frequency of atmospheric rivers in the future (e.g., Dettinger 2011;⁵⁵ Warner et al. 2015;⁵⁷ Gao et al. 2015;⁵⁸ see further discussion in Ch. 9: Extreme Storms). Sequences of these extreme storms have played a critical role in ending recent hydrological droughts along the U.S. West Coast.⁵⁹ However, as winter temperatures increase, the fraction of precipitation falling as snow will decrease, potentially disrupting western U.S. water management practices.

Significant U.S. seasonal precipitation deficits are not confidently projected outside of the Southwest. However, future higher tempera-

tures will *likely* lead to greater frequencies and magnitudes of agricultural droughts throughout the continental United States as the resulting increases in evapotranspiration outpace projected precipitation increases.² Figure 8.1 shows the weighted multimodel projection of the percent change in near-surface soil moisture at the end of the 21st century under the higher scenario (RCP8.5), indicating widespread drying over the entire continental United States. Previous National Climate Assessments^{34, 60} have discussed the implication of these future drier conditions in the context of the PDSI, finding that the future normal condition would be considered drought at the present time, and that the incidence of “extreme drought” (PDSI < -4) would be significantly increased. However, as described below, the PDSI may overestimate future soil moisture drying.

This projection is made “without attribution” (Ch. 4: Projections), but confidence that future soils will generally be drier at the surface is *medium*, as the mechanisms leading to increased evapotranspiration in a warmer climate are elementary scientific facts. However, the land surface component models in the CMIP5 climate models vary greatly in their sophistication, causing the projected magnitude of both the average soil moisture decrease and the increased risk for agricultural drought to be less certain. The weighted projected seasonal decreases in surface soil moisture are generally towards drier conditions, even in regions and seasons where precipitation is projected to experience large increases (Figure 7.6) due to increases in the evapotranspiration associated with higher temperature. Drying is assessed to be large relative to natural variations in much of the CONUS region in the summer. Significant spring and fall drying is also projected in the mountainous western states, with potential implications for forest and wildfire risk. Also, the combination of significant summer



and fall drying in the midwestern states has potential agricultural implications. The largest percent changes are projected in the southwestern United States and are consistent in magnitude with an earlier study of the Colorado River Basin using more sophisticated macroscale hydrological models.⁴²

In this assessment, we limit the direct CMIP5 weighted multimodel projection of soil moisture shown in Figure 8.1 to the surface (defined as the top 10 cm of the soil), as the land surface component sub-models vary greatly in their representation of the total depth of the soil. A more relevant projection to agricultural drought would be the soil moisture at the root

depth of typical U.S. crops. Cook et al.³⁸ find that future drying at a depth of 30 cm will be less than at 2 cm, but still significant and comparable to a modified PDSI formulation. Few of the CMIP5 land models have detailed ecological representations of evapotranspiration processes, causing the simulation of the soil moisture budget to be less constrained than reality.⁶¹ Over the western United States, unrealistically low elevations in the CMIP5 models due to resolution constraints present a further challenge in interpreting evapotranspiration changes. Nonetheless, Figure 8.1 shows a projected drying of surface soil moisture across nearly all of the coterminous United States in all seasons, even in regions and seasons where

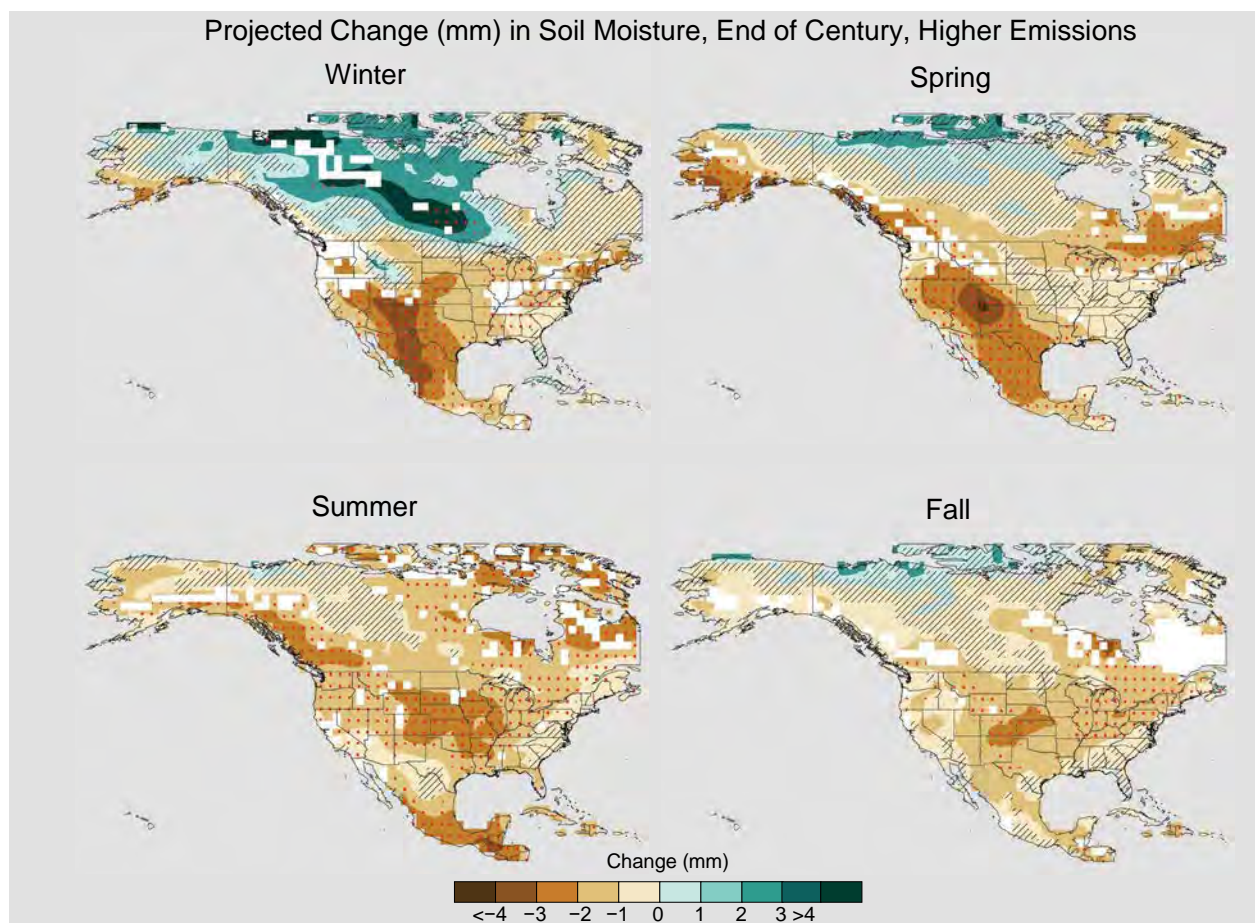


Figure 8.1: Projected end of the 21st century weighted CMIP5 multimodel average percent changes in near surface seasonal soil moisture (mrsos) under the higher scenario (RCP8.5). Stippling indicates that changes are assessed to be large compared to natural variations. Hashing indicates that changes are assessed to be small compared to natural variations. Blank regions (if any) are where projections are assessed to be inconclusive (Appendix B). (Figure source: NOAA NCEI and CICS-NC).

precipitation is projected to increase, consistent with increased evapotranspiration due to elevated temperatures.³⁸

Widespread reductions in mean snowfall across North America are projected by the CMIP5 models.⁶² Together with earlier snowmelt at altitudes high enough for snow, disruptions in western U.S. water delivery systems are expected to lead to more frequent hydrological drought conditions.^{40, 41, 50, 63, 64} Due to resolution constraints, the elevation of mountains as represented in the CMIP5 models is too low to adequately represent the effects of future temperature on snowpacks. However, increased model resolution has been demonstrated to have important impacts on future projections of snowpack water content in warmer climates and is enabled by recent advances in high performance computing.⁶⁵ Figure 8.2 and Table 8.2 show a projection of changes in western U.S. mountain winter (December, January, and February) hydrology obtained from a different high-resolution atmospheric model at the middle and end of the 21st century under the higher scenario (RCP8.5). These projections indicate dramatic reductions in all aspects of snow⁶⁶ and are similar to previous statistically downscaled pro-

jections.^{67, 68} Table 8.2 reveals that the reductions in snow water equivalent accelerate in the latter half of this century under the higher scenario (RCP8.5) and with substantial variations across the western United States. Changes in snow residence time, an alternative measure of snowpack relevant to the timing of runoff, is also shown to be sensitive to elevation, with widespread reductions across this region.⁶⁹ Given the larger projected increases in temperature at high altitudes compared to adjacent lower altitudes⁷⁰ and the resulting changes in both snowpack depth and melt timing in very warm future scenarios such as RCP8.5, and assuming no change to water resource management practices, several important western U.S. snowpack reservoirs effectively disappear by 2100 in this dynamical projection, resulting in chronic, long-lasting hydrological drought. This dramatic statement is also supported by two climate model studies: a multimodel statistical downscaling of the CMIP5 RCP8.5 ensemble that finds large areal reductions in snow-dominated regions of the western United States by mid-century and complete elimination of snow-dominated regions in certain watersheds,⁶⁸ and a large ensemble simulation of a global climate model.⁷¹

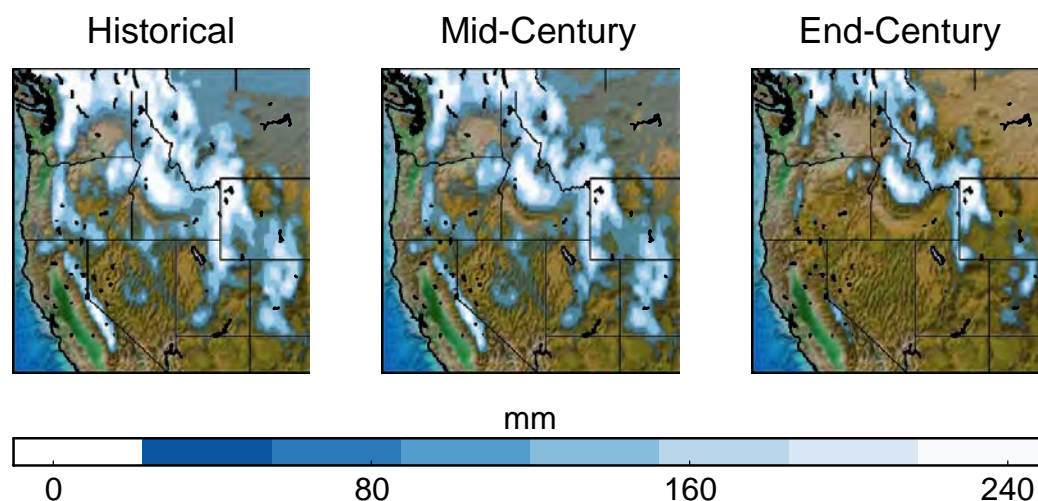


Figure 8.2: Projected changes in winter (DJF) snow water equivalent at the middle and end of this century under the higher scenario (RCP8.5) from a high-resolution version of the Community Atmospheric Model, CAM5.⁶⁶ (Figure source: H. Krishnan, LBNL).

Table 8.2. Projected changes in western U.S. mountain range winter (DJF) snow-related hydrology variables at the middle and end of this century. Projections are for the higher scenario (RCP8.5) from a high-resolution version of the Community Atmospheric Model, CAM5.⁶⁶

Mountain Range	Snow Water Equivalent (% Change)		Snow Cover (% Change)		Snowfall (% Change)		Surface Temperature (change in K)	
	2050	2100	2050	2100	2050	2100	2050	2100
Cascades	-41.5	-89.9	-21.6	-72.9	-10.7	-50.0	0.9	4.1
Klamath	-50.75	-95.8	-38.6	-89.0	-23.1	-78.7	0.8	3.5
Rockies	-17.3	-65.1	-8.2	-43.1	1.7	-8.2	1.4	5.5
Sierra Nevada	-21.8	-89.0	-21.9	-77.7	-4.7	-66.6	1.1	4.5
Wasatch and Uinta	-18.9	-78.7	-14.2	-61.4	4.1	-34.6	1.8	6.1
Western USA	-22.3	-70.1	-12.7	-51.5	-1.6	-21.4	1.3	5.2

As earlier spring melt and reduced snow water equivalent have been formally attributed to human-induced warming, substantial reductions in western U.S. winter and spring snowpack are projected (with attribution) to be *very likely* as the climate continues to warm (*very high confidence*). Under higher scenarios and assuming no change to current water-resources management, chronic, long-duration hydrological drought is increasingly possible by the end of this century (*very high confidence*).

8.2 Floods

Flooding damage in the United States can come from flash floods of smaller rivers and creeks, prolonged flooding along major rivers, urban flooding unassociated with proximity to a riverway, coastal flooding from storm surge which may be exacerbated by sea level rise, and the confluence of coastal storms and inland riverine flooding from the same precipitation event (Ch. 12: Sea Level Rise). Flash flooding is associated with extreme precipitation somewhere along the river which may occur upstream of the regions at risk. Flooding of major rivers in the United States with substantial winter snow accumulations usually occurs in the late winter or spring and can result from an unusually heavy seasonal snowfall followed by a “rain on snow” event or from a rapid onset of higher temperatures

that leads to rapid snow melting within the river basin. In the western coastal states, most flooding occurs in conjunction with extreme precipitation events referred to as “atmospheric rivers” (see Ch. 9: Extreme Storms),^{72, 73} with mountain snowpack being vulnerable to these typically warmer-than-normal storms and their potential for rain on existing snow cover.⁷⁴ Hurricanes and tropical storms are an important driver of flooding events in the eastern United States. Changes in streamflow rates depend on many factors, both human and natural, in addition to climate change. Deforestation, urbanization, dams, floodwater management activities, and changes in agricultural practices can all play a role in past and future changes in flood statistics. Projection of future changes is thus a complex multivariate problem.³⁴

The IPCC AR5⁷ did not attribute changes in flooding to anthropogenic influence nor report detectable changes in flooding magnitude, duration, or frequency. Trends in extreme high values of streamflow are mixed across the United States.^{34, 75, 76} Analysis of 200 U.S. stream gauges indicates areas of both increasing and decreasing flooding magnitude⁷⁷ but does not provide robust evidence that these trends are attributable to human influences. Significant increases in flood frequency have

been detected in about one-third of stream gauge stations examined for the central United States, with a much stronger signal of frequency change than is found for changes in flood magnitude in these gauges.⁷⁸ This apparent disparity with ubiquitous increases in observed extreme precipitation (Figure 7.2) can be partly explained by the seasonality of the two phenomena. Extreme precipitation events in the eastern half of the CONUS are larger in the summer and fall when soil moisture and seasonal streamflow levels are low and less favorable for flooding.⁷⁹ By contrast, high streamflow events are often larger in the spring and winter when soil moisture is high and snowmelt and frozen ground can enhance runoff.⁸⁰ Furthermore, floods may be poorly explained by daily precipitation characteristics alone; the relevant mechanisms are more complex, involving processes that are seasonally and geographically variable, including the seasonal cycles of soil moisture content and snowfall/snowmelt.⁸¹

Recent analysis of annual maximum streamflow shows statistically significant trends in the upper Mississippi River valley (increasing) and in the Northwest (decreasing).⁴⁴ In fact, across the midwestern United States, statistically significant increases in flooding are well documented.^{78, 82, 83, 84, 85, 86, 87, 88} These increases in flood risk and severity are not attributed to 20th century changes in agricultural practices^{87, 89} but instead are attributed mostly to the observed increases in precipitation shown in Figures 7.1 through 7.4.^{78, 84, 89, 90} Trends in maximum streamflow in the northeastern United States are less dramatic and less spatially coherent,^{44, 80} although one study found mostly increasing trends⁹¹ in that region, consistent with the increasing trends in observed extreme precipitation in the region (Ch. 6: Temperature Change).^{34, 80}

The nature of the proxy archives complicates the reconstruction of past flood events in a gridded fashion as has been done with droughts. However, reconstructions of past river outflows do exist. For instance, it has been suggested that the mid-20th century water allocations from the Colorado River were made during one of the wettest periods of the past five centuries.⁹² For the eastern United States, the Mississippi River has undergone century-scale variability in flood frequency—perhaps linked to the moisture availability in the central United States and the temperature structure of the Atlantic Ocean.⁹³

The complex mix of processes complicates the formal attribution of observed flooding trends to anthropogenic climate change and suggests that additional scientific rigor is needed in flood attribution studies.⁹⁴ As noted above, precipitation increases have been found to strongly influence changes in flood statistics. However, in U.S. regions, no formal attribution of precipitation changes to anthropogenic forcing has been made so far, so indirect attribution of flooding changes is not possible. Hence, no formal attribution of observed flooding changes to anthropogenic forcing has been claimed.⁷⁸

A projection study based on coupling an ensemble of regional climate model output to a hydrology model⁹⁵ finds that the magnitude of future very extreme runoff (which can lead to flooding) is decreased in most of the summer months in Washington State, Oregon, Idaho, and western Montana but substantially increases in the other seasons. Projected weighted increases in extreme runoff from the coast to the Cascade Mountains are particularly large in that study during the fall and winter which are not evident in the weighted seasonal averaged CMIP5 runoff projections.² For the West Coast of the United States, extremely heavy precipitation from intense atmospheric



river storms is an important factor in flood frequency and severity.^{55,96} Projections indicate greater frequency of heavy atmospheric rivers in the future (e.g., Dettinger et al. 2011;⁹⁶ Warner et al. 2015;⁵⁷ Gao et al. 2015;⁵⁸ see further discussion in Ch. 9: Extreme Storms). Translating these increases in atmospheric river frequency to their impact on flood frequency requires a detailed representation of western states topography in the global projection models and/or via dynamic downscaling to regional models and is a rapidly developing science. In a report prepared for the Federal Insurance and Mitigation Administration of the Federal Emergency Management Agency, a regression-based approach of scaling river gauge data based on seven commonly used climate change indices from the CMIP3 database⁹⁷ found that at the end of the 21st century the 1% annual chance floodplain area would increase in area by about 30%, with larger changes in the Northeast and Great Lakes regions and smaller changes in the central part of the country and the Gulf Coast.⁹⁸

Urban flooding results from heavy precipitation events that overwhelm the existing sewer infrastructure's ability to convey the resulting stormwater. Future increases in daily and sub-daily extreme precipitation rates will require significant upgrades to many communities' storm sewer systems, as will sea level rise in coastal cities and towns.^{99,100}

No studies have formally attributed (see Ch. 3: Detection and Attribution) long-term changes in observed flooding of major rivers in the United States to anthropogenic forcing. We conclude that there is *medium confidence* that detectable (though not attributable to anthropogenic forcing changes) increases in flood statistics have occurred in parts of the central United States. Key Finding 3 of Chapter 7: Precipitation Change states that the frequency and intensity of heavy precipitation events are

projected to continue to increase over the 21st century with *high confidence*. Given the connection between extreme precipitation and flooding, and the complexities of other relevant factors, we concur with the IPCC Special Report on Extremes (SREX) assessment of "medium confidence (based on physical reasoning) that projected increases in heavy rainfall would contribute to increases in local flooding in some catchments or regions".¹⁰¹

Existing studies of individual extreme flooding events are confined to changes in the locally responsible precipitation event and have not included detailed analyses of the events' hydrology. Gochis et al.¹⁰² describe the massive floods of 2013 along the Colorado front range, estimating that the streamflow amounts ranged from 50- to 500-year return values across the region. Hoerling et al.¹⁷ analyzed the 2013 northeastern Colorado heavy multi-day precipitation event and resulting flood, finding little evidence of an anthropogenic influence on its occurrence. However, Pall et al.¹⁰³ challenge their event attribution methodology with a more constrained study and find that the thermodynamic response of precipitation in this event due to anthropogenic forcing was substantially increased. The Pall et al.¹⁰³ approach does not rule out that the likelihood of the extremely rare large-scale meteorological pattern responsible for the flood may have changed.

8.3 Wildfires

A global phenomenon with natural (lightning) and human-caused ignition sources, wildfire represents a critical ecosystem process. Recent decades have seen a profound increase in forest fire activity over the western United States and Alaska.^{104, 105, 106, 107} The frequency of large wildfires is influenced by a complex combination of natural and human factors. Temperature, soil moisture, relative humidity, wind speed, and vegetation (fuel density) are



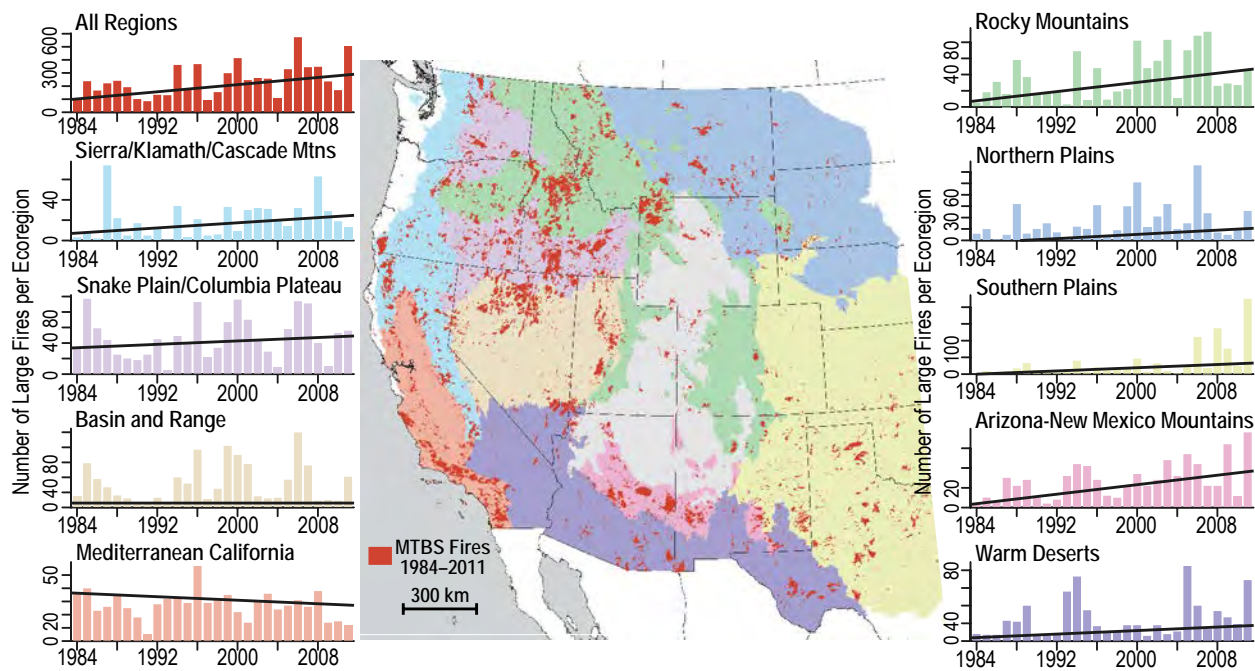


Figure 8.3: Trends in the annual number of large fires in the western United States for a variety of ecoregions. The black lines are fitted trend lines. Statistically significant at a 10% level for all regions except the Snake Plain/Columbia Plateau, Basin and Range, and Mediterranean California regions. (Figure source: Dennison et al.¹⁰⁸).

important aspects of the relationship between fire frequency and ecosystems. Forest management and fire suppression practices can also alter this relationship from what it was in the preindustrial era. Changes in these control parameters can interact with each other in complex ways with the potential for tipping points—in both fire frequency and in ecosystem properties—that may be crossed as the climate warms.

Figure 8.3 shows that the number of large fires has increased over the period 1984–2011, with high statistical significance in 7 out of 10 western U.S. regions across a large variety of vegetation, elevation, and climatic types.¹⁰⁸ State-level fire data over the 20th century¹⁰⁹ indicates that area burned in the western United States decreased from 1916 to about 1940, was at low levels until the 1970s, then increased into the more recent period. Modeled increases in temperatures and vapor pressure deficits due to anthropogenic climate change have increased forest fire activity in the western United States by increasing the aridity of forest fu-

els during the fire season.¹⁰⁴ Increases in these relevant climatic drivers were found to be responsible for over half the observed increase in western U.S. forest fuel aridity from 1979 to 2015 and doubled the forest fire area over the period 1984–2015.¹⁰⁴ Littell et al. (2009, 2010, 2016)^{109, 110, 111} found that two climatic mechanisms affect fire in the western United States: increased fuel flammability driven by warmer, drier conditions and increased fuel availability driven by antecedent moisture. Littell et al.¹¹¹ found a clear link between increased drought and increased fire risk. Yoon et al.¹¹² assessed the 2014 fire season, finding an increased risk of fire in California. While fire suppression practices can also lead to a significant increase in fire risk in lower-elevation and drier forest types, this is less important in higher-elevation and moister forests.^{113, 114, 115} Increases in future forest fire extent, frequency, and intensity depend strongly on local ecosystem properties and will vary greatly across the United States. Westerling et al.¹¹⁶ projected substantial increases in forest fire frequency in the Greater Yellowstone ecosystem by mid-century under

the older SRES A2 emissions scenario, and further stated that years without large fires in the region will become extremely rare. Stavros et al.¹¹⁷ projected increases in very large fires (greater than 50,000 acres) across the western United States by mid-century under both the lower and higher scenarios (RCP4.5 and RCP8.5, respectively). Likewise, Prestemon et al.¹¹⁸ projected significant increases in lightning-ignited wildfire in the Southeast by mid-century but with substantial differences between ecoregions. However, other factors, related to climate change such as water scarcity or insect infestations may act to stifle future forest fire activity by reducing growth or otherwise killing trees leading to fuel reduction.¹¹⁰

Historically, wildfires have been less frequent and of smaller extent in Alaska compared to the rest of the globe.^{119, 120} Shortened land snow cover seasons and higher temperatures have made the Arctic more vulnerable to wildfire.^{119, 120, 121} Total area burned and the number of large fires (those with area greater than 1,000 square km or 386 square miles) in Alaska exhibits significant interannual and decadal scale variability from influences of atmospheric circulation patterns and controlled burns, but have *likely* increased since 1959.¹²² The most recent decade has seen an unusually large number of severe wildfire years in Alaska, for which the risk of severe fires has *likely* increased by 33%–50% as a result of anthropogenic climate change¹²³ and is projected to increase by up to a factor of four by the end of the century under the mid-high scenario (RCP6.0).¹²¹ Historically less flammable tundra and cooler boreal forest regions could shift into historically unprecedented fire risk regimes as a consequence of temperatures increasing above the minimum thresholds required for burning. Alaska's fire season is also *likely* lengthening—a trend expected to continue.^{119, 124} Thresholds in temperature and precipitation shape Arctic fire regimes, and

projected increases in future lightning activity imply increased vulnerability to future climate change.^{119, 121} Alaskan tundra and forest wildfires will *likely* increase under warmer and drier conditions^{124, 125} and potentially result in a transition into a fire regime unprecedented in the last 10,000 years.¹²⁶ Total area burned is projected to increase between 25% and 53% by the end of the century.¹²⁷

Boreal forests and tundra contain large stores of carbon, approximately 50% of the total global soil carbon.¹²⁸ Increased fire activity could deplete these stores, releasing them to the atmosphere to serve as an additional source of atmospheric CO₂ and alter the carbon cycle if ecosystems change from higher to lower carbon densities.^{126, 128} Additionally, increased fires in Alaska may also enhance the degradation of Alaska's permafrost, blackening the ground, reducing surface albedo, and removing protective vegetation.

Both anthropogenic climate change and the legacy of land use/management have an influence on U.S. wildfires and are subtly and inextricably intertwined. Forest management practices have resulted in higher fuel densities in most U.S. forests, except in the Alaskan bush and the higher mountainous regions of the western United States. Nonetheless, there is *medium confidence* for a human-caused climate change contribution to increased forest fire activity in Alaska in recent decades with a *likely* further increase as the climate continues to warm, and *low to medium confidence* for a detectable human climate change contribution in the western United States based on existing studies. Recent literature does not contain a complete robust detection and attribution analysis of forest fires including estimates of natural decadal and multidecadal variability, as described in Chapter 3: Detection and Attribution, nor separate the contributions to observed trends from climate change and for-



est management. These assessment statements about attribution to human-induced climate change are instead multistep attribution statements (Ch. 3: Detection and Attribution) based on plausible model-based estimates of anthropogenic contributions to observed trends. The modeled contributions, in turn, are based on climate variables that are closely linked to fire risk and that, in most cases, have a detectable human influence, such as surface air temperature and snow melt timing.



TRACEABLE ACCOUNTS

Key Finding 1

Recent droughts and associated heat waves have reached record intensity in some regions of the United States; however, by geographical scale and duration, the Dust Bowl era of the 1930s remains the benchmark drought and extreme heat event in the historical record (*very high confidence*). While by some measures drought has decreased over much of the continental United States in association with long-term increases in precipitation, neither the precipitation increases nor inferred drought decreases have been confidently attributed to anthropogenic forcing.

Description of evidence base

Recent droughts are well characterized and described in the literature. The Dust Bowl is not as well documented, but available observational records support the key finding. The last sentence is an “absence of evidence” statement and does not imply “evidence of absence” of future anthropogenic changes. The inferred decreases in some measures of U.S. drought or types of drought (heat wave/flash droughts) are described in Andreadis and Lettenmaier¹² and Mo and Lettenmaier³.

Major uncertainties

Record-breaking temperatures are well documented with low uncertainty.¹²⁹ The magnitude of the Dust Bowl relative to present times varies with location. Uncertainty in the key finding is affected by the quality of pre-World War II observations but is relatively low.

Assessment of confidence based on evidence and agreement

Precipitation is well observed in the United States, leading to *very high confidence*.

Summary sentence or paragraph that integrates the above information

The key finding is a statement that recent U.S. droughts, while sometimes long and severe, are not unprecedented in the historical record.

Key Finding 2

The human effect on recent major U.S. droughts is complicated. Little evidence is found for a human influence on observed precipitation deficits, but much evidence is found for a human influence on surface soil moisture deficits due to increased evapotranspiration caused by higher temperatures (*high confidence*).

Description of evidence base

Observational records of meteorological drought are not long enough to detect statistically significant trends. Additionally, paleoclimatic evidence suggests that major droughts have occurred throughout the distant past. Surface soil moisture is not well observed throughout the CONUS, but numerous event attribution studies attribute enhanced reduction of surface soil moisture during dry periods to anthropogenic warming and enhanced evapotranspiration. Sophisticated land surface models have been demonstrated to reproduce the available observations and have allowed for century scale reconstructions.

Major uncertainties

Uncertainties stem from the length of precipitation observations and the lack of surface moisture observations.

Assessment of confidence based on evidence and agreement

Confidence is *high* for widespread future surface soil moisture deficits, as little change is projected for future summer and fall average precipitation. In the absence of increased precipitation (and in some cases with it), evapotranspiration increases due to increased temperatures will lead to less soil moisture overall, especially near the surface.

Summary sentence or paragraph that integrates the above information

The precipitation deficit portion of the key finding is a conservative statement reflecting the conflicting and limited event attribution literature on meteorological drought. The soil moisture portion of the key finding is limited to the surface and not the more relevant root depth and is supported by the studies cited in this chapter.



Key Finding 3

Future decreases in surface (top 10 cm) soil moisture from anthropogenic forcing over most of the United States are *likely* as the climate warms under the higher scenarios. (*Medium confidence*)

Description of evidence base

First principles establish that evaporation is at least linearly dependent on temperatures and accounts for much of the surface moisture decrease as temperature increases. Plant transpiration for many non-desert species controls plant temperature and responds to increased temperature by opening stomata to release more water vapor. This water comes from the soil at root depth as the plant exhausts its stored water supply (*very high confidence*). Furthermore, nearly all CMIP5 models exhibit U.S. surface soil moisture drying at the end of the century under the higher scenario (RCP8.5), and the multimodel average exhibits no significant annual soil moisture increases anywhere on the planet.²

Major uncertainties

While both evaporation and transpiration changes are of the same sign as temperature increases, the relative importance of each as a function of depth is less well quantified. The amount of transpiration varies considerably among plant species, and these are treated with widely varying degrees of sophistication in the land surface components of contemporary climate models. Uncertainty in the sign of the anthropogenic change of root depth soil moisture is low in regions and seasons of projected precipitation decreases (Ch. 7: Precipitation Changes). There is moderate to high uncertainty in the magnitude of the change in soil moisture at all depths and all regions and seasons. This key finding is a “projection without attribution” statement as such a drying is not part of the observed record. Projections of summertime mean CONUS precipitation exhibit no significant change. However, recent summertime precipitation trends are positive, leading to reduced agricultural drought conditions overall.¹² While statistically significant increases in precipitation have been identified over parts of the United States, these trends have not been clearly attributed to anthropogenic forcing (Ch. 7: Precipitation Change). Furthermore, North

American summer temperature increases under the higher scenario (RCP8.5) at the end of the century are projected to be substantially more than the current observed (and modeled) temperature increase. Because of the response of evapotranspiration to temperature increases, the CMIP5 multimodel average projection is for drier surface soils even in those high latitude regions (Alaska and Canada) that are confidently projected to experience increases in precipitation. Hence, in the CONUS region, with little or no projected summertime changes in precipitation, we conclude that surface soil moisture will *likely* decrease.

Assessment of confidence based on evidence and agreement

CMIP5 and regional models support the surface soil moisture key finding. Confidence is assessed as “medium” as this key finding—despite the high level of agreement among model projections—because of difficulties in observing long-term changes in this metric, and because, at present, there is no published evidence of detectable long-term decreases in surface soil moisture across the United States.

Summary sentence or paragraph that integrates the above information

In the northern United States, surface soil moisture (top 10 cm) is *likely* to decrease as evaporation outpaces increases in precipitation. In the Southwest, the combination of temperature increases and precipitation decreases causes surface soil moisture decreases to be *very likely*. In this region, decreases in soil moisture at the root depth are *likely*.

Key Finding 4

Substantial reductions in western U.S. winter and spring snowpack are projected as the climate warms. Earlier spring melt and reduced snow water equivalent have been formally attributed to human induced warming (*high confidence*) and will *very likely* be exacerbated as the climate continues to warm (*very high confidence*). Under higher scenarios, and assuming no change to current water resources management, chronic, long-duration hydrological drought is increasingly possible by the end of this century (*very high confidence*).



Description of evidence base

First principles tell us that as temperatures rise, minimum snow levels also must rise. Certain changes in western U.S. hydrology have already been attributed to human causes in several papers following Barnett et al.⁴¹ and are cited in the text. The CMIP3/5 models project widespread warming with future increases in atmospheric GHG concentrations, although these are underestimated in the current generation of global climate models (GCMs) at the high altitudes of the western United States due to constraints on orographic representation at current GCM spatial resolutions.

CMIP5 models were not designed or constructed for direct projection of locally relevant snowpack amounts. However, a high-resolution climate model, selected for its ability to simulate western U.S. snowpack amounts and extent, projects devastating changes in the hydrology of this region assuming constant water resource management practices.⁶⁶ This conclusion is also supported by a statistical downscaling result shown in Figure 3.1 of Walsh et al.³⁴ and Cayan et al.⁶⁷ and by the more recent statistical downscaling study of Klos et al.⁶⁸.

Major uncertainties

The major uncertainty is not so much “if” but rather “how much” as changes to precipitation phases (rain or snow) are sensitive to temperature increases that in turn depend on greenhouse gas (GHG) forcing changes. Also, changes to the lower-elevation catchments will be realized prior to those at higher elevations that, even at 25 km, are not adequately resolved. Uncertainty in the final statement also stems from the usage of one model but is tempered by similar findings from statistical downscaling studies. However, this simulation is a so-called “prescribed temperature” experiment with the usual uncertainties about climate sensitivity wired in by the usage of one particular ocean temperature change. Uncertainty in the equator-to-pole differential ocean warming rate is also a factor.

Assessment of confidence based on evidence and agreement

All CMIP5 models project large-scale warming in the western United States as GHG forcing increases. Warm-

ing is underestimated in most of the western United States due to elevation deficiencies that are a consequence of coarse model resolution.

Summary sentence or paragraph that integrates the above information

Warmer temperatures lead to less snow and more rain if total precipitation remains unchanged. Projected winter/spring precipitation changes are a mix of increases in northern states and decreases in the Southwest. In the northern Rocky Mountains, snowpack is projected to decrease even with a projected precipitation increase due to this phase change effect. This will lead to, at the very least, profound changes to the seasonal and sub-seasonal timing of the western U.S. hydrological cycle even where annual precipitation remains nearly unchanged with a strong potential for water shortages.

Key Finding 5

Detectable changes in some classes of flood frequency have occurred in parts of the United States and are a mix of increases and decreases. Extreme precipitation, one of the controlling factors in flood statistics, is observed to have generally increased and is projected to continue to do so across the United States in a warming atmosphere. However, formal attribution approaches have not established a significant connection of increased riverine flooding to human-induced climate change, and the timing of any emergence of a future detectable anthropogenic change in flooding is unclear. (*Medium confidence*)

Description of evidence base

Observed changes are a mix of increases and decreases and are documented by Walsh et al.³⁴ and other studies cited in the text. No attribution statements have been made.

Major uncertainties

Floods are highly variable both in space and time. The multivariate nature of floods complicates detection and attribution.



Assessment of confidence based on evidence and agreement

Confidence is limited to *medium* due to both the lack of an attributable change in observed flooding to date and the complicated multivariate nature of flooding. However, confidence is *high* in the projections of increased future extreme precipitation, the principal driver (among several) of many floods. It is unclear when an observed long-term increase in U.S. riverine flooding will be attributed to anthropogenic climate change. Hence, confidence is *medium* in this part of the key message at this time.

Summary sentence or paragraph that integrates the above information

The key finding is a relatively weak statement reflecting the lack of definitive detection and attribution of anthropogenic changes in U.S. flooding intensity, duration, and frequency.

Key Finding 6

The incidence of large forest fires in the western United States and Alaska has increased since the early 1980s (*high confidence*) and is projected to further increase in those regions as the climate warms with profound changes to certain ecosystems (*medium confidence*).

Description of evidence base

Studies by Dennison et al. (western United States)¹⁰⁸ and Kasischke and Turetsky (Alaska)¹²² document the observed increases in fire statistics. Projections of West-erling et al. (western United States)¹¹⁶ and Young et al.¹²¹ and others (Alaska) indicate increased fire risk. These observations and projections are consistent with drying due to warmer temperatures leading to increased flammability and longer fire seasons.

Major uncertainties

Analyses of other regions of the United States, which also could be subject to increased fire risk, do not seem to be readily available. Likewise, projections of the western U.S. fire risk are of limited areas. In terms of attribution, there is still some uncertainty as to how well non-climatic confounding factors such as forest-ry management and fire suppression practices have been accounted for, particularly for the western United States. Other climate change factors, such as increased water deficits and insect infestations, could reduce fuel loads, tending towards reducing fire frequency and/or intensity.

Assessment of confidence based on evidence and agreement

Confidence is *high* in the observations due to solid observational evidence. Confidence in projections would be higher if there were more available studies covering a broader area of the United States and a wider range of ecosystems.

Summary sentence or paragraph that integrates the above information

Wildfires have increased over parts of the western United States and Alaska in recent decades and are projected to continue to increase as a result of climate change. As a result, shifts in certain ecosystem types may occur.



REFERENCES

1. NOAA, 2008: Drought: Public Fact Sheet. National Oceanic and Atmospheric Administration, National Weather Service, Washington, D.C. <http://www.nws.noaa.gov/os/brochures/climate/DroughtPublic2.pdf>
2. Collins, M., R. Knutti, J. Arblaster, J.-L. Dufresne, T. Fichefet, P. Friedlingstein, X. Gao, W.J. Gutowski, T. Johns, G. Krinner, M. Shongwe, C. Tebaldi, A.J. Weaver, and M. Wehner, 2013: Long-term climate change: Projections, commitments and irreversibility. *Climate Change 2013: The Physical Science Basis. Contribution of Working Group I to the Fifth Assessment Report of the Intergovernmental Panel on Climate Change*. Stocker, T.F., D. Qin, G.-K. Plattner, M. Tignor, S.K. Allen, J. Boschung, A. Nauels, Y. Xia, V. Bex, and P.M. Midgley, Eds. Cambridge University Press, Cambridge, United Kingdom and New York, NY, USA, 1029–1136. <http://www.climatechange2013.org/report/full-report/>
3. Mo, K.C. and D.P. Lettenmaier, 2015: Heat wave flash droughts in decline. *Geophysical Research Letters*, **42**, 2823–2829. <http://dx.doi.org/10.1002/2015GL064018>
4. Bennet, H.H., F.H. Fowler, F.C. Harrington, R.C. Moore, J.C. Page, M.L. Cooke, H.A. Wallace, and R.G. Tugwell, 1936: *A Report of the Great Plains Area Drought Committee*. Hopkins Papers Box 13. Franklin D. Roosevelt Library, New Deal Network (FERI), Hyde Park, NY. <http://newdeal.feri.org/hopkins/hop27.htm>
5. Cook, E.R., C.A. Woodhouse, C.M. Eakin, D.M. Meko, and D.W. Stahle, 2004: Long-term aridity changes in the western United States. *Science*, **306**, 1015–1018. <http://dx.doi.org/10.1126/science.1102586>
6. Coats, S., B.I. Cook, J.E. Smerdon, and R. Seager, 2015: North American pancontinental droughts in model simulations of the last millennium. *Journal of Climate*, **28**, 2025–2043. <http://dx.doi.org/10.1175/JCLI-D-14-00634.1>
7. Bindoff, N.L., P.A. Stott, K.M. AchutaRao, M.R. Allen, N. Gillett, D. Gutzler, K. Hansingo, G. Hegerl, Y. Hu, S. Jain, I.I. Mokhov, J. Overland, J. Perlwitz, R. Sebbari, and X. Zhang, 2013: Detection and attribution of climate change: From global to regional. *Climate Change 2013: The Physical Science Basis. Contribution of Working Group I to the Fifth Assessment Report of the Intergovernmental Panel on Climate Change*. Stocker, T.F., D. Qin, G.-K. Plattner, M. Tignor, S.K. Allen, J. Boschung, A. Nauels, Y. Xia, V. Bex, and P.M. Midgley, Eds. Cambridge University Press, Cambridge, United Kingdom and New York, NY, USA, 867–952. <http://www.climatechange2013.org/report/full-report/>
8. Hegerl, G.C., F.W. Zwiers, P. Braconnot, N.P. Gillett, Y. Luo, J.A.M. Orsini, N. Nicholls, J.E. Penner, and P.A. Stott, 2007: Understanding and attributing climate change. *Climate Change 2007: The Physical Science Basis. Contribution of Working Group I to the Fourth Assessment Report of the Intergovernmental Panel on Climate Change*. Solomon, S., D. Qin, M. Manning, Z. Chen, M. Marquis, K.B. Averyt, M. Tignor, and H.L. Miller, Eds. Cambridge University Press, Cambridge, United Kingdom and New York, NY, USA, 663–745. http://www.ipcc.ch/publications_and_data/ar4/wg1/en/ch9.html
9. Sheffield, J., E.F. Wood, and M.L. Roderick, 2012: Little change in global drought over the past 60 years. *Nature*, **491**, 435–438. <http://dx.doi.org/10.1038/nature11575>
10. Dai, A., 2013: Increasing drought under global warming in observations and models. *Nature Climate Change*, **3**, 52–58. <http://dx.doi.org/10.1038/nclimate1633>
11. Masson-Delmotte, V., M. Schulz, A. Abe-Ouchi, J. Beer, A. Ganopolski, J.F. González Rouco, E. Jansen, K. Lambeck, J. Luterbacher, T. Naish, T. Osborn, B. Otto-Bliesner, T. Quinn, R. Ramesh, M. Rojas, X. Shao, and A. Timmermann, 2013: Information from paleoclimate archives. *Climate Change 2013: The Physical Science Basis. Contribution of Working Group I to the Fifth Assessment Report of the Intergovernmental Panel on Climate Change*. Stocker, T.F., D. Qin, G.-K. Plattner, M. Tignor, S.K. Allen, J. Boschung, A. Nauels, Y. Xia, V. Bex, and P.M. Midgley, Eds. Cambridge University Press, Cambridge, United Kingdom and New York, NY, USA, 383–464. <http://www.climatechange2013.org/report/full-report/>
12. Andreadis, K.M. and D.P. Lettenmaier, 2006: Trends in 20th century drought over the continental United States. *Geophysical Research Letters*, **33**, L10403. <http://dx.doi.org/10.1029/2006GL025711>
13. Seager, R., M. Hoerling, S. Schubert, H. Wang, B. Lyon, A. Kumar, J. Nakamura, and N. Henderson, 2015: Causes of the 2011–14 California drought. *Journal of Climate*, **28**, 6997–7024. <http://dx.doi.org/10.1175/JCLI-D-14-00860.1>
14. Trenberth, K.E., A. Dai, G. van der Schrier, P.D. Jones, J. Barichivich, K.R. Briffa, and J. Sheffield, 2014: Global warming and changes in drought. *Nature Climate Change*, **4**, 17–22. <http://dx.doi.org/10.1038/nclimate2067>
15. Cheng, L., M. Hoerling, A. AghaKouchak, B. Livneh, X.-W. Quan, and J. Eischeid, 2016: How has human-induced climate change affected California drought risk? *Journal of Climate*, **29**, 111–120. <http://dx.doi.org/10.1175/JCLI-D-15-0260.1>



16. Hoerling, M., M. Chen, R. Dole, J. Eischeid, A. Kumar, J.W. Nielsen-Gammon, P. Pegion, J. Perlwitz, X.-W. Quan, and T. Zhang, 2013: Anatomy of an extreme event. *Journal of Climate*, **26**, 2811–2832. <http://dx.doi.org/10.1175/JCLI-D-12-00270.1>
17. Hoerling, M., J. Eischeid, A. Kumar, R. Leung, A. Mariotti, K. Mo, S. Schubert, and R. Seager, 2014: Causes and predictability of the 2012 Great Plains drought. *Bulletin of the American Meteorological Society*, **95**, 269–282. <http://dx.doi.org/10.1175/BAMS-D-13-00055.1>
18. Angélil, O., D. Stone, M. Wehner, C.J. Paciorek, H. Krishnan, and W. Collins, 2017: An independent assessment of anthropogenic attribution statements for recent extreme temperature and rainfall events. *Journal of Climate*, **30**, 5–16. <http://dx.doi.org/10.1175/JCLI-D-16-0077.1>
19. Rupp, D.E., P.W. Mote, N. Massey, F.E.L. Otto, and M.R. Allen, 2013: Human influence on the probability of low precipitation in the central United States in 2012 [in “Explaining Extreme Events of 2013 from a Climate Perspective”]. *Bulletin of the American Meteorological Society*, **94** (9), S2–S6. <http://dx.doi.org/10.1175/BAMS-D-13-00085.1>
20. Mo, K.C. and D.P. Lettenmaier, 2016: Precipitation deficit flash droughts over the United States. *Journal of Hydrometeorology*, **17**, 1169–1184. <http://dx.doi.org/10.1175/jhm-d-15-0158.1>
21. Diffenbaugh, N.S. and M. Scherer, 2013: Likelihood of July 2012 U.S. temperatures in pre-industrial and current forcing regimes [in “Explaining Extreme Events of 2013 from a Climate Perspective”]. *Bulletin of the American Meteorological Society*, **94** (9), S6–S9. <http://dx.doi.org/10.1175/BAMS-D-13-00085.1>
22. Livneh, B. and M.P. Hoerling, 2016: The physics of drought in the U.S. Central Great Plains. *Journal of Climate*, **29**, 6783–6804. <http://dx.doi.org/10.1175/JCLI-D-15-0697.1>
23. Seager, R., M. Hoerling, D.S. Siegfried, h. Wang, B. Lyon, A. Kumar, J. Nakamura, and N. Henderson, 2014: Causes and Predictability of the 2011–14 California Drought. National Oceanic and Atmospheric Administration, Drought Task Force Narrative Team, 40 pp. <http://dx.doi.org/10.7289/V58K771F>
24. Swain, D., M. Tsiang, M. Haughen, D. Singh, A. Charland, B. Rajarthan, and N.S. Diffenbaugh, 2014: The extraordinary California drought of 2013/14: Character, context and the role of climate change [in “Explaining Extreme Events of 2013 from a Climate Perspective”]. *Bulletin of the American Meteorological Society*, **95** (9), S3–S6. <http://dx.doi.org/10.1175/1520-0477-95.9.S1.1>
25. Bond, N.A., M.F. Cronin, H. Freeland, and N. Mantua, 2015: Causes and impacts of the 2014 warm anomaly in the NE Pacific. *Geophysical Research Letters*, **42**, 3414–3420. <http://dx.doi.org/10.1002/2015GL063306>
26. Hartmann, D.L., 2015: Pacific sea surface temperature and the winter of 2014. *Geophysical Research Letters*, **42**, 1894–1902. <http://dx.doi.org/10.1002/2015GL063083>
27. Lee, M.-Y., C.-C. Hong, and H.-H. Hsu, 2015: Compounding effects of warm sea surface temperature and reduced sea ice on the extreme circulation over the extratropical North Pacific and North America during the 2013–2014 boreal winter. *Geophysical Research Letters*, **42**, 1612–1618. <http://dx.doi.org/10.1002/2014GL062956>
28. Diffenbaugh, N.S., D.L. Swain, and D. Touma, 2015: Anthropogenic warming has increased drought risk in California. *Proceedings of the National Academy of Sciences*, **112**, 3931–3936. <http://dx.doi.org/10.1073/pnas.1422385112>
29. Wang, H. and S. Schubert, 2014: Causes of the extreme dry conditions over California during early 2013 [in “Explaining Extreme Events of 2013 from a Climate Perspective”]. *Bulletin of the American Meteorological Society*, **95** (9), S7–S11. <http://dx.doi.org/10.1175/1520-0477-95.9.S1.1>
30. Mao, Y., B. Nijssen, and D.P. Lettenmaier, 2015: Is climate change implicated in the 2013–2014 California drought? A hydrologic perspective. *Geophysical Research Letters*, **42**, 2805–2813. <http://dx.doi.org/10.1002/2015GL063456>
31. Mote, P.W., D.E. Rupp, S. Li, D.J. Sharp, F. Otto, P.F. Uhe, M. Xiao, D.P. Lettenmaier, H. Cullen, and M.R. Allen, 2016: Perspectives on the causes of exceptionally low 2015 snowpack in the western United States. *Geophysical Research Letters*, **43**, 10,980–10,988. <http://dx.doi.org/10.1002/2016GL069965>
32. Funk, C., A. Hoell, and D. Stone, 2014: Examining the contribution of the observed global warming trend to the California droughts of 2012/13 and 2013/14 [in “Explaining Extreme Events of 2013 from a Climate Perspective”]. *Bulletin of the American Meteorological Society*, **95** (9), S11–S15. <http://dx.doi.org/10.1175/1520-0477-95.9.S1.1>
33. Williams, A.P., R. Seager, J.T. Abatzoglou, B.I. Cook, J.E. Smerdon, and E.R. Cook, 2015: Contribution of anthropogenic warming to California drought during 2012–2014. *Geophysical Research Letters*, **42**, 6819–6828. <http://dx.doi.org/10.1002/2015GL064924>
34. Walsh, J., D. Wuebbles, K. Hayhoe, J. Kossin, K. Kunkel, G. Stephens, P. Thorne, R. Vose, M. Wehner, J. Willis, D. Anderson, S. Doney, R. Feely, P. Hennon, V. Kharin, T. Knutson, F. Landerer, T. Lenton, J. Kennedy, and R. Somerville, 2014: Ch. 2: Our changing climate. *Climate Change Impacts in the United States: The Third National Climate Assessment*. Melillo, J.M., T.C. Richmond, and G.W. Yohe, Eds. U.S. Global Change Research Program, Washington, D.C., 19–67. <http://dx.doi.org/10.7930/J0KW5CXT>



35. Wehner, M., D.R. Easterling, J.H. Lawrimore, R.R. Heim, Jr., R.S. Vose, and B.D. Santer, 2011: Projections of future drought in the continental United States and Mexico. *Journal of Hydrometeorology*, **12**, 1359-1377. <http://dx.doi.org/10.1175/2011JHM1351.1>
36. Brown, P.M., E.K. Heyerdahl, S.G. Kitchen, and M.H. Weber, 2008: Climate effects on historical fires (1630–1900) in Utah. *International Journal of Wildland Fire*, **17**, 28-39. <http://dx.doi.org/10.1071/WF07023>
37. Milly, P.C.D. and K.A. Dunne, 2016: Potential evapotranspiration and continental drying. *Nature Climate Change*, **6**, 946-969. <http://dx.doi.org/10.1038/nclimate3046>
38. Cook, B.I., T.R. Ault, and J.E. Smerdon, 2015: Unprecedented 21st century drought risk in the American Southwest and Central Plains. *Science Advances*, **1**, e1400082. <http://dx.doi.org/10.1126/sciadv.1400082>
39. Berg, A., J. Sheffield, and P.C.D. Milly, 2017: Divergent surface and total soil moisture projections under global warming. *Geophysical Research Letters*, **44**, 236-244. <http://dx.doi.org/10.1002/2016GL071921>
40. Barnett, T.P. and D.W. Pierce, 2009: Sustainable water deliveries from the Colorado River in a changing climate. *Proceedings of the National Academy of Sciences*, **106**, 7334-7338. <http://dx.doi.org/10.1073/pnas.0812762106>
41. Barnett, T.P., D.W. Pierce, H.G. Hidalgo, C. Bonfils, B.D. Santer, T. Das, G. Bala, A.W. Wood, T. Nozawa, A.A. Mirin, D.R. Cayan, and M.D. Dettinger, 2008: Human-induced changes in the hydrology of the western United States. *Science*, **319**, 1080-1083. <http://dx.doi.org/10.1126/science.1152538>
42. Christensen, N.S. and D.P. Lettenmaier, 2007: A multimodel ensemble approach to assessment of climate change impacts on the hydrology and water resources of the Colorado River Basin. *Hydrology and Earth System Sciences*, **11**, 1417-1434. <http://dx.doi.org/10.5194/hess-11-1417-2007>
43. Hoerling, M., D. Lettenmaier, D. Cayan, and B. Udall, 2009: Reconciling future Colorado River flows. *Southwest Hydrology*, **8**, 20-21.31. http://www.swhydro.arizona.edu/archive/V8_N3/feature2.pdf
44. McCabe, G.J. and D.M. Wolock, 2014: Spatial and temporal patterns in conterminous United States streamflow characteristics. *Geophysical Research Letters*, **41**, 6889-6897. <http://dx.doi.org/10.1002/2014GL061980>
45. Stewart, I.T., D.R. Cayan, and M.D. Dettinger, 2005: Changes toward earlier streamflow timing across western North America. *Journal of Climate*, **18**, 1136-1155. <http://dx.doi.org/10.1175/JCLI3321.1>
46. Knowles, N., M.D. Dettinger, and D.R. Cayan, 2006: Trends in snowfall versus rainfall in the western United States. *Journal of Climate*, **19**, 4545-4559. <http://dx.doi.org/10.1175/JCLI3850.1>
47. Mote, P.W., 2003: Trends in snow water equivalent in the Pacific Northwest and their climatic causes. *Geophysical Research Letters*, **30**, 1601. <http://dx.doi.org/10.1029/2003GL017258>
48. Mote, P.W., A.F. Hamlet, M.P. Clark, and D.P. Lettenmaier, 2005: Declining mountain snowpack in western North America. *Bulletin of the American Meteorological Society*, **86**, 39-49. <http://dx.doi.org/10.1175/BAMS-86-1-39>
49. Hidalgo, H.G., T. Das, M.D. Dettinger, D.R. Cayan, D.W. Pierce, T.P. Barnett, G. Bala, A. Mirin, A.W. Wood, C. Bonfils, B.D. Santer, and T. Nozawa, 2009: Detection and attribution of streamflow timing changes to climate change in the western United States. *Journal of Climate*, **22**, 3838-3855. <http://dx.doi.org/10.1175/2009jcli2470.1>
50. Pierce, D.W., T.P. Barnett, H.G. Hidalgo, T. Das, C. Bonfils, B.D. Santer, G. Bala, M.D. Dettinger, D.R. Cayan, A. Mirin, A.W. Wood, and T. Nozawa, 2008: Attribution of declining western US snowpack to human effects. *Journal of Climate*, **21**, 6425-6444. <http://dx.doi.org/10.1175/2008JCLI2405.1>
51. Bonfils, C., B.D. Santer, D.W. Pierce, H.G. Hidalgo, G. Bala, T. Das, T.P. Barnett, D.R. Cayan, C. Doutriaux, A.W. Wood, A. Mirin, and T. Nozawa, 2008: Detection and attribution of temperature changes in the mountainous western United States. *Journal of Climate*, **21**, 6404-6424. <http://dx.doi.org/10.1175/2008JCLI2397.1>
52. Luce, C.H. and Z.A. Holden, 2009: Declining annual streamflow distributions in the Pacific Northwest United States, 1948–2006. *Geophysical Research Letters*, **36**, L16401. <http://dx.doi.org/10.1029/2009GL039407>
53. Luce, C.H., J.T. Abatzoglou, and Z.A. Holden, 2013: The missing mountain water: Slower westerlies decrease orographic enhancement in the Pacific Northwest USA. *Science*, **342**, 1360-1364. <http://dx.doi.org/10.1126/science.1242335>
54. Kormos, P.R., C.H. Luce, S.J. Wenger, and W.R. Berghuijs, 2016: Trends and sensitivities of low streamflow extremes to discharge timing and magnitude in Pacific Northwest mountain streams. *Water Resources Research*, **52**, 4990-5007. <http://dx.doi.org/10.1002/2015WR018125>
55. Dettinger, M., 2011: Climate change, atmospheric rivers, and floods in California—a multimodel analysis of storm frequency and magnitude changes. *Journal of the American Water Resources Association*, **47**, 514-523. <http://dx.doi.org/10.1111/j.1752-1688.2011.00546.x>



56. Guan, B., N.P. Molotch, D.E. Waliser, E.J. Fetzer, and P.J. Neiman, 2013: The 2010/2011 snow season in California's Sierra Nevada: Role of atmospheric rivers and modes of large-scale variability. *Water Resources Research*, **49**, 6731-6743. <http://dx.doi.org/10.1002/wrcr.20537>
57. Warner, M.D., C.F. Mass, and E.P. Salathé Jr., 2015: Changes in winter atmospheric rivers along the North American West Coast in CMIP5 climate models. *Journal of Hydrometeorology*, **16**, 118-128. <http://dx.doi.org/10.1175/JHM-D-14-0080.1>
58. Gao, Y., J. Lu, L.R. Leung, Q. Yang, S. Hagos, and Y. Qian, 2015: Dynamical and thermodynamical modulations on future changes of landfalling atmospheric rivers over western North America. *Geophysical Research Letters*, **42**, 7179-7186. <http://dx.doi.org/10.1002/2015GL065435>
59. Dettinger, M.D., 2013: Atmospheric rivers as drought busters on the U.S. West Coast. *Journal of Hydrometeorology*, **14**, 1721-1732. <http://dx.doi.org/10.1175/JHM-D-13-02.1>
60. Karl, T.R., J.T. Melillo, and T.C. Peterson, eds., 2009: *Global Climate Change Impacts in the United States*. Cambridge University Press: New York, NY, 189 pp. <http://downloads.globalchange.gov/usimpacts/pdfs/climate-impacts-report.pdf>
61. Williams, I.N. and M.S. Torn, 2015: Vegetation controls on surface heat flux partitioning, and land-atmosphere coupling. *Geophysical Research Letters*, **42**, 9416-9424. <http://dx.doi.org/10.1002/2015GL066305>
62. O'Gorman, P.A., 2014: Contrasting responses of mean and extreme snowfall to climate change. *Nature*, **512**, 416-418. <http://dx.doi.org/10.1038/nature13625>
63. Cayan, D.R., T. Das, D.W. Pierce, T.P. Barnett, M. Tyree, and A. Gershunov, 2010: Future dryness in the southwest US and the hydrology of the early 21st century drought. *Proceedings of the National Academy of Sciences*, **107**, 21271-21276. <http://dx.doi.org/10.1073/pnas.0912391107>
64. Das, T., D.W. Pierce, D.R. Cayan, J.A. Vano, and D.P. Lettenmaier, 2011: The importance of warm season warming to western U.S. streamflow changes. *Geophysical Research Letters*, **38**, L23403. <http://dx.doi.org/10.1029/2011GL049660>
65. Kapnick, S.B. and T.L. Delworth, 2013: Controls of global snow under a changed climate. *Journal of Climate*, **26**, 5537-5562. <http://dx.doi.org/10.1175/JCLI-D-12-00528.1>
66. Rhoades, A.M., P.A. Ullrich, and C.M. Zarzycki, 2017: Projecting 21st century snowpack trends in western USA mountains using variable-resolution CESM. *Climate Dynamics*, **Online First**, 1-28. <http://dx.doi.org/10.1007/s00382-017-3606-0>
67. Cayan, D., K. Kunkel, C. Castro, A. Gershunov, J. Barsugli, A. Ray, J. Overpeck, M. Anderson, J. Russell, B. Rajagopalan, I. Rangwala, and P. Duffy, 2013: Ch. 6: Future climate: Projected average. *Assessment of Climate Change in the Southwest United States: A Report Prepared for the National Climate Assessment*. Garfin, G., A. Jardine, R. Merideth, M. Black, and S. LeRoy, Eds. Island Press, Washington, D.C., 153-196. <http://swccar.org/sites/all/themes/files/SW-NCA-col-or-FINALweb.pdf>
68. Klos, P.Z., T.E. Link, and J.T. Abatzoglou, 2014: Extent of the rain-snow transition zone in the western U.S. under historic and projected climate. *Geophysical Research Letters*, **41**, 4560-4568. <http://dx.doi.org/10.1002/2014GL060500>
69. Luce, C.H., V. Lopez-Burgos, and Z. Holden, 2014: Sensitivity of snowpack storage to precipitation and temperature using spatial and temporal analog models. *Water Resources Research*, **50**, 9447-9462. <http://dx.doi.org/10.1002/2013WR014844>
70. Pierce, D.W. and D.R. Cayan, 2013: The uneven response of different snow measures to human-induced climate warming. *Journal of Climate*, **26**, 4148-4167. <http://dx.doi.org/10.1175/jcli-d-12-00534.1>
71. Fyfe, J.C., C. Derksen, L. Mudryk, G.M. Flato, B.D. Santer, N.C. Swart, N.P. Molotch, X. Zhang, H. Wan, V.K. Arora, J. Scinocca, and Y. Jiao, 2017: Large near-term projected snowpack loss over the western United States. *Nature Communications*, **8**, 14996. <http://dx.doi.org/10.1038/ncomms14996>
72. Neiman, P.J., L.J. Schick, F.M. Ralph, M. Hughes, and G.A. Wick, 2011: Flooding in western Washington: The connection to atmospheric rivers. *Journal of Hydrometeorology*, **12**, 1337-1358. <http://dx.doi.org/10.1175/2011JHM1358.1>
73. Ralph, F.M. and M.D. Dettinger, 2011: Storms, floods, and the science of atmospheric rivers. *Eos, Transactions, American Geophysical Union*, **92**, 265-266. <http://dx.doi.org/10.1029/2011EO320001>
74. Guan, B., D.E. Waliser, F.M. Ralph, E.J. Fetzer, and P.J. Neiman, 2016: Hydrometeorological characteristics of rain-on-snow events associated with atmospheric rivers. *Geophysical Research Letters*, **43**, 2964-2973. <http://dx.doi.org/10.1002/2016GL067978>
75. Archfield, S.A., R.M. Hirsch, A. Viglione, and G. Blöschl, 2016: Fragmented patterns of flood change across the United States. *Geophysical Research Letters*, **43**, 10,232-10,239. <http://dx.doi.org/10.1002/2016GL070590>
76. EPA, 2016: Climate Change Indicators in the United States, 2016. 4th edition. EPA 430-R-16-004. U.S. Environmental Protection Agency, Washington, D.C., 96 pp. https://www.epa.gov/sites/production/files/2016-08/documents/climate_indicators_2016.pdf

77. Hirsch, R.M. and K.R. Ryberg, 2012: Has the magnitude of floods across the USA changed with global CO₂ levels? *Hydrological Sciences Journal*, **57**, 1-9. <http://dx.doi.org/10.1080/02626667.2011.621895>
78. Mallakpour, I. and G. Villarini, 2015: The changing nature of flooding across the central United States. *Nature Climate Change*, **5**, 250-254. <http://dx.doi.org/10.1038/nclimate2516>
79. Wehner, M.F., 2013: Very extreme seasonal precipitation in the NARCCAP ensemble: Model performance and projections. *Climate Dynamics*, **40**, 59-80. <http://dx.doi.org/10.1007/s00382-012-1393-1>
80. Frei, A., K.E. Kunkel, and A. Matonse, 2015: The seasonal nature of extreme hydrological events in the northeastern United States. *Journal of Hydrometeorology*, **16**, 2065-2085. <http://dx.doi.org/10.1175/JHM-D-14-0237.1>
81. Berghuijs, W.R., R.A. Woods, C.J. Hutton, and M. Sivapalan, 2016: Dominant flood generating mechanisms across the United States. *Geophysical Research Letters*, **43**, 4382-4390. <http://dx.doi.org/10.1002/2016GL068070>
82. Groisman, P.Y., R.W. Knight, and T.R. Karl, 2001: Heavy precipitation and high streamflow in the contiguous United States: Trends in the twentieth century. *Bulletin of the American Meteorological Society*, **82**, 219-246. [http://dx.doi.org/10.1175/1520-0477\(2001\)082<0219:hpahsi>2.3.co;2](http://dx.doi.org/10.1175/1520-0477(2001)082<0219:hpahsi>2.3.co;2)
83. Mallakpour, I. and G. Villarini, 2016: Investigating the relationship between the frequency of flooding over the central United States and large-scale climate. *Advances in Water Resources*, **92**, 159-171. <http://dx.doi.org/10.1016/j.advwatres.2016.04.008>
84. Novotny, E.V. and H.G. Stefan, 2007: Stream flow in Minnesota: Indicator of climate change. *Journal of Hydrology*, **334**, 319-333. <http://dx.doi.org/10.1016/j.jhydrol.2006.10.011>
85. Ryberg, K.R., W. Lin, and A.V. Vecchia, 2014: Impact of climate variability on runoff in the north-central United States. *Journal of Hydrologic Engineering*, **19**, 148-158. [http://dx.doi.org/10.1061/\(ASCE\)HE.1943-5584.0000775](http://dx.doi.org/10.1061/(ASCE)HE.1943-5584.0000775)
86. Slater, L.J., M.B. Singer, and J.W. Kirchner, 2015: Hydrologic versus geomorphic drivers of trends in flood hazard. *Geophysical Research Letters*, **42**, 370-376. <http://dx.doi.org/10.1002/2014GL062482>
87. Tomer, M.D. and K.E. Schilling, 2009: A simple approach to distinguish land-use and climate-change effects on watershed hydrology. *Journal of Hydrology*, **376**, 24-33. <http://dx.doi.org/10.1016/j.jhydrol.2009.07.029>
88. Villarini, G. and A. Strong, 2014: Roles of climate and agricultural practices in discharge changes in an agricultural watershed in Iowa. *Agriculture, Ecosystems & Environment*, **188**, 204-211. <http://dx.doi.org/10.1016/j.agee.2014.02.036>
89. Frans, C., E. Istanbuluoglu, V. Mishra, F. Munoz-Arriola, and D.P. Lettenmaier, 2013: Are climatic or land cover changes the dominant cause of runoff trends in the Upper Mississippi River Basin? *Geophysical Research Letters*, **40**, 1104-1110. <http://dx.doi.org/10.1002/grl.50262>
90. Wang, D. and M. Hejazi, 2011: Quantifying the relative contribution of the climate and direct human impacts on mean annual streamflow in the contiguous United States. *Water Resources Research*, **47**, W00J12. <http://dx.doi.org/10.1029/2010WR010283>
91. Armstrong, W.H., M.J. Collins, and N.P. Snyder, 2014: Hydroclimatic flood trends in the northeastern United States and linkages with large-scale atmospheric circulation patterns. *Hydrological Sciences Journal*, **59**, 1636-1655. <http://dx.doi.org/10.1080/02626667.2013.862339>
92. Woodhouse, C.A., S.T. Gray, and D.M. Meko, 2006: Updated streamflow reconstructions for the Upper Colorado River Basin. *Water Resources Research*, **42**. <http://dx.doi.org/10.1029/2005WR004455>
93. Munoz, S.E., K.E. Gruley, A. Massie, D.A. Fike, S. Schroeder, and J.W. Williams, 2015: Cahokia's emergence and decline coincided with shifts of flood frequency on the Mississippi River. *Proceedings of the National Academy of Sciences*, **112**, 6319-6324. <http://dx.doi.org/10.1073/pnas.1501904112>
94. Merz, B., S. Vorogushyn, S. Uhlemann, J. Delgado, and Y. Hundecha, 2012: HESS Opinions "More efforts and scientific rigour are needed to attribute trends in flood time series". *Hydrology and Earth System Sciences*, **16**, 1379-1387. <http://dx.doi.org/10.5194/hess-16-1379-2012>
95. Najafi, M.R. and H. Moradkhani, 2015: Multi-model ensemble analysis of runoff extremes for climate change impact assessments. *Journal of Hydrology*, **525**, 352-361. <http://dx.doi.org/10.1016/j.jhydrol.2015.03.045>
96. Dettinger, M.D., F.M. Ralph, T. Das, P.J. Neiman, and D.R. Cayan, 2011: Atmospheric rivers, floods and the water resources of California. *Water*, **3**, 445-478. <http://dx.doi.org/10.3390/w3020445>
97. Tebaldi, C., K. Hayhoe, J.M. Arblaster, and G.A. Meehl, 2006: Going to the extremes: An intercomparison of model-simulated historical and future changes in extreme events. *Climatic Change*, **79**, 185-211. <http://dx.doi.org/10.1007/s10584-006-9051-4>

98. AECOM, 2013: The Impact of Climate Change and Population Growth on the National Flood Insurance Program Through 2100. 257 pp. http://www.acclimatise.uk.com/login/uploaded/resources/FEMA_NFIP_report.pdf
99. SFPUC, 2016: Flood Resilience: Report, Task Order 57 (Draft: May 2016). San Francisco Public Utilities Commission, San Francisco, CA. 302 pp. <http://sfwater.org/modules/showdocument.aspx?documentid=9176>
100. Winters, B.A., J. Angel, C. Ballerine, J. Byard, A. Flegel, D. Gambill, E. Jenkins, S. McConkey, M. Markus, B.A. Bender, and M.J. O'Toole, 2015: Report for the Urban Flooding Awareness Act. Illinois Department of Natural Resources, Springfield, IL. 89 pp. https://www.dnr.illinois.gov/WaterResources/Documents/Final_UFAA_Report.pdf
101. IPCC, 2012: Summary for policymakers. *Managing the Risks of Extreme Events and Disasters to Advance Climate Change Adaptation. A Special Report of Working Groups I and II of the Intergovernmental Panel on Climate Change*. Field, C.B., V. Barros, T.F. Stocker, D. Qin, D.J. Dokken, K.L. Ebi, M.D. Mastrandrea, K.J. Mach, G.-K. Plattner, S.K. Allen, M. Tignor, and P.M. Midgley, Eds. Cambridge University Press, Cambridge, UK and New York, NY, 3-21. http://www.ipcc.ch/pdf/special-reports/srex/SREX_FD_SPM_final.pdf
102. Gochis, D., R. Schumacher, K. Friedrich, N. Doesken, M. Kelsch, J. Sun, K. Ikeda, D. Lindsey, A. Wood, B. Dolan, S. Matrosov, A. Newman, K. Mahoney, S. Rutledge, R. Johnson, P. Kucera, P. Kennedy, D. Semper-Torres, M. Steiner, R. Roberts, J. Wilson, W. Yu, V. Chandrasekar, R. Rasmussen, A. Anderson, and B. Brown, 2015: The Great Colorado Flood of September 2013. *Bulletin of the American Meteorological Society*, **96** (12), 1461-1487. <http://dx.doi.org/10.1175/BAMS-D-13-00241.1>
103. Pall, P.C.M.P., M.F. Wehner, D.A. Stone, C.J. Paciorek, and W.D. Collins, 2017: Diagnosing anthropogenic contributions to heavy Colorado rainfall in September 2013. *Weather and Climate Extremes*, **17**, 1-6. <http://dx.doi.org/10.1016/j.wace.2017.03.004>
104. Abatzoglou, J.T. and A.P. Williams, 2016: Impact of anthropogenic climate change on wildfire across western US forests. *Proceedings of the National Academy of Sciences*, **113**, 11770-11775. <http://dx.doi.org/10.1073/pnas.1607171113>
105. Higuera, P.E., J.T. Abatzoglou, J.S. Littell, and P. Morgan, 2015: The changing strength and nature of fire-climate relationships in the northern Rocky Mountains, U.S.A., 1902-2008. *PLoS ONE*, **10**, e0127563. <http://dx.doi.org/10.1371/journal.pone.0127563>
106. Running, S.W., 2006: Is global warming causing more, larger wildfires? *Science*, **313**, 927-928. <http://dx.doi.org/10.1126/science.1130370>
107. Westerling, A.L., H.G. Hidalgo, D.R. Cayan, and T.W. Swetnam, 2006: Warming and earlier spring increase western U.S. forest wildfire activity. *Science*, **313**, 940-943. <http://dx.doi.org/10.1126/science.1128834>
108. Dennison, P.E., S.C. Brewer, J.D. Arnold, and M.A. Moritz, 2014: Large wildfire trends in the western United States, 1984-2011. *Geophysical Research Letters*, **41**, 2928-2933. <http://dx.doi.org/10.1002/2014GL059576>
109. Littell, J.S., D. McKenzie, D.L. Peterson, and A.L. Westerling, 2009: Climate and wildfire area burned in western U.S. ecoregions, 1916-2003. *Ecological Applications*, **19**, 1003-1021. <http://dx.doi.org/10.1890/07-1183.1>
110. Littell, J.S., E.E. Oneil, D. McKenzie, J.A. Hicke, J.A. Lutz, R.A. Norheim, and M.M. Elsner, 2010: Forest ecosystems, disturbance, and climatic change in Washington State, USA. *Climatic Change*, **102**, 129-158. <http://dx.doi.org/10.1007/s10584-010-9858-x>
111. Littell, J.S., D.L. Peterson, K.L. Riley, Y. Liu, and C.H. Luce, 2016: A review of the relationships between drought and forest fire in the United States. *Global Change Biology*, **22**, 2353-2369. <http://dx.doi.org/10.1111/gcb.13275>
112. Yoon, J.-H., B. Kravitz, P.J. Rasch, S.-Y.S. Wang, R.R. Gillies, and L. Higgs, 2015: Extreme fire season in California: A glimpse into the future? *Bulletin of the American Meteorological Society*, **96** (12), S5-S9. <http://dx.doi.org/10.1175/bams-d-15-00114.1>
113. Harvey, B.J., 2016: Human-caused climate change is now a key driver of forest fire activity in the western United States. *Proceedings of the National Academy of Sciences*, **113**, 11649-11650. <http://dx.doi.org/10.1073/pnas.1612926113>
114. Schoennagel, T., T.T. Veblen, and W.H. Romme, 2004: The interaction of fire, fuels, and climate across Rocky Mountain forests. *BioScience*, **54**, 661-676. [http://dx.doi.org/10.1641/0006-3568\(2004\)054\[0661:TIOFFA\]2.0.CO;2](http://dx.doi.org/10.1641/0006-3568(2004)054[0661:TIOFFA]2.0.CO;2)
115. Stephens, S.L., J.K. Agee, P.Z. Fulé, M.P. North, W.H. Romme, T.W. Swetnam, and M.G. Turner, 2013: Managing forests and fire in changing climates. *Science*, **342**, 41-42. <http://dx.doi.org/10.1126/science.1240294>
116. Westerling, A.L., M.G. Turner, E.A.H. Smithwick, W.H. Romme, and M.G. Ryan, 2011: Continued warming could transform Greater Yellowstone fire regimes by mid-21st century. *Proceedings of the National Academy of Sciences*, **108**, 13165-13170. <http://dx.doi.org/10.1073/pnas.1110199108>



117. Stavros, E.N., J.T. Abatzoglou, D. McKenzie, and N.K. Larkin, 2014: Regional projections of the likelihood of very large wildland fires under a changing climate in the contiguous Western United States. *Climatic Change*, **126**, 455-468. <http://dx.doi.org/10.1007/s10584-014-1229-6>
118. Prestemon, J.P., U. Shankar, A. Xiu, K. Talgo, D. Yang, E. Dixon, D. McKenzie, and K.L. Abt, 2016: Projecting wildfire area burned in the south-eastern United States, 2011–60. *International Journal of Wildland Fire*, **25**, 715-729. <http://dx.doi.org/10.1071/WF15124>
119. Flannigan, M., B. Stocks, M. Turetsky, and M. Wotton, 2009: Impacts of climate change on fire activity and fire management in the circumboreal forest. *Global Change Biology*, **15**, 549-560. <http://dx.doi.org/10.1111/j.1365-2486.2008.01660.x>
120. Hu, F.S., P.E. Higuera, P. Duffy, M.L. Chipman, A.V. Rocha, A.M. Young, R. Kelly, and M.C. Dietze, 2015: Arctic tundra fires: Natural variability and responses to climate change. *Frontiers in Ecology and the Environment*, **13**, 369-377. <http://dx.doi.org/10.1890/150063>
121. Young, A.M., P.E. Higuera, P.A. Duffy, and F.S. Hu, 2017: Climatic thresholds shape northern high-latitude fire regimes and imply vulnerability to future climate change. *Ecography*, **40**, 606-617. <http://dx.doi.org/10.1111/ecog.02205>
122. Kasischke, E.S. and M.R. Turetsky, 2006: Recent changes in the fire regime across the North American boreal region—Spatial and temporal patterns of burning across Canada and Alaska. *Geophysical Research Letters*, **33**, L09703. <http://dx.doi.org/10.1029/2006GL025677>
123. Partain, J.L., Jr., S. Alden, U.S. Bhatt, P.A. Bieniek, B.R. Brettschneider, R. Lader, P.Q. Olson, T.S. Rupp, H. Strader, R.L.T. Jr., J.E. Walsh, A.D. York, and R.H. Zieh, 2016: An assessment of the role of anthropogenic climate change in the Alaska fire season of 2015 [in “Explaining Extreme Events of 2015 from a Climate Perspective”]. *Bulletin of the American Meteorological Society*, **97** (12), S14-S18. <http://dx.doi.org/10.1175/BAMS-D-16-0149.1>
124. Sanford, T., R. Wang, and A. Kenwa, 2015: *The Age of Alaskan Wildfires*. Climate Central, Princeton, NJ, 32 pp. <http://assets.climatecentral.org/pdfs/AgeofAlaskanWildfires.pdf>
125. French, N.H.F., L.K. Jenkins, T.V. Loboda, M. Flannigan, R. Jandt, L.L. Bourgeau-Chavez, and M. Whitley, 2015: Fire in arctic tundra of Alaska: Past fire activity, future fire potential, and significance for land management and ecology. *International Journal of Wildland Fire*, **24**, 1045-1061. <http://dx.doi.org/10.1071/WF14167>
126. Kelly, R., M.L. Chipman, P.E. Higuera, I. Stefanova, L.B. Brubaker, and F.S. Hu, 2013: Recent burning of boreal forests exceeds fire regime limits of the past 10,000 years. *Proceedings of the National Academy of Sciences*, **110**, 13055-13060. <http://dx.doi.org/10.1073/pnas.1305069110>
127. Joly, K., P.A. Duffy, and T.S. Rupp, 2012: Simulating the effects of climate change on fire regimes in Arctic biomes: Implications for caribou and moose habitat. *Ecosphere*, **3**, 1-18. <http://dx.doi.org/10.1890/ES12-00012.1>
128. McGuire, A.D., L.G. Anderson, T.R. Christensen, S. Dallimore, L. Guo, D.J. Hayes, M. Heimann, T.D. Lorenson, R.W. MacDonald, and N. Roulet, 2009: Sensitivity of the carbon cycle in the Arctic to climate change. *Ecological Monographs*, **79**, 523-555. <http://dx.doi.org/10.1890/08-2025.1>
129. Meehl, G.A., C. Tebaldi, G. Walton, D. Easterling, and L. McDaniel, 2009: Relative increase of record high maximum temperatures compared to record low minimum temperatures in the US. *Geophysical Research Letters*, **36**, L23701. <http://dx.doi.org/10.1029/2009GL040736>
130. Rupp, D.E., P.W. Mote, N. Massey, C.J. Rye, R. Jones, and M.R. Allen, 2012: Did human influence on climate make the 2011 Texas drought more probable? [in “Explaining Extreme Events of 2011 from a Climate Perspective”]. *Bulletin of the American Meteorological Society*, **93**, 1052-1054. <http://dx.doi.org/10.1175/BAMS-D-12-00021.1>
131. Knutson, T.R., F. Zeng, and A.T. Wittenberg, 2014: Seasonal and annual mean precipitation extremes occurring during 2013: A U.S. focused analysis [in “Explaining Extreme Events of 2013 from a Climate Perspective”]. *Bulletin of the American Meteorological Society*, **95** (9), S19-S23. <http://dx.doi.org/10.1175/1520-0477-95.9.S1.1>





9

Extreme Storms

KEY FINDINGS

1. Human activities have contributed substantially to observed ocean–atmosphere variability in the Atlantic Ocean (*medium confidence*), and these changes have contributed to the observed upward trend in North Atlantic hurricane activity since the 1970s (*medium confidence*).
2. Both theory and numerical modeling simulations generally indicate an increase in tropical cyclone (TC) intensity in a warmer world, and the models generally show an increase in the number of very intense TCs. For Atlantic and eastern North Pacific hurricanes and western North Pacific typhoons, increases are projected in precipitation rates (*high confidence*) and intensity (*medium confidence*). The frequency of the most intense of these storms is projected to increase in the Atlantic and western North Pacific (*low confidence*) and in the eastern North Pacific (*medium confidence*).
3. Tornado activity in the United States has become more variable, particularly over the 2000s, with a decrease in the number of days per year with tornadoes and an increase in the number of tornadoes on these days (*medium confidence*). Confidence in past trends for hail and severe thunderstorm winds, however, is *low*. Climate models consistently project environmental changes that would putatively support an increase in the frequency and intensity of severe thunderstorms (a category that combines tornadoes, hail, and winds), especially over regions that are currently prone to these hazards, but confidence in the details of this projected increase is *low*.
4. There has been a trend toward earlier snowmelt and a decrease in snowstorm frequency on the southern margins of climatologically snowy areas (*medium confidence*). Winter storm tracks have shifted northward since 1950 over the Northern Hemisphere (*medium confidence*). Projections of winter storm frequency and intensity over the United States vary from increasing to decreasing depending on region, but model agreement is poor and confidence is *low*. Potential linkages between the frequency and intensity of severe winter storms in the United States and accelerated warming in the Arctic have been postulated, but they are complex, and, to some extent, contested, and confidence in the connection is currently *low*.
5. The frequency and severity of landfalling “atmospheric rivers” on the U.S. West Coast (narrow streams of moisture that account for 30%–40% of the typical snowpack and annual precipitation in the region and are associated with severe flooding events) will increase as a result of increasing evaporation and resulting higher atmospheric water vapor that occurs with increasing temperature. (*Medium confidence*)

Recommended Citation for Chapter

Kossin, J.P., T. Hall, T. Knutson, K.E. Kunkel, R.J. Trapp, D.E. Waliser, and M.F. Wehner, 2017: Extreme storms. In: *Climate Science Special Report: Fourth National Climate Assessment, Volume I* [Wuebbles, D.J., D.W. Fahey, K.A. Hibbard, D.J. Dokken, B.C. Stewart, and T.K. Maycock (eds.)]. U.S. Global Change Research Program, Washington, DC, USA, pp. 257-276, doi: 10.7930/J07S7KXX.

9.1 Introduction

Extreme storms have numerous impacts on lives and property. Quantifying how broad-scale average climate influences the behavior of extreme storms is particularly challenging, in part because extreme storms are comparatively rare short-lived events and occur within an environment of largely random variability. Additionally, because the physical mechanisms linking climate change and extreme storms can manifest in a variety of ways, even the sign of the changes in the extreme storms can vary in a warming climate. This makes detection and attribution of trends in extreme storm characteristics more difficult than detection and attribution of trends in the larger environment in which the storms evolve (e.g., Ch. 6: Temperature Change). Projecting changes in severe storms is also challenging because of model constraints in how they capture and represent small-scale, highly local physics. Despite the challenges, good progress is being made for a variety of storm types, such as tropical cyclones, severe convective storms (thunderstorms), winter storms, and atmospheric river events.

9.2 Tropical Cyclones (Hurricanes and Typhoons)

Detection and attribution (Ch. 3: Detection and Attribution) of past changes in tropical cyclone (TC) behavior remain a challenge due to the nature of the historical data, which are highly heterogeneous in both time and among the various regions that collect and analyze the data.^{1, 2, 3} While there are ongoing efforts to reanalyze and homogenize the data (e.g., Landsea et al. 2015;⁴ Kossin et al. 2013²), there is still low confidence that any reported long-term (multidecadal to centennial) increases in TC activity are robust, after accounting for past changes in observing capabilities [which is unchanged from the Intergovernmental Panel on Climate Change Fifth Assessment Report (IPCC AR5) assessment statement⁵]. This is not meant to

imply that no such increases have occurred, but rather that the data are not of a high enough quality to determine this with much confidence. Furthermore, it has been argued that within the period of highest data quality (since around 1980), the globally observed changes in the environment would not necessarily support a detectable trend in tropical cyclone intensity.² That is, the trend signal has not yet had time to rise above the background variability of natural processes.

Both theory and numerical modeling simulations (in general) indicate an increase in TC intensity in a warmer world, and the models generally show an increase in the number of very intense TCs.^{6, 7, 8, 9, 10} In some cases, climate models can be used to make attribution statements about TCs without formal detection (see also Ch. 3: Detection and Attribution). For example, there is evidence that, in addition to the effects of El Niño, anthropogenic forcing made the extremely active 2014 Hawaiian hurricane season substantially more likely, although no significant rising trend in TC frequency near Hawai'i was detected.¹¹

Changes in frequency and intensity are not the only measures of TC behavior that may be affected by climate variability and change, and there is evidence that the locations where TCs reach their peak intensity has migrated poleward over the past 30 years in the Northern and Southern Hemispheres, apparently in concert with environmental changes associated with the independently observed expansion of the tropics.¹² The poleward migration in the western North Pacific,¹³ which includes a number of U.S. territories, appears particularly consistent among the various available TC datasets and remains significant over the past 60–70 years after accounting for the known modes of natural variability in the region (Figure 9.1). The migration, which can substantially change patterns of TC hazard exposure and



mortality risk, is also evident in 21st century Coupled Model Intercomparison Project Phase 5 (CMIP5) projections following the RCP8.5 emissions trajectories, suggesting a possible link to human activities. Further analysis comparing observed past TC behavior with climate model historical forcing runs (and with model control runs simulating multidecadal internal climate variability alone) are needed to better understand this process, but it is expected that this will be an area of heightened future research.

In the Atlantic, observed multidecadal variability of the ocean and atmosphere, which TCs are shown to respond to, has been ascribed (Ch. 3: Detection and Attribution) to natural internal variability via meridional overturning ocean circulation changes,¹⁴ natural external variability caused by volcanic eruptions^{15,16} and Saharan dust outbreaks,^{17,18} and anthropogenic ex-

ternal forcing via greenhouse gases and sulfate aerosols.^{19,20,21} Determining the relative contributions of each mechanism to the observed multidecadal variability in the Atlantic, and even whether natural or anthropogenic factors have dominated, is presently a very active area of research and debate, and no consensus has yet been reached.^{22,23,24,25,26,27} Despite the level of disagreement about the relative magnitude of human influences, there is broad agreement that human factors have had an impact on the observed oceanic and atmospheric variability in the North Atlantic, and there is *medium confidence* that this has contributed to the observed increase in hurricane activity since the 1970s. This is essentially unchanged from the IPCC AR5 statement,⁶ although the post-AR5 literature has only served to further support this statement.²⁸ This is expected to remain an active research topic in the foreseeable future.

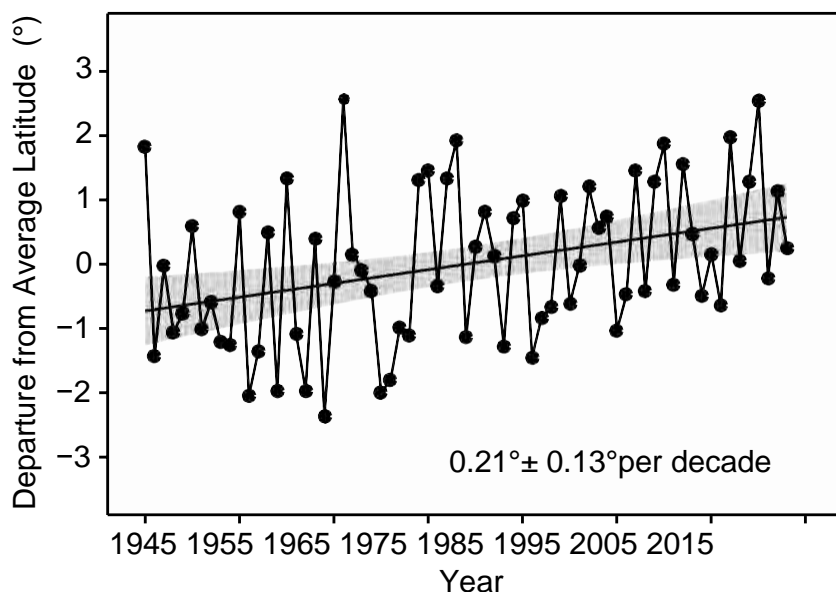


Figure 9.1: Poleward migration, in degrees of latitude, of the location of annual mean tropical cyclone (TC) peak lifetime intensity in the western North Pacific Ocean, after accounting for the known regional modes of interannual (El Niño–Southern Oscillation; ENSO) and interdecadal (Pacific Decadal Oscillation; PDO) variability. The time series shows residuals of the multivariate regression of annually averaged latitude of TC peak lifetime intensity onto the mean Niño-3.4 and PDO indices. Data are taken from the Joint Typhoon Warning Center (JTWC). Shading shows 95% confidence bounds for the trend. Annotated values at lower right show the mean migration rate and its 95% confidence interval in degrees per decade for the period 1945–2013. (Figure source: adapted from Kossin et al. 2016;¹³ © American Meteorological Society. Used with permission.)

The IPCC AR5 consensus TC projections for the late 21st century (IPCC Figure 14.17)⁸ include an increase in global mean TC intensity, precipitation rate, and frequency of very intense (Saffir-Simpson Category 4–5) TCs, and a decrease, or little change, in global TC frequency. Since the IPCC AR5, some studies have provided additional support for this consensus, and some have challenged an aspect of it. For example, a recent study⁹ projects increased mean hurricane intensities in the Atlantic Ocean basin and in most, but not all, other TC-supporting basins (see Table 3 in Knutson et al. 2015⁹). In their study, the global occurrence of Saffir–Simpson Category 4–5 storms was projected to increase significantly, with the most significant basin-scale changes projected for the Northeast Pacific basin, potentially increasing intense hurricane risk to Hawai‘i (Figure 9.2) over the coming century. However, another recent (post-AR5) study proposed that increased thermal stratification of the upper ocean in CMIP5 climate warming scenarios should substantially reduce the warming-induced intensification of TCs estimated in previous studies.²⁹ Follow-up studies, however, estimate that the effect of such increased stratification is relatively small, reducing the projected intensification of TCs by only about 10%–15%.^{30, 31}

Another recent study challenged the IPCC AR5 consensus projection of a decrease, or little change, in global tropical cyclone frequency by simulating increased global TC frequency over the 21st century under the higher scenario (RCP8.5).³² However, another modeling study has found that neither direct analysis of CMIP5-class simulations, nor indirect inferences from the simulations (such as those of Emanuel 2013³²), could reproduce the decrease in TC frequency projected in a warmer world by high-resolution TC-permitting climate models,³³ which adds uncertainty to the results of Emanuel.³²

In summary, despite new research that challenges one aspect of the AR5 consensus for late 21st century-projected TC activity, it remains *likely* that global mean tropical cyclone maximum wind speeds and precipitation rates will increase; and it is *more likely than not* that the global frequency of occurrence of TCs will either decrease or remain essentially the same. Confidence in projected global increases of intensity and tropical cyclone precipitation rates is *medium* and *high*, respectively, as there is better model consensus. Confidence is further heightened, particularly for projected increases in precipitation rates, by a robust physical understanding of the processes that lead to these increases. Confidence in projected increases in the frequency of very intense TCs is generally lower (*medium* in the eastern North Pacific and *low* in the western North Pacific and Atlantic) due to comparatively fewer studies available and due to the competing influences of projected reductions in overall storm frequency and increased mean intensity on the frequency of the most intense storms. Both the magnitude and sign of projected changes in individual ocean basins appears to depend on the large-scale pattern of changes to atmospheric circulation and ocean surface temperature (e.g., Knutson et al. 2015⁹). Projections of these regional patterns of change—apparently critical for TC projections—are uncertain, leading to uncertainty in regional TC projections.



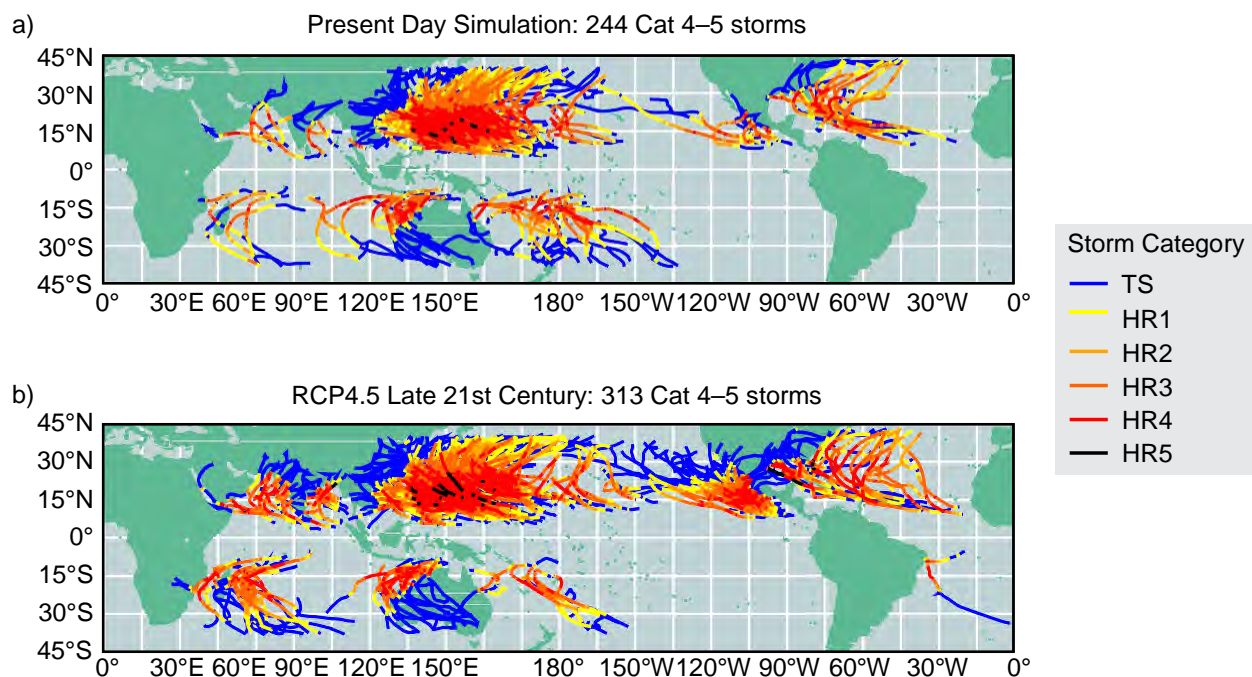


Figure 9.2: Tracks of simulated Saffir–Simpson Category 4–5 tropical cyclones for (a) present-day or (b) late-21st-century conditions, based on dynamical downscaling of climate conditions from the CMIP5 multimodel ensemble (lower scenario; RCP4.5). The tropical cyclones were initially simulated using a 50-km grid global atmospheric model, but each individual tropical cyclone was re-simulated at higher resolution using the GFDL hurricane model to provide more realistic storm intensities and structure. Storm categories or intensities are shown over the lifetime of each simulated storm, according to the Saffir–Simpson scale. The categories are depicted by the track colors, varying from tropical storm (blue) to Category 5 (black; see legend). (Figure source: Knutson et al. 2015;⁹© American Meteorological Society. Used with permission.)

Box 9.1: U.S. Landfalling Major Hurricane “Drought”

Hurricane Harvey made landfall as a major hurricane (Saffir–Simpson Category 3 or higher) in Texas in 2017, breaking what has sometimes been colloquially referred to as the “hurricane drought.” Prior to Harvey, the last major hurricane to make landfall in the continental United States was Wilma in 2005. The 11-year (2006–2016) absence of U.S. major hurricane landfall events is unprecedented in the historical records dating back to the mid-19th century and has occurred in tandem with average to above-average basin-wide major hurricane counts. Was the 11-year absence of U.S. landfalling major hurricanes due to random luck, or were there systematic changes in climate that drove this?

One recent study indicates that the absence of U.S. landfalling major hurricanes cannot readily be attributed to any sustained changes in the climate patterns that affect hurricanes.³⁴ Based on a statistical analysis of the historical North Atlantic hurricane database, the study found no evidence of a connection between the number of major U.S. landfalls from one year to the next and concluded that the 11-year absence of U.S. landfalling major hurricanes was random. A subsequent recent study did identify a systematic pattern of atmosphere/ocean conditions that vary in such a way that conditions conducive to hurricane intensification in the deep tropics occur in concert with conditions conducive to weakening near the U.S. coast.³⁵ This result suggests a possible relationship between climate and hurricanes; increasing basin-wide hurricane counts are associated with a decreasing fraction of major hurricanes making U.S. landfall, as major hurricanes approaching the U.S. coast are more likely to

Box 9.1 (continued)

weaken during active North Atlantic hurricane periods (such as the present period). It is unclear to what degree this relationship has affected absolute hurricane landfall counts during the recent active hurricane period from the mid-1990s, as the basin-wide number and landfalling fraction are in opposition (that is, there are more major hurricanes but a smaller fraction make landfall as major hurricanes). It is also unclear how this relationship may change as the climate continues to warm. Other studies have identified systematic interdecadal hurricane track variability that may affect landfalling hurricane and major hurricane frequency.^{36, 37, 38}

Another recent study³⁹ shows that the extent of the absence is sensitive to uncertainties in the historical data and even small variations in the definition of a major hurricane, which is somewhat arbitrary. It is also sensitive to the definition of U.S. landfall, which is a geopolitical-border-based constraint and has no physical meaning. In fact, many areas outside of the U.S. border have experienced major hurricane landfalls in the past 11 years. In this sense, the frequency of U.S. landfalling major hurricanes is not a particularly robust metric with which to study questions about hurricane activity and its relationship with climate variability. Furthermore, the 11-year absence of U.S. landfalling major hurricanes is not a particularly relevant metric in terms of coastal hazard exposure and risk. For example, Hurricanes Ike (2008), Irene (2011), Sandy (2012), and most recently Hurricane Matthew (2016) brought severe impacts to the U.S. coast despite not making landfall in the United States while classified as major hurricanes. In the case of Hurricane Sandy, extreme rainfall and storm surge (see also Ch. 12: Sea Level Rise) during landfall caused extensive destruction in and around the New York City area, despite Sandy's designation as a post-tropical cyclone at that time. In the case of Hurricane Matthew, the center came within about 40 miles of the Florida coast while Matthew was a major hurricane, which is close enough to significantly impact the coast but not close enough to break the "drought" as it is defined.

In summary, the absence of U.S. landfalling major hurricanes from Wilma in 2005 to Harvey in 2017 was anomalous. There is some evidence that systematic atmosphere/ocean variability has reduced the fraction of hurricanes making U.S. landfall since the mid-1990s, but this is at least partly countered by increased basin-wide numbers, and the net effect on landfall rates is unclear. Moreover, there is a large random element, and the metric itself suffers from lack of physical basis due to the arbitrary intensity threshold and geopolitically based constraints. Additionally, U.S. coastal risk, particularly from storm surge and freshwater flooding, depends strongly on storm size, propagation speed and direction, and rainfall rates. There is some danger, in the form of evoking complacency, in placing too much emphasis on an absence of a specific subset of hurricanes.

9.3 Severe Convective Storms (Thunderstorms)

Tornado and severe thunderstorm events cause significant loss of life and property: more than one-third of the \$1 billion weather disasters in the United States during the past 25 years were due to such events, and, relative to other extreme weather, the damages from convective weather hazards have undergone the largest increase since 1980.⁴⁰ A particular challenge in quantifying the existence and intensity of these events arises from the data

source: rather than measurements, the occurrence of tornadoes and severe thunderstorms is determined by visual sightings by eye-witnesses (such as "storm spotters" and law enforcement officials) or post-storm damage assessments. The reporting has been susceptible to changes in population density, modifications to reporting procedures and training, the introduction of video and social media, and so on. These have led to systematic, non-meteorological biases in the long-term data record.



Nonetheless, judicious use of the report database has revealed important information about tornado trends. Since the 1970s, the United States has experienced a decrease in the number of days per year on which tornadoes occur, but an increase in the number of tornadoes that form on such days.⁴¹ One important implication is that the frequency of days with large numbers of tornadoes – tornado outbreaks – appears to be increasing (Figure 9.3). The extent of the season over which such tornado activity occurs is increasing as well: although tornadoes in the United States are observed in all months of the year, an earlier calendar-day start to the season of high activity is emerging. In general, there is more interannual variability, or volatility, in tornado occurrence (see also Elsner et al. 2015⁴²).⁴³

Evaluations of hail and (non-tornadic) thunderstorm wind reports have thus far been less revealing. Although there is evidence of an increase in the number of hail days per year, the inherent uncertainty in reported hail size reduces the confidence in such a conclusion.⁴⁴

Thunderstorm wind reports have proven to be even less reliable, because, as compared to tornadoes and hail, there is less tangible visual evidence; thus, although the United States has lately experienced several significant thunderstorm wind events (sometimes referred to as “derechos”), the lack of studies that explore long-term trends in wind events and the uncertainties in the historical data preclude any robust assessment.

It is possible to bypass the use of reports by exploiting the fact that the temperature, humidity, and wind in the larger vicinity – or “environment” – of a developing thunderstorm ultimately control the intensity, morphology, and hazardous tendency of the storm. Thus, the premise is that quantifications of the vertical profiles of temperature, humidity, and wind can be used as a proxy for actual severe thunderstorm occurrence. In particular, a thresholded product of convective available potential energy (CAPE) and vertical wind shear over a surface-to-6 km layer (S06) constitutes one widely used means of

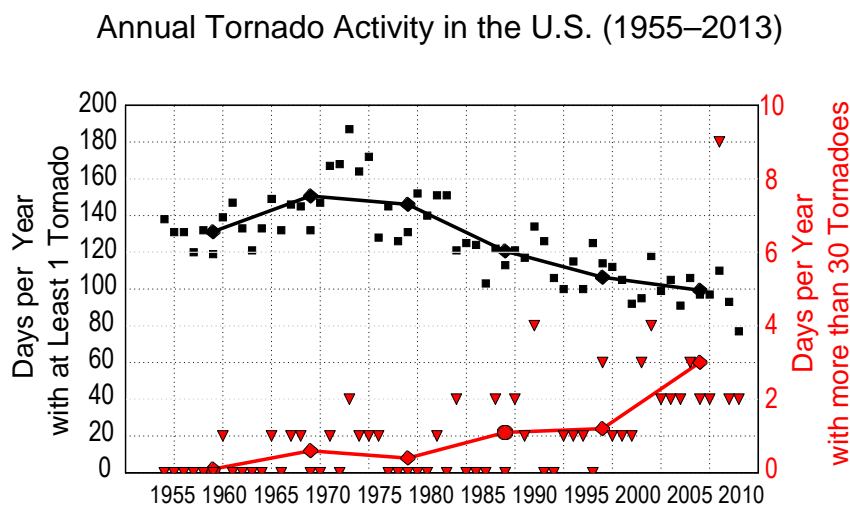


Figure 9.3: Annual tornado activity in the United States over the period 1955–2013. The black squares indicate the number of days per year with at least one tornado rated (E)F1 or greater, and the black circles and line show the decadal mean line of such *tornado days*. The red triangles indicate the number of days per year with more than 30 tornadoes rated (E)F1 or greater, and the red circles and line show the decadal mean of these *tornado outbreaks*. (Figure source: redrawn from Brooks et al. 2014⁴¹).

representing the frequency of severe thunderstorms.⁴⁵ This environmental-proxy approach avoids the biases and other issues with eyewitness storm reports and is readily evaluated using the relatively coarse global datasets and global climate models. It has the disadvantage of assuming that a thunderstorm will necessarily form and then realize its environmental potential.

Upon employing global climate models (GCMs) to evaluate CAPE and S06, a consistent finding among a growing number of proxy-based studies is a projected increase in the frequency of severe thunderstorm environments in the United States over the mid- to late 21st century.^{46, 47, 48, 49, 50, 51} The most robust projected increases in frequency are over the U.S. Midwest and southern Great Plains, during March-April-May (MAM).⁴⁶ Based on the increased frequency of very high CAPE, increases in storm intensity are also projected over this same period (see also Del Genio et al. 2007⁵²).

Key limitations of the environmental proxy approach are being addressed through the applications of high-resolution dynamical downscaling, wherein sufficiently fine model grids are used so that individual thunderstorms are explicitly resolved, rather than implicitly represented (as through environmental proxies). The individually modeled thunderstorms can then be quantified and assessed in terms of severity.^{53, 54, 55} The dynamical-downscaling results have thus far supported the basic findings of the environmental proxy studies, particularly in terms of the seasons and geographical regions projected to experience the largest increases in severe thunderstorm occurrence.⁴⁶

The computational expense of high-resolution dynamical downscaling makes it difficult to generate model ensembles over long time

periods, and thus to assess the uncertainty of the downscaled projections. Because these dynamical downscaling implementations focus on the statistics of storm occurrence rather than on faithful representations of individual events, they have generally been unconcerned with specific extreme convective events in history. So, for example, such downscaling does not address whether the intensity of an event like the Joplin, Missouri, tornado of May 22, 2011, would be amplified under projected future climates. Recently, the “pseudo-global warming” (PGW) methodology (see Schär et al. 1996⁵⁶), which is a variant of dynamical downscaling, has been adapted to address these and related questions. As an example, when the parent “supercell” of select historical tornado events forms under the climate conditions projected during the late 21st century, it does not evolve into a benign, unorganized thunderstorm but instead maintains its supercellular structure.⁵⁷ As measured by updraft strength, the intensity of these supercells under PGW is relatively higher, although not in proportion to the theoretical intensity based on the projected higher levels of CAPE. The adverse effects of enhanced precipitation loading under PGW has been offered as one possible explanation for such shortfalls in projected updraft strength.

9.4 Winter Storms

The frequency of large snowfall years has decreased in the southern United States and Pacific Northwest and increased in the northern United States (see Ch. 7: Precipitation Change). The winters of 2013/2014 and 2014/2015 have contributed to this trend. They were characterized by frequent storms and heavier-than-normal snowfalls in the Midwest and Northeast and drought in the western United States. These were related to blocking (a large-scale pressure pattern with little or no movement) of the wintertime circulation in the Pacific sector of the Northern



Hemisphere (e.g., Marinaro et al. 2015⁵⁸) that put the midwestern and northeastern United States in the primary winter storm track, while at the same time reducing the number of winter storms in California, causing severe drought conditions.⁵⁹ While some observational studies suggest a linkage between blocking affecting the U.S. climate and enhanced arctic warming (arctic amplification), specifically for an increase in highly amplified jet stream patterns in winter over the United States,⁶⁰ other studies show mixed results.^{61, 62, 63} Therefore, a definitive understanding of the effects of arctic amplification on midlatitude winter weather remains elusive. Other explanations have been offered for the weather patterns of recent winters, such as anomalously strong Pacific trade winds,⁶⁴ but these have not been linked to anthropogenic forcing (e.g., Delworth et al. 2015⁶⁵).

Analysis of storm tracks indicates that there has been an increase in winter storm frequency and intensity since 1950, with a slight shift in tracks toward the poles.^{66, 67, 68} Current global climate models (CMIP5) do in fact predict an increase in extratropical cyclone (ETC) frequency over the eastern United States, including the most intense ETCs, under the higher scenario (RCP8.5).⁶⁹ However, there are large model-to-model differences in the realism of ETC simulations and in the projected changes. Moreover, projected ETC changes have large regional variations, including a decreased total frequency in the North Atlantic, further highlighting the complexity of the response to climate change.

9.5 Atmospheric Rivers

The term “atmospheric rivers” (ARs) refers to the relatively narrow streams of moisture transport that often occur within and across midlatitudes⁷⁰ (Figure 9.4), in part because they often transport as much water as in the Amazon River.⁷¹ While ARs occupy less than 10% of the circumference of Earth at any given time, they account for 90% of the poleward moisture transport across midlatitudes (a more complete discussion of precipitation variability is found in Ch. 7: Precipitation Change). In many regions of the world, they account for a substantial fraction of the precipitation,⁷² and thus water supply, often delivered in the form of an extreme weather and precipitation event (Figure 9.4). For example, ARs account for 30%–40% of the typical snowpack in the Sierra Nevada mountains and annual precipitation in the U.S. West Coast states^{73, 74} — an essential summertime source of water for agriculture, consumption, and ecosystem health. However, this vital source of water is also associated with severe flooding — with observational evidence showing a close connection between historically high streamflow events and floods with landfalling AR events — in the west and other sectors of the United States.^{75, 76, 77} More recently, research has also demonstrated that ARs are often found to be critical in ending droughts in the western United States.⁷⁸



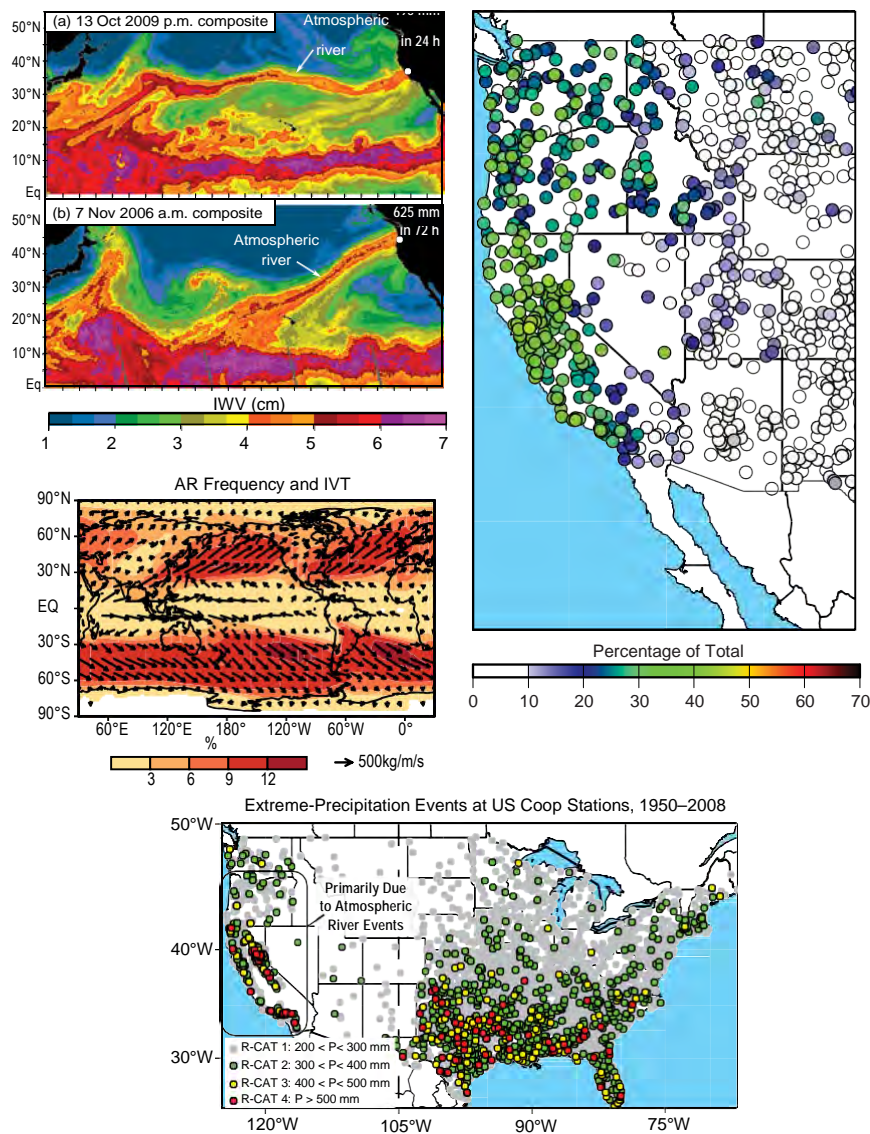


Figure 9.4: (upper left) Atmospheric rivers depicted in Special Sensor Microwave Imager (SSM/I) measurements of SSM/I total column water vapor leading to extreme precipitation events at landfall locations. (middle left) Annual mean frequency of atmospheric river occurrence (for example, 12% means about 1 every 8 days) and their integrated vapor transport (IVT).⁷² (bottom) ARs are the dominant synoptic storms for the U.S. West Coast in terms of extreme precipitation⁹³ and (right) supply a large fraction of the annual precipitation in the U.S. West Coast states.⁷³ [Figure source: (upper and middle left) Ralph et al. 2011,⁹⁴ (upper right) Guan and Waliser 2015,⁷² (lower left) Ralph and Dettinger 2012,⁹³ (lower right) Dettinger et al. 2011;⁷³ left panels, © American Meteorological Society. Used with permission.]

Given the important role that ARs play in the water supply of the western United States and their role in weather and water extremes in the west and occasionally other parts of the United States (e.g., Rutz et al. 2014⁷⁹), it is critical to examine how climate change and the expected intensification of the global water cycle and atmospheric transports (e.g., Held and Soden 2006;⁸⁰ Lavers et al. 2015⁸¹) are projected to impact ARs (e.g., Dettinger and Ingram 2013⁸²).

Under climate change conditions, ARs may be altered in a number of ways, namely their frequency, intensity, duration, and locations. In association with landfalling ARs, any of these would be expected to result in impacts on hazards and water supply given the discussion above. Assessments of ARs in climate change projections for the United States have been undertaken for central California from CMIP3,⁷³ and a number of studies have been

done for the West Coast of North America,^{83, 84, 85, 86, 87} and these studies have uniformly shown that ARs are likely to become more frequent and intense in the future. For example, one recent study reveals a large increase of AR days along the West Coast by the end of the 21st century under the higher scenario (RCP8.5), with fractional increases between 50% and 600%, depending on the seasons and landfall locations.⁸³ Results from these studies (and Lavers et al. 2013⁸⁸ for ARs impacting the United Kingdom) show that these AR changes were predominantly driven by increasing atmospheric specific humidity, with little discernible change in the low-level winds. The higher atmospheric water vapor content in a warmer climate is to be expected because of an increase in saturation water vapor pressure with air temperature (Ch. 2: Physical Drivers of Climate Change). While the thermodynamic effect appears to dominate the climate change impact on ARs, leading to projected increases in ARs, there is evidence for a dynamical effect (that is, location change) related to the projected poleward shift of the subtropical jet that diminished the thermodynamic effect in the southern portion of the West Coast of North America.⁸³

Presently, there is no clear consensus on whether the consistently projected increases in AR frequency and intensity will translate to increased precipitation in California. This is mostly because previous studies did not examine this explicitly and because the model resolution is poor and thus the topography is poorly represented, and the topography is a key aspect of forcing the precipitation out of the systems.⁸⁹ The evidence for considerable increases in the number and intensity of ARs depends (as do all climate variability studies based on dynamical models) on the model fidelity in representing ARs and their interactions with the global climate/circulation. Additional confidence comes from studies that

show qualitatively similar projected increases while also providing evidence that the models represent AR frequency, transports, and spatial distributions relatively well compared to observations.^{84, 85} A caveat associated with drawing conclusions from any given study or differences between two is that they typically use different detection methodologies that are typically tailored to a regional setting (cf. Guan and Waliser 2015⁷²). Additional research is warranted to examine these storms from a global perspective, with additional and more in-depth, process-oriented diagnostics/metrics. Stepping away from the sensitivities associated with defining atmospheric rivers, one study examined the intensification of the integrated vapor transport (IVT), which is easily and unambiguously defined.⁸¹ That study found that for the higher scenario (RCP8.5), multimodel mean IVT and the IVT associated with extremes above 95% percentile increase by 30%–40% in the North Pacific. These results, along with the uniform findings of the studies above examining projected changes in ARs for western North America and the United Kingdom, give *high confidence* that the frequency of AR storms will increase in association with rising global temperatures.



TRACEABLE ACCOUNTS

Key Finding 1

Human activities have contributed substantially to observed ocean–atmosphere variability in the Atlantic Ocean (*medium confidence*), and these changes have contributed to the observed upward trend in North Atlantic hurricane activity since the 1970s (*medium confidence*).

Description of evidence base

The Key Finding and supporting text summarizes extensive evidence documented in the climate science literature and is similar to statements made in previous national (NCA3)⁹⁰ and international⁹¹ assessments. Data limitations are documented in Kossin et al. 2013² and references therein. Contributions of natural and anthropogenic factors in observed multidecadal variability are quantified in Carlsaw et al. 2013;²² Zhang et al. 2013;²⁷ Tung and Zhou 2013;²⁶ Mann et al. 2014;²³ Stevens 2015;²⁵ Sobel et al. 2016;²⁴ Walsh et al. 2015.¹⁰

Major uncertainties

Key remaining uncertainties are due to known and substantial heterogeneities in the historical tropical cyclone data and lack of robust consensus in determining the precise relative contributions of natural and anthropogenic factors in past variability of the tropical environment.

Assessment of confidence based on evidence and agreement, including short description of nature of evidence and level of agreement

Confidence in this finding is rated as *medium*. Although the range of estimates of natural versus anthropogenic contributions in the literature is fairly broad, virtually all studies identify a measurable, and generally substantial, anthropogenic influence. This does constitute a consensus for human contribution to the increases in tropical cyclone activity since 1970.

Summary sentence or paragraph that integrates the above information

The key message and supporting text summarizes extensive evidence documented in the climate science peer-reviewed literature. The uncertainties and points

of consensus that were described in the NCA3 and IPCC assessments have continued.

Key Finding 2

Both theory and numerical modeling simulations generally indicate an increase in tropical cyclone (TC) intensity in a warmer world, and the models generally show an increase in the number of very intense TCs. For Atlantic and eastern North Pacific hurricanes and western North Pacific typhoons, increases are projected in precipitation rates (*high confidence*) and intensity (*medium confidence*). The frequency of the most intense of these storms is projected to increase in the Atlantic and western North Pacific (*low confidence*) and in the eastern North Pacific (*medium confidence*).

Description of evidence base

The Key Finding and supporting text summarizes extensive evidence documented in the climate science literature and is similar to statements made in previous national (NCA3)⁹⁰ and international⁹¹ assessments. Since these assessments, more recent downscaling studies have further supported these assessments (e.g., Knutson et al. 2015⁹), though pointing out that the changes (future increased intensity and tropical cyclone precipitation rates) may not occur in all ocean basins.

Major uncertainties

A key uncertainty remains in the lack of a supporting detectable anthropogenic signal in the historical data to add further confidence to these projections. As such, confidence in the projections is based on agreement among different modeling studies and physical understanding (for example, potential intensity theory for tropical cyclone intensities and the expectation of stronger moisture convergence, and thus higher precipitation rates, in tropical cyclones in a warmer environment containing greater amounts of environmental atmospheric moisture). Additional uncertainty stems from uncertainty in both the projected pattern and magnitude of future sea surface temperatures.⁹



Assessment of confidence based on evidence and agreement, including short description of nature of evidence and level of agreement

Confidence is rated as *high* in tropical cyclone rainfall projections and *medium* in intensity projections since there are a number of publications supporting these overall conclusions, fairly well-established theory, general consistency among different studies, varying methods used in studies, and still a fairly strong consensus among studies. However, a limiting factor for confidence in the results is the lack of a supporting detectable anthropogenic contribution in observed tropical cyclone data.

There is *low* to *medium confidence* for increased occurrence of the most intense tropical cyclones for most ocean basins, as there are relatively few formal studies that focus on these changes, and the change in occurrence of such storms would be enhanced by increased intensities, but reduced by decreased overall frequency of tropical cyclones.

Summary sentence or paragraph that integrates the above information

Models are generally in agreement that tropical cyclones will be more intense and have higher precipitation rates, at least in most ocean basins. Given the agreement between models and support of theory and mechanistic understanding, there is *medium* to *high confidence* in the overall projection, although there is some limitation on confidence levels due to the lack of a supporting detectable anthropogenic contribution to tropical cyclone intensities or precipitation rates.

Key Finding 3

Tornado activity in the United States has become more variable, particularly over the 2000s, with a decrease in the number of days per year with tornadoes and an increase in the number of tornadoes on these days (*medium confidence*). Confidence in past trends for hail and severe thunderstorm winds, however, is *low*. Climate models consistently project environmental changes that would putatively support an increase in the frequency and intensity of severe thunderstorms (a category that combines tornadoes, hail, and winds), especially over

regions that are currently prone to these hazards, but confidence in the details of this projected increase is *low*.

Description of evidence base

Evidence for the first and second statement comes from the U.S. database of tornado reports. There are well known biases in this database, but application of an intensity threshold [greater than or equal to a rating of 1 on the (Enhanced) Fujita scale], and the quantification of tornado activity in terms of tornado days instead of raw numbers of reports are thought to reduce these biases. It is not known at this time whether the variability and trends are necessarily due to climate change.

The third statement is based on projections from a wide range of climate models, including GCMs and RCMs, run over the past 10 years (e.g., see the review by Brooks 2013⁹²). The evidence is derived from an “environmental-proxy” approach, which herein means that severe thunderstorm occurrence is related to the occurrence of two key environmental parameters: CAPE and vertical wind shear. A limitation of this approach is the assumption that the thunderstorm will necessarily form and then realize its environmental potential. This assumption is indeed violated, albeit at levels that vary by region and season.

Major uncertainties

Regarding the first and second statements, there is still some uncertainty in the database, even when the data are filtered. The major uncertainty in the third statement equates to the aforementioned limitation (that is, the thunderstorm will necessarily form and then realize its environmental potential).

Assessment of confidence based on evidence and agreement, including short description of nature of evidence and level of agreement

Medium: That the variability in tornado activity has increased.

Medium: That the severe-thunderstorm environmental conditions will change with a changing climate, but

Low: on the precise (geographical and seasonal) realization of the environmental conditions as actual severe thunderstorms.

Summary sentence or paragraph that integrates the above information

With an established understanding of the data biases, careful analysis provides useful information about past changes in severe thunderstorm and tornado activity. This information suggests that tornado variability has increased in the 2000s, with a concurrent decrease in the number of days per year experiencing tornadoes and an increase in the number of tornadoes on these days. Similarly, the development of novel applications of climate models provides information about possible future severe storm and tornado activity, and although confidence in these projections is low, they do suggest that the projected environments are at least consistent with environments that would putatively support an increase in frequency and intensity of severe thunderstorms.

Key Finding 4

There has been a trend toward earlier snowmelt and a decrease in snowstorm frequency on the southern margins of climatologically snowy areas (*medium confidence*). Winter storm tracks have shifted northward since 1950 over the Northern Hemisphere (*medium confidence*). Projections of winter storm frequency and intensity over the United States vary from increasing to decreasing depending on region, but model agreement is poor and confidence is *low*. Potential linkages between the frequency and intensity of severe winter storms in the United States and accelerated warming in the Arctic have been postulated, but they are complex, and, to some extent, contested, and confidence in the connection is currently *low*.

Description of evidence base

The Key Finding and supporting text summarizes evidence documented in the climate science literature.

Evidence for changes in winter storm track changes are documented in a small number of studies.^{67, 68} Future changes are documented in one study,⁶⁹ but there are large model-to-model differences. The effects of arctic amplification on U.S. winter storms have been studied, but the results are mixed,^{60, 61, 62, 63} leading to considerable uncertainties.

Major uncertainties

Key remaining uncertainties relate to the sensitivity of observed snow changes to the spatial distribution of observing stations and to historical changes in station location and observing practices. There is conflicting evidence about the effects of arctic amplification on CONUS winter weather.

Assessment of confidence based on evidence and agreement, including short description of nature of evidence and level of agreement

There is *high confidence* that warming has resulted in earlier snowmelt and decreased snowfall on the warm margins of areas with consistent snowpack based on a number of observational studies. There is *medium confidence* that Northern Hemisphere storm tracks have shifted north based on a small number of studies. There is *low confidence* in future changes in winter storm frequency and intensity based on conflicting evidence from analysis of climate model simulations.

Summary sentence or paragraph that integrates the above information

Decreases in snowfall on southern and low elevation margins of currently climatologically snowy areas are likely but winter storm frequency and intensity changes are uncertain.

Key Finding 5

The frequency and severity of landfalling “atmospheric rivers” on the U.S. West Coast (narrow streams of moisture that account for 30%–40% of the typical snowpack and annual precipitation in the region and are associated with severe flooding events) will increase as a result of increasing evaporation and resulting higher atmospheric water vapor that occurs with increasing temperature (*medium confidence*).

Description of evidence base

The Key Finding and supporting text summarizes evidence documented in the climate science literature.

Evidence for the expectation of an increase in the frequency and severity of landfalling atmospheric rivers on the U.S. West Coast comes from the CMIP-based



climate change projection studies of Dettinger et al. 2011;⁷³ Warner et al. 2015;⁸⁷ Payne and Magnusdottir 2015;⁸⁵ Gao et al. 2015;⁸³ Radić et al. 2015;⁸⁶ and Hagos et al. 2016.⁸⁴ The close connection between atmospheric rivers and water availability and flooding is based on the present-day observation studies of Guan et al. 2010;⁷⁴ Dettinger et al. 2011;⁷³ Ralph et al. 2006;⁷⁷ Neiman et al. 2011;⁷⁶ Moore et al. 2012;⁷⁵ and Dettinger 2013.⁷⁸

Major uncertainties

A modest uncertainty remains in the lack of a supporting detectable anthropogenic signal in the historical data to add further confidence to these projections. However, the overall increase in atmospheric rivers projected/expected is based to a very large degree on the *very high confidence* that the atmospheric water vapor will increase. Thus, increasing water vapor coupled with little projected change in wind structure/intensity still indicates increases in the frequency/intensity of atmospheric rivers. A modest uncertainty arises in quantifying the expected change at a regional level (for example, northern Oregon vs. southern Oregon) given that there are some changes expected in the position of the jet stream that might influence the degree of increase for different locations along the West Coast. Uncertainty in the projections of the number and intensity of ARs is introduced by uncertainties in the models' ability to represent ARs and their interactions with climate.

Assessment of confidence based on evidence and agreement, including short description of nature of evidence and level of agreement

Confidence in this finding is rated as *medium* based on qualitatively similar projections among different studies.

Summary sentence or paragraph that integrates the above information

Increases in atmospheric river frequency and intensity are expected along the U.S. West Coast, leading to the likelihood of more frequent flooding conditions, with uncertainties remaining in the details of the spatial structure of these along the coast (for example, northern vs. southern California).



REFERENCES

1. Klotzbach, P.J. and C.W. Landsea, 2015: Extremely intense hurricanes: Revisiting Webster et al. (2005) after 10 years. *Journal of Climate*, **28**, 7621-7629. <http://dx.doi.org/10.1175/JCLI-D-15-0188.1>
2. Kossin, J.P., T.L. Olander, and K.R. Knapp, 2013: Trend analysis with a new global record of tropical cyclone intensity. *Journal of Climate*, **26**, 9960-9976. <http://dx.doi.org/10.1175/JCLI-D-13-00262.1>
3. Walsh, K.J.E., J.L. McBride, P.J. Klotzbach, S. Balachandran, S.J. Camargo, G. Holland, T.R. Knutson, J.P. Kossin, T.-c. Lee, A. Sobel, and M. Sugi, 2016: Tropical cyclones and climate change. *Wiley Interdisciplinary Reviews: Climate Change*, **7**, 65-89. <http://dx.doi.org/10.1002/wcc.371>
4. Landsea, C., J. Franklin, and J. Beven, 2015: The revised Atlantic hurricane database (HURDAT2). National Hurricane Center, Miami, FL.
5. Hartmann, D.L., A.M.G. Klein Tank, M. Rusticucci, L.V. Alexander, S. Brönnimann, Y. Charabi, F.J. Dentener, E.J. Dlugokencky, D.R. Easterling, A. Kaplan, B.J. Soden, P.W. Thorne, M. Wild, and P.M. Zhai, 2013: Observations: Atmosphere and surface. *Climate Change 2013: The Physical Science Basis. Contribution of Working Group I to the Fifth Assessment Report of the Intergovernmental Panel on Climate Change*. Stocker, T.F., D. Qin, G.-K. Plattner, M. Tignor, S.K. Allen, J. Boschung, A. Nauels, Y. Xia, V. Bex, and P.M. Midgley, Eds. Cambridge University Press, Cambridge, United Kingdom and New York, NY, USA, 159-254. <http://www.climatechange2013.org/report/full-report/>
6. Bindoff, N.L., P.A. Stott, K.M. AchutaRao, M.R. Allen, N. Gillett, D. Gutzler, K. Hansingo, G. Hegerl, Y. Hu, S. Jain, I.I. Mokhov, J. Overland, J. Perlwitz, R. Sebbari, and X. Zhang, 2013: Detection and attribution of climate change: From global to regional. *Climate Change 2013: The Physical Science Basis. Contribution of Working Group I to the Fifth Assessment Report of the Intergovernmental Panel on Climate Change*. Stocker, T.F., D. Qin, G.-K. Plattner, M. Tignor, S.K. Allen, J. Boschung, A. Nauels, Y. Xia, V. Bex, and P.M. Midgley, Eds. Cambridge University Press, Cambridge, United Kingdom and New York, NY, USA, 867-952. <http://www.climatechange2013.org/report/full-report/>
7. Camargo, S.J., 2013: Global and regional aspects of tropical cyclone activity in the CMIP5 models. *Journal of Climate*, **26**, 9880-9902. <http://dx.doi.org/10.1175/jcli-d-12-00549.1>
8. Christensen, J.H., K. Krishna Kumar, E. Aldrian, S.-I. An, I.F.A. Cavalcanti, M. de Castro, W. Dong, P. Goswami, A. Hall, J.K. Kanyanga, A. Kitoh, J. Kossin, N.-C. Lau, J. Renwick, D.B. Stephenson, S.-P. Xie, and T. Zhou, 2013: Climate phenomena and their relevance for future regional climate change. *Climate Change 2013: The Physical Science Basis. Contribution of Working Group I to the Fifth Assessment Report of the Intergovernmental Panel on Climate Change*. Stocker, T.F., D. Qin, G.-K. Plattner, M. Tignor, S.K. Allen, J. Boschung, A. Nauels, Y. Xia, V. Bex, and P.M. Midgley, Eds. Cambridge University Press, Cambridge, United Kingdom and New York, NY, USA, 1217-1308. <http://www.climatechange2013.org/report/full-report/>
9. Knutson, T.R., J.J. Sirutis, M. Zhao, R.E. Tuleya, M. Bender, G.A. Vecchi, G. Villarini, and D. Chavas, 2015: Global projections of intense tropical cyclone activity for the late twenty-first century from dynamical downscaling of CMIP5/RCP4.5 scenarios. *Journal of Climate*, **28**, 7203-7224. <http://dx.doi.org/10.1175/JCLI-D-15-0129.1>
10. Walsh, K.J.E., S.J. Camargo, G.A. Vecchi, A.S. Daloz, J. Elsner, K. Emanuel, M. Horn, Y.-K. Lim, M. Roberts, C. Patricola, E. Scoccimarro, A.H. Sobel, S. Strazzo, G. Villarini, M. Wehner, M. Zhao, J.P. Kossin, T. LaRow, K. Oouchi, S. Schubert, H. Wang, J. Bacmeister, P. Chang, F. Chauvin, C. Jablonowski, A. Kumar, H. Murakami, T. Ose, K.A. Reed, R. Saravanan, Y. Yamada, C.M. Zarzycki, P.L. Vidale, J.A. Jonas, and N. Henderson, 2015: Hurricanes and climate: The U.S. CLIVAR Working Group on Hurricanes. *Bulletin of the American Meteorological Society*, **96** (12), 997-1017. <http://dx.doi.org/10.1175/BAMS-D-13-00242.1>
11. Murakami, H., G.A. Vecchi, T.L. Delworth, K. Paffen-dorf, L. Jia, R. Gudgel, and F. Zeng, 2015: Investigating the influence of anthropogenic forcing and natural variability on the 2014 Hawaiian hurricane season [in "Explaining Extreme Events of 2014 from a Climate Perspective"]. *Bulletin of the American Meteorological Society*, **96** (12), S115-S119. <http://dx.doi.org/10.1175/BAMS-D-15-00119.1>
12. Kossin, J.P., K.A. Emanuel, and G.A. Vecchi, 2014: The poleward migration of the location of tropical cyclone maximum intensity. *Nature*, **509**, 349-352. <http://dx.doi.org/10.1038/nature13278>
13. Kossin, J.P., K.A. Emanuel, and S.J. Camargo, 2016: Past and projected changes in western North Pacific tropical cyclone exposure. *Journal of Climate*, **29**, 5725-5739. <http://dx.doi.org/10.1175/JCLI-D-16-0076.1>
14. Delworth, L.T. and E.M. Mann, 2000: Observed and simulated multidecadal variability in the Northern Hemisphere. *Climate Dynamics*, **16**, 661-676. <http://dx.doi.org/10.1007/s003820000075>

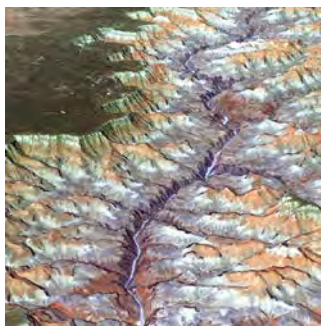
15. Evan, A.T., 2012: Atlantic hurricane activity following two major volcanic eruptions. *Journal of Geophysical Research*, **117**, D06101. <http://dx.doi.org/10.1029/2011JD016716>
16. Thompson, D.W.J. and S. Solomon, 2009: Understanding recent stratospheric climate change. *Journal of Climate*, **22**, 1934-1943. <http://dx.doi.org/10.1175/2008JCLI2482.1>
17. Evan, A.T., G.R. Foltz, D. Zhang, and D.J. Vimont, 2011: Influence of African dust on ocean-atmosphere variability in the tropical Atlantic. *Nature Geoscience*, **4**, 762-765. <http://dx.doi.org/10.1038/ngeo1276>
18. Evan, A.T., D.J. Vimont, A.K. Heidinger, J.P. Kossin, and R. Bennartz, 2009: The role of aerosols in the evolution of tropical North Atlantic Ocean temperature anomalies. *Science*, **324**, 778-781. <http://dx.doi.org/10.1126/science.1167404>
19. Booth, B.B.B., N.J. Dunstone, P.R. Halloran, T. Andrews, and N. Bellouin, 2012: Aerosols implicated as a prime driver of twentieth-century North Atlantic climate variability. *Nature*, **484**, 228-232. <http://dx.doi.org/10.1038/nature10946>
20. Dunstone, N.J., D.M. Smith, B.B.B. Booth, L. Hermanson, and R. Eade, 2013: Anthropogenic aerosol forcing of Atlantic tropical storms. *Nature Geoscience*, **6**, 534-539. <http://dx.doi.org/10.1038/ngeo1854>
21. Mann, M.E. and K.A. Emanuel, 2006: Atlantic hurricane trends linked to climate change. *Eos, Transactions, American Geophysical Union*, **87**, 233-244. <http://dx.doi.org/10.1029/2006EO240001>
22. Carslaw, K.S., L.A. Lee, C.L. Reddington, K.J. Pringle, A. Rap, P.M. Forster, G.W. Mann, D.V. Spracklen, M.T. Woodhouse, L.A. Regayre, and J.R. Pierce, 2013: Large contribution of natural aerosols to uncertainty in indirect forcing. *Nature*, **503**, 67-71. <http://dx.doi.org/10.1038/nature12674>
23. Mann, M.E., B.A. Steinman, and S.K. Miller, 2014: On forced temperature changes, internal variability, and the AMO. *Geophysical Research Letters*, **41**, 3211-3219. <http://dx.doi.org/10.1002/2014GL059233>
24. Sobel, A.H., S.J. Camargo, T.M. Hall, C.-Y. Lee, M.K. Tippett, and A.A. Wing, 2016: Human influence on tropical cyclone intensity. *Science*, **353**, 242-246. <http://dx.doi.org/10.1126/science.aaf6574>
25. Stevens, B., 2015: Rethinking the lower bound on aerosol radiative forcing. *Journal of Climate*, **28**, 4794-4819. <http://dx.doi.org/10.1175/JCLI-D-14-00656.1>
26. Tung, K.-K. and J. Zhou, 2013: Using data to attribute episodes of warming and cooling in instrumental records. *Proceedings of the National Academy of Sciences*, **110**, 2058-2063. <http://dx.doi.org/10.1073/pnas.1212471110>
27. Zhang, R., T.L. Delworth, R. Sutton, D.L.R. Hodson, K.W. Dixon, I.M. Held, Y. Kushnir, J. Marshall, Y. Ming, R. Msadek, J. Robson, A.J. Rosati, M. Ting, and G.A. Vecchi, 2013: Have aerosols caused the observed Atlantic multidecadal variability? *Journal of the Atmospheric Sciences*, **70**, 1135-1144. <http://dx.doi.org/10.1175/jas-d-12-0331.1>
28. Kossin, J.P., T.R. Karl, T.R. Knutson, K.A. Emanuel, K.E. Kunkel, and J.J. O'Brien, 2015: Reply to "Comments on 'Monitoring and understanding trends in extreme storms: State of knowledge'". *Bulletin of the American Meteorological Society*, **96** (12), 1177-1179. <http://dx.doi.org/10.1175/BAMS-D-14-00261.1>
29. Huang, P., I.I. Lin, C. Chou, and R.-H. Huang, 2015: Change in ocean subsurface environment to suppress tropical cyclone intensification under global warming. *Nature Communications*, **6**, 7188. <http://dx.doi.org/10.1038/ncomms8188>
30. Emanuel, K., 2015: Effect of upper-ocean evolution on projected trends in tropical cyclone activity. *Journal of Climate*, **28**, 8165-8170. <http://dx.doi.org/10.1175/JCLI-D-15-0401.1>
31. Tuleya, R.E., M. Bender, T.R. Knutson, J.J. Sirutis, B. Thomas, and I. Ginis, 2016: Impact of upper-tropospheric temperature anomalies and vertical wind shear on tropical cyclone evolution using an idealized version of the operational GFDL hurricane model. *Journal of the Atmospheric Sciences*, **73**, 3803-3820. <http://dx.doi.org/10.1175/JAS-D-16-0045.1>
32. Emanuel, K.A., 2013: Downscaling CMIP5 climate models shows increased tropical cyclone activity over the 21st century. *Proceedings of the National Academy of Sciences*, **110**, 12219-12224. <http://dx.doi.org/10.1073/pnas.1301293110>
33. Wehner, M., Prabhat, K.A. Reed, D. Stone, W.D. Collins, and J. Bacmeister, 2015: Resolution dependence of future tropical cyclone projections of CAM5.1 in the U.S. CLIVAR Hurricane Working Group idealized configurations. *Journal of Climate*, **28**, 3905-3925. <http://dx.doi.org/10.1175/JCLI-D-14-00311.1>
34. Hall, T. and K. Hereid, 2015: The frequency and duration of U.S. hurricane droughts. *Geophysical Research Letters*, **42**, 3482-3485. <http://dx.doi.org/10.1002/2015GL063652>
35. Kossin, J.P., 2017: Hurricane intensification along U.S. coast suppressed during active hurricane periods. *Nature*, **541**, 390-393. <http://dx.doi.org/10.1038/nature20783>
36. Colbert, A.J. and B.J. Soden, 2012: Climatological variations in North Atlantic tropical cyclone tracks. *Journal of Climate*, **25**, 657-673. <http://dx.doi.org/10.1175/jcli-d-11-00034.1>

37. Kossin, J.P. and D.J. Vimont, 2007: A more general framework for understanding Atlantic hurricane variability and trends. *Bulletin of the American Meteorological Society*, **88**, 1767-1781. <http://dx.doi.org/10.1175/bams-88-11-1767>
38. Wang, C., H. Liu, S.-K. Lee, and R. Atlas, 2011: Impact of the Atlantic warm pool on United States land-falling hurricanes. *Geophysical Research Letters*, **38**, L19702. <http://dx.doi.org/10.1029/2011gl049265>
39. Hart, R.E., D.R. Chavas, and M.P. Guishard, 2016: The arbitrary definition of the current Atlantic major hurricane landfall drought. *Bulletin of the American Meteorological Society*, **97**, 713-722. <http://dx.doi.org/10.1175/BAMS-D-15-00185.1>
40. Smith, A.B. and R.W. Katz, 2013: U.S. billion-dollar weather and climate disasters: Data sources, trends, accuracy and biases. *Natural Hazards*, **67**, 387-410. <http://dx.doi.org/10.1007/s11069-013-0566-5>
41. Brooks, H.E., G.W. Carbin, and P.T. Marsh, 2014: Increased variability of tornado occurrence in the United States. *Science*, **346**, 349-352. <http://dx.doi.org/10.1126/science.1257460>
42. Elsner, J.B., S.C. Elsner, and T.H. Jagger, 2015: The increasing efficiency of tornado days in the United States. *Climate Dynamics*, **45**, 651-659. <http://dx.doi.org/10.1007/s00382-014-2277-3>
43. Tippett, M.K., 2014: Changing volatility of U.S. annual tornado reports. *Geophysical Research Letters*, **41**, 6956-6961. <http://dx.doi.org/10.1002/2014GL061347>
44. Allen, J.T. and M.K. Tippett, 2015: The Characteristics of United States Hail Reports: 1955-2014. *Electronic Journal of Severe Storms Meteorology*.
45. Brooks, H.E., J.W. Lee, and J.P. Craven, 2003: The spatial distribution of severe thunderstorm and tornado environments from global reanalysis data. *Atmospheric Research*, **67-68**, 73-94. [http://dx.doi.org/10.1016/S0169-8095\(03\)00045-0](http://dx.doi.org/10.1016/S0169-8095(03)00045-0)
46. Diffenbaugh, N.S., M. Scherer, and R.J. Trapp, 2013: Robust increases in severe thunderstorm environments in response to greenhouse forcing. *Proceedings of the National Academy of Sciences*, **110**, 16361-16366. <http://dx.doi.org/10.1073/pnas.1307758110>
47. Gensini, V.A., C. Ramseyer, and T.L. Mote, 2014: Future convective environments using NARCCAP. *International Journal of Climatology*, **34**, 1699-1705. <http://dx.doi.org/10.1002/joc.3769>
48. Seeley, J.T. and D.M. Romps, 2015: The effect of global warming on severe thunderstorms in the United States. *Journal of Climate*, **28**, 2443-2458. <http://dx.doi.org/10.1175/JCLI-D-14-00382.1>
49. Trapp, R.J., N.S. Diffenbaugh, H.E. Brooks, M.E. Baldwin, E.D. Robinson, and J.S. Pal, 2007: Changes in severe thunderstorm environment frequency during the 21st century caused by anthropogenically enhanced global radiative forcing. *Proceedings of the National Academy of Sciences*, **104**, 19719-19723. <http://dx.doi.org/10.1073/pnas.0705494104>
50. Trapp, R.J., N.S. Diffenbaugh, and A. Gluhovsky, 2009: Transient response of severe thunderstorm forcing to elevated greenhouse gas concentrations. *Geophysical Research Letters*, **36**, L01703. <http://dx.doi.org/10.1029/2008GL036203>
51. Van Klooster, S.L. and P.J. Roebber, 2009: Surface-based convective potential in the contiguous United States in a business-as-usual future climate. *Journal of Climate*, **22**, 3317-3330. <http://dx.doi.org/10.1175/2009JCLI2697.1>
52. Del Genio, A.D., M.S. Yao, and J. Jonas, 2007: Will moist convection be stronger in a warmer climate? *Geophysical Research Letters*, **34**, L16703. <http://dx.doi.org/10.1029/2007GL030525>
53. Trapp, R.J., E.D. Robinson, M.E. Baldwin, N.S. Diffenbaugh, and B.R.J. Schwedler, 2011: Regional climate of hazardous convective weather through high-resolution dynamical downscaling. *Climate Dynamics*, **37**, 677-688. <http://dx.doi.org/10.1007/s00382-010-0826-y>
54. Robinson, E.D., R.J. Trapp, and M.E. Baldwin, 2013: The geospatial and temporal distributions of severe thunderstorms from high-resolution dynamical downscaling. *Journal of Applied Meteorology and Climatology*, **52**, 2147-2161. <http://dx.doi.org/10.1175/JAMC-D-12-0131.1>
55. Gensini, V.A. and T.L. Mote, 2014: Estimations of hazardous convective weather in the United States using dynamical downscaling. *Journal of Climate*, **27**, 6581-6589. <http://dx.doi.org/10.1175/JCLI-D-13-00777.1>
56. Schär, C., C. Frei, D. Lüthi, and H.C. Davies, 1996: Surrogate climate-change scenarios for regional climate models. *Geophysical Research Letters*, **23**, 669-672. <http://dx.doi.org/10.1029/96GL00265>
57. Trapp, R.J. and K.A. Hoogewind, 2016: The realization of extreme tornadic storm events under future anthropogenic climate change. *Journal of Climate*, **29**, 5251-5265. <http://dx.doi.org/10.1175/JCLI-D-15-0623.1>
58. Marinaro, A., S. Hilberg, D. Changnon, and J.R. Angel, 2015: The North Pacific-driven severe Midwest winter of 2013/14. *Journal of Applied Meteorology and Climatology*, **54**, 2141-2151. <http://dx.doi.org/10.1175/JAMC-D-15-0084.1>

59. Chang, E.K.M., C. Zheng, P. Lanigan, A.M.W. Yau, and J.D. Neelin, 2015: Significant modulation of variability and projected change in California winter precipitation by extratropical cyclone activity. *Geophysical Research Letters*, **42**, 5983-5991. <http://dx.doi.org/10.1002/2015GL064424>
60. Francis, J. and N. Skific, 2015: Evidence linking rapid Arctic warming to mid-latitude weather patterns. *Philosophical Transactions of the Royal Society A: Mathematical, Physical and Engineering Sciences*, **373**, 20140170. <http://dx.doi.org/10.1098/rsta.2014.0170>
61. Barnes, E.A. and L.M. Polvani, 2015: CMIP5 projections of Arctic amplification, of the North American/ North Atlantic circulation, and of their relationship. *Journal of Climate*, **28**, 5254-5271. <http://dx.doi.org/10.1175/JCLI-D-14-00589.1>
62. Perlwitz, J., M. Hoerling, and R. Dole, 2015: Arctic tropospheric warming: Causes and linkages to lower latitudes. *Journal of Climate*, **28**, 2154-2167. <http://dx.doi.org/10.1175/JCLI-D-14-00095.1>
63. Screen, J.A., C. Deser, and L. Sun, 2015: Projected changes in regional climate extremes arising from Arctic sea ice loss. *Environmental Research Letters*, **10**, 084006. <http://dx.doi.org/10.1088/1748-9326/10/8/084006>
64. Yang, X., G.A. Vecchi, T.L. Delworth, K. Paffendorf, L. Jia, R. Gudgel, F. Zeng, and S.D. Underwood, 2015: Extreme North America winter storm season of 2013/14: Roles of radiative forcing and the global warming hiatus [in "Explaining Extreme Events of 2014 from a Climate Perspective"]. *Bulletin of the American Meteorological Society*, **96** (12), S25-S28. <http://dx.doi.org/10.1175/BAMS-D-15-00133.1>
65. Delworth, T.L., F. Zeng, A. Rosati, G.A. Vecchi, and A.T. Wittenberg, 2015: A link between the hiatus in global warming and North American drought. *Journal of Climate*, **28**, 3834-3845. <http://dx.doi.org/10.1175/jcli-d-14-00616.1>
66. Vose, R.S., S. Applequist, M.A. Bourassa, S.C. Pryor, R.J. Barthelmie, B. Blanton, P.D. Bromirski, H.E. Brooks, A.T. DeGaetano, R.M. Dole, D.R. Easterling, R.E. Jensen, T.R. Karl, R.W. Katz, K. Klink, M.C. Kruk, K.E. Kunkel, M.C. MacCracken, T.C. Peterson, K. Shein, B.R. Thomas, J.E. Walsh, X.L. Wang, M.F. Wehner, D.J. Wuebbles, and R.S. Young, 2014: Monitoring and understanding changes in extremes: Extratropical storms, winds, and waves. *Bulletin of the American Meteorological Society*, **95**, 377-386. <http://dx.doi.org/10.1175/BAMS-D-12-00162.1>
67. Wang, X.L., Y. Feng, G.P. Compo, V.R. Swail, F.W. Zwiers, R.J. Allan, and P.D. Sardeshmukh, 2012: Trends and low frequency variability of extratropical cyclone activity in the ensemble of twentieth century reanalysis. *Climate Dynamics*, **40**, 2775-2800. <http://dx.doi.org/10.1007/s00382-012-1450-9>
68. Wang, X.L., V.R. Swail, and F.W. Zwiers, 2006: Climatology and changes of extratropical cyclone activity: Comparison of ERA-40 with NCEP-NCAR reanalysis for 1958-2001. *Journal of Climate*, **19**, 3145-3166. <http://dx.doi.org/10.1175/JCLI3781.1>
69. Colle, B.A., Z. Zhang, K.A. Lombardo, E. Chang, P. Liu, and M. Zhang, 2013: Historical evaluation and future prediction of eastern North American and western Atlantic extratropical cyclones in the CMIP5 models during the cool season. *Journal of Climate*, **26**, 6882-6903. <http://dx.doi.org/10.1175/JCLI-D-12-00498.1>
70. Zhu, Y. and R.E. Newell, 1998: A proposed algorithm for moisture fluxes from atmospheric rivers. *Monthly Weather Review*, **126**, 725-735. [http://dx.doi.org/10.1175/1520-0493\(1998\)126<0725:APAFMF>2.0.CO;2](http://dx.doi.org/10.1175/1520-0493(1998)126<0725:APAFMF>2.0.CO;2)
71. Newell, R.E., N.E. Newell, Y. Zhu, and C. Scott, 1992: Tropospheric rivers? - A pilot study. *Geophysical Research Letters*, **19**, 2401-2404. <http://dx.doi.org/10.1029/92GL02916>
72. Guan, B. and D.E. Waliser, 2015: Detection of atmospheric rivers: Evaluation and application of an algorithm for global studies. *Journal of Geophysical Research Atmospheres*, **120**, 12514-12535. <http://dx.doi.org/10.1002/2015JD024257>
73. Dettinger, M.D., F.M. Ralph, T. Das, P.J. Neiman, and D.R. Cayan, 2011: Atmospheric rivers, floods and the water resources of California. *Water*, **3**, 445-478. <http://dx.doi.org/10.3390/w3020445>
74. Guan, B., N.P. Molotch, D.E. Waliser, E.J. Fetzer, and P.J. Neiman, 2010: Extreme snowfall events linked to atmospheric rivers and surface air temperature via satellite measurements. *Geophysical Research Letters*, **37**, L20401. <http://dx.doi.org/10.1029/2010GL044696>
75. Moore, B.J., P.J. Neiman, F.M. Ralph, and F.E. Barthold, 2012: Physical processes associated with heavy flooding rainfall in Nashville, Tennessee, and vicinity during 1-2 May 2010: The role of an atmospheric river and mesoscale convective systems. *Monthly Weather Review*, **140**, 358-378. <http://dx.doi.org/10.1175/MWR-D-11-00126.1>
76. Neiman, P.J., L.J. Schick, F.M. Ralph, M. Hughes, and G.A. Wick, 2011: Flooding in western Washington: The connection to atmospheric rivers. *Journal of Hydrometeorology*, **12**, 1337-1358. <http://dx.doi.org/10.1175/2011JHM1358.1>
77. Ralph, F.M., P.J. Neiman, G.A. Wick, S.I. Gutman, M.D. Dettinger, D.R. Cayan, and A.B. White, 2006: Flooding on California's Russian River: Role of atmospheric rivers. *Geophysical Research Letters*, **33**, L13801. <http://dx.doi.org/10.1029/2006GL026689>
78. Dettinger, M.D., 2013: Atmospheric rivers as drought busters on the U.S. West Coast. *Journal of Hydrometeorology*, **14**, 1721-1732. <http://dx.doi.org/10.1175/JHM-D-13-02.1>

79. Rutz, J.J., W.J. Steenburgh, and F.M. Ralph, 2014: Climatological characteristics of atmospheric rivers and their inland penetration over the western United States. *Monthly Weather Review*, **142**, 905-921. <http://dx.doi.org/10.1175/MWR-D-13-00168.1>
80. Held, I.M. and B.J. Soden, 2006: Robust responses of the hydrological cycle to global warming. *Journal of Climate*, **19**, 5686-5699. <http://dx.doi.org/10.1175/jcli3990.1>
81. Lavers, D.A., F.M. Ralph, D.E. Waliser, A. Gershunov, and M.D. Dettinger, 2015: Climate change intensification of horizontal water vapor transport in CMIP5. *Geophysical Research Letters*, **42**, 5617-5625. <http://dx.doi.org/10.1002/2015GL064672>
82. Dettinger, M.D. and B.L. Ingram, 2013: The coming megafloods. *Scientific American*, 308, 64-71. <http://dx.doi.org/10.1038/scientificamerican0113-64>
83. Gao, Y., J. Lu, L.R. Leung, Q. Yang, S. Hagos, and Y. Qian, 2015: Dynamical and thermodynamical modulations on future changes of landfalling atmospheric rivers over western North America. *Geophysical Research Letters*, **42**, 7179-7186. <http://dx.doi.org/10.1002/2015GL065435>
84. Hagos, S.M., L.R. Leung, J.-H. Yoon, J. Lu, and Y. Gao, 2016: A projection of changes in landfalling atmospheric river frequency and extreme precipitation over western North America from the Large Ensemble CESM simulations. *Geophysical Research Letters*, **43**, 1357-1363. <http://dx.doi.org/10.1002/2015GL067392>
85. Payne, A.E. and G. Magnusdottir, 2015: An evaluation of atmospheric rivers over the North Pacific in CMIP5 and their response to warming under RCP 8.5. *Journal of Geophysical Research Atmospheres*, **120**, 11,173-11,190. <http://dx.doi.org/10.1002/2015JD023586>
86. Radić, V., A.J. Cannon, B. Menounos, and N. Gi, 2015: Future changes in autumn atmospheric river events in British Columbia, Canada, as projected by CMIP5 global climate models. *Journal of Geophysical Research Atmospheres*, **120**, 9279-9302. <http://dx.doi.org/10.1002/2015JD023279>
87. Warner, M.D., C.F. Mass, and E.P. Salathé Jr., 2015: Changes in winter atmospheric rivers along the North American West Coast in CMIP5 climate models. *Journal of Hydrometeorology*, **16**, 118-128. <http://dx.doi.org/10.1175/JHM-D-14-0080.1>
88. Lavers, D.A., R.P. Allan, G. Villarini, B. Lloyd-Hughes, D.J. Brayshaw, and A.J. Wade, 2013: Future changes in atmospheric rivers and their implications for winter flooding in Britain. *Environmental Research Letters*, **8**, 034010. <http://dx.doi.org/10.1088/1748-9326/8/3/034010>
89. Pierce, D.W., D.R. Cayan, T. Das, E.P. Maurer, N.L. Miller, Y. Bao, M. Kanamitsu, K. Yoshimura, M.A. Snyder, L.C. Sloan, G. Franco, and M. Tyree, 2013: The key role of heavy precipitation events in climate model disagreements of future annual precipitation changes in California. *Journal of Climate*, **26**, 5879-5896. <http://dx.doi.org/10.1175/jcli-d-12-00766.1>
90. Melillo, J.M., T.C. Richmond, and G.W. Yohe, eds., 2014: *Climate Change Impacts in the United States: The Third National Climate Assessment*. U.S. Global Change Research Program: Washington, D.C., 841 pp. <http://dx.doi.org/10.7930/J0Z31WJ2>
91. IPCC, 2013: *Climate Change 2013: The Physical Science Basis. Contribution of Working Group I to the Fifth Assessment Report of the Intergovernmental Panel on Climate Change*. Cambridge University Press, Cambridge, UK and New York, NY, 1535 pp. <http://www.climatechange2013.org/report/>
92. Brooks, H.E., 2013: Severe thunderstorms and climate change. *Atmospheric Research*, **123**, 129-138. <http://dx.doi.org/10.1016/j.atmosres.2012.04.002>
93. Ralph, F.M. and M.D. Dettinger, 2012: Historical and national perspectives on extreme West Coast precipitation associated with atmospheric rivers during December 2010. *Bulletin of the American Meteorological Society*, **93**, 783-790. <http://dx.doi.org/10.1175/BAMS-D-11-00188.1>
94. Ralph, F.M., P.J. Neiman, G.N. Kiladis, K. Weickmann, and D.W. Reynolds, 2011: A multiscale observational case study of a Pacific atmospheric river exhibiting tropical-extratropical connections and a mesoscale frontal wave. *Monthly Weather Review*, **139**, 1169-1189. <http://dx.doi.org/10.1175/2010mwr3596.1>





10

Changes in Land Cover and Terrestrial Biogeochemistry

KEY FINDINGS

1. Changes in land use and land cover due to human activities produce physical changes in land surface albedo, latent and sensible heat, and atmospheric aerosol and greenhouse gas concentrations. The combined effects of these changes have recently been estimated to account for $40\% \pm 16\%$ of the human-caused global radiative forcing from 1850 to present day (*high confidence*). In recent decades, land use and land cover changes have turned the terrestrial biosphere (soil and plants) into a net “sink” for carbon (drawing down carbon from the atmosphere), and this sink has steadily increased since 1980 (*high confidence*). Because of the uncertainty in the trajectory of land cover, the possibility of the land becoming a net carbon source cannot be excluded (*very high confidence*).
2. Climate change and induced changes in the frequency and magnitude of extreme events (e.g., droughts, floods, and heat waves) have led to large changes in plant community structure with subsequent effects on the biogeochemistry of terrestrial ecosystems. Uncertainties about how climate change will affect land cover change make it difficult to project the magnitude and sign of future climate feedbacks from land cover changes (*high confidence*).
3. Since 1901, regional averages of both the consecutive number of frost-free days and the length of the corresponding growing season have increased for the seven contiguous U.S. regions used in this assessment. However, there is important variability at smaller scales, with some locations actually showing decreases of a few days to as much as one to two weeks. Plant productivity has not increased commensurate with the increased number of frost-free days or with the longer growing season due to plant-specific temperature thresholds, plant–pollinator dependence, and seasonal limitations in water and nutrient availability (*very high confidence*). Future consequences of changes to the growing season for plant productivity are uncertain.
4. Recent studies confirm and quantify that surface temperatures are higher in urban areas than in surrounding rural areas for a number of reasons, including the concentrated release of heat from buildings, vehicles, and industry. In the United States, this urban heat island effect results in daytime temperatures 0.9° – 7.2° F (0.5° – 4.0° C) higher and nighttime temperatures 1.8° – 4.5° F (1.0° – 2.5° C) higher in urban areas, with larger temperature differences in humid regions (primarily in the eastern United States) and in cities with larger and denser populations. The urban heat island effect will strengthen in the future as the structure, spatial extent, and population density of urban areas change and grow (*high confidence*).

Recommended Citation for Chapter

Hibbard, K.A., F.M. Hoffman, D. Huntzinger, and T.O. West, 2017: Changes in land cover and terrestrial biogeochemistry. In: *Climate Science Special Report: Fourth National Climate Assessment, Volume I* [Wuebbles, D.J., D.W. Fahey, K.A. Hibbard, D.J. Dokken, B.C. Stewart, and T.K. Maycock (eds.)]. U.S. Global Change Research Program, Washington, DC, USA, pp. 277-302, doi: 10.7930/J0416V6X.

10.1 Introduction

Direct changes in land use by humans are contributing to radiative forcing by altering land cover and therefore albedo, contributing to climate change (Ch. 2: Physical Drivers of Climate Change). This forcing is spatially variable in both magnitude and sign; globally averaged, it is negative (climate cooling; Figure 2.3). Climate changes, in turn, are altering the biogeochemistry of land ecosystems through extended growing seasons, increased numbers of frost-free days, altered productivity in agricultural and forested systems, longer fire seasons, and urban-induced thunderstorms.^{1,2} Changes in land use and land cover interact with local, regional, and global

climate processes.³ The resulting ecosystem responses alter Earth's albedo, the carbon cycle, and atmospheric aerosols, constituting a mix of positive and negative feedbacks to climate change (Figure 10.1 and Chapter 2, Section 2.6.2).^{4,5} Thus, changes to terrestrial ecosystems or land cover are a direct driver of climate change and they are further altered by climate change in ways that affect both ecosystem productivity and, through feedbacks, the climate itself. The following sections describe advances since the Third National Climate Assessment (NCA3)⁶ in scientific understanding of land cover and associated biogeochemistry and their impacts on the climate system.

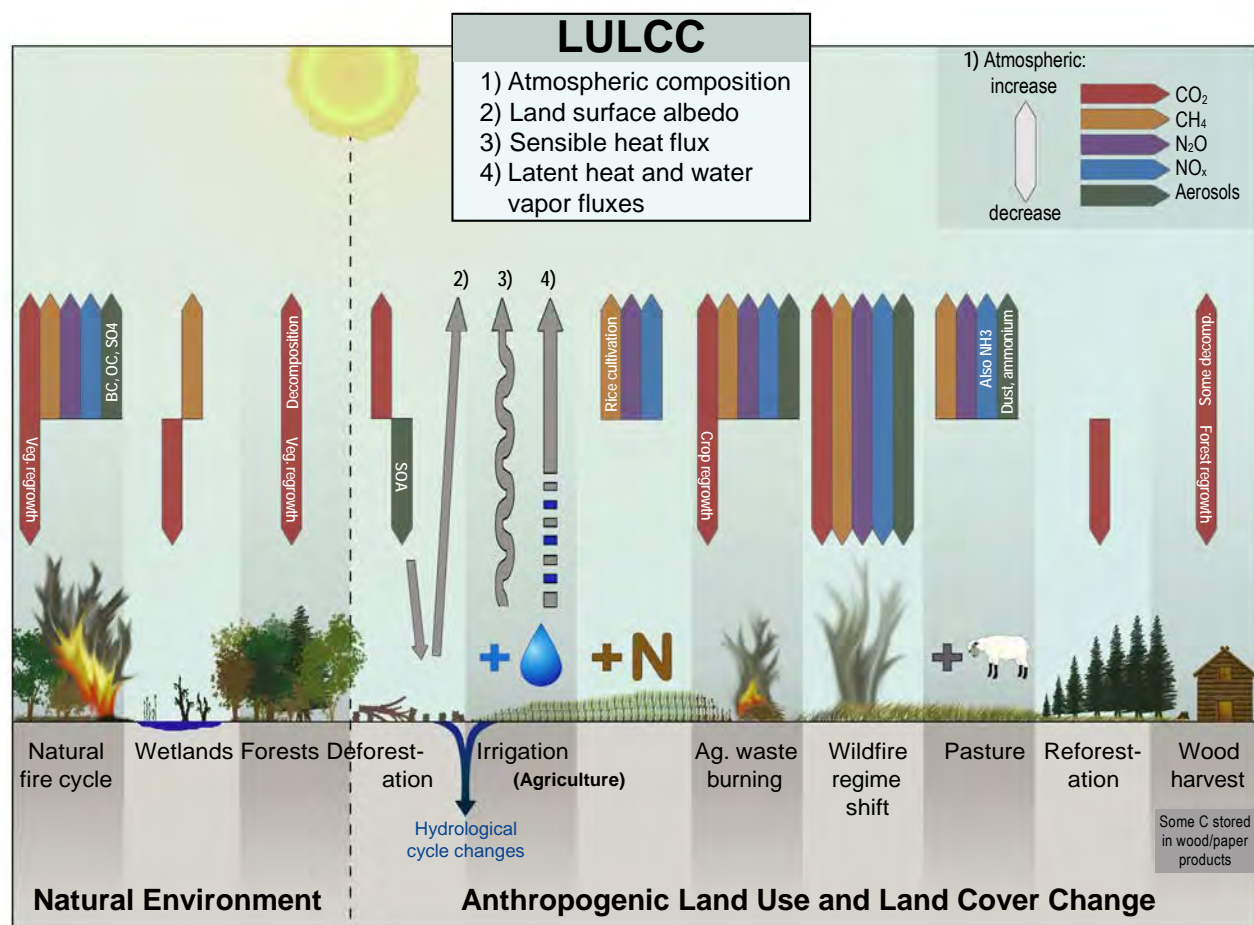


Figure 10.1: This graphical representation summarizes land-atmosphere interactions from natural and anthropogenic land-use and land-cover change (LULCC) contributions to radiative forcing. Emissions and sequestration of carbon and fluxes of nitrogen oxides, aerosols, and water shown here were used to calculate net radiative forcing from LULCC. (Figure source: Ward et al. 2014⁵).

10.2 Terrestrial Ecosystem Interactions with the Climate System

Other chapters of this report discuss changes in temperature (Ch. 6: Temperature Change), precipitation (Ch. 7: Precipitation Change), hydrology (Ch. 8: Droughts, Floods, and Wildfires), and extreme events (Ch. 9: Extreme Storms). Collectively, these processes affect the phenology, structure, productivity, and biogeochemical processes of all terrestrial ecosystems, and as such, climate change will alter land cover and ecosystem services.

10.2.1 Land Cover and Climate Forcing

Changes in land cover and land use have long been recognized as important contributors to global climate forcing (e.g., Feddema et al. 2005⁷). Historically, studies that account for the contribution of the land cover to radiative forcing have accounted for albedo forcings only and not those from changes in land surface geophysical properties (e.g., plant transpiration, evaporation from soils, plant community structure and function) or in aerosols. Physical climate effects from land-cover or land-use change do not lend themselves directly to quantification using the traditional radiative forcing concept. However, a framework to attribute the indirect contributions of land cover to radiative forcing and the climate system—including effects on seasonal and interannual soil moisture and latent/sensible heat, evapotranspiration, biogeochemical cycle (CO₂) fluxes from soils and plants, aerosol and aerosol precursor emissions, ozone precursor emissions, and snowpack—was reported in NRC.⁸ Predicting future consequences of changes in land cover on the climate system will require not only the traditional calculations of surface albedo but also surface net radiation partitioning between latent and sensible heat exchange and the effects of resulting changes in biogeochemical trace gas and aerosol fluxes. Future trajectories of land use and land cover change are uncertain and

will depend on population growth, changes in agricultural yield driven by the competing demands for production of fuel (i.e., bioenergy crops), food, feed, and fiber as well as urban expansion. The diversity of future land cover and land use changes as implemented by the models that developed the Representative Concentration Pathways (RCPs) to attain target goals of radiative forcing by 2100 is discussed by Hurtt et al.⁹ For example, the higher scenario (RCP8.5)¹⁰ features an increase of cultivated land by about 185 million hectares from 2000 to 2050 and another 120 million hectares from 2050 to 2100. In the mid-high scenario (RCP6.0)—the Asia Pacific Integrated Model (AIM),¹¹ urban land use increases due to population and economic growth while cropland area expands due to increasing food demand. Grassland areas decline while total forested area extent remains constant throughout the century.⁹ The Global Change Assessment Model (GCAM), under a lower scenario (RCP4.5), preserved and expanded forested areas throughout the 21st century. Agricultural land declined slightly due to this afforestation, yet food demand is met through crop yield improvements, dietary shifts, production efficiency, and international trade.^{9,12} As with the higher scenario (RCP8.5), the even lower scenario (RCP2.6)¹³ reallocated agricultural production from developed to developing countries, with increased bioenergy production.⁹ Continued land-use change is projected across all RCPs (2.6, 4.5, 6.0, and 8.5) and is expected to contribute between 0.9 and 1.9 W/m² to direct radiative forcing by 2100.⁵ The RCPs demonstrate that land-use management and change combined with policy, demographic, energy technological innovations and change, and lifestyle changes all contribute to future climate (see Ch. 4: Projections for more detail on RCPs).¹⁴

Traditional calculations of radiative forcing by land-cover change yield small forcing values



(Ch. 2: Physical Drivers of Climate Change) because they account only for changes in surface albedo (e.g., Myhre and Myhre 2003;¹⁵ Betts et al. 2007;¹⁶ Jones et al. 2015¹⁷). Recent assessments (Myhre et al. 2013⁴ and references therein) are beginning to calculate the relative contributions of land-use and land-cover change (LULCC) to radiative forcing in addition to albedo and/or aerosols.⁵ Radiative forcing data reported in this chapter are largely from observations (see Table 8.2 in Myhre et al. 2013⁴). Ward et al.⁵ performed an independent modeling study to partition radiative forcing from natural and anthropogenic land use and land cover change and related land management activities into contributions from carbon dioxide (CO₂), methane (CH₄), nitrous oxide (N₂O), aerosols, halocarbons, and ozone (O₃).

The more extended effects of land-atmosphere interactions from natural and anthropogenic land-use and land-cover change (LULCC; Figure 10.1) described above have recently been reviewed and estimated by atmospheric constituent (Figure 10.2).^{4,5} The combined albedo and greenhouse gas radiative forcing for land-cover change is estimated to account for 40% ± 16% of the human-caused global radiative forcing from 1850 to 2010 (Figure 10.2).⁵ These calculations for total radiative forcing (from LULCC sources and all other sources) are consistent with Myhre et al. 2013⁴ (2.23 W/m² and 2.22 W/m² for Ward et al. 2014⁵ and Myhre et al. 2013⁴, respectively). The contributions of CO₂, CH₄, N₂O, and aerosols/O₃/albedo effects to total LULCC radiative forcing are about 47%, 34%, 15%, and 4%, respectively, highlighting the importance of non-albedo contributions to LULCC and radiative forcing. The net radiative forcing due specifically to fire—after accounting for short-lived forcing agents (O₃ and aerosols), long-lived greenhouse gases, and land albedo change both now and in the future—is estimated to be near

zero due to regrowth of forests which offsets the release of CO₂ from fire.¹⁸

10.2.2 Land Cover and Climate Feedbacks

Earth system models differ significantly in projections of terrestrial carbon uptake,¹⁹ with large uncertainties in the effects of increasing atmospheric CO₂ concentrations (i.e., CO₂ fertilization) and nutrient downregulation on plant productivity, as well as the strength of carbon cycle feedbacks (Ch. 2: Physical Drivers of Climate Change).^{20,21} When CO₂ effects on photosynthesis and transpiration are removed from global gridded crop models, simulated response to climate across the models is comparable, suggesting that model parameterizations representing these processes remain uncertain.²²

A recent analysis shows large-scale greening in the Arctic and boreal regions of North America and browning in the boreal forests of eastern Alaska for the period 1984–2012.²³ Satellite observations and ecosystem models suggest that biogeochemical interactions of carbon dioxide (CO₂) fertilization, nitrogen (N) deposition, and land-cover change are responsible for 25%–50% of the global greening of the Earth and 4% of Earth's browning between 1982 and 2009.^{24,25} While several studies have documented significant increases in the rate of green-up periods, the lengthening of the growing season (Section 10.3.1) also alters the timing of green-up (onset of growth) and brown-down (senescence); however, where ecosystems become depleted of water resources as a result of a lengthening growing season, the actual period of productive growth can be truncated.²⁶

Large-scale die-off and disturbances resulting from climate change have potential effects beyond the biogeochemical and carbon cycle effects. Biogeophysical feedbacks can strengthen or reduce climate forcing. The low albedo



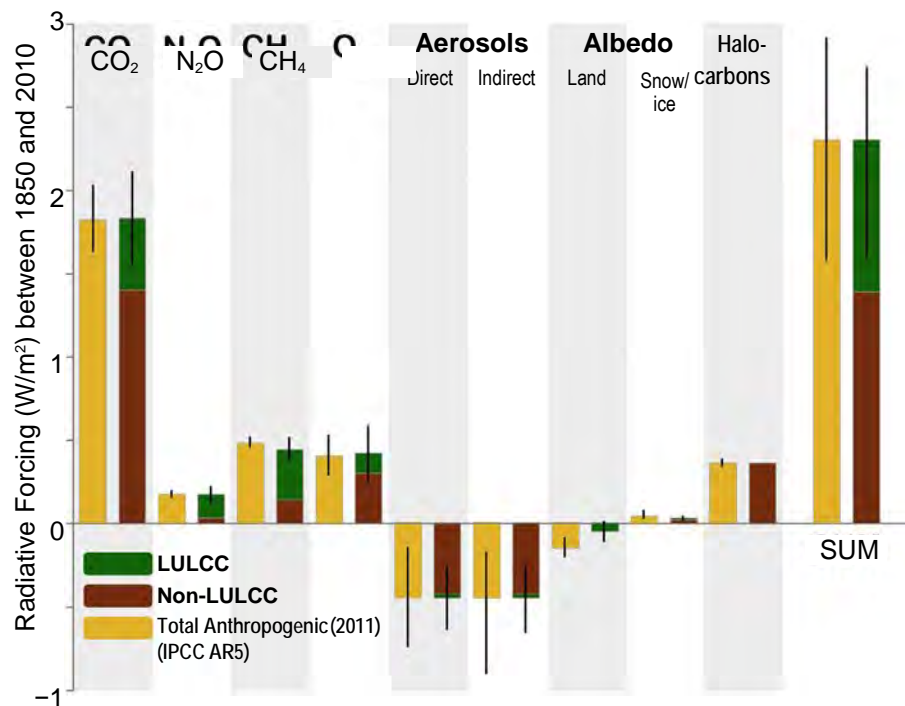


Figure 10.2: Anthropogenic radiative forcing (RF) contributions, separated by land-use and land-cover change (LULCC) and non-LULCC sources (green and maroon bars, respectively), are decomposed by atmospheric constituent to year 2010 in this diagram, using the year 1850 as the reference. Total anthropogenic RF contributions by atmospheric constituent⁴ (see also Figure 2.3) are shown for comparison (yellow bars). Error bars represent uncertainties for total anthropogenic RF (yellow bars) and for the LULCC components (green bars).⁵ The SUM bars indicate the net RF when all anthropogenic forcing agents are combined. (Figure source: Ward et al. 2014⁵).

of boreal forests provides a positive feedback, but those albedo effects are mitigated in tropical forests through evaporative cooling; for temperate forests, the evaporative effects are less clear.²⁷ Changes in surface albedo, evaporation, and surface roughness can have feedbacks to local temperatures that are larger than the feedback due to the change in carbon sequestration.²⁸ Forest management frameworks (e.g., afforestation, deforestation, and avoided deforestation) that account for biophysical (e.g., land surface albedo and surface roughness) properties can be used as climate protection or mitigation strategies.²⁹

10.2.3 Temperature Change

Interactions between temperature changes, land cover, and biogeochemistry are more complex than commonly assumed. Previous research suggested a fairly direct relationship between increasing temperatures, longer growing seasons (see Section 10.3.1),

increasing plant productivity (e.g., Walsh et al. 2014³⁰), and therefore also an increase in CO₂ uptake. Without water or nutrient limitations, increased CO₂ concentrations and warm temperatures have been shown to extend the growing season, which may contribute to longer periods of plant activity and carbon uptake, but do not affect reproduction rates.³¹ However, a longer growing season can also increase plant water demand, affecting regional water availability, and result in conditions that exceed plant physiological thresholds for growth, producing subsequent feedbacks to radiative forcing and climate. These consequences could offset potential benefits of a longer growing season (e.g., Georgakakos et al. 2014³²; Hibbard et al. 2014³³). For instance, increased dry conditions can lead to wildfire (e.g., Hatfield et al. 2014;³⁴ Joyce et al. 2014;³⁵ Ch. 8: Droughts, Floods and Wildfires) and urban temperatures can contribute to urban-induced thunderstorms in the southeast-



ern United States.³⁶ Temperature benefits of early onset of plant development in a longer growing season can be offset by 1) freeze damage caused by late-season frosts; 2) limits to growth because of shortening of the photoperiod later in the season; or 3) by shorter chilling periods required for leaf unfolding by many plants.^{37,38} MODIS data provided insight into the coterminous U.S. 2012 drought, when a warm spring reduced the carbon cycle impact of the drought by inducing earlier carbon uptake.³⁹ New evidence points to longer temperature-driven growing seasons for grasslands that may facilitate earlier onset of growth, but also that senescence is typically earlier.⁴⁰ In addition to changing CO₂ uptake, higher temperatures can also enhance soil decomposition rates, thereby adding more CO₂ to the atmosphere. Similarly, temperature, as well as changes in the seasonality and intensity of precipitation, can influence nutrient and water availability, leading to both shortages and excesses, thereby influencing rates and magnitudes of decomposition.¹

10.2.4 Water Cycle Changes

The global hydrological cycle is expected to intensify under climate change as a consequence of increased temperatures in the troposphere. The consequences of the increased water-holding capacity of a warmer atmosphere include longer and more frequent droughts and less frequent but more severe precipitation events and cyclonic activity (see Ch. 9: Extreme Storms for an in-depth discussion of extreme storms). More intense rain events and storms can lead to flooding and ecosystem disturbances, thereby altering ecosystem function and carbon cycle dynamics. For an extensive review of precipitation changes and droughts, floods, and wildfires, see Chapters 7 and 8 in this report, respectively.

From the perspective of the land biosphere, drought has strong effects on ecosystem

productivity and carbon storage by reducing photosynthesis and increasing the risk of wildfire, pest infestation, and disease susceptibility. Thus, droughts of the future will affect carbon uptake and storage, leading to feedbacks to the climate system (Chapter 2, Section 2.6.2; also see Chapter 11 for Arctic/climate/wildfire feedbacks).⁴¹ Reduced productivity as a result of extreme drought events can also extend for several years post-drought (i.e., drought legacy effects).^{42, 43, 44} In 2011, the most severe drought on record in Texas led to statewide regional tree mortality of 6.2%, or nearly nine times greater than the average annual mortality in this region (approximately 0.7%).⁴⁵ The net effect on carbon storage was estimated to be a redistribution of 24–30 TgC from the live to dead tree carbon pool, which is equal to 6%–7% of pre-drought live tree carbon storage in Texas state forestlands.⁴⁵ Another way to think about this redistribution is that the single Texas drought event equals approximately 36% of annual global carbon losses due to deforestation and land-use change.⁴⁶ The projected increases in temperatures and in the magnitude and frequency of heavy precipitation events, changes to snowpack, and changes in the subsequent water availability for agriculture and forestry may lead to similar rates of mortality or changes in land cover. Increasing frequency and intensity of drought across northern ecosystems reduces total observed organic matter export, has led to oxidized wetland soils, and releases stored contaminants into streams after rain events.⁴⁷

10.2.5 Biogeochemistry

Terrestrial biogeochemical cycles play a key role in Earth's climate system, including by affecting land-atmosphere fluxes of many aerosol precursors and greenhouse gases, including carbon dioxide (CO₂), methane (CH₄), and nitrous oxide (N₂O). As such, changes in the terrestrial ecosystem can drive climate change. At the same time, biogeochemical



cycles are sensitive to changes in climate and atmospheric composition.

Increased atmospheric CO₂ concentrations are often assumed to lead to increased plant production (known as CO₂ fertilization) and longer-term storage of carbon in biomass and soils. Whether increased atmospheric CO₂ will continue to lead to long-term storage of carbon in terrestrial ecosystems depends on whether CO₂ fertilization simply intensifies the rate of short-term carbon cycling (for example, by stimulating respiration, root exudation, and high turnover root growth), how water and other nutrients constrain CO₂ fertilization, or whether the additional carbon is used by plants to build more wood or tissues that, once senesced, decompose into long-lived soil organic matter. Under increased CO₂ concentrations, plants have been observed to optimize water use due to reduced stomatal conductance, thereby increasing water-use efficiency.⁴⁸ This change in water-use efficiency can affect plants' tolerance to stress and specifically to drought.⁴⁹ Due to the complex interactions of the processes that govern terrestrial biogeochemical cycling, terrestrial ecosystem responses to increasing CO₂ levels remain one of the largest uncertainties in long-term climate feedbacks and therefore in predicting longer-term climate change (Ch. 2: Physical Drivers of Climate Change).

Nitrogen is a principal nutrient for plant growth and can limit or stimulate plant productivity (and carbon uptake), depending on availability. As a result, increased nitrogen deposition and natural nitrogen-cycle responses to climate change will influence the global carbon cycle. For example, nitrogen limitation can inhibit the CO₂ fertilization response of plants to elevated atmospheric CO₂ (e.g., Norby et al. 2005;⁵⁰ Zaehle et al. 2010⁵¹). Conversely, increased decomposition of soil organic matter in response to climate warm-

ing increases nitrogen mineralization. This shift of nitrogen from soil to vegetation can increase ecosystem carbon storage.^{46, 52} While the effects of increased nitrogen deposition may counteract some nitrogen limitation on CO₂ fertilization, the importance of nitrogen in future carbon-climate interactions is not clear. Nitrogen dynamics are being integrated into the simulation of land carbon cycle modeling, but only two of the models in CMIP5 included coupled carbon-nitrogen interactions.⁵³

Many factors, including climate, atmospheric CO₂ concentrations, and nitrogen deposition rates influence the structure of the plant community and therefore the amount and biochemical quality of inputs into soils.^{54, 55} ⁵⁶ For example, though CO₂ losses from soils may decrease with greater nitrogen deposition, increased emissions of other greenhouse gases, such as methane (CH₄) and nitrous oxide (N₂O), can offset the reduction in CO₂.⁵⁷ The dynamics of soil organic carbon under the influence of climate change is poorly understood and therefore not well represented in models. As a result, there is high uncertainty in soil carbon stocks in model simulations.^{58, 59}

Future emissions of many aerosol precursors are expected to be affected by a number of climate-related factors, in part because of changes in aerosol and aerosol precursors from the terrestrial biosphere. For example, volatile organic compounds (VOCs) are a significant source of secondary organic aerosols, and biogenic sources of VOCs exceed emissions from the industrial and transportation sectors.⁶⁰ Isoprene is one of the most important biogenic VOCs, and isoprene emissions are strongly dependent on temperature and light, as well as other factors like plant type and leaf age.⁶⁰ Higher temperatures are expected to lead to an increase in biogenic VOC emissions. Atmospheric CO₂ concentration can also affect isoprene emissions (e.g., Rosenstiel et al. 2003⁶¹).



Changes in biogenic VOC emissions can impact aerosol formation and feedbacks with climate (Ch. 2: Physical Drivers of Climate Change, Section 2.6.1; Feedbacks via changes in atmospheric composition). Increased biogenic VOC emissions can also impact ozone and the atmospheric oxidizing capacity.⁶² Conversely, increases in nitrogen oxide (NO_x) pollution produce tropospheric ozone (O₃), which has damaging effects on vegetation. For example, a recent study estimated yield losses for maize and soybean production of up to 5% to 10% due to increases in O₃.⁶³

10.2.6 Extreme Events and Disturbance

This section builds on the physical overview provided in earlier chapters to frame how the intersections of climate, extreme events, and disturbance affect regional land cover and biogeochemistry. In addition to overall trends in temperature (Ch. 6: Temperature Change) and precipitation (Ch. 7: Precipitation Change), changes in modes of variability such as the Pacific Decadal Oscillation (PDO) and the El Niño–Southern Oscillation (ENSO) (Ch. 5: Circulation and Variability) can contribute to drought in the United States, which leads to unanticipated changes in disturbance regimes in the terrestrial biosphere (e.g., Kam et al. 2014⁶⁴). Extreme climatic events can increase the susceptibility of ecosystems to invasive plants and plant pests by promoting transport of propagules into affected regions, decreasing the resistance of native communities to establishment, and by putting existing native species at a competitive disadvantage.⁶⁵ For example, drought may exacerbate the rate of plant invasions by non-native species in rangelands and grasslands.⁴⁵ Land-cover changes such as encroachment and invasion of non-native species can in turn lead to increased frequency of disturbance such as fire. Disturbance events alter soil moisture, which, in addition to being affected by evapotranspiration and precipitation (Ch. 8: Droughts, Floods, and Wildfires),

is controlled by canopy and rooting architecture as well as soil physics. Invasive plants may be directly responsible for changes in fire regimes through increased biomass, changes in the distribution of flammable biomass, increased flammability, and altered timing of fuel drying, while others may be “fire followers” whose abundances increase as a result of shortening the fire return interval (e.g., Lambert et al. 2010⁶⁶). Changes in land cover resulting from alteration of fire return intervals, fire severity, and historical disturbance regimes affect long-term carbon exchange between the atmosphere and biosphere (e.g., Moore et al. 2016⁴⁵). Recent extensive diebacks and changes in plant cover due to drought have interacted with regional carbon cycle dynamics, including carbon release from biomass and reductions in carbon uptake from the atmosphere; however, plant regrowth may offset emissions.⁶⁷ The 2011–2015 meteorological drought in California (described in Ch. 8: Droughts, Floods, and Wildfires), combined with future warming, will lead to long-term changes in land cover, leading to increased probability of climate feedbacks (e.g., drought and wildfire) and in ecosystem shifts.⁶⁸ California’s recent drought has also resulted in measureable canopy water losses, posing long-term hazards to forest health and biophysical feedbacks to regional climate.⁴⁴ ^{69, 70} Multiyear or severe meteorological and hydrological droughts (see Ch. 8: Droughts, Floods, and Wildfires for definitions) can also affect stream biogeochemistry and riparian ecosystems by concentrating sediments and nutrients.⁶⁷

Changes in the variability of hurricanes and winter storm events (Ch. 9: Extreme Storms) also affect the terrestrial biosphere, as shown in studies comparing historic and future (projected) extreme events in the western United States and how these translate into changes in regional water balance, fire, and streamflow.



Composited across 10 global climate models (GCMs), summer (June–August) water-balance deficit in the future (2030–2059) increases compared to that under historical (1916–2006) conditions. Portions of the Southwest that have significant monsoon precipitation and some mountainous areas of the Pacific Northwest are exempt from this deficit.⁷¹ Projections for 2030–2059 suggest that extremely low flows that have historically occurred (1916–2006) in the Columbia Basin, upper Snake River, southeastern California, and southwestern Oregon are less likely to occur. Given the historical relationships between fire occurrence and drought indicators such as water-balance deficit and streamflow, climate change can be expected to have significant effects on fire occurrence and area burned.^{71, 72, 73}

Climate change in the northern high latitudes is directly contributing to increased fire occurrence (Ch. 11: Arctic Changes); in the coterminous United States, climate-induced changes in fires, changes in direct human ignitions, and land-management practices all significantly contribute to wildfire trends. Wildfires in the western United States are often ignited by lightning, but management practices such as fire suppression contribute to fuels and amplify the intensity and spread of wildfire. Fires initiated from unintentional ignition, such as by campfires, or intentional human-caused ignitions are also intensified by increasingly dry and vulnerable fuels, which build up with fire suppression or human settlements (See also Ch. 8: Droughts, Floods, and Wildfires).

10.3 Climate Indicators and Agricultural and Forest Responses

Recent studies indicate a correlation between the expansion of agriculture and the global amplitude of CO₂ uptake and emissions.^{74, 75} Conversely, agricultural production is increasingly disrupted by climate and extreme weather events, and these effects are expected

to be augmented by mid-century and beyond for most crops.^{76, 77} Precipitation extremes put pressure on agricultural soil and water assets and lead to increased irrigation, shrinking aquifers, and ground subsidence.

10.3.1 Changes in the Frost-Free and Growing Seasons

The concept that longer growing seasons are increasing productivity in some agricultural and forested ecosystems was discussed in the Third National Climate Assessment (NCA3).⁶ However, there are other consequences to a lengthened growing season that can offset gains in productivity. Here we discuss these emerging complexities as well as other aspects of how climate change is altering and interacting with terrestrial ecosystems. The growing season is the part of the year in which temperatures are favorable for plant growth. A basic metric by which this is measured is the frost-free period. The U.S. Department of Agriculture Natural Resources Conservation Service defines the frost-free period using a range of thresholds. They calculate the average date of the last day with temperature below 24°F (−4.4°C), 28°F (−2.2°C), and 32°F (0°C) in the spring and the average date of the first day with temperature below 24°F, 28°F, and 32°F in the fall, at various probabilities. They then define the frost-free period at three index temperatures (32°F, 28°F, and 24°F), also with a range of probabilities. A single temperature threshold (for example, temperature below 32°F) is often used when discussing growing season; however, different plant cover-types (e.g., forest, agricultural, shrub, and tundra) have different temperature thresholds for growth, and different requirements/thresholds for chilling.^{34, 78} For the purposes of this report, we use the metric with a 32°F (0°C) threshold to define the change in the number of “frost-free” days, and a temperature threshold of 41°F (5°C) as a first-order measure of



how the growing season length has changed over the observational record.⁷⁸

The NCA3 reported an increase in the growing season length of as much as several weeks as a result of higher temperatures occurring earlier and later in the year (e.g., Walsh et al. 2014;³⁰ Hatfield et al. 2014;³⁴ Joyce et al. 2014³⁵). NCA3 used a threshold of 32°F (0°C) (i.e., the frost-free period) to define the growing season. An update to this finding is presented in Figures 10.3 and 10.4, which show changes in the frost-free period and growing season, respectively, as defined above. Overall, the length of the frost-free period has increased in the contiguous United States during the past century (Figure 10.3). However, growing season changes are more variable: growing season length increased until the late 1930s, declined slightly until the early 1970s, increased again until about 1990, and remained quasi-stable thereafter (Figure 10.4). This contrasts somewhat with changes in the length of the frost-free period presented in NCA3, which showed a continuing increase after 1980. This difference is attributable to the temperature thresholds used in each indicator to define the start and end of these periods. Specifically, there are now more frost-free days (32°F threshold) in winter than the growing season (41°F threshold).

The lengthening of the growing season has been somewhat greater in the northern and western United States, which experienced increases of 1–2 weeks in many locations. In contrast, some areas in the Midwest, Southern Great Plains, and the Southeast had decreases of a week or more between the periods 1986–2015 and 1901–1960.² These differences reflect the more general pattern of warming and cooling nationwide (Ch. 6: Temperature Changes). Observations and models have verified that the growing season has generally

increased plant productivity over most of the United States.²⁵

Consistent with increases in growing season length and the coldest temperature of the year, plant hardiness zones have shifted northward in many areas.⁷⁹ The widespread increase in temperature has also impacted the distribution of other climate zones in parts of the United States. For instance, there have been moderate changes in the range of the temperate and continental climate zones of the eastern United States since 1950⁸⁰ as well as changes in the coverage of some extreme climate zones in the western United States. In particular, the spatial extent of the “alpine tundra” zone has decreased in high-elevation areas,⁸¹ while the extent of the “hot arid” zone has increased in the Southwest.⁸²

The period over which plants are actually productive, that is, their true growing season, is a function of multiple climate factors, including air temperature, number of frost-free days, and rainfall, as well as biophysical factors, including soil physics, daylight hours, and the biogeochemistry of ecosystems.⁸³ Temperature-induced changes in plant phenology, like flowering or spring leaf onset, could result in a timing mismatch (phenological asynchrony) with pollinator activity, affecting seasonal plant growth and reproduction and pollinator survival.^{84, 85, 86, 87} Further, while growing season length is generally referred to in the context of agricultural productivity, the factors that govern which plant types will grow in a given location are common to all plants whether they are in agricultural, natural, or managed landscapes. Changes in both the length and the seasonality of the growing season, in concert with local environmental conditions, can have multiple effects on agricultural productivity and land cover.

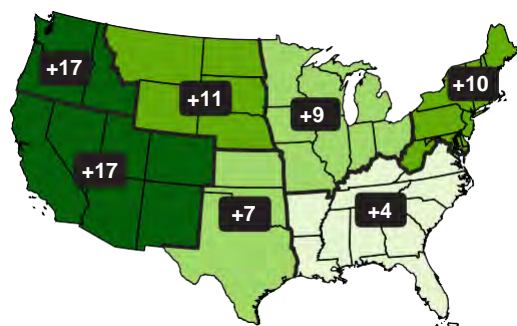


In the context of agriculture, a longer growing season could allow for the diversification of cropping systems or allow multiple harvests within a growing season. For example, shifts in cold hardiness zones across the contiguous United States suggest widespread expansion of thermally suitable areas for the cultivation of cold-intolerant perennial crops⁸⁸ as well as for biological invasion of non-native plants and plant pests.⁸⁹ However, changes in available water, conversion from dry to irrigated farming, and changes in sensible and latent heat exchange associated with these shifts need to be considered. Increasingly dry conditions under a longer growing season can alter terrestrial organic matter export and catalyze oxidation of wetland soils, releasing stored contaminants (for example, copper and nickel) into streamflow after rainfall.⁴⁷ Similarly, a longer growing season, particularly in years where water is limited, is not due to warming alone, but is exacerbated by higher atmospheric CO₂ concentrations that extend the active period of growth by plants.³¹ Longer growing seasons can also limit the types of crops that can be grown, encourage invasive species encroachment or weed growth, or in-

crease demand for irrigation, possibly beyond the limits of water availability. They could also disrupt the function and structure of a region's ecosystems and could, for example, alter the range and types of animal species in the area.

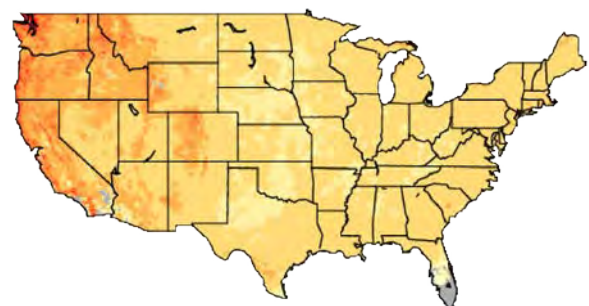
A longer and temporally shifted growing season also affects the role of terrestrial ecosystems in the carbon cycle. Neither seasonality of growing season (spring and summer) nor carbon, water, and energy fluxes should be interpreted separately when analyzing the impacts of climate extremes such as drought (Ch. 8: Droughts, Floods, and Wildfires).^{39, 90} Observations and data-driven model studies suggest that losses in net terrestrial carbon uptake during record warm springs followed by severely hot and dry summers can be largely offset by carbon gains in record-exceeding warmth and early arrival of spring.³⁹ Depending on soil physics and land cover, a cool spring, however, can deplete soil water resources less rapidly, making the subsequent impacts of precipitation deficits less severe.⁹⁰ Depletion of soil moisture through early plant activity in a warm spring can potentially amplify summer heating, a typical lagged direct

(a) Observed Increase in Frost-Free Season Length



Change in Annual Number of Days
 0–4 5–9 10–14 15+

(b) Projected Changes in Frost-free Season Length



Change in Annual Number of Days
 0 10 20 30 40 50 60 70 80 90

Figure 10.3: (a) Observed changes in the length of the frost-free season by region, where the frost-free season is defined as the number of days between the last spring occurrence and the first fall occurrence of a minimum temperature at or below 32°F. This change is expressed as the change in the average number of frost-free days in 1986–2015 compared to 1901–1960. (b) Projected changes in the length of the frost-free season at mid-century (2036–2065 as compared to 1976–2005) under the higher scenario (RCP8.5). Gray indicates areas that are not projected to experience a freeze in more than 10 of the 30 years (Figure source: (a) updated from Walsh et al. 2014;³⁰ (b) NOAA NCEI and CICS-NC, data source: LOCA dataset).

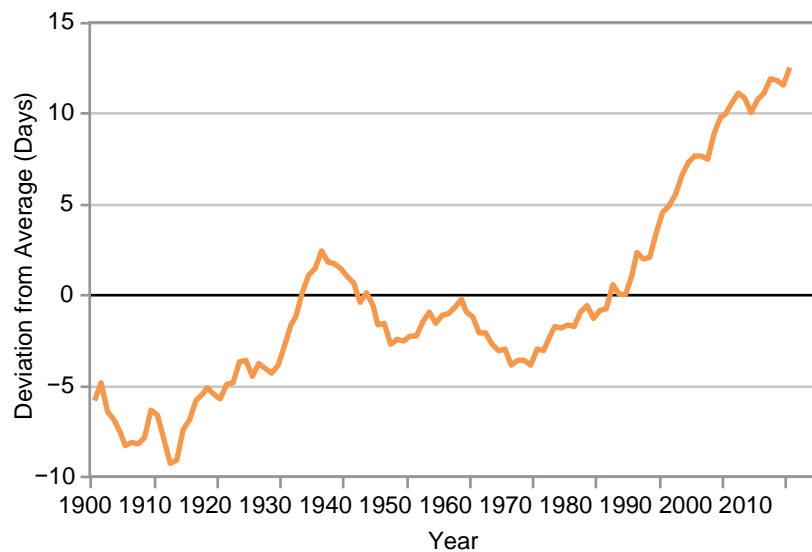


Figure 10.4: The length of the growing season in the contiguous 48 states compared with a long-term average (1895–2015), where “growing season” is defined by a daily minimum temperature threshold of 41°F. For each year, the line represents the number of days shorter or longer than the long-term average. The line was smoothed using an 11-year moving average. Choosing a different long-term average for comparison would not change the shape of the data over time. (Figure source: Kunkel 2016²).

effect of an extremely warm spring.⁴² Ecosystem responses to the phenological changes of timing and extent of growing season and subsequent biophysical feedbacks are therefore strongly dependent on the timing of climate extremes (Ch. 8: Droughts, Floods, and Wildfires; Ch. 9: Extreme Storms).⁹⁰

The global Coupled Model Intercomparison Project Phase 5 (CMIP5) analyses did not explicitly explore future changes to the growing season length. Many of the projected changes in North American climate are generally consistent across CMIP5 models, but there is substantial inter-model disagreement in projections of some metrics important to productivity in biophysical systems, including the sign of regional precipitation changes and extreme heat events across the northern United States.⁹¹

10.3.2 Water Availability and Drought

Drought is generally parameterized in most agricultural models as limited water availability and is an integrated response of both meteorological and agricultural drought, as described in Chapter 8: Droughts, Floods,

and Wildfires. However, physiological as well as biophysical processes that influence land cover and biogeochemistry interact with drought through stomatal closure induced by elevated atmospheric CO₂ levels.^{48, 49} This has direct impacts on plant transpiration, atmospheric latent heat fluxes, and soil moisture, thereby influencing local and regional climate. Drought is often offset by management through groundwater withdrawals, with increasing pressure on these resources to maintain plant productivity. This results in indirect climate effects by altering land surface exchange of water and energy with the atmosphere.⁹²

10.3.3 Forestry Considerations

Climate change and land-cover change in forested areas interact in many ways, such as through changes in mortality rates driven by changes in the frequency and magnitude of fire, insect infestations, and disease. In addition to the direct economic benefits of forestry, unquantified societal benefits include ecosystem services, like protection of watersheds and wildlife habitat, and recreation and human health value. United States forests and



related wood products also absorb and store the equivalent of 16% of all CO₂ emitted by fossil fuel burning in the United States each year.⁶ Climate change is expected to reduce the carbon sink strength of forests overall.

Effective management of forests offers the opportunity to reduce future climate change—for example, as given in proposals for Reduced Emissions from Deforestation and forest Degradation (REDD+; <https://www.forestcarbonpartnership.org/what-redd>) in developing countries and tropical ecosystems (see Ch. 14: Mitigation)—by capturing and storing carbon in forest ecosystems and long-term wood products.⁹³ Afforestation in the United States has the potential to capture and store 225 million tons of additional carbon per year from 2010 to 2110.^{94, 95} However, the projected maturation of United States forests⁹⁶ and land-cover change, driven in particular by the expansion of urban and suburban areas along with projected increased demands for food and bioenergy, threaten the extent of forests and their carbon storage potential.⁹⁷

Changes in growing season length, combined with drought and accompanying wildfire are reshaping California's mountain ecosystems. The California drought led to the lowest snowpack in 500 years, the largest wildfires in post-settlement history, greater than 23% stress mortality in Sierra mid-elevation forests, and associated post-fire erosion.⁶⁹ It is anticipated that slow recovery, possibly to different ecosystem types, with numerous shifts to species' ranges will result in long-term changes to land surface biophysical as well as ecosystem structure and function in this region (<http://www.fire.ca.gov/treetaskforce/>).⁶⁹

While changes in forest stocks, composition, and the ultimate use of forest products can influence net emissions and climate, the future net changes in forest stocks remain uncertain.^{9, 27, 98, 99, 100} This

uncertainty is due to a combination of uncertainties in future population size, population distribution and subsequent land-use change, harvest trends, wildfire management practices (for example, large-scale thinning of forests), and the impact of maturing U.S. forests.

10.4 Urban Environments and Climate Change

Urban areas exhibit several characteristics that affect land-surface and geophysical attributes, including building infrastructure (rougher, more uneven surfaces compared to rural or natural systems), increased emissions and concentrations of aerosols and other greenhouse gasses, and increased anthropogenic heat sources.^{101, 102} The understanding that urban areas modify their surrounding environment has been accepted for over a century, but the mechanisms through which this occurs have only begun to be understood and analyzed for more than 40 years.^{102, 103} Prior to the 1970s, the majority of urban climate research was observational and descriptive,¹⁰⁴ but since that time, more importance has been given to physical dynamics that are a function of land surface (for example, built environment and change to surface roughness); hydrologic, aerosol, and other greenhouse gas emissions; thermal properties of the built environment; and heat generated from human activities (Seto et al. 2016¹⁰⁵ and references therein).

There is now strong evidence that urban environments modify local microclimates, with implications for regional and global climate change.^{102, 104} Urban systems affect various climate attributes, including temperature, rainfall intensity and frequency, winter precipitation (snowfall), and flooding. New observational capabilities—including NASA's dual polarimetric radar, advanced satellite remote sensing (for example, the Global Precipitation Measurement Mission-GPM), and regionalized, coupled land-surface-atmospheric



modeling systems for urban systems – are now available to evaluate aspects of daytime and nighttime temperature fluctuations; urban precipitation; contribution of aerosols; how the urban built environment impacts the seasonality and type of precipitation (rain or snow) as well as the amount and distribution of precipitation; and the significance of the extent of urban metropolitan areas.^{101, 102, 106, 107}

The urban heat island (UHI) is characterized by increased surface and canopy temperatures as a result of heat-retaining asphalt and concrete, a lack of vegetation, and anthropogenic generation of heat and greenhouse gasses.¹⁰⁷ The heat gain due to the storage capacity of urban built structures, reductions in local evapotranspiration, and anthropogenically generated heat alter the spatio-temporal pattern of temperature and leads to the UHI phenomenon. The UHI physical processes that affect the climate system include generation of heat storage in buildings during the day, nighttime release of latent heat storage by buildings, and sensible heat generated by human activities, include heating of buildings, air conditioning, and traffic.¹⁰⁸

The strength of the effect is correlated with the spatial extent and population density of urban areas; however, because of varying definitions of urban vs. non-urban, impervious surface area is a more objective metric for estimating the extent and intensity of urbanization.¹⁰⁹ Based on land surface temperature measurements, on average, the UHI effect increases urban temperature by 5.2°F (2.9°C), but it has been measured at 14.4°F (8°C) in cities built in areas dominated by temperate forests.¹⁰⁹ In arid regions, however, urban areas can be more than 3.6°F (2°C) cooler than surrounding shrublands.¹¹⁰ Similarly, urban settings lose up to 12% of precipitation through impervious surface runoff, versus just over 3% loss to runoff in vegetated regions. Carbon losses

from the biosphere to the atmosphere through urbanization account for almost 2% of the continental terrestrial biosphere total, a significant proportion given that urban areas only account for around 1% of land in the United States.¹¹⁰ Similarly, statistical analyses of the relationship between climate and urban land use suggest an empirical relationship between the patterns of urbanization and precipitation deficits during the dry season. Causal factors for this reduction may include changes to runoff (for example, impervious-surface versus natural-surface hydrology) that extend beyond the urban heat island effect and energy-related aerosol emissions.¹¹¹

The urban heat island effect is more significant during the night and during winter than during the day, and it is affected by the shape, size, and geometry of buildings in urban centers as well as by infrastructure along gradients from urban to rural settlements.^{101, 105, 106} Recent research points to mounting evidence that urbanization also affects cycling of water, carbon, aerosols, and nitrogen in the climate system.¹⁰⁶

Coordinated modeling and observational studies have revealed other mechanisms by which the physical properties of urban areas can influence local weather and climate. It has been suggested that urban-induced wind convergence can determine storm initiation; aerosol concentrations and composition then influence the amount of cloud water and ice present in the clouds. Aerosols can also influence updraft and downdraft intensities, their life span, and surface precipitation totals.¹⁰⁷ A pair of studies investigated rainfall efficiency in sea-breeze thunderstorms and found that integrated moisture convergence in urban areas influenced storm initiation and mid-level moisture, thereby affecting precipitation dynamics.^{112, 113}



According to the World Bank, over 81% of the United States population currently resides in urban settings.¹¹⁴ Climate mitigation efforts to offset UHI are often stalled by the lack of quantitative data and understanding of the specific factors of urban systems that contribute to UHI. A recent study set out to quantitatively determine contributors to the intensity of UHI across North America.¹¹⁵ The study found that population strongly influenced nighttime UHI, but that daytime UHI varied spatially following precipitation gradients. The model applied in this study indicated that the spatial variation in the UHI signal was controlled most strongly by impacts on the atmospheric convection efficiency. Because of the impracticality of managing convection efficiency, results from Zhao et al.¹¹⁵ support albedo management as an efficient strategy to mitigate UHI on a large scale.



TRACEABLE ACCOUNTS

Key Finding 1

Changes in land use and land cover due to human activities produce physical changes in land surface albedo, latent and sensible heat, and atmospheric aerosol and greenhouse gas concentrations. The combined effects of these changes have recently been estimated to account for $40\% \pm 16\%$ of the human-caused global radiative forcing from 1850 to present day (*high confidence*). In recent decades, land use and land cover changes have turned the terrestrial biosphere (soil and plants) into a net “sink” for carbon (drawing down carbon from the atmosphere), and this sink has steadily increased since 1980 (*high confidence*). Because of the uncertainty in the trajectory of land cover, the possibility of the land becoming a net carbon source cannot be excluded (*very high confidence*).

Description of evidence base

Traditional methods that estimate albedo changes for calculating radiative forcing due to land-use change were identified by NRC.⁸ That report recommended that indirect contributions of land-cover change to climate-relevant variables, such as soil moisture, greenhouse gas (e.g., CO₂ and water vapor) sources and sinks, snow cover, aerosols, and aerosol and ozone precursor emissions also be considered. Several studies have documented physical land surface processes such as albedo, surface roughness, sensible and latent heat exchange, and land-use and land-cover change that interact with regional atmospheric processes (e.g., Marotz et al. 1975;¹¹⁶ Barnston and Schickendanz 1984;¹¹⁷ Alpert and Mandel 1986;¹¹⁸ Pielke and Zeng 1989;¹¹⁹ Feddema et al. 2005;⁷ Pielke et al. 2007¹²⁰); however, traditional calculations of radiative forcing by land-cover change in global climate model simulations yield small forcing values (Ch. 2: Physical Drivers of Climate Change) because they account only for changes in surface albedo (e.g., Myhre and Myhre 2003;¹⁵ Betts et al. 2007;¹⁶ Jones et al. 2015¹⁷).

Recent studies that account for the physical as well as biogeochemical changes in land cover and land use radiative forcing estimated that these drivers contribute 40% of present radiative forcing due to land-use/

land-cover change (0.9 W/m^2).^{4,5} These studies utilized AR5 and follow-on model simulations to estimate changes in land-cover and land-use climate forcing and feedbacks for the greenhouse gases—carbon dioxide, methane, and nitrous oxide—that contribute to total anthropogenic radiative forcing from land-use and land-cover change.^{4,5} This research is grounded in long-term observations that have been documented for over 40 years and recently implemented into global Earth system models.^{4, 20} For example, IPCC 2013: Summary for Policymakers states: “From 1750 to 2011, CO₂ emissions from fossil fuel combustion and cement production have released 375 [345 to 405] GtC to the atmosphere, while deforestation and other land-use changes are estimated to have released 180 [100 to 260] GtC. This results in cumulative anthropogenic emissions of 555 [470 to 640] GtC.”¹²¹ IPCC 2013, Working Group 1, Chapter 14 states for North America: “In summary, it is very likely that by mid-century the anthropogenic warming signal will be large compared to natural variability such as that stemming from the NAO, ENSO, PNA, PDO, and the NAMS in all North America regions throughout the year”.¹²²

Major uncertainties

Uncertainty exists in the future land-cover and land-use change as well as uncertainties in regional calculations of land-cover change and associated radiative forcing. The role of the land as a current sink has *very high confidence*; however, future strength of the land sink is uncertain.^{96, 97} The existing impact of land systems on climate forcing has *high confidence*.⁴ Based on current RCP scenarios for future radiative forcing targets ranging from 2.6 to 8.5 W/m², the future forcing has lower confidence because it is difficult to estimate changes in land cover and land use into the future.¹⁴ Compared to 2000, the CO₂-eq. emissions consistent with RCP8.5 more than double by 2050 and increase by three by 2100.¹⁰ About one quarter of this increase is due to increasing use of fertilizers and intensification of agricultural production, giving rise to the primary source of N₂O emissions. In addition, increases in livestock population, rice production, and enteric fermentation processes increase CH₄ emissions.¹⁰ Therefore,



if existing trends in land-use and land-cover change continue, the contribution of land cover to forcing will increase with *high confidence*. Overall, future scenarios from the RCPs suggest that land-cover change based on policy, bioenergy, and food demands could lead to significantly different distribution of land cover types (forest, agriculture, urban) by 2100.^{9, 10, 11, 12, 13, 14}

Summary sentence or paragraph that integrates the above information

The key finding is based on basic physics and biophysical models that have been well established for decades with regards to the contribution of land albedo to radiative forcing (NRC 2005). Recent assessments specifically address additional biogeochemical contributions of land-cover and land-use change to radiative forcing.^{4, 8} The role of current sink strength of the land is also uncertain.^{96, 97} The future distribution of land cover and contributions to total radiative forcing are uncertain and depend on policy, energy demand and food consumption, dietary demands.¹⁴

Key Finding 2

Climate change and induced changes in the frequency and magnitude of extreme events (e.g., droughts, floods, and heat waves) have led to large changes in plant community structure with subsequent effects on the biogeochemistry of terrestrial ecosystems. Uncertainties about how climate change will affect land cover change make it difficult to project the magnitude and sign of future climate feedbacks from land cover changes (*high confidence*).

Description of evidence base

From the perspective of the land biosphere, drought has strong effects on ecosystem productivity and carbon storage by reducing microbial activity and photosynthesis and by increasing the risk of wildfire, pest infestation, and disease susceptibility. Thus, future droughts will affect carbon uptake and storage, leading to feedbacks to the climate system.⁴¹ Reduced productivity as a result of extreme drought events can also extend for several years post-drought (i.e., drought legacy effects).^{42, 43, 44} Under increased CO₂ concentrations, plants have been observed to optimize water use due

to reduced stomatal conductance, thereby increasing water-use efficiency.⁴⁸ This change in water-use efficiency can affect plants' tolerance to stress and specifically to drought.⁴⁹

Recent severe droughts in the western United States (Texas and California) have led to significant mortality and carbon cycle dynamics (<http://www.fire.ca.gov/treetaskforce/>).^{45, 69} Carbon redistribution through mortality in the Texas drought was around 36% of global carbon losses due to deforestation and land use change.⁴⁶

Major uncertainties

Major uncertainties include how future land-use/land-cover changes will occur as a result of policy and/or mitigation strategies in addition to climate change. Ecosystem responses to phenological changes are strongly dependent on the timing of climate extremes.⁹⁰ Due to the complex interactions of the processes that govern terrestrial biogeochemical cycling, terrestrial ecosystem response to increasing CO₂ levels remains one of the largest uncertainties in long-term climate feedbacks and therefore in predicting longer-term climate change effects on ecosystems (e.g., Swann et al. 2016⁴⁹).

Summary sentence or paragraph that integrates the above information

The timing, frequency, magnitude, and extent of climate extremes strongly influence plant community structure and function, with subsequent effects on terrestrial biogeochemistry and feedbacks to the climate system. Future interactions between land cover and the climate system are uncertain and depend on human land-use decisions, the evolution of the climate system, and the timing, frequency, magnitude, and extent of climate extremes.

Key Finding 3

Since 1901, regional averages of both the consecutive number of frost-free days and the length of the corresponding growing season have increased for the seven contiguous U.S. regions used in this assessment. However, there is important variability at smaller scales, with



some locations actually showing decreases of a few days to as much as one to two weeks. Plant productivity has not increased commensurate with the increased number of frost-free days or with the longer growing season due to plant-specific temperature thresholds, plant–pollinator dependence, and seasonal limitations in water and nutrient availability (*very high confidence*). Future consequences of changes to the growing season for plant productivity are uncertain.

Description of evidence base

Data on the lengthening and regional variability of the growing season since 1901 were updated by Kunkel.² Many of these differences reflect the more general pattern of warming and cooling nationwide (Ch. 6: Temperature Changes). Without nutrient limitations, increased CO₂ concentrations and warm temperatures have been shown to extend the growing season, which may contribute to longer periods of plant activity and carbon uptake but do not affect reproduction rates.³¹ However, other confounding variables that coincide with climate change (for example, drought, increased ozone, and reduced photosynthesis due to increased or extreme heat) can offset increased growth associated with longer growing seasons²⁶ as well as changes in water availability and demand for water (e.g., Georgakakos et al. 2014;³² Hibbard et al. 2014³³). Increased dry conditions can lead to wildfire (e.g., Hatfield et al. 2014;³⁴ Joyce et al. 2014;³⁵ Ch. 8: Droughts, Floods and Wildfires) and urban temperatures can contribute to urban-induced thunderstorms in the southeastern United States.³⁶ Temperature benefits of early onset of plant development in a longer growing season can be offset by 1) freeze damage caused by late-season frosts; 2) limits to growth because of shortening of the photoperiod later in the season; or 3) by shorter chilling periods required for leaf unfolding by many plants.^{37, 38}

Major uncertainties

Uncertainties exist in future response of the climate system to anthropogenic forcings (land use/land cover as well as fossil fuel emissions) and associated feedbacks among variables such as temperature and precipitation interactions with carbon and nitrogen cycles as well as land-cover change that impact the length of

the growing season (Ch. 6: Temperature Changes and Ch. 8: Droughts, Floods and Wildfires).^{26, 31, 34}

Summary sentence or paragraph that integrates the above information

Changes in growing season length and interactions with climate, biogeochemistry, and land cover were covered in 12 chapters of NCA3⁶ but with sparse assessment of how changes in the growing season might offset plant productivity and subsequent feedbacks to the climate system. This key finding provides an assessment of the current state of the complex nature of the growing season.

Key Finding 4

Recent studies confirm and quantify higher surface temperatures in urban areas than in surrounding rural areas for a number of reasons, including the concentrated release of heat from buildings, vehicles, and industry. In the United States, this urban heat island effect results in daytime temperatures 0.9°–7.2°F (0.5°–4.0°C) higher and nighttime temperatures 1.8°–4.5°F (1.0°–2.5°C) higher in urban areas, with larger temperature differences in humid regions (primarily in the eastern United States) and in cities with larger and denser populations. The urban heat island effect will strengthen in the future as the structure, spatial extent, and population density of urban areas change and grow (*high confidence*).

Description of evidence base

Urban interactions with the climate system have been investigated for more than 40 years.^{102, 103} The heat gain due to the storage capacity of urban built structures, reduction in local evapotranspiration, and anthropogenically generated heat alter the spatio-temporal pattern of temperature and leads to the well-known urban heat island (UHI) phenomenon.^{101, 105, 106} The urban heat island (UHI) effect is correlated with the extent of impervious surfaces, which alter albedo or the saturation of radiation.¹⁰⁹ The urban-rural difference that defines the UHI is greatest for cities built in temperate forest ecosystems.¹⁰⁹ The average temperature increase is 2.9°C, except for urban areas in biomes with arid and semiarid climates.^{109, 110}



Major uncertainties

The largest uncertainties about urban forcings or feedbacks to the climate system are how urban settlements will evolve and how energy consumption and efficiencies, and their interactions with land cover and water, may change from present times.^{10, 14, 33, 105}

Summary sentence or paragraph that integrates the above information

Key Finding 4 is based on simulated and satellite land surface measurements analyzed by Imhoff et al.¹⁰⁹. Bounoua et al.,¹¹⁰ Shepherd,¹⁰⁷ Seto and Shepherd,¹⁰⁶ Grimmond et al.,¹⁰¹ and Seto et al.¹⁰⁵ provide specific references with regard to how building materials and spatio-temporal patterns of urban settlements influence radiative forcing and feedbacks of urban areas to the climate system.



REFERENCES

1. Galloway, J.N., W.H. Schlesinger, C.M. Clark, N.B. Grimm, R.B. Jackson, B.E. Law, P.E. Thornton, A.R. Townsend, and R. Martin, 2014: Ch. 15: Biogeochemical cycles. *Climate Change Impacts in the United States: The Third National Climate Assessment*. Melillo, J.M., Terese (T.C.) Richmond, and G.W. Yohe, Eds. U.S. Global Change Research Program, Washington, DC, 350-368. <http://dx.doi.org/10.7930/J0X63JT0>
2. Kunkel, K.E., 2016: Update to data originally published in: Kunkel, K.E., D. R. Easterling, K. Hubbard, K. Redmond, 2004: Temporal variations in frost-free season in the United States: 1895 - 2000. *Geophysical Research Letters*, **31**, L03201. <http://dx.doi.org/10.1029/2003gl018624>
3. Brown, D.G., C. Polsky, P. Bolstad, S.D. Brody, D. Hulse, R. Kroh, T.R. Loveland, and A. Thomson, 2014: Ch. 13: Land use and land cover change. *Climate Change Impacts in the United States: The Third National Climate Assessment*. Melillo, J.M., Terese (T.C.) Richmond, and G.W. Yohe, Eds. U.S. Global Change Research Program, Washington, DC, 318-332. <http://dx.doi.org/10.7930/J05Q4T1Q>
4. Myhre, G., D. Shindell, F.-M. Bréon, W. Collins, J. Fuglestvedt, J. Huang, D. Koch, J.-F. Lamarque, D. Lee, B. Mendoza, T. Nakajima, A. Robock, G. Stephens, T. Takemura, and H. Zhang, 2013: Anthropogenic and natural radiative forcing. *Climate Change 2013: The Physical Science Basis. Contribution of Working Group I to the Fifth Assessment Report of the Intergovernmental Panel on Climate Change*. Stocker, T.F., D. Qin, G.-K. Plattner, M. Tignor, S.K. Allen, J. Boschung, A. Nauels, Y. Xia, V. Bex, and P.M. Midgley, Eds. Cambridge University Press, Cambridge, United Kingdom and New York, NY, USA, 659-740. <http://www.climatechange2013.org/report/full-report/>
5. Ward, D.S., N.M. Mahowald, and S. Kloster, 2014: Potential climate forcing of land use and land cover change. *Atmospheric Chemistry and Physics*, **14**, 12701-12724. <http://dx.doi.org/10.5194/acp-14-12701-2014>
6. Melillo, J.M., T.C. Richmond, and G.W. Yohe, eds., 2014: *Climate Change Impacts in the United States: The Third National Climate Assessment*. U.S. Global Change Research Program: Washington, D.C., 841 pp. <http://dx.doi.org/10.7930/J0Z31WJ2>
7. Feddema, J.J., K.W. Oleson, G.B. Bonan, L.O. Mearns, L.E. Buja, G.A. Meehl, and W.M. Washington, 2005: The importance of land-cover change in simulating future climates. *Science*, **310**, 1674-1678. <http://dx.doi.org/10.1126/science.1118160>
8. NRC, 2005: *Radiative Forcing of Climate Change: Expanding the Concept and Addressing Uncertainties*. National Academies Press, Washington, D.C., 222 pp. <http://dx.doi.org/10.17226/11175>
9. Hurtt, G.C., L.P. Chini, S. Frolking, R.A. Betts, J. Feddema, G. Fischer, J.P. Fisk, K. Hibbard, R.A. Houghton, A. Janetos, C.D. Jones, G. Kindermann, T. Kinoshita, K. Klein Goldewijk, K. Riahi, E. Shevliakova, S. Smith, E. Stehfest, A. Thomson, P. Thornton, D.P. van Vuuren, and Y.P. Wang, 2011: Harmonization of land-use scenarios for the period 1500-2100: 600 years of global gridded annual land-use transitions, wood harvest, and resulting secondary lands. *Climatic Change*, **109**, 117. <http://dx.doi.org/10.1007/s10584-011-0153-2>
10. Riahi, K., S. Rao, V. Krey, C. Cho, V. Chirkov, G. Fischer, G. Kindermann, N. Nakicenovic, and P. Rafaj, 2011: RCP 8.5—A scenario of comparatively high greenhouse gas emissions. *Climatic Change*, **109**, 33. <http://dx.doi.org/10.1007/s10584-011-0149-y>
11. Fujimori, S., T. Masui, and Y. Matsuoka, 2014: Development of a global computable general equilibrium model coupled with detailed energy end-use technology. *Applied Energy*, **128**, 296-306. <http://dx.doi.org/10.1016/j.apenergy.2014.04.074>
12. Thomson, A.M., K.V. Calvin, S.J. Smith, G.P. Kyle, A. Volke, P. Patel, S. Delgado-Arias, B. Bond-Lamberty, M.A. Wise, and L.E. Clarke, 2011: RCP4.5: A pathway for stabilization of radiative forcing by 2100. *Climatic Change*, **109**, 77-94. <http://dx.doi.org/10.1007/s10584-011-0151-4>
13. van Vuuren, D.P., S. Deetman, M.G.J. den Elzen, A. Hof, M. Isaac, K. Klein Goldewijk, T. Kram, A. Mendoza Beltran, E. Stehfest, and J. van Vliet, 2011: RCP2.6: Exploring the possibility to keep global mean temperature increase below 2°C. *Climatic Change*, **109**, 95-116. <http://dx.doi.org/10.1007/s10584-011-0152-3>
14. van Vuuren, D.P., J. Edmonds, M. Kainuma, K. Riahi, A. Thomson, K. Hibbard, G.C. Hurtt, T. Kram, V. Krey, and J.F. Lamarque, 2011: The representative concentration pathways: An overview. *Climatic Change*, **109**, 5-31. <http://dx.doi.org/10.1007/s10584-011-0148-z>
15. Myhre, G. and A. Myhre, 2003: Uncertainties in radiative forcing due to surface albedo changes caused by land-use changes. *Journal of Climate*, **16**, 1511-1524. [http://dx.doi.org/10.1175/1520-0442\(2003\)016<1511:uirfdt>2.0.co;2](http://dx.doi.org/10.1175/1520-0442(2003)016<1511:uirfdt>2.0.co;2)
16. Betts, R.A., P.D. Falloon, K.K. Goldewijk, and N. Ramankutty, 2007: Biogeophysical effects of land use on climate: Model simulations of radiative forcing and large-scale temperature change. *Agricultural and Forest Meteorology*, **142**, 216-233. <http://dx.doi.org/10.1016/j.agrformet.2006.08.021>
17. Jones, A.D., K.V. Calvin, W.D. Collins, and J. Edmonds, 2015: Accounting for radiative forcing from albedo change in future global land-use scenarios. *Climatic Change*, **131**, 691-703. <http://dx.doi.org/10.1007/s10584-015-1411-5>



18. Ward, D.S. and N.M. Mahowald, 2015: Local sources of global climate forcing from different categories of land use activities. *Earth System Dynamics*, **6**, 175-194. <http://dx.doi.org/10.5194/esd-6-175-2015>
19. Lovenduski, N.S. and G.B. Bonan, 2017: Reducing uncertainty in projections of terrestrial carbon uptake. *Environmental Research Letters*, **12**, 044020. <http://dx.doi.org/10.1088/1748-9326/aa66b8>
20. Anav, A., P. Friedlingstein, M. Kidston, L. Bopp, P. Ciais, P. Cox, C. Jones, M. Jung, R. Myneni, and Z. Zhu, 2013: Evaluating the land and ocean components of the global carbon cycle in the CMIP5 earth system models. *Journal of Climate*, **26**, 6801-6843. <http://dx.doi.org/10.1175/jcli-d-12-00417.1>
21. Hoffman, F.M., J.T. Randerson, V.K. Arora, Q. Bao, P. Cadule, D. Ji, C.D. Jones, M. Kawamiya, S. Khattiwala, K. Lindsay, A. Obata, E. Shevliakova, K.D. Six, J.F. Tjiputra, E.M. Volodin, and T. Wu, 2014: Causes and implications of persistent atmospheric carbon dioxide biases in Earth System Models. *Journal of Geophysical Research Biogeosciences*, **119**, 141-162. <http://dx.doi.org/10.1002/2013JG002381>
22. Rosenzweig, C., J. Elliott, D. Deryng, A.C. Ruane, C. Müller, A. Arneth, K.J. Boote, C. Folberth, M. Glotter, N. Khabarov, K. Neumann, F. Piontek, T.A.M. Pugh, E. Schmid, E. Stehfest, H. Yang, and J.W. Jones, 2014: Assessing agricultural risks of climate change in the 21st century in a global gridded crop model inter-comparison. *Proceedings of the National Academy of Sciences*, **111**, 3268-3273. <http://dx.doi.org/10.1073/pnas.1222463110>
23. Ju, J. and J.G. Masek, 2016: The vegetation greenness trend in Canada and US Alaska from 1984–2012 Landsat data. *Remote Sensing of Environment*, **176**, 1-16. <http://dx.doi.org/10.1016/j.rse.2016.01.001>
24. Zhu, Z., S. Piao, R.B. Myneni, M. Huang, Z. Zeng, J.G. Canadell, P. Ciais, S. Sitch, P. Friedlingstein, A. Arneth, C. Cao, L. Cheng, E. Kato, C. Koven, Y. Li, X. Lian, Y. Liu, R. Liu, J. Mao, Y. Pan, S. Peng, J. Penuelas, B. Poulter, T.A.M. Pugh, B.D. Stocker, N. Viovy, X. Wang, Y. Wang, Z. Xiao, H. Yang, S. Zaehle, and N. Zeng, 2016: Greening of the Earth and its drivers. *Nature Climate Change*, **6**, 791-795. <http://dx.doi.org/10.1038/nclimate3004>
25. Mao, J., A. Ribes, B. Yan, X. Shi, P.E. Thornton, R. Seferian, P. Ciais, R.B. Myneni, H. Douville, S. Piao, Z. Zhu, R.E. Dickinson, Y. Dai, D.M. Ricciuto, M. Jin, F.M. Hoffman, B. Wang, M. Huang, and X. Lian, 2016: Human-induced greening of the northern extratropical land surface. *Nature Climate Change*, **6**, 959-963. <http://dx.doi.org/10.1038/nclimate3056>
26. Adams, H.D., A.D. Collins, S.P. Briggs, M. Vennetier, L.T. Dickman, S.A. Sevanto, N. Garcia-Forner, H.H. Powers, and N.G. McDowell, 2015: Experimental drought and heat can delay phenological development and reduce foliar and shoot growth in semiarid trees. *Global Change Biology*, **21**, 4210-4220. <http://dx.doi.org/10.1111/gcb.13030>
27. Bonan, G.B., 2008: Forests and climate change: Forcings, feedbacks, and the climate benefits of forests. *Science*, **320**, 1444-1449. <http://dx.doi.org/10.1126/science.1155121>
28. Jackson, R.B., J.T. Randerson, J.G. Canadell, R.G. Anderson, R. Avissar, D.D. Baldocchi, G.B. Bonan, K. Caldeira, N.S. Diffenbaugh, C.B. Field, B.A. Hungate, E.G. Jobbágy, L.M. Kueppers, D.N. Marcelo, and D.E. Pataki, 2008: Protecting climate with forests. *Environmental Research Letters*, **3**, 044006. <http://dx.doi.org/10.1088/1748-9326/3/4/044006>
29. Anderson, R.G., J.G. Canadell, J.T. Randerson, R.B. Jackson, B.A. Hungate, D.D. Baldocchi, G.A. Ban-Weiss, G.B. Bonan, K. Caldeira, L. Cao, N.S. Diffenbaugh, K.R. Gurney, L.M. Kueppers, B.E. Law, S. Luysaert, and T.L. O'Halloran, 2011: Biophysical considerations in forestry for climate protection. *Frontiers in Ecology and the Environment*, **9**, 174-182. <http://dx.doi.org/10.1890/090179>
30. Walsh, J., D. Wuebbles, K. Hayhoe, J. Kossin, K. Kunkel, G. Stephens, P. Thorne, R. Vose, M. Wehner, J. Willis, D. Anderson, S. Doney, R. Feely, P. Hennon, V. Kharin, T. Knutson, F. Landerer, T. Lenton, J. Kennedy, and R. Somerville, 2014: Ch. 2: Our changing climate. *Climate Change Impacts in the United States: The Third National Climate Assessment*. Melillo, J.M., T.C. Richmond, and G.W. Yohe, Eds. U.S. Global Change Research Program, Washington, D.C., 19-67. <http://dx.doi.org/10.7930/J0KW5CXT>
31. Reyes-Fox, M., H. Steltzer, M.J. Trlica, G.S. McMaster, A.A. Andales, D.R. LeCain, and J.A. Morgan, 2014: Elevated CO₂ further lengthens growing season under warming conditions. *Nature*, **510**, 259-262. <http://dx.doi.org/10.1038/nature13207>
32. Georgakakos, A., P. Fleming, M. Dettinger, C. Peters-Lidard, T.C. Richmond, K. Reckhow, K. White, and D. Yates, 2014: Ch. 3: Water resources. *Climate Change Impacts in the United States: The Third National Climate Assessment*. Melillo, J.M., T.C. Richmond, and G.W. Yohe, Eds. U.S. Global Change Research Program, Washington, D.C., 69-112. <http://dx.doi.org/10.7930/J0G44N6T>
33. Hibbard, K., T. Wilson, K. Averyt, R. Harriss, R. Newmark, S. Rose, E. Shevliakova, and V. Tidwell, 2014: Ch. 10: Energy, water, and land use. *Climate Change Impacts in the United States: The Third National Climate Assessment*. Melillo, J.M., Terese (T.C.) Richmond, and G.W. Yohe, Eds. U.S. Global Change Research Program, Washington, DC, 257-281. <http://dx.doi.org/10.7930/J0JW8BSF>



34. Hatfield, J., G. Takle, R. Grotjahn, P. Holden, R.C. Izaurralde, T. Mader, E. Marshall, and D. Liverman, 2014: Ch. 6: Agriculture. *Climate Change Impacts in the United States: The Third National Climate Assessment*. Melillo, J.M., Terese (T.C.) Richmond, and G.W. Yohe, Eds. U.S. Global Change Research Program, Washington, DC, 150-174. <http://dx.doi.org/10.7930/J02Z13FR>
35. Joyce, L.A., S.W. Running, D.D. Breshears, V.H. Dale, R.W. Malmshemer, R.N. Sampson, B. Sohngen, and C.W. Woodall, 2014: Ch. 7: Forests. *Climate Change Impacts in the United States: The Third National Climate Assessment*. Melillo, J.M., Terese (T.C.) Richmond, and G.W. Yohe, Eds. U.S. Global Change Research Program, Washington, DC, 175-194. <http://dx.doi.org/10.7930/J0Z60KZC>
36. Ashley, W.S., M.L. Bentley, and J.A. Stallins, 2012: Urban-induced thunderstorm modification in the southeast United States. *Climatic Change*, **113**, 481-498. <http://dx.doi.org/10.1007/s10584-011-0324-1>
37. Fu, Y.H., H. Zhao, S. Piao, M. Peaucelle, S. Peng, G. Zhou, P. Ciais, M. Huang, A. Menzel, J. Penuelas, Y. Song, Y. Vitisse, Z. Zeng, and I.A. Janssens, 2015: Declining global warming effects on the phenology of spring leaf unfolding. *Nature*, **526**, 104-107. <http://dx.doi.org/10.1038/nature15402>
38. Gu, L., P.J. Hanson, W. Mac Post, D.P. Kaiser, B. Yang, R. Nemani, S.G. Pallardy, and T. Meyers, 2008: The 2007 eastern US spring freezes: Increased cold damage in a warming world? *BioScience*, **58**, 253-262. <http://dx.doi.org/10.1641/b580311>
39. Wolf, S., T.F. Keenan, J.B. Fisher, D.D. Baldocchi, A.R. Desai, A.D. Richardson, R.L. Scott, B.E. Law, M.E. Litvak, N.A. Brunzell, W. Peters, and I.T. van der Laan-Luijckx, 2016: Warm spring reduced carbon cycle impact of the 2012 US summer drought. *Proceedings of the National Academy of Sciences*, **113**, 5880-5885. <http://dx.doi.org/10.1073/pnas.1519620113>
40. Fridley, J.D., J.S. Lynn, J.P. Grime, and A.P. Askew, 2016: Longer growing seasons shift grassland vegetation towards more-productive species. *Nature Climate Change*, **6**, 865-868. <http://dx.doi.org/10.1038/nclimate3032>
41. Schlesinger, W.H., M.C. Dietze, R.B. Jackson, R.P. Phillips, C.C. Rhoads, L.E. Rustad, and J.M. Vose, 2016: Forest biogeochemistry in response to drought. *Effects of Drought on Forests and Rangelands in the United States: A comprehensive science synthesis*. Vose, J., J.S. Clark, C. Luce, and T. Patel-Weynand, Eds. U.S. Department of Agriculture, Forest Service, Washington Office, Washington, DC, 97-106. <http://www.tree-search.fs.fed.us/pubs/50261>
42. Frank, D., M. Reichstein, M. Bahn, K. Thonicke, D. Frank, M.D. Mahecha, P. Smith, M. van der Velde, S. Vicca, F. Babst, C. Beer, N. Buchmann, J.G. Canadell, P. Ciais, W. Cramer, A. Ibrom, F. Miglietta, B. Poulter, A. Rammig, S.I. Seneviratne, A. Walz, M. Wattenbach, M.A. Zavala, and J. Zscheischler, 2015: Effects of climate extremes on the terrestrial carbon cycle: Concepts, processes and potential future impacts. *Global Change Biology*, **21**, 2861-2880. <http://dx.doi.org/10.1111/gcb.12916>
43. Reichstein, M., M. Bahn, P. Ciais, D. Frank, M.D. Mahecha, S.I. Seneviratne, J. Zscheischler, C. Beer, N. Buchmann, D.C. Frank, D. Papale, A. Rammig, P. Smith, K. Thonicke, M. van der Velde, S. Vicca, A. Walz, and M. Wattenbach, 2013: Climate extremes and the carbon cycle. *Nature*, **500**, 287-295. <http://dx.doi.org/10.1038/nature12350>
44. Anderegg, W.R.L., C. Schwalm, F. Biondi, J.J. Camarero, G. Koch, M. Litvak, K. Ogle, J.D. Shaw, E. Shevliakova, A.P. Williams, A. Wolf, E. Ziaco, and S. Pacala, 2015: Pervasive drought legacies in forest ecosystems and their implications for carbon cycle models. *Science*, **349**, 528-532. <http://dx.doi.org/10.1126/science.aab1833>
45. Moore, G.W., C.B. Edgar, J.G. Vogel, R.A. Washington-Allen, Rosaleen G. March, and R. Zehnder, 2016: Tree mortality from an exceptional drought spanning mesic to semiarid ecoregions. *Ecological Applications*, **26**, 602-611. <http://dx.doi.org/10.1890/15-0330>
46. Ciais, P., C. Sabine, G. Bala, L. Bopp, V. Brovkin, J. Canadell, A. Chhabra, R. DeFries, J. Galloway, M. Heimann, C. Jones, C. Le Quéré, R.B. Myneni, S. Piao, and P. Thornton, 2013: Carbon and other biogeochemical cycles. *Climate Change 2013: The Physical Science Basis. Contribution of Working Group I to the Fifth Assessment Report of the Intergovernmental Panel on Climate Change*. Stocker, T.F., D. Qin, G.-K. Plattner, M. Tignor, S.K. Allen, J. Boschung, A. Nauels, Y. Xia, V. Bex, and P.M. Midgley, Eds. Cambridge University Press, Cambridge, United Kingdom and New York, NY, USA, 465-570. <http://www.climatechange2013.org/report/full-report/>
47. Szokan-Emilson, E.J., B.W. Kielstra, S.E. Arnott, S.A. Watmough, J.M. Gunn, and A.J. Tanentzap, 2017: Dry conditions disrupt terrestrial-aquatic linkages in northern catchments. *Global Change Biology*, **23**, 117-126. <http://dx.doi.org/10.1111/gcb.13361>
48. Keenan, T.F., D.Y. Hollinger, G. Bohrer, D. Dragoni, J.W. Munger, H.P. Schmid, and A.D. Richardson, 2013: Increase in forest water-use efficiency as atmospheric carbon dioxide concentrations rise. *Nature*, **499**, 324-327. <http://dx.doi.org/10.1038/nature12291>
49. Swann, A.L.S., F.M. Hoffman, C.D. Koven, and J.T. Randerson, 2016: Plant responses to increasing CO2 reduce estimates of climate impacts on drought severity. *Proceedings of the National Academy of Sciences*, **113**, 10019-10024. <http://dx.doi.org/10.1073/pnas.1604581113>



50. Norby, R.J., E.H. DeLucia, B. Gielen, C. Calfapietra, C.P. Giardina, J.S. King, J. Ledford, H.R. McCarthy, D.J.P. Moore, R. Ceulemans, P. De Angelis, A.C. Finzi, D.F. Karnosky, M.E. Kubiske, M. Lukac, K.S. Pregitzer, G.E. Scarascia-Mugnozza, W.H. Schlesinger, and R. Oren, 2005: Forest response to elevated CO₂ is conserved across a broad range of productivity. *Proceedings of the National Academy of Sciences of the United States of America*, **102**, 18052-18056. <http://dx.doi.org/10.1073/pnas.0509478102>
51. Zaehle, S., P. Friedlingstein, and A.D. Friend, 2010: Terrestrial nitrogen feedbacks may accelerate future climate change. *Geophysical Research Letters*, **37**, L01401. <http://dx.doi.org/10.1029/2009GL041345>
52. Melillo, J.M., S. Butler, J. Johnson, J. Mohan, P. Steudler, H. Lux, E. Burrows, F. Bowles, R. Smith, L. Scott, C. Vario, T. Hill, A. Burton, Y.M. Zhou, and J. Tang, 2011: Soil warming, carbon-nitrogen interactions, and forest carbon budgets. *Proceedings of the National Academy of Sciences*, **108**, 9508-9512. <http://dx.doi.org/10.1073/pnas.1018189108>
53. Knutti, R. and J. Sedláček, 2013: Robustness and uncertainties in the new CMIP5 climate model projections. *Nature Climate Change*, **3**, 369-373. <http://dx.doi.org/10.1038/nclimate1716>
54. Jandl, R., M. Lindner, L. Vesterdal, B. Bauwens, R. Baritz, F. Hagedorn, D.W. Johnson, K. Minkinen, and K.A. Byrne, 2007: How strongly can forest management influence soil carbon sequestration? *Geoderma*, **137**, 253-268. <http://dx.doi.org/10.1016/j.geoderma.2006.09.003>
55. McLauchlan, K., 2006: The nature and longevity of agricultural impacts on soil carbon and nutrients: A review. *Ecosystems*, **9**, 1364-1382. <http://dx.doi.org/10.1007/s10021-005-0135-1>
56. Smith, P., S.J. Chapman, W.A. Scott, H.I.J. Black, M. Wattenbach, R. Milne, C.D. Campbell, A. Lilly, N. Ostle, P.E. Levy, D.G. Lumsdon, P. Millard, W. Towers, S. Zaehle, and J.U. Smith, 2007: Climate change cannot be entirely responsible for soil carbon loss observed in England and Wales, 1978-2003. *Global Change Biology*, **13**, 2605-2609. <http://dx.doi.org/10.1111/j.1365-2486.2007.01458.x>
57. Liu, L.L. and T.L. Greaver, 2009: A review of nitrogen enrichment effects on three biogenic GHGs: The CO₂ sink may be largely offset by stimulated N₂O and CH₄ emission. *Ecology Letters*, **12**, 1103-1117. <http://dx.doi.org/10.1111/j.1461-0248.2009.01351.x>
58. Todd-Brown, K.E.O., J.T. Randerson, W.M. Post, F.M. Hoffman, C. Tarnocai, E.A.G. Schuur, and S.D. Allison, 2013: Causes of variation in soil carbon simulations from CMIP5 Earth system models and comparison with observations. *Biogeosciences*, **10**, 1717-1736. <http://dx.doi.org/10.5194/bg-10-1717-2013>
59. Tian, H., C. Lu, J. Yang, K. Banger, D.N. Huntzinger, C.R. Schwalm, A.M. Michalak, R. Cook, P. Ciais, D. Hayes, M. Huang, A. Ito, A.K. Jain, H. Lei, J. Mao, S. Pan, W.M. Post, S. Peng, B. Poulter, W. Ren, D. Ricciuto, K. Schaefer, X. Shi, B. Tao, W. Wang, Y. Wei, Q. Yang, B. Zhang, and N. Zeng, 2015: Global patterns and controls of soil organic carbon dynamics as simulated by multiple terrestrial biosphere models: Current status and future directions. *Global Biogeochemical Cycles*, **29**, 775-792. <http://dx.doi.org/10.1002/2014GB005021>
60. Guenther, A., T. Karl, P. Harley, C. Wiedinmyer, P.I. Palmer, and C. Geron, 2006: Estimates of global terrestrial isoprene emissions using MEGAN (Model of Emissions of Gases and Aerosols from Nature). *Atmospheric Chemistry and Physics*, **6**, 3181-3210. <http://dx.doi.org/10.5194/acp-6-3181-2006>
61. Rosenstiel, T.N., M.J. Potosnak, K.L. Griffin, R. Fall, and R.K. Monson, 2003: Increased CO₂ uncouples growth from isoprene emission in an agriforest ecosystem. *Nature*, **421**, 256-259. <http://dx.doi.org/10.1038/nature01312>
62. Pyle, J.A., N. Warwick, X. Yang, P.J. Young, and G. Zeng, 2007: Climate/chemistry feedbacks and biogenic emissions. *Philosophical Transactions of the Royal Society A: Mathematical, Physical and Engineering Sciences*, **365**, 1727-40. <http://dx.doi.org/10.1098/rsta.2007.2041>
63. McGrath, J.M., A.M. Betzelberger, S. Wang, E. Shook, X.-G. Zhu, S.P. Long, and E.A. Ainsworth, 2015: An analysis of ozone damage to historical maize and soybean yields in the United States. *Proceedings of the National Academy of Sciences*, **112**, 14390-14395. <http://dx.doi.org/10.1073/pnas.1509777112>
64. Kam, J., J. Sheffield, and E.F. Wood, 2014: Changes in drought risk over the contiguous United States (1901-2012): The influence of the Pacific and Atlantic Oceans. *Geophysical Research Letters*, **41**, 5897-5903. <http://dx.doi.org/10.1002/2014GL060973>
65. Diez, J.M., C.M. D'Antonio, J.S. Dukes, E.D. Grosholz, J.D. Olden, C.J.B. Sorte, D.M. Blumenthal, B.A. Bradley, R. Early, I. Ibáñez, S.J. Jones, J.J. Lawler, and L.P. Miller, 2012: Will extreme climatic events facilitate biological invasions? *Frontiers in Ecology and the Environment*, **10**, 249-257. <http://dx.doi.org/10.1890/110137>
66. Lambert, A.M., C.M. D'Antonio, and T.L. Dudley, 2010: Invasive species and fire in California ecosystems. *Fremontia*, **38**, 29-36.
67. Vose, J., J.S. Clark, C. Luce, and T. Patel-Weynand, eds., 2016: *Effects of Drought on Forests and Rangelands in the United States: A Comprehensive Science Synthesis*. U.S. Department of Agriculture, Forest Service, Washington Office: Washington, DC, 289 pp. <http://www.treesearch.fs.fed.us/pubs/50261>



68. Diffenbaugh, N.S., D.L. Swain, and D. Touma, 2015: Anthropogenic warming has increased drought risk in California. *Proceedings of the National Academy of Sciences*, **112**, 3931-3936. <http://dx.doi.org/10.1073/pnas.1422385112>
69. Asner, G.P., P.G. Brodrick, C.B. Anderson, N. Vaughn, D.E. Knapp, and R.E. Martin, 2016: Progressive forest canopy water loss during the 2012-2015 California drought. *Proceedings of the National Academy of Sciences*, **113**, E249-E255. <http://dx.doi.org/10.1073/pnas.1523397113>
70. Mann, M.E. and P.H. Gleick, 2015: Climate change and California drought in the 21st century. *Proceedings of the National Academy of Sciences*, **112**, 3858-3859. <http://dx.doi.org/10.1073/pnas.1503667112>
71. Littell, J.S., D.L. Peterson, K.L. Riley, Y.-Q. Liu, and C.H. Luce, 2016: Fire and drought. *Effects of Drought on Forests and Rangelands in the United States: A comprehensive science synthesis*. Vose, J., J.S. Clark, C. Luce, and T. Patel-Weynand, Eds. U.S. Department of Agriculture, Forest Service, Washington Office, Washington, DC, 135-150. <http://www.treesearch.fs.fed.us/pubs/50261>
72. Littell, J.S., M.M. Elsner, G.S. Mauger, E.R. Lutz, A.F. Hamlet, and E.P. Salathé, 2011: Regional Climate and Hydrologic Change in the Northern U.S. Rockies and Pacific Northwest: Internally Consistent Projections of Future Climate for Resource Management. University of Washington, Seattle. <https://cig.uw.edu/publications/regional-climate-and-hydrologic-change-in-the-northern-u-s-rockies-and-pacific-northwest-internally-consistent-projections-of-future-climate-for-resource-management/>
73. Elsner, M.M., L. Cuo, N. Voisin, J.S. Deems, A.F. Hamlet, J.A. Vano, K.E.B. Mickelson, S.Y. Lee, and D.P. Lettenmaier, 2010: Implications of 21st century climate change for the hydrology of Washington State. *Climatic Change*, **102**, 225-260. <http://dx.doi.org/10.1007/s10584-010-9855-0>
74. Zeng, N., F. Zhao, G.J. Collatz, E. Kalnay, R.J. Salawitch, T.O. West, and L. Guanter, 2014: Agricultural green revolution as a driver of increasing atmospheric CO₂ seasonal amplitude. *Nature*, **515**, 394-397. <http://dx.doi.org/10.1038/nature13893>
75. Gray, J.M., S. Frolking, E.A. Kort, D.K. Ray, C.J. Kucharik, N. Ramankutty, and M.A. Friedl, 2014: Direct human influence on atmospheric CO₂ seasonality from increased cropland productivity. *Nature*, **515**, 398-401. <http://dx.doi.org/10.1038/nature13957>
76. Challinor, A.J., J. Watson, D.B. Lobell, S.M. Howden, D.R. Smith, and N. Chhetri, 2014: A meta-analysis of crop yield under climate change and adaptation. *Nature Climate Change*, **4**, 287-291. <http://dx.doi.org/10.1038/nclimate2153>
77. Lobell, D.B. and C. Tebaldi, 2014: Getting caught with our plants down: The risks of a global crop yield slowdown from climate trends in the next two decades. *Environmental Research Letters*, **9**, 074003. <http://dx.doi.org/10.1088/1748-9326/9/7/074003>
78. Zhang, X., L. Alexander, G.C. Hegerl, P. Jones, A.K. Tank, T.C. Peterson, B. Trewin, and F.W. Zwiers, 2011: Indices for monitoring changes in extremes based on daily temperature and precipitation data. *Wiley Interdisciplinary Reviews: Climate Change*, **2**, 851-870. <http://dx.doi.org/10.1002/wcc.147>
79. Daly, C., M.P. Widrlechner, M.D. Halbleib, J.I. Smith, and W.P. Gibson, 2012: Development of a new USDA plant hardiness zone map for the United States. *Journal of Applied Meteorology and Climatology*, **51**, 242-264. <http://dx.doi.org/10.1175/2010JAMC2536.1>
80. Chan, D. and Q. Wu, 2015: Significant anthropogenic-induced changes of climate classes since 1950. *Scientific Reports*, **5**, 13487. <http://dx.doi.org/10.1038/srep13487>
81. Diaz, H.F. and J.K. Eischeid, 2007: Disappearing "alpine tundra" Köppen climatic type in the western United States. *Geophysical Research Letters*, **34**, L18707. <http://dx.doi.org/10.1029/2007GL031253>
82. Grundstein, A., 2008: Assessing climate change in the contiguous United States using a modified Thornthwaite climate classification scheme. *The Professional Geographer*, **60**, 398-412. <http://dx.doi.org/10.1080/00330120802046695>
83. EPA, 2016: Climate Change Indicators in the United States, 2016. 4th edition. EPA 430-R-16-004. U.S. Environmental Protection Agency, Washington, D.C., 96 pp. https://www.epa.gov/sites/production/files/2016-08/documents/climate_indicators_2016.pdf
84. Yang, L.H. and V.H.W. Rudolf, 2010: Phenology, ontogeny and the effects of climate change on the timing of species interactions. *Ecology Letters*, **13**, 1-10. <http://dx.doi.org/10.1111/j.1461-0248.2009.01402.x>
85. Rafferty, N.E. and A.R. Ives, 2011: Effects of experimental shifts in flowering phenology on plant-pollinator interactions. *Ecology Letters*, **14**, 69-74. <http://dx.doi.org/10.1111/j.1461-0248.2010.01557.x>
86. Kudo, G. and T.Y. Ida, 2013: Early onset of spring increases the phenological mismatch between plants and pollinators. *Ecology*, **94**, 2311-2320. <http://dx.doi.org/10.1890/12-2003.1>
87. Forrest, J.R.K., 2015: Plant-pollinator interactions and phenological change: What can we learn about climate impacts from experiments and observations? *Oikos*, **124**, 4-13. <http://dx.doi.org/10.1111/oik.01386>

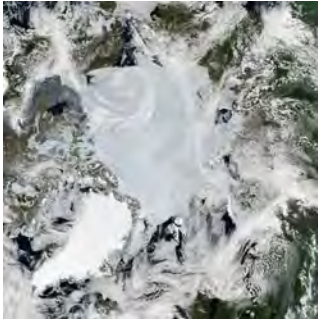


88. Parker, L.E. and J.T. Abatzoglou, 2016: Projected changes in cold hardiness zones and suitable over-winter ranges of perennial crops over the United States. *Environmental Research Letters*, **11**, 034001. <http://dx.doi.org/10.1088/1748-9326/11/3/034001>
89. Hellmann, J.J., J.E. Byers, B.G. Bierwagen, and J.S. Dukes, 2008: Five potential consequences of climate change for invasive species. *Conservation Biology*, **22**, 534-543. <http://dx.doi.org/10.1111/j.1523-1739.2008.00951.x>
90. Sippel, S., J. Zscheischler, and M. Reichstein, 2016: Ecosystem impacts of climate extremes crucially depend on the timing. *Proceedings of the National Academy of Sciences*, **113**, 5768-5770. <http://dx.doi.org/10.1073/pnas.1605667113>
91. Maloney, E.D., S.J. Camargo, E. Chang, B. Colle, R. Fu, K.L. Geil, Q. Hu, X. Jiang, N. Johnson, K.B. Karnauskas, J. Kinter, B. Kirtman, S. Kumar, B. Langenbrunner, K. Lombardo, L.N. Long, A. Mariotti, J.E. Meyerson, K.C. Mo, J.D. Neelin, Z. Pan, R. Seager, Y. Serra, A. Seth, J. Sheffield, J. Stroeve, J. Thibeault, S.-P. Xie, C. Wang, B. Wyman, and M. Zhao, 2014: North American climate in CMIP5 experiments: Part III: Assessment of twenty-first-century projections. *Journal of Climate*, **27**, 2230-2270. <http://dx.doi.org/10.1175/JCLI-D-13-00273.1>
92. Marston, L., M. Konar, X. Cai, and T.J. Troy, 2015: Virtual groundwater transfers from overexploited aquifers in the United States. *Proceedings of the National Academy of Sciences*, **112**, 8561-8566. <http://dx.doi.org/10.1073/pnas.1500457112>
93. Lippke, B., E. Oneil, R. Harrison, K. Skog, L. Gustavsson, and R. Sathre, 2011: Life cycle impacts of forest management and wood utilization on carbon mitigation: Knowns and unknowns. *Carbon Management*, **2**, 303-333. <http://dx.doi.org/10.4155/CMT.11.24>
94. EPA, 2005: Greenhouse Gas Mitigation Potential in U.S. Forestry and Agriculture. EPA 430-R-05-006. Environmental Protection Agency, Washington, D.C., 154 pp. https://www3.epa.gov/climatechange/Downloads/ccs/ghg_mitigation_forestry_ag_2005.pdf
95. King, S.L., D.J. Twedt, and R.R. Wilson, 2006: The role of the wetland reserve program in conservation efforts in the Mississippi River alluvial valley. *Wildlife Society Bulletin*, **34**, 914-920. [http://dx.doi.org/10.2193/0091-7648\(2006\)34\[914:TROTWR\]2.0.CO;2](http://dx.doi.org/10.2193/0091-7648(2006)34[914:TROTWR]2.0.CO;2)
96. Wear, D.N. and J.W. Coulston, 2015: From sink to source: Regional variation in U.S. forest carbon futures. *Scientific Reports*, **5**, 16518. <http://dx.doi.org/10.1038/srep16518>
97. McKinley, D.C., M.G. Ryan, R.A. Birdsey, C.P. Giardina, M.E. Harmon, L.S. Heath, R.A. Houghton, R.B. Jackson, J.F. Morrison, B.C. Murray, D.E. Pataki, and K.E. Skog, 2011: A synthesis of current knowledge on forests and carbon storage in the United States. *Ecological Applications*, **21**, 1902-1924. <http://dx.doi.org/10.1890/10-0697.1>
98. Pan, Y., R.A. Birdsey, J. Fang, R. Houghton, P.E. Kauppi, W.A. Kurz, O.L. Phillips, A. Shvidenko, S.L. Lewis, J.G. Canadell, P. Ciais, R.B. Jackson, S.W. Pacala, A.D. McGuire, S. Piao, A. Rautiainen, S. Sitch, and D. Hayes, 2011: A large and persistent carbon sink in the world's forests. *Science*, **333**, 988-993. <http://dx.doi.org/10.1126/science.1201609>
99. Hansen, M.C., P.V. Potapov, R. Moore, M. Hancher, S.A. Turubanova, A. Tyukavina, D. Thau, S.V. Stehman, S.J. Goetz, T.R. Loveland, A. Kommareddy, A. Egorov, L. Chini, C.O. Justice, and J.R.G. Townshend, 2013: High-resolution global maps of 21st-century forest cover change. *Science*, **342**, 850-853. <http://dx.doi.org/10.1126/science.1244693>
100. Williams, A.P., C.D. Allen, A.K. Macalady, D. Griffin, C.A. Woodhouse, D.M. Meko, T.W. Swetnam, S.A. Rauscher, R. Seager, H.D. Grissino-Mayer, J.S. Dean, E.R. Cook, C. Gangodagamage, M. Cai, and N.G. McDowell, 2013: Temperature as a potent driver of regional forest drought stress and tree mortality. *Nature Climate Change*, **3**, 292-297. <http://dx.doi.org/10.1038/nclimate1693>
101. Grimmond, C.S.B., H.C. Ward, and S. Kotthaus, 2016: Effects of urbanization on local and regional climate. *Routledge Handbook of Urbanization and Global Environmental Change*. Seto, K.C., W.D. Solecki, and C.A. Griffith, Eds. Routledge, London, 169-187.
102. Mitra, C. and J.M. Shepherd, 2016: Urban precipitation: A global perspective. *Routledge Handbook of Urbanization and Global Environment Change*. Seto, K.C., W.D. Solecki, and C.A. Griffith, Eds. Routledge, London, 152-168.
103. Landsberg, H.E., 1970: Man-made climatic changes: Man's activities have altered the climate of urbanized areas and may affect global climate in the future. *Science*, **170**, 1265-1274. <http://dx.doi.org/10.1126/science.170.3964.1265>
104. Mills, G., 2007: Cities as agents of global change. *International Journal of Climatology*, **27**, 1849-1857. <http://dx.doi.org/10.1002/joc.1604>
105. Seto, K.C., W.D. Solecki, and C.A. Griffith, eds., 2016: *Routledge Handbook on Urbanization and Global Environmental Change*. Routledge: London, 582 pp.
106. Seto, K.C. and J.M. Shepherd, 2009: Global urban land-use trends and climate impacts. *Current Opinion in Environmental Sustainability*, **1**, 89-95. <http://dx.doi.org/10.1016/j.cosust.2009.07.012>



107. Shepherd, J.M., 2013: Impacts of urbanization on precipitation and storms: Physical insights and vulnerabilities *Climate Vulnerability: Understanding and Addressing Threats to Essential Resources*. Academic Press, Oxford, 109-125. <http://dx.doi.org/10.1016/B978-0-12-384703-4.00503-7>
108. Hidalgo, J., V. Masson, A. Baklanov, G. Pigeon, and L. Gimeno, 2008: Advances in urban climate modeling. *Annals of the New York Academy of Sciences*, **1146**, 354-374. <http://dx.doi.org/10.1196/annals.1446.015>
109. Imhoff, M.L., P. Zhang, R.E. Wolfe, and L. Bounoua, 2010: Remote sensing of the urban heat island effect across biomes in the continental USA. *Remote Sensing of Environment*, **114**, 504-513. <http://dx.doi.org/10.1016/j.rse.2009.10.008>
110. Bounoua, L., P. Zhang, G. Mostovoy, K. Thome, J. Masek, M. Imhoff, M. Shepherd, D. Quattrochi, J. Santanello, J. Silva, R. Wolfe, and A.M. Toure, 2015: Impact of urbanization on US surface climate. *Environmental Research Letters*, **10**, 084010. <http://dx.doi.org/10.1088/1748-9326/10/8/084010>
111. Kaufmann, R.K., K.C. Seto, A. Schneider, Z. Liu, L. Zhou, and W. Wang, 2007: Climate response to rapid urban growth: Evidence of a human-induced precipitation deficit. *Journal of Climate*, **20**, 2299-2306. <http://dx.doi.org/10.1175/jcli4109.1>
112. Shepherd, J.M., B.S. Ferrier, and P.S. Ray, 2001: Rainfall morphology in Florida convergence zones: A numerical study. *Monthly Weather Review*, **129**, 177-197. [http://dx.doi.org/10.1175/1520-0493\(2001\)129<0177:rmifcz>2.0.co;2](http://dx.doi.org/10.1175/1520-0493(2001)129<0177:rmifcz>2.0.co;2)
113. van den Heever, S.C. and W.R. Cotton, 2007: Urban aerosol impacts on downwind convective storms. *Journal of Applied Meteorology and Climatology*, **46**, 828-850. <http://dx.doi.org/10.1175/jam2492.1>
114. World Bank, 2017: Urban population (% of total): United States (1960-2015). World Bank Open Data. <http://data.worldbank.org/indicator/SP.URB.TOTL.IN.ZS?locations=US>
115. Zhao, L., X. Lee, R.B. Smith, and K. Oleson, 2014: Strong contributions of local background climate to urban heat islands. *Nature*, **511**, 216-219. <http://dx.doi.org/10.1038/nature13462>
116. Marotz, G.A., J. Clark, J. Henry, and R. Standfast, 1975: Cloud fields over irrigated areas in southwestern Kansas—Data and speculations. *The Professional Geographer*, **27**, 457-461. <http://dx.doi.org/10.1111/j.0033-0124.1975.00457.x>
117. Barnston, A.G. and P.T. Schickedanz, 1984: The effect of irrigation on warm season precipitation in the southern Great Plains. *Journal of Climate and Applied Meteorology*, **23**, 865-888. [http://dx.doi.org/10.1175/1520-0450\(1984\)023<0865:TEOIO-W>2.0.CO;2](http://dx.doi.org/10.1175/1520-0450(1984)023<0865:TEOIO-W>2.0.CO;2)
118. Alpert, P. and M. Mandel, 1986: Wind variability—An indicator for a mesoclimatic change in Israel. *Journal of Climate and Applied Meteorology*, **25**, 1568-1576. [http://dx.doi.org/10.1175/1520-0450\(1986\)025<1568:wwifam>2.0.co;2](http://dx.doi.org/10.1175/1520-0450(1986)025<1568:wwifam>2.0.co;2)
119. Pielke, R.A., Sr. and X. Zeng, 1989: Influence on severe storm development of irrigated land. *National Weather Digest* **14**, 16-17.
120. Pielke, R.A., Sr., J. Adegoke, A. Beltrán-Przekurat, C.A. Hiemstra, J. Lin, U.S. Nair, D. Niyogi, and T.E. Nobis, 2007: An overview of regional land-use and land-cover impacts on rainfall. *Tellus B*, **59**, 587-601. <http://dx.doi.org/10.1111/j.1600-0889.2007.00251.x>
121. IPCC, 2013: Summary for policymakers. *Climate Change 2013: The Physical Science Basis. Contribution of Working Group I to the Fifth Assessment Report of the Intergovernmental Panel on Climate Change*. Stocker, T.F., D. Qin, G.-K. Plattner, M. Tignor, S.K. Allen, J. Boschung, A. Nauels, Y. Xia, V. Bex, and P.M. Midgley, Eds. Cambridge University Press, Cambridge, United Kingdom and New York, NY, USA, 1-30. <http://www.climatechange2013.org/report/>
122. Christensen, J.H., K. Krishna Kumar, E. Aldrian, S.-I. An, I.F.A. Cavalcanti, M. de Castro, W. Dong, P. Goswami, A. Hall, J.K. Kanyanga, A. Kitoh, J. Kosin, N.-C. Lau, J. Renwick, D.B. Stephenson, S.-P. Xie, and T. Zhou, 2013: Climate phenomena and their relevance for future regional climate change. *Climate Change 2013: The Physical Science Basis. Contribution of Working Group I to the Fifth Assessment Report of the Intergovernmental Panel on Climate Change*. Stocker, T.F., D. Qin, G.-K. Plattner, M. Tignor, S.K. Allen, J. Boschung, A. Nauels, Y. Xia, V. Bex, and P.M. Midgley, Eds. Cambridge University Press, Cambridge, United Kingdom and New York, NY, USA, 1217-1308. <http://www.climatechange2013.org/report/full-report/>





11

Arctic Changes and their Effects on Alaska and the Rest of the United States

KEY FINDINGS

1. Annual average near-surface air temperatures across Alaska and the Arctic have increased over the last 50 years at a rate more than twice as fast as the global average temperature (*very high confidence*).
2. Rising Alaskan permafrost temperatures are causing permafrost to thaw and become more discontinuous; this process releases additional carbon dioxide and methane, resulting in an amplifying feedback and additional warming (*high confidence*). The overall magnitude of the permafrost-carbon feedback is uncertain; however, it is clear that these emissions have the potential to compromise the ability to limit global temperature increases.
3. Arctic land and sea ice loss observed in the last three decades continues, in some cases accelerating (*very high confidence*). It is *virtually certain* that Alaska glaciers have lost mass over the last 50 years, with each year since 1984 showing an annual average ice mass less than the previous year. Based on gravitational data from satellites, average ice mass loss from Greenland was -269 Gt per year between April 2002 and April 2016, accelerating in recent years (*high confidence*). Since the early 1980s, annual average arctic sea ice has decreased in extent between 3.5% and 4.1% per decade, become thinner by between 4.3 and 7.5 feet, and began melting at least 15 more days each year. September sea ice extent has decreased between 10.7% and 15.9% per decade (*very high confidence*). Arctic-wide ice loss is expected to continue through the 21st century, *very likely* resulting in nearly sea ice-free late summers by the 2040s (*very high confidence*).
4. It is *very likely* that human activities have contributed to observed arctic surface temperature warming, sea ice loss, glacier mass loss, and Northern Hemisphere snow extent decline (*high confidence*).
5. Atmospheric circulation patterns connect the climates of the Arctic and the contiguous United States. Evidenced by recent record warm temperatures in the Arctic and emerging science, the midlatitude circulation has influenced observed arctic temperatures and sea ice (*high confidence*). However, confidence is *low* regarding whether or by what mechanisms observed arctic warming may have influenced the midlatitude circulation and weather patterns over the continental United States. The influence of arctic changes on U.S. weather over the coming decades remains an open question with the potential for significant impact.

Recommended Citation for Chapter

Taylor, P.C., W. Maslowski, J. Perlwitz, and D.J. Wuebbles, 2017: Arctic changes and their effects on Alaska and the rest of the United States. In: *Climate Science Special Report: Fourth National Climate Assessment, Volume I* [Wuebbles, D.J., D.W. Fahey, K.A. Hibbard, D.J. Dokken, B.C. Stewart, and T.K. Maycock (eds.)]. U.S. Global Change Research Program, Washington, DC, USA, pp. 303-332, doi: 10.7930/J00863GK.

11.1 Introduction

Climate changes in Alaska and across the Arctic continue to outpace changes occurring across the globe. The Arctic, defined as the area north of the Arctic Circle, is a vulnerable and complex system integral to Earth's climate. The vulnerability stems in part from the extensive cover of ice and snow, where the freezing point marks a critical threshold that when crossed has the potential to transform the region. Because of its high sensitivity to radiative forcing and its role in amplifying warming,¹ the arctic cryosphere is a key indicator of the global climate state. Accelerated melting of multiyear sea ice, mass loss from the Greenland Ice Sheet (GrIS), reduction of terrestrial snow cover, and permafrost degradation are stark examples of the rapid Arctic-wide response to global warming. These local arctic changes influence global sea level, ocean salinity, the carbon cycle, and potentially atmospheric and oceanic circulation patterns. Arctic climate change has altered the global climate in the past² and will influence climate in the future.

As an arctic nation, United States' decisions regarding climate change adaptation and mitigation, resource development, trade, national security, transportation, etc., depend on projections of future Alaskan and arctic climate. Aside from uncertainties due to natural variability, scientific uncertainty, and human activities including greenhouse gas emissions (see Ch. 4: Projections), additional unique uncertainties in our understanding of arctic processes thwart projections, including mixed-phase cloud processes;³ boundary layer processes;⁴ sea ice mechanics;⁴ and ocean currents, eddies, and tides that affect the advection of heat into and around the Arctic Ocean.⁵ ⁶The inaccessibility of the Arctic has made it difficult to sustain the high-quality observations of the atmosphere, ocean, land, and ice required to improve physically-based models.

Improved data quality and increased observational coverage would help address societally relevant arctic science questions.

Despite these challenges, our scientific knowledge is sufficiently advanced to effectively inform policy. This chapter documents significant scientific progress and knowledge about how the Alaskan and arctic climate has changed and will continue to change.

11.2 Arctic Changes

11.2.1 Alaska and Arctic Temperature

Surface temperature – an essential component of the arctic climate system – drives and signifies change, fundamentally controlling the melting of ice and snow. Further, the vertical profile of boundary layer temperature modulates the exchange of mass, energy, and momentum between the surface and atmosphere, influencing other components such as clouds.^{7, 8} Arctic temperatures exhibit spatial and interannual variability due to interactions and feedbacks between sea ice, snow cover, atmospheric heat transports, vegetation, clouds, water vapor, and the surface energy budget.⁹ ^{10, 11}Interannual variations in Alaskan temperatures are strongly influenced by decadal variability like the Pacific Decadal Oscillation (Ch. 5: Circulation and Variability).^{12, 13} However, observed temperature trends exceed this variability.

Arctic surface and atmospheric temperatures have substantially increased in the observational record. Multiple observation sources, including land-based surface stations since at least 1950 and available meteorological re-analysis datasets, provide evidence that arctic near-surface air temperatures have increased more than twice as fast as the global average.^{14, 15, 16, 17, 18} Showing enhanced arctic warming since 1981, satellite-observed arctic average surface skin temperatures have increased by $1.08^{\circ} \pm 0.13^{\circ}\text{F}$ ($+0.60^{\circ} \pm 0.07^{\circ}\text{C}$) per decade.¹⁹



As analyzed in Chapter 6: Temperature Change (Figure 6.1), strong near-surface air temperature warming has occurred across Alaska exceeding 1.5°F (0.8°C) over the last 30 years. Especially strong warming has occurred over Alaska's North Slope during autumn. For example, Utqiagvik's (formally Barrow) warming since 1979 exceeds 7°F (3.8°C) in September, 12°F (6.6°C) in October, and 10°F (5.5°C) in November.²⁰

Enhanced arctic warming is a robust feature of the climate response to anthropogenic forcing.^{21, 22} An anthropogenic contribution to arctic and Alaskan surface temperature warming over the past 50 years is *very likely*.^{23, 24, 25, 26, 27} One study argues that the natural forcing has not contributed to the long-term arctic warming in a discernable way.²⁷ Also, other anthropogenic forcings (mostly aerosols) have *likely* offset up to 60% of the high-latitude greenhouse gas warming since 1913,²⁷ suggesting that arctic warming to date would have been larger without the offsetting influence of aerosols. Other studies argue for a more significant contribution of natural variability to observed arctic temperature trends^{24, 28} and indicate that natural variability alone cannot explain observed warming. It is *very likely* that arctic surface temperatures will continue to increase faster than the global mean through the 21st century.^{25, 26, 27, 29}

11.2.2 Arctic Sea Ice Change

Arctic sea ice strongly influences Alaskan, arctic, and global climate by modulating exchanges of mass, energy, and momentum between the ocean and the atmosphere. Variations in arctic sea ice cover also influence atmospheric temperature and humidity, wind patterns, clouds, ocean temperature, thermal stratification, and ecosystem productivity.^{7, 10, 30, 31, 32, 33, 34, 35, 36, 37} Arctic sea ice exhibits significant interannual, spatial, and seasonal variability driven by atmospheric wind patterns

and cyclones, atmospheric temperature and humidity structure, clouds, radiation, sea ice dynamics, and the ocean.^{38, 39, 40, 41, 42, 43, 44}

Overwhelming evidence indicates that the character of arctic sea ice is rapidly changing. Observational evidence shows Arctic-wide sea ice decline since 1979, accelerating ice loss since 2000, and some of the fastest loss along the Alaskan coast.^{19, 20, 45, 46} Although sea ice loss is found in all months, satellite observations show the fastest loss in late summer and autumn.⁴⁵ Since 1979, the annual average arctic sea ice extent has *very likely* decreased at a rate of 3.5%–4.1% per decade.^{19, 37} Regional sea ice melt along the Alaskan coasts exceeds the arctic average rates with declines in the Beaufort and Chukchi Seas of –4.1% and –4.7% per decade, respectively.²⁰ The annual minimum and maximum sea ice extent have decreased over the last 35 years by –13.3% ± 2.6% and –2.7% ± 0.5% per decade, respectively.⁴⁷ The ten lowest September sea ice extents over the satellite period have all occurred in the last ten years, the lowest in 2012. The 2016 September sea ice minimum tied with 2007 for the second lowest on record, but rapid refreezing resulted in the 2016 September monthly average extent being the fifth lowest. Despite the rapid initial refreezing, sea ice extent was again in record low territory during fall–winter 2016/2017 due to anomalously warm temperatures in the marginal seas around Alaska,⁴⁷ contributing to a new record low in winter ice-volume (see <http://psc.apl.uw.edu/research/projects/arctic-sea-ice-volume-anomaly>).⁴⁸

Other important characteristics of arctic sea ice have also changed, including thickness, age, and volume. Sea ice thickness is monitored using an array of satellite, aircraft, and vessel measurements.^{37, 45} The mean thickness of the arctic sea ice during winter between 1980 and 2008 has decreased between 4.3 and 7.5 feet (1.3 and 2.3 meters).³⁷ The age distribution



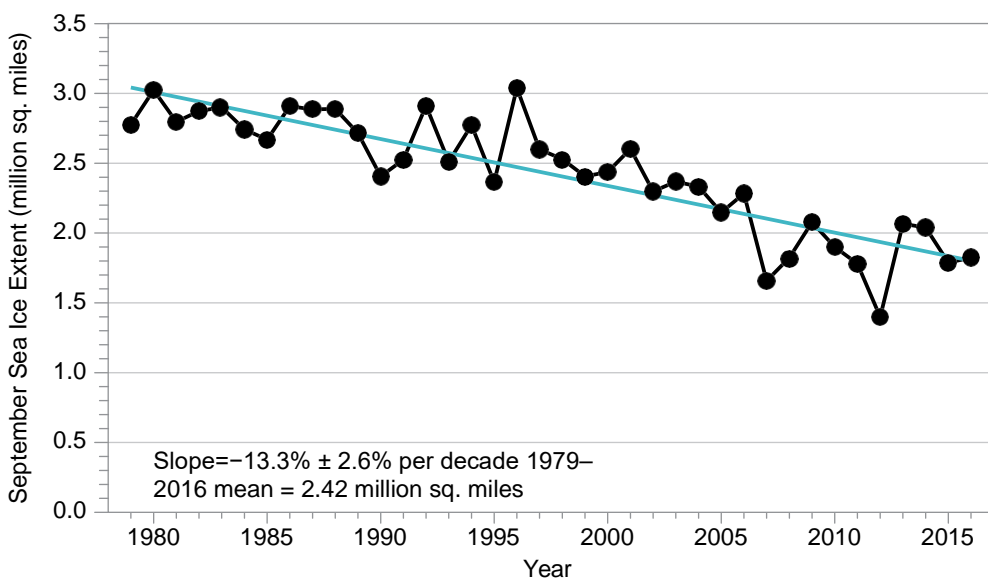
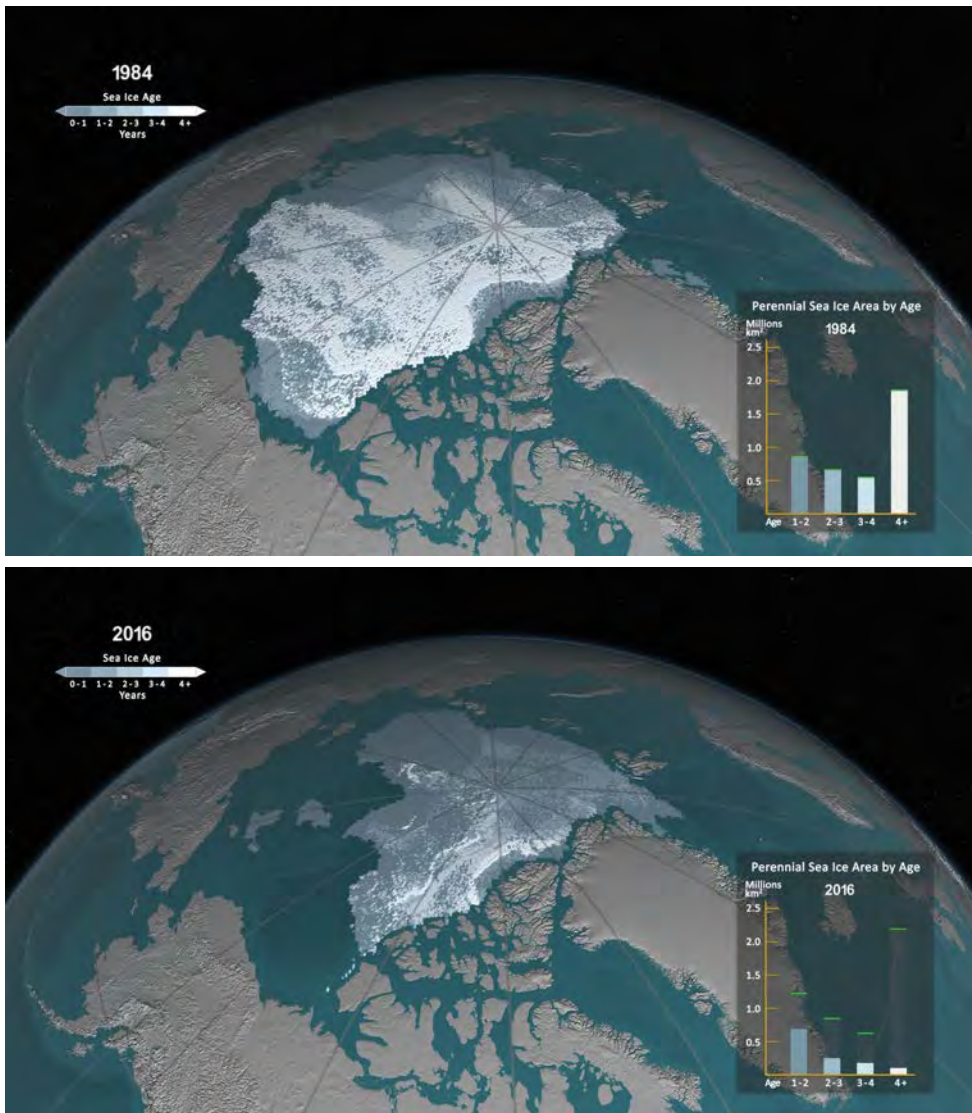


Figure 11.1: September sea ice extent and age shown for (a) 1984 and (b) 2016, illustrating significant reductions in sea ice extent and age (thickness). Bar graph in the lower right of each panel illustrates the sea ice area (unit: million km²) covered within each age category (>1 year), and the green bars represent the maximum value for each age range during the record. The year 1984 is representative of September sea ice characteristics during the 1980s. The years 1984 and 2016 are selected as endpoints in the time series; a movie of the complete time series is available at <http://svs.gsfc.nasa.gov/cgi-bin/details.cgi?aid=4489>. (c) Shows the satellite-era arctic sea ice areal extent trend from 1979 to 2016 for September (unit: million mi²). [Figure source: Panels (a),(b): NASA Science Visualization Studio; data: Tschudi et al. 2016;⁴⁹ Panel (c) data: Fetterer et al. 2016²⁰⁹].

of sea ice has become younger since 1988. In March 2016, first-year (multi-year) sea ice accounted for 78% (22%) of the total extent, whereas in the 1980s first-year (multi-year) sea ice accounted for 55% (45%).⁴⁷ Moreover, ice older than four years accounted for 16% of the March 1985 icepack but accounted for only 1.2% of the icepack in March 2016, indicating significant changes in sea ice volume.⁴⁷ The top two panels in Figure 11.1 show the September sea ice extent and age in 1984 and 2016, illustrating significant reductions in sea ice age.⁴⁹ While these panels show only two years (beginning point and ending point) of the complete time series, these two years are representative of the overall trends discussed and shown in the September sea ice extent time series in the bottom panel of Fig 11.1. Younger, thinner sea ice is more susceptible to melt, therefore reductions in age and thickness imply a larger interannual variability of extent.

Sea ice melt season—defined as the number of days between spring melt onset and fall freeze-up—has lengthened Arctic-wide by at least five days per decade since 1979, with larger regional changes.^{46, 50} Some of the largest observed changes in sea ice melt season (Figure 11.2) are found along Alaska’s northern and western coasts, lengthening the melt season by 20–30 days per decade and increasing the annual number of ice-free days by more than 90.⁵⁰ Summer sea ice retreat along coastal Alaska has led to longer open water seasons, making the Alaskan coastline more vulnerable to erosion.^{51, 52} Increased melt season length corresponds to increased absorption of solar radiation by the Arctic Ocean during summer and increases upper ocean temperature, delaying fall freeze-up. Overall, this process significantly contributes to reductions in arctic sea ice.^{42, 46} Wind-driven sea ice export through the Fram Strait has not increased over the last

80 years;³⁷ however, one recent study suggests that it may have increased since 1979.⁵³

It is *very likely* that there is an anthropogenic contribution to the observed arctic sea ice decline since 1979. A range of modeling studies analyzing the September sea ice extent trends in simulations with and without anthropogenic forcing conclude that these declines cannot be explained by natural variability alone.^{54, 55, 56, 57, 58, 59} Further, observational-based analyses considering a range of anthropogenic and natural forcing mechanisms for September sea ice loss reach the same conclusion.⁶⁰ Considering the occurrence of individual September sea ice anomalies, internal climate variability alone *very likely* could not have caused recently observed record low arctic sea ice extents, such as in September 2012.^{61, 62} The potential contribution of natural variability to arctic sea ice trends is significant.^{55, 63, 64} One recent study²⁸ indicates that internal variability dominates arctic atmospheric circulation trends, accounting for 30%–50% of the sea ice reductions since 1979, and up to 60% in September. However, previous studies indicate that the contributions from internal variability are smaller than 50%.^{54, 55} This apparent significant contribution of natural variability to sea ice decline indicates that natural variability alone cannot explain the observed sea ice decline and is consistent with the statement that it is *very likely* there is an anthropogenic contribution to the observed arctic sea ice decline since 1979.

Continued sea ice loss is expected across the Arctic, which is *very likely* to result in late summers becoming nearly ice-free (areal extent less than 10^6 km² or approximately 3.9×10^5 mi²) by the 2040s.^{21, 65} Natural variability,⁶⁶ future scenarios, and model uncertainties^{64, 67, 68} all influence sea ice projections. One study suggests that internal variability alone accounts for a 20-year prediction uncertainty in



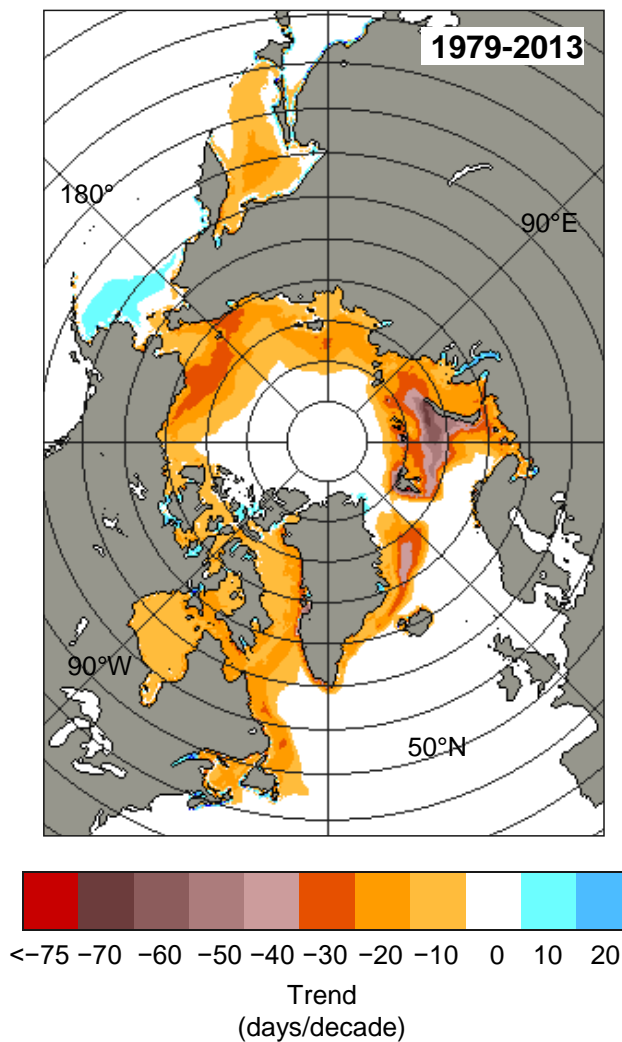


Figure 11.2: A 35-year trend in arctic sea ice melt season length, in days per decade, from passive microwave satellite observations, illustrating that the sea ice season has shortened by more than 60 days in coastal Alaska over the last 30 years. (Figure source: adapted from Parkinson 2014⁶⁰).

the timing of the first occurrence of an ice-free summer, whereas differences between a higher scenario (RCP8.5) and a lower scenario (RCP4.5) add only 5 years.⁶³ Projected September sea ice reductions by 2081–2100 range from 43% for an even lower scenario (RCP2.6) to 94% for RCP8.5.²¹ However, September sea ice projections over the next few decades are similar for the different anthropogenic forcing associated with these scenarios; scenario dependent sea ice loss only becomes apparent after 2050. Another study⁶⁹ indicates that the total sea ice loss scales roughly linearly with CO₂ emissions, such that an additional 1,000 GtC from present day levels corresponds to

ice-free conditions in September. A key message from the Third National Climate Assessment (NCA3)⁷⁰ was that arctic sea ice is disappearing. The fundamental conclusion of this assessment is unchanged; additional research corroborates the NCA3 statement.

11.2.3 Arctic Ocean and Marginal Seas *Sea Surface Temperature*

Arctic Ocean sea surface temperatures (SSTs) have increased since comprehensive records became available in 1982. Satellite-observed Arctic Ocean SSTs, poleward of 60°N, exhibit a trend of $0.16^{\circ} \pm 0.02^{\circ}\text{F}$ ($0.09^{\circ} \pm 0.01^{\circ}\text{C}$) per decade.¹⁹ Arctic Ocean SST is controlled by a

combination of factors, including solar radiation and energy transport from ocean currents and atmospheric winds. Summertime Arctic Ocean SST trends and patterns strongly couple with sea ice extent; however, clouds, ocean color, upper-ocean thermal structure, and atmospheric circulation also play a role.⁴⁰ Along coastal Alaska, SSTs in the Chukchi Sea exhibit a statistically significant (95% confidence) trend of $0.9^\circ \pm 0.5^\circ\text{F}$ ($0.5^\circ \pm 0.3^\circ\text{C}$) per decade.⁷²

Arctic Ocean temperatures also increased at depth.^{71, 73} Since 1970, Arctic Ocean Intermediate Atlantic Water—located between 150 and 900 meters—has warmed by $0.86^\circ \pm 0.09^\circ\text{F}$ ($0.48^\circ \pm 0.05^\circ\text{C}$) per decade; the most recent decade being the warmest.⁷³ The observed temperature level is unprecedented in the last 1,150 years for which proxy indicators provide records.^{74, 75} The influence of Intermediate Atlantic Water warming on future Alaska and arctic sea ice loss is unclear.^{38, 76}

Alaskan Sea Level Rise

The Alaskan coastline is vulnerable to sea level rise (SLR); however, strong regional variability exists in current trends and future projections. Some regions are experiencing relative sea level fall, whereas others are experiencing relative sea level rise, as measured by tide gauges that are part of NOAA's National Water Level Observation Network. These tide gauge data show sea levels rising fastest along the northern coast of Alaska but still slower than the global average, due to isostatic rebound (Ch. 12: Sea Level Rise).⁷⁷ However, considerable uncertainty in relative sea level rise exists due to a lack of tide gauges; for example, no tide gauges are located between Bristol Bay and Norton Sound or between Cape Lisburne and Prudhoe Bay. Under almost all future scenarios, SLR along most of the Alaskan coastline is projected to be less than the global average (Ch. 12: Sea Level Rise).

Salinity

Arctic Ocean salinity influences the freezing temperature of sea ice (less salty water freezes more readily) and the density profile representing the integrated effects of freshwater transport, river runoff, evaporation, and sea ice processes. Arctic Ocean salinity exhibits multidecadal variability, hampering the assessment of long-term trends.⁷⁸ Emerging evidence suggests that the Arctic Ocean and marginal sea salinity has decreased in recent years despite short-lived regional salinity increases between 2000 and 2005.⁷¹ Increased river runoff, rapid melting of sea and land ice, and changes in freshwater transport have influenced observed Arctic Ocean salinity.^{71, 79}

Ocean Acidification

Arctic Ocean acidification is occurring at a faster rate than the rest of the globe (see also Ch. 13: Ocean Changes).⁸⁰ Coastal Alaska and its ecosystems are especially vulnerable to ocean acidification because of the high sensitivity of Arctic Ocean water chemistry to changes in sea ice, respiration of organic matter, upwelling, and increasing river runoff.⁸⁰ Sea ice loss and a longer melt season contribute to increased vulnerability of the Arctic Ocean to acidification by lowering total alkalinity, permitting greater upwelling, and influencing the primary production characteristics in coastal Alaska.^{81, 82, 83, 84, 85, 86} Global-scale modeling studies suggest that the largest and most rapid changes in pH will continue along Alaska's coast, indicating that ocean acidification may increase enough by the 2030s to significantly influence coastal ecosystems.⁸⁰

11.2.4 Boreal Wildfires

Alaskan wildfire activity has increased in recent decades. This increase has occurred both in the boreal forest⁸⁷ and in the arctic tundra,⁸⁸ where fires historically were smaller and less frequent. A shortened snow cover season and higher temperatures over the last 50 years⁸⁹ make the Arctic more vulnerable to wildfire.⁸⁷



^{88, 90} Total area burned and the number of large fires (those with area greater than 1,000 km² or 386 mi²) in Alaska exhibit significant interannual and decadal variability, from influences of atmospheric circulation patterns and controlled burns, but have *likely* increased since 1959.⁹¹ The most recent decade has seen an unusually large number of years with anomalously large wildfires in Alaska.⁹² Studies indicate that anthropogenic climate change has *likely* lengthened the wildfire season and increased the risk of severe fires.⁹³ Further, wildfire risks are expected to increase through the end of the century due to warmer, drier conditions.^{90, 94} Using climate simulations to force an ecosystem model over Alaska (Alaska Frame-Based Ecosystem Code, ALFRESCO), the total area burned is projected to increase between 25% and 53% by 2100.⁹⁵ A transition into a regime of fire activity unprecedented in the last 10,000 years is possible.⁹⁶ We conclude that there is *medium confidence* for a human-caused climate change contribution to increased forest fire activity in Alaska in recent decades. See Chapter 8: Drought, Floods, and Wildfires for more details.

A significant amount of the total global soil carbon is found in the boreal forest and tundra ecosystems, including permafrost.^{97, 98, 99} Increased fire activity could deplete these stores, releasing them to the atmosphere to serve as an additional source of atmospheric CO₂.^{97, 100} Increased fires may also enhance the degradation of Alaska's permafrost by blackening the ground, reducing surface albedo, and removing protective vegetation.^{101, 102, 103, 104}

11.2.5 Snow Cover

Snow cover extent has significantly decreased across the Northern Hemisphere and Alaska over the last decade (see also Ch. 7: Precipitation Change and Ch. 10: Land Cover).^{105, 106} Northern Hemisphere June snow cover decreased by more than 65% between 1967 and 2012,^{37, 107} at

a trend of -17.2% per decade since 1979.⁸⁹ June snow cover dipped below 3 million square km (approximately 1.16 million square miles) for the fifth time in six years between 2010 and 2015, a threshold not crossed in the previous 43 years of record.⁸⁹ Early season snow cover in May, which affects the accumulation of solar insolation through the summer, has also declined at -7.3% per decade, due to reduced winter accumulation from warmer temperatures. Regional trends in snow cover duration vary, with some showing earlier onsets while others show later onsets.⁸⁹ In Alaska, the 2016 May statewide snow coverage of 595,000 square km (approximately 372,000 square miles) was the lowest on record dating back to 1967; the snow coverage of 2015 was the second lowest, and 2014 was the fourth lowest.

Human activities have *very likely* contributed to observed snow cover declines over the last 50 years. Attribution studies indicate that observed trends in Northern Hemisphere snow cover cannot be explained by natural forcing alone, but instead require anthropogenic forcing.^{24, 106, 108} Declining snow cover is expected to continue and will be affected by both the anthropogenic forcing and evolution of arctic ecosystems. The observed tundra shrub expansion and greening^{109, 110} affects melt by influencing snow depth, melt dynamics, and the local surface energy budget. Nevertheless, model simulations show that future reductions in snow cover influence biogeochemical feedbacks and warming more strongly than changes in vegetation cover and fire in the North American Arctic.¹¹¹

11.2.6 Continental Ice Sheets and Mountain Glaciers

Mass loss from ice sheets and glaciers influences sea level rise, the oceanic thermohaline circulation, and the global energy budget. Moreover, the relative contribution of GrIS to global sea level rise continues to increase, exceeding the contribution from thermal expansion.



sion (see Ch. 12: Sea Level Rise). Observational and modeling studies indicate that GrIS and glaciers in Alaska are out of mass balance with current climate conditions and are rapidly losing mass.^{37, 112} In recent years, mass loss has accelerated and is expected to continue.^{112, 113}

Dramatic changes have occurred across GrIS, particularly at its margins. GrIS average annual mass loss from January 2003 to May 2013 was -244 ± 6 Gt per year (approximately 0.26 inches per decade sea level equivalent).¹¹³ One study indicates that ice mass loss from Greenland was -269 Gt per year between April 2002 and April 2016.⁴⁷ Increased surface melt, runoff, and increased outlet glacier discharge from warmer air temperatures are primary contributing factors.^{114, 115, 116, 117, 118} The effects of warmer air and ocean temperatures on GrIS can be amplified by ice dynamical feedbacks, such as faster sliding, greater calving, and increased submarine melting.^{116, 119, 120, 121} Shallow ocean warming and regional ocean and atmospheric circulation changes also contribute to mass loss.^{122, 123, 124} The underlying mechanisms of the recent discharge speed-up remain unclear,^{125, 126} however, warmer subsurface ocean

and atmospheric temperatures^{118, 127, 128} and meltwater penetration to the glacier bed^{125, 129} *very likely* contribute.

Annual average ice mass from Arctic-wide glaciers has decreased every year since 1984,^{112, 130, 131} with significant losses in Alaska, especially over the past two decades (Figure 11.3).^{37, 132} Figure 11.4 illustrates observed changes from U.S. Geological Survey repeat photography of Alaska's Muir Glacier, retreating more than 4 miles between 1941 and 2004, and its tributary the Riggs Glacier. Total glacial ice mass in the Gulf of Alaska region has declined steadily since 2003.¹¹³ NASA's Gravity Recovery and Climate Experiment (GRACE) indicates mass loss from the northern and southern parts of the Gulf of Alaska region of -36 ± 4 Gt per year and -4 ± 3 Gt per year, respectively.¹¹³ Studies suggest an anthropogenic imprint on imbalances in Alaskan glaciers, indicating that melt will continue through the 21st century.^{112, 133, 134} Multiple datasets indicate that it is *virtually certain* that Alaskan glaciers have lost mass over the last 50 years and will continue to do so.¹³⁵

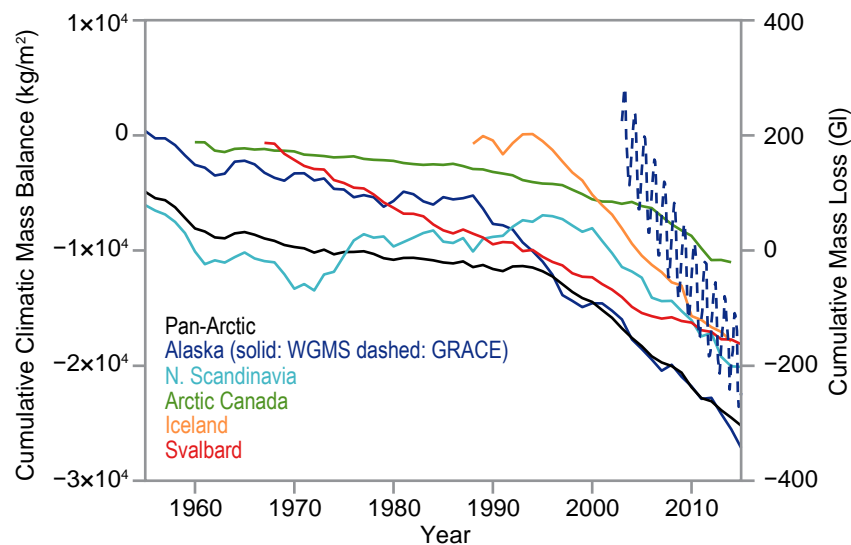


Figure 11.3: Time series of the cumulative climatic mass balance (units: kg/m^2) in five arctic regions and for the Pan-Arctic from the World Glacier Monitoring Service (WGMS;²¹⁰ Wolken et al.,²¹¹ solid lines, left y-axis), plus Alaskan glacial mass loss observed from NASA GRACE¹¹³ (dashed blue line, right y-axis). (Figure source: Harig and Simons 2016¹¹³ and Wolken et al. 2016;²¹¹ © American Meteorological Society, used with permission.)

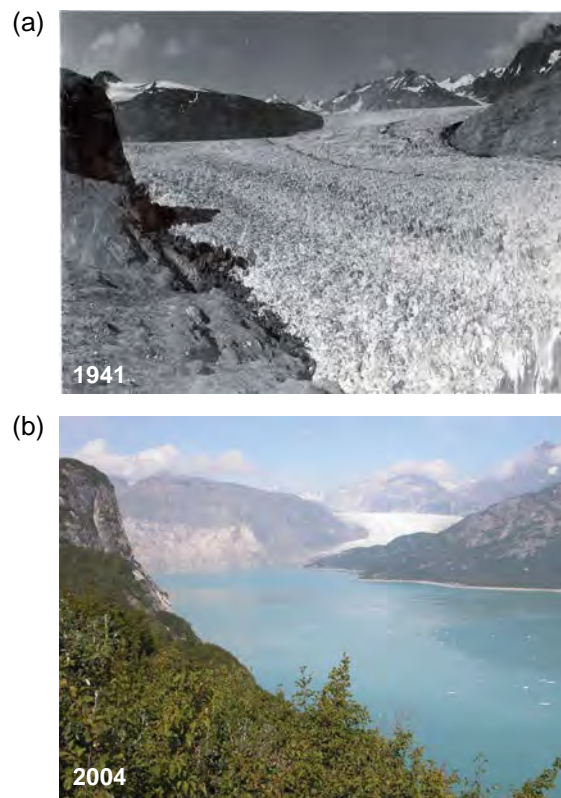


Figure 11.4: Two northeast-looking photographs of the Muir Glacier located in southeastern Alaska taken from a Glacier Bay Photo station in (a) 1941 and (b) 2004. U.S. Geological Survey repeat photography allows the tracking of glacier changes, illustrating that between 1941 and 2004 the Muir Glacier has retreated more than 4 miles to the northwest and out of view. Riggs Glacier (in view) is a tributary to Muir Glacier and has retreated by as much as 0.37 miles and thinned by more than 0.16 miles. The photographs also illustrate a significant change in the surface type between 1941 and 2004 as bare rock in the foreground has been replaced by dense vegetation (Figure source: USGS 2004²¹²).

11.3 Arctic Feedbacks on the Lower 48 and Globally

11.3.1 Linkages between Arctic Warming and Lower Latitudes

Midlatitude circulation influences arctic climate and climate change.^{11, 136, 137, 138, 139, 140, 141, 142, 143, 144, 145} Record warm arctic temperatures in winter 2016 resulted primarily from the transport of midlatitude air into the Arctic, demonstrating the significant midlatitude influence.¹⁴⁶ Emerging science demonstrates that warm, moist air intrusions from midlatitudes results in increased downwelling longwave radiation, warming the arctic surface and hindering wintertime sea ice growth.^{139, 141, 147, 148}

The extent to which enhanced arctic surface warming and sea ice loss influence the large-scale atmospheric circulation and midlatitude

weather and climate extremes has become an active research area.^{137, 146} Several pathways have been proposed (see references in Cohen et al.¹⁴⁹ and Barnes and Screen¹⁵⁰): reduced meridional temperature gradient, a more sinuous jet-stream, trapped atmospheric waves, modified storm tracks, weakened stratospheric polar vortex. While modeling studies link a reduced meridional temperature gradient to fewer cold temperature extremes in the continental United States,^{151, 152, 153, 154} other studies hypothesize that a slower jet stream may amplify Rossby waves and increase the frequency of atmospheric blocking, causing more persistent and extreme weather in midlatitudes.¹⁵⁵

Multiple observational studies suggest that the concurrent changes in the Arctic and Northern Hemisphere large-scale circula-

tion since the 1990s did not occur by chance, but were caused by arctic amplification.^{149, 150, 156} Reanalysis data suggest a relationship between arctic amplification and observed changes in persistent circulation phenomena like blocking and planetary wave amplitude.^{155, 157, 158} The recent multi-year California drought serves as an example of an event caused by persistent circulation phenomena (see Ch. 5: Circulation and Variability and Ch. 8: Drought, Floods, and Wildfires).^{159, 160, 161} Robust empirical evidence is lacking because the arctic sea ice observational record is too short¹⁶² or because the atmospheric response to arctic amplification depends on the prior state of the atmospheric circulation, reducing detectability.¹⁴⁶ Furthermore, it is not possible to draw conclusions regarding the direction of the relationship between arctic warming and midlatitude circulation based on empirical correlation and covariance analyses alone. Observational analyses have been combined with modeling studies to test causality statements.

Studies with simple models and Atmospheric General Circulation Models (AGCMs) provide evidence that arctic warming can affect midlatitude jet streams and location of storm tracks.^{137, 146, 150} In addition, analysis of CMIP5 models forced with increasing greenhouse gases suggests that the magnitude of arctic amplification affects the future midlatitude jet position, specifically during boreal winter.¹⁶³ However, the effect of arctic amplification on blocking is not clear (Ch. 5: Circulation and Variability).¹⁶⁴

Regarding attribution, AGCM simulations forced with observed changes in arctic sea ice suggest that the sea ice loss effect on observed recent midlatitude circulation changes and winter climate in the continental United States is small compared to natural large-scale atmospheric variability.^{142, 144, 154, 165} It is argued, however, that climate models do not properly

reproduce the linkages between arctic amplification and lower latitude climate due to model errors, including incorrect sea ice-atmosphere coupling and poor representation of stratospheric processes.^{137, 166}

In summary, emerging science demonstrates a strong influence of the midlatitude circulation on the Arctic, affecting temperatures and sea ice (*high confidence*). The influence of arctic changes on the midlatitude circulation and weather patterns are an area of active research. Currently, confidence is *low* regarding whether or by what mechanisms observed arctic warming may have influenced midlatitude circulation and weather patterns over the continental United States. The nature and magnitude of arctic amplification's influence on U.S. weather over the coming decades remains an open question.

11.3.2 Freshwater Effects on Ocean Circulation

The addition of freshwater to the Arctic Ocean from melting sea ice and land ice can influence important arctic climate system characteristics, including ocean salinity, altering ocean circulation, density stratification, and sea ice characteristics. Observations indicate that river runoff is increasing, driven by land ice melt, adding freshwater to the Arctic Ocean.¹⁶⁷ Melting arctic sea and land ice combined with time-varying atmospheric forcing^{79, 168} control Arctic Ocean freshwater export to the North Atlantic. Large-scale circulation variability in the central Arctic not only controls the redistribution and storage of freshwater in the Arctic⁷⁹ but also the export volume.¹⁶⁹ Increased freshwater fluxes can weaken open ocean convection and deep water formation in the Labrador and Irminger seas, weakening the Atlantic meridional overturning circulation (AMOC).^{170, 171} AMOC-associated poleward heat transport substantially contributes to North American and continental European climate; any AMOC slowdown could have implications for global



climate change as well (see Ch. 15: Potential Surprises).^{172, 173} Connections to subarctic ocean variations and the Atlantic Meridional Overturning Circulation have not been conclusively established and require further investigation (see Ch. 13: Ocean Changes).

11.3.3 Permafrost–Carbon Feedback

Alaska and arctic permafrost characteristics have responded to increased temperatures and reduced snow cover in most regions since the 1980s.¹³⁰ The permafrost warming rate varies regionally; however, colder permafrost is warming faster than warmer permafrost.^{37, 174} This feature is most evident across Alaska, where permafrost on the North Slope is warming more rapidly than in the interior. Permafrost temperatures across the North Slope at various depths ranging from 39 to 65 feet (12 to 20 meters) have warmed between 0.3° and 1.3°F (0.2° and 0.7°C) per decade over the observational period (Figure 11.5).¹⁷⁵ Permafrost active layer thickness increased across much of the Arctic while showing strong regional

variations.^{37, 130, 176} Further, recent geologic survey data indicate significant permafrost thaw slumping in northwestern Canada and across the circumpolar Arctic that indicate significant ongoing permafrost thaw, potentially priming the region for more rapid thaw in the future.¹⁷⁷ Continued degradation of permafrost and a transition from continuous to discontinuous permafrost is expected over the 21st century.^{37, 178, 179}

Permafrost contains large stores of carbon. Though the total contribution of these carbon stores to global methane emission is uncertain, Alaska’s permafrost contains rich and vulnerable organic carbon soils.^{99, 179, 180} Thus, warming Alaska permafrost is a concern for the global carbon cycle as it provides a possibility for a significant and potentially uncontrollable release of carbon, complicating the ability to limit global temperature increases. Current methane emissions from Alaskan arctic tundra and boreal forests contribute a small fraction of the global methane (CH₄) budget.¹⁸¹ Howev-

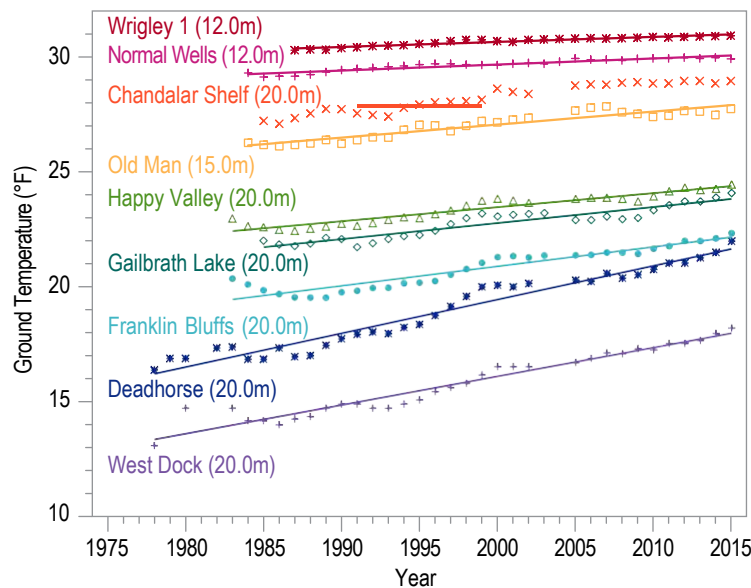


Figure 11.5: Time series of annual mean permafrost temperatures (units: °F) at various depths from 39 to 65 feet (12 to 20 meters) from 1977 through 2015 at several sites across Alaska, including the North Slope continuous permafrost region (purple/blue/green shades), and the discontinuous permafrost (orange/pink/red shades) in Alaska and northwestern Canada. Solid lines represent the linear trends drawn to highlight that permafrost temperatures are warming faster in the colder, coastal permafrost regions than the warmer interior regions. (Figure Source: adapted from Romanovsky et al. 2016;¹⁷⁵ © American Meteorological Society, used with permission.)

er, gas flux measurements have directly measured the release of CO₂ and CH₄ from arctic permafrost.¹⁸² Recent measurements indicate that cold season methane emissions (after snowfall) are greater than summer emissions in Alaska, and methane emissions in upland tundra are greater than in wetland tundra.¹⁸³

The permafrost–carbon feedback represents the additional release of CO₂ and CH₄ from thawing permafrost soils providing additional radiative forcing, a source of a potential surprise (Ch. 15: Potential Surprises).¹⁸⁴ Thawing permafrost makes previously frozen organic matter available for microbial decomposition, producing CO₂ and CH₄. The specific condition under which microbial decomposition occurs, aerobic or anaerobic, determines the proportion of CO₂ and CH₄ released. This distinction has potentially significant implications, as CH₄ has a 100-year global warming potential 35 times that of CO₂.¹⁸⁵ Emerging science indicates that 3.4 times more carbon is released under aerobic conditions than anaerobic conditions, and 2.3 times more carbon after accounting for the stronger greenhouse effect of CH₄.¹⁸⁶ Additionally, CO₂ and CH₄ production strongly depends on vegetation and soil properties.¹⁸⁴

Combined data and modeling studies indicate a positive permafrost–carbon feedback with a global sensitivity between –14 and –19 GtC per °C (approximately –25 to –34 GtC per °F) soil carbon loss^{187, 188} resulting in a total 120 ± 85 GtC release from permafrost by 2100 and an additional global temperature increase of 0.52° ± 0.38°F (0.29° ± 0.21°C) by the permafrost–carbon feedback.¹⁸⁹ More recently, Chadburn et al.¹⁹⁰ infer a –4 million km² per °C (or approximately 858,000 mi² per °F) reduction in permafrost area to globally averaged warming at stabilization by constraining climate models with the observed spatial distribution of permafrost; this sensitivity is 20% higher

than previous studies. In the coming decades, enhanced high-latitude plant growth and its associated CO₂ sink should partially offset the increased emissions from permafrost thaw;^{179, 189, 191} thereafter, decomposition is expected to dominate uptake. Permafrost thaw is occurring faster than models predict due to poorly understood deep soil, ice wedge, and thermokarst processes.^{188, 192, 193} Additionally, uncertainty stems from the surprising uptake of methane from mineral soils.¹⁹⁴ There is *high confidence* in the positive sign of the permafrost–carbon feedback, but *low confidence* in the feedback magnitude.

11.3.4 Methane Hydrate Instability

Significant stores of CH₄, in the form of methane hydrates (also called clathrates), lie within and below permafrost and under the global ocean on continental margins. The estimated total global inventory of methane hydrates ranges from 500 to 3,000 GtC^{195, 196, 197} with a central estimate of 1,800 GtC.¹⁹⁸ Methane hydrates are solid compounds formed at high pressures and cold temperatures, trapping methane gas within the crystalline structure of water. Methane hydrates within upper continental slopes of the Pacific, Atlantic, and Gulf of Mexico margins and beneath the Alaskan arctic continental shelf may be vulnerable to small increases in ocean temperature.^{197, 198, 199, 200, 201, 202, 203}

Rising sea levels and warming oceans have a competing influence on methane hydrate stability.^{199, 204} Studies indicate that the temperature effect dominates and that the overall influence is *very likely* a destabilizing effect.¹⁹⁸ Projected warming rates for the 21st century Arctic Ocean are not expected to lead to sudden or catastrophic destabilization of seafloor methane hydrates.²⁰⁵ Recent observations indicate increased CH₄ emission from the arctic seafloor near Svalbard; however, these emissions are not reaching the atmosphere.^{198, 206}



TRACEABLE ACCOUNTS

Key Finding 1

Annual average near-surface air temperatures across Alaska and the Arctic have increased over the last 50 years at a rate more than twice as fast as the global average temperature. (*Very high confidence*)

Description of evidence base

The Key Finding is supported by observational evidence from ground-based observing stations, satellites, and data-model temperature analyses from multiple sources and independent analysis techniques.^{14,15,16,17,18,19,20} For more than 40 years, climate models have predicted enhanced arctic warming, indicating a solid grasp on the underlying physics and positive feedbacks driving the accelerated arctic warming.^{1,21,22} Lastly, similar statements have been made in NCA3,⁷⁰ IPCC AR5,¹⁷ and in other arctic-specific assessments such as the Arctic Climate Impacts Assessment²⁰⁷ and Snow, Water, Ice and Permafrost in the Arctic.¹³⁰

Major Uncertainties

The lack of high quality and restricted spatial resolution of surface and ground temperature data over many arctic land regions and essentially no measurements over the Central Arctic Ocean hamper the ability to better refine the rate of arctic warming and completely restrict our ability to quantify and detect regional trends, especially over the sea ice. Climate models generally produce an arctic warming between two to three times the global mean warming. A key uncertainty is our quantitative knowledge of the contributions from individual feedback processes in driving the accelerated arctic warming. Reducing this uncertainty will help constrain projections of future arctic warming.

Assessment of confidence based on evidence and agreement, including short description of nature of evidence and level of agreement

Very high confidence that the arctic surface and air temperatures have warmed across Alaska and the Arctic at a much faster rate than the global average is provided by the multiple datasets analyzed by multiple independent groups indicating the same conclusion. Additionally, climate models capture the enhanced warming in

the Arctic, indicating a solid understanding of the underlying physical mechanisms.

If appropriate, estimate likelihood of impact or consequence, including short description of basis of estimate

It is *very likely* that the accelerated rate of arctic warming will have a significant consequence for the United States due to accelerated land and sea ice melt driving changes in the ocean including sea level rise threatening our coastal communities and freshening of sea water that is influencing marine ecology.

Summary sentence or paragraph that integrates the above information

Annual average near-surface air temperatures across Alaska and the Arctic have increased over the last 50 years at a rate more than twice the global average. Observational studies using ground-based observing stations and satellites analyzed by multiple independent groups support this finding. The enhanced sensitivity of the arctic climate system to anthropogenic forcing is also supported by climate modeling evidence, indicating a solid grasp on the underlying physics. These multiple lines of evidence provide *very high confidence* of enhanced arctic warming with potentially significant impacts on coastal communities and marine ecosystems.

Key Finding 2

Rising Alaskan permafrost temperatures are causing permafrost to thaw and become more discontinuous; this process releases additional carbon dioxide and methane, resulting in an amplifying feedback and additional warming (*high confidence*). The overall magnitude of the permafrost-carbon feedback is uncertain; however, it is clear that these emissions have the potential to compromise the ability to limit global temperature increases.

Description of evidence base

The Key Finding is supported by observational evidence of warming permafrost temperatures and a deepening active layer, in situ gas measurements and



laboratory incubation experiments of CO₂ and CH₄ release, and model studies.^{37, 179, 186, 187, 188, 192, 193} Alaska and arctic permafrost characteristics have responded to increased temperatures and reduced snow cover in most regions since the 1980s, with colder permafrost warming faster than warmer permafrost.^{37, 130, 175} Large carbon soil pools (more than 50% of the global below-ground organic carbon pool) are locked up in the permafrost soils,¹⁸⁰ with the potential to be released. Thawing permafrost makes previously frozen organic matter available for microbial decomposition. In situ gas flux measurements have directly measured the release of CO₂ and CH₄ from arctic permafrost.^{182, 183} The specific conditions of microbial decomposition, aerobic or anaerobic, determines the relative production of CO₂ and CH₄. This distinction is significant as CH₄ is a much more powerful greenhouse gas than CO₂.¹⁸⁵ However, incubation studies indicate that 3.4 times more carbon is released under aerobic conditions than anaerobic conditions, leading to a 2.3 times the stronger radiative forcing under aerobic conditions.¹⁸⁶ Combined data and modeling studies suggest a global sensitivity of the permafrost–carbon feedback warming global temperatures in 2100 by 0.52° ± 0.38°F (0.29° ± 0.21°C) alone.¹⁸⁹ Chadburn et al.¹⁹⁰ infer the sensitivity of permafrost area to globally averaged warming to be 4 million km² by constraining a group of climate models with the observed spatial distribution of permafrost; this sensitivity is 20% higher than previous studies. Permafrost thaw is occurring faster than models predict due to poorly understood deep soil, ice wedge, and thermokarst processes.^{188, 192, 193, 208} Additional uncertainty stems from the surprising uptake of methane from mineral soils¹⁹⁴ and dependence of emissions on vegetation and soil properties.¹⁸⁴ The observational and modeling evidence supports the Key Finding that the permafrost–carbon cycle is positive.

Major uncertainties

A major limiting factor is the sparse observations of permafrost in Alaska and remote areas across the Arctic. Major uncertainties are related to deep soil, ice wedging, and thermokarst processes and the dependence of CO₂ and CH₄ uptake and production on vegetation and soil properties. Uncertainties also exist in relevant

soil processes during and after permafrost thaw, especially those that control unfrozen soil carbon storage and plant carbon uptake and net ecosystem exchange. Many processes with the potential to drive rapid permafrost thaw (such as thermokarst) are not included in current earth system models.

Assessment of confidence based on evidence and agreement, including short description of nature of evidence and level of agreement

There is *high confidence* that permafrost is thawing, becoming discontinuous, and releasing CO₂ and CH₄. Physically-based arguments and observed increases in CO₂ and CH₄ emissions as permafrost thaws indicate that the feedback is positive. This confidence level is justified based on observations of rapidly changing permafrost characteristics.

If appropriate, estimate likelihood of impact or consequence, including short description of basis of estimate

Thawing permafrost *very likely* has significant impacts to the global carbon cycle and serves as a source of CO₂ and CH₄ emission that complicates the ability to limit global temperature increases.

Summary sentence or paragraph that integrates the above information

Permafrost is thawing, becoming more discontinuous, and releasing CO₂ and CH₄. Observational and modeling evidence indicates that permafrost has thawed and released additional CO₂ and CH₄ indicating that the permafrost–carbon cycle feedback is positive accounting for additional warming of approximately 0.08° to 0.50°C on top of climate model projections. Although the magnitude of the permafrost–carbon feedback is uncertain due to a range of poorly understood processes (deep soil and ice wedge processes, plant carbon uptake, dependence of uptake and emissions on vegetation and soil type, and the role of rapid permafrost thaw processes, such as thermokarst), emerging science and the newest estimates continue to indicate that this feedback is more likely on the larger side of the range. Impacts of permafrost thaw and the permafrost



carbon feedback complicates our ability to limit global temperature increases by adding a currently unconstrained radiative forcing to the climate system.

Key Finding 3

Arctic land and sea ice loss observed in the last three decades continues, in some cases accelerating (*very high confidence*). It is *virtually certain* that Alaska glaciers have lost mass over the last 50 years, with each year since 1984 showing an annual average ice mass less than the previous year. Based on gravitational data from satellites, average ice mass loss from Greenland was -269 Gt per year between April 2002 and April 2016, accelerating in recent years (*high confidence*). Since the early 1980s, annual average arctic sea ice has decreased in extent between 3.5% and 4.1% per decade, become thinner by between 4.3 and 7.5 feet, and began melting at least 15 more days each year. September sea ice extent has decreased between 10.7% and 15.9% per decade (*very high confidence*). Arctic-wide ice loss is expected to continue through the 21st century, *very likely* resulting in nearly sea ice-free late summers by the 2040s (*very high confidence*).

Description of evidence base

The Key Finding is supported by observational evidence from multiple ground-based and satellite-based observational techniques (including passive microwave, laser and radar altimetry, and gravimetry) analyzed by independent groups using different techniques reaching similar conclusions.^{19, 37, 45, 47, 112, 113, 134, 135} Additionally, the U.S. Geological Survey repeat photography database shows the glacier retreat for many Alaskan glaciers (Figure 11.4: Muir Glacier). Several independent model analysis studies using a wide array of climate models and different analysis techniques indicate that sea ice loss will continue across the Arctic, *very likely* resulting in late summers becoming nearly ice-free by the 2040s.^{21, 59, 65}

Major uncertainties

Key uncertainties remain in the quantification and modeling of key physical processes that contribute to the acceleration of land and sea ice melting. Climate models are unable to capture the rapid pace of ob-

served sea and land ice melt over the last 15 years; a major factor is our inability to quantify and accurately model the physical processes driving the accelerated melting. The interactions between atmospheric circulation, ice dynamics and thermodynamics, clouds, and specifically the influence on the surface energy budget are key uncertainties. Mechanisms controlling marine-terminating glacier dynamics—specifically the roles of atmospheric warming, seawater intrusions under floating ice shelves, and the penetration of surface meltwater to the glacier bed—are key uncertainties in projecting Greenland Ice Sheet melt.

Assessment of confidence based on evidence and agreement, including short description of nature of evidence and level of agreement

There is *very high confidence* that arctic sea and land ice melt is accelerating and mountain glacier ice mass is declining given the multiple observational sources and analysis techniques documented in the peer-reviewed climate science literature.

If appropriate, estimate likelihood of impact or consequence, including short description of basis of estimate

It is *very likely* that accelerating arctic land and sea ice melt impacts the United States. Accelerating Arctic Ocean sea ice melt increases coastal erosion in Alaska and makes Alaskan fisheries more susceptible to ocean acidification by changing Arctic Ocean chemistry. Greenland Ice Sheet and Alaska mountain glacier melt drives sea level rise threatening coastal communities in the United States and worldwide, influencing marine ecology, and potentially altering the thermohaline circulation.

Summary sentence or paragraph that integrates the above information

Arctic land and sea ice loss observed in the last three decades continues, in some cases accelerating. A diverse range of observational evidence from multiple data sources and independent analysis techniques provide consistent evidence of substantial declines in arctic sea ice extent, thickness, and volume since at least 1979, mountain glacier melt over the last 50 years, and



accelerating mass loss from Greenland. An array of different models and independent analyses indicate that future declines in ice across the Arctic are expected resulting in late summers in the Arctic becoming ice free by the 2040s.

Key Finding 4

It is *very likely* that human activities have contributed to observed arctic surface temperature warming, sea ice loss, glacier mass loss, and Northern Hemisphere snow extent decline (*high confidence*).

Description of evidence base

The Key Finding is supported by many attribution studies using a wide array of climate models documenting the anthropogenic influence on arctic temperature, sea ice, mountain glaciers, and snow extent.^{23, 24, 25, 26, 27, 29, 54, 55, 56, 57, 58, 59, 61, 62, 106, 108, 133} Observation-based analyses also support an anthropogenic influence.^{60, 69} Najafi et al.²⁷ show that the greenhouse warming signal in the Arctic could be even stronger, as a significant portion of greenhouse gas induced warming (approximately 60%) has been offset by anthropogenic aerosol emissions. The emerging science of extreme event attribution indicates that natural variability alone could not have caused the recently observed record low arctic sea ice extents, such as in September 2012.^{61, 62} Natural variability in the Arctic is significant,^{63, 64} however the majority of studies indicate that the contribution from individual sources of internal variability to observed trends in arctic temperature and sea ice are less than 50%^{28, 54, 55} and alone cannot explain the observed trends over the satellite era. This Key Finding marks an increased confidence relative to the IPCC AR5²⁴ moving from *likely* to *very likely*. In our assessment, the new understanding of the anthropogenic forcing,²⁷ its relationship to arctic climate change,⁶⁹ arctic climate variability,^{28, 63, 64} and especially extreme event attribution studies^{61, 62} reaffirms previous studies and warrants the increased likelihood of an anthropogenic influence on arctic climate change. Multiple lines evidence, independent analysis techniques, models, and studies support the Key Finding.

Major uncertainties

A major limiting factor in our ability to attribute arctic sea ice and glacier melt to human activities is the significant natural climate variability in the Arctic. Longer data records and a better understanding of the physical mechanisms that drive natural climate variability in the Arctic are required to reduce this uncertainty. Another major uncertainty is the ability of climate models to capture the relevant physical processes and climate changes at a fine spatial scale, especially those at the land and ocean surface in the Arctic.

Assessment of confidence based on evidence and agreement, including short description of nature of evidence and level of agreement

There is *high confidence* that human activities have contributed to arctic surface temperature warming, sea ice loss since 1979, glacier mass loss, and Northern Hemisphere snow extent given multiple independent analysis techniques from independent groups using many different climate models indicate the same conclusion.

If appropriate, estimate likelihood of impact or consequence, including short description of basis of estimate

Arctic sea ice and glacier mass loss impacts the United States by affecting coastal erosion in Alaska and key Alaskan fisheries through an increased vulnerability to ocean acidification. Glacier mass loss is a significant driver of sea level rise threatening coastal communities in the United States and worldwide, influencing marine ecology, and potentially altering the Atlantic Meridional Overturning Circulation.¹⁷²

Summary sentence or paragraph that integrates the above information

Evidenced by the multiple independent studies, analysis techniques, and the array of different climate models used over the last 20 years, it is *very likely* that human activities have contributed to arctic surface temperature warming, sea ice loss since 1979, glacier mass loss, and Northern Hemisphere snow extent decline observed across the Arctic. Key uncertainties remain in the understanding and modeling of arctic climate variability; however, many independent studies indicate



that internal variability alone cannot explain the trends or extreme events observed in arctic temperature and sea ice over the satellite era.

Key Finding 5

Atmospheric circulation patterns connect the climates of the Arctic and the contiguous United States. Evidenced by recent record warm temperatures in the Arctic and emerging science, the midlatitude circulation has influenced observed arctic temperatures and sea ice (*high confidence*). However, confidence is *low* regarding whether or by what mechanisms observed arctic warming may have influenced the midlatitude circulation and weather patterns over the continental United States. The influence of arctic changes on U.S. weather over the coming decades remains an open question with the potential for significant impact.

Description of evidence base

The midlatitude circulation influences the Arctic through the transport of warm, moist air, altering the Arctic surface energy budget.^{138, 142, 143, 144} The intrusion of warm, moist air from midlatitudes increases downwelling longwave radiation, warming the arctic surface and hindering wintertime sea ice growth.^{139, 147} Emerging research provides a new understanding of the importance of synoptic time scales and the episodic nature of midlatitude air intrusions.^{139, 141, 148} The combination of recent observational and model-based evidence as well as the physical understanding of the mechanisms of midlatitude circulation effects on arctic climate supports this Key Finding.

In addition, research on the impact of arctic climate on midlatitude circulation is rapidly evolving, including observational analysis and modeling studies. Multiple observational studies provide evidence for concurrent changes in the Arctic and Northern Hemisphere large-scale circulation changes.^{149, 150, 156} Further, modeling studies demonstrate that arctic warming can influence the midlatitude jet stream and storm track.^{137, 146, 150, 163} However, attribution studies indicate that the observed midlatitude circulation changes over the continental United States are smaller than natural variability and are therefore not detectable in the observational re-

cord.^{142, 144, 154, 165} This disagreement between independent studies using different analysis techniques and the lack of understanding of the physical mechanism(s) supports this Key Finding.

Major uncertainties

A major limiting factor is our understanding and modeling of natural climate variability in the Arctic. Longer data records and a better understanding of the physical mechanisms that drive natural climate variability in the Arctic are required to reduce this uncertainty. The inability of climate models to accurately capture interactions between sea ice and the atmospheric circulation and polar stratospheric processes limits our current understanding.

Assessment of confidence based on evidence and agreement, including short description of nature of evidence and level of agreement

High confidence in the impact of midlatitude circulation on arctic changes from the consistency between observations and models as well as a solid physical understanding.

Low confidence on the detection of an impact of arctic warming on midlatitude climate is based on short observational data record, model uncertainty, and lack of physical understanding.

Summary sentence or paragraph that integrates the above information

The midlatitude circulation has influenced observed arctic temperatures, supported by recent observational and model-based evidence as well as the physical understanding from emerging science. In turn, confidence is low regarding the mechanisms by which observed arctic warming has influenced the midlatitude circulation and weather patterns over the continental United States, due to the disagreement between numerous studies and a lack of understanding of the physical mechanism(s). Resolving the remaining questions requires longer data records and improved understanding and modeling of physics in the Arctic. The influence of arctic changes on U.S. weather over the coming decades remains an open question with the potential for significant impact.



REFERENCES

1. Manabe, S. and R.T. Wetherald, 1975: The effects of doubling the CO₂ concentration on the climate of a General Circulation Model. *Journal of the Atmospheric Sciences*, **32**, 3-15. [http://dx.doi.org/10.1175/1520-0469\(1975\)032<0003:teodtc>2.0.co;2](http://dx.doi.org/10.1175/1520-0469(1975)032<0003:teodtc>2.0.co;2)
2. Knies, J., P. Cabedo-Sanz, S.T. Belt, S. Baranwal, S. Fietz, and A. Rosell-Melé, 2014: The emergence of modern sea ice cover in the Arctic Ocean. *Nature Communications*, **5**, 5608. <http://dx.doi.org/10.1038/ncomms6608>
3. Wyser, K., C.G. Jones, P. Du, E. Girard, U. Willén, J. Cassano, J.H. Christensen, J.A. Curry, K. Dethloff, J.-E. Haugen, D. Jacob, M. Körtzow, R. Laprise, A. Lynch, S. Pfeifer, A. Rinke, M. Serreze, M.J. Shaw, M. Tjernström, and M. Zagar, 2008: An evaluation of Arctic cloud and radiation processes during the SHEBA year: Simulation results from eight Arctic regional climate models. *Climate Dynamics*, **30**, 203-223. <http://dx.doi.org/10.1007/s00382-007-0286-1>
4. Bourassa, M.A., S.T. Gille, C. Bitz, D. Carlson, I. Cerovecki, C.A. Clayson, M.F. Cronin, W.M. Drennan, C.W. Fairall, R.N. Hoffman, G. Magnusdottir, R.T. Pinker, I.A. Renfrew, M. Serreze, K. Speer, L.D. Talley, and G.A. Wick, 2013: High-latitude ocean and sea ice surface fluxes: Challenges for climate research. *Bulletin of the American Meteorological Society*, **94**, 403-423. <http://dx.doi.org/10.1175/BAMS-D-11-00244.1>
5. Maslowski, W., J. Clement Kinney, M. Higgins, and A. Roberts, 2012: The future of Arctic sea ice. *Annual Review of Earth and Planetary Sciences*, **40**, 625-654. <http://dx.doi.org/10.1146/annurev-earth-042711-105345>
6. Maslowski, W., J. Clement Kinney, S.R. Okkonen, R. Osinski, A.F. Roberts, and W.J. Williams, 2014: The large scale ocean circulation and physical processes controlling Pacific-Arctic interactions. *The Pacific Arctic Region: Ecosystem Status and Trends in a Rapidly Changing Environment*. Grebmeier, M.J. and W. Maslowski, Eds. Springer Netherlands, Dordrecht, 101-132. http://dx.doi.org/10.1007/978-94-017-8863-2_5
7. Kay, J.E. and A. Gettelman, 2009: Cloud influence on and response to seasonal Arctic sea ice loss. *Journal of Geophysical Research*, **114**, D18204. <http://dx.doi.org/10.1029/2009JD011773>
8. Taylor, P.C., S. Kato, K.-M. Xu, and M. Cai, 2015: Covariance between Arctic sea ice and clouds within atmospheric state regimes at the satellite footprint level. *Journal of Geophysical Research Atmospheres*, **120**, 12656-12678. <http://dx.doi.org/10.1002/2015JD023520>
9. Overland, J., E. Hanna, I. Hanssen-Bauer, S.-J. Kim, J. Wlask, M. Wang, and U.S. Bhatt, 2015: [The Arctic] Arctic air temperature [in "State of the Climate in 2014"]. *Bulletin of the American Meteorological Society*, **96** (12), S128-S129. <http://dx.doi.org/10.1175/2015BAMSStateoftheClimate.1>
10. Johannessen, O.M., S.I. Kuzmina, L.P. Bobylev, and M.W. Miles, 2016: Surface air temperature variability and trends in the Arctic: New amplification assessment and regionalisation. *Tellus A*, **68**, 28234. <http://dx.doi.org/10.3402/tellusa.v68.28234>
11. Overland, J.E. and M. Wang, 2016: Recent extreme Arctic temperatures are due to a split polar vortex. *Journal of Climate*, **29**, 5609-5616. <http://dx.doi.org/10.1175/JCLI-D-16-0320.1>
12. Hartmann, B. and G. Wendler, 2005: The significance of the 1976 Pacific climate shift in the climatology of Alaska. *Journal of Climate*, **18**, 4824-4839. <http://dx.doi.org/10.1175/JCLI3532.1>
13. McAfee, S.A., 2014: Consistency and the lack thereof in Pacific Decadal Oscillation impacts on North American winter climate. *Journal of Climate*, **27**, 7410-7431. <http://dx.doi.org/10.1175/JCLI-D-14-00143.1>
14. Serreze, M.C., A.P. Barrett, J.C. Stroeve, D.N. Kindig, and M.M. Holland, 2009: The emergence of surface-based Arctic amplification. *The Cryosphere*, **3**, 11-19. <http://dx.doi.org/10.5194/tc-3-11-2009>
15. Bekryaev, R.V., I.V. Polyakov, and V.A. Alexeev, 2010: Role of polar amplification in long-term surface air temperature variations and modern Arctic warming. *Journal of Climate*, **23**, 3888-3906. <http://dx.doi.org/10.1175/2010jcli3297.1>
16. Screen, J.A. and I. Simmonds, 2010: The central role of diminishing sea ice in recent Arctic temperature amplification. *Nature*, **464**, 1334-1337. <http://dx.doi.org/10.1038/nature09051>
17. Hartmann, D.L., A.M.G. Klein Tank, M. Rusticucci, L.V. Alexander, S. Brönnimann, Y. Charabi, F.J. Dentener, E.J. Dlugokencky, D.R. Easterling, A. Kaplan, B.J. Soden, P.W. Thorne, M. Wild, and P.M. Zhai, 2013: Observations: Atmosphere and surface. *Climate Change 2013: The Physical Science Basis. Contribution of Working Group I to the Fifth Assessment Report of the Intergovernmental Panel on Climate Change*. Stocker, T.F., D. Qin, G.-K. Plattner, M. Tignor, S.K. Allen, J. Boschung, A. Nauels, Y. Xia, V. Bex, and P.M. Midgley, Eds. Cambridge University Press, Cambridge, United Kingdom and New York, NY, USA, 159-254. <http://www.climatechange2013.org/report/full-report/>



18. Overland, J., E. Hanna, I. Hanssen-Bauer, S.-J. Kim, J. Walsh, M. Wang, and U. Bhatt, 2014: Air temperature [in Arctic Report Card 2014]. ftp://ftp.oar.noaa.gov/arctic/documents/ArcticReportCard_full_report2014.pdf
19. Comiso, J.C. and D.K. Hall, 2014: Climate trends in the Arctic as observed from space. *Wiley Interdisciplinary Reviews: Climate Change*, **5**, 389-409. <http://dx.doi.org/10.1002/wcc.277>
20. Wendler, G., B. Moore, and K. Galloway, 2014: Strong temperature increase and shrinking sea ice in Arctic Alaska. *The Open Atmospheric Science Journal*, **8**, 7-15. <http://dx.doi.org/10.2174/1874282301408010007>
21. Collins, M., R. Knutti, J. Arblaster, J.-L. Dufresne, T. Fichet, P. Friedlingstein, X. Gao, W.J. Gutowski, T. Johns, G. Krinner, M. Shongwe, C. Tebaldi, A.J. Weaver, and M. Wehner, 2013: Long-term climate change: Projections, commitments and irreversibility. *Climate Change 2013: The Physical Science Basis. Contribution of Working Group I to the Fifth Assessment Report of the Intergovernmental Panel on Climate Change*. Stocker, T.F., D. Qin, G.-K. Plattner, M. Tignor, S.K. Allen, J. Boschung, A. Nauels, Y. Xia, V. Bex, and P.M. Midgley, Eds. Cambridge University Press, Cambridge, United Kingdom and New York, NY, USA, 1029-1136. <http://www.climatechange2013.org/report/full-report/>
22. Taylor, P.C., M. Cai, A. Hu, J. Meehl, W. Washington, and G.J. Zhang, 2013: A decomposition of feedback contributions to polar warming amplification. *Journal of Climate*, **26**, 7023-7043. <http://dx.doi.org/10.1175/JCLI-D-12-00696.1>
23. Gillett, N.P., D.A. Stone, P.A. Stott, T. Nozawa, A.Y. Karpechko, G.C. Hegerl, M.F. Wehner, and P.D. Jones, 2008: Attribution of polar warming to human influence. *Nature Geoscience*, **1**, 750-754. <http://dx.doi.org/10.1038/ngeo338>
24. Bindoff, N.L., P.A. Stott, K.M. AchutaRao, M.R. Allen, N. Gillett, D. Gutzler, K. Hansingo, G. Hegerl, Y. Hu, S. Jain, I.I. Mokhov, J. Overland, J. Perlwitz, R. Sebbari, and X. Zhang, 2013: Detection and attribution of climate change: From global to regional. *Climate Change 2013: The Physical Science Basis. Contribution of Working Group I to the Fifth Assessment Report of the Intergovernmental Panel on Climate Change*. Stocker, T.F., D. Qin, G.-K. Plattner, M. Tignor, S.K. Allen, J. Boschung, A. Nauels, Y. Xia, V. Bex, and P.M. Midgley, Eds. Cambridge University Press, Cambridge, United Kingdom and New York, NY, USA, 867-952. <http://www.climatechange2013.org/report/full-report/>
25. Fyfe, J.C., K. von Salzen, N.P. Gillett, V.K. Arora, G.M. Flato, and J.R. McConnell, 2013: One hundred years of Arctic surface temperature variation due to anthropogenic influence. *Scientific Reports*, **3**, 2645. <http://dx.doi.org/10.1038/srep02645>
26. Chylek, P., N. Hengartner, G. Lesins, J.D. Klett, O. Humlum, M. Wyatt, and M.K. Dubey, 2014: Isolating the anthropogenic component of Arctic warming. *Geophysical Research Letters*, **41**, 3569-3576. <http://dx.doi.org/10.1002/2014GL060184>
27. Najafi, M.R., F.W. Zwiers, and N.P. Gillett, 2015: Attribution of Arctic temperature change to greenhouse-gas and aerosol influences. *Nature Climate Change*, **5**, 246-249. <http://dx.doi.org/10.1038/nclimate2524>
28. Ding, Q., A. Schweiger, M. Lheureux, D.S. Battisti, S. Po-Chedley, N.C. Johnson, E. Blanchard-Wrigglesworth, K. Harnos, Q. Zhang, R. Eastman, and E.J. Steig, 2017: Influence of high-latitude atmospheric circulation changes on summertime Arctic sea ice. *Nature Climate Change*, **7**, 289-295. <http://dx.doi.org/10.1038/nclimate3241>
29. Christensen, J.H., K. Krishna Kumar, E. Aldrian, S.-I. An, I.F.A. Cavalcanti, M. de Castro, W. Dong, P. Goswami, A. Hall, J.K. Kanyanga, A. Kitoh, J. Kosin, N.-C. Lau, J. Renwick, D.B. Stephenson, S.-P. Xie, and T. Zhou, 2013: Climate phenomena and their relevance for future regional climate change. *Climate Change 2013: The Physical Science Basis. Contribution of Working Group I to the Fifth Assessment Report of the Intergovernmental Panel on Climate Change*. Stocker, T.F., D. Qin, G.-K. Plattner, M. Tignor, S.K. Allen, J. Boschung, A. Nauels, Y. Xia, V. Bex, and P.M. Midgley, Eds. Cambridge University Press, Cambridge, United Kingdom and New York, NY, USA, 1217-1308. <http://www.climatechange2013.org/report/full-report/>
30. Boisvert, L.N., T. Markus, and T. Vihma, 2013: Moisture flux changes and trends for the entire Arctic in 2003-2011 derived from EOS Aqua data. *Journal of Geophysical Research Oceans*, **118**, 5829-5843. <http://dx.doi.org/10.1002/jgrc.20414>
31. Boisvert, L.N., D.L. Wu, and C.L. Shie, 2015: Increasing evaporation amounts seen in the Arctic between 2003 and 2013 from AIRS data. *Journal of Geophysical Research Atmospheres*, **120**, 6865-6881. <http://dx.doi.org/10.1002/2015JD023258>
32. Boisvert, L.N., D.L. Wu, T. Vihma, and J. Susskind, 2015: Verification of air/surface humidity differences from AIRS and ERA-Interim in support of turbulent flux estimation in the Arctic. *Journal of Geophysical Research Atmospheres*, **120**, 945-963. <http://dx.doi.org/10.1002/2014JD021666>
33. Kay, J.E., K. Raeder, A. Gettelman, and J. Anderson, 2011: The boundary layer response to recent Arctic sea ice loss and implications for high-latitude climate feedbacks. *Journal of Climate*, **24**, 428-447. <http://dx.doi.org/10.1175/2010JCLI3651.1>
34. Pavelsky, T.M., J. Boé, A. Hall, and E.J. Fetzer, 2011: Atmospheric inversion strength over polar oceans in winter regulated by sea ice. *Climate Dynamics*, **36**, 945-955. <http://dx.doi.org/10.1007/s00382-010-0756-8>



35. Solomon, A., M.D. Shupe, O. Persson, H. Morrison, T. Yamaguchi, P.M. Caldwell, and G.d. Boer, 2014: The sensitivity of springtime Arctic mixed-phase stratocumulus clouds to surface-layer and cloud-top inversion-layer moisture sources. *Journal of the Atmospheric Sciences*, **71**, 574-595. <http://dx.doi.org/10.1175/JAS-D-13-0179.1>
36. Taylor, P.C., R.G. Ellingson, and M. Cai, 2011: Geographical distribution of climate feedbacks in the NCAR CCSM3.0. *Journal of Climate*, **24**, 2737-2753. <http://dx.doi.org/10.1175/2010JCLI3788.1>
37. Vaughan, D.G., J.C. Comiso, I. Allison, J. Carrasco, G. Kaser, R. Kwok, P. Mote, T. Murray, F. Paul, J. Ren, E. Rignot, O. Solomina, K. Steffen, and T. Zhang, 2013: Observations: Cryosphere. *Climate Change 2013: The Physical Science Basis. Contribution of Working Group I to the Fifth Assessment Report of the Intergovernmental Panel on Climate Change*. Stocker, T.F., D. Qin, G.-K. Plattner, M. Tignor, S.K. Allen, J. Boschung, A. Nauels, Y. Xia, V. Bex, and P.M. Midgley, Eds. Cambridge University Press, Cambridge, United Kingdom and New York, NY, USA, 317-382. <http://www.climatechange2013.org/report/full-report/>
38. Carmack, E., I. Polyakov, L. Padman, I. Fer, E. Hunke, J. Hutchings, J. Jackson, D. Kelley, R. Kwok, C. Layton, H. Mellling, D. Perovich, O. Persson, B. Ruddick, M.-L. Timmermans, J. Toole, T. Ross, S. Vavrus, and P. Winsor, 2015: Toward quantifying the increasing role of oceanic heat in sea ice loss in the new Arctic. *Bulletin of the American Meteorological Society*, **96** (12), 2079-2105. <http://dx.doi.org/10.1175/BAMS-D-13-00177.1>
39. Kwok, R. and N. Untersteiner, 2011: The thinning of Arctic sea ice. *Physics Today*, **64**, 36-41. <http://dx.doi.org/10.1063/1.3580491>
40. Ogi, M. and I.G. Rigor, 2013: Trends in Arctic sea ice and the role of atmospheric circulation. *Atmospheric Science Letters*, **14**, 97-101. <http://dx.doi.org/10.1002/asl2.423>
41. Ogi, M. and J.M. Wallace, 2007: Summer minimum Arctic sea ice extent and the associated summer atmospheric circulation. *Geophysical Research Letters*, **34**, L12705. <http://dx.doi.org/10.1029/2007GL029897>
42. Stroeve, J.C., V. Kattsov, A. Barrett, M. Serreze, T. Pavlova, M. Holland, and W.N. Meier, 2012: Trends in Arctic sea ice extent from CMIP5, CMIP3 and observations. *Geophysical Research Letters*, **39**, L16502. <http://dx.doi.org/10.1029/2012GL052676>
43. Stroeve, J.C., M.C. Serreze, M.M. Holland, J.E. Kay, J. Malanik, and A.P. Barrett, 2012: The Arctic's rapidly shrinking sea ice cover: A research synthesis. *Climatic Change*, **110**, 1005-1027. <http://dx.doi.org/10.1007/s10584-011-0101-1>
44. Taylor, P.C., R.G. Ellingson, and M. Cai, 2011: Seasonal variations of climate feedbacks in the NCAR CCSM3. *Journal of Climate*, **24**, 3433-3444. <http://dx.doi.org/10.1175/2011jcli3862.1>
45. Stroeve, J., A. Barrett, M. Serreze, and A. Schweiger, 2014: Using records from submarine, aircraft and satellites to evaluate climate model simulations of Arctic sea ice thickness. *The Cryosphere*, **8**, 1839-1854. <http://dx.doi.org/10.5194/tc-8-1839-2014>
46. Stroeve, J.C., T. Markus, L. Boisvert, J. Miller, and A. Barrett, 2014: Changes in Arctic melt season and implications for sea ice loss. *Geophysical Research Letters*, **41**, 1216-1225. <http://dx.doi.org/10.1002/2013GL058951>
47. Perovich, D., W. Meier, M. Tschudi, S. Farrell, S. Gerland, S. Hendricks, T. Krumpfen, and C. Hass, 2016: Sea ice [in Arctic Report Card 2016]. <http://www.arctic.noaa.gov/Report-Card/Report-Card-2016/ArtMID/5022/ArticleID/286/Sea-Ice>
48. Schweiger, A., R. Lindsay, J. Zhang, M. Steele, H. Stern, and R. Kwok, 2011: Uncertainty in modeled Arctic sea ice volume. *Journal of Geophysical Research*, **116**, C00D06. <http://dx.doi.org/10.1029/2011JC007084>
49. Tschudi, M., C. Fowler, J. Maslanik, J.S. Stewart, and W. Meier, 2016: EASE-Grid Sea Ice Age, Version 3. In: NASA (ed.). National Snow and Ice Data Center Distributed Active Archive Center, Boulder, CO.
50. Parkinson, C.L., 2014: Spatially mapped reductions in the length of the Arctic sea ice season. *Geophysical Research Letters*, **41**, 4316-4322. <http://dx.doi.org/10.1002/2014GL060434>
51. Chapin III, F.S., S.F. Trainor, P. Cochran, H. Huntington, C. Markon, M. McCammon, A.D. McGuire, and M. Serreze, 2014: Ch. 22: Alaska. *Climate Change Impacts in the United States: The Third National Climate Assessment*. Melillo, J.M., Terese (T.C.) Richmond, and G.W. Yohe, Eds. U.S. Global Change Research Program, Washington, DC, 514-536. <http://dx.doi.org/10.7930/J00Z7150>
52. Gibbs, A.E. and B.M. Richmond, 2015: National Assessment of Shoreline Change: Historical Shoreline Change Along the North Coast of Alaska, U.S.-Canadian Border to Icy Cape. U.S. Geological Survey, 96 pp. <http://dx.doi.org/10.3133/ofr20151048>
53. Smedsrud, L.H., M.H. Halvorsen, J.C. Stroeve, R. Zhang, and K. Kloster, 2017: Fram Strait sea ice export variability and September Arctic sea ice extent over the last 80 years. *The Cryosphere*, **11**, 65-79. <http://dx.doi.org/10.5194/tc-11-65-2017>
54. Day, J.J., J.C. Hargreaves, J.D. Annan, and A. Abe-Ouchi, 2012: Sources of multi-decadal variability in Arctic sea ice extent. *Environmental Research Letters*, **7**, 034011. <http://dx.doi.org/10.1088/1748-9326/7/3/034011>



55. Kay, J.E., M.M. Holland, and A. Jahn, 2011: Inter-annual to multi-decadal Arctic sea ice extent trends in a warming world. *Geophysical Research Letters*, **38**, L15708. <http://dx.doi.org/10.1029/2011GL048008>
56. Min, S.-K., X. Zhang, F.W. Zwiers, and T. Agnew, 2008: Human influence on Arctic sea ice detectable from early 1990s onwards. *Geophysical Research Letters*, **35**, L21701. <http://dx.doi.org/10.1029/2008GL035725>
57. Stroeve, J., M.M. Holland, W. Meier, T. Scambos, and M. Serreze, 2007: Arctic sea ice decline: Faster than forecast. *Geophysical Research Letters*, **34**, L09501. <http://dx.doi.org/10.1029/2007GL029703>
58. Vinnikov, K.Y., A. Robock, R.J. Stouffer, J.E. Walsh, C.L. Parkinson, D.J. Cavalieri, J.F.B. Mitchell, D. Garrett, and V.F. Zakharov, 1999: Global warming and Northern Hemisphere sea ice extent. *Science*, **286**, 1934-1937. <http://dx.doi.org/10.1126/science.286.5446.1934>
59. Wang, M. and J.E. Overland, 2012: A sea ice free summer Arctic within 30 years: An update from CMIP5 models. *Geophysical Research Letters*, **39**, L18501. <http://dx.doi.org/10.1029/2012GL052868>
60. Notz, D. and J. Marotzke, 2012: Observations reveal external driver for Arctic sea-ice retreat. *Geophysical Research Letters*, **39**, L08502. <http://dx.doi.org/10.1029/2012GL051094>
61. Kirchmeier-Young, M.C., F.W. Zwiers, and N.P. Gillett, 2017: Attribution of extreme events in Arctic sea ice extent. *Journal of Climate*, **30**, 553-571. <http://dx.doi.org/10.1175/jcli-d-16-0412.1>
62. Zhang, R. and T.R. Knutson, 2013: The role of global climate change in the extreme low summer Arctic sea ice extent in 2012 [in "Explaining Extreme Events of 2012 from a Climate Perspective"]. *Bulletin of the American Meteorological Society*, **94** (9), S23-S26. <http://dx.doi.org/10.1175/BAMS-D-13-00085.1>
63. Jahn, A., J.E. Kay, M.M. Holland, and D.M. Hall, 2016: How predictable is the timing of a summer ice-free Arctic? *Geophysical Research Letters*, **43**, 9113-9120. <http://dx.doi.org/10.1002/2016GL070067>
64. Swart, N.C., J.C. Fyfe, E. Hawkins, J.E. Kay, and A. Jahn, 2015: Influence of internal variability on Arctic sea-ice trends. *Nature Climate Change*, **5**, 86-89. <http://dx.doi.org/10.1038/nclimate2483>
65. Snape, T.J. and P.M. Forster, 2014: Decline of Arctic sea ice: Evaluation and weighting of CMIP5 projections. *Journal of Geophysical Research Atmospheres*, **119**, 546-554. <http://dx.doi.org/10.1002/2013JD020593>
66. Wettstein, J.J. and C. Deser, 2014: Internal variability in projections of twenty-first-century Arctic sea ice loss: Role of the large-scale atmospheric circulation. *Journal of Climate*, **27**, 527-550. <http://dx.doi.org/10.1175/JCLI-D-12-00839.1>
67. Gagné, M.È., N.P. Gillett, and J.C. Fyfe, 2015: Impact of aerosol emission controls on future Arctic sea ice cover. *Geophysical Research Letters*, **42**, 8481-8488. <http://dx.doi.org/10.1002/2015GL065504>
68. Stroeve, J. and D. Notz, 2015: Insights on past and future sea-ice evolution from combining observations and models. *Global and Planetary Change*, **135**, 119-132. <http://dx.doi.org/10.1016/j.gloplacha.2015.10.011>
69. Notz, D. and J. Stroeve, 2016: Observed Arctic sea-ice loss directly follows anthropogenic CO₂ emission. *Science*, **354**, 747-750. <http://dx.doi.org/10.1126/science.aag2345>
70. Melillo, J.M., T.C. Richmond, and G.W. Yohe, eds., 2014: *Climate Change Impacts in the United States: The Third National Climate Assessment*. U.S. Global Change Research Program: Washington, D.C., 841 pp. <http://dx.doi.org/10.7930/J0Z31WJ2>
71. Rhein, M., S.R. Rintoul, S. Aoki, E. Campos, D. Chambers, R.A. Feely, S. Gulev, G.C. Johnson, S.A. Josey, A. Kostianoy, C. Mauritzen, D. Roemmich, L.D. Talley, and F. Wang, 2013: Observations: Ocean. *Climate Change 2013: The Physical Science Basis. Contribution of Working Group I to the Fifth Assessment Report of the Intergovernmental Panel on Climate Change*. Stocker, T.F., D. Qin, G.-K. Plattner, M. Tignor, S.K. Allen, J. Boschung, A. Nauels, Y. Xia, V. Bex, and P.M. Midgley, Eds. Cambridge University Press, Cambridge, United Kingdom and New York, NY, USA, 255-316. <http://www.climatechange2013.org/report/full-report/>
72. Timmermans, M.-L. and A. Proshutinsky, 2015: [The Arctic] Sea surface temperature [in "State of the Climate in 2014"]. *Bulletin of the American Meteorological Society*, **96** (12), S147-S148. <http://dx.doi.org/10.1175/2015BAMSStateoftheClimate.1>
73. Polyakov, I.V., A.V. Pnyushkov, and L.A. Timokhov, 2012: Warming of the intermediate Atlantic water of the Arctic Ocean in the 2000s. *Journal of Climate*, **25**, 8362-8370. <http://dx.doi.org/10.1175/JCLI-D-12-00266.1>
74. Jungclauss, J.H., K. Lohmann, and D. Zanchettin, 2014: Enhanced 20th-century heat transfer to the Arctic simulated in the context of climate variations over the last millennium. *Climate of the Past*, **10**, 2201-2213. <http://dx.doi.org/10.5194/cp-10-2201-2014>
75. Spielhagen, R.F., K. Werner, S.A. Sørensen, K. Zamelczyk, E. Kandiano, G. Budeus, K. Husum, T.M. Marchitto, and M. Hald, 2011: Enhanced modern heat transfer to the Arctic by warm Atlantic water. *Science*, **331**, 450-453. <http://dx.doi.org/10.1126/science.1197397>



76. Döscher, R., T. Vihma, and E. Maksimovich, 2014: Recent advances in understanding the Arctic climate system state and change from a sea ice perspective: A review. *Atmospheric Chemistry and Physics*, **14**, 13571-13600. <http://dx.doi.org/10.5194/acp-14-13571-2014>
77. Church, J.A., P.U. Clark, A. Cazenave, J.M. Gregory, S. Jevrejeva, A. Levermann, M.A. Merrifield, G.A. Milne, R.S. Nerem, P.D. Nunn, A.J. Payne, W.T. Pfeffer, D. Stammer, and A.S. Unnikrishnan, 2013: Sea level change. *Climate Change 2013: The Physical Science Basis. Contribution of Working Group I to the Fifth Assessment Report of the Intergovernmental Panel on Climate Change*. Stocker, T.F., D. Qin, G.-K. Plattner, M. Tignor, S.K. Allen, J. Boschung, A. Nauels, Y. Xia, V. Bex, and P.M. Midgley, Eds. Cambridge University Press, Cambridge, United Kingdom and New York, NY, USA, 1137-1216. <http://www.climate-change2013.org/report/full-report/>
78. Rawlins, M.A., M. Steele, M.M. Holland, J.C. Adam, J.E. Cherry, J.A. Francis, P.Y. Groisman, L.D. Hinzman, T.G. Huntington, D.L. Kane, J.S. Kimball, R. Kwok, R.B. Lammers, C.M. Lee, D.P. Lettenmaier, K.C. McDonald, E. Podest, J.W. Pundsack, B. Rudels, M.C. Serreze, A. Shiklomanov, Ø. Skagseth, T.J. Troy, C.J. Vörösmarty, M. Wensnahan, E.F. Wood, R. Woodgate, D. Yang, K. Zhang, and T. Zhang, 2010: Analysis of the Arctic system for freshwater cycle intensification: Observations and expectations. *Journal of Climate*, **23**, 5715-5737. <http://dx.doi.org/10.1175/2010JCLI3421.1>
79. Köhl, A. and N. Serra, 2014: Causes of decadal changes of the freshwater content in the Arctic Ocean. *Journal of Climate*, **27**, 3461-3475. <http://dx.doi.org/10.1175/JCLI-D-13-00389.1>
80. Mathis, J.T., J.N. Cross, W. Evans, and S.C. Doney, 2015: Ocean acidification in the surface waters of the Pacific-Arctic boundary regions. *Oceanography*, **28**, 122-135. <http://dx.doi.org/10.5670/oceanog.2015.36>
81. Arrigo, K.R., G. van Dijken, and S. Pabi, 2008: Impact of a shrinking Arctic ice cover on marine primary production. *Geophysical Research Letters*, **35**, L19603. <http://dx.doi.org/10.1029/2008GL035028>
82. Bates, N.R., R. Garley, K.E. Frey, K.L. Shake, and J.T. Mathis, 2014: Sea-ice melt CO₂-carbonate chemistry in the western Arctic Ocean: Meltwater contributions to air-sea CO₂ gas exchange, mixed-layer properties and rates of net community production under sea ice. *Biogeosciences*, **11**, 6769-6789. <http://dx.doi.org/10.5194/bg-11-6769-2014>
83. Cai, W.-J., L. Chen, B. Chen, Z. Gao, S.H. Lee, J. Chen, D. Pierrot, K. Sullivan, Y. Wang, X. Hu, W.-J. Huang, Y. Zhang, S. Xu, A. Murata, J.M. Grebmeier, E.P. Jones, and H. Zhang, 2010: Decrease in the CO₂ uptake capacity in an ice-free Arctic Ocean basin. *Science*, **329**, 556-559. <http://dx.doi.org/10.1126/science.1189338>
84. Hunt, G.L., Jr., K.O. Coyle, L.B. Eisner, E.V. Farley, R.A. Heintz, F. Mueter, J.M. Napp, J.E. Overland, P.H. Ressler, S. Salo, and P.J. Stabeno, 2011: Climate impacts on eastern Bering Sea foodwebs: A synthesis of new data and an assessment of the Oscillating Control Hypothesis. *ICES Journal of Marine Science*, **68**, 1230-1243. <http://dx.doi.org/10.1093/icesjms/fsr036>
85. Mathis, J.T., R.S. Pickart, R.H. Byrne, C.L. McNeil, G.W.K. Moore, L.W. Juranek, X. Liu, J. Ma, R.A. Easley, M.M. Elliot, J.N. Cross, S.C. Reisdorph, F. Bahr, J. Morison, T. Lichendorf, and R.A. Feely, 2012: Storm-induced upwelling of high pCO₂ waters onto the continental shelf of the western Arctic Ocean and implications for carbonate mineral saturation states. *Geophysical Research Letters*, **39**, L16703. <http://dx.doi.org/10.1029/2012GL051574>
86. Stabeno, P.J., E.V. Farley, Jr., N.B. Kachel, S. Moore, C.W. Mordy, J.M. Napp, J.E. Overland, A.I. Pinchuk, and M.F. Sigler, 2012: A comparison of the physics of the northern and southern shelves of the eastern Bering Sea and some implications for the ecosystem. *Deep Sea Research Part II: Topical Studies in Oceanography*, **65-70**, 14-30. <http://dx.doi.org/10.1016/j.dsr2.2012.02.019>
87. Flannigan, M., B. Stocks, M. Turetsky, and M. Wotton, 2009: Impacts of climate change on fire activity and fire management in the circumboreal forest. *Global Change Biology*, **15**, 549-560. <http://dx.doi.org/10.1111/j.1365-2486.2008.01660.x>
88. Hu, F.S., P.E. Higuera, P. Duffy, M.L. Chipman, A.V. Rocha, A.M. Young, R. Kelly, and M.C. Dietze, 2015: Arctic tundra fires: Natural variability and responses to climate change. *Frontiers in Ecology and the Environment*, **13**, 369-377. <http://dx.doi.org/10.1890/150063>
89. Derksen, C., R. Brown, L. Mudryk, and K. Luojus, 2015: Terrestrial snow cover [in Arctic Report Card 2015]. ftp://ftp.oar.noaa.gov/arctic/documents/ArcticReportCard_full_report2015.pdf
90. Young, A.M., P.E. Higuera, P.A. Duffy, and F.S. Hu, 2017: Climatic thresholds shape northern high-latitude fire regimes and imply vulnerability to future climate change. *Ecography*, **40**, 606-617. <http://dx.doi.org/10.1111/ecog.02205>
91. Kasischke, E.S. and M.R. Turetsky, 2006: Recent changes in the fire regime across the North American boreal region—Spatial and temporal patterns of burning across Canada and Alaska. *Geophysical Research Letters*, **33**, L09703. <http://dx.doi.org/10.1029/2006GL025677>
92. Sanford, T., R. Wang, and A. Kenwa, 2015: *The Age of Alaskan Wildfires*. Climate Central, Princeton, NJ, 32 pp. <http://assets.climatecentral.org/pdfs/AgeofAlaskanWildfires.pdf>

98. Partain, J.L., Jr., S. Alden, U.S. Bhatt, P.A. Bieniek, B.R. Brettschneider, R. Lader, P.Q. Olsson, T.S. Rupp, H. Strader, R.L.T. Jr., J.E. Walsh, A.D. York, and R.H. Zieh, 2016: An assessment of the role of anthropogenic climate change in the Alaska fire season of 2015 [in "Explaining Extreme Events of 2015 from a Climate Perspective"]. *Bulletin of the American Meteorological Society*, **97** (12), S14-S18. <http://dx.doi.org/10.1175/BAMS-D-16-0149.1>
99. French, N.H.F., L.K. Jenkins, T.V. Loboda, M. Flannigan, R. Jandt, L.L. Bourgeau-Chavez, and M. Whitley, 2015: Fire in arctic tundra of Alaska: Past fire activity, future fire potential, and significance for land management and ecology. *International Journal of Wildland Fire*, **24**, 1045-1061. <http://dx.doi.org/10.1071/WF14167>
95. Joly, K., P.A. Duffy, and T.S. Rupp, 2012: Simulating the effects of climate change on fire regimes in Arctic biomes: Implications for caribou and moose habitat. *Ecosphere*, **3**, 1-18. <http://dx.doi.org/10.1890/ES12-00012.1>
96. Kelly, R., M.L. Chipman, P.E. Higuera, I. Stefanova, L.B. Brubaker, and F.S. Hu, 2013: Recent burning of boreal forests exceeds fire regime limits of the past 10,000 years. *Proceedings of the National Academy of Sciences*, **110**, 13055-13060. <http://dx.doi.org/10.1073/pnas.1305069110>
97. McGuire, A.D., L.G. Anderson, T.R. Christensen, S. Dallimore, L. Guo, D.J. Hayes, M. Heimann, T.D. Lorenson, R.W. MacDonald, and N. Roulet, 2009: Sensitivity of the carbon cycle in the Arctic to climate change. *Ecological Monographs*, **79**, 523-555. <http://dx.doi.org/10.1890/08-2025.1>
98. Mishra, U., J.D. Jastrow, R. Matamala, G. Hugelius, C.D. Koven, J.W. Harden, C.L. Ping, G.J. Michaelson, Z. Fan, R.M. Miller, A.D. McGuire, C. Tarnocai, P. Kuhry, W.J. Riley, K. Schaefer, E.A.G. Schuur, M.T. Jorgenson, and L.D. Hinzman, 2013: Empirical estimates to reduce modeling uncertainties of soil organic carbon in permafrost regions: A review of recent progress and remaining challenges. *Environmental Research Letters*, **8**, 035020. <http://dx.doi.org/10.1088/1748-9326/8/3/035020>
99. Mishra, U. and W.J. Riley, 2012: Alaskan soil carbon stocks: Spatial variability and dependence on environmental factors. *Biogeosciences*, **9**, 3637-3645. <http://dx.doi.org/10.5194/bg-9-3637-2012>
100. Kelly, R., H. Genet, A.D. McGuire, and F.S. Hu, 2016: Palaeodata-informed modelling of large carbon losses from recent burning of boreal forests. *Nature Climate Change*, **6**, 79-82. <http://dx.doi.org/10.1038/nclimate2832>
101. Brown, D.R.N., M.T. Jorgenson, T.A. Douglas, V.E. Romanovsky, K. Kielland, C. Hiemstra, E.S. Euskirchen, and R.W. Ruess, 2015: Interactive effects of wildfire and climate on permafrost degradation in Alaskan lowland forests. *Journal of Geophysical Research Biogeosciences*, **120**, 1619-1637. <http://dx.doi.org/10.1002/2015JG003033>
102. Myers-Smith, I.H., J.W. Harden, M. Wilmking, C.C. Fuller, A.D. McGuire, and F.S. Chapin Iii, 2008: Wetland succession in a permafrost collapse: interactions between fire and thermokarst. *Biogeosciences*, **5**, 1273-1286. <http://dx.doi.org/10.5194/bg-5-1273-2008>
103. Swanson, D.K., 1996: Susceptibility of permafrost soils to deep thaw after forest fires in interior Alaska, U.S.A., and some ecologic implications. *Arctic and Alpine Research*, **28**, 217-227. <http://dx.doi.org/10.2307/1551763>
104. Yoshikawa, K., W.R. Bolton, V.E. Romanovsky, M. Fukuda, and L.D. Hinzman, 2002: Impacts of wildfire on the permafrost in the boreal forests of Interior Alaska. *Journal of Geophysical Research*, **107**, 8148. <http://dx.doi.org/10.1029/2001JD000438>
105. Derksen, C. and R. Brown, 2012: Snow [in Arctic Report Card 2012]. ftp://ftp.oar.noaa.gov/arctic/documents/ArcticReportCard_full_report2012.pdf
106. Kunkel, K.E., D.A. Robinson, S. Champion, X. Yin, T. Estilow, and R.M. Frankson, 2016: Trends and extremes in Northern Hemisphere snow characteristics. *Current Climate Change Reports*, **2**, 65-73. <http://dx.doi.org/10.1007/s40641-016-0036-8>
107. Brown, R.D. and D.A. Robinson, 2011: Northern Hemisphere spring snow cover variability and change over 1922-2010 including an assessment of uncertainty. *The Cryosphere*, **5**, 219-229. <http://dx.doi.org/10.5194/tc-5-219-2011>
108. Rupp, D.E., P.W. Mote, N.L. Bindoff, P.A. Stott, and D.A. Robinson, 2013: Detection and attribution of observed changes in Northern Hemisphere spring snow cover. *Journal of Climate*, **26**, 6904-6914. <http://dx.doi.org/10.1175/JCLI-D-12-00563.1>
109. Mao, J., A. Ribes, B. Yan, X. Shi, P.E. Thornton, R. Seferian, P. Ciais, R.B. Myneni, H. Douville, S. Piao, Z. Zhu, R.E. Dickinson, Y. Dai, D.M. Ricciuto, M. Jin, F.M. Hoffman, B. Wang, M. Huang, and X. Lian, 2016: Human-induced greening of the northern extratropical land surface. *Nature Climate Change*, **6**, 959-963. <http://dx.doi.org/10.1038/nclimate3056>



110. Myers-Smith, I.H., B.C. Forbes, M. Wilking, M. Hallinger, T. Lantz, D. Blok, K.D. Tape, M. Macias-Fauria, U. Sass-Klaassen, E. Lévesque, S. Boudreau, P. Ropars, L. Hermanutz, A. Trant, L.S. Collier, S. Weijers, J. Rozema, S.A. Rayback, N.M. Schmidt, G. Schaepman-Strub, S. Wipf, C. Rixen, C.B. Ménard, S. Venn, S. Goetz, L. Andreu-Hayles, S. Elmendorf, V. Ravolainen, J. Welker, P. Grogan, H.E. Epstein, and D.S. Hik, 2011: Shrub expansion in tundra ecosystems: Dynamics, impacts and research priorities. *Environmental Research Letters*, **6**, 045509. <http://dx.doi.org/10.1088/1748-9326/6/4/045509>
111. Euskirchen, E.S., A.P. Bennett, A.L. Breen, H. Genet, M.A. Lindgren, T.A. Kurkowski, A.D. McGuire, and T.S. Rupp, 2016: Consequences of changes in vegetation and snow cover for climate feedbacks in Alaska and northwest Canada. *Environmental Research Letters*, **11**, 105003. <http://dx.doi.org/10.1088/1748-9326/11/10/105003>
112. Zemp, M., H. Frey, I. Gärtner-Roer, S.U. Nussbaumer, M. Hoelzle, F. Paul, W. Haeberli, F. Denzinger, A.P. Ahlström, B. Anderson, S. Bajracharya, C. Baroni, L.N. Braun, B.E. Cáceres, G. Casassa, G. Cobos, L.R. Dávila, H. Delgado Granados, M.N. Demuth, L. Espizua, A. Fischer, K. Fujita, B. Gadek, A. Ghazanfar, J.O. Hagen, P. Holmlund, N. Karimi, Z. Li, M. Pelto, P. Pitte, V.V. Popovnin, C.A. Portocarrero, R. Prinz, C.V. Sangewar, I. Severskiy, O. Sigurðsson, A. Soruco, R. Usabaliev, and C. Vincent, 2015: Historically unprecedented global glacier decline in the early 21st century. *Journal of Glaciology*, **61**, 745-762. <http://dx.doi.org/10.3189/2015jogG15j017>
113. Harig, C. and F.J. Simons, 2016: Ice mass loss in Greenland, the Gulf of Alaska, and the Canadian Archipelago: Seasonal cycles and decadal trends. *Geophysical Research Letters*, **43**, 3150-3159. <http://dx.doi.org/10.1002/2016GL067759>
114. Howat, I.M., I. Joughin, M. Fahnestock, B.E. Smith, and T.A. Scambos, 2008: Synchronous retreat and acceleration of southeast Greenland outlet glaciers 2000-06: Ice dynamics and coupling to climate. *Journal of Glaciology*, **54**, 646-660. <http://dx.doi.org/10.3189/002214308786570908>
115. Khan, S.A., K.H. Kjaer, M. Bevis, J.L. Bamber, J. Wahr, K.K. Kjeldsen, A.A. Bjork, N.J. Korsgaard, L.A. Stearns, M.R. van den Broeke, L. Liu, N.K. Larsen, and I.S. Muresan, 2014: Sustained mass loss of the northeast Greenland ice sheet triggered by regional warming. *Nature Climate Change*, **4**, 292-299. <http://dx.doi.org/10.1038/nclimate2161>
116. Rignot, E., M. Koppes, and I. Velicogna, 2010: Rapid submarine melting of the calving faces of West Greenland glaciers. *Nature Geoscience*, **3**, 187-191. <http://dx.doi.org/10.1038/ngeo765>
117. Straneo, F., R.G. Curry, D.A. Sutherland, G.S. Hamilton, C. Cenedese, K. Vage, and L.A. Stearns, 2011: Impact of fjord dynamics and glacial runoff on the circulation near Helheim Glacier. *Nature Geoscience*, **4**, 322-327. <http://dx.doi.org/10.1038/ngeo1109>
118. van den Broeke, M., J. Bamber, J. Ettema, E. Rignot, E. Schrama, W.J. van de Berg, E. van Meijgaard, I. Velicogna, and B. Wouters, 2009: Partitioning recent Greenland mass loss. *Science*, **326**, 984-986. <http://dx.doi.org/10.1126/science.1178176>
119. Bartholomew, I.D., P. Nienow, A. Sole, D. Mair, T. Cowton, M.A. King, and S. Palmer, 2011: Seasonal variations in Greenland Ice Sheet motion: Inland extent and behaviour at higher elevations. *Earth and Planetary Science Letters*, **307**, 271-278. <http://dx.doi.org/10.1016/j.epsl.2011.04.014>
120. Holland, D.M., R.H. Thomas, B. de Young, M.H. Ribergaard, and B. Lyberth, 2008: Acceleration of Jakobshavn Isbrae triggered by warm subsurface ocean waters. *Nature Geoscience*, **1**, 659-664. <http://dx.doi.org/10.1038/ngeo316>
121. Joughin, I., S.B. Das, M.A. King, B.E. Smith, I.M. Howat, and T. Moon, 2008: Seasonal speedup along the western flank of the Greenland Ice Sheet. *Science*, **320**, 781-783. <http://dx.doi.org/10.1126/science.1153288>
122. Dupont, T.K. and R.B. Alley, 2005: Assessment of the importance of ice-shelf buttressing to ice-sheet flow. *Geophysical Research Letters*, **32**, L04503. <http://dx.doi.org/10.1029/2004GL022024>
123. Lim, Y.-K., D.S. Siegfried, M.J.N. Sophie, N.L. Jae, M.M. Andrea, I.C. Richard, Z. Bin, and V. Isabella, 2016: Atmospheric summer teleconnections and Greenland Ice Sheet surface mass variations: Insights from MERRA-2. *Environmental Research Letters*, **11**, 024002. <http://dx.doi.org/10.1088/1748-9326/11/2/024002>
124. Tedesco, M., T. Mote, X. Fettweis, E. Hanna, J. Jeyaratnam, J.F. Booth, R. Datta, and K. Briggs, 2016: Arctic cut-off high drives the poleward shift of a new Greenland melting record. *Nature Communications*, **7**, 11723. <http://dx.doi.org/10.1038/ncomms11723>
125. Johannessen, O.M., A. Korabely, V. Miles, M.W. Miles, and K.E. Solberg, 2011: Interaction between the warm subsurface Atlantic water in the Sermilik Fjord and Helheim Glacier in southeast Greenland. *Surveys in Geophysics*, **32**, 387-396. <http://dx.doi.org/10.1007/s10712-011-9130-6>
126. Straneo, F., G.S. Hamilton, D.A. Sutherland, L.A. Stearns, F. Davidson, M.O. Hammill, G.B. Stenson, and A. Rosing-Asvid, 2010: Rapid circulation of warm subtropical waters in a major glacial fjord in East Greenland. *Nature Geoscience*, **3**, 182-186. <http://dx.doi.org/10.1038/ngeo764>

127. Andresen, C.S., F. Straneo, M.H. Ribergaard, A.A. Bjork, T.J. Andersen, A. Kuijpers, N. Norgaard-Pedersen, K.H. Kjaer, F. Schjoth, K. Weckstrom, and A.P. Ahlstrom, 2012: Rapid response of Helheim Glacier in Greenland to climate variability over the past century. *Nature Geoscience*, **5**, 37-41. <http://dx.doi.org/10.1038/ngeo1349>
128. Velicogna, I., 2009: Increasing rates of ice mass loss from the Greenland and Antarctic ice sheets revealed by GRACE. *Geophysical Research Letters*, **36**, L19503. <http://dx.doi.org/10.1029/2009GL040222>
129. Mernild, S.H., J.K. Malmros, J.C. Yde, and N.T. Knudsen, 2012: Multi-decadal marine- and land-terminating glacier recession in the Ammassalik region, southeast Greenland. *The Cryosphere*, **6**, 625-639. <http://dx.doi.org/10.5194/tc-6-625-2012>
130. AMAP, 2011: Snow, Water, Ice and Permafrost in the Arctic (SWIPA): Climate Change and the Cryosphere. Oslo, Norway. 538 pp. <http://www.amap.no/documents/download/1448>
131. Pelto, M.S., 2015: [Global Climate] Alpine glaciers [in "State of the Climate in 2014"]. *Bulletin of the American Meteorological Society*, **96** (12), S19-S20. <http://dx.doi.org/10.1175/2015BAMSStateoftheClimate.1>
132. Sharp, M., G. Wolken, D. Burgess, J.G. Cogley, L. Copland, L. Thomson, A. Arendt, B. Wouters, J. Kohler, L.M. Andreassen, S. O'Neel, and M. Pelto, 2015: [Global Climate] Glaciers and ice caps outside Greenland [in "State of the Climate in 2014"]. *Bulletin of the American Meteorological Society*, **96** (12), S135-S137. <http://dx.doi.org/10.1175/2015BAMSStateoftheClimate.1>
133. Marzeion, B., J.G. Cogley, K. Richter, and D. Parkes, 2014: Attribution of global glacier mass loss to anthropogenic and natural causes. *Science*, **345**, 919-921. <http://dx.doi.org/10.1126/science.1254702>
134. Mengel, M., A. Levermann, K. Frieler, A. Robinson, B. Marzeion, and R. Winkelmann, 2016: Future sea level rise constrained by observations and long-term commitment. *Proceedings of the National Academy of Sciences*, **113**, 2597-2602. <http://dx.doi.org/10.1073/pnas.1500515113>
135. Larsen, C.F., E. Burgess, A.A. Arendt, S. O'Neel, A.J. Johnson, and C. Kienholz, 2015: Surface melt dominates Alaska glacier mass balance. *Geophysical Research Letters*, **42**, 5902-5908. <http://dx.doi.org/10.1002/2015GL064349>
136. Ding, Q., J.M. Wallace, D.S. Battisti, E.J. Steig, A.J.E. Gallant, H.-J. Kim, and L. Geng, 2014: Tropical forcing of the recent rapid Arctic warming in northeastern Canada and Greenland. *Nature*, **509**, 209-212. <http://dx.doi.org/10.1038/nature13260>
137. Francis, J.A., S.J. Vavrus, and J. Cohen, 2017: Amplified Arctic warming and mid-latitude weather: Emerging connections. *Wiley Interdisciplinary Review: Climate Change*, **8**, e474. <http://dx.doi.org/10.1002/wcc.474>
138. Graverson, R.G., 2006: Do changes in the midlatitude circulation have any impact on the Arctic surface air temperature trend? *Journal of Climate*, **19**, 5422-5438. <http://dx.doi.org/10.1175/JCLI3906.1>
139. Lee, S., 2014: A theory for polar amplification from a general circulation perspective. *Asia-Pacific Journal of Atmospheric Sciences*, **50**, 31-43. <http://dx.doi.org/10.1007/s13143-014-0024-7>
140. Lee, S., T. Gong, N. Johnson, S.B. Feldstein, and D. Pollard, 2011: On the possible link between tropical convection and the Northern Hemisphere Arctic surface air temperature change between 1958 and 2001. *Journal of Climate*, **24**, 4350-4367. <http://dx.doi.org/10.1175/2011JCLI4003.1>
141. Park, H.-S., S. Lee, S.-W. Son, S.B. Feldstein, and Y. Kosaka, 2015: The impact of poleward moisture and sensible heat flux on Arctic winter sea ice variability. *Journal of Climate*, **28**, 5030-5040. <http://dx.doi.org/10.1175/JCLI-D-15-0074.1>
142. Perlwitz, J., M. Hoerling, and R. Dole, 2015: Arctic tropospheric warming: Causes and linkages to lower latitudes. *Journal of Climate*, **28**, 2154-2167. <http://dx.doi.org/10.1175/JCLI-D-14-00095.1>
143. Rigor, I.G., J.M. Wallace, and R.L. Colony, 2002: Response of sea ice to the Arctic oscillation. *Journal of Climate*, **15**, 2648-2663. [http://dx.doi.org/10.1175/1520-0442\(2002\)015<2648:ROSITT>2.0.CO;2](http://dx.doi.org/10.1175/1520-0442(2002)015<2648:ROSITT>2.0.CO;2)
144. Screen, J.A., C. Deser, and I. Simmonds, 2012: Local and remote controls on observed Arctic warming. *Geophysical Research Letters*, **39**, L10709. <http://dx.doi.org/10.1029/2012GL051598>
145. Screen, J.A. and J.A. Francis, 2016: Contribution of sea-ice loss to Arctic amplification is regulated by Pacific Ocean decadal variability. *Nature Climate Change*, **6**, 856-860. <http://dx.doi.org/10.1038/nclimate3011>
146. Overland, J., E. Hanna, I. Hanssen-Bauer, S.-J. Kim, J. Walsh, M. Wang, U. Bhatt, and R.L. Thoman, 2016: Surface air temperature [in Arctic Report Card 2016]. <http://arctic.noaa.gov/Report-Card/Report-Card-2016/ArtMID/5022/ArticleID/271/Surface-Air-Temperature>
147. Liu, Y. and J.R. Key, 2014: Less winter cloud aids summer 2013 Arctic sea ice return from 2012 minimum. *Environmental Research Letters*, **9**, 044002. <http://dx.doi.org/10.1088/1748-9326/9/4/044002>
148. Woods, C. and R. Caballero, 2016: The role of moist intrusions in winter Arctic warming and sea ice decline. *Journal of Climate*, **29**, 4473-4485. <http://dx.doi.org/10.1175/jcli-d-15-0773.1>



149. Cohen, J., J.A. Screen, J.C. Furtado, M. Barlow, D. Whittleston, D. Coumou, J. Francis, K. Dethloff, D. Entekhabi, J. Overland, and J. Jones, 2014: Recent Arctic amplification and extreme mid-latitude weather. *Nature Geoscience*, **7**, 627-637. <http://dx.doi.org/10.1038/ngeo2234>
150. Barnes, E.A. and J.A. Screen, 2015: The impact of Arctic warming on the midlatitude jet-stream: Can it? Has it? Will it? *Wiley Interdisciplinary Reviews: Climate Change*, **6**, 277-286. <http://dx.doi.org/10.1002/wcc.337>
151. Ayarzagüena, B. and J.A. Screen, 2016: Future Arctic sea ice loss reduces severity of cold air outbreaks in midlatitudes. *Geophysical Research Letters*, **43**, 2801-2809. <http://dx.doi.org/10.1002/2016GL068092>
152. Screen, J.A., C. Deser, and L. Sun, 2015: Reduced risk of North American cold extremes due to continued Arctic sea ice loss. *Bulletin of the American Meteorological Society*, **96** (12), 1489-1503. <http://dx.doi.org/10.1175/BAMS-D-14-00185.1>
153. Screen, J.A., C. Deser, and L. Sun, 2015: Projected changes in regional climate extremes arising from Arctic sea ice loss. *Environmental Research Letters*, **10**, 084006. <http://dx.doi.org/10.1088/1748-9326/10/8/084006>
154. Sun, L., J. Perlwitz, and M. Hoerling, 2016: What caused the recent "Warm Arctic, Cold Continents" trend pattern in winter temperatures? *Geophysical Research Letters*, **43**, 5345-5352. <http://dx.doi.org/10.1002/2016GL069024>
155. Francis, J.A. and S.J. Vavrus, 2012: Evidence linking Arctic amplification to extreme weather in mid-latitudes. *Geophysical Research Letters*, **39**, L06801. <http://dx.doi.org/10.1029/2012GL051000>
156. Vihma, T., 2014: Effects of Arctic sea ice decline on weather and climate: A review. *Surveys in Geophysics*, **35**, 1175-1214. <http://dx.doi.org/10.1007/s10712-014-9284-0>
157. Francis, J. and N. Skific, 2015: Evidence linking rapid Arctic warming to mid-latitude weather patterns. *Philosophical Transactions of the Royal Society A: Mathematical, Physical and Engineering Sciences*, **373**, 20140170. <http://dx.doi.org/10.1098/rsta.2014.0170>
158. Francis, J.A. and S.J. Vavrus, 2015: Evidence for a wavier jet stream in response to rapid Arctic warming. *Environmental Research Letters*, **10**, 014005. <http://dx.doi.org/10.1088/1748-9326/10/1/014005>
159. Seager, R., M. Hoerling, S. Schubert, H. Wang, B. Lyon, A. Kumar, J. Nakamura, and N. Henderson, 2015: Causes of the 2011-14 California drought. *Journal of Climate*, **28**, 6997-7024. <http://dx.doi.org/10.1175/JCLI-D-14-00860.1>
160. Swain, D., M. Tsiang, M. Haughen, D. Singh, A. Charland, B. Rajarthan, and N.S. Diffenbaugh, 2014: The extraordinary California drought of 2013/14: Character, context and the role of climate change [in "Explaining Extreme Events of 2013 from a Climate Perspective"]. *Bulletin of the American Meteorological Society*, **95** (9), S3-S6. <http://dx.doi.org/10.1175/1520-0477-95.9.S1.1>
161. Teng, H. and G. Branstator, 2017: Causes of extreme ridges that induce California droughts. *Journal of Climate*, **30**, 1477-1492. <http://dx.doi.org/10.1175/jcli-d-16-0524.1>
162. Overland, J., J.A. Francis, R. Hall, E. Hanna, S.-J. Kim, and T. Vihma, 2015: The melting Arctic and midlatitude weather patterns: Are they connected? *Journal of Climate*, **28**, 7917-7932. <http://dx.doi.org/10.1175/JCLI-D-14-00822.1>
163. Barnes, E.A. and L.M. Polvani, 2015: CMIP5 projections of Arctic amplification, of the North American/North Atlantic circulation, and of their relationship. *Journal of Climate*, **28**, 5254-5271. <http://dx.doi.org/10.1175/JCLI-D-14-00589.1>
164. Hoskins, B. and T. Woollings, 2015: Persistent extratropical regimes and climate extremes. *Current Climate Change Reports*, **1**, 115-124. <http://dx.doi.org/10.1007/s40641-015-0020-8>
165. Sigmond, M. and J.C. Fyfe, 2016: Tropical Pacific impacts on cooling North American winters. *Nature Climate Change*, **6**, 970-974. <http://dx.doi.org/10.1038/nclimate3069>
166. Cohen, J., J. Jones, J.C. Furtado, and E. Tziperman, 2013: Warm Arctic, cold continents: A common pattern related to Arctic sea ice melt, snow advance, and extreme winter weather. *Oceanography*, **26**, 150-160. <http://dx.doi.org/10.5670/oceanog.2013.70>
167. Nummelin, A., M. Ilicak, C. Li, and L.H. Smedsrud, 2016: Consequences of future increased Arctic runoff on Arctic Ocean stratification, circulation, and sea ice cover. *Journal of Geophysical Research Oceans*, **121**, 617-637. <http://dx.doi.org/10.1002/2015JC011156>
168. Giles, K.A., S.W. Laxon, A.L. Ridout, D.J. Wingham, and S. Bacon, 2012: Western Arctic Ocean freshwater storage increased by wind-driven spin-up of the Beaufort Gyre. *Nature Geoscience*, **5**, 194-197. <http://dx.doi.org/10.1038/ngeo1379>
169. Morison, J., R. Kwok, C. Peralta-Ferriz, M. Alkire, I. Rigor, R. Andersen, and M. Steele, 2012: Changing Arctic Ocean freshwater pathways. *Nature*, **481**, 66-70. <http://dx.doi.org/10.1038/nature10705>
170. Rahmstorf, S., J.E. Box, G. Feulner, M.E. Mann, A. Robinson, S. Rutherford, and E.J. Schaffernicht, 2015: Exceptional twentieth-century slowdown in Atlantic Ocean overturning circulation. *Nature Climate Change*, **5**, 475-480. <http://dx.doi.org/10.1038/nclimate2554>



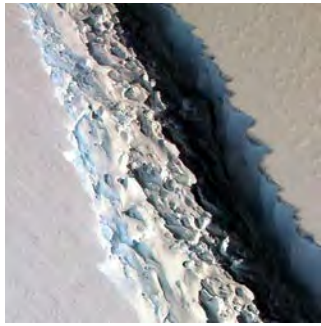
171. Yang, Q., T.H. Dixon, P.G. Myers, J. Bonin, D. Chambers, and M.R. van den Broeke, 2016: Recent increases in Arctic freshwater flux affects Labrador Sea convection and Atlantic overturning circulation. *Nature Communications*, **7**, 10525. <http://dx.doi.org/10.1038/ncomms10525>
172. Liu, W., S.-P. Xie, Z. Liu, and J. Zhu, 2017: Overlooked possibility of a collapsed Atlantic Meridional Overturning Circulation in warming climate. *Science Advances*, **3**, e1601666. <http://dx.doi.org/10.1126/sciadv.1601666>
173. Smeed, D.A., G.D. McCarthy, S.A. Cunningham, E. Frajka-Williams, D. Rayner, W.E. Johns, C.S. Meinen, M.O. Baringer, B.I. Moat, A. Ducez, and H.L. Bryden, 2014: Observed decline of the Atlantic meridional overturning circulation 2004–2012. *Ocean Science*, **10**, 29-38. <http://dx.doi.org/10.5194/os-10-29-2014>
174. Romanovsky, V.E., S.L. Smith, H.H. Christiansen, N.I. Shiklomanov, D.A. Streletskiy, D.S. Drozdov, G.V. Malkova, N.G. Oberman, A.L. Kholodov, and S.S. Marchenko, 2015: [The Arctic] Terrestrial permafrost [in "State of the Climate in 2014"]. *Bulletin of the American Meteorological Society*, **96** (12), S139-S141. <http://dx.doi.org/10.1175/2015BAMSStateoftheClimate.1>
175. Romanovsky, V.E., S.L. Smith, K. Isaksen, N.I. Shiklomanov, D.A. Streletskiy, A.L. Kholodov, H.H. Christiansen, D.S. Drozdov, G.V. Malkova, and S.S. Marchenko, 2016: [The Arctic] Terrestrial permafrost [in "State of the Climate in 2015"]. *Bulletin of the American Meteorological Society*, **97**, S149-S152. <http://dx.doi.org/10.1175/2016BAMSStateoftheClimate.1>
176. Shiklomanov, N.E., D.A. Streletskiy, and F.E. Nelson, 2012: Northern Hemisphere component of the global Circumpolar Active Layer Monitory (CALM) program. In *Proceedings of the 10th International Conference on Permafrost*, Salekhard, Russia. Kane, D.L. and K.M. Hinkel, Eds., 377-382. http://research.iarc.uaf.edu/NICOP/proceedings/10th/TICOP_vol1.pdf
177. Kokelj, S.V., T.C. Lantz, J. Tunnicliffe, R. Segal, and D. Lacelle, 2017: Climate-driven thaw of permafrost preserved glacial landscapes, northwestern Canada. *Geology*, **45**, 371-374. <http://dx.doi.org/10.1130/g38626.1>
178. Grosse, G., S. Goetz, A.D. McGuire, V.E. Romanovsky, and E.A.G. Schuur, 2016: Changing permafrost in a warming world and feedbacks to the Earth system. *Environmental Research Letters*, **11**, 040201. <http://dx.doi.org/10.1088/1748-9326/11/4/040201>
179. Schuur, E.A.G., A.D. McGuire, C. Schadel, G. Grosse, J.W. Harden, D.J. Hayes, G. Hugelius, C.D. Koven, P. Kuhry, D.M. Lawrence, S.M. Natali, D. Olefeldt, V.E. Romanovsky, K. Schaefer, M.R. Turetsky, C.C. Treat, and J.E. Vonk, 2015: Climate change and the permafrost carbon feedback. *Nature*, **520**, 171-179. <http://dx.doi.org/10.1038/nature14338>
180. Tarnocai, C., J.G. Canadell, E.A.G. Schuur, P. Kuhry, G. Mazhitova, and S. Zimov, 2009: Soil organic carbon pools in the northern circumpolar permafrost region. *Global Biogeochemical Cycles*, **23**, GB2023. <http://dx.doi.org/10.1029/2008GB003327>
181. Chang, R.Y.-W., C.E. Miller, S.J. Dinardo, A. Karion, C. Sweeney, B.C. Daube, J.M. Henderson, M.E. Mountain, J. Eluszkiewicz, J.B. Miller, L.M.P. Bruhwiler, and S.C. Wofsy, 2014: Methane emissions from Alaska in 2012 from CARVE airborne observations. *Proceedings of the National Academy of Sciences*, **111**, 16694-16699. <http://dx.doi.org/10.1073/pnas.1412953111>
182. Schuur, E.A.G., J.G. Vogel, K.G. Crummer, H. Lee, J.O. Sickman, and T.E. Osterkamp, 2009: The effect of permafrost thaw on old carbon release and net carbon exchange from tundra. *Nature*, **459**, 556-559. <http://dx.doi.org/10.1038/nature08031>
183. Zona, D., B. Gioli, R. Commane, J. Lindaas, S.C. Wofsy, C.E. Miller, S.J. Dinardo, S. Dengel, C. Sweeney, A. Karion, R.Y.-W. Chang, J.M. Henderson, P.C. Murphy, J.P. Goodrich, V. Moreaux, A. Liljedahl, J.D. Watts, J.S. Kimball, D.A. Lipson, and W.C. Oechel, 2016: Cold season emissions dominate the Arctic tundra methane budget. *Proceedings of the National Academy of Sciences*, **113**, 40-45. <http://dx.doi.org/10.1073/pnas.1516017113>
184. Treat, C.C., S.M. Natali, J. Ernakovich, C.M. Iversen, M. Lupascu, A.D. McGuire, R.J. Norby, T. Roy Chowdhury, A. Richter, H. Šantrůčková, C. Schädel, E.A.G. Schuur, V.L. Sloan, M.R. Turetsky, and M.P. Waldrop, 2015: A pan-Arctic synthesis of CH₄ and CO₂ production from anoxic soil incubations. *Global Change Biology*, **21**, 2787-2803. <http://dx.doi.org/10.1111/gcb.12875>
185. Myhre, G., D. Shindell, F.-M. Bréon, W. Collins, J. Fuglestvedt, J. Huang, D. Koch, J.-F. Lamarque, D. Lee, B. Mendoza, T. Nakajima, A. Robock, G. Stephens, T. Takemura, and H. Zhang, 2013: Anthropogenic and natural radiative forcing. *Climate Change 2013: The Physical Science Basis. Contribution of Working Group I to the Fifth Assessment Report of the Intergovernmental Panel on Climate Change*. Stocker, T.F., D. Qin, G.-K. Plattner, M. Tignor, S.K. Allen, J. Boschung, A. Nauels, Y. Xia, V. Bex, and P.M. Midgley, Eds. Cambridge University Press, Cambridge, United Kingdom and New York, NY, USA, 659-740. <http://www.climatechange2013.org/report/full-report/>
186. Schädel, C., M.K.F. Bader, E.A.G. Schuur, C. Biasi, R. Bracho, P. Capek, S. De Baets, K. Diakova, J. Ernakovich, C. Estop-Aragones, D.E. Graham, I.P. Hartley, C.M. Iversen, E. Kane, C. Knoblauch, M. Lupascu, P.J. Martikainen, S.M. Natali, R.J. Norby, J.A. O'Donnell, T.R. Chowdhury, H. Šantrůčková, G. Shaver, V.L. Sloan, C.C. Treat, M.R. Turetsky, M.P. Waldrop, and K.P. Wickland, 2016: Potential carbon emissions dominated by carbon dioxide from thawed permafrost soils. *Nature Climate Change*, **6**, 950-953. <http://dx.doi.org/10.1038/nclimate3054>



187. Koven, C.D., D.M. Lawrence, and W.J. Riley, 2015: Permafrost carbon-climate feedback is sensitive to deep soil carbon decomposability but not deep soil nitrogen dynamics. *Proceedings of the National Academy of Sciences*, **112**, 3752-3757. <http://dx.doi.org/10.1073/pnas.1415123112>
188. Koven, C.D., E.A.G. Schuur, C. Schädel, T.J. Bohn, E.J. Burke, G. Chen, X. Chen, P. Ciais, G. Grosse, J.W. Harden, D.J. Hayes, G. Hugelius, E.E. Jafarov, G. Krinner, P. Kuhry, D.M. Lawrence, A.H. MacDougall, S.S. Marchenko, A.D. McGuire, S.M. Natali, D.J. Nicolsky, D. Olefeldt, S. Peng, V.E. Romanovsky, K.M. Schaefer, J. Strauss, C.C. Treat, and M. Turetsky, 2015: A simplified, data-constrained approach to estimate the permafrost carbon-climate feedback. *Philosophical Transactions of the Royal Society A: Mathematical, Physical and Engineering Sciences*, **373**, 20140423. <http://dx.doi.org/10.1098/rsta.2014.0423>
189. Schaefer, K., H. Lantuit, E.R. Vladimirov, E.A.G. Schuur, and R. Witt, 2014: The impact of the permafrost carbon feedback on global climate. *Environmental Research Letters*, **9**, 085003. <http://dx.doi.org/10.1088/1748-9326/9/8/085003>
190. Chadburn, S.E., E.J. Burke, P.M. Cox, P. Friedlingstein, G. Hugelius, and S. Westermann, 2017: An observation-based constraint on permafrost loss as a function of global warming. *Nature Climate Change*, **7**, 340-344. <http://dx.doi.org/10.1038/nclimate3262>
191. Friedlingstein, P., P. Cox, R. Betts, L. Bopp, W.v. Bloh, V. Brovkin, P. Cadule, S. Doney, M. Eby, I. Fung, G. Bala, J. John, C. Jones, F. Joos, T. Kato, M. Kawamiya, W. Knorr, K. Lindsay, H.D. Matthews, T. Raddatz, P. Rayner, C. Reick, E. Roeckner, K.-G. Schnitzler, R. Schnur, K. Strassmann, A.J. Weaver, C. Yoshikawa, and N. Zeng, 2006: Climate-carbon cycle feedback analysis: Results from the C⁴MIP model intercomparison. *Journal of Climate*, **19**, 3337-3353. <http://dx.doi.org/10.1175/JCLI3800.1>
192. Fisher, J.B., M. Sikka, W.C. Oechel, D.N. Huntzinger, J.R. Melton, C.D. Koven, A. Ahlström, M.A. Arain, I. Baker, J.M. Chen, P. Ciais, C. Davidson, M. Dietze, B. El-Masri, D. Hayes, C. Huntingford, A.K. Jain, P.E. Levy, M.R. Lomas, B. Poulter, D. Price, A.K. Sahoo, K. Schaefer, H. Tian, E. Tomelleri, H. Verbeeck, N. Viovy, R. Wania, N. Zeng, and C.E. Miller, 2014: Carbon cycle uncertainty in the Alaskan Arctic. *Biogeosciences*, **11**, 4271-4288. <http://dx.doi.org/10.5194/bg-11-4271-2014>
193. Liljedahl, A.K., J. Boike, R.P. Daanen, A.N. Fedorov, G.V. Frost, G. Grosse, L.D. Hinzman, Y. Iijima, J.C. Jorgenson, N. Matveyeva, M. Necsoiu, M.K. Reynolds, V.E. Romanovsky, J. Schulla, K.D. Tape, D.A. Walker, C.J. Wilson, H. Yabuki, and D. Zona, 2016: Pan-Arctic ice-wedge degradation in warming permafrost and its influence on tundra hydrology. *Nature Geoscience*, **9**, 312-318. <http://dx.doi.org/10.1038/ngeo2674>
194. Oh, Y., B. Stackhouse, M.C.Y. Lau, X. Xu, A.T. Trugman, J. Moch, T.C. Onstott, C.J. Jørgensen, L. D'Imperio, B. Elberling, C.A. Emmerton, V.L. St. Louis, and D. Medvigy, 2016: A scalable model for methane consumption in Arctic mineral soils. *Geophysical Research Letters*, **43**, 5143-5150. <http://dx.doi.org/10.1002/2016GL069049>
195. Archer, D., 2007: Methane hydrate stability and anthropogenic climate change. *Biogeosciences*, **4**, 521-544. <http://dx.doi.org/10.5194/bg-4-521-2007>
196. Piñero, E., M. Marquardt, C. Hensen, M. Haeckel, and K. Wallmann, 2013: Estimation of the global inventory of methane hydrates in marine sediments using transfer functions. *Biogeosciences*, **10**, 959-975. <http://dx.doi.org/10.5194/bg-10-959-2013>
197. Ruppel, C.D. *Methane hydrates and contemporary climate change*. Nature Education Knowledge, 2011.3.
198. Ruppel, C.D. and J.D. Kessler, 2017: The interaction of climate change and methane hydrates. *Reviews of Geophysics*, **55**, 126-168. <http://dx.doi.org/10.1002/2016RG000534>
199. Bollmann, M., T. Bosch, F. Colijn, R. Ebbinghaus, R. Froese, K. Güssow, S. Khalilian, S. Krastel, A. Körtzinger, M. Langenbuch, M. Latif, B. Matthiessen, F. Melzner, A. Oschlies, S. Petersen, A. Proelß, M. Quaas, J. Reichenbach, T. Requate, T. Reusch, P. Rosenstiel, J.O. Schmidt, K. Schrottke, H. Sichelschmidt, U. Siebert, R. Soltwedel, U. Sommer, K. Statterger, H. Sterr, R. Sturm, T. Treude, A. Vafeidis, C.v. Bernem, J.v. Beusekom, R. Voss, M. Visbeck, M. Wahl, K. Wallmann, and F. Weinberger, 2010: *World Ocean Review: Living With the Oceans*. maribus gGmbH, 232 pp. http://worldoceanreview.com/wp-content/downloads/wor1/WOR1_english.pdf
200. Brothers, L.L., B.M. Herman, P.E. Hart, and C.D. Ruppel, 2016: Subsea ice-bearing permafrost on the U.S. Beaufort Margin: 1. Minimum seaward extent defined from multichannel seismic reflection data. *Geochemistry, Geophysics, Geosystems*, **17**, 4354-4365. <http://dx.doi.org/10.1002/2016GC006584>
201. Johnson, H.P., U.K. Miller, M.S. Salmi, and E.A. Solomon, 2015: Analysis of bubble plume distributions to evaluate methane hydrate decomposition on the continental slope. *Geochemistry, Geophysics, Geosystems*, **16**, 3825-3839. <http://dx.doi.org/10.1002/2015GC005955>
202. Ruppel, C.D., B.M. Herman, L.L. Brothers, and P.E. Hart, 2016: Subsea ice-bearing permafrost on the U.S. Beaufort Margin: 2. Borehole constraints. *Geochemistry, Geophysics, Geosystems*, **17**, 4333-4353. <http://dx.doi.org/10.1002/2016GC006582>
203. Skarke, A., C. Ruppel, M. Kodis, D. Brothers, and E. Lobecker, 2014: Widespread methane leakage from the sea floor on the northern US Atlantic margin. *Nature Geoscience*, **7**, 657-661. <http://dx.doi.org/10.1038/ngeo2232>

204. Hunter, S.J., D.S. Goldobin, A.M. Haywood, A. Ridgwell, and J.G. Rees, 2013: Sensitivity of the global submarine hydrate inventory to scenarios of future climate change. *Earth and Planetary Science Letters*, **367**, 105-115. <http://dx.doi.org/10.1016/j.epsl.2013.02.017>
205. Kretschmer, K., A. Biastoch, L. Rüpke, and E. Burwicz, 2015: Modeling the fate of methane hydrates under global warming. *Global Biogeochemical Cycles*, **29**, 610-625. <http://dx.doi.org/10.1002/2014GB005011>
206. Graves, C.A., L. Steinle, G. Rehder, H. Niemann, D.P. Connelly, D. Lowry, R.E. Fisher, A.W. Stott, H. Sahling, and R.H. James, 2015: Fluxes and fate of dissolved methane released at the seafloor at the landward limit of the gas hydrate stability zone offshore western Svalbard. *Journal of Geophysical Research Oceans*, **120**, 6185-6201. <http://dx.doi.org/10.1002/2015JC011084>
207. ACIA, 2005: Arctic Climate Impact Assessment. ACIA Secretariat and Cooperative Institute for Arctic Research, 1042 pp. <http://www.acia.uaf.edu/pages/scientific.html>
208. Hollesen, J., H. Matthiesen, A.B. Møller, and B. Elberling, 2015: Permafrost thawing in organic Arctic soils accelerated by ground heat production. *Nature Climate Change*, **5**, 574-578. <http://dx.doi.org/10.1038/nclimate2590>
209. Fetterer, F., K. Knowles, W. Meier, and M. Savoie, 2016, updated daily: Sea Ice Index, Version 2. National Snow and Ice Data Center, Boulder, CO.
210. WGMS, 2016: Fluctuations of Glaciers Database. World Glacier Monitoring Service, Zurich, Switzerland.
211. Wolken, G., M. Sharp, L.M. Andreassen, A. Arendt, D. Burgess, J.G. Cogley, L. Copland, J. Kohler, S. O'Neel, M. Pelto, L. Thomson, and B. Wouters, 2016: [The Arctic] Glaciers and ice caps outside Greenland [in "State of the Climate in 2015"]. *Bulletin of the American Meteorological Society*, **97**, S142-S145. <http://dx.doi.org/10.1175/2016BAMSStateoftheClimate.1>
212. USGS, 2004: Repeat Photography of Alaskan Glaciers: Muir Glacier (USGS Photograph by Bruce F. Molnia). Department of the Interior, U.S. Geological Survey. https://www2.usgs.gov/climate_landuse/glaciers/repeat_photography.asp





12

Sea Level Rise

KEY FINDINGS

1. Global mean sea level (GMSL) has risen by about 7–8 inches (about 16–21 cm) since 1900, with about 3 of those inches (about 7 cm) occurring since 1993 (*very high confidence*). Human-caused climate change has made a substantial contribution to GMSL rise since 1900 (*high confidence*), contributing to a rate of rise that is greater than during any preceding century in at least 2,800 years (*medium confidence*).
2. Relative to the year 2000, GMSL is *very likely* to rise by 0.3–0.6 feet (9–18 cm) by 2030, 0.5–1.2 feet (15–38 cm) by 2050, and 1.0–4.3 feet (30–130 cm) by 2100 (*very high confidence in lower bounds; medium confidence in upper bounds for 2030 and 2050; low confidence in upper bounds for 2100*). Future pathways have little effect on projected GMSL rise in the first half of the century, but significantly affect projections for the second half of the century (*high confidence*). Emerging science regarding Antarctic ice sheet stability suggests that, for high emission scenarios, a GMSL rise exceeding 8 feet (2.4 m) by 2100 is physically possible, although the probability of such an extreme outcome cannot currently be assessed. Regardless of pathway, it is *extremely likely* that GMSL rise will continue beyond 2100 (*high confidence*).
3. Relative sea level (RSL) rise in this century will vary along U.S. coastlines due, in part, to changes in Earth’s gravitational field and rotation from melting of land ice, changes in ocean circulation, and vertical land motion (*very high confidence*). For almost all future GMSL rise scenarios, RSL rise is *likely* to be greater than the global average in the U.S. Northeast and the western Gulf of Mexico. In intermediate and low GMSL rise scenarios, RSL rise is *likely* to be less than the global average in much of the Pacific Northwest and Alaska. For high GMSL rise scenarios, RSL rise is *likely* to be higher than the global average along all U.S. coastlines outside Alaska. Almost all U.S. coastlines experience more than global mean sea level rise in response to Antarctic ice loss, and thus would be particularly affected under extreme GMSL rise scenarios involving substantial Antarctic mass loss (*high confidence*).
4. As sea levels have risen, the number of tidal floods each year that cause minor impacts (also called “nuisance floods”) have increased 5- to 10-fold since the 1960s in several U.S. coastal cities (*very high confidence*). Rates of increase are accelerating in over 25 Atlantic and Gulf Coast cities (*very high confidence*). Tidal flooding will continue increasing in depth, frequency, and extent this century (*very high confidence*).

KEY FINDINGS *(continued)*

5. Assuming storm characteristics do not change, sea level rise will increase the frequency and extent of extreme flooding associated with coastal storms, such as hurricanes and nor'easters (*very high confidence*). A projected increase in the intensity of hurricanes in the North Atlantic (*medium confidence*) could increase the probability of extreme flooding along most of the U.S. Atlantic and Gulf Coast states beyond what would be projected based solely on RSL rise. However, there is *low confidence* in the projected increase in frequency of intense Atlantic hurricanes, and the associated flood risk amplification and flood effects could be offset or amplified by such factors as changes in overall storm frequency or tracks.

Recommended Citation for Chapter

Sweet, W.V., R. Horton, R.E. Kopp, A.N. LeGrande, and A. Romanou, 2017: Sea level rise. In: *Climate Science Special Report: Fourth National Climate Assessment, Volume I* [Wuebbles, D.J., D.W. Fahey, K.A. Hibbard, D.J. Dokken, B.C. Stewart, and T.K. Maycock (eds.)]. U.S. Global Change Research Program, Washington, DC, USA, pp. 333-363, doi: 10.7930/J0VM49F2.

12.1 Introduction

Sea level rise is closely linked to increasing global temperatures. Thus, even as uncertainties remain about just how much sea level may rise this century, it is virtually certain that sea level rise this century and beyond will pose a growing challenge to coastal communities, infrastructure, and ecosystems from increased (permanent) inundation, more frequent and extreme coastal flooding, erosion of coastal landforms, and saltwater intrusion within coastal rivers and aquifers. Assessment of vulnerability to rising sea levels requires consideration of physical causes, historical evidence, and projections. A risk-based perspective on sea level rise points to the need for emphasis on how changing sea levels alter the coastal zone and interact with coastal flood risk at local scales.

This chapter reviews the physical factors driving changes in global mean sea level (GMSL) and those causing additional regional variations in relative sea level (RSL). It presents geological and instrumental observations of historical sea level changes and an assessment of the human contribution to sea level change. It then describes a range of scenarios for fu-

ture levels and rates of sea level change, and the relationship of these scenarios to the Representative Concentration Pathways (RCPs). Finally, it assesses the impact of changes in sea level on extreme water levels.

While outside the scope of this chapter, it is important to note the myriad of other potential impacts associated with RSL rise, wave action, and increases in coastal flooding. These impacts include loss of life, damage to infrastructure and the built environment, salinization of coastal aquifers, mobilization of pollutants, changing sediment budgets, coastal erosion, and ecosystem changes such as marsh loss and threats to endangered flora and fauna.¹ While all of these impacts are inherently important, some also have the potential to influence local rates of RSL rise and the extent of wave-driven and coastal flooding impacts. For example, there is evidence that wave action and flooding of beaches and marshes can induce changes in coastal geomorphology, such as sediment build up, that may iteratively modify the future flood risk profile of communities and ecosystems.²



12.2 Physical Factors Contributing to Sea Level Rise

Sea level change is driven by a variety of mechanisms operating at different spatial and temporal scales (see Kopp et al. 2015³ for a review). GMSL rise is primarily driven by two factors: 1) increased volume of seawater due to thermal expansion of the ocean as it warms, and 2) increased mass of water in the ocean due to melting ice from mountain glaciers and the Antarctic and Greenland ice sheets.⁴ The overall amount (mass) of ocean water, and thus sea level, is also affected to a lesser extent by changes in global land-water storage, which reflects changes in the impoundment of water in dams and reservoirs and river runoff from groundwater extraction, inland sea and wetland drainage, and global precipitation patterns, such as occur during phases of the El Niño–Southern Oscillation (ENSO).^{4, 5, 6, 7, 8}

Sea level and its changes are not uniform globally for several reasons. First, atmosphere–ocean dynamics—driven by ocean circulation, winds, and other factors—are associated with differences in the height of the sea surface, as are differences in density arising from the distribution of heat and salinity in the ocean. Changes in any of these factors will affect sea surface height. For example, a weakening of the Gulf Stream transport in the mid-to-late 2000s may have contributed to enhanced sea level rise in the ocean environment extending to the northeastern U.S. coast,^{9, 10, 11} a trend that many models project will continue into the future.¹²

Second, the locations of land ice melting and land water reservoir changes impart distinct regional “static-equilibrium fingerprints” on sea level, based on gravitational, rotational, and crustal deformation effects (Figure 12.1a–d).¹³ For example, sea level falls near a melting ice sheet because of the reduced gravitational attraction of the ocean toward the icesheet;

reciprocally, it rises by greater than the global average far from the melting ice sheet.

Third, the Earth’s mantle is still moving in response to the loss of the great North American (Laurentide) and European ice sheets of the Last Glacial Maximum; the associated changes in the height of the land, the shape of the ocean basin, and the Earth’s gravitational field give rise to glacial-isostatic adjustment (Figure 12.1e). For example, in areas once covered by the thickest parts of the great ice sheets of the Last Glacial Maximum, such as in Hudson Bay and in Scandinavia, post-glacial rebound of the land is causing RSL to fall. Along the flanks of the ice sheets, such as along most of the east coast of the United States, subsidence of the bulge that flanked the ice sheet is causing RSL to rise.

Finally, a variety of other factors can cause local vertical land movement. These include natural sediment compaction, compaction caused by local extraction of groundwater and fossil fuels, and processes related to plate tectonics, such as earthquakes and more gradual seismic creep (Figure 12.1f).^{14, 15}

Compared to many climate variables, the trend signal for sea level change tends to be large relative to natural variability. However, at inter-annual timescales, changes in ocean dynamics, density, and wind can cause substantial sea level variability in some regions. For example, there has been a multidecadal suppression of sea level rise off the Pacific coast¹⁶ and large year-to-year variations in sea level along the Northeast U.S. coast.¹⁷ Local rates of land height change have also varied dramatically on decadal timescales in some locations, such as along the western Gulf Coast, where rates of subsurface extraction of fossil fuels and groundwater have varied over time.¹⁸



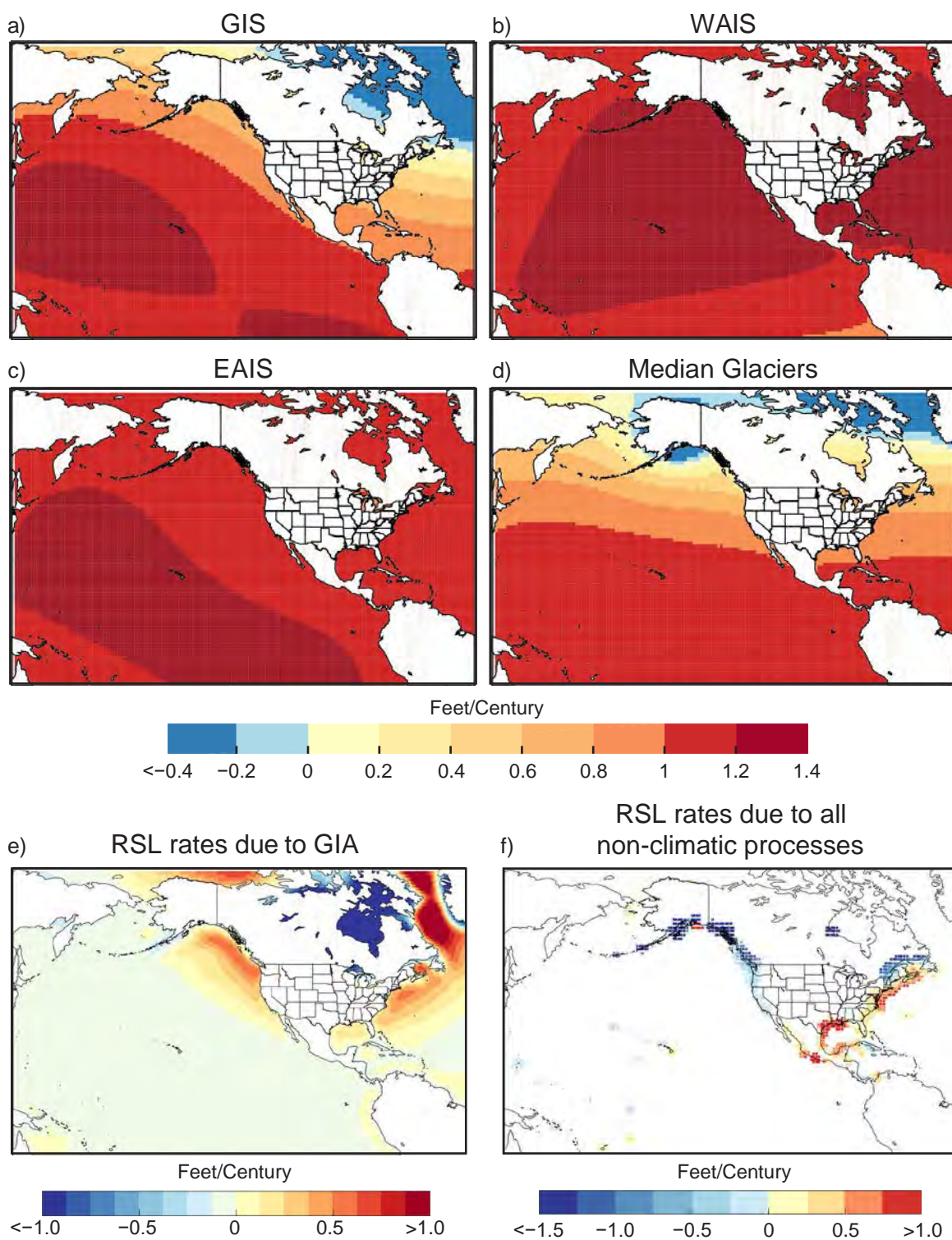


Figure 12.1: (a–d) Static-equilibrium fingerprints of the relative sea level (RSL) effect of land ice melt, in units of feet of RSL change per feet of global mean sea level (GMSL) change, for mass loss from (a) Greenland, (b) West Antarctica, (c) East Antarctica, and (d) the median projected combination of melting glaciers, after Kopp et al.^{3, 76} (e) Model projections of the rate of RSL rise due to glacial-isostatic adjustment (units of feet/century), after Kopp et al.³ (f) Tide gauge-based estimates of the non-climatic, long term contribution to RSL rise, including the effects of glacial isostatic adjustment, tectonics, and sediment compaction (units of feet/century).⁷⁶ (Figure source: (a)–(d) Kopp et al. 2015,³ (e) adapted from Kopp et al. 2015,³ (f) adapted from Sweet et al. 2017⁷¹).

12.3 Paleo Sea Level

Geological records of temperature and sea level indicate that during past warm periods over the last several millions of years, GMSL was higher than it is today.^{19, 20} During the Last Interglacial stage, about 125,000 years ago, global average sea surface temperature was about $0.5^{\circ} \pm 0.3^{\circ}\text{C}$ ($0.9^{\circ} \pm 0.5^{\circ}\text{F}$) above the preindustrial level [that is, comparable to the average over 1995–2014, when global mean temperature was about 0.8°C (1.4°F) above the preindustrial levels].²¹ Polar temperatures were comparable to those projected for 1° – 2°C (1.8° – 3.6°F) of global mean warming above the preindustrial level. At this time, GMSL was about 6–9 meters (about 20–30 feet) higher than today (Figure 12.2a).^{22, 23} This geological benchmark may indicate the probable long-term response of GMSL to the minimum magnitude of temperature change projected for the current century.

Similarly, during the mid-Pliocene warm period, about 3 million years ago, global mean temperature was about 1.8° – 3.6°C (3.2° – 6.5°F) above the preindustrial level.²⁴ Estimates of GMSL are less well constrained than during the Last Interglacial, due to the smaller number of local geological sea level reconstruction and the possibility of significant vertical land motion over millions of years.²⁰ Some reconstructions place mid-Pliocene GMSL at about 10–30 meters (about 30–100 feet) higher than today.²⁵ Sea levels this high would require a significantly reduced Antarctic ice sheet, highlighting the risk of significant Antarctic ice sheet loss under such levels of warming (Figure 12.2a).

For the period since the Last Glacial Maximum, about 26,000 to 19,000 years ago,²⁶ geologists can produce detailed reconstructions of sea levels as well as rates of sea level change. To do this, they use proxies such as the heights of fossil coral reefs and the populations of

different salinity-sensitive microfossils within salt marsh sediments.²⁷ During the main portion of the deglaciation, from about 17,000 to 8,000 years ago, GMSL rose at an average rate of about 12 mm/year (0.5 inches/year).²⁸ However, there were periods of faster rise. For example, during Meltwater Pulse 1a, lasting from about 14,600 to 14,300 years ago, GMSL may have risen at an average rate about 50 mm/year (2 inches/year).²⁹

Since the disappearance of the last remnants of the North American (Laurentide) Ice Sheet about 7,000 years ago³⁰ to about the start of the 20th century, however, GMSL has been relatively stable. During this period, total GMSL rise is estimated to have been about 4 meters (about 13 feet), most of which occurred between 7,000 and 4,000 years ago.²⁸ The Third National Climate Assessment (NCA3) noted, based on a geological data set from North Carolina,³¹ that the 20th century GMSL rise was much faster than at any time over the past 2,000 years. Since NCA3, high-resolution sea level reconstructions have been developed for multiple locations, and a new global analysis of such reconstructions strengthens this finding.³² Over the last 2,000 years, prior to the industrial era, GMSL exhibited small fluctuations of about ± 8 cm (3 inches), with a significant decline of about 8 cm (3 inches) between the years 1000 and 1400 CE coinciding with about 0.2°C (0.4°F) of global mean cooling.³² The rate of rise in the last century, about 14 cm/century (5.5 inches/century), was greater than during any preceding century in at least 2,800 years (Figure 12.2b).³²



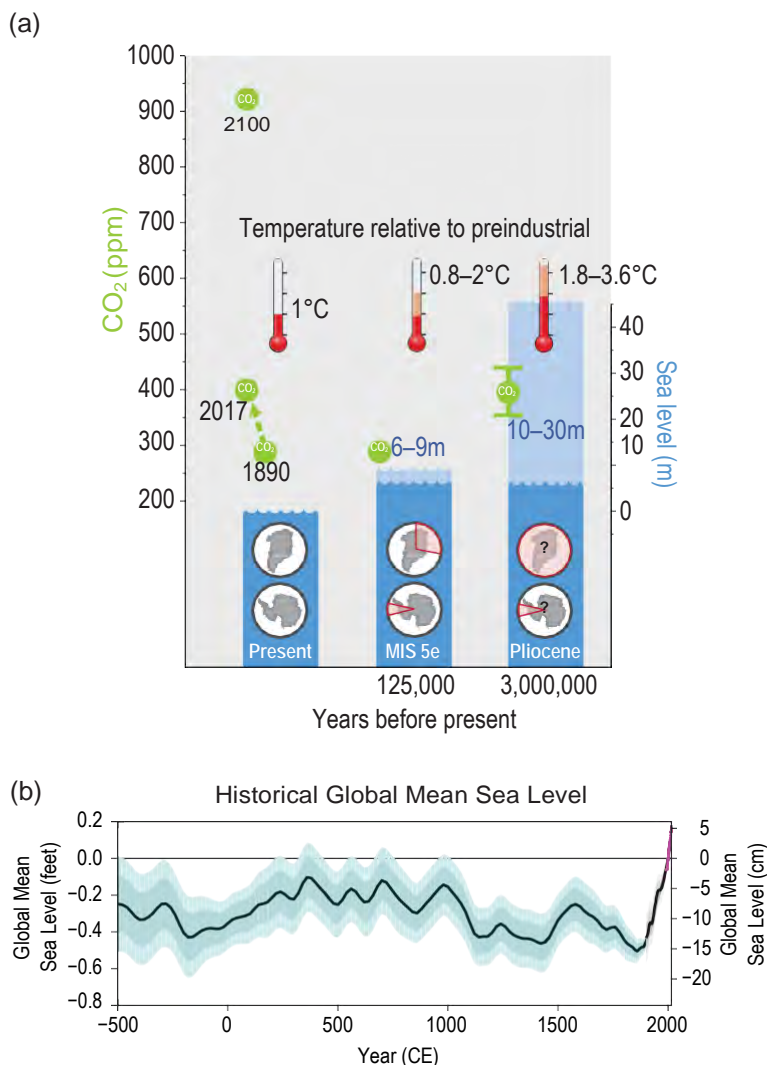


Figure 12.2: (a) The relationship between peak global mean temperature, atmospheric CO₂, maximum global mean sea level (GMSL), and source(s) of meltwater for two periods in the past with global mean temperature comparable to or warmer than present. Light blue shading indicates uncertainty of GMSL maximum. Red pie charts over Greenland and Antarctica denote fraction, not location, of ice retreat. Atmospheric CO₂ levels in 2100 are shown under RCP8.5. (b) GMSL rise from -500 to 1900 CE, from Kopp et al.'s³² geological and tide gauge-based reconstruction (blue), from 1900 to 2010 from Hay et al.'s³³ tide gauge-based reconstruction (black), and from 1992 to 2015 from the satellite-based reconstruction updated from Nerem et al.³⁵ (magenta). (Figure source: (a) adapted from Dutton et al. 2015²⁰ and (b) Sweet et al. 2017⁷¹).



12.4 Recent Past Trends (20th and 21st Centuries)

12.4.1 Global Tide Gauge Network and Satellite Observations

A global tide gauge network provides the century-long observations of local RSL, whereas satellite altimetry provides broader coverage of sea surface heights outside the polar regions starting in 1993. GMSL can be estimated through statistical analyses of either data set. GMSL trends over the 1901–1990 period vary slightly (Hay et al. 2015:³³ 1.2 ± 0.2 mm/year [0.05 inches/year]; Church and White 2011:³⁴ 1.5 ± 0.2 mm/year [0.06 inches/year]) with differences amounting to about 1 inch over 90 years. Thus, these results indicate about 11–14 cm (4–5 inches) of GMSL rise from 1901 to 1990.

Tide gauge analyses indicate that GMSL rose at a considerably faster rate of about 3 mm/year (0.12 inches/year) since 1993,^{33, 34} a result supported by satellite data indicating a trend of 3.4 ± 0.4 mm/year (0.13 ± 0.02 inches/year) over 1993–2015 (update to Nerem et al. 2010³⁵). These results indicate an additional GMSL rise of about 7 cm (about 3 inches) since 1990 (Figure 12.2b, Figure 12.3a) and about 16–21 cm (about 7–8 inches) since 1900. Satellite (altimetry and gravity) and in situ water column (Argo floats) measurements show that, since 2005, about one third of GMSL rise has been from steric changes (primarily thermal expansion) and about two thirds from the addition of mass to the ocean, which represents a growing land-ice contribution (compared to steric) and a departure from the relative contributions earlier in the 20th century (Figure 12.3a).^{4, 36, 37, 38, 39, 40}

In addition to land ice, the mass-addition contribution also includes net changes in global land-water storage. This term varied in sign over the course of the last century, with human-induced changes in land-water storage

being negative (perhaps as much as about -0.6 mm/year [-0.02 inches/year]) during the period of heavy dam construction in the middle of the last century, and turning positive in the 1990s as groundwater withdrawal came to dominate.⁸ On decadal timescales, precipitation variability can dominate human-induced changes in land water storage; recent satellite-gravity estimates suggest that, over 2002–2014, a human-caused land-water contribution to GMSL of 0.4 mm/year (0.02 inches/year) was more than offset by -0.7 mm/year (-0.03 inches/year) due to natural variability.⁵

Comparison of results from a variety of approaches supports the conclusion that a substantial fraction of GMSL rise since 1900 is attributable to human-caused climate change.^{32, 41, 42, 43, 44, 45, 46, 47, 48} For example, based on the long term historical relationship between temperature and rate of GMSL change, Kopp et al.³² found that GMSL rise would *extremely likely* have been less than 59% of observed in the absence of 20th century global warming, and that it is *very likely* that GMSL has been higher since 1960 than it would have been without 20th century global warming (Figure 12.3b). Similarly, using a variety of models for individual components, Slangen et al.⁴¹ found that about 80% of the GMSL rise they simulated for 1970–2005 and about half of that which they simulated for 1900–2005 was attributable to anthropogenic forcing.



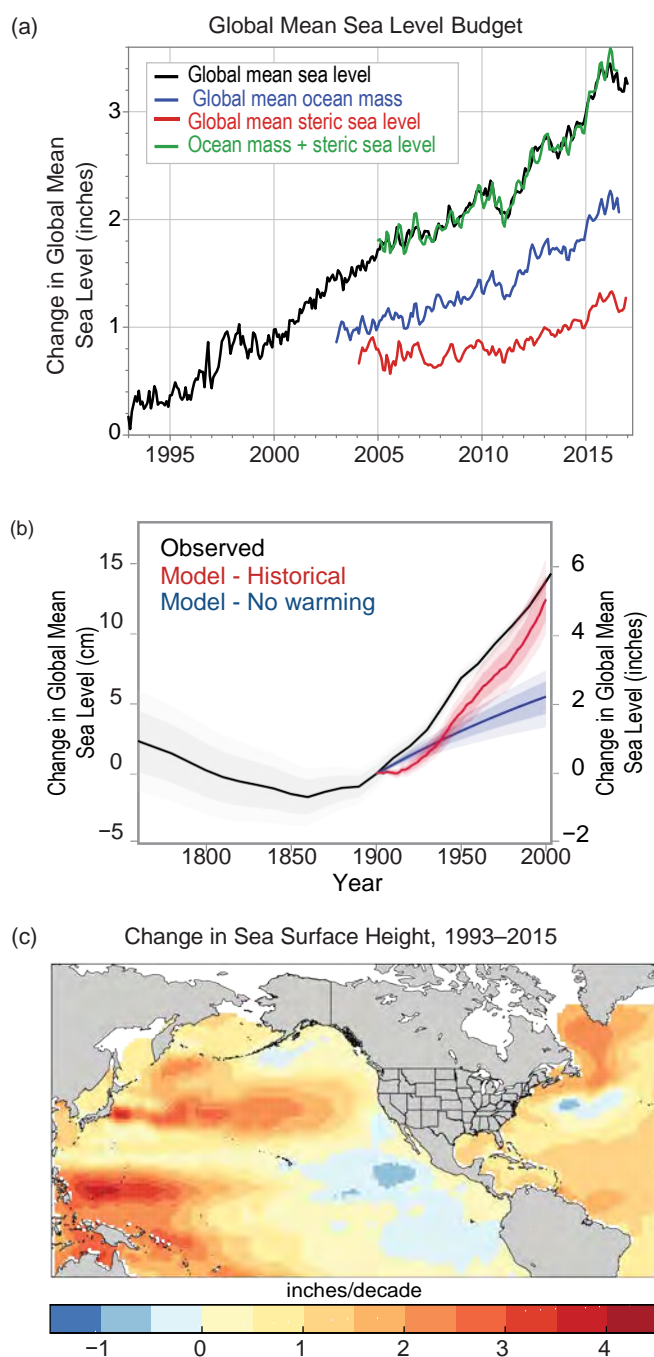


Figure 12.3: (a) Contributions of ocean mass changes from land ice and land water storage (measured by satellite gravimetry) and ocean volume changes (or steric, primarily from thermal expansion measured by in situ ocean profilers) and their comparison to global mean sea level (GMSL) change (measured by satellite altimetry) since 1993. (b) An estimate of modeled GMSL rise in the absence of 20th century warming (blue), from the same model with observed warming (red), and compared to observed GMSL change (black). Heavy/light shading indicates the 17th–83rd and 5th–95th percentiles. (c) Rates of change from 1993 to 2015 in sea surface height from satellite altimetry data; updated from Kopp et al.³ using data updated from Church and White.³⁴ (Figure source: (a) adapted and updated from Leuliette and Nerem 2016,⁴⁰ (b) adapted from Kopp et al. 2016³² and (c) adapted and updated from Kopp et al. 2015³).

Over timescales of a few decades, ocean-atmosphere dynamics drive significant variability in sea surface height, as can be observed by satellite (Figure 12.3c) and in tide gauge records that have been adjusted to account for background rates of rise due to long term factors like glacio-isostatic adjustments. For example, the U.S. Pacific Coast experienced a slower-than-global increase between about 1980 and 2011, while the western tropical Pacific experienced a faster-than-global increase in the 1990s and 2000s. This pattern was associated with changes in average winds linked to the Pacific Decadal Oscillation (PDO)^{16, 49, 50} and appears to have reversed since about 2012.⁵¹ Along the Atlantic coast, the U.S. Northeast has experienced a faster-than-global increase since the 1970s, while the U.S. Southeast has experienced a slower-than-global increase since the 1970s. This pattern appears to be tied to changes in the Gulf Stream,^{10, 12, 52, 53} although whether these changes represent natural variability or a long-term trend remains uncertain.⁵⁴

12.4.2 Ice Sheet Gravity and Altimetry and Visual Observations

Since NCA3, Antarctica and Greenland have continued to lose ice mass, with mounting evidence accumulating that mass loss is accelerating. Studies using repeat gravimetry (GRACE satellites), repeat altimetry, GPS monitoring, and mass balance calculations generally agree on accelerating mass loss in Antarctica.^{55, 56, 57, 58} Together, these indicate a mass loss of roughly 100 Gt/year (gigatonnes/year) over the last decade (a contribution to GMSL of about 0.3 mm/year [0.01 inches/year]). Positive accumulation rate anomalies in East Antarctica, especially in Dronning Maud Land,⁵⁹ have contributed to the trend of slight growth there (e.g., Seo et al. 2015;⁵⁷ Martín-Español et al. 2016⁵⁸), but this is more than offset by mass loss elsewhere, especially in West Antarctica along the coast facing the Amundsen Sea,^{60, 61}

Totten Glacier in East Antarctica,^{62, 63} and along the Antarctic Peninsula.^{57, 58, 64} Floating ice shelves around Antarctica are losing mass at an accelerating rate.⁶⁵ Mass loss from floating ice shelves does not directly affect GMSL, but does allow faster flow of ice from the ice sheet into the ocean.

Estimates of mass loss in Greenland based on mass balance from input-output, repeat gravimetry, repeat altimetry, and aerial imagery as discussed in Chapter 11: Arctic Changes reveal a recent acceleration.⁶⁶ Mass loss averaged approximately 75 Gt/year (about 0.2 mm/year [0.01 inches/year] GMSL rise) from 1900 to 1983, continuing at a similar rate of approximately 74 Gt/year through 2003 before accelerating to 186 Gt/year (0.5 mm/year [0.02 inches/year] GMSL rise) from 2003 to 2010.⁶⁷ Strong interannual variability does exist (see Ch. 11: Arctic Changes), such as during the exceptional melt year from April 2012 to April 2013, which resulted in mass loss of approximately 560 Gt (1.6 mm/year [0.06 inches/year]).⁶⁸ More recently (April 2014–April 2015), annual mass losses have resumed the accelerated rate of 186 Gt/year.^{67, 69} Mass loss over the last century has reversed the long-term trend of slow thickening linked to the continuing evolution of the ice sheet from the end of the last ice age.⁷⁰



12.5 Projected Sea Level Rise

12.5.1 Scenarios of Global Mean Sea Level Rise

No single physical model is capable of accurately representing all of the major processes contributing to GMSL and regional/local RSL rise. Accordingly, the U.S. Interagency Sea Level Rise Task Force (henceforth referred to as “Interagency”)⁷¹ has revised the GMSL rise scenarios for the United States and now provides six scenarios that can be used for assessment and risk-framing purposes (Figure 12.4a; Table 12.1). The low scenario of 30 cm (about 1 foot) GMSL rise by 2100 is consistent with a continuation of the recent approximately 3 mm/year (0.12 inches/year) rate of rise through to 2100 (Table 12.2), while the five other scenarios span a range of GMSL rise be-

tween 50 and 250 cm (1.6 and 8.2 feet) in 2100, with corresponding rise rates between 5 mm/year (0.2 inches/year) to 44 mm/year (1.7 inches/year) towards the end of this century (Table 12.2). The highest scenario of 250 cm is consistent with several literature estimates of the maximum physically plausible level of 21st century sea level rise (e.g., Pfeffer et al. 2008,⁷² updated with Sriver et al. 2012⁷³ estimates of thermal expansion and Bamber and Aspinall 2013⁷⁴ estimates of Antarctic contribution, and incorporating land water storage, as discussed in Miller et al. 2013⁷⁵ and Kopp et al. 2014⁷⁶). It is also consistent with the high end of recent projections of Antarctic ice sheet melt discussed below.⁷⁷ The Interagency

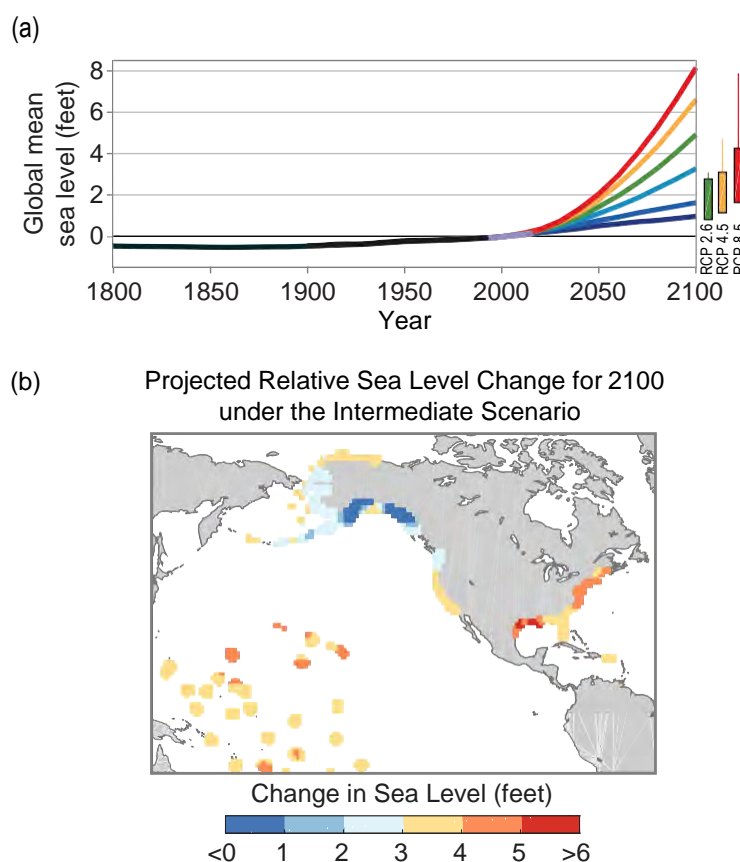


Figure 12.4: (a) Global mean sea level (GMSL) rise from 1800 to 2100, based on Figure 12.2b from 1800 to 2015, the six Interagency⁷¹ GMSL scenarios (navy blue, royal blue, cyan, green, orange, and red curves), the *very likely* ranges in 2100 for different RCPs (colored boxes), and lines augmenting the *very likely* ranges by the difference between the median Antarctic contribution of Kopp et al.⁷⁶ and the various median Antarctic projections of DeConto and Pollard.⁷⁷ (b) Relative sea level (RSL) rise (feet) in 2100 projected for the Interagency Intermediate Scenario (1-meter [3.3 feet] GMSL rise by 2100) (Figure source: Sweet et al. 2017⁷¹).

Table 12.1. The Interagency GMSL rise scenarios in meters (feet) relative to 2000. All values are 19-year averages of GMSL centered at the identified year. To convert from a 1991–2009 tidal datum to the 1983–2001 tidal datum, add 2.4 cm (0.9 inches).

Scenario	2020	2030	2050	2100
Low	0.06 (0.2)	0.09 (0.3)	0.16 (0.5)	0.30 (1.0)
Intermediate-Low	0.08 (0.3)	0.13 (0.4)	0.24 (0.8)	0.50 (1.6)
Intermediate	0.10 (0.3)	0.16 (0.5)	0.34 (1.1)	1.0 (3.3)
Intermediate-High	0.10 (0.3)	0.19 (0.6)	0.44 (1.4)	1.5 (4.9)
High	0.11 (0.4)	0.21 (0.7)	0.54 (1.8)	2.0 (6.6)
Extreme	0.11 (0.4)	0.24 (0.8)	0.63 (2.1)	2.5 (8.2)

Table 12.2. Rates of GMSL rise in the Interagency scenarios in mm/year (inches/year). All values represent 19-year average rates of change, centered at the identified year.

Scenario	2020	2030	2050	2090
Low	3 (0.1)	3 (0.1)	3 (0.1)	3 (0.1)
Intermediate-Low	5 (0.2)	5 (0.2)	5 (0.2)	5 (0.2)
Intermediate	6 (0.2)	7 (0.3)	10 (0.4)	15 (0.6)
Intermediate-High	7 (0.3)	10 (0.4)	15 (0.6)	24 (0.9)
High	8 (0.3)	13 (0.5)	20 (0.8)	35 (1.4)
Extreme	10 (0.4)	15 (0.6)	25 (1.0)	44 (1.7)

Table 12.3. Interpretations of the Interagency GMSL rise scenarios

Scenario	Interpretation
Low	Continuing current rate of GMSL rise, as calculated since 1993 Low end of <i>very likely</i> range under RCP2.6
Intermediate-Low	Modest increase in rate Middle of <i>likely</i> range under RCP2.6 Low end of <i>likely</i> range under RCP4.5 Low end of <i>very likely</i> range under RCP8.5
Intermediate	High end of <i>very likely</i> range under RCP4.5 High end of <i>likely</i> range under RCP8.5 Middle of <i>likely</i> range under RCP4.5 when accounting for possible ice cliff instabilities
Intermediate-High	Slightly above high end of <i>very likely</i> range under RCP8.5 Middle of <i>likely</i> range under RCP8.5 when accounting for possible ice cliff instabilities
High	High end of <i>very likely</i> range under RCP8.5 when accounting for possible ice cliff instabilities
Extreme	Consistent with estimates of physically possible “worst case”



GMSL scenario interpretations are shown in Table 12.3.

The Interagency scenario approach is similar to local RSL rise scenarios of Hall et al.⁷⁸ used for all coastal U.S. Department of Defense installations worldwide. The Interagency approach starts with a probabilistic projection framework to generate time series and regional projections consistent with each GMSL rise scenario for 2100.⁷⁶ That framework combines probabilistic estimates of contributions to GMSL and regional RSL rise from ocean processes, cryospheric processes, geological processes, and anthropogenic land-water storage. Pooling the Kopp et al.⁷⁶ projections across even lower, lower, and higher scenarios (RCP2.6, 4.5, and 8.5), the probabilistic projections are filtered to identify pathways consistent with each of these 2100 levels, with the median (and 17th and 83rd percentiles) picked from each of the filtered subsets.

12.5.2 Probabilities of Different Sea Level Rise Scenarios

Several studies have estimated the probabilities of different amounts of GMSL rise under different pathways (e.g., Church et al. 2013;⁴ Kopp et al. 2014;⁷⁶ Slangen et al. 2014;⁷⁹ Jevrejeva et al. 2014;⁸⁰ Grinsted et al. 2015;⁸¹ Kopp et al. 2016;³² Mengel et al. 2016;⁸² Jackson and

Jevrejeva 2016⁸³) using a variety of methods, including both statistical and physical models. Most of these studies are in general agreement that GMSL rise by 2100 is *very likely* to be between about 25–80 cm (0.8–2.6 feet) under an even lower scenario (RCP2.6), 35–95 cm (1.1–3.1 feet) under a lower scenario (RCP4.5), and 50–130 cm (1.6–4.3 feet) under a higher scenario (RCP8.5), although some projections extend the *very likely* range for RCP8.5 as high as 160–180 cm (5–6 feet) (Kopp et al. 2014,⁷⁶ sensitivity study).^{80, 83} Based on Kopp et al.,⁷⁶ the probability of exceeding the amount of GMSL in 2100 under the Interagency scenarios is shown in Table 12.4.

The Antarctic projections of Kopp et al.,⁷⁶ the GMSL projections of which underlie Table 12.4, are consistent with a statistical-physical model of the onset of marine ice sheet instability calibrated to observations of ongoing retreat in the Amundsen Embayment sector of West Antarctica.⁸⁴ Ritz et al.'s⁸⁴ 95th percentile Antarctic contribution to GMSL of 30 cm by 2100 is comparable to Kopp et al.'s⁷⁶ 95th percentile projection of 33 cm under the higher scenario (RCP8.5). However, emerging science suggests that these projections may understate the probability of faster-than-expected ice sheet melt, particularly for high-end warming scenarios. While these probability estimates

Table 12.4. Probability of exceeding the Interagency GMSL scenarios in 2100 per Kopp et al.⁷⁶ New evidence regarding the Antarctic ice sheet, if sustained, may significantly increase the probability of the intermediate-high, high, and extreme scenarios, particularly under the higher scenario (RCP8.5), but these results have not yet been incorporated into a probabilistic analysis.

Scenario	RCP2.6	RCP4.5	RCP8.5
Low	94%	98%	100%
Intermediate-Low	49%	73%	96%
Intermediate	2%	3%	17%
Intermediate-High	0.4%	0.5%	1.3%
High	0.1%	0.1%	0.3%
Extreme	0.05%	0.05%	0.1%



are consistent with the assumption that the relationship between global temperature and GMSL in the coming century will be similar to that observed over the last two millennia,^{32, 85} emerging positive feedbacks (self-amplifying cycles) in the Antarctic Ice Sheet especially^{86, 87} may invalidate that assumption. Physical feedbacks that until recently were not incorporated into ice sheet models⁸⁸ could add about 0–10 cm (0–0.3 feet), 20–50 cm (0.7–1.6 feet) and 60–110 cm (2.0–3.6 feet) to central estimates of current century sea level rise under even lower, lower, and higher scenarios (RCP2.6, RCP4.5 and RCP8.5, respectively).⁷⁷ In addition to marine ice sheet instability, examples of these interrelated processes include ice cliff instability and ice shelf hydrofracturing. Processes underway in Greenland may also be leading to accelerating high-end melt risk. Much of the research has focused on changes in surface albedo driven by the melt-associated unmasking and concentration of impurities in snow and ice.⁶⁹ However, ice dynamics at the bottom of the ice sheet may be important as well, through interactions with surface runoff or a warming ocean. As an example of the latter, Jakobshavn Isbræ, Kangerdlugssuaq Glacier, and the Northeast Greenland ice stream may be vulnerable to marine ice sheet instability.⁶⁶

12.5.3 Sea Level Rise after 2100

GMSL rise will not stop in 2100, and so it is useful to consider extensions of GMSL rise projections beyond this point. By 2200, the 0.3–

2.5 meter (1.0–8.2 feet) range spanned by the six Interagency GMSL scenarios in year 2100 increases to about 0.4–9.7 meters (1.3–31.8 feet), as shown in Table 12.5. These six scenarios imply average rates of GMSL rise over the first half of the next century of 1.4 mm/year (0.06 inch/year), 4.6 mm/yr (0.2 inch/year), 16 mm/year (0.6 inch/year), 32 mm/year (1.3 inches/year), 46 mm/yr (1.8 inches/year) and 60 mm/year (2.4 inches/year), respectively. Excluding the possible effects of still emerging science regarding ice cliffs and ice shelves, it is very likely that by 2200 GMSL will have risen by 0.3–2.4 meters (1.0–7.9 feet) under an even lower scenario (RCP2.6), 0.4–2.7 meters (1.3–8.9 feet) under a lower scenario (RCP4.5), and 1.0–3.7 meters (3.3–12 feet) under the higher scenario (RCP8.5).⁷⁶

Under most projections, GMSL rise will also not stop in 2200. The concept of a “sea level rise commitment” refers to the long-term projected sea level rise were the planet’s temperature to be stabilized at a given level (e.g., Levermann et al. 2013;⁸⁹ Golledge et al. 2015⁹⁰). The paleo sea level record suggests that even 2°C (3.6°F) of global average warming above the preindustrial temperature may represent a commitment to several meters of rise. One modeling study suggesting a 2,000-year commitment of 2.3 m/°C (4.2 feet/°F)⁸⁹ indicates that emissions through 2100 would lock in a likely 2,000-year GMSL rise commitment of about 0.7–4.2 meters (2.3–14 feet) under an even lower scenario (RCP2.6), about 1.7–5.6

Table 12.5. Post-2100 extensions of the Interagency GMSL rise scenarios in meters (feet)

Scenario	2100	2120	2150	2200
Low	0.30 (1.0)	0.34 (1.1)	0.37 (1.2)	0.39 (1.3)
Intermediate-Low	0.50 (1.6)	0.60 (2.0)	0.73 (2.4)	0.95 (3.1)
Intermediate	1.0 (3.3)	1.3 (4.3)	1.8 (5.9)	2.8 (9.2)
Intermediate-High	1.5 (4.9)	2.0 (6.6)	3.1 (10)	5.1 (17)
High	2.0 (6.6)	2.8 (9.2)	4.3 (14)	7.5 (25)
Extreme	2.5 (8.2)	3.6 (12)	5.5 (18)	9.7 (32)



meters (5.6–19 feet) under a lower scenario (RCP4.5), and about 4.3–9.9 meters (14–33 feet) under the higher scenario (RCP8.5).⁹¹ However, as with the 21st century projections, emerging science regarding the sensitivity of the Antarctic Ice Sheet may increase the estimated sea level rise over the next millennium, especially for a higher scenario.⁷⁷ Large-scale climate geoengineering might reduce these commitments,^{92, 93} but may not be able to avoid lock-in of significant change.^{94, 95, 96, 97} Once changes are realized, they will be effectively irreversible for many millennia, even if humans artificially accelerate the removal of CO₂ from the atmosphere.⁷⁷

The 2,000-year commitment understates the full sea level rise commitment, due to the long response time of the polar ice sheets. Paleo sea level records (Figure 12.2a) suggest that 1°C of warming may already represent a long-term commitment to more than 6 meters (20 feet) of GMSL rise.^{20, 22, 23} A 10,000-year modeling study⁹⁸ suggests that 2°C warming represents a 10,000-year commitment to about 25 meters (80 feet) of GMSL rise, driven primarily by a loss of about one-third of the Antarctic ice sheet and three-fifths of the Greenland ice sheet, while 21st century emissions consistent with a higher scenario (RCP8.5) represent a 10,000-year commitment to about 38 meters (125 feet) of GMSL rise, including a complete loss of the Greenland ice sheet over about 6,000 years.

12.5.4 Regional Projections of Sea Level Change

Because the different factors contributing to sea level change give rise to different spatial patterns, projecting future RSL change at specific locations requires not just an estimate of GMSL change but estimates of the different processes contributing to GMSL change – each of which has a different associated spatial pattern – as well as of the processes contributing exclusively to regional or local change. Based

on the process-level projections of the Inter-agency GMSL scenarios, several key regional patterns are apparent in future U.S. RSL rise as shown for the Intermediate (1 meter [3.3 feet] GMSL rise by 2100 scenario) in Figure 12.4b.

1. RSL rise due to Antarctic Ice Sheet melt is greater than GMSL rise along all U.S. coastlines due to static-equilibrium effects.
2. RSL rise due to Greenland Ice Sheet melt is less than GMSL rise along the coastline of the continental United States due to static-equilibrium effects. This effect is especially strong in the Northeast.
3. RSL rise is additionally augmented in the Northeast by the effects of glacial isostatic adjustment.
4. The Northeast is also exposed to rise due to changes in the Gulf Stream and reductions in the Atlantic meridional overturning circulation (AMOC). Were the AMOC to collapse entirely – an outcome viewed as unlikely in the 21st century – it could result in as much as approximately 0.5 meters (1.6 feet) of additional regional sea level rise (see Ch. 15: Potential Surprises for further discussion).^{99, 100}
5. The western Gulf of Mexico and parts of the U.S. Atlantic Coast south of New York are currently experiencing significant RSL rise caused by the withdrawal of groundwater (along the Atlantic Coast) and of both fossil fuels and groundwater (along the Gulf Coast). Continuation of these practices will further amplify RSL rise.
6. The presence of glaciers in Alaska and their proximity to the Pacific Northwest reduces RSL rise in these regions, due to both the ongoing glacial isostatic adjustment to past glacier shrinkage and to



the static-equilibrium effects of projected future losses.

7. Because they are far from all glaciers and ice sheets, RSL rise in Hawai'i and other Pacific islands due to any source of melting land ice is amplified by the static-equilibrium effects.

12.6 Extreme Water Levels

12.6.1 Observations

Coastal flooding during extreme high-water events has become deeper due to local RSL rise and more frequent from a fixed-elevation perspective.^{78, 101, 102, 103} Trends in annual frequencies surpassing local emergency preparedness thresholds for minor tidal flooding (i.e., “nuisance” levels of about 30–60 cm [1–2 feet]) that begin to flood infrastructure and trigger coastal flood “advisories” by NOAA’s National Weather Service have increased 5- to 10-fold or more since the 1960s along the U.S. coastline,¹⁰⁴ as shown in Figure 12.5a. Locations experiencing such trend changes (based upon fits of flood days per year of Sweet and Park 2014¹⁰⁵) include Atlantic City and Sandy Hook, NJ; Philadelphia, PA; Baltimore and Annapolis, MD; Norfolk, VA; Wilmington, NC; Charleston, SC; Savannah, GA; Mayport and Key West, FL; Port Isabel, TX, La Jolla, CA; and Honolulu, HI. In fact, over the last several decades, minor tidal flood rates have been accelerating within several (more than 25) East and Gulf Coast cities with established elevation thresholds for minor (nuisance) flood impacts, fastest where elevation thresholds are lower, local RSL rise is higher, and extreme variability less.^{104, 105, 106}

Trends in extreme water levels (for example, monthly maxima) in excess of mean sea levels (for example, monthly means) exist, but are not commonplace.^{48, 101, 107, 108, 109} More common are regional time dependencies in high-water probabilities, which can co-vary on an interan-

nual basis with climatic and other patterns.^{101, 110, 111, 112, 113, 114, 115} These patterns are often associated with anomalous oceanic and atmospheric conditions.^{116, 117} For instance, the probability of experiencing minor tidal flooding is compounded during El Niño periods along portions of the West and Mid-Atlantic Coasts¹⁰⁵ from a combination of higher sea levels and enhanced synoptic forcing and storm surge frequency.^{112, 118, 119, 120}

12.6.2 Influence of Projected Sea Level Rise on Coastal Flood Frequencies

The extent and depth of minor-to-major coastal flooding during high-water events will continue to increase in the future as local RSL rises.^{71, 76, 78, 105, 121, 122, 123, 124, 125} Relative to fixed elevations, the frequency of high-water events will increase the fastest where extreme variability is less and the rate of local RSL rise is higher.^{71, 76, 105, 121, 124, 126} Under the RCP-based probabilistic RSL projections of Kopp et al. 2014,⁷⁶ at tide gauge locations along the contiguous U.S. coastline, a median 8-fold increase (range of 1.1- to 430-fold increase) is expected by 2050 in the annual number of floods exceeding the elevation of the current 100-year flood event (measured with respect to a 1991–2009 baseline sea level).¹²⁴ Under the same forcing, the frequency of minor tidal flooding (with contemporary recurrence intervals generally <1 year¹⁰⁴) will increase even more so in the coming decades^{105, 127} and eventually occur on a daily basis (Figure 12.5b). With only about 0.35 m (<14 inches) of additional local RSL rise (with respect to the year 2000), annual frequencies of moderate level flooding—those locally with a 5-year recurrence interval (Figure 12.5c) and associated with a NOAA coastal flood warning of serious risk to life and property—will increase 25-fold at the majority of NOAA tide gauge locations along the U.S. coastline (outside of Alaska) by or about (± 5 years) 2080, 2060, 2040, and 2030 under the Interagency Low, Intermediate-Low,



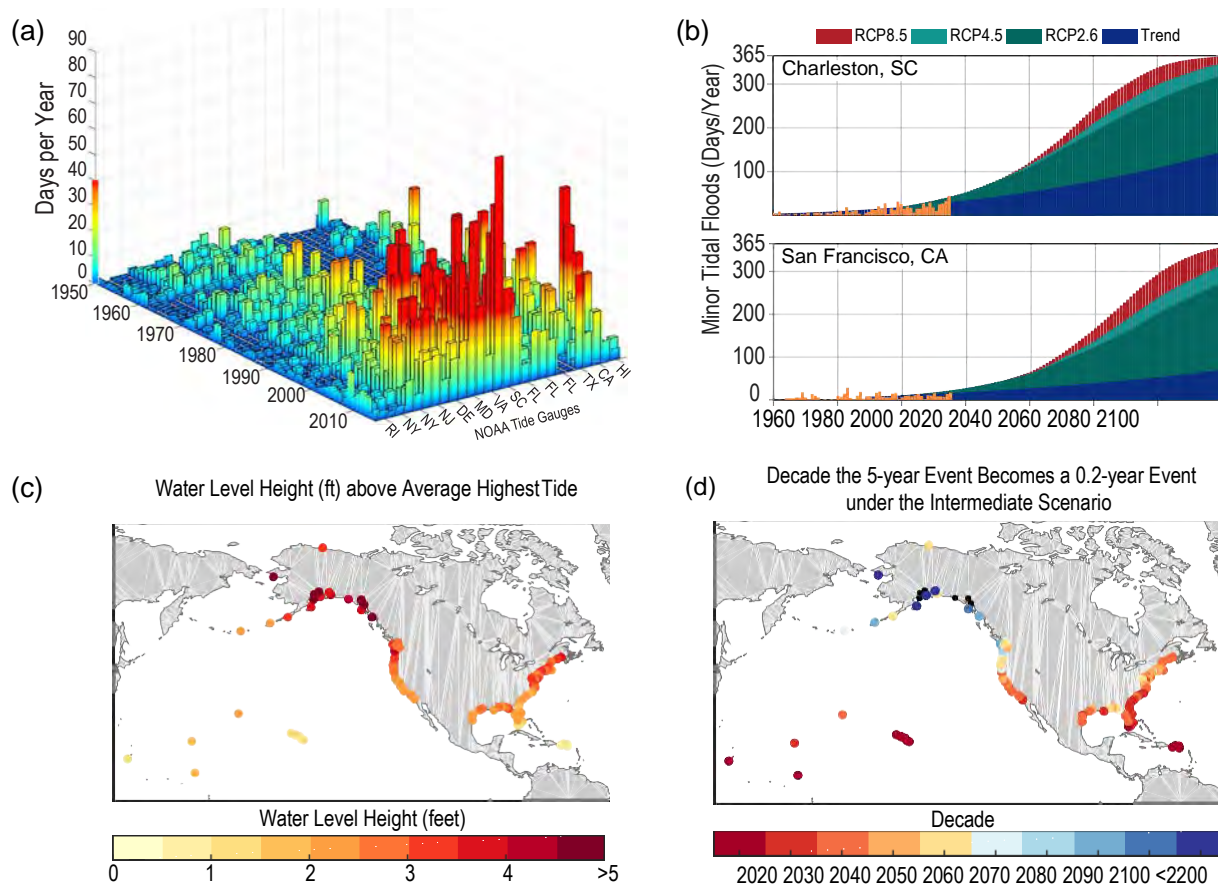


Figure 12.5: (a) Tidal floods (days per year) exceeding NOAA thresholds for minor impacts at 28 NOAA tide gauges through 2015. (b) Historical exceedances (orange), future projections through 2100 based upon the continuation of the historical trend (blue), and future projections under median RCP2.6, 4.5 and 8.5 conditions, for two of the locations—Charleston, SC and San Francisco, CA. (c) Water level heights above average highest tide associated with a local 5-year recurrence probability, and (d) the future decade when the 5-year event becomes a 0.2-year (5 or more times per year) event under the Interagency Intermediate scenario; black dots imply that a 5-year to 0.2-year frequency change does not unfold by 2200 under the Intermediate scenario. (Figure source: (a) adapted from Sweet and Marra 2016,¹⁶⁵ (b) adapted from Sweet and Park 2014,¹⁰⁵ (c) and (d) Sweet et al. 2017⁷¹).

Intermediate, and Intermediate-High GMSL scenarios, respectively.⁷¹ Figure 12.5d, which shows the decade in which the frequency of such moderate level flooding will increase 25-fold under the Interagency Intermediate Scenario, highlights that the mid- and Southeast Atlantic, western Gulf of Mexico, California, and the Island States and Territories are most susceptible to rapid changes in potentially damaging flood frequencies.

12.6.3 Waves and Impacts

The combination of a storm surge at high tide with additional dynamic effects from waves^{128, 129} creates the most damaging coastal hydraulic conditions.¹³⁰ Simply with higher-than-nor-

mal sea levels, wave action increases the likelihood for extensive coastal erosion^{131, 132, 133} and low-island overwash.¹³⁴ Wave runup is often the largest water level component during extreme events, especially along island coastlines where storm surge is constrained by bathymetry.^{78, 121, 123} On an interannual basis, wave impacts are correlated across the Pacific Ocean with phases of ENSO.^{135, 136} Over the last half century, there has been an increasing trend in wave height and power within the North Pacific Ocean^{137, 138} that is modulated by the PDO.^{137, 139} Resultant increases in wave run-up have been more of a factor than RSL rise in terms of impacts along the U.S. Northwest Pacific Coast over the last several

decades.¹⁴⁰ In the Northwest Atlantic Ocean, no long-term trends in wave power have been observed over the last half century,¹⁴¹ though hurricane activity drives interannual variability.¹⁴² In terms of future conditions this century, increases in mean and maximum seasonal wave heights are projected within parts of the northeast Pacific, northwest Atlantic, and Gulf of Mexico.^{138, 143, 144, 145}

12.6.4 Sea Level Rise, Changing Storm Characteristics, and Their Interdependencies

Future probabilities of extreme coastal floods will depend upon the amount of local RSL rise, changes in coastal storm characteristics, and their interdependencies. For instance, there have been more storms producing concurrent locally extreme storm surge and rainfall (not captured in tide gauge data) along the U.S. East and Gulf Coasts over the last 65 years, with flooding further compounded by local RSL rise.¹⁶⁶ Hemispheric-scale extratropical cyclones may experience a northward shift this century, with some studies projecting an overall decrease in storm number (Colle et al. 2015¹¹⁷ and references therein). The research is mixed about strong extratropical storms; studies find potential increases in frequency and intensity in some regions, like within the

Northeast,¹⁴⁶ whereas others project decreases in strong extratropical storms in some regions (e.g., Zappa et al. 2013¹⁴⁷).

For tropical cyclones, model projections for the North Atlantic mostly agree that intensities and precipitation rates will increase this century (see Ch. 9: Extreme Storms), although some model evidence suggests that track changes could dampen the effect in the U.S. Mid-Atlantic and Northeast.¹⁴⁸ Assuming other storm characteristics do not change, sea level rise will increase the frequency and extent of extreme flooding associated with coastal storms, such as hurricanes and nor'easters. A projected increase in the intensity of hurricanes in the North Atlantic could increase the probability of extreme flooding along most of the U.S. Atlantic and Gulf Coast states beyond what would be projected based solely on RSL rise.^{110, 149, 150, 151} In addition, RSL increases are projected to cause a nonlinear increase in storm surge heights in shallow bathymetry environments^{152, 153, 154, 155, 156} and extend wave propagation and impacts landward.^{152, 153} However, there is low confidence in the magnitude of the increase in intensity and the associated flood risk amplification, and it could be offset or amplified by other factors, such as changes in storm frequency or tracks (e.g., Knutson et al. 2013,¹⁵⁷ 2015¹⁵⁸).



TRACEABLE ACCOUNTS

Key Finding 1

Global mean sea level (GMSL) has risen by about 7–8 inches (about 16–21 cm) since 1900, with about 3 of those inches (about 7 cm) occurring since 1993 (*very high confidence*). Human-caused climate change has made a substantial contribution to GMSL rise since 1900 (*high confidence*), contributing to a rate of rise that is greater than during any preceding century in at least 2,800 years (*medium confidence*).

Description of evidence base

Multiple researchers, using different statistical approaches, have integrated tide gauge records to estimate GMSL rise since the late nineteenth century (e.g., Church and White 2006,¹⁵⁹ 2011;³⁴ Hay et al. 2015;³³ Jevrejeva et al. 2009).⁴² The most recent published rate estimates are 1.2 ± 0.2^{33} or 1.5 ± 0.2^{34} mm/year over 1901–1990. Thus, these results indicate about 11–14 cm (4–5 inches) of GMSL rise from 1901 to 1990. Tide gauge analyses indicate that GMSL rose at a considerably faster rate of about 3 mm/year (0.12 inches/year) since 1993,^{33,34} a result supported by satellite data indicating a trend of 3.4 ± 0.4 mm/year (0.13 inches/year) over 1993–2015 (update to Nerem et al. 2010³⁵) (Figure 12.3a). These results indicate an additional GMSL rise of about 7 cm (about 3 inches) rise since 1990. Thus, total GMSL rise since 1900 is about 16–21 cm (about 7–8 inches).

The finding regarding the historical context of the 20th century change is based upon Kopp et al.³², who conducted a meta-analysis of geological RSL reconstructions spanning the last 3,000 years from 24 locations around the world as well as tide gauge data from 66 sites and the tide gauge based GMSL reconstruction of Hay et al.³³ By constructing a spatio-temporal statistical model of these data sets, they identified the common global sea level signal over the last three millennia and its uncertainties. They found a 95% probability that the average rate of GMSL change over 1900–2000 was greater than during any preceding century in at least 2,800 years.

The finding regarding the substantial human contribution is based upon several lines of evidence. Kopp et al.,³² based on the long term historical relationship between temperature and the rate of sea level change, found that it is *extremely likely* that GMSL rise would have been <59% of observed in the absence of 20th century global warming, and that it is *very likely* that GMSL has been higher since 1960 than it would have been without 20th century global warming. Using a variety of models for individual components, Slangen et al.⁴¹ found that $69\% \pm 31\%$ out of the $87\% \pm 20\%$ of GMSL rise over 1970–2005 that their models simulated was attributable to anthropogenic forcing, and that $37\% \pm 38\%$ out of $74\% \pm 22\%$ simulated was attributable over 1900–2005. Jevrejeva et al.,⁴² using the relationship between forcing and GMSL over 1850 and 2001 and CMIP3 models, found that $\sim 75\%$ of GMSL rise in the 20th century is attributable to anthropogenic forcing. Marcos and Amores,⁴⁵ using CMIP5 models, found that $\sim 87\%$ of ocean heat uptake since 1970 in the top 700 m of the ocean has been due to anthropogenic forcing. Slangen et al.,⁴⁶ using CMIP5, found that anthropogenic forcing was required to explain observed thermosteric SLR over 1957–2005. Marzeion et al.⁴⁷ found that $25\% \pm 35\%$ of glacial loss over 1851–2010, and $69\% \pm 24\%$ over 1991–2010, was attributable to anthropogenic forcing. Dangendorf et al.,⁴³ based on time series analysis, found that >45% of observed GMSL trend since 1900 cannot (with 99% probability) be explained by multi-decadal natural variability. Becker et al.,⁴⁴ based on time series analysis, found a 99% probability that at least 1.0 or 1.3 mm/year of GMSL rise over 1880–2010 is anthropogenic.

Major uncertainties

Uncertainties in reconstructed GMSL change relate to the sparsity of tide gauge records, particularly before the middle of the twentieth century, and to different statistical approaches for estimating GMSL change from these sparse records. Uncertainties in reconstructed GMSL change before the twentieth century also relate to the sparsity of geological proxies for sea



level change, the interpretation of these proxies, and the dating of these proxies. Uncertainty in attribution relates to the reconstruction of past changes and the magnitude of unforced variability.

Assessment of confidence based on evidence and agreement, including short description of nature of evidence and level of agreement

Confidence is *very high* in the rate of GMSL rise since 1900, based on multiple different approaches to estimating GMSL rise from tide gauges and satellite altimetry. Confidence is *high* in the substantial human contribution to GMSL rise since 1900, based on both statistical and physical modeling evidence. It is *medium* that the magnitude of the observed rise since 1900 is unprecedented in the context of the previous 2,800 years, based on meta-analysis of geological proxy records.

Summary sentence or paragraph that integrates the above information

This key finding is based upon multiple analyses of tide gauge and satellite altimetry records, on a meta-analysis of multiple geological proxies for pre-instrumental sea level change, and on both statistical and physical analyses of the human contribution to GMSL rise since 1900.

Key Finding 2

Relative to the year 2000, GMSL is *very likely* to rise by 0.3–0.6 feet (9–18 cm) by 2030, 0.5–1.2 feet (15–38 cm) by 2050, and 1.0–4.3 feet (30–130 cm) by 2100 (*very high confidence in lower bounds; medium confidence in upper bounds for 2030 and 2050; low confidence in upper bounds for 2100*). Future pathways have little effect on projected GMSL rise in the first half of the century, but significantly affect projections for the second half of the century (*high confidence*). Emerging science regarding Antarctic ice sheet stability suggests that, for high emission scenarios, a GMSL rise exceeding 8 feet (2.4 m) by 2100 is physically possible, although the probability of such an extreme outcome cannot currently be assessed. Regardless of pathway, it is *extremely likely* that GMSL rise will continue beyond 2100 (*high confidence*).

Description of evidence base

The lower bound of the *very likely* range is based on a continuation of the observed approximately 3 mm/year rate of GMSL rise. The upper end of the *very likely* range is based upon estimates for the higher scenario (RCP8.5) from three studies producing fully probabilistic projections across multiple RCPs. Kopp et al. 2014⁷⁶ fused multiple sources of information accounting for the different individual processes contributing to GMSL rise. Kopp et al. 2016³² constructed a semi-empirical sea level model calibrated to the Common Era sea level reconstruction. Mengel et al.⁸² constructed a set of semi-empirical models of the different contributing processes. All three studies show negligible RCP dependence in the first half of this century, becoming more prominent in the second half of the century. A sensitivity study by Kopp et al. 2014,⁷⁶ as well as studies by Jevrejeva et al.⁸⁰ and by Jackson and Jevrejeva,⁸³ used frameworks similar to Kopp et al. 2016³² but incorporated directly an expert elicitation study on ice sheet stability.⁷⁴ (This study was incorporated in Kopp et al. 2014's⁷⁶ main results with adjustments for consistency with Church et al. 2013⁴). These studies extend the *very likely* range for the higher scenario (RCP8.5) as high as 160–180 cm (5–6 feet) (Kopp et al. 2014,⁷⁶ sensitivity study).^{80, 83}

To estimate the effect of incorporating the DeConto and Pollard⁷⁷ projections of Antarctic ice sheet melt, we note that Kopp et al. (2014)'s⁷⁶ median projection of Antarctic melt in 2100 is 4 cm (1.6 inches) (RCP2.6), 5 cm (2 inches) (RCP4.5), or 6 cm (2.4 inches) (RCP8.5). By contrast, DeConto and Pollard's⁷⁷ ensemble mean projections are (varying the assumptions for the size of Pliocene mass loss and the bias correction in the Amundsen Sea) 2–14 cm (0.1–0.5 foot) for an even lower scenario (RCP2.6), 26–58 cm (0.9–1.9 feet) for a lower scenario (RCP4.5), and 64–114 cm (2.1–3.7 ft) for the higher scenario (RCP8.5). Thus, we conclude that DeConto and Pollard's⁷⁷ projection would lead to a –10 cm (–0.1–0.3 ft) increase in median RCP2.6 projections, a 21–53 cm (0.7–1.7 feet) increase in median RCP4.5 projections, and a 58–108 cm (1.9–3.5 feet) increase in median RCP8.5 projections.



Very likely ranges, 2030 relative to 2000 in cm (feet)

	Kopp et al. (2014) ⁷⁶	Kopp et al. (2016) ³²	Mengel et al. (2016) ⁸²
RCP8.5	11–18 (0.4–0.6)	8–15 (0.3–0.5)	7–12 (0.2–0.4)
RCP4.5	10–18 (0.3–0.6)	8–15 (0.3–0.5)	7–12 (0.2–0.4)
RCP2.6	10–18 (0.3–0.6)	8–15 (0.3–0.5)	7–12 (0.2–0.4)

Very likely ranges, 2050 relative to 2000 in cm (feet)

	Kopp et al. (2014) ⁷⁶	Kopp et al. (2016) ³²	Mengel et al. (2016) ⁸²
RCP8.5	21–38 (0.7–1.2)	16–34 (0.5–1.1)	15–28 (0.5–0.9)
RCP4.5	18–35 (0.6–1.1)	15–31 (0.5–1.0)	14–25 (0.5–0.8)
RCP2.6	18–33 (0.6–1.1)	14–29 (0.5–1.0)	13–23 (0.4–0.8)

Very likely ranges, 2100 relative to 2000 in cm (feet)

	Kopp et al. (2014) ⁷⁶	Kopp et al. (2016) ³²	Mengel et al. (2016) ⁸²
RCP8.5	55–121 (1.8–4.0)	52–131 (1.7–4.3)	57–131 (1.9–4.3)
RCP4.5	36–93 (1.2–3.1)	33–85 (1.1–2.8)	37–77 (1.2–2.5)
RCP2.6	29–82 (1.0–2.7)	24–61 (0.8–2.0)	28–56 (0.9–1.8)

Major uncertainties

Since NCA3, multiple different approaches have been used to generate probabilistic projections of GMSL rise, conditional upon the RCPs. These approaches are in general agreement. However, emerging results indicate that marine-based sectors of the Antarctic Ice Sheet are more unstable than previous modeling indicated. The rate of ice sheet mass changes remains challenging to project.

Assessment of confidence based on evidence and agreement, including short description of nature of evidence and level of agreement

There is *very high* confidence that future GMSL rise over the next several decades will be at least as fast as a con-

tinuation of the historical trend over the last quarter century would indicate. There is *medium* confidence in the upper end of very likely ranges for 2030 and 2050.

Due to possibly large ice sheet contributions, there is *low* confidence in the upper end of very likely ranges for 2100. Based on multiple projection methods, there is *high confidence* that differences between emission scenarios are small before 2050 but significant beyond 2050.

Summary sentence or paragraph that integrates the above information

This key finding is based upon multiple methods for estimating the probability of future sea level change and on new modeling results regarding the stability of marine based ice in Antarctica.

Key Finding 3

Relative sea level (RSL) rise in this century will vary along U.S. coastlines due, in part, to changes in Earth's gravitational field and rotation from melting of land ice, changes in ocean circulation, and vertical land motion (*very high confidence*). For almost all future GMSL rise scenarios, RSL rise is *likely* to be greater than the global average in the U.S. Northeast and the western Gulf of Mexico. In intermediate and low GMSL rise scenarios, RSL rise is *likely* to be less than the global average in much of the Pacific Northwest and Alaska. For high GMSL rise scenarios, RSL rise is *likely* to be higher than the global average along all U.S. coastlines outside Alaska. Almost all U.S. coastlines experience more than global-mean sea-level rise in response to Antarctic ice loss, and thus would be particularly affected under extreme GMSL rise scenarios involving substantial Antarctic mass loss (*high confidence*).

Description of evidence base

The processes that cause geographic variability in RSL change are reviewed by Kopp et al.³ Long tide gauge data sets show the RSL rise caused by vertical land motion due to glacio-isostatic adjustment and fluid withdrawal along many U.S. coastlines.^{160,161} These observations are corroborated by glacio-isostatic adjustment models, by GPS observations, and by geological data (e.g., Engelhart and Horton 2012¹⁶²). The physics of the



gravitational, rotational and flexural “static-equilibrium fingerprint” response of sea level to redistribution of mass from land ice to the oceans is well established.^{13, 163} GCM studies indicate the potential for a Gulf Stream contribution to sea level rise in the U.S. Northeast.^{12, 164} Kopp et al.⁷⁶ and Slangen et al.⁴⁶ accounted for land motion (only glacial isostatic adjustment for Slangen et al.), fingerprint, and ocean dynamic responses. Comparing projections of local RSL change and GMSL change in these studies indicate that local rise is likely to be greater than the global average along the U.S. Atlantic and Gulf Coasts and less than the global average in most of the Pacific Northwest. Sea level rise projections in this report are developed by an Interagency Sea Level Rise Task Force.⁷¹

Major uncertainties

Since NCA3, multiple authors have produced global or regional studies synthesizing the major process that causes global and local sea level change to diverge. The largest sources of uncertainty in the geographic variability of sea level change are ocean dynamic sea level change and, for those regions where sea level fingerprints for Greenland and Antarctica differ from the global mean in different directions, the relative contributions of these two sources to projected sea level change.

Assessment of confidence based on evidence and agreement, including short description of nature of evidence and level of agreement

Because of the enumerated physical processes, there is *very high* confidence that RSL change will vary across U.S. coastlines. There is *high* confidence in the likely differences of RSL change from GMSL change under different levels of GMSL change, based on projections incorporating the different relevant processes.

Summary sentence or paragraph that integrates the above information

The part of the key finding regarding the existence of geographic variability is based upon a broader observational, modeling, and theoretical literature. The specific differences are based upon the scenarios described by the Interagency Sea Level Rise Task Force.⁷¹

Key Finding 4

As sea levels have risen, the number of tidal floods each year that cause minor impacts (also called “nuisance floods”) have increased 5- to 10-fold since the 1960s in several U.S. coastal cities (*very high confidence*). Rates of increase are accelerating in over 25 Atlantic and Gulf Coast cities (*very high confidence*). Tidal flooding will continue increasing in depth, frequency, and extent this century (*very high confidence*).

Description of evidence base

Sweet et al.¹⁰⁴ examined 45 NOAA tide gauge locations with hourly data since 1980 and Sweet and Park¹⁰⁵ examined a subset of these (27 locations) with hourly data prior to 1950, all with a National Weather Service elevation threshold established for minor “nuisance” flood impacts. Using linear or quadratic fits of annual number of days exceeding the minor thresholds, Sweet and Park¹⁰⁵ find increases in trend-derived values between 1960 and 2010 greater than 10-fold at 8 locations, greater than 5-fold at 6 locations, and greater than 3-fold at 7 locations. Sweet et al.,¹⁰⁴ Sweet and Park,¹⁰⁵ and Ezer and Atkinson¹⁰⁶ find that annual minor tidal flood frequencies since 1980 are accelerating along locations on the East and Gulf Coasts (>25 locations¹⁰⁴) due to continued exceedance of a typical high-water distribution above elevation thresholds for minor impacts.

Historical changes over the last 60 years in flood probabilities have occurred most rapidly where RSL rates were highest and where tide ranges and extreme variability is less (Sweet and Park 2014). In terms of future rates of changes in extreme event probabilities relative to fixed elevations, Hunter,¹²⁶ Tebaldi et al.,¹²¹ Kopp et al.,⁷⁶ Sweet and Park¹⁰⁵ and Sweet et al.⁷¹ all find that locations with less extreme variability and higher RSL rise rates are most prone.

Major uncertainties

Minor flooding probabilities have been only assessed where a tide gauge is present with >30 years of data and where a NOAA National Weather Service elevation threshold for impacts has been established. There are likely many other locations experiencing similar flood-



ing patterns, but an expanded assessment is not possible at this time.

Assessment of confidence based on evidence and agreement, including short description of nature of evidence and level of agreement

There is *very high* confidence that exceedance probabilities of high tide flooding at dozens of local-specific elevation thresholds have significantly increased over the last half century, often in an accelerated fashion, and that exceedance probabilities will continue to increase this century.

Summary sentence or paragraph that integrates the above information

This key finding is based upon several studies finding historic and projecting future changes in high-water probabilities for local-specific elevation thresholds for flooding.

Key Finding 5

Assuming storm characteristics do not change, sea level rise will increase the frequency and extent of extreme flooding associated with coastal storms, such as hurricanes and nor'easters (*very high confidence*). A projected increase in the intensity of hurricanes in the North Atlantic (*medium confidence*) could increase the probability of extreme flooding along most of the U.S. Atlantic and Gulf Coast states beyond what would be projected based solely on RSL rise. However, there is *low confidence* in the projected increase in frequency of intense Atlantic hurricanes, and the associated flood risk amplification and flood effects could be offset or amplified by such factors as changes in overall storm frequency or tracks.

Description of evidence base

The frequency, extent, and depth of extreme event-driven (for example, 5- to 100-year event probabilities) coastal flooding relative to existing infrastructure will continue to increase in the future as local RSL rises.^{71, 76, 78, 103, 121, 122, 123, 124} Extreme flood probabilities will increase regardless of change in storm characteristics, which may exacerbate such changes. Model-based projections of tropical storms and related major storm

surges within the North Atlantic mostly agree that intensities and frequencies of the most intense storms will increase this century.^{110, 149, 150, 151, 157} However, the projection of increased hurricane intensity is more robust across models than the projection of increased frequency of the most intense storms, since a number of models project a substantial decrease in the overall number of tropical storms and hurricanes in the North Atlantic. Changes in the frequency of intense hurricanes depends on changes in both the overall frequency of tropical cyclones storms and their intensities. High-resolution models generally project an increase in mean hurricane intensity in the Atlantic (e.g., Knutson et al. 2013¹⁵⁷). In addition, there is model evidence for a change in tropical cyclone tracks in warm years that minimizes the increase in landfalling hurricanes in the U.S. Mid-Atlantic or Northeast.¹⁴⁸

Major uncertainties

Uncertainties remain large with respect to the precise change in future risk of a major coastal impact at a specific location from changes in the most intense tropical cyclone characteristics and tracks beyond changes imposed from local sea level rise.

Assessment of confidence based on evidence and agreement, including short description of nature of evidence and level of agreement

There is *low confidence* that the flood risk at specific locations will be amplified from a major tropical storm this century.

Summary sentence or paragraph that integrates the above information

This key finding is based upon several modeling studies of future hurricane characteristics and associated increases in major storm surge risk amplification.



REFERENCES

1. Wong, P.P., I.J. Losada, J.-P. Gattuso, J. Hinkel, A. Khattabi, K.L. McInnes, Y. Saito, and A. Sallenger, 2014: Coastal systems and low-lying areas. *Climate Change 2014: Impacts, Adaptation, and Vulnerability. Part A: Global and Sectoral Aspects. Contribution of Working Group II to the Fifth Assessment Report of the Intergovernmental Panel on Climate Change*. Field, C.B., V.R. Barros, D.J. Dokken, K.J. Mach, M.D. Mastrandrea, T.E. Bilir, M. Chatterjee, K.L. Ebi, Y.O. Estrada, R.C. Genova, B. Girma, E.S. Kissel, A.N. Levy, S. MacCracken, P.R. Mastrandrea, and L.L. White, Eds. Cambridge University Press, Cambridge, United Kingdom and New York, NY, USA, 361-409. <http://www.ipcc.ch/report/ar5/wg2/>
2. Lentz, E.E., E.R. Thieler, N.G. Plant, S.R. Stippa, R.M. Horton, and D.B. Gesch, 2016: Evaluation of dynamic coastal response to sea-level rise modifies inundation likelihood. *Nature Climate Change*, **6**, 696-700. <http://dx.doi.org/10.1038/nclimate2957>
3. Kopp, R.E., C.C. Hay, C.M. Little, and J.X. Mitrovica, 2015: Geographic variability of sea-level change. *Current Climate Change Reports*, **1**, 192-204. <http://dx.doi.org/10.7282/T37W6F4P>
4. Church, J.A., P.U. Clark, A. Cazenave, J.M. Gregory, S. Jevrejeva, A. Levermann, M.A. Merrifield, G.A. Milne, R.S. Nerem, P.D. Nunn, A.J. Payne, W.T. Pfeffer, D. Stammer, and A.S. Unnikrishnan, 2013: Sea level change. *Climate Change 2013: The Physical Science Basis. Contribution of Working Group I to the Fifth Assessment Report of the Intergovernmental Panel on Climate Change*. Stocker, T.F., D. Qin, G.-K. Plattner, M. Tignor, S.K. Allen, J. Boschung, A. Nauels, Y. Xia, V. Bex, and P.M. Midgley, Eds. Cambridge University Press, Cambridge, United Kingdom and New York, NY, USA, 1137-1216. <http://www.climatechange2013.org/report/full-report/>
5. Reager, J.T., A.S. Gardner, J.S. Famiglietti, D.N. Wiese, A. Eicker, and M.-H. Lo, 2016: A decade of sea level rise slowed by climate-driven hydrology. *Science*, **351**, 699-703. <http://dx.doi.org/10.1126/science.aad8386>
6. Rietbroek, R., S.-E. Brunnabend, J. Kusche, J. Schröter, and C. Dahle, 2016: Revisiting the contemporary sea-level budget on global and regional scales. *Proceedings of the National Academy of Sciences*, **113**, 1504-1509. <http://dx.doi.org/10.1073/pnas.1519132113>
7. Wada, Y., M.-H. Lo, P.J.F. Yeh, J.T. Reager, J.S. Famiglietti, R.-J. Wu, and Y.-H. Tseng, 2016: Fate of water pumped from underground and contributions to sea-level rise. *Nature Climate Change*, **6**, 777-780. <http://dx.doi.org/10.1038/nclimate3001>
8. Wada, Y., J.T. Reager, B.F. Chao, J. Wang, M.-H. Lo, C. Song, Y. Li, and A.S. Gardner, 2017: Recent changes in land water storage and its contribution to sea level variations. *Surveys in Geophysics*, **38**, 131-152. <http://dx.doi.org/10.1007/s10712-016-9399-6>
9. Boon, J.D., 2012: Evidence of sea level acceleration at U.S. and Canadian tide stations, Atlantic Coast, North America. *Journal of Coastal Research*, 1437-1445. <http://dx.doi.org/10.2112/JCOASTRES-D-12-00102.1>
10. Ezer, T., 2013: Sea level rise, spatially uneven and temporally unsteady: Why the U.S. East Coast, the global tide gauge record, and the global altimeter data show different trends. *Geophysical Research Letters*, **40**, 5439-5444. <http://dx.doi.org/10.1002/2013GL057952>
11. Sallenger, A.H., K.S. Doran, and P.A. Howd, 2012: Hotspot of accelerated sea-level rise on the Atlantic coast of North America. *Nature Climate Change*, **2**, 884-888. <http://dx.doi.org/10.1038/nclimate1597>
12. Yin, J. and P.B. Goddard, 2013: Oceanic control of sea level rise patterns along the East Coast of the United States. *Geophysical Research Letters*, **40**, 5514-5520. <http://dx.doi.org/10.1002/2013GL057992>
13. Mitrovica, J.X., N. Gomez, E. Morrow, C. Hay, K. Letychev, and M.E. Tamisiea, 2011: On the robustness of predictions of sea level fingerprints. *Geophysical Journal International*, **187**, 729-742. <http://dx.doi.org/10.1111/j.1365-246X.2011.05090.x>
14. Zervas, C., S. Gill, and W.V. Sweet, 2013: Estimating Vertical Land Motion From Long-term Tide Gauge Records. National Oceanic and Atmospheric Administration, National Ocean Service, 22 pp. https://tidesandcurrents.noaa.gov/publications/Technical_Report_NOS_CO-OPS_065.pdf
15. Wöppelmann, G. and M. Marcos, 2016: Vertical land motion as a key to understanding sea level change and variability. *Reviews of Geophysics*, **54**, 64-92. <http://dx.doi.org/10.1002/2015RG000502>
16. Bromirski, P.D., A.J. Miller, R.E. Flick, and G. Auad, 2011: Dynamical suppression of sea level rise along the Pacific coast of North America: Indications for imminent acceleration. *Journal of Geophysical Research*, **116**, C07005. <http://dx.doi.org/10.1029/2010JC006759>
17. Goddard, P.B., J. Yin, S.M. Griffies, and S. Zhang, 2015: An extreme event of sea-level rise along the Northeast coast of North America in 2009-2010. *Nature Communications*, **6**, 6346. <http://dx.doi.org/10.1038/ncomms7346>
18. Galloway, D., D.R. Jones, and S.E. Ingebritsen, 1999: Land Subsidence in the United States. U.S. Geological Survey, Reston, VA. 6 pp. <https://pubs.usgs.gov/circ/circ1182/>



19. Miller, K.G., M.A. Kominz, J.V. Browning, J.D. Wright, G.S. Mountain, M.E. Katz, P.J. Sugarman, B.S. Cramer, N. Christie-Blick, and S.F. Pekar, 2005: The Phanerozoic record of global sea-level change. *Science*, **310**, 1293-1298. <http://dx.doi.org/10.1126/science.1116412>
20. Dutton, A., A.E. Carlson, A.J. Long, G.A. Milne, P.U. Clark, R. DeConto, B.P. Horton, S. Rahmstorf, and M.E. Raymo, 2015: Sea-level rise due to polar ice-sheet mass loss during past warm periods. *Science*, **349**, aaa4019. <http://dx.doi.org/10.1126/science.aaa4019>
21. Hoffman, J.S., P.U. Clark, A.C. Parnell, and F. He, 2017: Regional and global sea-surface temperatures during the last interglaciation. *Science*, **355**, 276-279. <http://dx.doi.org/10.1126/science.aai8464>
22. Dutton, A. and K. Lambeck, 2012: Ice volume and sea level during the Last Interglacial. *Science*, **337**, 216-219. <http://dx.doi.org/10.1126/science.1205749>
23. Kopp, R.E., F.J. Simons, J.X. Mitrovica, A.C. Maloof, and M. Oppenheimer, 2009: Probabilistic assessment of sea level during the last interglacial stage. *Nature*, **462**, 863-867. <http://dx.doi.org/10.1038/nature08686>
24. Haywood, A.M., D.J. Hill, A.M. Dolan, B.L. Ot- to-Bliesner, F. Bragg, W.L. Chan, M.A. Chandler, C. Contoux, H.J. Dowsett, A. Jost, Y. Kamae, G. Lohmann, D.J. Lunt, A. Abe-Ouchi, S.J. Pickering, G. Ramstein, N.A. Rosenbloom, U. Salzmann, L. Sohl, C. Stepanek, H. Ueda, Q. Yan, and Z. Zhang, 2013: Large-scale features of Pliocene climate: Results from the Pliocene Model Intercomparison Project. *Climate of the Past*, **9**, 191-209. <http://dx.doi.org/10.5194/cp-9-191-2013>
25. Miller, K.G., J.D. Wright, J.V. Browning, A. Kulpecz, M. Kominz, T.R. Naish, B.S. Cramer, Y. Rosenthal, W.R. Peltier, and S. Sosdian, 2012: High tide of the warm Pliocene: Implications of global sea level for Antarctic deglaciation. *Geology*, **40**, 407-410. <http://dx.doi.org/10.1130/g32869.1>
26. Clark, P.U., A.S. Dyke, J.D. Shakun, A.E. Carlson, J. Clark, B. Wohlfarth, J.X. Mitrovica, S.W. Hostetler, and A.M. McCabe, 2009: The last glacial maximum. *Science*, **325**, 710-714. <http://dx.doi.org/10.1126/science.1172873>
27. Shennan, I., A.J. Long, and B.P. Horton, eds., 2015: *Handbook of Sea-Level Research*. John Wiley & Sons, Ltd, 581 pp. <http://dx.doi.org/10.1002/9781118452547>
28. Lambeck, K., H. Rouby, A. Purcell, Y. Sun, and M. Sambridge, 2014: Sea level and global ice volumes from the Last Glacial Maximum to the Holocene. *Proceedings of the National Academy of Sciences*, **111**, 15296-15303. <http://dx.doi.org/10.1073/pnas.1411762111>
29. Deschamps, P., N. Durand, E. Bard, B. Hamelin, G. Camoin, A.L. Thomas, G.M. Henderson, J.i. Okuno, and Y. Yokoyama, 2012: Ice-sheet collapse and sea-level rise at the Bolling warming 14,600 years ago. *Nature*, **483**, 559-564. <http://dx.doi.org/10.1038/nature10902>
30. Carlson, A.E., A.N. LeGrande, D.W. Oppo, R.E. Came, G.A. Schmidt, F.S. Anslow, J.M. Licciardi, and E.A. Obbink, 2008: Rapid early Holocene deglaciation of the Laurentide ice sheet. *Nature Geoscience*, **1**, 620-624. <http://dx.doi.org/10.1038/ngeo285>
31. Kemp, A.C., B.P. Horton, J.P. Donnelly, M.E. Mann, M. Vermeer, and S. Rahmstorf, 2011: Climate related sea-level variations over the past two millennia. *Proceedings of the National Academy of Sciences*, **108**, 11017-11022. <http://dx.doi.org/10.1073/pnas.1015619108>
32. Kopp, R.E., A.C. Kemp, K. Bittermann, B.P. Horton, J.P. Donnelly, W.R. Gehrels, C.C. Hay, J.X. Mitrovica, E.D. Morrow, and S. Rahmstorf, 2016: Temperature-driven global sea-level variability in the Common Era. *Proceedings of the National Academy of Sciences*, **113**, E1434-E1441. <http://dx.doi.org/10.1073/pnas.1517056113>
33. Hay, C.C., E. Morrow, R.E. Kopp, and J.X. Mitrovica, 2015: Probabilistic reanalysis of twentieth-century sea-level rise. *Nature*, **517**, 481-484. <http://dx.doi.org/10.1038/nature14093>
34. Church, J.A. and N.J. White, 2011: Sea-level rise from the late 19th to the early 21st century. *Surveys in Geophysics*, **32**, 585-602. <http://dx.doi.org/10.1007/s10712-011-9119-1>
35. Nerem, R.S., D.P. Chambers, C. Choe, and G.T. Mitchum, 2010: Estimating mean sea level change from the TOPEX and Jason altimeter missions. *Marine Geodesy*, **33**, 435-446. <http://dx.doi.org/10.1080/01490419.2010.491031>
36. Llovel, W., J.K. Willis, F.W. Landerer, and I. Fukumori, 2014: Deep-ocean contribution to sea level and energy budget not detectable over the past decade. *Nature Climate Change*, **4**, 1031-1035. <http://dx.doi.org/10.1038/nclimate2387>
37. Leuliette, E.W., 2015: The balancing of the sea-level budget. *Current Climate Change Reports*, **1**, 185-191. <http://dx.doi.org/10.1007/s40641-015-0012-8>
38. Merrifield, M.A., P. Thompson, E. Leuliette, G.T. Mitchum, D.P. Chambers, S. Jevrejeva, R.S. Nerem, M. Menéndez, W. Sweet, B. Hamlington, and J.J. Marra, 2015: [Global Oceans] Sea level variability and change [in "State of the Climate in 2014"]. *Bulletin of the American Meteorological Society*, **96** (12), S82-S85. <http://dx.doi.org/10.1175/2015BAMSStateoftheClimate.1>



39. Chambers, D.P., A. Cazenave, N. Champollion, H. Dieng, W. Llovel, R. Forsberg, K. von Schuckmann, and Y. Wada, 2017: Evaluation of the global mean sea level budget between 1993 and 2014. *Surveys in Geophysics*, **38**, 309–327. <http://dx.doi.org/10.1007/s10712-016-9381-3>
40. Leuliette, E.W. and R.S. Nerem, 2016: Contributions of Greenland and Antarctica to global and regional sea level change. *Oceanography*, **29**, 154–159. <http://dx.doi.org/10.5670/oceanog.2016.107>
41. Slangen, A.B.A., J.A. Church, C. Agosta, X. Fettweis, B. Marzeion, and K. Richter, 2016: Anthropogenic forcing dominates global mean sea-level rise since 1970. *Nature Climate Change*, **6**, 701–705. <http://dx.doi.org/10.1038/nclimate2991>
42. Jevrejeva, S., A. Grinsted, and J.C. Moore, 2009: Anthropogenic forcing dominates sea level rise since 1850. *Geophysical Research Letters*, **36**, L20706. <http://dx.doi.org/10.1029/2009GL040216>
43. Dangendorf, S., M. Marcos, A. Müller, E. Zorita, R. Riva, K. Berk, and J. Jensen, 2015: Detecting anthropogenic footprints in sea level rise. *Nature Communications*, **6**, 7849. <http://dx.doi.org/10.1038/ncomms8849>
44. Becker, M., M. Karpytchev, and S. Lennartz-Sassinek, 2014: Long-term sea level trends: Natural or anthropogenic? *Geophysical Research Letters*, **41**, 5571–5580. <http://dx.doi.org/10.1002/2014GL061027>
45. Marcos, M. and A. Amores, 2014: Quantifying anthropogenic and natural contributions to thermosteric sea level rise. *Geophysical Research Letters*, **41**, 2502–2507. <http://dx.doi.org/10.1002/2014GL059766>
46. Slangen, A.B.A., J.A. Church, X. Zhang, and D. Monselesan, 2014: Detection and attribution of global mean thermosteric sea level change. *Geophysical Research Letters*, **41**, 5951–5959. <http://dx.doi.org/10.1002/2014GL061356>
47. Marzeion, B., J.G. Cogley, K. Richter, and D. Parkes, 2014: Attribution of global glacier mass loss to anthropogenic and natural causes. *Science*, **345**, 919–921. <http://dx.doi.org/10.1126/science.1254702>
48. Marcos, M., B. Marzeion, S. Dangendorf, A.B.A. Slangen, H. Palanisamy, and L. Fenoglio-Marc, 2017: Internal variability versus anthropogenic forcing on sea level and its components. *Surveys in Geophysics*, **38**, 329–348. <http://dx.doi.org/10.1007/s10712-016-9373-3>
49. Zhang, X. and J.A. Church, 2012: Sea level trends, interannual and decadal variability in the Pacific Ocean. *Geophysical Research Letters*, **39**, L21701. <http://dx.doi.org/10.1029/2012GL053240>
50. Merrifield, M.A., 2011: A shift in western tropical Pacific sea level trends during the 1990s. *Journal of Climate*, **24**, 4126–4138. <http://dx.doi.org/10.1175/2011JCLI3932.1>
51. Hamlington, B.D., S.H. Cheon, P.R. Thompson, M.A. Merrifield, R.S. Nerem, R.R. Leben, and K.Y. Kim, 2016: An ongoing shift in Pacific Ocean sea level. *Journal of Geophysical Research Oceans*, **121**, 5084–5097. <http://dx.doi.org/10.1002/2016JC011815>
52. Kopp, R.E., 2013: Does the mid-Atlantic United States sea level acceleration hot spot reflect ocean dynamic variability? *Geophysical Research Letters*, **40**, 3981–3985. <http://dx.doi.org/10.1002/grl.50781>
53. Kopp, R.E., B.P. Horton, A.C. Kemp, and C. Tebaldi, 2015: Past and future sea-level rise along the coast of North Carolina, USA. *Climatic Change*, **132**, 693–707. <http://dx.doi.org/10.1007/s10584-015-1451-x>
54. Rahmstorf, S., J.E. Box, G. Feulner, M.E. Mann, A. Robinson, S. Rutherford, and E.J. Schaffernicht, 2015: Exceptional twentieth-century slowdown in Atlantic Ocean overturning circulation. *Nature Climate Change*, **5**, 475–480. <http://dx.doi.org/10.1038/nclimate2554>
55. Shepherd, A., E.R. Ivins, A. Geruo, V.R. Barletta, M.J. Bentley, S. Bettadpur, K.H. Briggs, D.H. Bromwich, R. Forsberg, N. Galin, M. Horwath, S. Jacobs, I. Joughin, M.A. King, J.T.M. Lenaerts, J. Li, S.R.M. Ligtenberg, A. Luckman, S.B. Luthcke, M. McMillan, R. Meister, G. Milne, J. Mouginot, A. Muir, J.P. Nicolas, J. Paden, A.J. Payne, H. Pritchard, E. Rignot, H. Rott, L. Sandberg Sørensen, T.A. Scambos, B. Scheuchl, E.J.O. Schrama, B. Smith, A.V. Sundal, J.H. van Angelen, W.J. van de Berg, M.R. van den Broeke, D.G. Vaughan, I. Velicogna, J. Wahr, P.L. Whitehouse, D.J. Wingham, D. Yi, D. Young, and H.J. Zwally, 2012: A reconciled estimate of ice-sheet mass balance. *Science*, **338**, 1183–1189. <http://dx.doi.org/10.1126/science.1228102>
56. Scambos, T. and C. Shuman, 2016: Comment on ‘Mass gains of the Antarctic ice sheet exceed losses’ by H. J. Zwally and others. *Journal of Glaciology*, **62**, 599–603. <http://dx.doi.org/10.1017/jog.2016.59>
57. Seo, K.-W., C.R. Wilson, T. Scambos, B.-M. Kim, D.E. Waliser, B. Tian, B.-H. Kim, and J. Eom, 2015: Surface mass balance contributions to acceleration of Antarctic ice mass loss during 2003–2013. *Journal of Geophysical Research Solid Earth*, **120**, 3617–3627. <http://dx.doi.org/10.1002/2014JB011755>
58. Martín-Español, A., A. Zammit-Mangion, P.J. Clarke, T. Flament, V. Helm, M.A. King, S.B. Luthcke, E. Petrie, F. Rémy, N. Schön, B. Wouters, and J.L. Bamber, 2016: Spatial and temporal Antarctic Ice Sheet mass trends, glacio-isostatic adjustment, and surface processes from a joint inversion of satellite altimeter, gravity, and GPS data. *Journal of Geophysical Research Earth Surface*, **121**, 182–200. <http://dx.doi.org/10.1002/2015JF003550>



59. Helm, V., A. Humbert, and H. Miller, 2014: Elevation and elevation change of Greenland and Antarctica derived from CryoSat-2. *The Cryosphere*, **8**, 1539-1559. <http://dx.doi.org/10.5194/tc-8-1539-2014>
60. Sutterley, T.C., I. Velicogna, E. Rignot, J. Mouginot, T. Flament, M.R. van den Broeke, J.M. van Wessem, and C.H. Reijmer, 2014: Mass loss of the Amundsen Sea embayment of West Antarctica from four independent techniques. *Geophysical Research Letters*, **41**, 8421-8428. <http://dx.doi.org/10.1002/2014GL061940>
61. Mouginot, J., E. Rignot, and B. Scheuchl, 2014: Sustained increase in ice discharge from the Amundsen Sea Embayment, West Antarctica, from 1973 to 2013. *Geophysical Research Letters*, **41**, 1576-1584. <http://dx.doi.org/10.1002/2013GL059069>
62. Khazendar, A., M.P. Schodlok, I. Fenty, S.R.M. Ligtenberg, E. Rignot, and M.R. van den Broeke, 2013: Observed thinning of Totten Glacier is linked to coastal polynya variability. *Nature Communications*, **4**, 2857. <http://dx.doi.org/10.1038/ncomms3857>
63. Li, X., E. Rignot, M. Morlighem, J. Mouginot, and B. Scheuchl, 2015: Grounding line retreat of Totten Glacier, East Antarctica, 1996 to 2013. *Geophysical Research Letters*, **42**, 8049-8056. <http://dx.doi.org/10.1002/2015GL065701>
64. Wouters, B., A. Martín-Español, V. Helm, T. Flament, J.M. van Wessem, S.R.M. Ligtenberg, M.R. van den Broeke, and J.L. Bamber, 2015: Dynamic thinning of glaciers on the Southern Antarctic Peninsula. *Science*, **348**, 899-903. <http://dx.doi.org/10.1126/science.aaa5727>
65. Paolo, F.S., H.A. Fricker, and L. Padman, 2015: Volume loss from Antarctic ice shelves is accelerating. *Science*, **348**, 327-331. <http://dx.doi.org/10.1126/science.aaa0940>
66. Khan, S.A., K.H. Kjaer, M. Bevis, J.L. Bamber, J. Wahr, K.K. Kjeldsen, A.A. Bjork, N.J. Korsgaard, L.A. Stearns, M.R. van den Broeke, L. Liu, N.K. Larsen, and I.S. Muresan, 2014: Sustained mass loss of the northeast Greenland ice sheet triggered by regional warming. *Nature Climate Change*, **4**, 292-299. <http://dx.doi.org/10.1038/nclimate2161>
67. Kjeldsen, K.K., N.J. Korsgaard, A.A. Bjørk, S.A. Khan, J.E. Box, S. Funder, N.K. Larsen, J.L. Bamber, W. Colgan, M. van den Broeke, M.-L. Siggaard-Andersen, C. Nuth, A. Schomacker, C.S. Andresen, E. Willerslev, and K.H. Kjaer, 2015: Spatial and temporal distribution of mass loss from the Greenland Ice Sheet since AD 1900. *Nature*, **528**, 396-400. <http://dx.doi.org/10.1038/nature16183>
68. Tedesco, M., X. Fettweis, T. Mote, J. Wahr, P. Alexander, J.E. Box, and B. Wouters, 2013: Evidence and analysis of 2012 Greenland records from spaceborne observations, a regional climate model and reanalysis data. *The Cryosphere*, **7**, 615-630. <http://dx.doi.org/10.5194/tc-7-615-2013>
69. Tedesco, M., S. Doherty, X. Fettweis, P. Alexander, J. Jeyaratnam, and J. Stroeve, 2016: The darkening of the Greenland ice sheet: Trends, drivers, and projections (1981–2100). *The Cryosphere*, **10**, 477-496. <http://dx.doi.org/10.5194/tc-10-477-2016>
70. MacGregor, J.A., W.T. Colgan, M.A. Fahnestock, M. Morlighem, G.A. Catania, J.D. Paden, and S.P. Gogineni, 2016: Holocene deceleration of the Greenland Ice Sheet. *Science*, **351**, 590-593. <http://dx.doi.org/10.1126/science.aab1702>
71. Sweet, W.V., R.E. Kopp, C.P. Weaver, J. Obeysekera, R.M. Horton, E.R. Thieler, and C. Zervas, 2017: Global and Regional Sea Level Rise Scenarios for the United States. National Oceanic and Atmospheric Administration, National Ocean Service, Silver Spring, MD. 75 pp. https://tidesandcurrents.noaa.gov/publications/techrpt83_Global_and_Regional_SLR_Scenarios_for_the_US_final.pdf
72. Pfeffer, W.T., J.T. Harper, and S. O'Neel, 2008: Kinematic constraints on glacier contributions to 21st-century sea-level rise. *Science*, **321**, 1340-1343. <http://dx.doi.org/10.1126/science.1159099>
73. Srivier, R.L., N.M. Urban, R. Olson, and K. Keller, 2012: Toward a physically plausible upper bound of sea-level rise projections. *Climatic Change*, **115**, 893-902. <http://dx.doi.org/10.1007/s10584-012-0610-6>
74. Bamber, J.L. and W.P. Aspinall, 2013: An expert judgement assessment of future sea level rise from the ice sheets. *Nature Climate Change*, **3**, 424-427. <http://dx.doi.org/10.1038/nclimate1778>
75. Miller, K.G., R.E. Kopp, B.P. Horton, J.V. Browning, and A.C. Kemp, 2013: A geological perspective on sea-level rise and its impacts along the U.S. mid-Atlantic coast. *Earth's Future*, **1**, 3-18. <http://dx.doi.org/10.1002/2013EF000135>
76. Kopp, R.E., R.M. Horton, C.M. Little, J.X. Mitrovica, M. Oppenheimer, D.J. Rasmussen, B.H. Strauss, and C. Tebaldi, 2014: Probabilistic 21st and 22nd century sea-level projections at a global network of tide-gauge sites. *Earth's Future*, **2**, 383-406. <http://dx.doi.org/10.1002/2014EF000239>
77. DeConto, R.M. and D. Pollard, 2016: Contribution of Antarctica to past and future sea-level rise. *Nature*, **531**, 591-597. <http://dx.doi.org/10.1038/nature17145>
78. Hall, J.A., S. Gill, J. Obeysekera, W. Sweet, K. Knutti, and J. Marburger, 2016: Regional Sea Level Scenarios for Coastal Risk Management: Managing the Uncertainty of Future Sea Level Change and Extreme Water Levels for Department of Defense Coastal Sites Worldwide. U.S. Department of Defense, Strategic Environmental Research and Development Program, Alexandria VA. 224 pp. <https://www.usfsp.edu/icar/files/2015/08/CARSWG-SLR-FINAL-April-2016.pdf>



79. Slangen, A.B.A., M. Carson, C.A. Katsman, R.S.W. van de Wal, A. Köhl, L.L.A. Vermeersen, and D. Stammer, 2014: Projecting twenty-first century regional sea-level changes. *Climatic Change*, **124**, 317-332. <http://dx.doi.org/10.1007/s10584-014-1080-9>
80. Jevrejeva, S., A. Grinsted, and J.C. Moore, 2014: Upper limit for sea level projections by 2100. *Environmental Research Letters*, **9**, 104008. <http://dx.doi.org/10.1088/1748-9326/9/10/104008>
81. Grinsted, A., S. Jevrejeva, R.E.M. Riva, and D. Dahl-Jensen, 2015: Sea level rise projections for northern Europe under RCP8.5. *Climate Research*, **64**, 15-23. <http://dx.doi.org/10.3354/cr01309>
82. Mengel, M., A. Levermann, K. Frieler, A. Robinson, B. Marzeion, and R. Winkelmann, 2016: Future sea level rise constrained by observations and long-term commitment. *Proceedings of the National Academy of Sciences*, **113**, 2597-2602. <http://dx.doi.org/10.1073/pnas.1500515113>
83. Jackson, L.P. and S. Jevrejeva, 2016: A probabilistic approach to 21st century regional sea-level projections using RCP and High-end scenarios. *Global and Planetary Change*, **146**, 179-189. <http://dx.doi.org/10.1016/j.gloplacha.2016.10.006>
84. Ritz, C., T.L. Edwards, G. Durand, A.J. Payne, V. Peyaud, and R.C.A. Hindmarsh, 2015: Potential sea-level rise from Antarctic ice-sheet instability constrained by observations. *Nature*, **528**, 115-118. <http://dx.doi.org/10.1038/nature16147>
85. Rahmstorf, S., 2007: A semi-empirical approach to projecting future sea-level rise. *Science*, **315**, 368-370. <http://dx.doi.org/10.1126/science.1135456>
86. Rignot, E., J. Mouginot, M. Morlighem, H. Seroussi, and B. Scheuchl, 2014: Widespread, rapid grounding line retreat of Pine Island, Thwaites, Smith, and Kohler Glaciers, West Antarctica, from 1992 to 2011. *Geophysical Research Letters*, **41**, 3502-3509. <http://dx.doi.org/10.1002/2014GL060140>
87. Joughin, I., B.E. Smith, and B. Medley, 2014: Marine ice sheet collapse potentially under way for the Thwaites Glacier Basin, West Antarctica. *Science*, **344**, 735-738. <http://dx.doi.org/10.1126/science.1249055>
88. Pollard, D., R.M. DeConto, and R.B. Alley, 2015: Potential Antarctic Ice Sheet retreat driven by hydrofracturing and ice cliff failure. *Earth and Planetary Science Letters*, **412**, 112-121. <http://dx.doi.org/10.1016/j.epsl.2014.12.035>
89. Levermann, A., P.U. Clark, B. Marzeion, G.A. Milne, D. Pollard, V. Radic, and A. Robinson, 2013: The multimillennial sea-level commitment of global warming. *Proceedings of the National Academy of Sciences*, **110**, 13745-13750. <http://dx.doi.org/10.1073/pnas.1219414110>
90. Golledge, N.R., D.E. Kowalewski, T.R. Naish, R.H. Levy, C.J. Fogwill, and E.G.W. Gasson, 2015: The multi-millennial Antarctic commitment to future sea-level rise. *Nature*, **526**, 421-425. <http://dx.doi.org/10.1038/nature15706>
91. Strauss, B.H., S. Kulp, and A. Levermann, 2015: Carbon choices determine US cities committed to futures below sea level. *Proceedings of the National Academy of Sciences*, **112**, 13508-13513. <http://dx.doi.org/10.1073/pnas.1511186112>
92. Irvine, P.J., D.J. Lunt, E.J. Stone, and A. Ridgwell, 2009: The fate of the Greenland Ice Sheet in a geo-engineered, high CO₂ world. *Environmental Research Letters*, **4**, 045109. <http://dx.doi.org/10.1088/1748-9326/4/4/045109>
93. Applegate, P.J. and K. Keller, 2015: How effective is albedo modification (solar radiation management geoengineering) in preventing sea-level rise from the Greenland Ice Sheet? *Environmental Research Letters*, **10**, 084018. <http://dx.doi.org/10.1088/1748-9326/10/8/084018>
94. Lenton, T.M., 2011: Early warning of climate tipping points. *Nature Climate Change*, **1**, 201-209. <http://dx.doi.org/10.1038/nclimate1143>
95. Barrett, S., T.M. Lenton, A. Millner, A. Tavoni, S. Carpenter, J.M. Anderies, F.S. Chapin, III, A.-S. Crepin, G. Daily, P. Ehrlich, C. Folke, V. Galaz, T. Hughes, N. Kautsky, E.F. Lambin, R. Naylor, K. Nyborg, S. Polasky, M. Scheffer, J. Wilen, A. Xepapadeas, and A. de Zeeuw, 2014: Climate engineering reconsidered. *Nature Climate Change*, **4**, 527-529. <http://dx.doi.org/10.1038/nclimate2278>
96. Markusson, N., F. Ginn, N. Singh Ghaleigh, and V. Scott, 2014: 'In case of emergency press here': Framing geoengineering as a response to dangerous climate change. *Wiley Interdisciplinary Reviews: Climate Change*, **5**, 281-290. <http://dx.doi.org/10.1002/wcc.263>
97. Sillmann, J., T.M. Lenton, A. Levermann, K. Ott, M. Hulme, F. Benduhn, and J.B. Horton, 2015: Climate emergencies do not justify engineering the climate. *Nature Climate Change*, **5**, 290-292. <http://dx.doi.org/10.1038/nclimate2539>
98. Clark, P.U., J.D. Shakun, S.A. Marcott, A.C. Mix, M. Eby, S. Kulp, A. Levermann, G.A. Milne, P.L. Pfister, B.D. Santer, D.P. Schrag, S. Solomon, T.F. Stocker, B.H. Strauss, A.J. Weaver, R. Winkelmann, D. Archer, E. Bard, A. Goldner, K. Lambeck, R.T. Pierrehumbert, and G.-K. Plattner, 2016: Consequences of twenty-first-century policy for multi-millennial climate and sea-level change. *Nature Climate Change*, **6**, 360-369. <http://dx.doi.org/10.1038/nclimate2923>



99. Gregory, J.M. and J.A. Lowe, 2000: Predictions of global and regional sea-level rise using AOGCMs with and without flux adjustment. *Geophysical Research Letters*, **27**, 3069-3072. <http://dx.doi.org/10.1029/1999GL011228>
100. Levermann, A., A. Griesel, M. Hofmann, M. Montoya, and S. Rahmstorf, 2005: Dynamic sea level changes following changes in the thermohaline circulation. *Climate Dynamics*, **24**, 347-354. <http://dx.doi.org/10.1007/s00382-004-0505-y>
101. Menéndez, M. and P.L. Woodworth, 2010: Changes in extreme high water levels based on a quasi-global tide-gauge data set. *Journal of Geophysical Research*, **115**, C10011. <http://dx.doi.org/10.1029/2009JC005997>
102. Kemp, A.C. and B.P. Horton, 2013: Contribution of relative sea-level rise to historical hurricane flooding in New York City. *Journal of Quaternary Science*, **28**, 537-541. <http://dx.doi.org/10.1002/jqs.2653>
103. Sweet, W.V., C. Zervas, S. Gill, and J. Park, 2013: Hurricane Sandy inundation probabilities of today and tomorrow [in "Explaining Extreme Events of 2012 from a Climate Perspective"]. *Bulletin of the American Meteorological Society*, **94** (9), S17-S20. <http://dx.doi.org/10.1175/BAMS-D-13-00085.1>
104. Sweet, W., J. Park, J. Marra, C. Zervas, and S. Gill, 2014: Sea Level Rise and Nuisance Flood Frequency Changes around the United States. NOAA Technical Report NOS CO-OPS 073. National Oceanic and Atmospheric Administration, National Ocean Service, Silver Spring, MD. 58 pp. http://tidesandcurrents.noaa.gov/publications/NOAA_Technical_Report_NOS_COOPS_073.pdf
105. Sweet, W.V. and J. Park, 2014: From the extreme to the mean: Acceleration and tipping points of coastal inundation from sea level rise. *Earth's Future*, **2**, 579-600. <http://dx.doi.org/10.1002/2014EF000272>
106. Ezer, T. and L.P. Atkinson, 2014: Accelerated flooding along the U.S. East Coast: On the impact of sea-level rise, tides, storms, the Gulf Stream, and the North Atlantic Oscillations. *Earth's Future*, **2**, 362-382. <http://dx.doi.org/10.1002/2014EF000252>
107. Talke, S.A., P. Orton, and D.A. Jay, 2014: Increasing storm tides in New York Harbor, 1844–2013. *Geophysical Research Letters*, **41**, 3149-3155. <http://dx.doi.org/10.1002/2014GL059574>
108. Wahl, T. and D.P. Chambers, 2015: Evidence for multidecadal variability in US extreme sea level records. *Journal of Geophysical Research Oceans*, **120**, 1527-1544. <http://dx.doi.org/10.1002/2014JC010443>
109. Reed, A.J., M.E. Mann, K.A. Emanuel, N. Lin, B.P. Horton, A.C. Kemp, and J.P. Donnelly, 2015: Increased threat of tropical cyclones and coastal flooding to New York City during the anthropogenic era. *Proceedings of the National Academy of Sciences*, **112**, 12610-12615. <http://dx.doi.org/10.1073/pnas.1513127112>
110. Grinsted, A., J.C. Moore, and S. Jevrejeva, 2013: Projected Atlantic hurricane surge threat from rising temperatures. *Proceedings of the National Academy of Sciences*, **110**, 5369-5373. <http://dx.doi.org/10.1073/pnas.1209980110>
111. Marcos, M., F.M. Calafat, Á. Berihuete, and S. Dangendorf, 2015: Long-term variations in global sea level extremes. *Journal of Geophysical Research Oceans*, **120**, 8115-8134. <http://dx.doi.org/10.1002/2015JC011173>
112. Woodworth, P.L. and M. Menéndez, 2015: Changes in the mesoscale variability and in extreme sea levels over two decades as observed by satellite altimetry. *Journal of Geophysical Research Oceans*, **120**, 64-77. <http://dx.doi.org/10.1002/2014JC010363>
113. Wahl, T. and D.P. Chambers, 2016: Climate controls multidecadal variability in U. S. extreme sea level records. *Journal of Geophysical Research Oceans*, **121**, 1274-1290. <http://dx.doi.org/10.1002/2015JC011057>
114. Mawdsley, R.J. and I.D. Haigh, 2016: Spatial and temporal variability and long-term trends in skew surges globally. *Frontiers in Marine Science*, **3**, Art. 26. <http://dx.doi.org/10.3389/fmars.2016.00029>
115. Sweet, W., M. Menendez, A. Genz, J. Obeysekera, J. Park, and J. Marra, 2016: In tide's way: Southeast Florida's September 2015 sunny-day flood [in "Explaining Extreme Events of 2015 from a Climate Perspective"]. *Bulletin of the American Meteorological Society*, **97** (12), S25-S30. <http://dx.doi.org/10.1175/BAMS-D-16-0117.1>
116. Feser, F., M. Barcikowska, O. Krueger, F. Schenk, R. Weisse, and L. Xia, 2015: Storminess over the North Atlantic and northwestern Europe—A review. *Quarterly Journal of the Royal Meteorological Society*, **141**, 350-382. <http://dx.doi.org/10.1002/qj.2364>
117. Colle, B.A., J.F. Booth, and E.K.M. Chang, 2015: A review of historical and future changes of extratropical cyclones and associated impacts along the US East Coast. *Current Climate Change Reports*, **1**, 125-143. <http://dx.doi.org/10.1007/s40641-015-0013-7>
118. Sweet, W.V. and C. Zervas, 2011: Cool-season sea level anomalies and storm surges along the U.S. East Coast: Climatology and comparison with the 2009/10 El Niño. *Monthly Weather Review*, **139**, 2290-2299. <http://dx.doi.org/10.1175/MWR-D-10-05043.1>
119. Thompson, P.R., G.T. Mitchum, C. Vonesch, and J. Li, 2013: Variability of winter storminess in the eastern United States during the twentieth century from tide gauges. *Journal of Climate*, **26**, 9713-9726. <http://dx.doi.org/10.1175/JCLI-D-12-00561.1>



120. Hamlington, B.D., R.R. Leben, K.Y. Kim, R.S. Nerem, L.P. Atkinson, and P.R. Thompson, 2015: The effect of the El Niño–Southern Oscillation on U.S. regional and coastal sea level. *Journal of Geophysical Research Oceans*, **120**, 3970-3986. <http://dx.doi.org/10.1002/2014JC010602>
121. Tebaldi, C., B.H. Strauss, and C.E. Zervas, 2012: Modelling sea level rise impacts on storm surges along US coasts. *Environmental Research Letters*, **7**, 014032. <http://dx.doi.org/10.1088/1748-9326/7/1/014032>
122. Horton, R.M., V. Gornitz, D.A. Bader, A.C. Ruane, R. Goldberg, and C. Rosenzweig, 2011: Climate hazard assessment for stakeholder adaptation planning in New York City. *Journal of Applied Meteorology and Climatology*, **50**, 2247-2266. <http://dx.doi.org/10.1175/2011JAMC2521.1>
123. Woodruff, J.D., J.L. Irish, and S.J. Camargo, 2013: Coastal flooding by tropical cyclones and sea-level rise. *Nature*, **504**, 44-52. <http://dx.doi.org/10.1038/nature12855>
124. Buchanan, M.K., R.E. Kopp, M. Oppenheimer, and C. Tebaldi, 2016: Allowances for evolving coastal flood risk under uncertain local sea-level rise. *Climatic Change*, **137**, 347-362. <http://dx.doi.org/10.1007/s10584-016-1664-7>
125. Dahl, K.A., M.F. Fitzpatrick, and E. Spanger-Siegfried, 2017: Sea level rise drives increased tidal flooding frequency at tide gauges along the U.S. East and Gulf Coasts: Projections for 2030 and 2045. *PLoS ONE*, **12**, e0170949. <http://dx.doi.org/10.1371/journal.pone.0170949>
126. Hunter, J., 2012: A simple technique for estimating an allowance for uncertain sea-level rise. *Climatic Change*, **113**, 239-252. <http://dx.doi.org/10.1007/s10584-011-0332-1>
127. Moftakhari, H.R., A. AghaKouchak, B.F. Sanders, D.L. Feldman, W. Sweet, R.A. Matthew, and A. Luke, 2015: Increased nuisance flooding along the coasts of the United States due to sea level rise: Past and future. *Geophysical Research Letters*, **42**, 9846-9852. <http://dx.doi.org/10.1002/2015GL066072>
128. Stockdon, H.F., R.A. Holman, P.A. Howd, and A.H. Sallenger, Jr., 2006: Empirical parameterization of setup, swash, and runup. *Coastal Engineering*, **53**, 573-588. <http://dx.doi.org/10.1016/j.coastaleng.2005.12.005>
129. Sweet, W.V., J. Park, S. Gill, and J. Marra, 2015: New ways to measure waves and their effects at NOAA tide gauges: A Hawaiian-network perspective. *Geophysical Research Letters*, **42**, 9355-9361. <http://dx.doi.org/10.1002/2015GL066030>
130. Moritz, H., K. White, B. Gouldby, W. Sweet, P. Ruggiero, M. Gravens, P. O'Brien, H. Moritz, T. Wahl, N.C. Nadal-Caraballo, and W. Veatch, 2015: USACE adaptation approach for future coastal climate conditions. *Proceedings of the Institution of Civil Engineers - Maritime Engineering*, **168**, 111-117. <http://dx.doi.org/10.1680/jmaen.15.00015>
131. Barnard, P.L., J. Allan, J.E. Hansen, G.M. Kaminsky, P. Ruggiero, and A. Doria, 2011: The impact of the 2009–10 El Niño Modoki on U.S. West Coast beaches. *Geophysical Research Letters*, **38**, L13604. <http://dx.doi.org/10.1029/2011GL047707>
132. Theuerkauf, E.J., A.B. Rodriguez, S.R. Fegley, and R.A. Luettich, 2014: Sea level anomalies exacerbate beach erosion. *Geophysical Research Letters*, **41**, 5139-5147. <http://dx.doi.org/10.1002/2014GL060544>
133. Serafin, K.A. and P. Ruggiero, 2014: Simulating extreme total water levels using a time-dependent, extreme value approach. *Journal of Geophysical Research Oceans*, **119**, 6305-6329. <http://dx.doi.org/10.1002/2014JC010093>
134. Hoeke, R.K., K.L. McInnes, J.C. Kruger, R.J. McNaught, J.R. Hunter, and S.G. Smithers, 2013: Widespread inundation of Pacific islands triggered by distant-source wind-waves. *Global and Planetary Change*, **108**, 128-138. <http://dx.doi.org/10.1016/j.gloplacha.2013.06.006>
135. Stopa, J.E. and K.F. Cheung, 2014: Periodicity and patterns of ocean wind and wave climate. *Journal of Geophysical Research Oceans*, **119**, 5563-5584. <http://dx.doi.org/10.1002/2013JC009729>
136. Barnard, P.L., A.D. Short, M.D. Harley, K.D. Splinter, S. Vitousek, I.L. Turner, J. Allan, M. Banno, K.R. Bryan, A. Doria, J.E. Hansen, S. Kato, Y. Kuriyama, E. Randall-Goodwin, P. Ruggiero, I.J. Walker, and DK Heathfield, 2015: Coastal vulnerability across the Pacific dominated by El Niño/Southern Oscillation. *Nature Geoscience*, **8**, 801-807. <http://dx.doi.org/10.1038/ngeo2539>
137. Bromirski, P.D., D.R. Cayan, J. Helly, and P. Witmann, 2013: Wave power variability and trends across the North Pacific. *Journal of Geophysical Research Oceans*, **118**, 6329-6348. <http://dx.doi.org/10.1002/2013JC009189>
138. Erikson, L.H., C.A. Hegermiller, P.L. Barnard, P. Ruggiero, and M. van Ormondt, 2015: Projected wave conditions in the Eastern North Pacific under the influence of two CMIP5 climate scenarios. *Ocean Modelling*, **96 (12)**, Part 1, 171-185. <http://dx.doi.org/10.1016/j.oceomod.2015.07.004>
139. Aucan, J., R. Hoeke, and M.A. Merrifield, 2012: Wave-driven sea level anomalies at the Midway tide gauge as an index of North Pacific storminess over the past 60 years. *Geophysical Research Letters*, **39**, L17603. <http://dx.doi.org/10.1029/2012GL052993>



140. Ruggiero, P., 2013: Is the intensifying wave climate of the U.S. Pacific Northwest increasing flooding and erosion risk faster than sea-level rise? *Journal of Waterway, Port, Coastal, and Ocean Engineering*, **139**, 88-97. [http://dx.doi.org/10.1061/\(ASCE\)WW.1943-5460.0000172](http://dx.doi.org/10.1061/(ASCE)WW.1943-5460.0000172)
141. Bromirski, P.D. and D.R. Cayan, 2015: Wave power variability and trends across the North Atlantic influenced by decadal climate patterns. *Journal of Geophysical Research Oceans*, **120**, 3419-3443. <http://dx.doi.org/10.1002/2014JC010440>
142. Bromirski, P.D. and J.P. Kossin, 2008: Increasing hurricane wave power along the U.S. Atlantic and Gulf coasts. *Journal of Geophysical Research*, **113**, C07012. <http://dx.doi.org/10.1029/2007JC004706>
143. Graham, N.E., D.R. Cayan, P.D. Bromirski, and R.E. Flick, 2013: Multi-model projections of twenty-first century North Pacific winter wave climate under the IPCC A2 scenario. *Climate Dynamics*, **40**, 1335-1360. <http://dx.doi.org/10.1007/s00382-012-1435-8>
144. Wang, X.L., Y. Feng, and V.R. Swail, 2014: Changes in global ocean wave heights as projected using multimodel CMIP5 simulations. *Geophysical Research Letters*, **41**, 1026-1034. <http://dx.doi.org/10.1002/2013GL058650>
145. Shope, J.B., C.D. Storlazzi, L.H. Erikson, and C.A. Hegermiller, 2016: Changes to extreme wave climates of islands within the western tropical Pacific throughout the 21st century under RCP 4.5 and RCP 8.5, with implications for island vulnerability and sustainability. *Global and Planetary Change*, **141**, 25-38. <http://dx.doi.org/10.1016/j.gloplacha.2016.03.009>
146. Colle, B.A., Z. Zhang, K.A. Lombardo, E. Chang, P. Liu, and M. Zhang, 2013: Historical evaluation and future prediction of eastern North American and western Atlantic extratropical cyclones in the CMIP5 models during the cool season. *Journal of Climate*, **26**, 6882-6903. <http://dx.doi.org/10.1175/JCLI-D-12-00498.1>
147. Zappa, G., L.C. Shaffrey, K.I. Hodges, P.G. Sansom, and D.B. Stephenson, 2013: A multimodel assessment of future projections of North Atlantic and European extratropical cyclones in the CMIP5 climate models. *Journal of Climate*, **26**, 5846-5862. <http://dx.doi.org/10.1175/jcli-d-12-00573.1>
148. Hall, T. and E. Yonekura, 2013: North American tropical cyclone landfall and SST: A statistical model study. *Journal of Climate*, **26**, 8422-8439. <http://dx.doi.org/10.1175/jcli-d-12-00756.1>
149. Lin, N., K. Emanuel, M. Oppenheimer, and E. Vanmarcke, 2012: Physically based assessment of hurricane surge threat under climate change. *Nature Climate Change*, **2**, 462-467. <http://dx.doi.org/10.1038/nclimate1389>
150. Little, C.M., R.M. Horton, R.E. Kopp, M. Oppenheimer, and S. Yip, 2015: Uncertainty in twenty-first-century CMIP5 sea level projections. *Journal of Climate*, **28**, 838-852. <http://dx.doi.org/10.1175/JCLI-D-14-00453.1>
151. Lin, N., R.E. Kopp, B.P. Horton, and J.P. Donnelly, 2016: Hurricane Sandy's flood frequency increasing from year 1800 to 2100. *Proceedings of the National Academy of Sciences*, **113**, 12071-12075. <http://dx.doi.org/10.1073/pnas.1604386113>
152. Smith, J.M., M.A. Cialone, T.V. Wamsley, and T.O. McAlpin, 2010: Potential impact of sea level rise on coastal surges in southeast Louisiana. *Ocean Engineering*, **37**, 37-47. <http://dx.doi.org/10.1016/j.oceaneng.2009.07.008>
153. Atkinson, J., J.M. Smith, and C. Bender, 2013: Sea-level rise effects on storm surge and nearshore waves on the Texas coast: Influence of landscape and storm characteristics. *Journal of Waterway, Port, Coastal, and Ocean Engineering*, **139**, 98-117. [http://dx.doi.org/10.1061/\(ASCE\)WW.1943-5460.0000187](http://dx.doi.org/10.1061/(ASCE)WW.1943-5460.0000187)
154. Bilskie, M.V., S.C. Hagen, S.C. Medeiros, and D.L. Passeri, 2014: Dynamics of sea level rise and coastal flooding on a changing landscape. *Geophysical Research Letters*, **41**, 927-934. <http://dx.doi.org/10.1002/2013GL058759>
155. Passeri, D.L., S.C. Hagen, S.C. Medeiros, M.V. Bilskie, K. Alizad, and D. Wang, 2015: The dynamic effects of sea level rise on low-gradient coastal landscapes: A review. *Earth's Future*, **3**, 159-181. <http://dx.doi.org/10.1002/2015EF000298>
156. Bilskie, M.V., S.C. Hagen, K. Alizad, S.C. Medeiros, D.L. Passeri, H.F. Needham, and A. Cox, 2016: Dynamic simulation and numerical analysis of hurricane storm surge under sea level rise with geomorphologic changes along the northern Gulf of Mexico. *Earth's Future*, **4**, 177-193. <http://dx.doi.org/10.1002/2015EF000347>
157. Knutson, T.R., J.J. Sirutis, G.A. Vecchi, S. Garner, M. Zhao, H.-S. Kim, M. Bender, R.E. Tuleya, I.M. Held, and G. Villarini, 2013: Dynamical downscaling projections of twenty-first-century Atlantic hurricane activity: CMIP3 and CMIP5 model-based scenarios. *Journal of Climate*, **27**, 6591-6617. <http://dx.doi.org/10.1175/jcli-d-12-00539.1>
158. Knutson, T.R., J.J. Sirutis, M. Zhao, R.E. Tuleya, M. Bender, G.A. Vecchi, G. Villarini, and D. Chavas, 2015: Global projections of intense tropical cyclone activity for the late twenty-first century from dynamical downscaling of CMIP5/RCP4.5 scenarios. *Journal of Climate*, **28**, 7203-7224. <http://dx.doi.org/10.1175/JCLI-D-15-0129.1>
159. Church, J.A. and N.J. White, 2006: A 20th century acceleration in global sea-level rise. *Geophysical Research Letters*, **33**, L01602. <http://dx.doi.org/10.1029/2005GL024826>



160. PSMSL, 2016: Obtaining tide gauge data. Permanent Service for Mean Sea Level. <http://www.psmsl.org/data/obtaining/>
161. Holgate, S.J., A. Matthews, P.L. Woodworth, L.J. Rickards, M.E. Tamisiea, E. Bradshaw, P.R. Foden, K.M. Gordon, S. Jevrejeva, and J. Pugh, 2013: New data systems and products at the Permanent Service for Mean Sea Level. *Journal of Coastal Research*, **29**, 493-504. <http://dx.doi.org/10.2112/JCOASTRES-D-12-00175.1>
162. Engelhart, S.E. and B.P. Horton, 2012: Holocene sea level database for the Atlantic coast of the United States. *Quaternary Science Reviews*, **54**, 12-25. <http://dx.doi.org/10.1016/j.quascirev.2011.09.013>
163. Farrell, W.E. and J.A. Clark, 1976: On postglacial sea level. *Geophysical Journal International*, **46**, 647-667. <http://dx.doi.org/10.1111/j.1365-246X.1976.tb01252.x>
164. Yin, J., M.E. Schlesinger, and R.J. Stouffer, 2009: Model projections of rapid sea-level rise on the northeast coast of the United States. *Nature Geoscience*, **2**, 262-266. <http://dx.doi.org/10.1038/ngeo462>
165. Sweet, W.V. and J.J. Marra, 2016: State of U.S. Nuisance Tidal Flooding. Supplement to State of the Climate: National Overview for May 2016. National Oceanic and Atmospheric Administration, National Centers for Environmental Information, 5 pp. <http://www.ncdc.noaa.gov/monitoring-content/sotc/national/2016/may/sweet-marra-nuisance-flooding-2015.pdf>
166. Wahl, T., S. Jain, J. Bender, S.D. Meyers, and M.E. Luther, 2015: Increasing risk of compound flooding from storm surge and rainfall for major US cities. *Nature Climate Change*, **5**, 1093-1097. <http://dx.doi.org/10.1038/nclimate2736>





13

Ocean Acidification and Other Ocean Changes

KEY FINDINGS

1. The world's oceans have absorbed about 93% of the excess heat caused by greenhouse gas warming since the mid-20th century, making them warmer and altering global and regional climate feedbacks. Ocean heat content has increased at all depths since the 1960s and surface waters have warmed by about $1.3^{\circ} \pm 0.1^{\circ}\text{F}$ ($0.7^{\circ} \pm 0.08^{\circ}\text{C}$) per century globally since 1900 to 2016. Under a higher scenario, a global increase in average sea surface temperature of $4.9^{\circ} \pm 1.3^{\circ}\text{F}$ ($2.7^{\circ} \pm 0.7^{\circ}\text{C}$) by 2100 is projected, with even higher changes in some U.S. coastal regions. (*Very high confidence*)
2. The potential slowing of the Atlantic meridional overturning circulation (AMOC; of which the Gulf Stream is one component) – as a result of increasing ocean heat content and freshwater driven buoyancy changes – could have dramatic climate feedbacks as the ocean absorbs less heat and CO_2 from the atmosphere. This slowing would also affect the climates of North America and Europe. Any slowing documented to date cannot be directly tied to anthropogenic forcing primarily due to lack of adequate observational data and to challenges in modeling ocean circulation changes. Under a higher scenario (RCP8.5) in CMIP5 simulations, the AMOC weakens over the 21st century by 12% to 54% (*low confidence*).
3. The world's oceans are currently absorbing more than a quarter of the CO_2 emitted to the atmosphere annually from human activities, making them more acidic (*very high confidence*), with potential detrimental impacts to marine ecosystems. In particular, higher-latitude systems typically have a lower buffering capacity against pH change, exhibiting seasonally corrosive conditions sooner than low-latitude systems. Acidification is regionally increasing along U.S. coastal systems as a result of upwelling (for example, in the Pacific Northwest) (*high confidence*), changes in freshwater inputs (for example, in the Gulf of Maine) (*medium confidence*), and nutrient input (for example, in agricultural watersheds and urbanized estuaries) (*high confidence*). The rate of acidification is unparalleled in at least the past 66 million years (*medium confidence*). Under the higher scenario (RCP8.5), the global average surface ocean acidity is projected to increase by 100% to 150% (*high confidence*).
4. Increasing sea surface temperatures, rising sea levels, and changing patterns of precipitation, winds, nutrients, and ocean circulation are contributing to overall declining oxygen concentrations at intermediate depths in various ocean locations and in many coastal areas. Over the last half century, major oxygen losses have occurred in inland seas, estuaries, and in the coastal and open ocean (*high confidence*). Ocean oxygen levels are projected to decrease by as much as 3.5% under the higher scenario (RCP8.5) by 2100 relative to preindustrial values (*high confidence*).

Recommended Citation for Chapter

Jewett, L. and A. Romanou, 2017: Ocean acidification and other ocean changes. In: *Climate Science Special Report: Fourth National Climate Assessment, Volume I* [Wuebbles, D.J., D.W. Fahey, K.A. Hibbard, D.J. Dokken, B.C. Stewart, and T.K. Maycock (eds.)]. U.S. Global Change Research Program, Washington, DC, USA, pp. 364-392, doi: 10.7930/J0QV3JQB.

13.0 A Changing Ocean

Anthropogenic perturbations to the global Earth system have included important alterations in the chemical composition, temperature, and circulation of the oceans. Some of these changes will be distinguishable from the background natural variability in nearly half of the global open ocean within a decade, with important consequences for marine ecosystems and their services.¹ However, the time-frame for detection will vary depending on the parameter featured.^{2,3}

13.1 Ocean Warming

13.1.1 General Background

Approximately 93% of excess heat energy trapped since the 1970s has been absorbed into the oceans, lessening atmospheric warming and leading to a variety of changes in ocean conditions, including sea level rise and ocean circulation (see Ch. 2: Physical Drivers of Climate Change, Ch. 6: Temperature Change, and Ch. 12: Sea Level Rise in this report).^{1,4} This is the result of the high heat capacity of seawater relative to the atmosphere, the relative area of the ocean compared to the land, and the ocean circulation that enables the transport of heat into deep waters. This large heat absorption by the oceans moderates the effects of increased anthropogenic greenhouse emissions on terrestrial climates while altering the fundamental physical properties of the ocean and indirectly impacting chemical properties such as the biological pump through increased stratification.^{1,5} Although upper ocean temperature varies over short- and medium timescales (for example, seasonal and regional patterns), there are clear long-term increases in surface temperature and ocean heat content over the past 65 years.^{4,6,7}

13.1.2 Ocean Heat Content

Ocean heat content (OHC) is an ideal variable to monitor changing climate as it is calculated using the entire water column, so ocean

warming can be documented and compared between particular regions, ocean basins, and depths. However, for years prior to the 1970s, estimates of ocean uptake are confined to the upper ocean (up to 700 m) due to sparse spatial and temporal coverage and limited vertical capabilities of many of the instruments in use. OHC estimates are improved for time periods after 1970 with increased sampling coverage and depth.^{4,8} Estimates of OHC have been calculated going back to the 1950s using averages over longer time intervals (i.e., decadal or 5-year intervals) to compensate for sparse data distributions, allowing for clear long-term trends to emerge (e.g., Levitus et al. 2012⁷).

From 1960 to 2015, OHC significantly increased for both 0–700 and 700–2,000 m depths, for a total ocean warming of about $33.5 \pm 7.0 \times 10^{22}$ J (a net heating of 0.37 ± 0.08 W/m²; Figure 13.1).⁶ During this period, there is evidence of an acceleration of ocean warming beginning in 1998,⁹ with a total heat increase of about 15.2×10^{22} J.⁶ Robust ocean warming occurs in the upper 700 m and is slow to penetrate into the deep ocean. However, the 700–2,000 m depths constitute an increasing portion of the total ocean energy budget as compared to the surface ocean (Figure 13.1).⁶ The role of the deep ocean (below 2,000 m [6,600 ft]) in ocean heat uptake remains uncertain, both in the magnitude but also the sign of the uptake.^{10,11} Penetration of surface waters to the deep ocean is a slow process, which means that while it takes only about a decade for near-surface temperatures to respond to increased heat energy, the deep ocean will continue to warm, and as a result sea levels will rise for centuries to millennia even if all further emissions cease.⁴



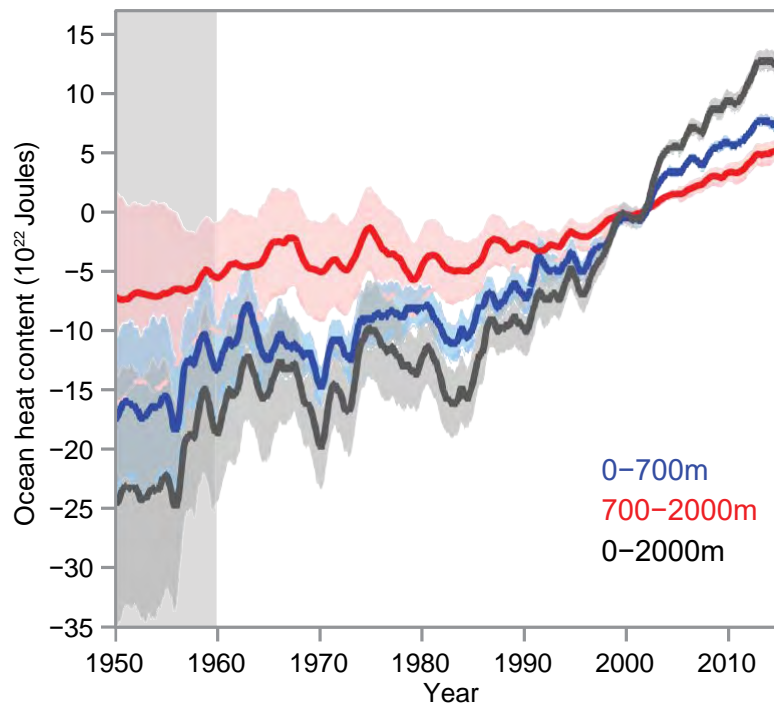


Figure 13.1: Global Ocean heat content change time series. Ocean heat content from 0 to 700 m (blue), 700 to 2,000 m (red), and 0 to 2,000 m (dark gray) from 1955 to 2015 with an uncertainty interval of ± 2 standard deviations shown in shading. All time series of the analysis performed by Cheng et al.⁶ are smoothed by a 12-month running mean filter, relative to the 1997–2005 base period. (Figure source: Cheng et al. 2017⁶).

Several sources have documented warming in all ocean basins from 0–2,000 m depths over the past 50 years (Figure 13.2).^{6,7,12} Annual fluctuations in surface temperatures and OHC are attributed to the combination of a long-term secular trend and decadal and smaller time scale variations, such as the Pacific Decadal Oscillation (PDO) and the Atlantic Multidecadal Oscillation (AMO) (Ch. 5: Circulation & Variability; Ch. 12: Sea Level Rise).^{13,14} The transport of heat to the deep ocean is likely linked to the strength of the Atlantic Meridional Overturning Circulation (see Section 13.2.1), where the Atlantic and Southern Ocean accounts for the dominant portion of total OHC change at the 700–2,000 m depth.^{6,8,9,15} Decadal variabil-

ity in ocean heat uptake is mostly attributed to ENSO phases (with El Niños warming and La Niñas cooling). For instance, La Niña conditions over the past decade have led to colder ocean temperatures in the eastern tropical Pacific.^{6,8,9,16} For the Pacific and Indian Oceans, the decadal shifts are primarily observed in the upper 350 m depth, likely due to shallow subtropical circulation, leading to an abrupt increase of OHC in the Indian Ocean carried by the Indonesian throughflow from the Pacific Ocean over the last decade.⁹ Although there is natural variability in ocean temperature, there remain clear increasing trends due to anthropogenic influences.



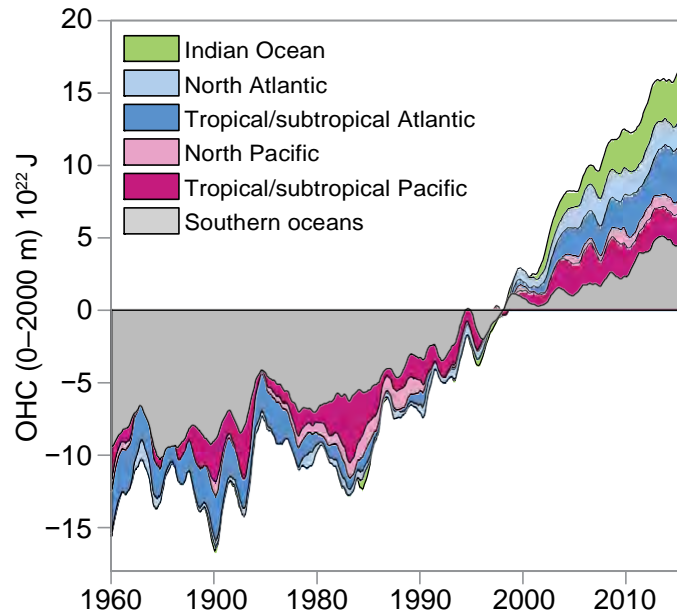


Figure 13.2: Ocean heat content changes from 1960 to 2015 for different ocean basins for 0 to 2,000 m depths. Time series is relative to the 1997–1999 base period and smoothed by a 12-month running filter by Cheng et al.⁶ The curves are additive, and the ocean heat content changes in different ocean basins are shaded in different colors (Figure source: Cheng et al. 2017⁶).

13.1.3 Sea Surface Temperature and U.S. Regional Warming

In addition to OHC, sea surface temperature (SST) measurements are widely available. SST measurements are useful because 1) the measurements have been taken over 150 years (albeit using different platforms, instruments, and depths through time); 2) SST reflects the lower boundary condition of the atmosphere; and 3) SST can be used to predict specific regional impacts of global warming on terrestrial and coastal systems.^{15, 17, 18} Globally, surface ocean temperatures have increased by $1.3^{\circ} \pm 0.1^{\circ}\text{F}$ ($0.70^{\circ} \pm 0.08^{\circ}\text{C}$) per century from 1900 to 2016 for the Extended Reconstructed Sea Surface Temperature version 4 (ERSST v4) record.¹⁹ All U.S. coastal waters have warmed by more than 0.7°F (0.4°C) over this period as shown in both Table 13.1 and Chapter 6: Temperature Change, Figure 6.6. During the past 60 years, the rates of increase of SSTs for the coastal waters of three U.S. regions were above the global average rate. These included the waters around Alaska, the Northeast, and the Southwest (Table 13.1). Over the last decade, some regions have experienced

increased high ocean temperature anomalies. SST in the Northeast has warmed faster than 99% of the global ocean since 2004, and a peak temperature for the region in 2012 was part of a large “ocean heat wave” in the Northwest Atlantic that persisted for nearly 18 months.^{20, 21} Projections indicate that the Northeast will continue to warm more quickly than other ocean regions through the end of the century.²² In the Northwest, a resilient ridge of high pressure over the North American West Coast suppressed storm activity and mixing, which intensified heat in the upper ocean in a phenomenon known as “The Blob”.²³ Anomalous warm waters persisted in the coastal waters of the Alaskan and Pacific Northwest from 2013 until 2015. Under a higher scenario (RCP8.5), SSTs are projected to increase by an additional 4.9°F (2.7°C) by 2100 (Figure 13.3), whereas for a lower scenario (RCP4.5) the SST increase would be 2.3°F (1.3°C).²⁴ In all U.S. coastal regions, the warming since 1901 is detectable compared to natural variability and attributable to anthropogenic forcing, according to an analysis of the CMIP5 models (Ch. 6: Temperature Change, Figure 6.5).

Table 13.1. Historical sea surface temperature trends (°C per century) and projected trends by 2080 (°C) for eight U.S. coastal regions and globally. Historical temperature trends are presented for the 1900–2016 and 1950–2016 periods with 95% confidence level, observed using the Extended Reconstructed Sea Surface Temperature version 4 (ERSSTv4).¹⁹ Global and regional predictions are calculated for lower and higher scenarios (RCP4.5 and RCP8.5, respectively) with 80% spread of all the CMIP5 members compared to the 1976–2005 period.¹⁵¹ The historical trends were analyzed for the latitude and longitude in the table, while the projected trends were analyzed for the California Current instead of the Northwest and Southwest separately and for the Bering Sea in Alaska (NOAA).

Region	Latitude and Longitude	Historical Trend (°C/100 years)		Projected Trend 2080 (relative to 1976–2005 climate) (°C)	
		1900–2016	1950–2016	RCP4.5	RCP8.5
Global		0.70 ± 0.08	1.00 ± 0.11	1.3 ± 0.6	2.7 ± 0.7
Alaska	50°–66°N, 150°–170°W	0.82 ± 0.26	1.22 ± 0.59	2.5 ± 0.6	3.7 ± 1.0
Northwest (NW)	40°–50°N, 120°–132°W	0.64 ± 0.30	0.68 ± 0.70	1.7 ± 0.4	2.8 ± 0.6
Southwest (SW)	30°–40°N, 116°–126°W	0.73 ± 0.33	1.02 ± 0.79		
Hawaii (HI)	18°–24°N, 152°–162°W	0.58 ± 0.19	0.46 ± 0.39	1.6 ± 0.4	2.8 ± 0.6
Northeast (NE)	36°–46°N, 64°–76°W	0.63 ± 0.31	1.10 ± 0.71	2.0 ± 0.3	3.2 ± 0.6
Southeast (SE)	24°–34°N, 64°–80°W	0.40 ± 0.18	0.13 ± 0.34	1.6 ± 0.3	2.7 ± 0.4
Gulf of Mexico (GOM)	20°–30°N, 80°–96°W	0.52 ± 0.14	0.37 ± 0.27	1.6 ± 0.3	2.8 ± 0.3
Caribbean	10°–20°N, 66°–86°W	0.76 ± 0.15	0.77 ± 0.32	1.5 ± 0.4	2.6 ± 0.3



CMIP5 ENSMN RCP8.5 Anomaly (2050–2099)–(1956–2005)

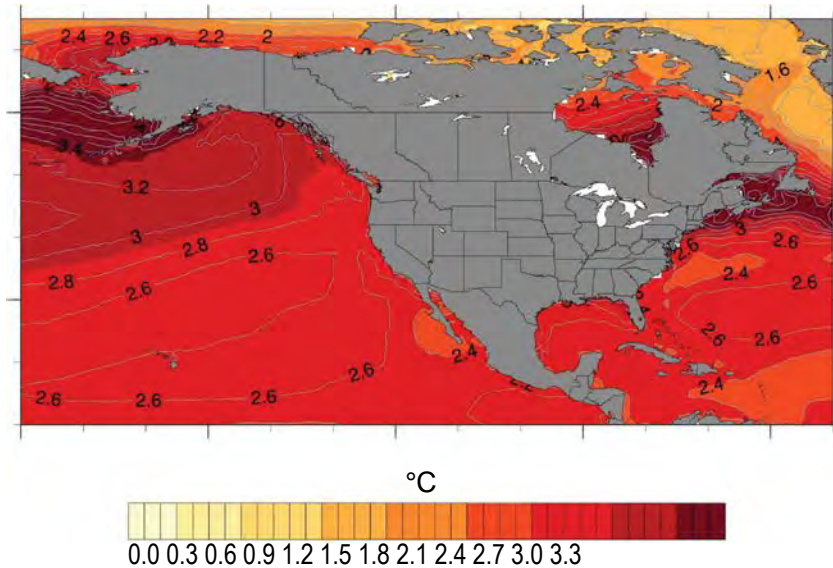


Figure 13.3: Projected changes in sea surface temperature (°C) for the coastal United States under the higher scenario (RCP8.5). Projected anomalies for the 2050–2099 period are calculated using a comparison from the average sea surface temperatures over 1956–2005. Projected changes are examined using the Coupled Model Intercomparison Project Phase 5 (CMIP5) suite of model simulations. (Figure source: NOAA).

13.1.4 Ocean Heat Feedback

The residual heat not taken up by the oceans increases land surface temperatures (approximately 3%) and atmospheric temperatures (approximately 1%), and melts both land and sea ice (approximately 3%), leading to sea level rise (see Ch. 12: Sea Level Rise).^{4, 6, 25} The meltwater from land and sea ice amplifies further subsurface ocean warming and ice shelf melting, primarily due to increased thermal stratification, which reduces the ocean’s efficiency in transporting heat to deep waters.⁴ Surface ocean stratification has increased by about 4% during the period 1971–2010²⁶ due to thermal heating and freshening from increased freshwater inputs (precipitation and evaporation changes and land and sea ice melting). The increase of ocean stratification will contribute to further feedback of ocean warming and, indirectly, mean sea level. In addition, increases in stratification are associated with suppression of tropical cyclone intensification,²⁷ retreat of the polar ice sheets,²⁸ and reductions of the convective mixing at higher latitudes that transports heat to the

deep ocean through the Atlantic Meridional Overturning Circulation.²⁹ Ocean heat uptake therefore represents an important feedback that will have a significant influence on future shifts in climate (see Ch. 2: Physical Drivers of Climate Change).

13.2 Ocean Circulation

13.2.1 Atlantic Meridional Overturning Circulation

The Atlantic Meridional Overturning Circulation (AMOC) refers to the three-dimensional, time-dependent circulation of the Atlantic Ocean, which has been a high priority topic of study in recent decades. The AMOC plays an important role in climate through its transport of heat, freshwater, and carbon (e.g., Johns et al. 2011;³⁰ McDonagh et al. 2015;³¹ Talley et al. 2016³²). AMOC-associated poleward heat transport substantially contributes to North American and continental European climate (see Ch. 5: Circulation and Variability). The Gulf Stream, in contrast to other western boundary currents, is expected to slow down because of the weakening of the AMOC, which would impact the Euro-

pean climate.³³ Variability in the AMOC has been attributed to wind forcing on intra-annual time scales and to geostrophic forces on interannual to decadal timescales.³⁴ Increased freshwater fluxes from melting Arctic Sea and land ice can weaken open ocean convection and deep-water formation in the Labrador and Irminger Seas, which could weaken the AMOC (Ch. 11: Arctic Changes; also see Ch. 5, Section 5.2.3: North Atlantic Oscillation and Northern Annular Mode).^{29,33}

While one recent study has suggested that the AMOC has slowed since preindustrial times²⁹ and another suggested slowing on faster time scales,³⁵ there is at present insufficient observational evidence to support a finding of long term slowdown of AMOC strength over the 20th century⁴ or within the last 50 years³⁴ as decadal ocean variability can obscure long-term trends. Some studies show long-term trends,^{36,37} but the combination of sparse data and large seasonal variability may also lead to incorrect interpretations (e.g., Kanzow et al. 2010³⁸). Several recent high resolution modeling studies constrained with the limited existing observational data³⁹ and/or with reconstructed freshwater fluxes⁴⁰ suggest that the recently observed AMOC slowdown at 26°N (off the Florida coast) since 2004 (e.g., as described in Smeed et al. 2014³⁵) is mainly due to natural variability, and that anthropogenic forcing has not yet caused a significant AMOC slowdown. In addition, direct observations of the AMOC in the South Atlantic fail to unambiguously demonstrate anthropogenic trends (e.g., Dong et al. 2015;⁴¹ Garzoli et al. 2013⁴²).

Under a higher scenario (RCP8.5) in CMIP5 simulations, it is very likely that the AMOC will weaken over the 21st century. The projected decline ranges from 12% to 54%,⁴³ with the range width reflecting substantial uncertainty in quantitative projections of AMOC behavior. In lower scenarios (like RCP4.5), CMIP5 mod-

els predict a 20% weakening of the AMOC during the first half of the 21st century and a stabilization and slight recovery after that.⁴⁴ The projected slowdown of the AMOC will be counteracted by the warming of the deep ocean (below 700 m [2,300 ft]), which will tend to strengthen the AMOC.⁴⁵ The situation is further complicated due to the known bias in coupled climate models related to the direction of the salinity transport in models versus observations, which is an indicator of AMOC stability (e.g., Drijhout et al. 2011;⁴⁶ Bryden et al. 2011;⁴⁷ Garzoli et al. 2013⁴²). Some argue that coupled climate models should be corrected for this known bias and that AMOC variations could be even larger than the gradual decrease most models predict if the AMOC were to shut down completely and “flip states”.⁴⁸ Any AMOC slowdown could result in less heat and CO₂ absorbed by the ocean from the atmosphere, which is a positive feedback to climate change (also see Ch. 2: Physical Drivers of Climate Change).^{49, 50, 51}

13.2.2 Changes in Salinity Structure

As a response to warming, increased atmospheric moisture leads to stronger evaporation or precipitation in terrestrial and oceanic environments and melting of land and sea ice. Approximately 80% of precipitation/evaporation events occur over the ocean, leading to patterns of higher salt content or freshwater anomalies and changes in ocean circulation (see Ch. 2: Physical Drivers of Climate Change and Ch. 6: Temperature Change).⁵² Over 1950–2010, average global amplification of the surface salinity pattern amounted to 5.3%; where fresh regions in the ocean became fresher and salty regions became saltier.⁵³ However, the long-term trends of these physical and chemical changes to the ocean are difficult to isolate from natural large-scale variability. In particular, ENSO displays particular salinity and precipitation/evaporation patterns that skew the trends. More research and data are neces-



sary to better model changes to ocean salinity. Several models have shown a similar spatial structure of surface salinity changes, including general salinity increases in the subtropical gyres, a strong basin-wide salinity increase in the Atlantic Ocean, and reduced salinity in the western Pacific warm pools and the North Pacific subpolar regions.^{52, 53} There is also a stronger distinction between the upper salty thermocline and fresh intermediate depth through the century. The regional changes in salinity to ocean basins will have an overall impact on ocean circulation and net primary production, leading to corresponding carbon export (see Ch. 2: Physical Drivers of Climate Change). In particular, the freshening of the Arctic Ocean due to melting of land and sea ice can lead to buoyancy changes which could slow down the AMOC (see Section 13.2.1).

13.2.3 Changes in Upwelling

Significant changes to ocean stratification and circulation can also be observed regionally, along the eastern ocean boundaries and at the equator. In these areas, wind-driven upwelling brings colder, nutrient- and carbon-rich water to the surface; this upwelled water is more efficient in heat and anthropogenic CO₂ uptake. There is some evidence that coastal upwelling in mid- to high-latitude eastern boundary regions has increased in intensity and/or frequency,⁵⁴ but in more tropical areas of the western Atlantic, such as in the Caribbean Sea, it has decreased between 1990 and 2010.^{55, 56} This has led to a decrease in primary productivity in the southern Caribbean Sea.⁵⁵ Within the continental United States, the California Current is experiencing fewer (by about 23%–40%) but stronger upwelling events.^{57, 58, 59} Stronger offshore upwelling combined with cross-shelf advection brings nutrients from the deeper ocean but also increased offshore transport.⁶⁰ The net nutrient load in the coastal regions is responsible for increased productivity and ecosystem function.

IPCC 2013 concluded that there is low confidence in the current understanding of how eastern upwelling systems will be altered under future climate change because of the obscuring role of multidecadal climate variability.²⁶ However, subsequent studies show that by 2100, upwelling is predicted to start earlier in the year, end later, and intensify in three of the four major eastern boundary upwelling systems (not in the California Current).⁶¹ In the California Current, upwelling is projected to intensify in spring but weaken in summer, with changes emerging from the envelope of natural variability primarily in the second half of the 21st century.⁶² Southern Ocean upwelling will intensify while the Atlantic equatorial upwelling systems will weaken.^{57, 61} The intensification is attributed to the strengthening of regional coastal winds as observations already show,⁵⁸ and model projections under the higher scenario (RCP8.5) estimate wind intensifying near poleward boundaries (including northern California Current) and weakening near equatorward boundaries (including southern California Current) for the 21st century.^{61, 63}

13.3 Ocean Acidification

13.3.1 General Background

In addition to causing changes in climate, increasing atmospheric levels of carbon dioxide (CO₂) from the burning of fossil fuels and other human activities, including changes in land use, have a direct effect on ocean carbonate chemistry that is termed ocean acidification.^{64, 65} Surface ocean waters absorb part of the increasing CO₂ in the atmosphere, which causes a variety of chemical changes in seawater: an increase in the partial pressure of CO₂ (pCO_{2,sw}), dissolved inorganic carbon (DIC), and the concentration of hydrogen and bicarbonate ions and a decrease in the concentration of carbonate ions (Figure 13.4). In brief, CO₂ is an acid gas that combines with water to form carbonic acid, which then dissociates



to hydrogen and bicarbonate ions. Increasing concentrations of seawater hydrogen ions result in a decrease of carbonate ions through their conversion to bicarbonate ions. The concentration of carbonate ions in seawater affects saturation states for calcium carbonate compounds, which many marine species use to build their shells and skeletons. Ocean acidity refers to the concentration of hydrogen ions in ocean seawater regardless of ocean pH, which is fundamentally basic (e.g., $\text{pH} > 7$). Ocean

surface waters have become 30% more acidic over the last 150 years as they have absorbed large amounts of CO_2 from the atmosphere,⁶⁶ and anthropogenically sourced CO_2 is gradually invading into oceanic deep waters. Since the preindustrial period, the oceans have absorbed approximately 29% of all CO_2 emitted to the atmosphere.⁶⁷ Oceans currently absorb about 26% of the human-caused CO_2 anthropogenically emitted into the atmosphere.⁶⁷

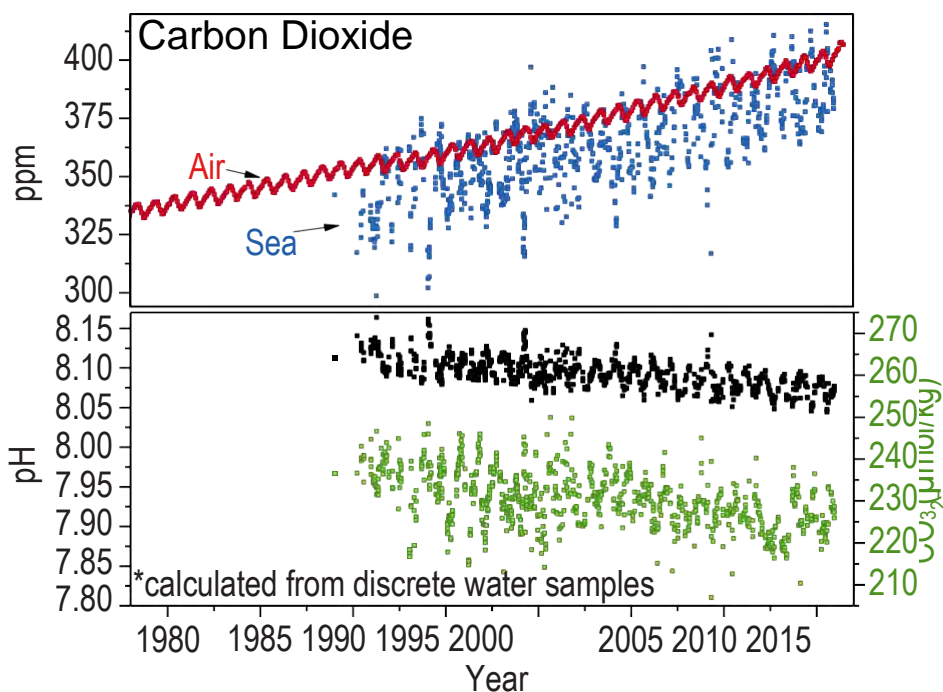


Figure 13.4: Trends in surface (< 50 m) ocean carbonate chemistry calculated from observations obtained at the Hawai'i Ocean Time-series (HOT) Program in the North Pacific over 1988–2015. The upper panel shows the linked increase in atmospheric (red points) and seawater (blue points) CO_2 concentrations. The bottom panel shows a decline in seawater pH (black points, primary y-axis) and carbonate ion concentration (green points, secondary y-axis). Ocean chemistry data were obtained from the Hawai'i Ocean Time-series Data Organization & Graphical System (HOT-DOGS, <http://hahana.soest.hawaii.edu/hot/hot-dogs/index.html>). (Figure source: NOAA).

13.3.2 Open Ocean Acidification

Surface waters in the open ocean experience changes in carbonate chemistry reflective of large-scale physical oceanic processes (see Ch. 2: Physical Drivers of Climate Change). These processes include both the global uptake of atmospheric CO₂ and the shoaling of naturally acidified subsurface waters due to vertical mixing and upwelling. In general, the rate of ocean acidification in open ocean surface waters at a decadal time-scale closely approximates the rate of atmospheric CO₂ increase.⁶⁸ Large, multidecadal phenomena such as the Atlantic Multidecadal Oscillation and Pacific Decadal Oscillation can add variability to the observed rate of change.⁶⁸

13.3.3 Coastal Acidification

Coastal shelf and nearshore waters are influenced by the same processes as open ocean surface waters such as absorption of atmospheric CO₂ and upwelling, as well as a number of additional, local-level processes, including freshwater, nutrient, sulfur, and nitrogen inputs.^{69,70} Coastal acidification generally exhibits higher-frequency variability and short-term episodic events relative to open-ocean acidification.^{71,72,73,74} Upwelling is of particular importance in coastal waters, especially along the U.S. West Coast. Deep waters that shoal with upwelling are enriched in CO₂ due to uptake of anthropogenic atmospheric CO₂ when last in contact with the atmosphere, coupled with deep water respiration processes and lack of gas exchange with the atmosphere.^{65,75} Freshwater inputs to coastal waters change seawater chemistry in ways that make it more susceptible to acidification, largely by freshening ocean waters and contributing varying amounts of dissolved inorganic carbon (DIC), total alkalinity (TA), dissolved and particulate organic carbon, and nutrients from riverine and estuarine sources. Coastal waters of the East Coast and mid-Atlantic are far more influenced by freshwater inputs than are Pacific

Coast waters.⁷⁶ Coastal waters can episodically experience riverine and glacial melt plumes that create conditions in which seawater can dissolve calcium carbonate structures.^{77,78} While these processes have persisted historically, climate-induced increases in glacial melt and high-intensity precipitation events can yield larger freshwater plumes than have occurred in the past. Nutrient runoff can increase coastal acidification by creating conditions that enhance biological respiration. In brief, nutrient loading typically promotes phytoplankton blooms, which, when they die, are consumed by bacteria. Bacteria respire CO₂ and thus bacterial blooms can result in acidification events whose intensity depends on local hydrographic conditions, including water column stratification and residence time.⁷² Long-term changes in nutrient loading, precipitation, and/or ice melt may also impart long-term, secular changes in the magnitude of coastal acidification.

13.3.4 Latitudinal Variation

Ocean carbon chemistry is highly influenced by water temperature, largely because the solubility of CO₂ in seawater increases as water temperature declines. Thus, cold, high-latitude surface waters can retain more CO₂ than warm, lower-latitude surface waters.^{76,79} Because carbonate minerals also more readily dissolve in colder waters, these waters can more regularly become undersaturated with respect to calcium carbonate whereby mineral dissolution is energetically favored. This chemical state, often referred to as seawater being “corrosive” to calcium carbonate, is important when considering the ecological implications of ocean acidification as many species make structures such as shells and skeletons from calcium carbonate. Seawater conditions undersaturated with respect to calcium carbonate are common at depth, but currently and historically rare at the surface and near-surface.⁸⁰ Some high-latitude surface



and near-surface waters now experience such corrosive conditions, which are rarely documented in low-latitude surface or near-surface systems. For example, corrosive conditions at a range of ocean depths have been documented in the Arctic and northeastern Pacific Oceans.^{74, 79, 81, 82} Storm-induced upwelling could cause undersaturation in tropical areas in the future.⁸³ It is important to note that low-latitude waters are experiencing a greater absolute rate of change in calcium carbonate saturation state than higher latitudes, though these low-latitude waters are not approaching the undersaturated state except within near-shore or some benthic habitats.⁸⁴

13.3.5 Paleo Evidence

Evidence suggests that the current rate of ocean acidification is the fastest in the last 66 million years (the K-Pg boundary) and possibly even the last 300 million years (when the first pelagic calcifiers evolved providing proxy information and also a strong carbonate buffer, characteristic of the modern ocean).^{85, 86} The Paleo-Eocene Thermal Maximum (PETM; around 56 million years ago) is often referenced as the closest analogue to the present, although the overall rate of change in CO₂ conditions during that event (estimated between 0.6 and 1.1 GtC/year) was much lower than the current increase in atmospheric CO₂ of 10 GtC/year.^{86, 87} The relatively slower rate of atmospheric CO₂ increase at the PETM likely led to relatively small changes in carbonate ion concentration in seawater compared with the contemporary acidification rate, due to the ability of rock weathering to buffer the change over the longer time period.⁸⁶ Some of the presumed acidification events in Earth's history have been linked to selective extinction events suggestive of how guilds of species may respond to the current acidification event.⁸⁵

13.3.6 Projected Changes

Projections indicate that by the end of the century under higher scenarios, such as SRES A1FI or RCP8.5, open-ocean surface pH will decline from the current average level of 8.1 to a possible average of 7.8 (Figure 13.5).¹ When the entire ocean volume is considered under the same scenario, the volume of waters undersaturated with respect to calcium carbonate could expand from 76% in the 1990s to 91% in 2100, resulting in a shallowing of the saturation horizons—depths below which undersaturation occurs.^{1, 88} Saturation horizons, which naturally vary among ocean basins, influence ocean carbon cycles and organisms with calcium carbonate structures, especially as they shoal into the zones where most biota lives.^{81, 89} As discussed above, for a variety of reasons, not all ocean and coastal regions will experience acidification in the same way depending on other compounding factors. For instance, recent observational data from the Arctic Basin show that the Beaufort Sea became undersaturated, for part of the year, with respect to aragonite in 2001, while other continental shelf seas in the Arctic Basin are projected to do so closer to the middle of the century (e.g., the Chukchi Sea in about 2033 and Bering Sea in about 2062).⁹⁰ Deviation from the global average rate of acidification will be especially true in coastal and estuarine areas where the rate of acidification is influenced by other drivers than atmospheric CO₂, some of which are under the control of local management decisions (for example, nutrient pollution loads).



Surface pH in 2090s (RCP8.5, changes from 1990s)

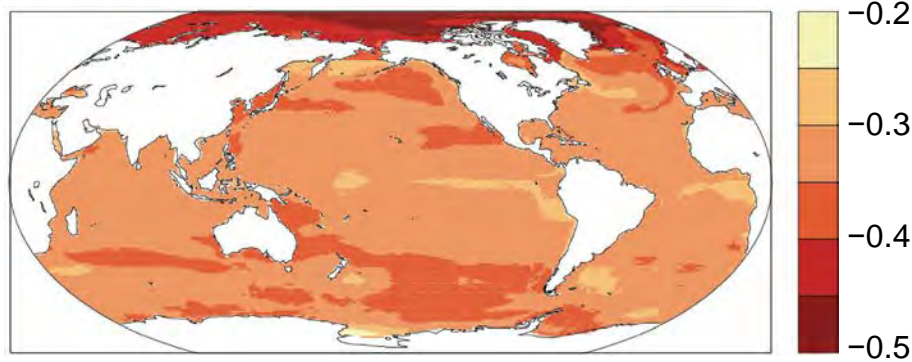


Figure 13.5: Predicted change in sea surface pH in 2090–2099 relative to 1990–1999 under the higher scenario (RCP8.5), based on the Community Earth System Models–Large Ensemble Experiments CMIP5 (Figure source: adapted from Bopp et al. 2013²⁴).

13.4 Ocean Deoxygenation

13.4.1 General Background

Oxygen is essential to most life in the ocean, governing a host of biogeochemical and biological processes. Oxygen influences metabolic, physiological, reproductive, behavioral, and ecological processes, ultimately shaping the composition, diversity, abundance, and distribution of organisms from microbes to whales. Increasingly, climate-induced oxygen loss (deoxygenation) associated with ocean warming and reduced ventilation to deep waters has become evident locally, regionally, and globally. Deoxygenation can also be attributed to anthropogenic nutrient input, especially in the coastal regions, where the nutrients can lead to the proliferation of primary production and, consequently, enhanced drawdown of dissolved oxygen by microbes.⁹¹ In addition, acidification (Section 13.2) can co-occur with deoxygenation as a result of warming-enhanced biological respiration.⁹² As aerobic organisms respire, O_2 is consumed and CO_2 is produced. Understanding the combined effect of both low O_2 and low pH on marine ecosystems is an area of active research.⁹³ Warming also raises biological metabolic rates which, in combination with intensified coastal and estuarine stratification, exacerbates eutrophication-induced hypoxia. We now see earlier

onset and longer periods of seasonal hypoxia in many eutrophic sites, most of which occur in areas that are also warming.⁹¹

13.4.2 Climate Drivers of Ocean Deoxygenation

Global ocean deoxygenation is a direct effect of warming. Ocean warming reduces the solubility of oxygen (that is, warmer water can hold less oxygen) and changes physical mixing (for example, upwelling and circulation) of oxygen in the oceans. The increased temperature of global oceans accounts for about 15% of current global oxygen loss,⁹⁴ although changes in temperature and oxygen are not uniform throughout the ocean.¹⁵ Warming also exerts direct influence on thermal stratification and enhances salinity stratification through ice melt and climate change-associated precipitation effects. Intensified stratification leads to reduced ventilation (mixing of oxygen into the ocean interior) and accounts for up to 85% of global ocean oxygen loss.⁹⁴ Effects of ocean temperature change and stratification on oxygen loss are strongest in intermediate or mode waters at bathyal depths (in general, 200–3,000 m) and also nearshore and in the open ocean; these changes are especially evident in tropical and subtropical waters globally, in the Eastern Pacific,⁹⁵ and in the Southern Ocean.⁹⁴

There are also other, less direct effects of global temperature increase. Warming on land reduces terrestrial plant water efficiency (through effects on stomata; see Ch. 8: Drought, Floods, and Wildfires, Key Message 3), leading to greater runoff, on average, into coastal zones (see Ch. 8: Drought, Floods, and Wildfires for other hydrological effects of warming) and further enhancing hypoxia potential because greater runoff can mean more nutrient transport (See Ch. 2: Physical Drivers of Climate Change).^{96, 97} Estuaries, especially ones with minimal tidal mixing, are particularly vulnerable to oxygen-depleted dead zones from the enhanced runoff and stratification. Warming can induce dissociation of frozen methane in gas hydrates buried on continental margins, leading to further drawdown of oxygen through aerobic methane oxidation in the water column.⁹⁸ On eastern ocean boundaries, warming can enhance the land–sea temperature differential, causing increased upwelling due to higher winds with (a) greater nutrient input leading to production, sinking, decay, and biochemical drawdown of oxygen and (b) upwelling of naturally low-oxygen, high-CO₂ waters onto the upper slope and shelf environments.^{58, 65} However, in the California Current, upwelling intensification has occurred only in the poleward regions (north of San Francisco), and the drivers may not be associated with land–sea temperature differences.⁶³ Taken together, the effects of warming are manifested as low-oxygen water in open oceans are being transported to and upwelled along coastal regions. These low-oxygen upwelled waters are then coupled with eutrophication-induced hypoxia, further reducing oxygen content in coastal areas.

Changes in precipitation, winds, circulation, airborne nutrients, and sea level can also contribute to ocean deoxygenation. Projected increases in precipitation in some regions will intensify stratification, reducing vertical

mixing and ventilation, and intensify nutrient input to coastal waters through excess runoff, which leads to increased algal biomass and concurrent dissolved oxygen consumption via community respiration.⁹⁹ Coastal wetlands that might remove these nutrients before they reach the ocean may be lost through rising sea level, further exacerbating hypoxia.⁹⁷ Some observations of oxygen decline are linked to regional changes in circulation involving low-oxygen water masses. Enhanced fluxes of airborne iron and nitrogen are interacting with natural climate variability and contributing to fertilization, enhanced respiration, and oxygen loss in the tropical Pacific.¹⁰⁰

13.4.3 Biogeochemical Feedbacks of Deoxygenation to Climate and Elemental Cycles

Climate patterns and ocean circulation have a large effect on global nitrogen and oxygen cycles, which in turn affect phosphorus and trace metal availability and generate feedbacks to the atmosphere and oceanic production. Global ocean productivity may be affected by climate-driven changes below the tropical and subtropical thermocline which control the volume of suboxic waters (< 5 micromolar O₂), and consequently the loss of fixed nitrogen through denitrification.^{101, 102} The extent of suboxia in the open ocean also regulates the production of the greenhouse gas nitrous oxide (N₂O); as oxygen declines, greater N₂O production may intensify global warming, as N₂O is about 310 times more effective at trapping heat than CO₂ (see Ch. 2: Physical Drivers of Climate Change, Section 2.3.2).^{103, 104} Production of hydrogen sulfide (H₂S, which is highly toxic) and intensified phosphorus recycling can occur at low oxygen levels.¹⁰⁵ Other feedbacks may emerge as oxygen minimum zone (OMZ) shoaling diminishes the depths of diurnal vertical migrations by fish and invertebrates, and as their huge biomass and associated oxygen consumption deplete oxygen.¹⁰⁶



13.4.4 Past Trends

Over hundreds of millions of years, oxygen has varied dramatically in the atmosphere and ocean and has been linked to biodiversity gains and losses.^{107, 108} Variation in oxygenation in the paleo record is very sensitive to climate – with clear links to temperature and often CO₂ variation.¹⁰⁹ OMZs expand and contract in synchrony with warming and cooling events, respectively.¹¹⁰ Episodic climate events that involve rapid temperature increases over decades, followed by a cool period lasting a few hundred years, lead to major fluctuations in the intensity of Pacific and Indian Ocean OMZs (i.e., DO of < 20 μM). These events are associated with rapid variations in North Atlantic deep water formation.¹¹¹ Ocean oxygen fluctuates on glacial-interglacial timescales of thousands of years in the Eastern Pacific.^{112, 113}

13.4.5 Modern Observations (last 50+ years)

Long-term oxygen records made over the last 50 years reflect oxygen declines in inland seas,^{114, 115, 116} in estuaries,^{117, 118} and in coastal waters.^{119, 120, 121, 122} The number of coastal, eutrophication-induced hypoxic sites in the United States has grown dramatically over the past 40 years.¹²³ Over larger scales, global syntheses show hypoxic waters have expanded by 4.5 million km² at a depth of 200 m,⁹⁵ with widespread loss of oxygen in the Southern

Ocean,⁹⁴ Western Pacific,¹²⁴ and North Atlantic.¹²⁵ Overall oxygen declines have been greater in coastal oceans than in the open ocean¹²⁶ and often greater inshore than offshore.¹²⁷ The emergence of a deoxygenation signal in regions with naturally high oxygen variability will unfold over longer time periods (20–50 years from now).¹²⁸

13.4.6 Projected Changes

Global Models

Global models generally agree that ocean deoxygenation is occurring; this finding is also reflected in in situ observations from past 50 years. Compilations of 10 Earth System models predict a global average loss of oxygen of –3.5% (higher scenario, RCP8.5) to –2.4% (lower scenario, RCP4.5) by 2100, but much stronger losses regionally, and in intermediate and mode waters (Figure 13.6).²⁴ The North Pacific, North Atlantic, Southern Ocean, subtropical South Pacific, and South Indian Oceans all are expected to experience deoxygenation, with O₂ decreases of as much as 17% in the North Pacific by 2100 for the RCP8.5 pathway. However, the tropical Atlantic and tropical Indian Oceans show increasing O₂ concentrations. In the many areas where oxygen is declining, high natural variability makes it difficult to identify anthropogenically forced trends.¹²⁸



Projected Change in Dissolved Oxygen

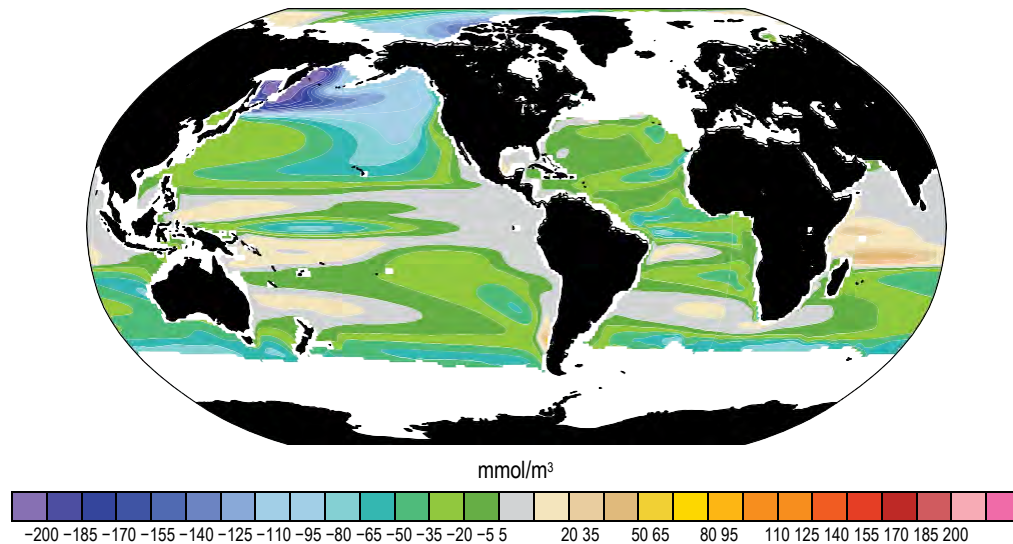


Figure 13.6: Predicted change in dissolved oxygen on the $\sigma_{\theta} = 26.5$ (average depth of approximately 290 m) potential density surface, between the 1981–2000 and 2081–2100, based on the Community Earth System Models–Large Ensemble Experiments (Figure source: redrawn from Long et al. 2016¹²⁸).

Regional Models

Regional models are critical because many oxygen drivers are local, influenced by bathymetry, winds, circulation, and fresh water and nutrient inputs. Most eastern boundary upwelling areas are predicted to experience intensified upwelling to 2100,⁶¹ although on the West Coast projections for increasing upwelling for the northern California Current occur only north of San Francisco (see Section 13.2.3).

Particularly notable for the western United States, variation in trade winds in the eastern Pacific Ocean can affect nutrient inputs, leading to centennial periods of oxygen decline or oxygen increase distinct from global oxygen decline.¹²⁹ Oxygen dynamics in the Eastern Tropical Pacific are highly sensitive to equatorial circulation changes.¹³⁰

Regional modeling also shows that year-to-year variability in precipitation in the central United States affects the nitrate–N flux by the Mississippi River and the extent of hypox-

ia in the Gulf of Mexico.¹³¹ A host of climate influences linked to warming and increased precipitation are predicted to lower dissolved oxygen in Chesapeake Bay.¹³²

13.5 Other Coastal Changes

13.5.1 Sea Level Rise

Sea level is an important variable that affects coastal ecosystems. Global sea level rose rapidly at the end of the last glaciation, as glaciers and the polar ice sheets thinned and melted at their fringes. On average around the globe, sea level is estimated to have risen at rates exceeding 2.5 mm/year between about 8,000 and 6,000 years before present. These rates steadily decreased to less than 2.0 mm/year through about 4,000 years ago and stabilized at less than 0.4 mm/year through the late 1800s. Global sea level rise has accelerated again within the last 100 years, and now averages about 1 to 2 mm/year.¹³³ See Chapter 12: Sea Level Rise for more thorough analysis of how sea level rise has already and will affect the U.S. coasts.

13.5.2 Wet and Dry Deposition

Dust transported from continental desert regions to the marine environment deposits nutrients such as iron, nitrogen, phosphorus, and trace metals that stimulate growth of phytoplankton and increase marine productivity.¹³⁴ U.S. continental and coastal regions experience large dust deposition fluxes originating from the Saharan desert to the East and from Central Asia and China to the Northwest.¹³⁵ Changes in drought frequency or intensity resulting from anthropogenically forced climate change, as well as other anthropogenic activities such as agricultural practices and land-use changes may play an important role in the future viability and strength of these dust sources (e.g., Mulitza et al. 2010¹³⁶).

Additionally, oxidized nitrogen, released during high-temperature combustion over land, and reduced nitrogen, released from intensive agriculture, are emitted in high population areas in North America and are carried away and deposited through wet or dry deposition over coastal and open ocean ecosystems via local wind circulation. Wet deposition of pollutants produced in urban areas is known to play an important role in changes of ecosystem structure in coastal and open ocean systems through intermediate changes in the biogeochemistry, for instance in dissolved oxygen or various forms of carbon.¹³⁷

13.5.3 Primary Productivity

Marine phytoplankton represent about half of the global net primary production (NPP) (approximately 50 ± 28 GtC / year), fixing atmospheric CO₂ into a bioavailable form for utilization by higher trophic levels (see also Ch. 2: Physical Drivers of Climate Change).¹³⁸ ¹³⁹ As such, NPP represents a critical component in the role of the oceans in climate feedback. The effect of climate change on primary productivity varies across the coasts depending on local conditions. For instance, nutrients

that stimulate phytoplankton growth are impacted by various climate conditions, such as increased stratification which limits the transport of nutrient-rich deep water to the surface, changes in circulation leading to variability in dry and wet deposition of nutrients to coasts, and altered precipitation/evaporation which changes runoff of nutrients from coastal communities. The effect of the multiple physical factors on NPP is complex and leads to model uncertainties.¹⁴⁰ There is considerable variation in model projections for NPP, from estimated decreases or no changes, to the potential increases by 2100.^{141, 142, 143} Simulations from nine Earth system models projected total NPP in 2090 to decrease by 2%–16% and export production (that is, particulate flux to the deep ocean) to drop by 7%–18% as compared to 1990 (RCP8.5).¹⁴² More information on phytoplankton species response and associated ecosystem dynamics is needed as any reduction of NPP and the associated export production would have an impact on carbon cycling and marine ecosystems.

13.5.4 Estuaries

Estuaries are critical ecosystems of biological, economic, and social importance in the United States. They are highly dynamic, influenced by the interactions of atmospheric, freshwater, terrestrial, oceanic, and benthic components. Of the 28 national estuarine research reserves in the United States and Puerto Rico, all are being impacted by climate change to varying levels.¹⁴⁴ In particular, sea level rise, saltwater intrusion, and the degree of freshwater discharge influence the forces and processes within these estuaries.¹⁴⁵ Sea level rise and subsidence are leading to drowning of existing salt marshes and/or subsequent changes in the relative area of the marsh plain, if adaptive upslope movement is impeded due to urbanization along shorelines. Several model scenarios indicate a decline in salt marsh habitat quality and an accelerated degradation as the



rate of sea level rise increases in the latter half of the century.^{146, 147} The increase in sea level as well as alterations to oceanic and atmospheric circulation can result in extreme wave conditions and storm surges, impacting coastal communities.¹⁴⁴ Additional climate change impacts to the physical and chemical estuarine processes include more extreme sea surface temperatures (higher highs and lower lows compared to the open ocean due to shallower depths and influence from land temperatures), changes in flow rates due to changes in precipitation, and potentially greater extents of salinity intrusion.



TRACEABLE ACCOUNTS

Key Finding 1

The world's oceans have absorbed about 93% of the excess heat caused by greenhouse gas warming since the mid-20th century, making them warmer and altering global and regional climate feedbacks. Ocean heat content has increased at all depths since the 1960s and surface waters have warmed by about $1.3^{\circ} \pm 0.1^{\circ}\text{F}$ ($0.7^{\circ} \pm 0.08^{\circ}\text{C}$) per century globally since 1900 to 2016. Under a higher scenario, a global increase in average sea surface temperature of $4.9^{\circ} \pm 1.3^{\circ}\text{F}$ ($2.7^{\circ} \pm 0.7^{\circ}\text{C}$) by 2100 is projected, with even higher changes in some U.S. coastal regions. (*Very high confidence*)

Description of evidence base

The key finding and supporting text summarizes the evidence documented in climate science literature, including Rhein et al. 2013.⁴ Oceanic warming has been documented in a variety of data sources, most notably the World Ocean Circulation Experiment (WOCE) (<http://www.nodc.noaa.gov/woce/wdiu/>) and Argo databases (<https://www.nodc.noaa.gov/argo/>) and Extended Reconstructed Sea Surface Temperature (ERSST) v4 (<https://www.ncdc.noaa.gov/data-access/marineocean-data/extended-reconstructed-sea-surface-temperature-ersst-v4>). There is particular confidence in calculated warming for the time period since 1971 due to increased spatial and depth coverage and the level of agreement among independent SST observations from satellites, surface drifters and ships, and independent studies using differing analyses, bias corrections, and data sources.^{6,7,11} Other observations such as the increase in mean sea level rise (see Ch. 12: Sea Level Rise) and reduced Arctic/Antarctic ice sheets (see Ch. 11: Arctic Changes) further confirm the increase in thermal expansion. For the purpose of extending the selected time periods back from 1900 to 2016 and analyzing U.S. regional SSTs, the ERSST version 4 (ERSSTv4)¹⁹ is used. For the centennial time scale changes over 1900–2016, warming trends in all regions are statistically significant with the 95% confidence level. U.S. regional SST warming is similar between calculations using ERSSTv4 in this report and those published by Belkin,¹⁴⁸ suggesting confidence in these findings. The projected increase in SST is based

on evidence from the latest generation of Earth System Models (CMIP5).

Major uncertainties

Uncertainties in the magnitude of ocean warming stem from the disparate measurements of ocean temperature over the last century. There is low uncertainty in warming trends of the upper ocean temperature from 0–700 m depth, whereas there is more uncertainty for deeper ocean depths of 700–2,000 m due to the short record of measurements from those areas. Data on warming trends at depths greater than 2,000 m are even more sparse. There are also uncertainties in the timing and reasons for particular decadal and interannual variations in ocean heat content and the contributions that different ocean basins play in the overall ocean heat uptake.

Summary sentence or paragraph that integrates the above information

There is *very high confidence* in measurements that show increases in the ocean heat content and warming of the ocean, based on the agreement of different methods. However, long-term data in total ocean heat uptake in the deep ocean are sparse leading to limited knowledge of the transport of heat between and within ocean basins.

Key Finding 2

The potential slowing of the Atlantic Meridional Overturning Circulation (AMOC; of which the Gulf Stream is one component)—as a result of increasing ocean heat content and freshwater driven buoyancy changes—could have dramatic climate feedbacks as the ocean absorbs less heat and CO₂ from the atmosphere.⁵¹ This slowing would also affect the climates of North America and Europe. Any slowing documented to date cannot be directly tied to anthropogenic forcing primarily due to lack of adequate observational data and to challenges in modeling ocean circulation changes. Under a higher scenario (RCP8.5) in CMIP5 simulations, the AMOC weakens over the 21st century by 12% to 54% (*low confidence*).



Description of evidence base

Investigations both through direct observations and models since 2013⁴ have raised significant concerns about whether there is enough evidence to determine the existence of an overall slowdown in the AMOC. As a result, more robust international observational campaigns are underway currently to measure AMOC circulation. Direct observations have determined a statistically significant slowdown at the 95% confidence level at 26°N (off Florida; see Baringer et al. 2016¹⁴⁹) but modeling studies constrained with observations cannot attribute this to anthropogenic forcing.³⁹ The study²⁹ which seemed to indicate broad-scale slowing has since been discounted due to its heavy reliance on sea surface temperature cooling as proxy for slowdown rather than actual direct observations. Since Rhein et al. 2013,⁴ more observations have led to increased statistical confidence in the measurement of the AMOC. Current observation trends indicate the AMOC slowing down at the 95% confidence level at 26°N and 41°N but a more limited in situ estimate at 35°S, shows an increase in the AMOC.^{35, 149} There is no one collection spot for AMOC-related data, but the U.S. Climate Variability and Predictability Program (US CLIVAR) has a U.S. AMOC priority focus area and a webpage with relevant data sites (<https://usclivar.org/amoc/amoc-time-series>).

The IPCC 2013 WG1 projections indicate a high likelihood of AMOC slowdown in the next 100 years, however overall understanding is limited by both a lack of direct observations (which is being remedied) and a lack of model skill to resolve deep ocean dynamics. As a result, this key finding was given an overall assessment of *low confidence*.

Major uncertainties

As noted, uncertainty about the overall trend of the AMOC is high given opposing trends in northern and southern ocean time series observations. Although earth system models do indicate a high likelihood of AMOC slowdown as a result of a warming, climate projections are subject to high uncertainty. This uncertainty stems from intermodel differences, internal variability that is different in each model, uncertainty in stratification changes, and most importantly uncer-

tainty in both future freshwater input at high latitudes as well as the strength of the subpolar gyre circulation.

Summary sentence or paragraph that integrates the above information

The increased focus on direct measurements of the AMOC should lead to a better understanding of 1) how it is changing and its variability by region, and 2) whether those changes are attributable to climate drivers through both model improvements and incorporation of those expanded observations into the models.

Key Finding 3

The world's oceans are currently absorbing more than a quarter of the CO₂ emitted to the atmosphere annually from human activities, making them more acidic (*very high confidence*), with potential detrimental impacts to marine ecosystems. In particular, higher-latitude systems typically have a lower buffering capacity against pH change, exhibiting seasonally corrosive conditions sooner than low-latitude systems. Acidification is regionally increasing along U.S. coastal systems as a result of upwelling (for example, in the Pacific Northwest) (*high confidence*), changes in freshwater inputs (for example, in the Gulf of Maine) (*medium confidence*), and nutrient input (for example, in agricultural watersheds and urbanized estuaries) (*high confidence*). The rate of acidification is unparalleled in at least the past 66 million years (*medium confidence*). Under the higher scenario (RCP8.5), the global average surface ocean acidity is projected to increase by 100% to 150% (*high confidence*).

Description of evidence base

Evidence on the magnitude of the ocean sink is obtained from multiple biogeochemical and transport ocean models and two observation-based estimates from the 1990s for the uptake of the anthropogenic CO₂. Estimates of the carbonate system (DIC and alkalinity) were based on multiple survey cruises in the global ocean in the 1990s (WOCE – now GO-SHIP, JGOFS). Coastal carbon and acidification surveys have been executed along the U.S. coastal large marine ecosystem since at least 2007, documenting significantly elevated pCO₂ and low pH conditions relative to oce-



anic waters. The data are available from the National Centers for Environmental Information (<https://www.ncei.noaa.gov/>). Other sources of biogeochemical bottle data can be found from HOT-DOGS ALOHA (<http://hahana.soest.hawaii.edu/hot/hot-dogs>) or CCHDO (<https://cchdo.ucsd.edu/>). Rates of change associated with the Palaeocene-Eocene Thermal Maximum (PETM, 56 million years ago) were derived using stable carbon and oxygen isotope records preserved in the sedimentary record from the New Jersey shelf using time series analysis and carbon cycle–climate modelling. This evidence supports a carbon release during the onset of the PETM over no less than 4,000 years, yielding a maximum sustained carbon release rate of less than 1.1 GtC per year.⁸⁶ The projected increase in global surface ocean acidity is based on evidence from ten of the latest generation earth system models which include six distinct biogeochemical models that were included in the latest IPCC AR5 2013.

Major uncertainties

In 2014 the ocean sink was 2.6 ± 0.5 GtC (9.5 GtCO₂), equivalent to 26% of the total emissions attributed to fossil fuel use and land use changes.⁶⁷ Estimates of the PETM ocean acidification event evidenced in the geological record remains a matter of some debate within the community. Evidence for the 1.1 GtC per year cited by Zeebe et al.,⁸⁶ could be biased as a result of brief pulses of carbon input above average rates of emissions were they to transpire over timescales $\lesssim 40$ years.

Summary sentence or paragraph that integrates the above information

There is *very high confidence* in evidence that the oceans absorb about a quarter of the carbon dioxide emitted in the atmosphere and hence become more acidic. The magnitude of the ocean carbon sink is known at a *high confidence* level because it is estimated using a series of disparate data sources and analysis methods, while the magnitude of the interannual variability is based only on model studies. There is *medium confidence* that the current rate of climate acidification is unprecedented in the past 66 million years. There is also *high confidence* that oceanic pH will continue to decrease.

Key Finding 4

Increasing sea surface temperatures, rising sea levels, and changing patterns of precipitation, winds, nutrients, and ocean circulation are contributing to overall declining oxygen concentrations at intermediate depths in various ocean locations and in many coastal areas. Over the last half century, major oxygen losses have occurred in inland seas, estuaries, and in the coastal and open ocean (*high confidence*). Ocean oxygen levels are projected to decrease by as much as 3.5% under the higher scenario (RCP8.5) by 2100 relative to preindustrial values (*high confidence*).

Description of evidence base

The key finding and supporting text summarizes the evidence documented in climate science literature including Rhein et al. 2013,⁴ Bopp et al. 2013,²⁴ and Schmidt et al. 2017.¹⁵⁰ Evidence arises from extensive global measurements of the WOCE after 1989 and individual profiles before that.⁹⁴ The first basin-wide dissolved oxygen surveys were performed in the 1920s.¹⁵⁰ The confidence level is based on globally integrated O₂ distributions in a variety of ocean models. Although the global mean exhibits low interannual variability, regional contrasts are large.

Major uncertainties

Uncertainties (as estimated from the intermodel spread) in the global mean are moderate mainly because ocean oxygen content exhibits low interannual variability when globally averaged. Uncertainties in long-term decreases of the global averaged oxygen concentration amount to 25% in the upper 1,000 m for the 1970–1992 period and 28% for the 1993–2003 period. Remaining uncertainties relate to regional variability driven by mesoscale eddies and intrinsic climate variability such as ENSO.

Summary sentence or paragraph that integrates the above information

Major ocean deoxygenation is taking place in bodies of water inland, at estuaries, and in the coastal and the open ocean (*high confidence*). Regionally, the phenomenon is exacerbated by local changes in weather, ocean circulation, and continental inputs to the oceans.



REFERENCES

1. Gattuso, J.-P., A. Magnan, R. Billé, W.W.L. Cheung, E.L. Howes, F. Joos, D. Allemand, L. Bopp, S.R. Cooley, C.M. Eakin, O. Hoegh-Guldberg, R.P. Kelly, H.-O. Pörtner, A.D. Rogers, J.M. Baxter, D. Laffoley, D. Osborn, A. Rankovic, J. Rochette, U.R. Sumaila, S. Treyer, and C. Turley, 2015: Contrasting futures for ocean and society from different anthropogenic CO₂ emissions scenarios. *Science*, **349**, aac4722. <http://dx.doi.org/10.1126/science.aac4722>
2. Henson, S.A., J.L. Sarmiento, J.P. Dunne, L. Bopp, I. Lima, S.C. Doney, J. John, and C. Beaulieu, 2010: Detection of anthropogenic climate change in satellite records of ocean chlorophyll and productivity. *Biogeosciences*, **7**, 621-640. <http://dx.doi.org/10.5194/bg-7-621-2010>
3. Henson, S.A., C. Beaulieu, and R. Lampitt, 2016: Observing climate change trends in ocean biogeochemistry: When and where. *Global Change Biology*, **22**, 1561-1571. <http://dx.doi.org/10.1111/gcb.13152>
4. Rhein, M., S.R. Rintoul, S. Aoki, E. Campos, D. Chambers, R.A. Feely, S. Gulev, G.C. Johnson, S.A. Josey, A. Kostianoy, C. Mauritzen, D. Roemmich, L.D. Talley, and F. Wang, 2013: Observations: Ocean. *Climate Change 2013: The Physical Science Basis. Contribution of Working Group I to the Fifth Assessment Report of the Intergovernmental Panel on Climate Change*. Stocker, T.F., D. Qin, G.-K. Plattner, M. Tignor, S.K. Allen, J. Boschung, A. Nauels, Y. Xia, V. Bex, and P.M. Midgley, Eds. Cambridge University Press, Cambridge, United Kingdom and New York, NY, USA, 255-316. <http://www.climatechange2013.org/report/full-report/>
5. Rossby, C.-G., 1959: Current problems in meteorology. *The Atmosphere and the Sea in Motion*. Bolin, B., Ed. Rockefeller Institute Press, New York, 9-50.
6. Cheng, L., K.E. Trenberth, J. Fasullo, T. Boyer, J. Abraham, and J. Zhu, 2017: Improved estimates of ocean heat content from 1960 to 2015. *Science Advances*, **3**, e1601545. <http://dx.doi.org/10.1126/sciadv.1601545>
7. Levitus, S., J.I. Antonov, T.P. Boyer, O.K. Baranova, H.E. Garcia, R.A. Locarnini, A.V. Mishonov, J.R. Reagan, D. Seidov, E.S. Yarosh, and M.M. Zweng, 2012: World ocean heat content and thermosteric sea level change (0–2000 m), 1955–2010. *Geophysical Research Letters*, **39**, L10603. <http://dx.doi.org/10.1029/2012GL051106>
8. Abraham, J.P., M. Baringer, N.L. Bindoff, T. Boyer, L.J. Cheng, J.A. Church, J.L. Conroy, C.M. Domingues, J.T. Fasullo, J. Gilson, G. Goni, S.A. Good, J.M. Gorman, V. Gouretski, M. Ishii, G.C. Johnson, S. Kizu, J.M. Lyman, A.M. Macdonald, W.J. Minkowycz, S.E. Moffitt, M.D. Palmer, A.R. Piola, F. Reseghetti, K. Schuckmann, K.E. Trenberth, I. Velicogna, and J.K. Willis, 2013: A review of global ocean temperature observations: Implications for ocean heat content estimates and climate change. *Reviews of Geophysics*, **51**, 450-483. <http://dx.doi.org/10.1002/rog.20022>
9. Lee, S.-K., W. Park, M.O. Baringer, A.L. Gordon, B. Huber, and Y. Liu, 2015: Pacific origin of the abrupt increase in Indian Ocean heat content during the warming hiatus. *Nature Geoscience*, **8**, 445-449. <http://dx.doi.org/10.1038/ngeo2438>
10. Purkey, S.G. and G.C. Johnson, 2010: Warming of global abyssal and deep Southern Ocean waters between the 1990s and 2000s: Contributions to global heat and sea level rise budgets. *Journal of Climate*, **23**, 6336-6351. <http://dx.doi.org/10.1175/2010JCLI3682.1>
11. Llovel, W., J.K. Willis, F.W. Landerer, and I. Fukumori, 2014: Deep-ocean contribution to sea level and energy budget not detectable over the past decade. *Nature Climate Change*, **4**, 1031-1035. <http://dx.doi.org/10.1038/nclimate2387>
12. Boyer, T., C.M. Domingues, S.A. Good, G.C. Johnson, J.M. Lyman, M. Ishii, V. Gouretski, J.K. Willis, J. Antonov, S. Wijffels, J.A. Church, R. Cowley, and N.L. Bindoff, 2016: Sensitivity of global upper-ocean heat content estimates to mapping methods, XBT bias corrections, and baseline climatologies. *Journal of Climate*, **29**, 4817-4842. <http://dx.doi.org/10.1175/jcli-d-15-0801.1>
13. Trenberth, K.E., J.T. Fasullo, and M.A. Balmaseda, 2014: Earth's energy imbalance. *Journal of Climate*, **27**, 3129-3144. <http://dx.doi.org/10.1175/jcli-d-13-00294.1>
14. Steinman, B.A., M.E. Mann, and S.K. Miller, 2015: Atlantic and Pacific Multidecadal Oscillations and Northern Hemisphere temperatures. *Science*, **347**, 988-991. <http://dx.doi.org/10.1126/science.1257856>
15. Roemmich, D., J. Church, J. Gilson, D. Monselesan, P. Sutton, and S. Wijffels, 2015: Unabated planetary warming and its ocean structure since 2006. *Nature Climate Change*, **5**, 240-245. <http://dx.doi.org/10.1038/nclimate2513>
16. Kosaka, Y. and S.-P. Xie, 2013: Recent global-warming hiatus tied to equatorial Pacific surface cooling. *Nature*, **501**, 403-407. <http://dx.doi.org/10.1038/nature12534>



17. Yan, X.-H., T. Boyer, K. Trenberth, T.R. Karl, S.-P. Xie, V. Nieves, K.-K. Tung, and D. Roemmich, 2016: The global warming hiatus: Slowdown or redistribution? *Earth's Future*, **4**, 472-482. <http://dx.doi.org/10.1002/2016EF000417>
18. Matthews, J.B.R., 2013: Comparing historical and modern methods of sea surface temperature measurement – Part 1: Review of methods, field comparisons and dataset adjustments. *Ocean Science*, **9**, 683-694. <http://dx.doi.org/10.5194/os-9-683-2013>
19. Huang, B., V.F. Banzon, E. Freeman, J. Lawrimore, W. Liu, T.C. Peterson, T.M. Smith, P.W. Thorne, S.D. Woodruff, and H.-M. Zhang, 2015: Extended Reconstructed Sea Surface Temperature Version 4 (ERSST.v4). Part I: Upgrades and intercomparisons. *Journal of Climate*, **28**, 911-930. <http://dx.doi.org/10.1175/JCLI-D-14-00006.1>
20. Pershing, A.J., M.A. Alexander, C.M. Hernandez, L.A. Kerr, A. Le Bris, K.E. Mills, J.A. Nye, N.R. Record, H.A. Scannell, J.D. Scott, G.D. Sherwood, and A.C. Thomas, 2015: Slow adaptation in the face of rapid warming leads to collapse of the Gulf of Maine cod fishery. *Science*, **350**, 809-812. <http://dx.doi.org/10.1126/science.aac9819>
21. Mills, K.E., A.J. Pershing, C.J. Brown, Y. Chen, F.-S. Chiang, D.S. Holland, S. Lehuta, J.A. Nye, J.C. Sun, A.C. Thomas, and R.A. Wahle, 2013: Fisheries management in a changing climate: Lessons from the 2012 ocean heat wave in the Northwest Atlantic. *Oceanography*, **26** (2), 191-195. <http://dx.doi.org/10.5670/oceanog.2013.27>
22. Saba, V.S., S.M. Griffies, W.G. Anderson, M. Winton, M.A. Alexander, T.L. Delworth, J.A. Hare, M.J. Harrison, A. Rosati, G.A. Vecchi, and R. Zhang, 2016: Enhanced warming of the Northwest Atlantic Ocean under climate change. *Journal of Geophysical Research Oceans*, **121**, 118-132. <http://dx.doi.org/10.1002/2015JC011346>
23. Bond, N.A., M.F. Cronin, H. Freeland, and N. Mantua, 2015: Causes and impacts of the 2014 warm anomaly in the NE Pacific. *Geophysical Research Letters*, **42**, 3414-3420. <http://dx.doi.org/10.1002/2015GL063306>
24. Bopp, L., L. Resplandy, J.C. Orr, S.C. Doney, J.P. Dunne, M. Gehlen, P. Halloran, C. Heinze, T. Ilyina, R. Séférian, J. Tjiputra, and M. Vichi, 2013: Multiple stressors of ocean ecosystems in the 21st century: Projections with CMIP5 models. *Biogeosciences*, **10**, 6225-6245. <http://dx.doi.org/10.5194/bg-10-6225-2013>
25. Nieves, V., J.K. Willis, and W.C. Patzert, 2015: Recent hiatus caused by decadal shift in Indo-Pacific heating. *Science*, **349**, 532-535. <http://dx.doi.org/10.1126/science.aaa4521>
26. Ciais, P., C. Sabine, G. Bala, L. Bopp, V. Brovkin, J. Canadell, A. Chhabra, R. DeFries, J. Galloway, M. Heimann, C. Jones, C. Le Quéré, R.B. Myneni, S. Piao, and P. Thornton, 2013: Carbon and other biogeochemical cycles. *Climate Change 2013: The Physical Science Basis. Contribution of Working Group I to the Fifth Assessment Report of the Intergovernmental Panel on Climate Change*. Stocker, T.F., D. Qin, G.-K. Plattner, M. Tignor, S.K. Allen, J. Boschung, A. Nauels, Y. Xia, V. Bex, and P.M. Midgley, Eds. Cambridge University Press, Cambridge, United Kingdom and New York, NY, USA, 465-570. <http://www.climatechange2013.org/report/full-report/>
27. Mei, W., S.-P. Xie, F. Primeau, J.C. McWilliams, and C. Pasquero, 2015: Northwestern Pacific typhoon intensity controlled by changes in ocean temperatures. *Science Advances*, **1**, e1500014. <http://dx.doi.org/10.1126/sciadv.1500014>
28. Straneo, F. and P. Heimbach, 2013: North Atlantic warming and the retreat of Greenland's outlet glaciers. *Nature*, **504**, 36-43. <http://dx.doi.org/10.1038/nature12854>
29. Rahmstorf, S., J.E. Box, G. Feulner, M.E. Mann, A. Robinson, S. Rutherford, and E.J. Schaffernicht, 2015: Exceptional twentieth-century slowdown in Atlantic Ocean overturning circulation. *Nature Climate Change*, **5**, 475-480. <http://dx.doi.org/10.1038/nclimate2554>
30. Johns, W.E., M.O. Baringer, L.M. Beal, S.A. Cunningham, T. Kanzow, H.L. Bryden, J.J.M. Hirschi, J. Marotzke, C.S. Meinen, B. Shaw, and R. Curry, 2011: Continuous, array-based estimates of Atlantic ocean heat transport at 26.5°N. *Journal of Climate*, **24**, 2429-2449. <http://dx.doi.org/10.1175/2010jcli3997.1>
31. McDonagh, E.L., B.A. King, H.L. Bryden, P. Courtois, Z. Szuts, M. Baringer, S.A. Cunningham, C. Atkinson, and G. McCarthy, 2015: Continuous estimate of Atlantic oceanic freshwater flux at 26.5°N. *Journal of Climate*, **28**, 8888-8906. <http://dx.doi.org/10.1175/jcli-d-14-00519.1>
32. Talley, L.D., R.A. Feely, B.M. Sloyan, R. Wanninkhof, M.O. Baringer, J.L. Bullister, C.A. Carlson, S.C. Doney, R.A. Fine, E. Firing, N. Gruber, D.A. Hansell, M. Ishii, G.C. Johnson, K. Katsumata, R.M. Key, M. Kramp, C. Langdon, A.M. Macdonald, J.T. Mathis, E.L. McDonagh, S. Mecking, F.J. Millero, C.W. Morry, T. Nakano, C.L. Sabine, W.M. Smethie, J.H. Swift, T. Tanhua, A.M. Thurnherr, M.J. Warner, and J.-Z. Zhang, 2016: Changes in ocean heat, carbon content, and ventilation: A review of the first decade of GO-SHIP global repeat hydrography. *Annual Review of Marine Science*, **8**, 185-215. <http://dx.doi.org/10.1146/annurev-marine-052915-100829>
33. Yang, H., G. Lohmann, W. Wei, M. Dima, M. Ionita, and J. Liu, 2016: Intensification and poleward shift of subtropical western boundary currents in a warming climate. *Journal of Geophysical Research Oceans*, **121**, 4928-4945. <http://dx.doi.org/10.1002/2015JC011513>

34. Buckley, M.W. and J. Marshall, 2016: Observations, inferences, and mechanisms of the Atlantic Meridional Overturning Circulation: A review. *Reviews of Geophysics*, **54**, 5-63. <http://dx.doi.org/10.1002/2015RG000493>
35. Smeed, D.A., G.D. McCarthy, S.A. Cunningham, E. Frajka-Williams, D. Rayner, W.E. Johns, C.S. Meinen, M.O. Baringer, B.I. Moat, A. Ducez, and H.L. Bryden, 2014: Observed decline of the Atlantic meridional overturning circulation 2004–2012. *Ocean Science*, **10**, 29-38. <http://dx.doi.org/10.5194/os-10-29-2014>
36. Longworth, H.R., H.L. Bryden, and M.O. Baringer, 2011: Historical variability in Atlantic meridional baroclinic transport at 26.5°N from boundary dynamic height observations. *Deep Sea Research Part II: Topical Studies in Oceanography*, **58**, 1754-1767. <http://dx.doi.org/10.1016/j.dsr2.2010.10.057>
37. Bryden, H.L., H.R. Longworth, and S.A. Cunningham, 2005: Slowing of the Atlantic meridional overturning circulation at 25°N. *Nature*, **438**, 655-657. <http://dx.doi.org/10.1038/nature04385>
38. Kanzow, T., S.A. Cunningham, W.E. Johns, J.J.-M. Hirschi, J. Marotzke, M.O. Baringer, C.S. Meinen, M.P. Chidichimo, C. Atkinson, L.M. Beal, H.L. Bryden, and J. Collins, 2010: Seasonal variability of the Atlantic meridional overturning circulation at 26.5°N. *Journal of Climate*, **23**, 5678-5698. <http://dx.doi.org/10.1175/2010jcli3389.1>
39. Jackson, L.C., K.A. Peterson, C.D. Roberts, and R.A. Wood, 2016: Recent slowing of Atlantic overturning circulation as a recovery from earlier strengthening. *Nature Geoscience*, **9**, 518-522. <http://dx.doi.org/10.1038/ngeo2715>
40. Böning, C.W., E. Behrens, A. Biastoch, K. Getzlaff, and J.L. Bamber, 2016: Emerging impact of Greenland meltwater on deepwater formation in the North Atlantic Ocean. *Nature Geoscience*, **9**, 523-527. <http://dx.doi.org/10.1038/ngeo2740>
41. Dong, S., G. Goni, and F. Bringas, 2015: Temporal variability of the South Atlantic Meridional Overturning Circulation between 20°S and 35°S. *Geophysical Research Letters*, **42**, 7655-7662. <http://dx.doi.org/10.1002/2015GL065603>
42. Garzoli, S.L., M.O. Baringer, S. Dong, R.C. Perez, and Q. Yao, 2013: South Atlantic meridional fluxes. *Deep Sea Research Part I: Oceanographic Research Papers*, **71**, 21-32. <http://dx.doi.org/10.1016/j.dsr.2012.09.003>
43. Collins, M., R. Knutti, J. Arblaster, J.-L. Dufresne, T. Fichefet, P. Friedlingstein, X. Gao, W.J. Gutowski, T. Johns, G. Krinner, M. Shongwe, C. Tebaldi, A.J. Weaver, and M. Wehner, 2013: Long-term climate change: Projections, commitments and irreversibility. *Climate Change 2013: The Physical Science Basis. Contribution of Working Group I to the Fifth Assessment Report of the Intergovernmental Panel on Climate Change*. Stocker, T.F., D. Qin, G.-K. Plattner, M. Tignor, S.K. Allen, J. Boschung, A. Nauels, Y. Xia, V. Bex, and P.M. Midgley, Eds. Cambridge University Press, Cambridge, United Kingdom and New York, NY, USA, 1029-1136. <http://www.climatechange2013.org/report/full-report/>
44. Cheng, W., J.C.H. Chiang, and D. Zhang, 2013: Atlantic Meridional Overturning Circulation (AMOC) in CMIP5 models: RCP and historical simulations. *Journal of Climate*, **26**, 7187-7197. <http://dx.doi.org/10.1175/jcli-d-12-00496.1>
45. Patara, L. and C.W. Böning, 2014: Abyssal ocean warming around Antarctica strengthens the Atlantic overturning circulation. *Geophysical Research Letters*, **41**, 3972-3978. <http://dx.doi.org/10.1002/2014GL059923>
46. Drijfhout, S.S., S.L. Weber, and E. van der Swaluw, 2011: The stability of the MOC as diagnosed from model projections for pre-industrial, present and future climates. *Climate Dynamics*, **37**, 1575-1586. <http://dx.doi.org/10.1007/s00382-010-0930-z>
47. Bryden, H.L., B.A. King, and G.D. McCarthy, 2011: South Atlantic overturning circulation at 24°S. *Journal of Marine Research*, **69**, 38-55. <http://dx.doi.org/10.1357/002224011798147633>
48. Liu, W., S.-P. Xie, Z. Liu, and J. Zhu, 2017: Overlooked possibility of a collapsed Atlantic Meridional Overturning Circulation in warming climate. *Science Advances*, **3**, e1601666. <http://dx.doi.org/10.1126/sciadv.1601666>
49. Zickfeld, K., M. Eby, and A.J. Weaver, 2008: Carbon-cycle feedbacks of changes in the Atlantic meridional overturning circulation under future atmospheric CO₂. *Global Biogeochemical Cycles*, **22**, GB3024. <http://dx.doi.org/10.1029/2007GB003118>
50. Halloran, P.R., B.B.B. Booth, C.D. Jones, F.H. Lambert, D.J. McNeall, I.J. Totterdell, and C. Völker, 2015: The mechanisms of North Atlantic CO₂ uptake in a large Earth System Model ensemble. *Biogeosciences*, **12**, 4497-4508. <http://dx.doi.org/10.5194/bg-12-4497-2015>
51. Romanou, A., J. Marshall, M. Kelley, and J. Scott, 2017: Role of the ocean's AMOC in setting the uptake efficiency of transient tracers. *Geophysical Research Letters*, **44**, 5590-5598. <http://dx.doi.org/10.1002/2017GL072972>



52. Durack, P.J. and S.E. Wijffels, 2010: Fifty-year trends in global ocean salinities and their relationship to broad-scale warming. *Journal of Climate*, **23**, 4342-4362. <http://dx.doi.org/10.1175/2010jcli3377.1>
53. Skliris, N., R. Marsh, S.A. Josey, S.A. Good, C. Liu, and R.P. Allan, 2014: Salinity changes in the World Ocean since 1950 in relation to changing surface freshwater fluxes. *Climate Dynamics*, **43**, 709-736. <http://dx.doi.org/10.1007/s00382-014-2131-7>
54. García-Reyes, M., W.J. Sydeman, D.S. Schoeman, R.R. Rykaczewski, B.A. Black, A.J. Smit, and S.J. Bograd, 2015: Under pressure: Climate change, upwelling, and eastern boundary upwelling ecosystems. *Frontiers in Marine Science*, **2**, Art. 109. <http://dx.doi.org/10.3389/fmars.2015.00109>
55. Taylor, G.T., F.E. Muller-Karger, R.C. Thunell, M.I. Scranton, Y. Astor, R. Varela, L.T. Ghinaglia, L. Lorenzoni, K.A. Fanning, S. Hameed, and O. Doherty, 2012: Ecosystem responses in the southern Caribbean Sea to global climate change. *Proceedings of the National Academy of Sciences*, **109**, 19315-19320. <http://dx.doi.org/10.1073/pnas.1207514109>
56. Astor, Y.M., L. Lorenzoni, R. Thunell, R. Varela, F. Muller-Karger, L. Troccoli, G.T. Taylor, M.I. Scranton, E. Tappa, and D. Rueda, 2013: Interannual variability in sea surface temperature and $f\text{CO}_2$ changes in the Cariaco Basin. *Deep Sea Research Part II: Topical Studies in Oceanography*, **93**, 33-43. <http://dx.doi.org/10.1016/j.dsr2.2013.01.002>
57. Hoegh-Guldberg, O., R. Cai, E.S. Poloczanska, P.G. Brewer, S. Sundby, K. Hilmi, V.J. Fabry, and S. Jung, 2014: The Ocean—Supplementary material. *Climate Change 2014: Impacts, Adaptation, and Vulnerability. Part B: Regional Aspects. Contribution of Working Group II to the Fifth Assessment Report of the Intergovernmental Panel of Climate Change*. Barros, V.R., C.B. Field, D.J. Dokken, M.D. Mastrandrea, K.J. Mach, T.E. Bilir, M. Chatterjee, K.L. Ebi, Y.O. Estrada, R.C. Genova, B. Girma, E.S. Kissel, A.N. Levy, S. MacCracken, P.R. Mastrandrea, and L.L. White, Eds. Cambridge University Press, Cambridge, United Kingdom and New York, NY, USA, 1655-1731. http://ipcc.ch/pdf/assessment-report/ar5/wg2/supplementary/WGI-IAR5-Chap30_OLSM.pdf
58. Sydeman, W.J., M. García-Reyes, D.S. Schoeman, R.R. Rykaczewski, S.A. Thompson, B.A. Black, and S.J. Bograd, 2014: Climate change and wind intensification in coastal upwelling ecosystems. *Science*, **345**, 77-80. <http://dx.doi.org/10.1126/science.1251635>
59. Jacox, M.G., A.M. Moore, C.A. Edwards, and J. Fiechter, 2014: Spatially resolved upwelling in the California Current System and its connections to climate variability. *Geophysical Research Letters*, **41**, 3189-3196. <http://dx.doi.org/10.1002/2014GL059589>
60. Bakun, A., B.A. Black, S.J. Bograd, M. García-Reyes, A.J. Miller, R.R. Rykaczewski, and W.J. Sydeman, 2015: Anticipated effects of climate change on coastal upwelling ecosystems. *Current Climate Change Reports*, **1**, 85-93. <http://dx.doi.org/10.1007/s40641-015-0008-4>
61. Wang, D., T.C. Gouhier, B.A. Menge, and A.R. Gan-guly, 2015: Intensification and spatial homogenization of coastal upwelling under climate change. *Nature*, **518**, 390-394. <http://dx.doi.org/10.1038/nature14235>
62. Brady, R.X., M.A. Alexander, N.S. Lovenduski, and R.R. Rykaczewski, 2017: Emergent anthropogenic trends in California Current upwelling. *Geophysical Research Letters*, **44**, 5044-5052. <http://dx.doi.org/10.1002/2017GL072945>
63. Rykaczewski, R.R., J.P. Dunne, W.J. Sydeman, M. García-Reyes, B.A. Black, and S.J. Bograd, 2015: Poleward displacement of coastal upwelling-favorable winds in the ocean's eastern boundary currents through the 21st century. *Geophysical Research Letters*, **42**, 6424-6431. <http://dx.doi.org/10.1002/2015GL064694>
64. Orr, J.C., V.J. Fabry, O. Aumont, L. Bopp, S.C. Doney, R.A. Feely, A. Gnanadesikan, N. Gruber, A. Ishida, F. Joos, R.M. Key, K. Lindsay, E. Maier-Reimer, R. Matear, P. Monfray, A. Mouchet, R.G. Najjar, G.-K. Plattner, K.B. Rodgers, C.L. Sabine, J.L. Sarmiento, R. Schlitzer, R.D. Slater, I.J. Totterdell, M.-F. Weirig, Y. Yamanaka, and A. Yool, 2005: Anthropogenic ocean acidification over the twenty-first century and its impact on calcifying organisms. *Nature*, **437**, 681-686. <http://dx.doi.org/10.1038/nature04095>
65. Feely, R.A., S.C. Doney, and S.R. Cooley, 2009: Ocean acidification: Present conditions and future changes in a high- CO_2 world. *Oceanography*, **22**, 36-47. <http://dx.doi.org/10.5670/oceanog.2009.95>
66. Feely, R.A., C.L. Sabine, K. Lee, W. Berelson, J. Kley-pas, V.J. Fabry, and F.J. Millero, 2004: Impact of anthropogenic CO_2 on the CaCO_3 system in the oceans. *Science*, **305**, 362-366. <http://dx.doi.org/10.1126/science.1097329>



67. Le Quéré, C., R.M. Andrew, J.G. Canadell, S. Sitch, J.I. Korsbakken, G.P. Peters, A.C. Manning, T.A. Boden, P.P. Tans, R.A. Houghton, R.F. Keeling, S. Alin, O.D. Andrews, P. Anthoni, L. Barbero, L. Bopp, F. Chevallier, L.P. Chini, P. Ciais, K. Currie, C. Delire, S.C. Doney, P. Friedlingstein, T. Gkritzalis, I. Harris, J. Hauck, V. Haverd, M. Hoppema, K. Klein Goldewijk, A.K. Jain, E. Kato, A. Körtzinger, P. Landschützer, N. Lefèvre, A. Lenton, S. Lienert, D. Lombardozzi, J.R. Melton, N. Metzl, F. Millero, P.M.S. Monteiro, D.R. Munro, J.E.M.S. Nabel, S.I. Nakaoka, K. O'Brien, A. Olsen, A.M. Omar, T. Ono, D. Pierrot, B. Poulter, C. Rödenbeck, J. Salisbury, U. Schuster, J. Schwinger, R. Séférian, I. Skjelvan, B.D. Stocker, A.J. Sutton, T. Takahashi, H. Tian, B. Tilbrook, I.T. van der Laan-Luijk, G.R. van der Werf, N. Viovy, A.P. Walker, A.J. Wiltshire, and S. Zaehle, 2016: Global carbon budget 2016. *Earth System Science Data*, **8**, 605-649. <http://dx.doi.org/10.5194/essd-8-605-2016>
68. Bates, N.R., Y.M. Astor, M.J. Church, K. Currie, J.E. Dore, M. González-Dávila, L. Lorenzoni, F. Muller-Karger, J. Olafsson, and J.M. Santana-Casiano, 2014: A time-series view of changing ocean chemistry due to ocean uptake of anthropogenic CO₂ and ocean acidification. *Oceanography*, **27**, 126-141. <http://dx.doi.org/10.5670/oceanog.2014.16>
69. Duarte, C.M., I.E. Hendriks, T.S. Moore, Y.S. Olsen, A. Steckbauer, L. Ramajo, J. Carstensen, J.A. Trotter, and M. McCulloch, 2013: Is ocean acidification an open-ocean syndrome? Understanding anthropogenic impacts on seawater pH. *Estuaries and Coasts*, **36**, 221-236. <http://dx.doi.org/10.1007/s12237-013-9594-3>
70. Doney, S.C., N. Mahowald, I. Lima, R.A. Feely, F.T. Mackenzie, J.F. Lamarque, and P.J. Rasch, 2007: Impact of anthropogenic atmospheric nitrogen and sulfur deposition on ocean acidification and the inorganic carbon system. *Proc Natl Acad Sci U S A*, **104**, 14580-5. <http://dx.doi.org/10.1073/pnas.0702218104>
71. Borges, A.V. and N. Gypens, 2010: Carbonate chemistry in the coastal zone responds more strongly to eutrophication than ocean acidification. *Limnology and Oceanography*, **55**, 346-353. <http://dx.doi.org/10.4319/lo.2010.55.1.0346>
72. Waldbusser, G.G. and J.E. Salisbury, 2014: Ocean acidification in the coastal zone from an organism's perspective: Multiple system parameters, frequency domains, and habitats. *Annual Review of Marine Science*, **6**, 221-247. <http://dx.doi.org/10.1146/annurev-marine-121211-172238>
73. Hendriks, I.E., C.M. Duarte, Y.S. Olsen, A. Steckbauer, L. Ramajo, T.S. Moore, J.A. Trotter, and M. McCulloch, 2015: Biological mechanisms supporting adaptation to ocean acidification in coastal ecosystems. *Estuarine, Coastal and Shelf Science*, **152**, A1-A8. <http://dx.doi.org/10.1016/j.ecss.2014.07.019>
74. Sutton, A.J., C.L. Sabine, R.A. Feely, W.J. Cai, M.F. Cronin, M.J. McPhaden, J.M. Morell, J.A. Newton, J.H. Noh, S.R. Ólafsdóttir, J.E. Salisbury, U. Send, D.C. Vandemark, and R.A. Weller, 2016: Using present-day observations to detect when anthropogenic change forces surface ocean carbonate chemistry outside preindustrial bounds. *Biogeosciences*, **13**, 5065-5083. <http://dx.doi.org/10.5194/bg-13-5065-2016>
75. Harris, K.E., M.D. DeGrandpre, and B. Hales, 2013: Aragonite saturation state dynamics in a coastal upwelling zone. *Geophysical Research Letters*, **40**, 2720-2725. <http://dx.doi.org/10.1002/grl.50460>
76. Gledhill, D.K., M.M. White, J. Salisbury, H. Thomas, I. Mlsna, M. Liebman, B. Mook, J. Grear, A.C. Candelmo, R.C. Chambers, C.J. Gobler, C.W. Hunt, A.L. King, N.N. Price, S.R. Signorini, E. Stancioff, C. Stymiest, R.A. Wahle, J.D. Waller, N.D. Rebeck, Z.A. Wang, T.L. Capson, J.R. Morrison, S.R. Cooley, and S.C. Doney, 2015: Ocean and coastal acidification off New England and Nova Scotia. *Oceanography*, **28**, 182-197. <http://dx.doi.org/10.5670/oceanog.2015.41>
77. Evans, W., J.T. Mathis, and J.N. Cross, 2014: Calcium carbonate corrosivity in an Alaskan inland sea. *Biogeosciences*, **11**, 365-379. <http://dx.doi.org/10.5194/bg-11-365-2014>
78. Salisbury, J., M. Green, C. Hunt, and J. Campbell, 2008: Coastal acidification by rivers: A threat to shellfish? *Eos, Transactions, American Geophysical Union*, **89**, 513-513. <http://dx.doi.org/10.1029/2008EO500001>
79. Bates, N.R. and J.T. Mathis, 2009: The Arctic Ocean marine carbon cycle: Evaluation of air-sea CO₂ exchanges, ocean acidification impacts and potential feedbacks. *Biogeosciences*, **6**, 2433-2459. <http://dx.doi.org/10.5194/bg-6-2433-2009>
80. Jiang, L.-Q., R.A. Feely, B.R. Carter, D.J. Greeley, D.K. Gledhill, and K.M. Arzayus, 2015: Climatological distribution of aragonite saturation state in the global oceans. *Global Biogeochemical Cycles*, **29**, 1656-1673. <http://dx.doi.org/10.1002/2015GB005198>
81. Feely, R.A., C.L. Sabine, J.M. Hernandez-Ayon, D. Ianson, and B. Hales, 2008: Evidence for upwelling of corrosive "acidified" water onto the continental shelf. *Science*, **320**, 1490-1492. <http://dx.doi.org/10.1126/science.1155676>
82. Qi, D., L. Chen, B. Chen, Z. Gao, W. Zhong, R.A. Feely, L.G. Anderson, H. Sun, J. Chen, M. Chen, L. Zhan, Y. Zhang, and W.-J. Cai, 2017: Increase in acidifying water in the western Arctic Ocean. *Nature Climate Change*, **7**, 195-199. <http://dx.doi.org/10.1038/nclimate3228>
83. Manzello, D., I. Enochs, S. Musielewicz, R. Carlton, and D. Gledhill, 2013: Tropical cyclones cause CaCO₃ undersaturation of coral reef seawater in a high-CO₂ world. *Journal of Geophysical Research Oceans*, **118**, 5312-5321. <http://dx.doi.org/10.1002/jgrc.20378>

84. Friedrich, T., A. Timmermann, A. Abe-Ouchi, N.R. Bates, M.O. Chikamoto, M.J. Church, J.E. Dore, D.K. Gledhill, M. Gonzalez-Davila, M. Heinemann, T. Ilyina, J.H. Jungclaus, E. McLeod, A. Mouchet, and J.M. Santana-Casiano, 2012: Detecting regional anthropogenic trends in ocean acidification against natural variability. *Nature Climate Change*, **2**, 167-171. <http://dx.doi.org/10.1038/nclimate1372>
85. Hönisch, B., A. Ridgwell, D.N. Schmidt, E. Thomas, S.J. Gibbs, A. Sluijs, R. Zeebe, L. Kump, R.C. Martindale, S.E. Greene, W. Kiessling, J. Ries, J.C. Zachos, D.L. Royer, S. Barker, T.M. Marchitto, Jr., R. Moyer, C. Pelejero, P. Ziveri, G.L. Foster, and B. Williams, 2012: The geological record of ocean acidification. *Science*, **335**, 1058-1063. <http://dx.doi.org/10.1126/science.1208277>
86. Zeebe, R.E., A. Ridgwell, and J.C. Zachos, 2016: Anthropogenic carbon release rate unprecedented during the past 66 million years. *Nature Geoscience*, **9**, 325-329. <http://dx.doi.org/10.1038/ngeo2681>
87. Wright, J.D. and M.F. Schaller, 2013: Evidence for a rapid release of carbon at the Paleocene-Eocene thermal maximum. *Proceedings of the National Academy of Sciences*, **110**, 15908-15913. <http://dx.doi.org/10.1073/pnas.1309188110>
88. Caldeira, K. and M.E. Wickett, 2005: Ocean model predictions of chemistry changes from carbon dioxide emissions to the atmosphere and ocean. *Journal of Geophysical Research: Oceans*, **110**, C09S04. <http://dx.doi.org/10.1029/2004JC002671>
89. Feely, R.A., S.R. Alin, B. Carter, N. Bednaršek, B. Hales, F. Chan, T.M. Hill, B. Gaylord, E. Sanford, R.H. Byrne, C.L. Sabine, D. Greeley, and L. Juranek, 2016: Chemical and biological impacts of ocean acidification along the west coast of North America. *Estuarine, Coastal and Shelf Science*, **183**, Part A, 260-270. <http://dx.doi.org/10.1016/j.ecss.2016.08.043>
90. Mathis, J.T., S.R. Cooley, N. Lucey, S. Colt, J. Ekstrom, T. Hurst, C. Hauri, W. Evans, J.N. Cross, and R.A. Feely, 2015: Ocean acidification risk assessment for Alaska's fishery sector. *Progress in Oceanography*, **136**, 71-91. <http://dx.doi.org/10.1016/j.pocean.2014.07.001>
91. Altieri, A.H. and K.B. Gedan, 2015: Climate change and dead zones. *Global Change Biology*, **21**, 1395-1406. <http://dx.doi.org/10.1111/gcb.12754>
92. Breitburg, D.L., J. Salisbury, J.M. Bernhard, W.-J. Cai, S. Dupont, S.C. Doney, K.J. Kroeker, L.A. Levin, W.C. Long, L.M. Milke, S.H. Miller, B. Phelan, U. Passow, B.A. Seibel, A.E. Todgham, and A.M. Tarrant, 2015: And on top of all that... Coping with ocean acidification in the midst of many stressors. *Oceanography*, **28**, 48-61. <http://dx.doi.org/10.5670/oceanog.2015.31>
93. Gobler, C.J., E.L. DePasquale, A.W. Griffith, and H. Baumann, 2014: Hypoxia and acidification have additive and synergistic negative effects on the growth, survival, and metamorphosis of early life stage bivalves. *PLoS ONE*, **9**, e83648. <http://dx.doi.org/10.1371/journal.pone.0083648>
94. Helm, K.P., N.L. Bindoff, and J.A. Church, 2011: Observed decreases in oxygen content of the global ocean. *Geophysical Research Letters*, **38**, L23602. <http://dx.doi.org/10.1029/2011GL049513>
95. Stramma, L., S. Schmidtko, L.A. Levin, and G.C. Johnson, 2010: Ocean oxygen minima expansions and their biological impacts. *Deep Sea Research Part I: Oceanographic Research Papers*, **57**, 587-595. <http://dx.doi.org/10.1016/j.dsr.2010.01.005>
96. Reay, D.S., F. Dentener, P. Smith, J. Grace, and R.A. Feely, 2008: Global nitrogen deposition and carbon sinks. *Nature Geoscience*, **1**, 430-437. <http://dx.doi.org/10.1038/ngeo230>
97. Rabalais, N.N., R.E. Turner, R.J. Díaz, and D. Justić, 2009: Global change and eutrophication of coastal waters. *ICES Journal of Marine Science*, **66**, 1528-1537. <http://dx.doi.org/10.1093/icesjms/fsp047>
98. Boetius, A. and F. Wenzhofer, 2013: Seafloor oxygen consumption fuelled by methane from cold seeps. *Nature Geoscience*, **6**, 725-734. <http://dx.doi.org/10.1038/ngeo1926>
99. Lee, M., E. Shevliakova, S. Malyshev, P.C.D. Milly, and P.R. Jaffé, 2016: Climate variability and extremes, interacting with nitrogen storage, amplify eutrophication risk. *Geophysical Research Letters*, **43**, 7520-7528. <http://dx.doi.org/10.1002/2016GL069254>
100. Ito, T., A. Nenes, M.S. Johnson, N. Meskhidze, and C. Deutsch, 2016: Acceleration of oxygen decline in the tropical Pacific over the past decades by aerosol pollutants. *Nature Geoscience*, **9**, 443-447. <http://dx.doi.org/10.1038/ngeo2717>
101. Codispoti, L.A., J.A. Brandes, J.P. Christensen, A.H. Devol, S.W.A. Naqvi, H.W. Paerl, and T. Yoshinari, 2001: The oceanic fixed nitrogen and nitrous oxide budgets: Moving targets as we enter the anthropocene? *Scientia Marina*, **65**, 85-105. <http://dx.doi.org/10.3989/scimar.2001.65s285>
102. Deutsch, C., H. Brix, T. Ito, H. Frenzel, and L. Thompson, 2011: Climate-forced variability of ocean hypoxia. *Science*, **333**, 336-339. <http://dx.doi.org/10.1126/science.1202422>
103. Gruber, N., 2008: Chapter 1 - The marine nitrogen cycle: Overview and challenges. *Nitrogen in the Marine Environment (2nd Edition)*. Academic Press, San Diego, 1-50. <http://dx.doi.org/10.1016/B978-0-12-372522-6.00001-3>



104. EPA, 2017: Inventory of U.S. Greenhouse Gas Emissions and Sinks: 1990-2015. EPA 430-P-17-001. U.S. Environmental Protection Agency, Washington, D.C., 633 pp. https://www.epa.gov/sites/production/files/2017-02/documents/2017_complete_report.pdf
105. Wallmann, K., 2003: Feedbacks between oceanic redox states and marine productivity: A model perspective focused on benthic phosphorus cycling. *Global Biogeochemical Cycles*, **17**, 1084. <http://dx.doi.org/10.1029/2002GB001968>
106. Bianchi, D., E.D. Galbraith, D.A. Carozza, K.A.S. Mislán, and C.A. Stock, 2013: Intensification of open-ocean oxygen depletion by vertically migrating animals. *Nature Geoscience*, **6**, 545-548. <http://dx.doi.org/10.1038/ngeo1837>
107. Knoll, A.H. and S.B. Carroll, 1999: Early animal evolution: Emerging views from comparative biology and geology. *Science*, **284**, 2129-2137. <http://dx.doi.org/10.1126/science.284.5423.2129>
108. McFall-Ngai, M., M.G. Hadfield, T.C.G. Bosch, H.V. Carey, T. Domazet-Lošo, A.E. Douglas, N. Dubilier, G. Eberl, T. Fukami, S.F. Gilbert, U. Hentschel, N. King, S. Kjelleberg, A.H. Knoll, N. Kremer, S.K. Mazmanian, J.L. Metcalf, K. Nealson, N.E. Pierce, J.F. Rawls, A. Reid, E.G. Ruby, M. Rumpho, J.G. Sanders, D. Tautz, and J.J. Wernegreen, 2013: Animals in a bacterial world, a new imperative for the life sciences. *Proceedings of the National Academy of Sciences*, **110**, 3229-3236. <http://dx.doi.org/10.1073/pnas.1218525110>
109. Falkowski, P.G., T. Algeo, L. Codispoti, C. Deutsch, S. Emerson, B. Hales, R.B. Huey, W.J. Jenkins, L.R. Kump, L.A. Levin, T.W. Lyons, N.B. Nelson, O.S. Schofield, R. Summons, L.D. Talley, E. Thomas, F. Whitney, and C.B. Pilcher, 2011: Ocean deoxygenation: Past, present, and future. *Eos, Transactions, American Geophysical Union*, **92**, 409-410. <http://dx.doi.org/10.1029/2011EO460001>
110. Robinson, R.S., A. Mix, and P. Martinez, 2007: Southern Ocean control on the extent of denitrification in the southeast Pacific over the last 70 ka. *Quaternary Science Reviews*, **26**, 201-212. <http://dx.doi.org/10.1016/j.quascirev.2006.08.005>
111. Schmittner, A., E.D. Galbraith, S.W. Hostetler, T.F. Pedersen, and R. Zhang, 2007: Large fluctuations of dissolved oxygen in the Indian and Pacific oceans during Dansgaard-Oeschger oscillations caused by variations of North Atlantic Deep Water subduction. *Paleoceanography*, **22**, PA3207. <http://dx.doi.org/10.1029/2006PA001384>
112. Galbraith, E.D., M. Kienast, T.F. Pedersen, and S.E. Calvert, 2004: Glacial-interglacial modulation of the marine nitrogen cycle by high-latitude O₂ supply to the global thermocline. *Paleoceanography*, **19**, PA4007. <http://dx.doi.org/10.1029/2003PA001000>
113. Moffitt, S.E., R.A. Moffitt, W. Sauthoff, C.V. Davis, K. Hewett, and T.M. Hill, 2015: Paleooceanographic insights on recent oxygen minimum zone expansion: Lessons for modern oceanography. *PLoS ONE*, **10**, e0115246. <http://dx.doi.org/10.1371/journal.pone.0115246>
114. Justić, D., T. Legović, and L. Rottini-Sandrini, 1987: Trends in oxygen content 1911-1984 and occurrence of benthic mortality in the northern Adriatic Sea. *Estuarine, Coastal and Shelf Science*, **25**, 435-445. [http://dx.doi.org/10.1016/0272-7714\(87\)90035-7](http://dx.doi.org/10.1016/0272-7714(87)90035-7)
115. Zaitsev, Y.P., 1992: Recent changes in the trophic structure of the Black Sea. *Fisheries Oceanography*, **1**, 180-189. <http://dx.doi.org/10.1111/j.1365-2419.1992.tb00036.x>
116. Conley, D.J., J. Carstensen, J. Aigars, P. Axe, E. Bonsdorff, T. Eremina, B.-M. Haahti, C. Humborg, P. Jonsson, J. Kotta, C. Lännegren, U. Larsson, A. Maximov, M.R. Medina, E. Lysiak-Pastuszak, N. Remeikaitė-Nikiėnė, J. Walve, S. Wilhelms, and L. Zillén, 2011: Hypoxia is increasing in the coastal zone of the Baltic Sea. *Environmental Science & Technology*, **45**, 6777-6783. <http://dx.doi.org/10.1021/es201212r>
117. Brush, G.S., 2009: Historical land use, nitrogen, and coastal eutrophication: A paleoecological perspective. *Estuaries and Coasts*, **32**, 18-28. <http://dx.doi.org/10.1007/s12237-008-9106-z>
118. Gilbert, D., B. Sundby, C. Gobeil, A. Mucci, and G.-H. Tremblay, 2005: A seventy-two-year record of diminishing deep-water oxygen in the St. Lawrence estuary: The northwest Atlantic connection. *Limnology and Oceanography*, **50**, 1654-1666. <http://dx.doi.org/10.4319/lo.2005.50.5.1654>
119. Rabalais, N.N., R.E. Turner, B.K. Sen Gupta, D.F. Boesch, P. Chapman, and M.C. Murrell, 2007: Hypoxia in the northern Gulf of Mexico: Does the science support the plan to reduce, mitigate, and control hypoxia? *Estuaries and Coasts*, **30**, 753-772. <http://dx.doi.org/10.1007/bf02841332>
120. Rabalais, N.N., R.J. Diaz, L.A. Levin, R.E. Turner, D. Gilbert, and J. Zhang, 2010: Dynamics and distribution of natural and human-caused hypoxia. *Biogeosciences*, **7**, 585-619. <http://dx.doi.org/10.5194/bg-7-585-2010>
121. Booth, J.A.T., E.E. McPhee-Shaw, P. Chua, E. Kingsley, M. Denny, R. Phillips, S.J. Bograd, L.D. Zeidberg, and W.F. Gilly, 2012: Natural intrusions of hypoxic, low pH water into nearshore marine environments on the California coast. *Continental Shelf Research*, **45**, 108-115. <http://dx.doi.org/10.1016/j.csr.2012.06.009>
122. Baden, S.P., L.O. Loo, L. Pihl, and R. Rosenberg, 1990: Effects of eutrophication on benthic communities including fish — Swedish west coast. *Ambio*, **19**, 113-122. <http://www.jstor.org/stable/4313676>

123. Diaz, R.J. and R. Rosenberg, 2008: Spreading dead zones and consequences for marine ecosystems. *Science*, **321**, 926-929. <http://dx.doi.org/10.1126/science.1156401>
124. Takatani, Y., D. Sasano, T. Nakano, T. Midorikawa, and M. Ishii, 2012: Decrease of dissolved oxygen after the mid-1980s in the western North Pacific subtropical gyre along the 137°E repeat section. *Global Biogeochemical Cycles*, **26**, GB2013. <http://dx.doi.org/10.1029/2011GB004227>
125. Stendardo, I. and N. Gruber, 2012: Oxygen trends over five decades in the North Atlantic. *Journal of Geophysical Research*, **117**, C11004. <http://dx.doi.org/10.1029/2012JC007909>
126. Gilbert, D., N.N. Rabalais, R.J. Diaz, and J. Zhang, 2010: Evidence for greater oxygen decline rates in the coastal ocean than in the open ocean. *Biogeosciences*, **7**, 2283-2296. <http://dx.doi.org/10.5194/bg-7-2283-2010>
127. Bograd, S.J., M.P. Buil, E.D. Lorenzo, C.G. Castro, I.D. Schroeder, R. Goericke, C.R. Anderson, C. Benitez-Nelson, and F.A. Whitney, 2015: Changes in source waters to the Southern California Bight. *Deep Sea Research Part II: Topical Studies in Oceanography*, **112**, 42-52. <http://dx.doi.org/10.1016/j.dsr2.2014.04.009>
128. Long, M.C., C. Deutsch, and T. Ito, 2016: Finding forced trends in oceanic oxygen. *Global Biogeochemical Cycles*, **30**, 381-397. <http://dx.doi.org/10.1002/2015GB005310>
129. Deutsch, C., W. Berelson, R. Thunell, T. Weber, C. Tems, J. McManus, J. Crusius, T. Ito, T. Baumgartner, V. Ferreira, J. Mey, and A. van Geen, 2014: Centennial changes in North Pacific anoxia linked to tropical trade winds. *Science*, **345**, 665-668. <http://dx.doi.org/10.1126/science.1252332>
130. Montes, I., B. Dewitte, E. Gutknecht, A. Paulmier, I. Dadou, A. Oschlies, and V. Garçon, 2014: High-resolution modeling of the eastern tropical Pacific oxygen minimum zone: Sensitivity to the tropical oceanic circulation. *Journal of Geophysical Research Oceans*, **119**, 5515-5532. <http://dx.doi.org/10.1002/2014JC009858>
131. Donner, S.D. and D. Scavia, 2007: How climate controls the flux of nitrogen by the Mississippi River and the development of hypoxia in the Gulf of Mexico. *Limnology and Oceanography*, **52**, 856-861. <http://dx.doi.org/10.4319/lo.2007.52.2.0856>
132. Najjar, R.G., C.R. Pyke, M.B. Adams, D. Breitburg, C. Hershner, M. Kemp, R. Howarth, M.R. Mulholland, M. Paolisso, D. Secor, K. Sellner, D. Wardrop, and R. Wood, 2010: Potential climate-change impacts on the Chesapeake Bay. *Estuarine, Coastal and Shelf Science*, **86**, 1-20. <http://dx.doi.org/10.1016/j.ecss.2009.09.026>
133. Thompson, P.R., B.D. Hamlington, F.W. Landerer, and S. Adhikari, 2016: Are long tide gauge records in the wrong place to measure global mean sea level rise? *Geophysical Research Letters*, **43**, 10,403-10,411. <http://dx.doi.org/10.1002/2016GL070552>
134. Jickells, T. and C.M. Moore, 2015: The importance of atmospheric deposition for ocean productivity. *Annual Review of Ecology, Evolution, and Systematics*, **46**, 481-501. <http://dx.doi.org/10.1146/annurev-ecolsys-112414-054118>
135. Chiapello, I., 2014: Dust observations and climatology. *Mineral Dust: A Key Player in the Earth System*. Knippertz, P. and J.-B.W. Stuut, Eds. Springer Netherlands, Dordrecht, 149-177. http://dx.doi.org/10.1007/978-94-017-8978-3_7
136. Mulitza, S., D. Heslop, D. Pittauerova, H.W. Fischer, I. Meyer, J.-B. Stuut, M. Zabel, G. Mollenhauer, J.A. Collins, H. Kuhnert, and M. Schulz, 2010: Increase in African dust flux at the onset of commercial agriculture in the Sahel region. *Nature*, **466**, 226-228. <http://dx.doi.org/10.1038/nature09213>
137. Paerl, H.W., R.L. Dennis, and D.R. Whitall, 2002: Atmospheric deposition of nitrogen: Implications for nutrient over-enrichment of coastal waters. *Estuaries*, **25**, 677-693. <http://dx.doi.org/10.1007/bf02804899>
138. Carr, M.-E., M.A.M. Friedrichs, M. Schmeltz, M. Noguchi Aita, D. Antoine, K.R. Arrigo, I. Asanuma, O. Aumont, R. Barber, M. Behrenfeld, R. Bidigare, E.T. Buitenhuis, J. Campbell, A. Ciotti, H. Dierssen, M. Dowell, J. Dunne, W. Esaias, B. Gentili, W. Gregg, S. Groom, N. Hoepffner, J. Ishizaka, T. Kameda, C. Le Quéré, S. Lohrenz, J. Marra, F. Mélin, K. Moore, A. Morel, T.E. Reddy, J. Ryan, M. Scardi, T. Smyth, K. Turpie, G. Tilstone, K. Waters, and Y. Yamanaka, 2006: A comparison of global estimates of marine primary production from ocean color. *Deep Sea Research Part II: Topical Studies in Oceanography*, **53**, 741-770. <http://dx.doi.org/10.1016/j.dsr2.2006.01.028>
139. Franz, B.A., M.J. Behrenfeld, D.A. Siegel, and S.R. Signorini, 2016: Global ocean phytoplankton [in "State of the Climate in 2015"]. *Bulletin of the American Meteorological Society*, **97**, S87-S89. <http://dx.doi.org/10.1175/2016BAMSStateoftheClimate.1>
140. Chavez, F.P., M. Messié, and J.T. Pennington, 2011: Marine primary production in relation to climate variability and change. *Annual Review of Marine Science*, **3**, 227-260. <http://dx.doi.org/10.1146/annurev.marine.010908.163917>
141. Frölicher, T.L., K.B. Rodgers, C.A. Stock, and W.W.L. Cheung, 2016: Sources of uncertainties in 21st century projections of potential ocean ecosystem stressors. *Global Biogeochemical Cycles*, **30**, 1224-1243. <http://dx.doi.org/10.1002/2015GB005338>

142. Fu, W., J.T. Randerson, and J.K. Moore, 2016: Climate change impacts on net primary production (NPP) and export production (EP) regulated by increasing stratification and phytoplankton community structure in the CMIP5 models. *Biogeosciences*, **13**, 5151-5170. <http://dx.doi.org/10.5194/bg-13-5151-2016>
143. Laufkötter, C., M. Vogt, N. Gruber, M. Aita-Noguchi, O. Aumont, L. Bopp, E. Buitenhuis, S.C. Doney, J. Dunne, T. Hashioka, J. Hauck, T. Hirata, J. John, C. Le Quéré, I.D. Lima, H. Nakano, R. Seferian, I. Totterdell, M. Vichi, and C. Völker, 2015: Drivers and uncertainties of future global marine primary production in marine ecosystem models. *Biogeosciences*, **12**, 6955-6984. <http://dx.doi.org/10.5194/bg-12-6955-2015>
144. Robinson, P., A.K. Leight, D.D. Trueblood, and B. Wood, 2013: Climate sensitivity of the National Estuarine Research Reserve System. NERRS, NOAA National Ocean Service, Silver Spring, Maryland. 79 pp. https://coast.noaa.gov/data/docs/nerrs/Research_DataSyntheses_130725_climate%20sensitivity%20of%20nerrs_Final-Rpt-in-Layout_FINAL.pdf
145. Monbaliu, J., Z. Chen, D. Felts, J. Ge, F. Hissel, J. Kappenberg, S. Narayan, R.J. Nicholls, N. Ohle, D. Schuster, J. Sothmann, and P. Willems, 2014: Risk assessment of estuaries under climate change: Lessons from Western Europe. *Coastal Engineering*, **87**, 32-49. <http://dx.doi.org/10.1016/j.coastaleng.2014.01.001>
146. Schile, L.M., J.C. Callaway, J.T. Morris, D. Stralberg, V.T. Parker, and M. Kelly, 2014: Modeling tidal marsh distribution with sea-level rise: Evaluating the role of vegetation, sediment, and upland habitat in marsh resiliency. *PLoS ONE*, **9**, e88760. <http://dx.doi.org/10.1371/journal.pone.0088760>
147. Swanson, K.M., J.Z. Drexler, C.C. Fuller, and D.H. Schoellhamer, 2015: Modeling tidal freshwater marsh sustainability in the Sacramento-San Joaquin delta under a broad suite of potential future scenarios. *San Francisco Estuary and Watershed Science*, **13**, 21. <http://dx.doi.org/10.15447/sfews.2015v13iss1art3>
148. Belkin, I., 2016: Chapter 5.2: Sea surface temperature trends in large marine ecosystems. *Large Marine Ecosystems: Status and Trends*. United Nations Environment Programme, Nairobi, 101-109. http://wedocs.unep.org/bitstream/handle/20.500.11822/13456/UNEP_DEWA_TWAP%20VOLUME%204%20REPORT_FINAL_4_MAY.pdf?sequence=1&isAllowed=y,%20English%20-%20Summary
149. Baringer, M.O., M. Lankhorst, D. Volkov, S. Garzoli, S. Dong, U. Send, and C. Meinen, 2016: Meridional oceanic overturning circulation and heat transport in the Atlantic Ocean [in "State of the Climate in 2015"]. *Bulletin of the American Meteorological Society*, **97**, S84-S87. <http://dx.doi.org/10.1175/2015BAMSStateoftheClimate.1>
150. Schmidtko, S., L. Stramma, and M. Visbeck, 2017: Decline in global oceanic oxygen content during the past five decades. *Nature*, **542**, 335-339. <http://dx.doi.org/10.1038/nature21399>
151. Scott, J.D., M.A. Alexander, D.R. Murray, D. Swales, and J. Eischeid, 2016: The climate change web portal: A system to access and display climate and earth system model output from the CMIP5 archive. *Bulletin of the American Meteorological Society*, **97**, 523-530. <http://dx.doi.org/10.1175/bams-d-15-00035.1>





14

Perspectives on Climate Change Mitigation

KEY FINDINGS

1. Reducing net emissions of CO₂ is necessary to limit near-term climate change and long-term warming. Other greenhouse gases (for example, methane) and black carbon aerosols exert stronger warming effects than CO₂ on a per ton basis, but they do not persist as long in the atmosphere; therefore, mitigation of non-CO₂ species contributes substantially to near-term cooling benefits but cannot be relied upon for ultimate stabilization goals. (*Very high confidence*)
2. Stabilizing global mean temperature to less than 3.6°F (2°C) above preindustrial levels requires substantial reductions in net global CO₂ emissions prior to 2040 relative to present-day values and likely requires net emissions to become zero or possibly negative later in the century. After accounting for the temperature effects of non-CO₂ species, cumulative global CO₂ emissions must stay below about 800 GtC in order to provide a two-thirds likelihood of preventing 3.6°F (2°C) of warming. Given estimated cumulative emissions since 1870, no more than approximately 230 GtC may be emitted in the future to remain under this temperature threshold. Assuming global emissions are equal to or greater than those consistent with the RCP4.5 scenario, this cumulative carbon threshold would be exceeded in approximately two decades. (*High confidence*)
3. Achieving global greenhouse gas emissions reductions before 2030 consistent with targets and actions announced by governments in the lead up to the 2015 Paris climate conference would hold open the possibility of meeting the long-term temperature goal of limiting global warming to 3.6°F (2°C) above preindustrial levels, whereas there would be virtually no chance if net global emissions followed a pathway well above those implied by country announcements. Actions in the announcements are, by themselves, insufficient to meet a 3.6°F (2°C) goal; the likelihood of achieving that goal depends strongly on the magnitude of global emissions reductions after 2030. (*High confidence*)
4. Further assessments of the technical feasibilities, costs, risks, co-benefits, and governance challenges of climate intervention or geoengineering strategies, which are as yet unproven at scale, are a necessary step before judgments about the benefits and risks of these approaches can be made with high confidence. (*High confidence*)

Recommended Citation for Chapter

DeAngelo, B., J. Edmonds, D.W. Fahey, and B.M. Sanderson, 2017: Perspectives on climate change mitigation. In: *Climate Science Special Report: Fourth National Climate Assessment, Volume I* [Wuebbles, D.J., D.W. Fahey, K.A. Hibbard, D.J. Dokken, B.C. Stewart, and T.K. Maycock (eds.)]. U.S. Global Change Research Program, Washington, DC, USA, pp. 393-410, doi: 10.7930/J0M32SZG.

Introduction

This chapter provides scientific context for key issues regarding the long-term mitigation of climate change. As such, this chapter first addresses the science underlying the timing of when and how CO₂ and other greenhouse gas (GHG) mitigation activities that occur in the present affect the climate of the future. When do we see the benefits of a GHG emission reduction activity? Chapter 4: Projections provides further context for this topic. Relatedly, the present chapter discusses the significance of the relationship between net cumulative CO₂ emissions and eventual global warming levels. The chapter reviews recent analyses of global emissions pathways associated with preventing 3.6°F (2°C) or 2.7°F (1.5°C) of warming relative to preindustrial times. And finally, this chapter briefly reviews the status of climate intervention proposals and how these types of mitigation actions could possibly play a role in avoiding future climate change.

14.1 The Timing of Benefits from Mitigation Actions

14.1.1 Lifetime of Greenhouse Gases and Inherent Delays in the Climate System

Carbon dioxide (CO₂) concentrations in the atmosphere are directly affected by human activities in the form of CO₂ emissions. Atmospheric CO₂ concentrations adjust to human emissions of CO₂ over long time scales, spanning from decades to millennia.^{1,2} The IPCC estimated that 15% to 40% of CO₂ emitted until 2100 will remain in the atmosphere longer than 1,000 years.¹ The persistence of warming is longer than the atmospheric lifetime of CO₂ and other GHGs, owing in large part to the thermal inertia of the ocean.³ Climate change resulting from anthropogenic CO₂ emissions, and any associated risks to the environment, human health and society, are thus essentially irreversible on human timescales.⁴ The world is committed to some degree of irreversible

warming and associated climate change resulting from emissions to date.

The long lifetime in the atmosphere of CO₂² and some other key GHGs, coupled with the time lag in the response of the climate system to atmospheric forcing,⁵ has timing implications for the benefits (i.e., avoided warming or risk) of mitigation actions. Large reductions in emissions of the long-lived GHGs are estimated to have modest temperature effects in the *near term* (e.g., over one to two decades) because total atmospheric concentration levels require long periods to adjust,⁶ but are necessary in the *long term* to achieve any objective of preventing warming of any desired magnitude. Near-term projections of global mean surface temperature are therefore not strongly influenced by changes in near-term emissions but rather dominated by natural variability, the Earth system response to past and current GHG emissions, and by model spread (i.e., the different climate outcomes associated with different models using the same emissions pathway).⁷ Long-term projections of global surface temperature (after mid-century), on the other hand, show that the choice of global emissions pathway, and thus the long-term mitigation pathway the world chooses, is the dominant source of future uncertainty in climate outcomes.^{3,8}

Some studies have nevertheless shown the potential for some near-term benefits of mitigation. For example, one study found that, even at the regional scale, heat waves would already be significantly more severe by the 2030s in a non-mitigation scenario compared to a moderate mitigation scenario.⁹ The mitigation of non-CO₂ GHGs with short atmospheric lifetimes (such as methane, some hydrofluorocarbons [HFCs], and ozone) and black carbon (an aerosol that absorbs solar radiation; see Ch. 2: Physical Drivers of Climate Change), collectively referred to as short-lived climate pollutants



(SLCPs), has been highlighted as a particular way to achieve more rapid climate benefits (e.g., Zaelke and Borgford-Parnell 2015¹⁰). SLCPs are substances that not only have an atmospheric lifetime shorter (for example, weeks to a decade) than CO₂ but also exert a stronger radiative forcing (and hence temperature effect) compared to CO₂ on a per ton basis.¹¹ For these reasons, mitigation of SLCP emissions produces more rapid radiative responses. In the case of black carbon, with an atmospheric lifetime of a few days to weeks,¹² emissions (and therefore reductions of those emissions) produce strong regional effects. Mitigation of black carbon and methane also generate direct health co-benefits.^{13, 14} Reductions and/or avoidances of SLCP emissions could be a significant contribution to staying at or below a 3.6°F (2°C) increase or any other chosen global mean temperature increase.^{15, 16, 17, 18} The recent Kigali Amendment to the Montreal Protocol seeks to phase down global HFC production and consumption in order to avoid substantial GHG emissions in coming decades. Stringent and continuous SLCP mitigation could potentially increase allowable CO₂ budgets for avoiding warming beyond any desired future level, by up to 25% under certain scenarios.¹⁸ However, given that economic and technological factors tend to couple CO₂ and many SLCP emissions to varying degrees, significant SLCP emissions reductions would be a co-benefit of CO₂ mitigation.

14.1.2 Stock and Stabilization: Cumulative CO₂ and the Role of Other Greenhouse Gases

Net cumulative CO₂ emissions in the industrial era will largely determine long-term, global mean temperature change. A robust feature of model climate change simulations is a nearly linear relationship between cumulative CO₂ emissions and global mean temperature increases, irrespective of the details and exact timing of the emissions pathway (see Figure 14.1; see also Ch. 4: Projections). Limiting and stabilizing warming to any level implies that there is a physical upper limit to the cumulative amount of CO₂ that can be added to the atmosphere.³ Eventually stabilizing the global temperature requires CO₂ emissions to approach zero.¹⁹ Thus, for a 3.6°F (2°C) or any desired global mean warming goal, an estimated range of cumulative CO₂ emissions from the current period onward can be calculated. The key sources of uncertainty for any compatible, forward looking CO₂ budget associated with a given future warming objective include the climate sensitivity, the response of the carbon cycle including feedbacks (for example, the release of GHGs from permafrost thaw), the amount of past CO₂ emissions, and the influence of past and future non-CO₂ species.^{3, 19} Increasing the probability that any given temperature goal will be reached therefore implies tighter constraints on cumulative CO₂ emissions. Relatedly, for any given cumulative CO₂ budget, higher emissions in the near term imply the need for steeper reductions in the long term.



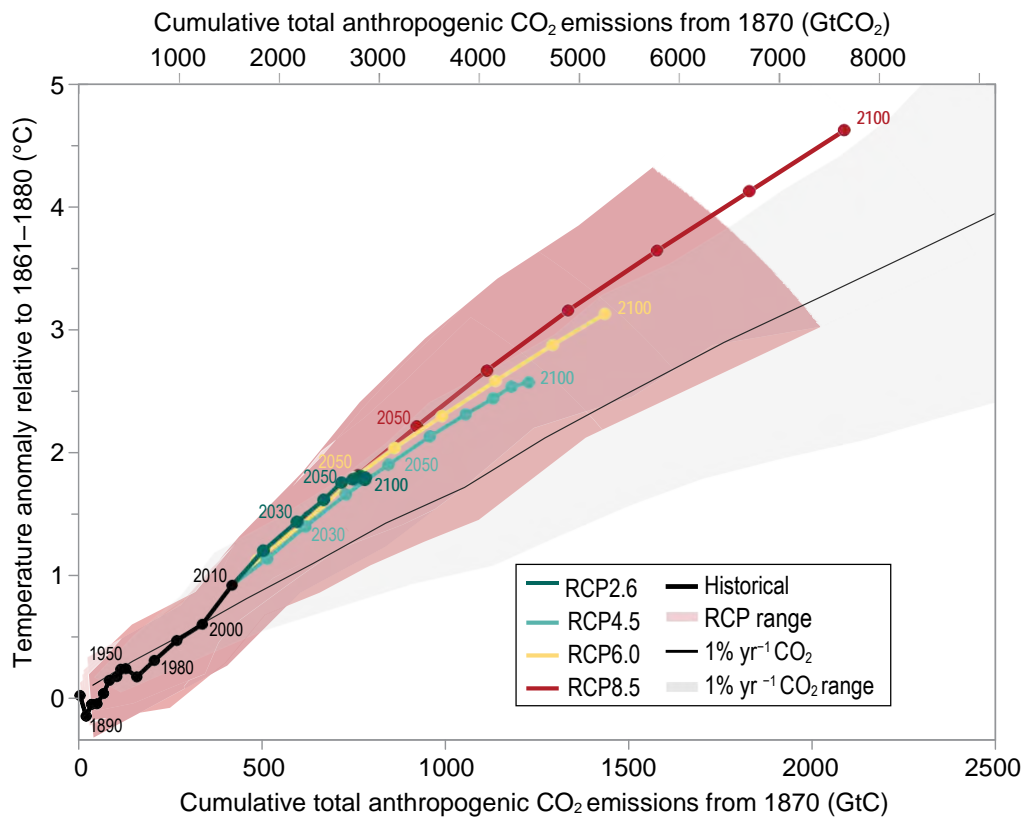


Figure 14.1: Global mean temperature change for a number of scenarios as a function of cumulative CO₂ emissions from preindustrial conditions, with time progressing along each individual line for each scenario. (Figure source: IPCC 2013;⁴²©IPCC. Used with permission).

Between 1870 and 2015, human activities, primarily the burning of fossil fuels and deforestation, emitted about 560 GtC in the form of CO₂ into the atmosphere.²⁰ According to best estimates in the literature, 1,000 GtC is the total cumulative amount of CO₂ that could be emitted yet still provide a two-thirds likelihood of preventing 3.6°F (2°C) of global mean warming since preindustrial times.^{3, 21} That estimate, however, ignores the additional radiative forcing effects of non-CO₂ species (that is, the net positive forcing resulting from the forcing of other well-mixed GHGs, including halocarbons, plus the other ozone precursor gases and aerosols). Considering both historical and projected non-CO₂ effects reduces the estimated cumulative CO₂ budget compatible with any future warming goal,¹⁸ and in the case of 3.6°F (2°C) it reduces the aforemen-

tioned estimate to 790 GtC.³ Given this more comprehensive estimate, limiting the global average temperature increase to below 3.6°F (2°C) means approximately 230 GtC more CO₂ could be emitted globally. To illustrate, if one assumes future global emissions follow a pathway consistent with the lower scenario (RCP4.5), this cumulative carbon threshold is exceeded by around 2037, while under the higher scenario (RCP8.5) this occurs by around 2033. To limit the global average temperature increase to 2.7°F (1.5°C), the estimated cumulative CO₂ budget is about 590 GtC (assuming linear scaling with the compatible 3.6°F (2°C) budget that also considers non-CO₂ effects), meaning only about 30 GtC more of CO₂ could be emitted. Further emissions of 30 GtC (in the form of CO₂) are projected to occur in the next few years (Table 14.1).



Table 14.1: Dates illustrating when cumulative CO₂ emissions thresholds associated with eventual warming of 3.6°F or 2.7°F above preindustrial levels might be reached. RCP4.5 and RCP8.5 refer, respectively, to emissions consistent with the lower and higher scenarios used throughout this report. The estimated cumulative CO₂ emissions (measured in Gigatons (Gt) of carbon) associated with different probabilities (e.g., 66%) of preventing 3.6°F (2°C) of warming are from the IPCC.³ The cumulative emissions compatible with 2.7°F (1.5°C) are linearly derived from the estimates associated with 3.6°F (2°C). The cumulative CO₂ estimates take into account the additional net warming effects associated with past and future non-CO₂ emissions consistent with the RCP scenarios. Historical CO₂ emissions from 1870–2015 (including fossil fuel combustion, land use change, and cement manufacturing) are from Le Quéré et al.²⁰ See Traceable Accounts for further details.

Dates by when cumulative carbon emissions (GtC) since 1870 reach amount commensurate with 3.6°F (2°C), when accounting for non-CO ₂ forcings			
	66% = 790 GtC	50% = 820 GtC	33% = 900 GtC
RCP4.5	2037	2040	2047
RCP8.5	2033	2035	2040
Dates by when cumulative carbon emissions (GtC) since 1870 reach amount commensurate with 2.7°F (1.5°C), when accounting for non-CO ₂ forcings			
	66% = 593 GtC	50% = 615 GtC	33% = 675 GtC
RCP4.5	2019	2021	2027
RCP8.5	2019	2021	2025

14.2 Pathways Centered Around 3.6°F (2°C)

The idea of a 3.6°F (2°C) goal can be found in the scientific literature as early as 1975. Nordhaus²² justified it by simply stating, “If there were global temperatures more than 2 or 3°C above the current average temperature, this would take the climate outside of the range of observations which have been made over the last several hundred thousand years.” Since that time, the concept of a 3.6°F (2°C) goal gained attention in both scientific and policy discourse. For example, the Stockholm Environment Institute²³ published a report stating that 3.6°F (2°C) “can be viewed as an upper limit beyond which the risks of grave damage to ecosystems, and of non-linear responses, are expected to increase rapidly.” And in 2007, the IPCC Fourth Assessment Report stated, among other things: “Confidence has increased that a 1 to 2°C increase in global mean temperature above 1990 levels (about 1.5 to 2.5°C above pre-industrial) poses

significant risks to many unique and threatened systems including many biodiversity hotspots.” Most recently, the Paris Agreement of 2015 took on the long-term goal of “holding the increase in the global average temperature to well below 2°C above pre-industrial levels and pursuing efforts to limit the temperature increase to 1.5°C above pre-industrial levels.” Many countries announced GHG emissions reduction targets and related actions (formally called Intended Nationally Determined Contributions [INDCs]) in the lead up to the Paris meeting; these announcements addressed emissions through 2025 or 2030 and take a wide range of forms. A number of studies have generated projections of future GHG emissions based on these announcements and evaluated whether, if implemented, the resulting emissions reductions would limit the increase in global average temperatures to 3.6°F (2°C) above preindustrial levels. In June 2017, the United States announced its intent to withdraw from the Paris Agreement. The scenarios



assessed below were published prior to this announcement and therefore do not reflect the implications of this announcement.

Estimates of global emissions and temperature implications from emissions pathways consistent with targets and actions announced by governments in the lead up to the 2015 Paris climate conference^{24, 25, 26, 27, 28} generally find that 1) these targets and actions would reduce GHG emissions growth by 2030 relative to a situation where these goals did not exist, though emissions are still not expected to be lower in 2030 than in 2015; and 2) the targets and actions would be a step towards limiting global mean temperature increase to 3.6°F (2°C), but by themselves, would be insufficient for this goal. According to one study, emissions pathways consistent with governments' announcements imply a median warming of 4.7°–5.6°F (2.6°–3.1°C) by 2100, though year 2100 temperature estimates depend on assumed emissions between 2030 and 2100.²⁴ For example, Climate Action Tracker,²⁶ using alternative post-2030 assumptions, put the range at 5.9°–7.0°F (3.3°–3.9°C).

Emissions pathways consistent with the targets and actions announced by governments in the lead up to the 2015 Paris conference

have been evaluated in the context of the likelihood of global mean surface temperature change (Figure 14.2). It was found that the likelihood of limiting the global mean temperature increase to 3.6°F (2°C) or less was enhanced by these announced actions, but depended strongly on assumptions about subsequent policies and measures. Under a scenario in which countries maintain the same pace of decarbonization past 2030 as they announced in their first actions (leading up to 2025 or 2030) there is some likelihood (less than 10%) of preventing a global mean surface temperature change of 3.6°F (2°C) relative to preindustrial levels; this scenario thus holds open the possibility of achieving this goal, whereas there would be virtually no chance if emissions climbed to levels above those implied by country announcements (Figure 14.2).²⁷ Greater emissions reductions beyond 2030 (based on higher decarbonization rates past 2030) increase the likelihood of limiting warming to 3.6°F (2°C) or lower to about 30%, and almost eliminate the likelihood of a global mean temperature increase greater than 7°F (4°C). Scenarios that assume even greater emissions reductions past 2030 would be necessary to have at least a 50% probability of limiting warming to 3.6°F (2°C)²⁷ as discussed and illustrated further below.



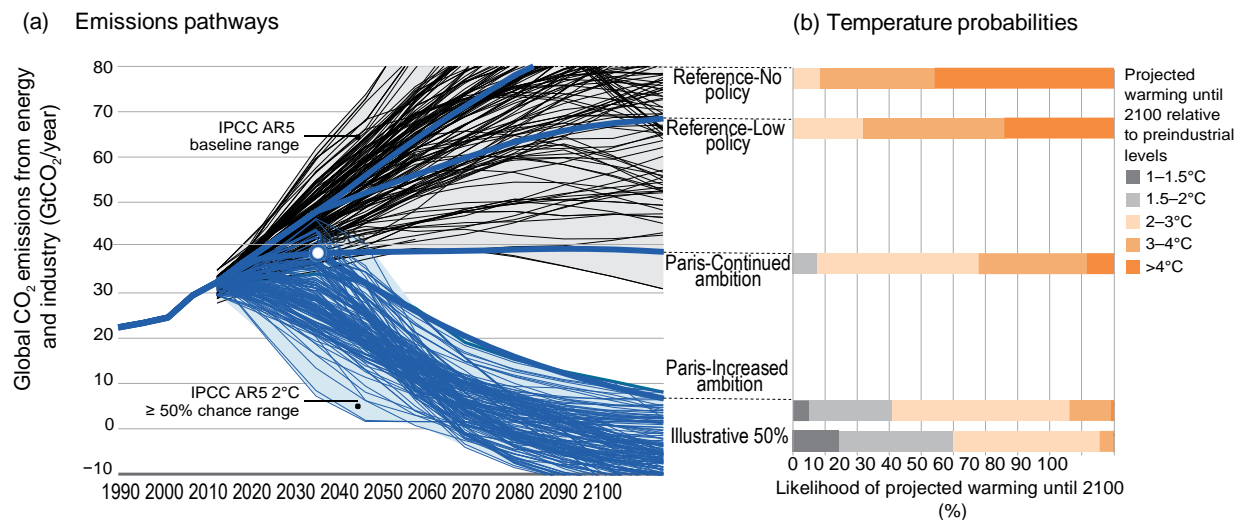


Figure 14.2: Global CO₂ emissions and probabilistic temperature outcomes of government announcements associated with the lead up to the Paris climate conference. (a) Global CO₂ emissions from energy and industry (includes CO₂ emissions from all fossil fuel production and use and industrial processes such as cement manufacture that also produce CO₂ as a byproduct) for emissions pathways following no policy, current policy, meeting the governments' announcements with constant country decarbonization rates past 2030, and meeting the governments' announcements with higher rates of decarbonization past 2030. INDCs refer to Intended Nationally Determined Contributions which is the term used for the governments' announced actions in the lead up to Paris. (b) Likelihoods of different levels of increase in global mean surface temperature during the 21st century relative to preindustrial levels for the four scenarios. Although (a) shows only CO₂ emissions from energy and industry, temperature outcomes are based on the full suite of GHG, aerosol, and short-lived species emissions across the full set of human activities and physical Earth systems. (Figure source: Fawcett et al. 2015²⁷).

There is a limited range of pathways which enable the world to remain below 3.6°F (2°C) of warming (see Figure 14.3), and almost all but the most rapid near-term mitigation pathways are heavily reliant on the implementation of CO₂ removal from the atmosphere later in the century or other climate intervention, discussed below. If global emissions are in line with the first round of announced government actions by 2030, then the world likely needs to reduce effective GHG emissions to zero by

2080 and be significantly net negative by the end of the century (relying on as yet unproven technologies to remove GHGs from the atmosphere) in order to stay below 3.6°F (2°C) of warming. Avoiding 2.7°F (1.5°C) of warming requires more aggressive action still, with net zero emissions achieved by 2050 and net negative emissions thereafter. In either case, faster near-term emissions reductions significantly decrease the requirements for net negative emissions in the future.



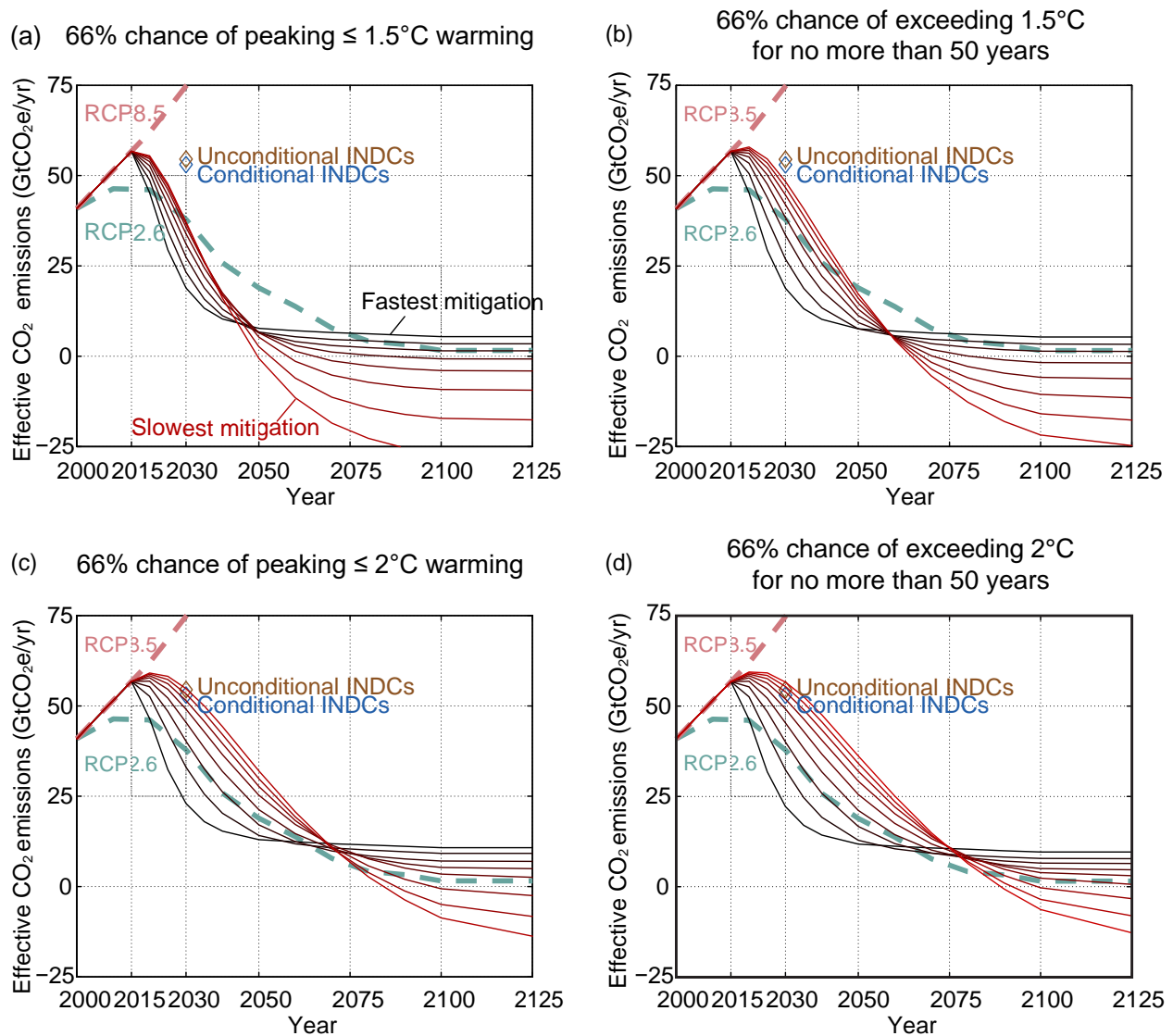


Figure 14.3: Global emissions pathways for GHGs, expressed as CO₂-equivalent emissions, which would be consistent with different temperature goals (relative to preindustrial temperatures). INDCs refer to Intended Nationally Determined Contributions which is the term used for the governments' announced actions in the lead up to Paris. (a) shows a set of pathways where global mean temperatures would likely (66%) not exceed 2.7°F (1.5°C). A number of pathways are consistent with the goal, ranging from the red curve (slowest near-term mitigation with large negative emissions requirements in the future) to the black curve with rapid near-term mitigation and less future negative emissions. (b) shows similar pathways with a 66% chance of exceeding 2.7°F (1.5°C) for only 50 years, where (c) and (d) show similar emission pathways for 3.6°F (2°C). (Figure source: Sanderson et al. 2016²⁵).



14.3 The Potential Role of Climate Intervention in Mitigation Strategies

Limiting the global mean temperature increase through emissions reductions or adapting to the impacts of a greater-than-3.6°F (2°C) warmer world have been acknowledged as severely challenging tasks by the international science and policy communities. Consequently, there is increased interest by some scientists and policy makers in exploring additional measures designed to reduce net radiative forcing through other, as yet untested actions, which are often referred to as geoengineering or climate intervention (CI) actions. CI approaches are generally divided into two categories: carbon dioxide removal (CDR)²⁹ and solar radiation management (SRM).³⁰ CDR and SRM methods may have future roles in helping meet global temperature goals. Both methods would reduce global average temperature by reducing net global radiative forcing: CDR through reducing atmospheric CO₂ concentrations and SRM through increasing Earth's albedo.

The evaluation of the suitability and advisability of potential CI actions requires a decision framework that includes important dimensions beyond scientific and technical considerations. Among these dimensions to be considered are the potential development of global and national governance and oversight procedures, geopolitical relations, legal considerations, environmental, economic and societal impacts, ethical considerations, and the relationships to global climate policy and current GHG mitigation and adaptation actions. It is clear that these social science and other non-physical science dimensions are likely to be a major part of the decision framework and ultimately control the adoption and effectiveness of CI actions. This report only acknowledges these mostly non-physical scientific dimensions and must forego a detailed discussion.

By removing CO₂ from the atmosphere, CDR directly addresses the principal cause of climate change. Potential CDR approaches include direct air capture, currently well-understood biological methods on land (for example, afforestation), less well-understood and potentially risky methods in the ocean (for example, ocean fertilization), and accelerated weathering (for example, forming calcium carbonate on land or in the oceans).²⁹ While CDR is technically possible, the primary challenge is achieving the required scale of removal in a cost-effective manner, which in part presumes a comparison to the costs of other, more traditional GHG mitigation options.^{31, 32} In principle, at large scale, CDR could measurably reduce CO₂ concentrations (that is, cause negative emissions). Point-source capture (as opposed to CO₂ capture from ambient air) and removal of CO₂ is a particularly effective CDR method. The climate value of avoided CO₂ emissions is essentially equivalent to that of the atmospheric removal of the same amount. To realize sustained climate benefits from CDR, however, the removal of CO₂ from the atmosphere must be essentially permanent—at least several centuries to millennia. In addition to high costs, CDR has the additional limitation of long implementation times.

By contrast, SRM approaches offer the only known CI methods of cooling Earth within a few years after inception. An important limitation of SRM is that it would not address damage to ocean ecosystems from increasing ocean acidification due to continued CO₂ uptake. SRM could theoretically have a significant global impact even if implemented by a small number of nations, and by nations that are not also the major emitters of GHGs; this could be viewed either as a benefit or risk of SRM.³⁰

Proposed SRM concepts increase Earth's albedo through injection of sulfur gases or aerosols into the stratosphere (thereby simulating



the effects of explosive volcanic eruptions) or marine cloud brightening through aerosol injection near the ocean surface. Injection of solid particles is an alternative to sulfur and yet other SRM methods could be deployed in space. Studies have evaluated the expected effort and effectiveness of various SRM methods.^{30,33} For example, model runs were performed in the GeoMIP project using the full CMIP5 model suite to illustrate the effect of reducing top-of-the-atmosphere insolation to offset climate warming from CO₂.³⁴ The idealized runs, which assumed an abrupt, globally-uniform insolation reduction in a 4 × CO₂ atmosphere, show that temperature increases are largely offset, most sea ice loss is avoided, average precipitation changes are small, and net primary productivity increases. However, important regional changes in climate variables are likely in SRM scenarios as discussed below.

As global ambitions increase to avoid or remove CO₂ emissions, probabilities of large increases in global temperatures by 2100 are proportionately reduced.²⁷ Scenarios in which large-scale CDR is used to meet a 3.6°F (2°C) limit while allowing business-as-usual consumption of fossil fuels are likely not feasible with present technologies. Model SRM scenarios have been developed that show reductions in radiative forcing up to 1 W/m² with annual stratospheric injections of 1 Mt of sulfur from aircraft or other platforms.^{35,36} Preliminary studies suggest that this could be accomplished at an implementation cost as low as a few billion dollars per year using current technology, enabling an individual country or subnational entity to conduct activities having significant global climate impacts.

SRM scenarios could in principle be designed to follow a particular radiative forcing trajectory, with adjustments made in response to monitoring of the climate effects.³⁷ SRM

could be used as an interim measure to avoid peaks in global average temperature and other climate parameters. The assumption is often made that SRM measures, once implemented, must continue indefinitely in order to avoid the rapid climate change that would occur if the measures were abruptly stopped. SRM could be used, however, as an interim measure to buy time for the implementation of emissions reductions and/or CDR, and SRM could be phased out as emissions reductions and CDR are phased in, to avoid abrupt changes in radiative forcing.³⁷

SRM via marine cloud brightening derives from changes in cloud albedo from injection of aerosols into low-level clouds, primarily over the oceans. Clouds with smaller and more numerous droplets reflect more sunlight than clouds with fewer and larger droplets. Current models provide more confidence in the effects of stratospheric injection than in marine cloud brightening and in achieving scales large enough to reduce global forcing.³⁰

CDR and SRM have substantial uncertainties regarding their effectiveness and unintended consequences. For example, CDR on a large scale may disturb natural systems and have important implications for land-use changes. For SRM actions, even if the reduction in global average radiative forcing from SRM was exactly equal to the radiative forcing from GHGs, the regional and temporal patterns of these forcings would have important differences. While SRM could rapidly lower global mean temperatures, the effects on precipitation patterns, light availability, crop yields, acid rain, pollution levels, temperature gradients, and atmospheric circulation in response to such actions are less well understood. Also, the reduction in sunlight from SRM may have effects on agriculture and ecosystems. In general, restoring regional preindustrial temperature and precipitation conditions through



SRM actions is not expected to be possible based on ensemble modeling studies.³⁸ As a consequence, optimizing the climate and geopolitical value of SRM actions would likely involve tradeoffs between regional temperature and precipitation changes.³⁹ Alternatively, intervention options have been proposed to address particular regional impacts.⁴⁰

GHG forcing has the potential to push the climate farther into unprecedented states for human civilization and increase the likelihood of “surprises” (see Ch. 15: Potential Surprises). CI could prevent climate change from reaching a state with more unpredictable consequences. The potential for rapid changes upon initiation (or ceasing) of a CI action would require adaptation on timescales significantly more rapid than what would otherwise be necessary. The NAS^{29, 30} and the Royal Society⁴¹ recognized that research on the feasibilities and consequences of CI actions is incomplete and call for continued research to improve knowledge of the feasibility, risks, and benefits of CI techniques.



TRACEABLE ACCOUNTS

Key Finding 1

Reducing net emissions of CO₂ is necessary to limit near-term climate change and long-term warming. Other greenhouse gases (for example, methane) and black carbon aerosols exert stronger warming effects than CO₂ on a per ton basis, but they do not persist as long in the atmosphere; therefore, mitigation of non-CO₂ species contributes substantially to near-term cooling benefits but cannot be relied upon for ultimate stabilization goals. (*Very high confidence*)

Description of evidence base

Joos et al.² and Ciais et al. (see Box 6.1 in particular)¹ describe the climate response of CO₂ pulse emissions, and Solomon et al.,⁴ NRC,¹⁹ and Collins et al.³ describe the long-term warming and other climate effects associated with CO₂ emissions. Paltsev et al.⁸ and Collins et al.³ describe the near-term vs. long-term nature of climate outcomes resulting from GHG mitigation. Myhre et al.¹¹ synthesize numerous studies detailing information about the radiative forcing effects and atmospheric lifetimes of all GHGs and aerosols (see in particular Appendix 8A therein). A recent body of literature has emerged highlighting the particular role that non-CO₂ mitigation can play in providing near-term cooling benefits (e.g., Shindell et al. 2012;¹⁷ Zaelke and Borgford-Parnell 2015;¹⁰ Rogelj et al. 2015¹⁸). For each of the individual statements made in Key Finding 1, there are numerous literature sources that provide consistent grounds on which to make these statements with *very high confidence*.

Major uncertainties

The Key Finding is comprised of qualitative statements that are traceable to the literature described above and in this chapter. Uncertainties affecting estimates of the exact timing and magnitude of the climate response following emissions (or avoidance of those emissions) of CO₂ and other GHGs involve the quantity of emissions, climate sensitivity, some uncertainty about the removal time or atmospheric lifetime of CO₂ and other GHGs, and the choice of model carrying out future simulations. The role of black carbon in climate change is

more uncertain compared to the role of the well-mixed GHGs (see Bond et al. 2013¹²).

Assessment of confidence based on evidence and agreement, including short description of nature of evidence and level of agreement

Key Finding 1 is comprised of qualitative statements based on a body of literature for which there is a high level of agreement. There is a well-established understanding, based in the literature, of the atmospheric lifetime and warming effects of CO₂ vs. other GHGs after emission, and in turn how atmospheric concentration levels respond following the emission of CO₂ and other GHGs.

Summary sentence or paragraph that integrates the above information

The qualitative statements contained in Key Finding 1 reflect aspects of fundamental scientific understanding, well grounded in the literature, that provide a relevant framework for considering the role of CO₂ and non-CO₂ species in mitigating climate change.

Key Finding 2

Stabilizing global mean temperature to less than 3.6°F (2°C) above preindustrial levels requires substantial reductions in net global CO₂ emissions prior to 2040 relative to present-day values and likely requires net emissions to become zero or possibly negative later in the century. After accounting for the temperature effects of non-CO₂ species, cumulative global CO₂ emissions must stay below about 800 GtC in order to provide a two-thirds likelihood of preventing 3.6°F (2°C) of warming. Given estimated cumulative emissions since 1870, no more than approximately 230 GtC may be emitted in the future to remain under this temperature threshold. Assuming global emissions are equal to or greater than those consistent with the RCP4.5 scenario, this cumulative carbon threshold would be exceeded in approximately two decades. (*High confidence*)

Description of evidence base

Key Finding 2 is a case study, focused on a pathway associated with 3.6°F (2°C) of warming, based on the more general concepts described in the chapter. As such, the



evidence for the relationship between cumulative CO₂ emissions and global mean temperature response^{3,19,21} also supports Key Finding 3.

Numerous studies have provided best estimates of cumulative CO₂ compatible with 3.6°F (2°C) of warming above preindustrial levels, including a synthesis by the IPCC.³ Sanderson et al.²⁵ provide further recent evidence to support the statement that net CO₂ emissions would need to approach zero or become negative later in the century in order to avoid this level of warming. Rogelj et al. 2015¹⁸ and the IPCC³ demonstrate that the consideration of non-CO₂ species has the effect of further constraining the amount of cumulative CO₂ emissions compatible with 3.6°F (2°C) of warming.

Table 14.1 shows the IPCC estimates associated with different probabilities (66% [the one highlighted in Key Finding 2], 50%, and 33%) of cumulative CO₂ emissions compatible with warming of 3.6°F (2°C) above preindustrial levels, and the cumulative CO₂ emissions compatible with 2.7°F (1.5°C) are in turn linearly derived from those, based on the understanding that cumulative emissions scale linearly with global mean temperature response. The IPCC estimates take into account the additional radiative forcing effects—past and future—of non-CO₂ species based on the emissions pathways consistent with the RCP scenarios (available here: <https://tntcat.iiasa.ac.at/RcpDb/dsd?Action=htmlpage&page=about#description>).

The authors calculated the dates shown in Table 14.1, which supports the last statement in Key Finding 2, based on Le Quéré et al.²⁰ and the publicly available RCP database. Le Quéré et al.²⁰ provide the widely used reference for historical global, annual CO₂ emissions from 1870 to 2015 (land-use change emissions were estimated up to year 2010 so are assumed to be constant between 2010 and 2015). Future CO₂ emissions are based on the lower and higher scenarios (RCP4.5 and RCP8.5, respectively); annual numbers between model-projected years (2020, 2030, 2040, etc.) are linearly interpolated.

Major uncertainties

There are large uncertainties about the course of future CO₂ and non-CO₂ emissions, but the fundamental point that CO₂ emissions need to eventually approach zero or possibly become net negative to stabilize warming below 3.6°F (2°C) holds regardless of future emissions scenario. There are also large uncertainties about the magnitude of past (since 1870 in this case) CO₂ and non-CO₂ emissions, which in turn influence the uncertainty about compatible cumulative emissions from the present day forward. Further uncertainties regarding non-CO₂ species, including aerosols, include their radiative forcing effects. The uncertainty in achieving the temperature targets for a given emissions pathway is, in large part, reflected by the range of probabilities shown in Table 14.1.

Assessment of confidence based on evidence and agreement, including short description of nature of evidence and level of agreement

There is *very high* confidence in the first statement of Key Finding 2 because it is based on a number of sources with a high level of agreement. The role of non-CO₂ species in particular introduces uncertainty in the second statement of Key Finding 2 regarding compatible cumulative CO₂ emissions that take into account past and future radiative forcing effects of non-CO₂ species; though this estimate is based on a synthesis of numerous studies by the IPCC. The last statement of Key Finding 2 is straightforward based on the best available estimates of historical emissions in combination with the widely used future projections of the RCP scenarios.

Summary sentence or paragraph that integrates the above information

Fundamental scientific understanding of the climate system provides a framework for considering potential pathways for achieving a target of preventing 3.6°F (2°C) of warming. There are uncertainties about cumulative CO₂ emissions compatible with this goal, in large part because of uncertainties about the role of non-CO₂ species, but it appears, based on past emissions and future projections, that the cumulative carbon threshold for this goal could be reached or exceeded in about two decades.



Key Finding 3

Achieving global greenhouse gas emissions reductions before 2030 consistent with targets and actions announced by governments in the lead up to the 2015 Paris climate conference would hold open the possibility of meeting the long-term temperature goal of limiting global warming to 3.6°F (2°C) above preindustrial levels, whereas there would be virtually no chance if global net emissions followed a pathway well above those implied by country announcements. Actions in the announcements are, by themselves, insufficient to meet a 3.6°F (2°C) goal; the likelihood of achieving that goal depends strongly on the magnitude of global emissions reductions after 2030. (*High confidence*)

Description of evidence base

The primary source supporting this key finding is Fawcett et al.;²⁷ it is also supported by Rogelj et al.,²⁴ Sanderson et al.,²⁵ and the Climate Action Tracker.²⁶ Each of these analyses evaluated the global climate implications of the aggregation of the individual country contributions thus far put forward under the Paris Agreement.

Major uncertainties

The largest uncertainty lies in the assumption of achieving emissions reductions consistent with the announcements prior to December 2015; these reductions are assumed to be achieved but could either be over- or underachieved. This in turn creates uncertainty about the extent of emissions reductions that would be needed after the first round of government announcements in order to achieve the 2°C or any other target. The response of the climate system, the climate sensitivity, is also a source of uncertainty; the Fawcett et al. analysis used the IPCC AR5 range, 1.5° to 4.5°C.

Assessment of confidence based on evidence and agreement, including short description of nature of evidence and level of agreement

There is *high* confidence in this key finding because a number of analyses have examined the implications of these announcements and have come to similar conclusions, as captured in this key finding.

Summary sentence or paragraph that integrates the above information

Different analyses have estimated the implications for global mean temperature of the emissions reductions consistent with the actions announced by governments in the lead up to the 2015 Paris climate conference and have reached similar conclusions. Assuming emissions reductions indicated in these announcements are achieved, along with a range of climate sensitivities, these contributions provide some likelihood of meeting the long-term goal of limiting global warming to well below 3.6°F (2°C) above preindustrial levels, but much depends on assumptions about what happens after 2030.

Key Finding 4

Further assessments of the technical feasibilities, costs, risks, co-benefits, and governance challenges of climate intervention or geoengineering strategies, which are as yet unproven at scale, are a necessary step before judgments about the benefits and risks of these approaches can be made with high confidence. (*High confidence*)

Description of evidence base

Key Finding 4 contains qualitative statements based on the growing literature addressing this topic, including from such bodies as the National Academy of Sciences and the Royal Society, coupled with judgment by the authors about the future interest level in this topic.

Major uncertainties

The major uncertainty is how public perception and interest among policymakers in climate intervention may change over time, even independently from the perceived level of progress made towards reducing CO₂ and other GHG emissions over time.

Assessment of confidence based on evidence and agreement, including short description of nature of evidence and level of agreement

There is *high* confidence that climate intervention strategies may gain greater attention, especially if efforts to slow the buildup of atmospheric CO₂ and other GHGs are considered inadequate by many in the scientific and policy communities.



Summary sentence or paragraph that integrates the above information

The key finding is a qualitative statement based on the growing literature on this topic. The uncertainty moving forward is the comfort level and desire among numerous stakeholders to research and potentially carry out these climate intervention strategies, particularly in light of how progress by the global community to reduce GHG emissions is perceived.



REFERENCES

1. Ciais, P., C. Sabine, G. Bala, L. Bopp, V. Brovkin, J. Canadell, A. Chhabra, R. DeFries, J. Galloway, M. Heimann, C. Jones, C. Le Quéré, R.B. Myneni, S. Piao, and P. Thornton, 2013: Carbon and other biogeochemical cycles. *Climate Change 2013: The Physical Science Basis. Contribution of Working Group I to the Fifth Assessment Report of the Intergovernmental Panel on Climate Change*. Stocker, T.F., D. Qin, G.-K. Plattner, M. Tignor, S.K. Allen, J. Boschung, A. Nauels, Y. Xia, V. Bex, and P.M. Midgley, Eds. Cambridge University Press, Cambridge, United Kingdom and New York, NY, USA, 465–570. <http://www.climatechange2013.org/report/full-report/>
2. Joos, F., R. Roth, J.S. Fuglestedt, G.P. Peters, I.G. Enting, W. von Bloh, V. Brovkin, E.J. Burke, M. Eby, N.R. Edwards, T. Friedrich, T.L. Frölicher, P.R. Halloran, P.B. Holden, C. Jones, T. Kleinen, F.T. Mackenzie, K. Matsumoto, M. Meinshausen, G.K. Plattner, A. Reisinger, J. Segschneider, G. Shaffer, M. Steinacher, K. Strassmann, K. Tanaka, A. Timmermann, and A.J. Weaver, 2013: Carbon dioxide and climate impulse response functions for the computation of greenhouse gas metrics: A multi-model analysis. *Atmospheric Chemistry and Physics*, **13**, 2793–2825. <http://dx.doi.org/10.5194/acp-13-2793-2013>
3. Collins, M., R. Knutti, J. Arblaster, J.-L. Dufresne, T. Fichefet, P. Friedlingstein, X. Gao, W.J. Gutowski, T. Johns, G. Krinner, M. Shongwe, C. Tebaldi, A.J. Weaver, and M. Wehner, 2013: Long-term climate change: Projections, commitments and irreversibility. *Climate Change 2013: The Physical Science Basis. Contribution of Working Group I to the Fifth Assessment Report of the Intergovernmental Panel on Climate Change*. Stocker, T.F., D. Qin, G.-K. Plattner, M. Tignor, S.K. Allen, J. Boschung, A. Nauels, Y. Xia, V. Bex, and P.M. Midgley, Eds. Cambridge University Press, Cambridge, United Kingdom and New York, NY, USA, 1029–1136. <http://www.climatechange2013.org/report/full-report/>
4. Solomon, S., G.K. Plattner, R. Knutti, and P. Friedlingstein, 2009: Irreversible climate change due to carbon dioxide emissions. *Proceedings of the National Academy of Sciences of the United States of America*, **106**, 1704–1709. <http://dx.doi.org/10.1073/pnas.0812721106>
5. Tebaldi, C. and P. Friedlingstein, 2013: Delayed detection of climate mitigation benefits due to climate inertia and variability. *Proceedings of the National Academy of Sciences*, **110**, 17229–17234. <http://dx.doi.org/10.1073/pnas.1300005110>
6. Prather, M.J., J.E. Penner, J.S. Fuglestedt, A. Kurosawa, J.A. Lowe, N. Höhne, A.K. Jain, N. Andronova, L. Pinguelli, C. Pires de Campos, S.C.B. Raper, R.B. Skeie, P.A. Stott, J. van Aardenne, and F. Wagner, 2009: Tracking uncertainties in the causal chain from human activities to climate. *Geophysical Research Letters*, **36**, L05707. <http://dx.doi.org/10.1029/2008GL036474>
7. Kirtman, B., S.B. Power, J.A. Adedoyin, G.J. Boer, R. Bojariu, I. Camilloni, F.J. Doblas-Reyes, A.M. Fiore, M. Kimoto, G.A. Meehl, M. Prather, A. Sarr, C. Schär, R. Sutton, G.J. van Oldenborgh, G. Vecchi, and H.J. Wang, 2013: Near-term climate change: Projections and predictability. *Climate Change 2013: The Physical Science Basis. Contribution of Working Group I to the Fifth Assessment Report of the Intergovernmental Panel on Climate Change*. Stocker, T.F., D. Qin, G.-K. Plattner, M. Tignor, S.K. Allen, J. Boschung, A. Nauels, Y. Xia, V. Bex, and P.M. Midgley, Eds. Cambridge University Press, Cambridge, UK and New York, NY, USA, 953–1028. <http://www.climatechange2013.org/report/full-report/>
8. Paltsev, S., E. Monier, J. Scott, A. Sokolov, and J. Reilly, 2015: Integrated economic and climate projections for impact assessment. *Climatic Change*, **131**, 21–33. <http://dx.doi.org/10.1007/s10584-013-0892-3>
9. Tebaldi, C. and M.F. Wehner, 2016: Benefits of mitigation for future heat extremes under RCP4.5 compared to RCP8.5. *Climatic Change*, **First online**, 1–13. <http://dx.doi.org/10.1007/s10584-016-1605-5>
10. Zaelke, D. and N. Borgford-Parnell, 2015: The importance of phasing down hydrofluorocarbons and other short-lived climate pollutants. *Journal of Environmental Studies and Sciences*, **5**, 169–175. <http://dx.doi.org/10.1007/s13412-014-0215-7>
11. Myhre, G., D. Shindell, F.-M. Bréon, W. Collins, J. Fuglestedt, J. Huang, D. Koch, J.-F. Lamarque, D. Lee, B. Mendoza, T. Nakajima, A. Robock, G. Stephens, T. Takemura, and H. Zhang, 2013: Anthropogenic and natural radiative forcing. *Climate Change 2013: The Physical Science Basis. Contribution of Working Group I to the Fifth Assessment Report of the Intergovernmental Panel on Climate Change*. Stocker, T.F., D. Qin, G.-K. Plattner, M. Tignor, S.K. Allen, J. Boschung, A. Nauels, Y. Xia, V. Bex, and P.M. Midgley, Eds. Cambridge University Press, Cambridge, United Kingdom and New York, NY, USA, 659–740. <http://www.climatechange2013.org/report/full-report/>
12. Bond, T.C., S.J. Doherty, D.W. Fahey, P.M. Forster, T. Berntsen, B.J. DeAngelo, M.G. Flanner, S. Ghan, B. Kärcher, D. Koch, S. Kinne, Y. Kondo, P.K. Quinn, M.C. Sarofim, M.G. Schultz, M. Schulz, C. Venkataraman, H. Zhang, S. Zhang, N. Bellouin, S.K. Guttikunda, P.K. Hopke, M.Z. Jacobson, J.W. Kaiser, Z. Klimont, U. Lohmann, J.P. Schwarz, D. Shindell, T. Storelvmo, S.G. Warren, and C.S. Zender, 2013: Bounding the role of black carbon in the climate system: A scientific assessment. *Journal of Geophysical Research Atmospheres*, **118**, 5380–5552. <http://dx.doi.org/10.1002/jgrd.50171>

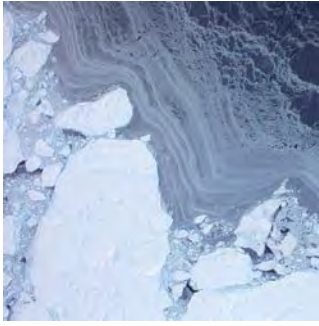


13. Anenberg, S.C., J. Schwartz, D. Shindell, M. Amann, G. Faluvegi, Z. Klimont, G. Janssens-Maenhout, L. Pozzoli, R. Van Dingenen, E. Vignati, L. Emberson, N.Z. Muller, J.J. West, M. Williams, V. Demkine, W.K. Hicks, J. Kuylensstierna, F. Raes, and V. Ramanathan, 2012: Global air quality and health co-benefits of mitigating near-term climate change through methane and black carbon emission controls. *Environmental Health Perspectives*, **120**, 831-839. <http://dx.doi.org/10.1289/ehp.1104301>
14. Rao, S., Z. Klimont, J. Leitao, K. Riahi, R. van Dingenen, L.A. Reis, K. Calvin, F. Dentener, L. Drouet, S. Fujimori, M. Harmsen, G. Luderer, C. Heyes, J. Strefler, M. Tavoni, and D.P. van Vuuren, 2016: A multi-model assessment of the co-benefits of climate mitigation for global air quality. *Environmental Research Letters*, **11**, 124013. <http://dx.doi.org/10.1088/1748-9326/11/12/124013>
15. Hayhoe, K.A.S., H.S. Kheshgi, A.K. Jain, and D.J. Wuebbles, 1998: Tradeoffs in fossil fuel use: The effects of CO₂, CH₄, and SO₂ aerosol emissions on climate. *World Resources Review*, **10**.
16. Shah, N., M. Wei, E.L. Virginie, and A.A. Phadke, 2015: Benefits of Leapfrogging to Superefficiency and Low Global Warming Potential Refrigerants in Room Air Conditioning. Lawrence Berkeley National Laboratory, Energy Technology Area, Berkeley, CA. 39 pp. <https://eetd.lbl.gov/publications/benefits-of-leapfrogging-to-superef-0>
17. Shindell, D., J.C.I. Kuylensstierna, E. Vignati, R. van Dingenen, M. Amann, Z. Klimont, S.C. Anenberg, N. Muller, G. Janssens-Maenhout, F. Raes, J. Schwartz, G. Faluvegi, L. Pozzoli, K. Kupiainen, L. Hoggland-Isaksson, L. Emberson, D. Streets, V. Ramanathan, K. Hicks, N.T.K. Oanh, G. Milly, M. Williams, V. Demkine, and D. Fowler, 2012: Simultaneously mitigating near-term climate change and improving human health and food security. *Science*, **335**, 183-189. <http://dx.doi.org/10.1126/science.1210026>
18. Rogelj, J., M. Meinshausen, M. Schaeffer, R. Knutti, and K. Riahi, 2015: Impact of short-lived non-CO₂ mitigation on carbon budgets for stabilizing global warming. *Environmental Research Letters*, **10**, 075001. <http://dx.doi.org/10.1088/1748-9326/10/7/075001>
19. NRC, 2011: *Climate Stabilization Targets: Emissions, Concentrations, and Impacts over Decades to Millennia*. National Research Council. The National Academies Press, Washington, D.C., 298 pp. <http://dx.doi.org/10.17226/12877>
20. Le Quéré, C., R.M. Andrew, J.G. Canadell, S. Sitch, J.I. Korsbakken, G.P. Peters, A.C. Manning, T.A. Boden, P.P. Tans, R.A. Houghton, R.F. Keeling, S. Alin, O.D. Andrews, P. Anthoni, L. Barbero, L. Bopp, F. Chevallier, L.P. Chini, P. Ciais, K. Currie, C. Delire, S.C. Doney, P. Friedlingstein, T. Gkritzalis, I. Harris, J. Hauck, V. Haverd, M. Hoppema, K. Klein Goldewijk, A.K. Jain, E. Kato, A. Körtzinger, P. Landschützer, N. Lefèvre, A. Lenton, S. Lienert, D. Lombardozi, J.R. Melton, N. Metzl, F. Millero, P.M.S. Monteiro, D.R. Munro, J.E.M.S. Nabel, S.I. Nakaoka, K. O'Brien, A. Olsen, A.M. Omar, T. Ono, D. Pierrot, B. Poulter, C. Rödenbeck, J. Salisbury, U. Schuster, J. Schwinger, R. Séférian, I. Skjelvan, B.D. Stocker, A.J. Sutton, T. Takahashi, H. Tian, B. Tilbrook, I.T. van der Laan-Luijkx, G.R. van der Werf, N. Viovy, A.P. Walker, A.J. Wiltshire, and S. Zaehle, 2016: Global carbon budget 2016. *Earth System Science Data*, **8**, 605-649. <http://dx.doi.org/10.5194/essd-8-605-2016>
21. Allen, M.R., D.J. Frame, C. Huntingford, C.D. Jones, J.A. Lowe, M. Meinshausen, and N. Meinshausen, 2009: Warming caused by cumulative carbon emissions towards the trillionth tonne. *Nature*, **458**, 1163-1166. <http://dx.doi.org/10.1038/nature08019>
22. Nordhaus, W.D., 1975: Can We Control Carbon Dioxide? International Institute for Applied Systems Analysis (IIASA), Laxenburg, Austria. 47 pp. <http://pure.iiasa.ac.at/365/>
23. Stockholm Environment Institute, 1990: Targets and Indicators of Climatic Change. Rijsberman, F.R. and R.J. Swart (Eds.). Stockholm Environment Institute, Stockholm, Sweden. 166 pp. <https://www.sei-international.org/mediamanager/documents/Publications/SEI-Report-TargetsAndIndicatorsOfClimatic-Change-1990.pdf>
24. Rogelj, J., M. den Elzen, N. Höhne, T. Fransen, H. Fekete, H. Winkler, R. Schaeffer, F. Sha, K. Riahi, and M. Meinshausen, 2016: Paris Agreement climate proposals need a boost to keep warming well below 2 °C. *Nature*, **534**, 631-639. <http://dx.doi.org/10.1038/nature18307>
25. Sanderson, B.M., B.C. O'Neill, and C. Tebaldi, 2016: What would it take to achieve the Paris temperature targets? *Geophysical Research Letters*, **43**, 7133-7142. <http://dx.doi.org/10.1002/2016GL069563>
26. Climate Action Tracker, 2016: Climate Action Tracker. <http://climateactiontracker.org/global.html>
27. Fawcett, A.A., G.C. Iyer, L.E. Clarke, J.A. Edmonds, N.E. Hultman, H.C. McJeon, J. Rogelj, R. Schuler, J. Alsalam, G.R. Asrar, J. Creason, M. Jeong, J. McFarland, A. Mundra, and W. Shi, 2015: Can Paris pledges avert severe climate change? *Science*, **350**, 1168-1169. <http://dx.doi.org/10.1126/science.aad5761>



28. UNFCCC, 2015: Paris Agreement. United Nations Framework Convention on Climate Change, [Bonn, Germany]. 25 pp. http://unfccc.int/files/essential_background/convention/application/pdf/english_paris_agreement.pdf
29. NAS, 2015: *Climate Intervention: Carbon Dioxide Removal and Reliable Sequestration*. The National Academies Press, Washington, DC, 154 pp. <http://dx.doi.org/10.17226/18805>
30. NAS, 2015: *Climate Intervention: Reflecting Sunlight to Cool Earth*. The National Academies Press, Washington, DC, 260 pp. <http://dx.doi.org/10.17226/18988>
31. Fuss, S., J.G. Canadell, G.P. Peters, M. Tavoni, R.M. Andrew, P. Ciais, R.B. Jackson, C.D. Jones, F. Kraxner, N. Nakicenovic, C. Le Quere, M.R. Raupach, A. Sharifi, P. Smith, and Y. Yamagata, 2014: Betting on negative emissions. *Nature Climate Change*, **4**, 850-853. <http://dx.doi.org/10.1038/nclimate2392>
32. Smith, P., S.J. Davis, F. Creutzig, S. Fuss, J. Minx, B. Gabrielle, E. Kato, R.B. Jackson, A. Cowie, E. Kriegler, D.P. van Vuuren, J. Rogelj, P. Ciais, J. Milne, J.G. Canadell, D. McCollum, G. Peters, R. Andrew, V. Krey, G. Shrestha, P. Friedlingstein, T. Gasser, A. Grubler, W.K. Heidug, M. Jonas, C.D. Jones, F. Kraxner, E. Littleton, J. Lowe, J.R. Moreira, N. Nakicenovic, M. Obersteiner, A. Patwardhan, M. Rogner, E. Rubin, A. Sharifi, A. Torvanger, Y. Yamagata, J. Edmonds, and C. Yongsung, 2016: Biophysical and economic limits to negative CO₂ emissions. *Nature Climate Change*, **6**, 42-50. <http://dx.doi.org/10.1038/nclimate2870>
33. Keith, D.W., R. Duren, and D.G. MacMartin, 2014: Field experiments on solar geoengineering: Report of a workshop exploring a representative research portfolio. *Philosophical Transactions of the Royal Society A: Mathematical, Physical and Engineering Sciences*, **372**, 20140175. <http://dx.doi.org/10.1098/rsta.2014.0175>
34. Kravitz, B., K. Caldeira, O. Boucher, A. Robock, P.J. Rasch, K. Alterskjær, D.B. Karam, J.N.S. Cole, C.L. Curry, J.M. Haywood, P.J. Irvine, D. Ji, A. Jones, J.E. Kristjánsson, D.J. Lunt, J.C. Moore, U. Niemeier, H. Schmidt, M. Schulz, B. Singh, S. Tilmes, S. Watanabe, S. Yang, and J.-H. Yoon, 2013: Climate model response from the Geoengineering Model Intercomparison Project (GeoMIP). *Journal of Geophysical Research Atmospheres*, **118**, 8320-8332. <http://dx.doi.org/10.1002/jgrd.50646>
35. Pierce, J.R., D.K. Weisenstein, P. Heckendorn, T. Peter, and D.W. Keith, 2010: Efficient formation of stratospheric aerosol for climate engineering by emission of condensable vapor from aircraft. *Geophysical Research Letters*, **37**, L18805. <http://dx.doi.org/10.1029/2010GL043975>
36. Tilmes, S., B.M. Sanderson, and B.C. O'Neill, 2016: Climate impacts of geoengineering in a delayed mitigation scenario. *Geophysical Research Letters*, **43**, 8222-8229. <http://dx.doi.org/10.1002/2016GL070122>
37. Keith, D.W. and D.G. MacMartin, 2015: A temporary, moderate and responsive scenario for solar geoengineering. *Nature Climate Change*, **5**, 201-206. <http://dx.doi.org/10.1038/nclimate2493>
38. Ricke, K.L., M.G. Morgan, and M.R. Allen, 2010: Regional climate response to solar-radiation management. *Nature Geoscience*, **3**, 537-541. <http://dx.doi.org/10.1038/ngeo915>
39. MacMartin, D.G., D.W. Keith, B. Kravitz, and K. Caldeira, 2013: Management of trade-offs in geoengineering through optimal choice of non-uniform radiative forcing. *Nature Climate Change*, **3**, 365-368. <http://dx.doi.org/10.1038/nclimate1722>
40. MacCracken, M.C., 2016: The rationale for accelerating regionally focused climate intervention research. *Earth's Future*, **4**, 649-657. <http://dx.doi.org/10.1002/2016EF000450>
41. Shepherd, J.G., K. Caldeira, P. Cox, J. Haigh, D. Keith, B. Launder, G. Mace, G. MacKerron, J. Pyle, S. Rayner, C. Redgwell, and A. Watson, 2009: *Geoengineering the Climate: Science, Governance and Uncertainty*. Royal Society, 82 pp. http://eprints.soton.ac.uk/156647/1/Geoengineering_the_climate.pdf
42. IPCC, 2013: Summary for policymakers. *Climate Change 2013: The Physical Science Basis. Contribution of Working Group I to the Fifth Assessment Report of the Intergovernmental Panel on Climate Change*. Stocker, T.F., D. Qin, G.-K. Plattner, M. Tignor, S.K. Allen, J. Boschung, A. Nauels, Y. Xia, V. Bex, and P.M. Midgley, Eds. Cambridge University Press, Cambridge, United Kingdom and New York, NY, USA, 1-30. <http://www.climatechange2013.org/report/>





15

Potential Surprises: Compound Extremes and Tipping Elements

KEY FINDINGS

1. Positive feedbacks (self-reinforcing cycles) within the climate system have the potential to accelerate human-induced climate change and even shift the Earth's climate system, in part or in whole, into new states that are very different from those experienced in the recent past (for example, ones with greatly diminished ice sheets or different large-scale patterns of atmosphere or ocean circulation). Some feedbacks and potential state shifts can be modeled and quantified; others can be modeled or identified but not quantified; and some are probably still unknown. (*Very high confidence* in the potential for state shifts and in the incompleteness of knowledge about feedbacks and potential state shifts).
2. The physical and socioeconomic impacts of compound extreme events (such as simultaneous heat and drought, wildfires associated with hot and dry conditions, or flooding associated with high precipitation on top of snow or waterlogged ground) can be greater than the sum of the parts (*very high confidence*). Few analyses consider the spatial or temporal correlation between extreme events.
3. While climate models incorporate important climate processes that can be well quantified, they do not include all of the processes that can contribute to feedbacks, compound extreme events, and abrupt and/or irreversible changes. For this reason, future changes outside the range projected by climate models cannot be ruled out (*very high confidence*). Moreover, the systematic tendency of climate models to underestimate temperature change during warm paleoclimates suggests that climate models are more likely to underestimate than to overestimate the amount of long-term future change (*medium confidence*).

Recommended Citation for Chapter

Kopp, R.E., K. Hayhoe, D.R. Easterling, T. Hall, R. Horton, K.E. Kunkel, and A.N. LeGrande, 2017: Potential surprises – compound extremes and tipping elements. In: *Climate Science Special Report: Fourth National Climate Assessment, Volume I* [Wuebbles, D.J., D.W. Fahey, K.A. Hibbard, D.J. Dokken, B.C. Stewart, and T.K. Maycock (eds.)]. U.S. Global Change Research Program, Washington, DC, USA, pp. 411-429, doi: 10.7930/J0GB227J.

15.1 Introduction

The Earth system is made up of many components that interact in complex ways across a broad range of temporal and spatial scales. As a result of these interactions the behavior of the system cannot be predicted by looking at individual components in isolation. Negative feedbacks, or self-stabilizing cycles, within and between components of the Earth system can dampen changes (Ch. 2: Physical Drivers of Climate Change). However, their stabilizing effects render such feedbacks of less concern from a risk perspective than positive feedbacks, or self-reinforcing cycles. Positive feedbacks magnify both natural and anthropogenic changes. Some Earth system components, such as arctic sea ice and the polar ice sheets, may exhibit thresholds beyond which these self-reinforcing cycles can drive the component, or the entire system, into a radically different state. Although the probabilities of these state shifts may be difficult to assess, their consequences could be high, potentially exceeding anything anticipated by climate model projections for the coming century.

Humanity's effect on the Earth system, through the large-scale combustion of fossil fuels and widespread deforestation and the resulting release of carbon dioxide (CO₂) into the atmosphere, as well as through emissions of other greenhouse gases and radiatively active substances from human activities, is unprecedented (Ch. 2: Physical Drivers of Climate Change). These forcings are driving changes in temperature and other climate variables. Previous chapters have covered a variety of observed and projected changes in such variables, including averages and extremes of temperature, precipitation, sea level, and storm events (see Chapters 1, 4–13).

While the distribution of climate model projections provides insight into the range of possible future changes, this range is limited

by the fact that models do not include or fully represent all of the known processes and components of the Earth system (e.g., ice sheets or arctic carbon reservoirs),¹ nor do they include all of the interactions between these components that contribute to the self-stabilizing and self-reinforcing cycles mentioned above (e.g., the dynamics of the interactions between ice sheets, the ocean, and the atmosphere). They also do not include currently unknown processes that may become increasingly relevant under increasingly large climate forcings. This limitation is emphasized by the systematic tendency of climate models to underestimate temperature change during warm paleoclimates (Section 15.5). Therefore, there is significant potential for humanity's effect on the planet to result in unanticipated surprises and a broad consensus that the further and faster the Earth system is pushed towards warming, the greater the risk of such surprises.

Scientists have been surprised by the Earth system many times in the past. The discovery of the ozone hole is a clear example. Prior to groundbreaking work by Molina and Rowland², chlorofluorocarbons (CFCs) were viewed as chemically inert; the chemistry by which they catalyzed stratospheric ozone depletion was unknown. Within eleven years of Molina and Rowland's work, British Antarctic Survey scientists reported ground observations showing that spring ozone concentrations in the Antarctic, driven by chlorine from human-emitted CFCs, had fallen by about one-third since the late 1960s.³ The problem quickly moved from being an "unknown unknown" to a "known known," and by 1987, the Montreal Protocol was adopted to phase out these ozone-depleting substances.

Another surprise has come from arctic sea ice. While the potential for powerful positive ice-albedo feedbacks has been understood since the late 19th century, climate models



have struggled to capture the magnitude of these feedbacks and to include all the relevant dynamics that affect sea ice extent. As of 2007, the observed decline in arctic sea ice from the start of the satellite era in 1979 outpaced the declines projected by almost all the models used by the Intergovernmental Panel on Climate Change’s Fourth Assessment Report (AR4),⁴ and it was not until AR4 that the IPCC first raised the prospect of an ice-free summer Arctic during this century.⁵ More recent studies are more consistent with observations and have moved the date of an ice-free summer Arctic up to approximately mid-century (see Ch. 11: Arctic Changes).⁶ But continued rapid declines – 2016 featured the lowest annually averaged arctic sea ice extent on record, and the 2017 winter maximum was also the lowest on record – suggest that climate models may still be underestimating or missing relevant feedback processes. These processes could include, for example, effects of melt ponds, changes in storminess and ocean wave impacts, and warming of near surface waters.^{7, 8, 9}

This chapter focuses primarily on two types of potential surprises. The first arises from potential changes in correlations between extreme events that may not be surprising on their own but together can increase the likelihood of compound extremes, in which multiple events occur simultaneously or in rapid sequence. Increasingly frequent compound extremes – either of multiple types of events (such as paired extremes of droughts and intense rainfall) or over greater spatial or temporal scales (such as a drought occurring in multiple major agricultural regions around the world or lasting for multiple decades) – are often not captured by analyses that focus solely on one type of extreme.

The second type of surprise arises from self-reinforcing cycles, which can give rise to “tipping elements” – subcomponents of the Earth

system that can be stable in multiple different states and can be “tipped” between these states by small changes in forcing, amplified by positive feedbacks. Examples of potential tipping elements include ice sheets, modes of atmosphere–ocean circulation like the El Niño–Southern Oscillation, patterns of ocean circulation like the Atlantic meridional overturning circulation, and large-scale ecosystems like the Amazon rainforest.^{10, 11} While compound extremes and tipping elements constitute at least partially “known unknowns,” the paleoclimate record also suggests the possibility of “unknown unknowns.” These possibilities arise in part from the tendency of current climate models to underestimate past responses to forcing, for reasons that may or may not be explained by current hypotheses (e.g., hypotheses related to positive feedbacks that are unrepresented or poorly represented in existing models).

15.2 Risk Quantification and Its Limits

Quantifying the risk of low-probability, high-impact events, based on models or observations, usually involves examining the tails of a probability distribution function (PDF). Robust detection, attribution, and projection of such events into the future is challenged by multiple factors, including an observational record that often does not represent the full range of physical possibilities in the climate system, as well as the limitations of the statistical tools, scientific understanding, and models used to describe these processes.¹²

The 2013 Boulder, Colorado, floods and the Dust Bowl of the 1930s in the central United States are two examples of extreme events whose magnitude and/or extent are unprecedented in the observational record. Statistical approaches such as Extreme Value Theory can be used to model and estimate the magnitude of rare events that may not have occurred in the observational record, such as the “1,000-



year flood event” (i.e., a flood event with a 0.1% chance of occurrence in any given year) (e.g., Smith 1987¹³). While useful for many applications, these are not physical models: they are statistical models that are typically based on the assumption that observed patterns of natural variability (that is, the sample from which the models derive their statistics) are both valid and stationary beyond the observational period. Extremely rare events can also be assessed based upon paleoclimate records and physical modeling. In the paleoclimatic record, numerous abrupt changes have occurred since the last deglaciation, many larger than those recorded in the instrumental record. For example, tree ring records of drought in the western United States show abrupt, long-lasting megadroughts that were similar to but more intense and longer-lasting than the 1930s Dust Bowl.¹⁴

Since models are based on physics rather than observational data, they are not inherently constrained to any given time period or set of physical conditions. They have been used to study the Earth in the distant past and even the climate of other planets (e.g., Lunt et al. 2012;¹⁵ Navarro et al. 2014¹⁶). Looking to the future, thousands of years’ worth of simulations can be generated and explored to characterize small-probability, high-risk extreme events, as well as correlated extremes (see Section 15.3). However, the likelihood that such model events represent real risks is limited by well-known uncertainties in climate modeling related to parameterizations, model resolution, and limits to scientific understanding (Ch. 4: Projections). For example, conventional convective parameterizations in global climate models systematically underestimate extreme precipitation.¹⁷ In addition, models often do not accurately capture or even include the processes, such as permafrost feedbacks, by which abrupt, non-reversible change may occur (see Section 15.4). An analysis focusing

on physical climate predictions over the last 20 years found a tendency for scientific assessments such as those of the IPCC to under-predict rather than over-predict changes that were subsequently observed.¹⁸

15.3 Compound Extremes

An important aspect of surprise is the potential for compound extreme events. These can be events that occur at the same time or in sequence (such as consecutive floods in the same region) and in the same geographic location or at multiple locations within a given country or around the world (such as the 2009 Australian floods and wildfires). They may consist of multiple extreme events or of events that by themselves may not be extreme but together produce a multi-event occurrence (such as a heat wave accompanied by drought¹⁹). It is possible for the net impact of these events to be less than the sum of the individual events if their effects cancel each other out. For example, increasing CO₂ concentrations and acceleration of the hydrological cycle may mitigate the future impact of extremes in gross primary productivity that currently impact the carbon cycle.²⁰ However, from a risk perspective, the primary concern relates to compound extremes with additive or even multiplicative effects.

Some areas are susceptible to multiple types of extreme events that can occur simultaneously. For example, certain regions are susceptible to both flooding from coastal storms and riverine flooding from snow melt, and a compound event would be the occurrence of both simultaneously. Compound events can also result from shared forcing factors, including natural cycles like the El Niño–Southern Oscillation (ENSO); large-scale circulation patterns, such as the ridge observed during the 2011–2017 California drought (e.g., Swain et al. 2016²¹; see also Ch. 8: Droughts, Floods, and Wildfires); or relatively greater regional sensitivity



to global change, as may occur in “hot spots” such as the western United States.²² Finally, compound events can result from mutually reinforcing cycles between individual events, such as the relationship between drought and heat, linked through soil moisture and evaporation, in water-limited areas.²³

In a changing climate, the probability of compound events can be altered if there is an underlying trend in conditions such as mean temperature, precipitation, or sea level that alters the baseline conditions or vulnerability of a region. It can also be altered if there is a change in the frequency or intensity of individual extreme events relative to the changing mean (for example, stronger storm surges, more frequent heat waves, or heavier precipitation events).

The occurrence of warm/dry and warm/wet conditions is discussed extensively in the literature; at the global scale, these conditions have increased since the 1950s,²⁴ and analysis of NOAA’s billion-dollar disasters illustrates the correlation between temperature and precipitation extremes during the costliest climate and weather events since 1980 (Figure 15.1, right). In the future, hot summers will become more frequent, and although it is not always clear for every region whether drought frequency will change, droughts in already dry regions, such as the southwestern United States, are likely to be more intense in a warmer world due to faster evaporation and associated surface drying.^{25, 26, 27} For other regions, however, the picture is not as clear. Recent examples of heat/drought events (in the southern Great Plains in 2011 or in California, 2012–2016) have highlighted the inadequacy of traditional univariate risk assessment methods.²⁸ Yet a bivariate analysis for the contiguous United States of precipitation deficits and positive temperature anomalies finds no significant trend in the last 30 years.²⁹

Another compound event frequently discussed in the literature is the increase in wildfire risk resulting from the combined effects of high precipitation variability (wet seasons followed by dry), elevated temperature, and low humidity. If followed by heavy rain, wildfires can in turn increase the risk of landslides and erosion. They can also radically increase emissions of greenhouse gases, as demonstrated by the amount of carbon dioxide produced by the Fort McMurray fires of May 2016—more than 10% of Canada’s annual emissions.

A third example of a compound event involves flooding arising from wet conditions due to precipitation or to snowmelt, which could be exacerbated by warm temperatures. These wet conditions lead to high groundwater levels, saturated soils, and/or elevated river flows, which can increase the risk of flooding associated with a given storm days or even months later.²³

Compound events may surprise in two ways. The first is if known types of compound events recur, but are stronger, longer-lasting, and/or more widespread than those experienced in the observational record or projected by model simulations for the future. One example would be simultaneous drought events in different agricultural regions across the country, or even around the world, that challenge the ability of human systems to provide adequate affordable food. Regions that lack the ability to adapt would be most vulnerable to this risk (e.g., Fraser et al. 2013³⁰). Another example would be the concurrent and more severe heavy precipitation events that have occurred in the U.S. Midwest in recent years. After record insurance payouts following the events, in 2014 several insurance companies, led by Farmers Insurance, sued the city of Chicago and surrounding counties for failing to adequately prepare for the impacts of a changing climate. Although the suit was



dropped later that same year, their point was made: in some regions of the United States, the insurance industry is not able to cope with the increasing frequency and/or concurrence of certain types of extreme events.

The second way in which compound events could surprise would be the emergence of new types of compound events not observed in the historical record or predicted by model simulations, due to model limitations (in terms of both their spatial resolution as well as their ability to explicitly resolve the physical processes that would result in such compound

events), an increase in the frequency of such events from human-induced climate change, or both. An example is Hurricane Sandy, where sea level rise, anomalously high ocean temperatures, and high tides combined to strengthen both the storm and the magnitude of the associated storm surge.³¹ At the same time, a blocking ridge over Greenland—a feature whose strength and frequency may be related to both Greenland surface melt and reduced summer sea ice in the Arctic (see also Ch. 11: Arctic Changes)³²—redirected the storm inland to what was, coincidentally, an exceptionally high-exposure location.

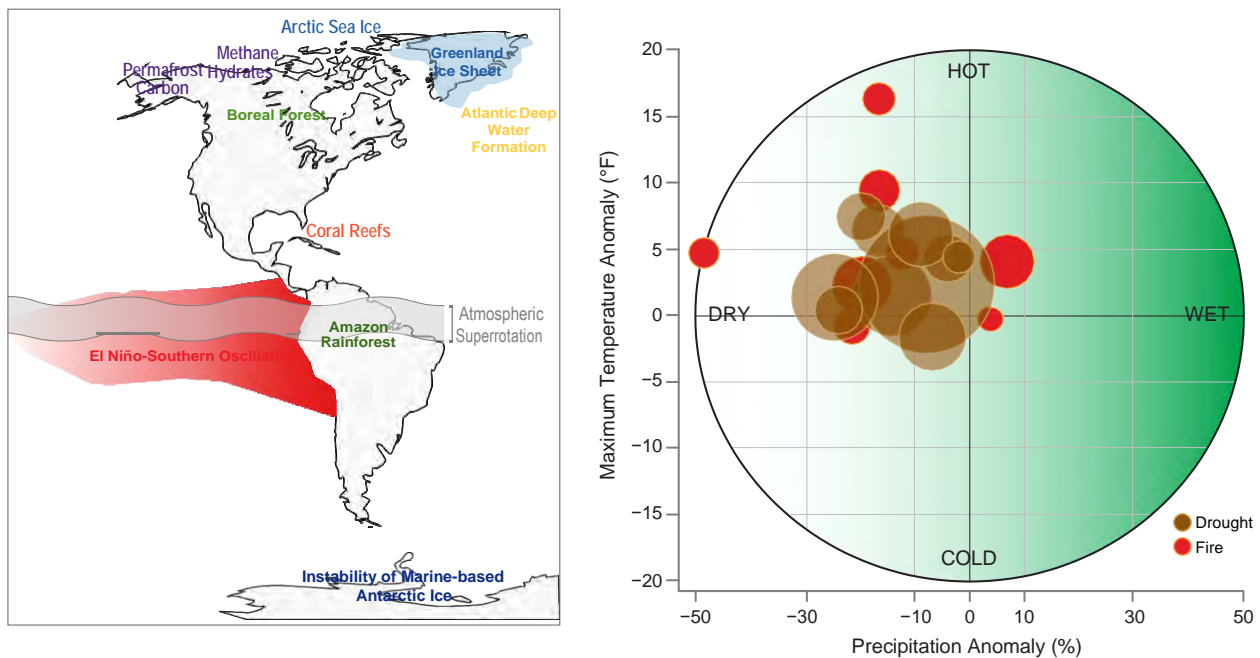


Figure 15.1: (left) Potential climatic tipping elements affecting the Americas (Figure source: adapted from Lenton et al. 2008¹⁰). (right) Wildfire and drought events from the NOAA Billion Dollar Weather Events list (1980–2016), and associated temperature and precipitation anomalies. Dot size scales with the magnitude of impact, as reflected by the cost of the event. These high-impact events occur preferentially under hot, dry conditions.

15.4 Climatic Tipping Elements

Different parts of the Earth system exhibit *critical thresholds*, sometimes called “tipping points” (e.g., Lenton et al. 2008;¹⁰ Collins et al. 2013;²⁵ NRC 2013;³³ Kopp et al. 2016¹¹). These parts, known as *tipping elements*, have the potential to enter into self-amplifying cycles that commit them to shifting from their current state into a new state: for example, from one in which the summer Arctic Ocean is covered by ice, to one in which it is ice-free. In some potential tipping elements, these state shifts occur abruptly; in others, the commitment to a

state shift may occur rapidly, but the state shift itself may take decades, centuries, or even millennia to play out. Often the forcing that commits a tipping element to a shift in state is unknown. Sometimes, it is even unclear whether a proposed tipping element actually exhibits tipping behavior. Through a combination of physical modeling, paleoclimate observations, and expert elicitations, scientists have identified a number of possible tipping elements in atmosphere–ocean circulation, the cryosphere, the carbon cycle, and ecosystems (Figure 15.1, left; Table 15.1).

Table 15.1: Potential tipping elements (adapted from Kopp et al. 2016¹¹).

Candidate Climatic Tipping Element	State Shift	Main Impact Pathways
Atmosphere–ocean circulation		
Atlantic meridional overturning circulation	Major reduction in strength	Regional temperature and precipitation; global mean temperature; regional sea level
El Niño–Southern Oscillation	Increase in amplitude	Regional temperature and precipitation
Equatorial atmospheric superrotation	Initiation	Cloud cover; climate sensitivity
Regional North Atlantic Ocean convection	Major reduction in strength	Regional temperature and precipitation
Cryosphere		
Antarctic Ice Sheet	Major decrease in ice volume	Sea level; albedo; freshwater forcing on ocean circulation
Arctic sea ice	Major decrease in summertime and/or perennial area	Regional temperature and precipitation; albedo
Greenland Ice Sheet	Major decrease in ice volume	Sea level; albedo; freshwater forcing on ocean circulation
Carbon cycle		
Methane hydrates	Massive release of carbon	Greenhouse gas emissions
Permafrost carbon	Massive release of carbon	Greenhouse gas emissions
Ecosystem		
Amazon rainforest	Dieback, transition to grasslands	Greenhouse gas emissions; biodiversity
Boreal forest	Dieback, transition to grasslands	Greenhouse gas emissions; albedo; biodiversity
Coral reefs	Die-off	Biodiversity



One important tipping element is the Atlantic meridional overturning circulation (AMOC), a major component of global ocean circulation. Driven by the sinking of cold, dense water in the North Atlantic near Greenland, its strength is projected to decrease with warming due to freshwater input from increased precipitation, glacial melt, and melt of the Greenland Ice Sheet (see also discussion in Ch. 11: Arctic Changes).³⁴ A decrease in AMOC strength is probable and may already be culpable for the “warming hole” observed in the North Atlantic,^{34,35} although it is still unclear whether this decrease represents a forced change or internal variability.³⁶ Given sufficient freshwater input, there is even the possibility of complete AMOC collapse. Most models do not predict such a collapse in the 21st century,³³ although one study that used observations to bias-correct climate model simulations found that CO₂ concentrations of 700 ppm led to a AMOC collapse within 300 years.³⁷

A slowing or collapse of the AMOC would have several consequences for the United States. A decrease in AMOC strength would accelerate sea level rise off the northeastern United States,³⁸ while a full collapse could result in as much as approximately 1.6 feet (0.5 m) of regional sea level rise,^{39,40} as well as a cooling of approximately 0°–4°F (0°–2°C) over the country.^{37,41} These changes would occur in addition to preexisting global and regional sea level and temperature change. A slowdown of the AMOC would also lead to a reduction of ocean carbon dioxide uptake, and thus an acceleration of global-scale warming.⁴²

Another tipping element is the atmospheric-oceanic circulation of the equatorial Pacific that, through a set of feedbacks, drives the state shifts of the El Niño–Southern Oscillation. This is an example of a tipping element that already shifts on a sub-decadal, interannual timescale,

primarily in response to internal noise. Climate model experiments suggest that warming will reduce the threshold needed to trigger extremely strong El Niño and La Niña events.⁴³ ⁴⁴ As evident from recent El Niño and La Niña events, such a shift would negatively impact many regions and sectors across the United States (for more on ENSO impacts, see Ch. 5: Circulation and Variability).

A third potential tipping element is arctic sea ice, which may exhibit abrupt state shifts into summer ice-free or year-round ice-free states.^{45,46} As discussed above, climate models have historically underestimated the rate of arctic sea ice loss. This is likely due to insufficient representation of critical positive feedbacks in models. Such feedbacks could include: greater high-latitude storminess and ocean wave penetration as sea ice declines; more northerly incursions of warm air and water; melting associated with increasing water vapor; loss of multiyear ice; and albedo decreases on the sea ice surface (e.g., Schröder et al. 2014;⁷ Asplin et al. 2012;⁸ Perovich et al. 2008⁹). At the same time, however, the point at which the threshold for an abrupt shift would be crossed also depends on the role of natural variability in a changing system; the relative importance of potential stabilizing negative feedbacks, such as more efficient heat transfer from the ocean to the atmosphere in fall and winter as sea declines; and how sea ice in other seasons, as well as the climate system more generally, responds once the first “ice-free” summer occurs (e.g., Ding et al. 2017⁴⁷). It is also possible that summer sea ice may not abruptly collapse, but instead respond in a manner proportional to the increase in temperature.^{48,49,50,51} Moreover, an abrupt decrease in winter sea ice may result simply as the gradual warming of Arctic Ocean causes it to cross a critical temperature for ice formation, rather than from self-reinforcing cycles.⁵²



Two possible tipping elements in the carbon cycle also lie in the Arctic. The first is buried in the permafrost, which contains an estimated 1,300–1,600 GtC (see also Ch. 11: Arctic Changes).⁵³ As the Arctic warms, about 5–15% is estimated to be vulnerable to release in this century.⁵³ Locally, the heat produced by the decomposition of organic carbon could serve as a positive feedback, accelerating carbon release.⁵⁴ However, the release of permafrost carbon, as well as whether that carbon is initially released as CO₂ or as the more potent greenhouse gas CH₄, is limited by many factors, including the freeze–thaw cycle, the rate with which heat diffuses into the permafrost, the potential for organisms to cycle permafrost carbon into new biomass, and oxygen availability. Though the release of permafrost carbon would probably not be fast enough to trigger a runaway self-amplifying cycle leading to a permafrost-free Arctic,⁵³ it still has the potential to significantly amplify both local and global warming, reduce the budget of human-caused CO₂ emissions consistent with global temperature targets, and drive continued warming even if human-caused emissions stopped altogether.^{55, 56}

The second possible arctic carbon cycle tipping element is the reservoir of methane hydrates frozen into the sediments of continental shelves of the Arctic Ocean (see also Ch. 11: Arctic Changes). There is an estimated 500 to 3,000 GtC in methane hydrates,^{57, 58, 59} with a most recent estimate of 1,800 GtC (equivalently, 2,400 Gt CH₄).⁶⁰ If released as methane rather than CO₂, this would be equivalent to about 82,000 Gt CO₂ using a global warming potential of 34.⁶¹ While the existence of this reservoir has been known and discussed for several decades (e.g., Kvenvolden 1988⁶²), only recently has it been hypothesized that warming bottom water temperatures may destabilize the hydrates over timescales shorter than mil-

lennia, leading to their release into the water column and eventually the atmosphere (e.g., Archer 2007;⁵⁷ Kretschmer et al. 2015⁶³). Recent measurements of the release of methane from these sediments in summer find that, while methane hydrates on the continental shelf and upper slope are undergoing dissociation, the resulting emissions are not reaching the ocean surface in sufficient quantity to affect the atmospheric methane budget significantly, if at all.^{60, 64} Estimates of plausible hydrate releases to the atmosphere over the next century are only a fraction of present-day anthropogenic methane emissions.^{60, 63, 65}

These estimates of future emissions from permafrost and hydrates, however, neglect the possibility that humans may insert themselves into the physical feedback systems. With an estimated 53% of global fossil fuel reserves in the Arctic becoming increasingly accessible in a warmer world,⁶⁶ the risks associated with this carbon being extracted and burned, further exacerbating the influence of humans on global climate, are evident.^{67, 68} Of less concern but still relevant, arctic ocean waters themselves are a source of methane, which could increase as sea ice decreases.⁶⁹

The Antarctic and Greenland Ice Sheets are clear tipping elements. The Greenland Ice Sheet exhibits multiple stable states as a result of feedbacks involving the elevation of the ice sheet, atmosphere–ocean–sea ice dynamics, and albedo.^{70, 71, 72, 73} At least one study suggests that warming of 2.9°F (1.6°C) above a preindustrial baseline could commit Greenland to an 85% reduction in ice volume and a 20 foot (6 m) contribution to global mean sea level over millennia.⁷¹ One 10,000-year modeling study⁷⁴ suggests that following the higher RCP8.5 scenario (see Ch. 4: Projections) over the 21st century would lead to complete loss of the Greenland Ice Sheet over 6,000 years.



In Antarctica, the amount of ice that sits on bedrock below sea level is enough to raise global mean sea level by 75.5 feet (23 m).⁷⁵ This ice is vulnerable to collapse over centuries to millennia due to a range of feedbacks involving ocean-ice sheet-bedrock interactions.^{74,76,77,78,79,80} Observational evidence suggests that ice dynamics already in progress have committed the planet to as much as 3.9 feet (1.2 m) worth of sea level rise from the West Antarctic Ice Sheet alone, although that amount is projected to occur over the course of many centuries.^{81,82} Plausible physical modeling indicates that, under the higher RCP8.5 scenario, Antarctic ice could contribute 3.3 feet (1 m) or more to global mean sea level over the remainder of this century,⁸³ with some authors arguing that rates of change could be even faster.⁸⁴ Over 10,000 years, one modeling study suggests that 3.6°F (2°C) of sustained warming could lead to about 70 feet (25 m) of global mean sea level rise from Antarctica alone.⁷⁴

Finally, tipping elements also exist in large-scale ecosystems. For example, boreal forests such as those in southern Alaska may expand northward in response to arctic warming. Because forests are darker than the tundra they replace, their expansion amplifies regional warming, which in turn accelerates their expansion.⁸⁵ As another example, coral reef ecosystems, such as those in Florida, are maintained by stabilizing ecological feedbacks among corals, coralline red algae, and grazing fish and invertebrates. However, these stabilizing feedbacks can be undermined by warming, increased risk of bleaching events, spread of disease, and ocean acidification, leading to abrupt reef collapse.⁸⁶ More generally, many ecosystems can undergo rapid regime shifts in response to a range of stressors, including climate change (e.g., Scheffer et al. 2001;⁸⁷ Folke et al. 2004⁸⁸).

15.5 Paleoclimatic Hints of Additional Potential Surprises

The paleoclimatic record provides evidence for additional state shifts whose driving mechanisms are as yet poorly understood. As mentioned, global climate models tend to underestimate both the magnitude of global mean warming in response to higher CO₂ levels as well as its amplification at high latitudes, compared to reconstructions of temperature and CO₂ from the geological record. Three case studies—all periods well predating the first appearance of *Homo sapiens* around 200,000 years ago⁸⁹—illustrate the limitations of current scientific understanding in capturing the full range of self-reinforcing cycles that operate within the Earth system, particularly over millennial time scales.

The first of these, the late Pliocene, occurred about 3.6 to 2.6 million years ago. Climate model simulations for this period systematically underestimate warming north of 30°N.⁹⁰ During the second of these, the middle Miocene (about 17–14.5 million years ago), models also fail to simultaneously replicate global mean temperature—estimated from proxies to be approximately 14° ± 4°F (8° ± 2°C) warmer than preindustrial—and the approximately 40% reduction in the pole-to-equator temperature gradient relative to today.⁹¹ Although about one-third of the global mean temperature increase during the Miocene can be attributed to changes in geography and vegetation, geological proxies indicate CO₂ concentrations of around 400 ppm,^{91,92} similar to today. This suggests the possibility of as yet unmodeled feedbacks, perhaps related to a significant change in the vertical distribution of heat in the tropical ocean.⁹³

The last of these case studies, the early Eocene, occurred about 56–48 million years ago. This period is characterized by the absence of permanent land ice, CO₂ concentrations peaking



around $1,400 \pm 470$ ppm,⁹⁴ and global temperatures about $25^{\circ}\text{F} \pm 5^{\circ}\text{F}$ ($14^{\circ}\text{C} \pm 3^{\circ}\text{C}$) warmer than the preindustrial.⁹⁵ Like the late Pliocene and the middle Miocene, this period also exhibits about half the pole-to-equator temperature gradient of today.^{15,96} About one-third of the temperature difference is attributable to changes in geography, vegetation, and ice sheet coverage.⁹⁵ However, to reproduce both the elevated global mean temperature and the reduced pole-to-equator temperature gradient, climate models would require CO₂ concentrations that exceed those indicated by the proxy record by two to five times¹⁵ – suggesting once again the presence of as yet poorly understood processes and feedbacks.

One possible explanation for this discrepancy is a planetary state shift that, above a particular CO₂ threshold, leads to a significant increase in the sensitivity of the climate to CO₂. Paleo-data for the last 800,000 years suggest a gradual increase in climate sensitivity with global mean temperature over glacial-interglacial cycles,^{97,98} although these results are based on a time period with CO₂ concentra-

tions lower than today. At higher CO₂ levels, one modeling study⁹⁵ suggests that an abrupt change in atmospheric circulation (the onset of equatorial atmospheric superrotation) between 1,120 and 2,240 ppm CO₂ could lead to a reduction in cloudiness and an approximate doubling of climate sensitivity. However, the critical threshold for such a transition is poorly constrained. If it occurred in the past at a lower CO₂ level, it might explain the Eocene discrepancy and potentially also the Miocene discrepancy: but in that case, it could also pose a plausible threat within the 21st century under the higher RCP8.5 scenario.

Regardless of the particular mechanism, the systematic paleoclimatic model-data mismatch for past warm climates suggests that climate models are omitting at least one, and probably more, processes crucial to future warming, especially in polar regions. For this reason, future changes outside the range projected by climate models cannot be ruled out, and climate models are more likely to underestimate than to overestimate the amount of long-term future change.



TRACEABLE ACCOUNTS

Key Finding 1

Positive feedbacks (self-reinforcing cycles) within the climate system have the potential to accelerate human-induced climate change and even shift the Earth's climate system, in part or in whole, into new states that are very different from those experienced in the recent past (for example, ones with greatly diminished ice sheets or different large-scale patterns of atmosphere or ocean circulation). Some feedbacks and potential state shifts can be modeled and quantified; others can be modeled or identified but not quantified; and some are probably still unknown. (*Very high confidence* in the potential for state shifts and in the incompleteness of knowledge about feedbacks and potential state shifts).

Description of evidence base

This key finding is based on a large body of scientific literature recently summarized by Lenton et al.,¹⁰ NRC,³³ and Kopp et al.¹¹ As NRC³³ (page vii) states, “A study of Earth’s climate history suggests the inevitability of ‘tipping points’—thresholds beyond which major and rapid changes occur when crossed—that lead to abrupt changes in the climate system” and (page xi), “Can all tipping points be foreseen? Probably not. Some will have no precursors, or may be triggered by naturally occurring variability in the climate system. Some will be difficult to detect, clearly visible only after they have been crossed and an abrupt change becomes inevitable.” As IPCC AR5 WG1 Chapter 12, section 12.5.5²⁵ further states, “A number of components or phenomena within the Earth system have been proposed as potentially possessing critical thresholds (sometimes referred to as tipping points) beyond which abrupt or nonlinear transitions to a different state ensues.” Collins et al.²⁵ further summarizes critical thresholds that can be modeled and others that can only be identified.

Major uncertainties

The largest uncertainties are 1) whether proposed tipping elements actually undergo critical transitions; 2) the magnitude and timing of forcing that will be required to initiate critical transitions in tipping elements; 3) the speed of the transition once it has been triggered; 4) the characteristics of the new state that re-

sults from such transition; and 5) the potential for new tipping elements to exist that are yet unknown.

Assessment of confidence based on evidence and agreement, including short description of nature of evidence and level of agreement

There is *very high confidence* in the likelihood of the existence of positive feedbacks, and the tipping elements statement is based on a large body of literature published over the last 25 years that draws from basic physics, observations, paleoclimate data, and modeling.

There is *very high confidence* that some feedbacks can be quantified, others are known but cannot be quantified, and others may yet exist that are currently unknown.

Summary sentence or paragraph that integrates the above information

The key finding is based on NRC³³ and IPCC AR5 WG1 Chapter 12 section 12.5.5,²⁵ which made a thorough assessment of the relevant literature.

Key Finding 2

The physical and socioeconomic impacts of compound extreme events (such as simultaneous heat and drought, wildfires associated with hot and dry conditions, or flooding associated with high precipitation on top of snow or waterlogged ground) can be greater than the sum of the parts (*very high confidence*). Few analyses consider the spatial or temporal correlation between extreme events.

Description of evidence base

This key finding is based on a large body of scientific literature summarized in the 2012 IPCC Special Report on Extremes.²³ The report’s Summary for Policymakers (page 6) states, “exposure and vulnerability are key determinants of disaster risk and of impacts when risk is realized... extreme impacts on human, ecological, or physical systems can result from individual extreme weather or climate events. Extreme impacts can also result from non-extreme events where exposure and vulnerability are high or from a compounding of events or their impacts. For example, drought, coupled with extreme heat and low humidity, can increase the risk of wildfire.”



Major uncertainties

The largest uncertainties are in the temporal congruence of the events and the compounding nature of their impacts.

Assessment of confidence based on evidence and agreement, including short description of nature of evidence and level of agreement

There is *very high confidence* that the impacts of multiple events could exceed the sum of the impacts of events occurring individually.

Summary sentence or paragraph that integrates the above information

The key finding is based on the 2012 IPCC SREX report, particularly section 3.1.3 on compound or multiple events, which presents a thorough assessment of the relevant literature.

Key Finding 3

While climate models incorporate important climate processes that can be well quantified, they do not include all of the processes that can contribute to feedbacks, compound extreme events, and abrupt and/or irreversible changes. For this reason, future changes outside the range projected by climate models cannot be ruled out (*very high confidence*). Moreover, the systematic tendency of climate models to underestimate temperature change during warm paleoclimates suggests that climate models are more likely to underestimate than to overestimate the amount of long-term future change (*medium confidence*).

Description of evidence base

This key finding is based on the conclusions of IPCC AR5 WG1,⁹⁹ specifically Chapter 9;¹ the state of the art of global models is briefly summarized in Chapter 4: Projections of this report. The second half of this key finding is based upon the tendency of global climate models to underestimate, relative to geological reconstructions, the magnitude of both long-term global mean warming and the amplification of warming at high latitudes in past warm climates (e.g., Salzmann et al. 2013;⁹⁰ Goldner et al. 2014;⁹¹ Caballeo and Huber 2013;⁹⁵ Lunt et al. 2012¹⁵).

Major uncertainties

The largest uncertainties are structural: are the models including all the important components and relationships necessary to model the feedbacks and if so, are these correctly represented in the models?

Assessment of confidence based on evidence and agreement, including short description of nature of evidence and level of agreement

There is *very high confidence* that the models are incomplete representations of the real world; and there is *medium confidence* that their tendency is to under- rather than over-estimate the amount of long-term future change.

Summary sentence or paragraph that integrates the above information

The key finding is based on the IPCC AR5 WG1 Chapter 9,¹ as well as systematic paleoclimatic model/data comparisons.



REFERENCES

1. Flato, G., J. Marotzke, B. Abiodun, P. Braconnot, S.C. Chou, W. Collins, P. Cox, F. Driouech, S. Emori, V. Eyring, C. Forest, P. Gleckler, E. Guilyardi, C. Jakob, V. Kattsov, C. Reason, and M. Rummukainen, 2013: Evaluation of climate models. *Climate Change 2013: The Physical Science Basis. Contribution of Working Group I to the Fifth Assessment Report of the Intergovernmental Panel on Climate Change*. Stocker, T.F., D. Qin, G.-K. Plattner, M. Tignor, S.K. Allen, J. Boschung, A. Nauels, Y. Xia, V. Bex, and P.M. Midgley, Eds. Cambridge University Press, Cambridge, United Kingdom and New York, NY, USA, 741–866. <http://www.climatechange2013.org/report/full-report/>
2. Molina, M.J. and F.S. Rowland, 1974: Stratospheric sink for chlorofluoromethanes: Chlorine atom-catalysed destruction of ozone. *Nature*, **249**, 810-812. <http://dx.doi.org/10.1038/249810a0>
3. Farman, J.C., B.G. Gardiner, and J.D. Shanklin, 1985: Large losses of total ozone in Antarctica reveal seasonal ClO_x/NO_x interaction. *Nature*, **315**, 207-210. <http://dx.doi.org/10.1038/315207a0>
4. Stroeve, J., M.M. Holland, W. Meier, T. Scambos, and M. Serreze, 2007: Arctic sea ice decline: Faster than forecast. *Geophysical Research Letters*, **34**, L09501. <http://dx.doi.org/10.1029/2007GL029703>
5. Meehl, G.A., T.F. Stocker, W.D. Collins, P. Friedlingstein, A.T. Gaye, J.M. Gregory, A. Kitoh, R. Knutti, J.M. Murphy, A. Noda, S.C.B. Raper, I.G. Watterson, A.J. Weaver, and Z.-C. Zhao, 2007: Global Climate Projections. *Climate Change 2007: The Physical Science Basis. Contribution of Working Group I to the Fourth Assessment Report of the Intergovernmental Panel on Climate Change*. Solomon, S., D. Qin, M. Manning, Z. Chen, M. Marquis, K.B. Averyt, M. Tignor, and H.L. Miller, Eds. Cambridge University Press, Cambridge, United Kingdom and New York, NY, USA, 747-845.
6. Stroeve, J.C., V. Kattsov, A. Barrett, M. Serreze, T. Pavlova, M. Holland, and W.N. Meier, 2012: Trends in Arctic sea ice extent from CMIP5, CMIP3 and observations. *Geophysical Research Letters*, **39**, L16502. <http://dx.doi.org/10.1029/2012GL052676>
7. Schröder, D., D.L. Feltham, D. Flocco, and M. Tsamados, 2014: September Arctic sea-ice minimum predicted by spring melt-pond fraction. *Nature Climate Change*, **4**, 353-357. <http://dx.doi.org/10.1038/nclimate2203>
8. Asplin, M.G., R. Galley, D.G. Barber, and S. Prinsenberg, 2012: Fracture of summer perennial sea ice by ocean swell as a result of Arctic storms. *Journal of Geophysical Research*, **117**, C06025. <http://dx.doi.org/10.1029/2011JC007221>
9. Perovich, D.K., J.A. Richter-Menge, K.F. Jones, and B. Light, 2008: Sunlight, water, and ice: Extreme Arctic sea ice melt during the summer of 2007. *Geophysical Research Letters*, **35**, L11501. <http://dx.doi.org/10.1029/2008GL034007>
10. Lenton, T.M., H. Held, E. Kriegler, J.W. Hall, W. Lucht, S. Rahmstorf, and H.J. Schellnhuber, 2008: Tipping elements in the Earth's climate system. *Proceedings of the National Academy of Sciences*, **105**, 1786-1793. <http://dx.doi.org/10.1073/pnas.0705414105>
11. Kopp, R.E., R.L. Shwom, G. Wagner, and J. Yuan, 2016: Tipping elements and climate-economic shocks: Pathways toward integrated assessment. *Earth's Future*, **4**, 346-372. <http://dx.doi.org/10.1002/2016EF000362>
12. Zwiers, F.W., L.V. Alexander, G.C. Hegerl, T.R. Knutson, J.P. Kossin, P. Naveau, N. Nicholls, C. Schär, S.I. Seneviratne, and X. Zhang, 2013: Climate extremes: Challenges in estimating and understanding recent changes in the frequency and intensity of extreme climate and weather events. *Climate Science for Serving Society: Research, Modeling and Prediction Priorities*. Arrar, G.R. and J.W. Hurrell, Eds. Springer Netherlands, Dordrecht, 339-389. http://dx.doi.org/10.1007/978-94-007-6692-1_13
13. Smith, J.A., 1987: Estimating the upper tail of flood frequency distributions. *Water Resources Research*, **23**, 1657-1666. <http://dx.doi.org/10.1029/WR023i008p01657>
14. Woodhouse, C.A. and J.T. Overpeck, 1998: 2000 years of drought variability in the central United States. *Bulletin of the American Meteorological Society*, **79**, 2693-2714. [http://dx.doi.org/10.1175/1520-0477\(1998\)079<2693:YODVIT>2.0.CO;2](http://dx.doi.org/10.1175/1520-0477(1998)079<2693:YODVIT>2.0.CO;2)
15. Lunt, D.J., T. Dunkley Jones, M. Heinemann, M. Huber, A. LeGrande, A. Winguth, C. Loptson, J. Marotzke, C.D. Roberts, J. Tindall, P. Valdes, and C. Winguth, 2012: A model-data comparison for a multi-model ensemble of early Eocene atmosphere-ocean simulations: EoMIP. *Climate of the Past*, **8**, 1717-1736. <http://dx.doi.org/10.5194/cp-8-1717-2012>
16. Navarro, T., J.B. Madeleine, F. Forget, A. Spiga, E. Millour, F. Montmessin, and A. Määttänen, 2014: Global climate modeling of the Martian water cycle with improved microphysics and radiatively active water ice clouds. *Journal of Geophysical Research Planets*, **119**, 1479-1495. <http://dx.doi.org/10.1002/2013JE004550>
17. Kang, I.-S., Y.-M. Yang, and W.-K. Tao, 2015: GCMs with implicit and explicit representation of cloud microphysics for simulation of extreme precipitation frequency. *Climate Dynamics*, **45**, 325-335. <http://dx.doi.org/10.1007/s00382-014-2376-1>



18. Brysse, K., N. Oreskes, J. O'Reilly, and M. Oppenheimer, 2013: Climate change prediction: Erring on the side of least drama? *Global Environmental Change*, **23**, 327-337. <http://dx.doi.org/10.1016/j.gloenvcha.2012.10.008>
19. Quarantelli, E.L., 1986: Disaster Crisis Management. University of Delaware, Newark, DE. 10 pp. <http://udspace.udel.edu/handle/19716/487>
20. Zscheischler, J., M. Reichstein, J. von Buttler, M. Mu, J.T. Randerson, and M.D. Mahecha, 2014: Carbon cycle extremes during the 21st century in CMIP5 models: Future evolution and attribution to climatic drivers. *Geophysical Research Letters*, **41**, 8853-8861. <http://dx.doi.org/10.1002/2014GL062409>
21. Swain, D.L., D.E. Horton, D. Singh, and N.S. Diffenbaugh, 2016: Trends in atmospheric patterns conducive to seasonal precipitation and temperature extremes in California. *Science Advances*, **2**, e1501344. <http://dx.doi.org/10.1126/sciadv.1501344>
22. Diffenbaugh, N.S. and F. Giorgi, 2012: Climate change hotspots in the CMIP5 global climate model ensemble. *Climatic Change*, **114**, 813-822. <http://dx.doi.org/10.1007/s10584-012-0570-x>
23. IPCC, 2012: Managing the Risks of Extreme Events and Disasters to Advance Climate Change Adaptation. A Special Report of Working Groups I and II of the Intergovernmental Panel on Climate Change. Field, C.B., V. Barros, T.F. Stocker, D. Qin, D.J. Dokken, K.L. Ebi, M.D. Mastrandrea, K.J. Mach, G.-K. Plattner, S.K. Allen, M. Tignor, and P.M. Midgley (Eds.). Cambridge University Press, Cambridge, UK and New York, NY. 582 pp. https://www.ipcc.ch/pdf/special-reports/srex/SREX_Full_Report.pdf
24. Hao, Z., A. AghaKouchak, and T.J. Phillips, 2013: Changes in concurrent monthly precipitation and temperature extremes. *Environmental Research Letters*, **8**, 034014. <http://dx.doi.org/10.1088/1748-9326/8/3/034014>
25. Collins, M., R. Knutti, J. Arblaster, J.-L. Dufresne, T. Fife, P. Friedlingstein, X. Gao, W.J. Gutowski, T. Johns, G. Krinner, M. Shongwe, C. Tebaldi, A.J. Weaver, and M. Wehner, 2013: Long-term climate change: Projections, commitments and irreversibility. *Climate Change 2013: The Physical Science Basis. Contribution of Working Group I to the Fifth Assessment Report of the Intergovernmental Panel on Climate Change*. Stocker, T.F., D. Qin, G.-K. Plattner, M. Tignor, S.K. Allen, J. Boschung, A. Nauels, Y. Xia, V. Bex, and P.M. Midgley, Eds. Cambridge University Press, Cambridge, United Kingdom and New York, NY, USA, 1029-1136. <http://www.climatechange2013.org/report/full-report/>
26. Trenberth, K.E., A. Dai, G. van der Schrier, P.D. Jones, J. Barichivich, K.R. Briffa, and J. Sheffield, 2014: Global warming and changes in drought. *Nature Climate Change*, **4**, 17-22. <http://dx.doi.org/10.1038/nclimate2067>
27. Cook, B.I., T.R. Ault, and J.E. Smerdon, 2015: Unprecedented 21st century drought risk in the American Southwest and Central Plains. *Science Advances*, **1**, e1400082. <http://dx.doi.org/10.1126/sciadv.1400082>
28. AghaKouchak, A., L. Cheng, O. Mazdiyasn, and A. Farahmand, 2014: Global warming and changes in risk of concurrent climate extremes: Insights from the 2014 California drought. *Geophysical Research Letters*, **41**, 8847-8852. <http://dx.doi.org/10.1002/2014GL062308>
29. Serinaldi, F., 2016: Can we tell more than we can know? The limits of bivariate drought analyses in the United States. *Stochastic Environmental Research and Risk Assessment*, **30**, 1691-1704. <http://dx.doi.org/10.1007/s00477-015-1124-3>
30. Fraser, E.D.G., E. Simelton, M. Termansen, S.N. Gosling, and A. South, 2013: "Vulnerability hotspots": Integrating socio-economic and hydrological models to identify where cereal production may decline in the future due to climate change induced drought. *Agricultural and Forest Meteorology*, **170**, 195-205. <http://dx.doi.org/10.1016/j.agrformet.2012.04.008>
31. Reed, A.J., M.E. Mann, K.A. Emanuel, N. Lin, B.P. Horton, A.C. Kemp, and J.P. Donnelly, 2015: Increased threat of tropical cyclones and coastal flooding to New York City during the anthropogenic era. *Proceedings of the National Academy of Sciences*, **112**, 12610-12615. <http://dx.doi.org/10.1073/pnas.1513127112>
32. Liu, J., Z. Chen, J. Francis, M. Song, T. Mote, and Y. Hu, 2016: Has Arctic sea ice loss contributed to increased surface melting of the Greenland Ice Sheet? *Journal of Climate*, **29**, 3373-3386. <http://dx.doi.org/10.1175/JCLI-D-15-0391.1>
33. NRC, 2013: *Abrupt Impacts of Climate Change: Anticipating Surprises*. The National Academies Press, Washington, DC, 222 pp. <http://dx.doi.org/10.17226/18373>
34. Rahmstorf, S., J.E. Box, G. Feulner, M.E. Mann, A. Robinson, S. Rutherford, and E.J. Schaffernicht, 2015: Exceptional twentieth-century slowdown in Atlantic Ocean overturning circulation. *Nature Climate Change*, **5**, 475-480. <http://dx.doi.org/10.1038/nclimate2554>
35. Drijfhout, S., G.J.v. Oldenborgh, and A. Cimadoribus, 2012: Is a decline of AMOC causing the warming hole above the North Atlantic in observed and modeled warming patterns? *Journal of Climate*, **25**, 8373-8379. <http://dx.doi.org/10.1175/jcli-d-12-00490.1>
36. Cheng, J., Z. Liu, S. Zhang, W. Liu, L. Dong, P. Liu, and H. Li, 2016: Reduced interdecadal variability of Atlantic Meridional Overturning Circulation under global warming. *Proceedings of the National Academy of Sciences*, **113**, 3175-3178. <http://dx.doi.org/10.1073/pnas.1519827113>



37. Liu, W., S.-P. Xie, Z. Liu, and J. Zhu, 2017: Overlooked possibility of a collapsed Atlantic Meridional Overturning Circulation in warming climate. *Science Advances*, **3**, e1601666. <http://dx.doi.org/10.1126/sciadv.1601666>
38. Yin, J. and P.B. Goddard, 2013: Oceanic control of sea level rise patterns along the East Coast of the United States. *Geophysical Research Letters*, **40**, 5514-5520. <http://dx.doi.org/10.1002/2013GL057992>
39. Gregory, J.M. and J.A. Lowe, 2000: Predictions of global and regional sea-level rise using AOGCMs with and without flux adjustment. *Geophysical Research Letters*, **27**, 3069-3072. <http://dx.doi.org/10.1029/1999GL011228>
40. Levermann, A., A. Griesel, M. Hofmann, M. Montoya, and S. Rahmstorf, 2005: Dynamic sea level changes following changes in the thermohaline circulation. *Climate Dynamics*, **24**, 347-354. <http://dx.doi.org/10.1007/s00382-004-0505-y>
41. Jackson, L.C., R. Kahana, T. Graham, M.A. Ringer, T. Woollings, J.V. Mecking, and R.A. Wood, 2015: Global and European climate impacts of a slowdown of the AMOC in a high resolution GCM. *Climate Dynamics*, **45**, 3299-3316. <http://dx.doi.org/10.1007/s00382-015-2540-2>
42. Pérez, F.F., H. Mercier, M. Vazquez-Rodriguez, P. Lherminier, A. Velo, P.C. Pardo, G. Roson, and A.F. Rios, 2013: Atlantic Ocean CO₂ uptake reduced by weakening of the meridional overturning circulation. *Nature Geoscience*, **6**, 146-152. <http://dx.doi.org/10.1038/ngeo1680>
43. Cai, W., S. Borlace, M. Lengaigne, P. van Rensch, M. Collins, G. Vecchi, A. Timmermann, A. Santoso, M.J. McPhaden, L. Wu, M.H. England, G. Wang, E. Guilyardi, and F.-F. Jin, 2014: Increasing frequency of extreme El Niño events due to greenhouse warming. *Nature Climate Change*, **4**, 111-116. <http://dx.doi.org/10.1038/nclimate2100>
44. Cai, W., G. Wang, A. Santoso, M.J. McPhaden, L. Wu, F.-F. Jin, A. Timmermann, M. Collins, G. Vecchi, M. Lengaigne, M.H. England, D. Dommenget, K. Takahashi, and E. Guilyardi, 2015: Increased frequency of extreme La Niña events under greenhouse warming. *Nature Climate Change*, **5**, 132-137. <http://dx.doi.org/10.1038/nclimate2492>
45. Lindsay, R.W. and J. Zhang, 2005: The thinning of Arctic sea ice, 1988-2003: Have we passed a tipping point? *Journal of Climate*, **18**, 4879-4894. <http://dx.doi.org/10.1175/jcli3587.1>
46. Eisenman, I. and J.S. Wettlaufer, 2009: Nonlinear threshold behavior during the loss of Arctic sea ice. *Proceedings of the National Academy of Sciences*, **106**, 28-32. <http://dx.doi.org/10.1073/pnas.0806887106>
47. Ding, Q., A. Schweiger, M. Lheureux, D.S. Battisti, S. Po-Chedley, N.C. Johnson, E. Blanchard-Wrigglesworth, K. Harnos, Q. Zhang, R. Eastman, and E.J. Steig, 2017: Influence of high-latitude atmospheric circulation changes on summertime Arctic sea ice. *Nature Climate Change*, **7**, 289-295. <http://dx.doi.org/10.1038/nclimate3241>
48. Armour, K.C., I. Eisenman, E. Blanchard-Wrigglesworth, K.E. McCusker, and C.M. Bitz, 2011: The reversibility of sea ice loss in a state-of-the-art climate model. *Geophysical Research Letters*, **38**, L16705. <http://dx.doi.org/10.1029/2011GL048739>
49. Ridley, J.K., J.A. Lowe, and H.T. Hewitt, 2012: How reversible is sea ice loss? *The Cryosphere*, **6**, 193-198. <http://dx.doi.org/10.5194/tc-6-193-2012>
50. Li, C., D. Notz, S. Tietsche, and J. Marotzke, 2013: The transient versus the equilibrium response of sea ice to global warming. *Journal of Climate*, **26**, 5624-5636. <http://dx.doi.org/10.1175/JCLI-D-12-00492.1>
51. Wagner, T.J.W. and I. Eisenman, 2015: How climate model complexity influences sea ice stability. *Journal of Climate*, **28**, 3998-4014. <http://dx.doi.org/10.1175/JCLI-D-14-00654.1>
52. Bathiany, S., D. Notz, T. Mauritsen, G. Raedel, and V. Brovkin, 2016: On the potential for abrupt Arctic winter sea ice loss. *Journal of Climate*, **29**, 2703-2719. <http://dx.doi.org/10.1175/JCLI-D-15-0466.1>
53. Schuur, E.A.G., A.D. McGuire, C. Schadel, G. Grosse, J.W. Harden, D.J. Hayes, G. Hugelius, C.D. Koven, P. Kuhry, D.M. Lawrence, S.M. Natali, D. Olefeldt, V.E. Romanovsky, K. Schaefer, M.R. Turetsky, C.C. Treat, and J.E. Vonk, 2015: Climate change and the permafrost carbon feedback. *Nature*, **520**, 171-179. <http://dx.doi.org/10.1038/nature14338>
54. Hollesen, J., H. Matthiesen, A.B. Møller, and B. Elberling, 2015: Permafrost thawing in organic Arctic soils accelerated by ground heat production. *Nature Climate Change*, **5**, 574-578. <http://dx.doi.org/10.1038/nclimate2590>
55. MacDougall, A.H., C.A. Avis, and A.J. Weaver, 2012: Significant contribution to climate warming from the permafrost carbon feedback. *Nature Geoscience*, **5**, 719-721. <http://dx.doi.org/10.1038/ngeo1573>
56. MacDougall, A.H., K. Zickfeld, R. Knutti, and H.D. Matthews, 2015: Sensitivity of carbon budgets to permafrost carbon feedbacks and non-CO₂ forcings. *Environmental Research Letters*, **10**, 125003. <http://dx.doi.org/10.1088/1748-9326/10/12/125003>
57. Archer, D., 2007: Methane hydrate stability and anthropogenic climate change. *Biogeosciences*, **4**, 521-544. <http://dx.doi.org/10.5194/bg-4-521-2007>
58. Ruppel, C.D. *Methane hydrates and contemporary climate change*. Nature Education Knowledge, 2011. 3.



59. Piñero, E., M. Marquardt, C. Hensen, M. Haeckel, and K. Wallmann, 2013: Estimation of the global inventory of methane hydrates in marine sediments using transfer functions. *Biogeosciences*, **10**, 959-975. <http://dx.doi.org/10.5194/bg-10-959-2013>
60. Ruppel, C.D. and J.D. Kessler, 2017: The interaction of climate change and methane hydrates. *Reviews of Geophysics*, **55**, 126-168. <http://dx.doi.org/10.1002/2016RG000534>
61. Myhre, G., D. Shindell, F.-M. Bréon, W. Collins, J. Fuglestvedt, J. Huang, D. Koch, J.-F. Lamarque, D. Lee, B. Mendoza, T. Nakajima, A. Robock, G. Stephens, T. Takemura, and H. Zhang, 2013: Anthropogenic and natural radiative forcing. *Climate Change 2013: The Physical Science Basis. Contribution of Working Group I to the Fifth Assessment Report of the Intergovernmental Panel on Climate Change*. Stocker, T.F., D. Qin, G.-K. Plattner, M. Tignor, S.K. Allen, J. Boschung, A. Nauels, Y. Xia, V. Bex, and P.M. Midgley, Eds. Cambridge University Press, Cambridge, United Kingdom and New York, NY, USA, 659-740. <http://www.climatechange2013.org/report/full-report/>
62. Kvenvolden, K.A., 1988: Methane hydrate – A major reservoir of carbon in the shallow geosphere? *Chemical Geology*, **71**, 41-51. [http://dx.doi.org/10.1016/0009-2541\(88\)90104-0](http://dx.doi.org/10.1016/0009-2541(88)90104-0)
63. Kretschmer, K., A. Biastoch, L. Rüpke, and E. Burwicz, 2015: Modeling the fate of methane hydrates under global warming. *Global Biogeochemical Cycles*, **29**, 610-625. <http://dx.doi.org/10.1002/2014GB005011>
64. Myhre, C.L., B. Ferré, S.M. Platt, A. Silyakova, O. Hermansen, G. Allen, I. Pisso, N. Schmidbauer, A. Stohl, J. Pitt, P. Jansson, J. Greinert, C. Percival, A.M. Fjaeraa, S.J. O'Shea, M. Gallagher, M. Le Breton, K.N. Bower, S.J.B. Bauguitte, S. Dalsøren, S. Vadakkepuliambatta, R.E. Fisher, E.G. Nisbet, D. Lowry, G. Myhre, J.A. Pyle, M. Cain, and J. Mienert, 2016: Extensive release of methane from Arctic seabed west of Svalbard during summer 2014 does not influence the atmosphere. *Geophysical Research Letters*, **43**, 4624-4631. <http://dx.doi.org/10.1002/2016GL068999>
65. Stranne, C., M. O'Regan, G.R. Dickens, P. Crill, C. Miller, P. Preto, and M. Jakobsson, 2016: Dynamic simulations of potential methane release from East Siberian continental slope sediments. *Geochemistry, Geophysics, Geosystems*, **17**, 872-886. <http://dx.doi.org/10.1002/2015GC006119>
66. Lee, S.-Y. and G.D. Holder, 2001: Methane hydrates potential as a future energy source. *Fuel Processing Technology*, **71**, 181-186. [http://dx.doi.org/10.1016/S0378-3820\(01\)00145-X](http://dx.doi.org/10.1016/S0378-3820(01)00145-X)
67. Jakob, M. and J. Hilaire, 2015: Climate science: Unburnable fossil-fuel reserves. *Nature*, **517**, 150-152. <http://dx.doi.org/10.1038/517150a>
68. McGlade, C. and P. Ekins, 2015: The geographical distribution of fossil fuels unused when limiting global warming to 2°C. *Nature*, **517**, 187-190. <http://dx.doi.org/10.1038/nature14016>
69. Kort, E.A., S.C. Wofsy, B.C. Daube, M. Diao, J.W. Elkins, R.S. Gao, E.J. Hintsa, D.F. Hurst, R. Jimenez, F.L. Moore, J.R. Spackman, and M.A. Zondlo, 2012: Atmospheric observations of Arctic Ocean methane emissions up to 82° north. *Nature Geoscience*, **5**, 318-321. <http://dx.doi.org/10.1038/ngeo1452>
70. Ridley, J., J.M. Gregory, P. Huybrechts, and J. Lowe, 2010: Thresholds for irreversible decline of the Greenland ice sheet. *Climate Dynamics*, **35**, 1049-1057. <http://dx.doi.org/10.1007/s00382-009-0646-0>
71. Robinson, A., R. Calov, and A. Ganopolski, 2012: Multistability and critical thresholds of the Greenland ice sheet. *Nature Climate Change*, **2**, 429-432. <http://dx.doi.org/10.1038/nclimate1449>
72. Levermann, A., P.U. Clark, B. Marzeion, G.A. Milne, D. Pollard, V. Radic, and A. Robinson, 2013: The multimillennial sea-level commitment of global warming. *Proceedings of the National Academy of Sciences*, **110**, 13745-13750. <http://dx.doi.org/10.1073/pnas.1219414110>
73. Koenig, S.J., R.M. DeConto, and D. Pollard, 2014: Impact of reduced Arctic sea ice on Greenland ice sheet variability in a warmer than present climate. *Geophysical Research Letters*, **41**, 3933-3942. <http://dx.doi.org/10.1002/2014GL059770>
74. Clark, P.U., J.D. Shakun, S.A. Marcott, A.C. Mix, M. Eby, S. Kulp, A. Levermann, G.A. Milne, P.L. Pfister, B.D. Santer, D.P. Schrag, S. Solomon, T.F. Stocker, B.H. Strauss, A.J. Weaver, R. Winkelmann, D. Archer, E. Bard, A. Goldner, K. Lambeck, R.T. Pierrehumbert, and G.-K. Plattner, 2016: Consequences of twenty-first-century policy for multi-millennial climate and sea-level change. *Nature Climate Change*, **6**, 360-369. <http://dx.doi.org/10.1038/nclimate2923>
75. Fretwell, P., H.D. Pritchard, D.G. Vaughan, J.L. Bamber, N.E. Barrand, R. Bell, C. Bianchi, R.G. Bingham, D.D. Blankenship, G. Casassa, G. Catania, D. Callens, H. Conway, A.J. Cook, H.F.J. Corr, D. Damaske, V. Damm, F. Ferraccioli, R. Forsberg, S. Fujita, Y. Gim, P. Gogineni, J.A. Griggs, R.C.A. Hindmarsh, P. Holmlund, J.W. Holt, R.W. Jacobel, A. Jenkins, W. Jokat, T. Jordan, E.C. King, J. Kohler, W. Krabill, M. Riger-Kusk, K.A. Langley, G. Leitchenkov, C. Leuschen, B.P. Luyendyk, K. Matsuoka, J. Mouginot, F.O. Nitsche, Y. Nogi, O.A. Nost, S.V. Popov, E. Rignot, D.M. Rippin, A. Rivera, J. Roberts, N. Ross, M.J. Siegert, A.M. Smith, D. Steinhage, M. Studinger, B. Sun, B.K. Tinto, B.C. Welch, D. Wilson, D.A. Young, C. Xiangbin, and A. Zirizzotti, 2013: Bedmap2: Improved ice bed, surface and thickness datasets for Antarctica. *The Cryosphere*, **7**, 375-393. <http://dx.doi.org/10.5194/tc-7-375-2013>



76. Schoof, C., 2007: Ice sheet grounding line dynamics: Steady states, stability, and hysteresis. *Journal of Geophysical Research*, **112**, F03S28. <http://dx.doi.org/10.1029/2006JF000664>
77. Gomez, N., J.X. Mitrovica, P. Huybers, and P.U. Clark, 2010: Sea level as a stabilizing factor for marine-ice-sheet grounding lines. *Nature Geoscience*, **3**, 850-853. <http://dx.doi.org/10.1038/ngeo1012>
78. Ritz, C., T.L. Edwards, G. Durand, A.J. Payne, V. Peyraud, and R.C.A. Hindmarsh, 2015: Potential sea-level rise from Antarctic ice-sheet instability constrained by observations. *Nature*, **528**, 115-118. <http://dx.doi.org/10.1038/nature16147>
79. Mengel, M. and A. Levermann, 2014: Ice plug prevents irreversible discharge from East Antarctica. *Nature Climate Change*, **4**, 451-455. <http://dx.doi.org/10.1038/nclimate2226>
80. Pollard, D., R.M. DeConto, and R.B. Alley, 2015: Potential Antarctic Ice Sheet retreat driven by hydrofracturing and ice cliff failure. *Earth and Planetary Science Letters*, **412**, 112-121. <http://dx.doi.org/10.1016/j.epsl.2014.12.035>
81. Joughin, I., B.E. Smith, and B. Medley, 2014: Marine ice sheet collapse potentially under way for the Thwaites Glacier Basin, West Antarctica. *Science*, **344**, 735-738. <http://dx.doi.org/10.1126/science.1249055>
82. Rignot, E., J. Mouginot, M. Morlighem, H. Seroussi, and B. Scheuchl, 2014: Widespread, rapid grounding line retreat of Pine Island, Thwaites, Smith, and Kohler Glaciers, West Antarctica, from 1992 to 2011. *Geophysical Research Letters*, **41**, 3502-3509. <http://dx.doi.org/10.1002/2014GL060140>
83. DeConto, R.M. and D. Pollard, 2016: Contribution of Antarctica to past and future sea-level rise. *Nature*, **531**, 591-597. <http://dx.doi.org/10.1038/nature17145>
84. Hansen, J., M. Sato, P. Hearty, R. Ruedy, M. Kelley, V. Masson-Delmotte, G. Russell, G. Tselioudis, J. Cao, E. Rignot, I. Velicogna, B. Tormey, B. Donovan, E. Kandiano, K. von Schuckmann, P. Kharecha, A.N. Legrande, M. Bauer, and K.W. Lo, 2016: Ice melt, sea level rise and superstorms: Evidence from paleoclimate data, climate modeling, and modern observations that 2°C global warming could be dangerous. *Atmospheric Chemistry and Physics*, **16**, 3761-3812. <http://dx.doi.org/10.5194/acp-16-3761-2016>
85. Jones, C., J. Lowe, S. Liddicoat, and R. Betts, 2009: Committed terrestrial ecosystem changes due to climate change. *Nature Geoscience*, **2**, 484-487. <http://dx.doi.org/10.1038/ngeo555>
86. Hoegh-Guldberg, O., P.J. Mumby, A.J. Hooten, R.S. Steneck, P. Greenfield, E. Gomez, C.D. Harvell, P.F. Sale, A.J. Edwards, K. Caldeira, N. Knowlton, C.M. Eakin, R. Iglesias-Prieto, N. Muthiga, R.H. Bradbury, A. Dubi, and M.E. Hatziolos, 2007: Coral reefs under rapid climate change and ocean acidification. *Science*, **318**, 1737-1742. <http://dx.doi.org/10.1126/science.1152509>
87. Scheffer, M., S. Carpenter, J.A. Foley, C. Folke, and B. Walker, 2001: Catastrophic shifts in ecosystems. *Nature*, **413**, 591-596. <http://dx.doi.org/10.1038/35098000>
88. Folke, C., S. Carpenter, B. Walker, M. Scheffer, T. Elmqvist, L. Gunderson, and C.S. Holling, 2004: Regime shifts, resilience, and biodiversity in ecosystem management. *Annual Review of Ecology, Evolution, and Systematics*, **35**, 557-581. <http://dx.doi.org/10.1146/annurev.ecolsys.35.021103.105711>
89. Tattersall, I., 2009: Human origins: Out of Africa. *Proceedings of the National Academy of Sciences*, **106**, 16018-16021. <http://dx.doi.org/10.1073/pnas.0903207106>
90. Salzmann, U., A.M. Dolan, A.M. Haywood, W.-L. Chan, J. Voss, D.J. Hill, A. Abe-Ouchi, B. Otto-Bliesner, F.J. Bragg, M.A. Chandler, C. Contoux, H.J. Dowsett, A. Jost, Y. Kamae, G. Lohmann, D.J. Lunt, S.J. Pickering, M.J. Pound, G. Ramstein, N.A. Rosenbloom, L. Sohl, C. Stepanek, H. Ueda, and Z. Zhang, 2013: Challenges in quantifying Pliocene terrestrial warming revealed by data-model discord. *Nature Climate Change*, **3**, 969-974. <http://dx.doi.org/10.1038/nclimate2008>
91. Goldner, A., N. Herold, and M. Huber, 2014: The challenge of simulating the warmth of the mid-Miocene climatic optimum in CESM1. *Climate of the Past*, **10**, 523-536. <http://dx.doi.org/10.5194/cp-10-523-2014>
92. Foster, G.L., C.H. Lear, and J.W.B. Rae, 2012: The evolution of pCO₂, ice volume and climate during the middle Miocene. *Earth and Planetary Science Letters*, **341-344**, 243-254. <http://dx.doi.org/10.1016/j.epsl.2012.06.007>
93. LaRiviere, J.P., A.C. Ravelo, A. Crimmins, P.S. Dekens, H.L. Ford, M. Lyle, and M.W. Wara, 2012: Late Miocene decoupling of oceanic warmth and atmospheric carbon dioxide forcing. *Nature*, **486**, 97-100. <http://dx.doi.org/10.1038/nature11200>
94. Anagnostou, E., E.H. John, K.M. Edgar, G.L. Foster, A. Ridgwell, G.N. Inglis, R.D. Pancost, D.J. Lunt, and P.N. Pearson, 2016: Changing atmospheric CO₂ concentration was the primary driver of early Cenozoic climate. *Nature*, **533**, 380-384. <http://dx.doi.org/10.1038/nature17423>
95. Caballero, R. and M. Huber, 2013: State-dependent climate sensitivity in past warm climates and its implications for future climate projections. *Proceedings of the National Academy of Sciences*, **110**, 14162-14167. <http://dx.doi.org/10.1073/pnas.1303365110>



96. Huber, M. and R. Caballero, 2011: The early Eocene equable climate problem revisited. *Climate of the Past*, **7**, 603-633. <http://dx.doi.org/10.5194/cp-7-603-2011>
97. von der Heydt, A.S., P. Köhler, R.S.W. van de Wal, and H.A. Dijkstra, 2014: On the state dependency of fast feedback processes in (paleo) climate sensitivity. *Geophysical Research Letters*, **41**, 6484-6492. <http://dx.doi.org/10.1002/2014GL061121>
98. Friedrich, T., A. Timmermann, M. Tigchelaar, O. Elison Timm, and A. Ganopolski, 2016: Nonlinear climate sensitivity and its implications for future greenhouse warming. *Science Advances*, **2**, e1501923. <http://dx.doi.org/10.1126/sciadv.1501923>
99. IPCC, 2013: *Climate Change 2013: The Physical Science Basis. Contribution of Working Group I to the Fifth Assessment Report of the Intergovernmental Panel on Climate Change*. Cambridge University Press, Cambridge, UK and New York, NY, 1535 pp. <http://www.climatechange2013.org/report/>





Appendix A

Observational Datasets Used in Climate Studies

Recommended Citation for Chapter

Wuebbles, D.J., 2017: Observational datasets used in climate studies. In: *Climate Science Special Report: Fourth National Climate Assessment, Volume I* [Wuebbles, D.J., D.W. Fahey, K.A. Hibbard, D.J. Dokken, B.C. Stewart, and T.K. Maycock (eds.)]. U.S. Global Change Research Program, Washington, DC, USA, pp. 430-435, doi: 10.7930/J0BK19HT.

Climate Datasets

Observations, including those from satellites, mobile platforms, field campaigns, and ground-based networks, provide the basis of knowledge on many temporal and spatial scales for understanding the changes occurring in Earth's climate system. These observations also inform the development, calibration, and evaluation of numerical models of the physics, chemistry, and biology being used in analyzing past changes in climate and for making future projections. As all observational data collected by support from Federal agencies are required to be made available free of charge with machine readable metadata, everyone can access these products for their personal analysis and research and for informing decisions. Many of these datasets are accessible through web services.

Many long-running observations worldwide have provided us with long-term records necessary for investigating climate change and its impacts. These include important climate variables such as surface temperature, sea ice extent, sea level rise, and streamflow. Perhaps one of the most iconic climatic datasets, that of atmospheric carbon dioxide measured at Mauna Loa, Hawai'i, has been recorded

since the 1950s. The U.S. and Global Historical Climatology Networks have been used as authoritative sources of recorded surface temperature increases, with some stations having continuous records going back many decades. Satellite radar altimetry data (for example, TOPEX/JASON1 & 2 satellite data) have informed the development of the University of Colorado's 20+ year record of global sea level changes. In the United States, the USGS (U.S. Geological Survey) National Water Information System contains, in some instances, decades of daily streamflow records which inform not only climate but land-use studies as well. The U.S. Bureau of Reclamation and U.S. Army Corp of Engineers have maintained data about reservoir levels for decades where applicable. Of course, datasets based on short-term observations are used in conjunction with longer-term records for climate study, and the U.S. programs are aimed at providing continuous data records. Methods have been developed and applied to process these data so as to account for biases, collection method, earth surface geometry, the urban heat island effect, station relocations, and uncertainty (e.g., see Vose et al. 2012;¹ Rennie et al. 2014;² Karl et al. 2015³).



Even observations not designed for climate have informed climate research. These include ship logs containing descriptions of ice extent, readings of temperature and precipitation provided in newspapers, and harvest records. Today, observations recorded both manually and in automated fashions inform research and are used in climate studies.

The U.S. Global Change Research Program (USGCRP) has established the Global Change Information System (GCIS) to better coordinate and integrate the use of federal information products on changes in the global environment and the implications of those changes for society. The GCIS is an open-source, web-based resource for traceable global change data, information, and products. Designed for use by scientists, decision makers, and the public, the GCIS provides coordinated links to a select group of information products produced, maintained, and disseminated by government agencies and organizations. Currently the GCIS is aimed at the datasets used in Third National Climate Assessment (NCA3) and the USGCRP Climate and Health Assessment. It will be updated for the datasets used in this report (The Climate Science Special Report, CSSR).

Temperature and Precipitation Observational Datasets

For analyses of surface temperature or precipitation, including determining changes over the globe or the United States, the starting point is accumulating observations of surface air temperature or precipitation taken at observing stations all over the world, and, in the case of temperature, sea surface temperatures (SSTs) taken by ships and buoys. These are direct measurements of the air temperature, sea surface temperature, and precipitation. The observations are quality assured to exclude clearly erroneous values. For tempera-

ture, additional analyses are performed on the data to correct for known biases in the way the temperatures were measured. These biases include the change to the observations that result from changes in observing practices or changes in the location or local environment of an observing station. One example is with SSTs where there was a change in practice from throwing a bucket over the side of the ship, pulling up seawater and measuring the temperature of the water in the bucket to measuring the temperature of the water in the engine intake. The bucket temperatures are systematically cooler than engine intake water and must be corrected.

For evaluating the globally averaged temperature, data are then compared to a long-term average for the location where the observations were taken (e.g., a 30-year average for an individual observing station) to create a deviation from that average, commonly referred to as an anomaly. Using anomalies allows the spatial averaging of stations in different climates and elevations to produce robust estimates of the spatially averaged temperature or precipitation for a given area.

To calculate the temperature or precipitation for a large area, like the globe or the United States, the area is divided into “grid boxes” usually in latitude/longitude space. For example, one common grid size has 5° x 5° latitude/longitude boxes, where each side of a grid box is 5° of longitude and 5° of latitude in length. All data anomalies in a given grid box are averaged together to produce a gridbox average. Some grid boxes contain no observations, but nearby grid boxes do contain observations, so temperatures or precipitation for the grid boxes with no observations are estimated as a function of the nearby grid boxes with observations for that date.



Calculating the temperature or precipitation value for the larger area, either the globe or the United States, is done by averaging the values for all the grid boxes to produce one number for each day, month, season, or year resulting in a time series. The time series in each of the grid boxes are also used to calculate long-term trends in the temperature or precipitation for each grid box. This provides a picture of how temperatures and precipitation are changing in different locations.

Evidence for changes in the climate of the United States arises from multiple analyses of data from *in situ*, satellite, and other records undertaken by many groups over several decades. The primary dataset for surface temperatures and precipitation in the United States is nClimGrid,^{4,5} though trends are similar in the U.S. Historical Climatology Network, the Global Historical Climatology Network, and other datasets. For temperature, several atmospheric reanalyses (e.g., 20th Century Reanalysis, Climate Forecast System Reanalysis, ERA-Interim, and Modern Era Reanalysis for Research and Applications) confirm rapid warming at the surface since 1979, with observed trends closely tracking

the ensemble mean of the reanalyses.¹ Several recently improved satellite datasets document changes in middle tropospheric temperatures.^{6,7,8} Longer-term changes are depicted using multiple paleo analyses (e.g., Wahl and Smerdon 2012;⁹ Trouet et al. 2013¹⁰).

Satellite Temperature Datasets

A special look is given to the satellite temperature datasets because of controversies associated with these datasets. Satellite-borne microwave sounders such as the Microwave Sounding Unit (MSU) and Advanced Microwave Sounding Unit (AMSU) instruments operating on NOAA polar-orbiting platforms take measurements of the temperature of thick layers of the atmosphere with near global coverage. Because the long-term data record requires the piecing together of measurements made by 16 different satellites, accurate instrument intercalibration is of critical importance. Over the mission lifetime of most satellites, the instruments drift in both calibration and local measurement time. Adjustments to counter the effects of these drifts need to be developed and applied before a long-term record can be assembled. For tropospheric measurements,

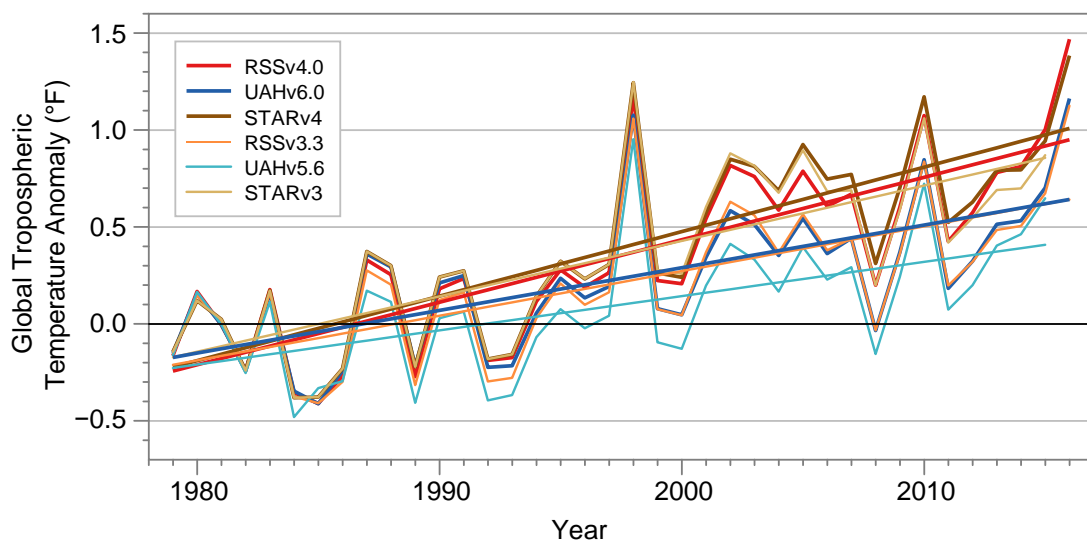


Figure A.1: Annual global (80°S–80°N) mean time series of tropospheric temperature for five recent datasets (see below). Each time series is adjusted so the mean value for the first three years is zero. This accentuates the differences in the long-term changes between the datasets. (Figure source: Remote Sensing Systems).

Table A.1.: Global Trends in Temperature Total Troposphere (TTT) since 1979 and 2000 (in °F per decade).

Dataset	Trend (1979–2015) (°F/Decade)	Trend (2000–2015) (°F/Decade)
RSS V4.0	0.301	0.198
UAH V6Beta5	0.196	0.141
STAR V4.0	0.316	0.157
RSS V3.3	0.208	0.105
UAH V5.6	0.176	0.211
STAR V3.0	0.286	0.061

the most challenging of these adjustments is the adjustment for drifting measurement time, which requires knowledge of the diurnal cycle in both atmospheric and surface temperature. Current versions of the sounder-based datasets account for the diurnal cycle by either using diurnal cycles deduced from model output^{11, 12} or by attempting to derive the diurnal cycle from the satellite measurements themselves (an approach plagued by sampling issues and possible calibration drifts).^{13, 14} Recently a hybrid approach has been developed, RSS Version 4.0,⁶ that results in an increased warming signal relative to the other approach-

es, particularly since 2000. Each of these methods has strengths and weaknesses, but none has sufficient accuracy to construct an unsailable long-term record of atmospheric temperature change. The resulting datasets show a greater spread in decadal-scale trends than do the surface temperature datasets for the same period, suggesting that they may be less reliable. Figure A.1 shows annual time series for the global mean tropospheric temperature for some recent versions of the satellite datasets. These data have been adjusted to remove the influence of stratospheric cooling.¹⁵ Linear trend values are shown in Table A.1.



DATA SOURCES

All Satellite Data are “Temperature Total Troposphere” time series calculated from TMT and TLS

$(1.1 * \text{TMT}) - (0.1 * \text{TLS})$. This combination reduces the effect of the lower stratosphere on the tropospheric temperature. (Fu, Qiang et al. “Contribution of stratospheric cooling to satellite-inferred tropospheric temperature trends.” *Nature* 429.6987 (2004): 55-58.)

UAH. UAH Version 6.0Beta5. Yearly (yyyy) text files of TMT and TLS are available from

<https://www.nsstc.uah.edu/data/msu/v6.0beta/tmt/>

<https://www.nsstc.uah.edu/data/msu/v6.0beta/tls/>

Downloaded 5/15/2016.

UAH. UAH Version 5.6. Yearly (yyyy) text files of TMT and TLS are available from

<http://vortex.nsstc.uah.edu/data/msu/t2/>

<http://vortex.nsstc.uah.edu/data/msu/t4/>

Downloaded 5/15/2016.

RSS. RSS Version 4.0.

ftp://ftp.remss.com/msu/data/netcdf/RSS_Tb_Anom_Maps_ch_TTT_V4_0.nc

Downloaded 5/15/2016

RSS. RSS Version 3.3.

ftp://ftp.remss.com/msu/data/netcdf/RSS_Tb_Anom_Maps_ch_TTT_V3.3.nc

Downloaded 5/15/2016

NOAA STAR. Star Version 3.0.

ftp://ftp.star.nesdis.noaa.gov/pub/smcd/emb/mscat/data/MSU_AMSU_v3.0/Monthly_Atmospheric_Layer_Mean_Temperature/Merged_Deep-Layer_Temperature/NESDIS-STAR_TCDR_MSU-AMSUA_V03R00_TMT_S197811_E201709_C20171002.nc

ftp://ftp.star.nesdis.noaa.gov/pub/smcd/emb/mscat/data/MSU_AMSU_v3.0/Monthly_Atmospheric_Layer_Mean_Temperature/Merged_Deep-Layer_Temperature/NESDIS-STAR_TCDR_MSU-AMSUA_V03R00_TLS_S197811_E201709_C20171002.nc

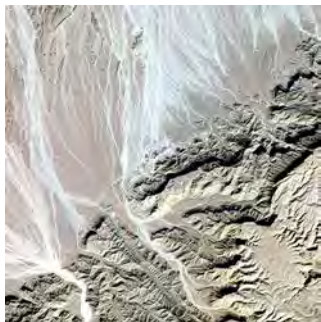
Downloaded 5/18/2016.



REFERENCES

- Vose, R.S., D. Arndt, V.F. Banzon, D.R. Easterling, B. Gleason, B. Huang, E. Kearns, J.H. Lawrimore, M.J. Menne, T.C. Peterson, R.W. Reynolds, T.M. Smith, C.N. Williams, and D.L. Wuertz, 2012: NOAA's merged land-ocean surface temperature analysis. *Bulletin of the American Meteorological Society*, **93**, 1677-1685. <http://dx.doi.org/10.1175/BAMS-D-11-00241.1>
- Rennie, J.J., J.H. Lawrimore, B.E. Gleason, P.W. Thorne, C.P. Morice, M.J. Menne, C.N. Williams, Jr., W.G. de Almeida, J.R. Christy, M. Flannery, M. Ishihara, K. Kamiguchi, A.M.G. Klein-Tank, A. Mhanda, D.H. Lister, V. Razuvaev, M. Renom, M. Rusticucci, J. Tandy, S.J. Worley, V. Venema, W. Angel, M. Brunet, B. Dattore, H. Diamond, M.A. Lazzara, F. Le Blancq, J. Luterbacher, H. Mächel, J. Revadekar, R.S. Vose, and X. Yin, 2014: The international surface temperature initiative global land surface databank: Monthly temperature data release description and methods. *Geoscience Data Journal*, **1**, 75-102. <http://dx.doi.org/10.1002/gdj3.8>
- Karl, T.R., A. Arguez, B. Huang, J.H. Lawrimore, J.R. McMahon, M.J. Menne, T.C. Peterson, R.S. Vose, and H.-M. Zhang, 2015: Possible artifacts of data biases in the recent global surface warming hiatus. *Science*, **348**, 1469-1472. <http://dx.doi.org/10.1126/science.aaa5632>
- Vose, R.S., S. Applequist, M. Squires, I. Durre, M.J. Menne, C.N. Williams, Jr., C. Fenimore, K. Gleason, and D. Arndt, 2014: Improved historical temperature and precipitation time series for U.S. climate divisions. *Journal of Applied Meteorology and Climatology*, **53**, 1232-1251. <http://dx.doi.org/10.1175/JAMC-D-13-0248.1>
- Vose, R.S., M. Squires, D. Arndt, I. Durre, C. Fenimore, K. Gleason, M.J. Menne, J. Partain, C.N. Williams Jr., P.A. Bieniek, and R.L. Thoman, 2017: Deriving historical temperature and precipitation time series for Alaska climate divisions via climatologically aided interpolation. *Journal of Service Climatology* **10**, 20. <https://www.stateclimate.org/sites/default/files/upload/pdf/journal-articles/2017-Ross-et-al.pdf>
- Mears, C.A. and F.J. Wentz, 2016: Sensitivity of satellite-derived tropospheric temperature trends to the diurnal cycle adjustment. *Journal of Climate*, **29**, 3629-3646. <http://dx.doi.org/10.1175/JCLI-D-15-0744.1>
- Spencer, R.W., J.R. Christy, and W.D. Braswell, 2017: UAH Version 6 global satellite temperature products: Methodology and results. *Asia-Pacific Journal of Atmospheric Sciences*, **53**, 121-130. <http://dx.doi.org/10.1007/s13143-017-0010-y>
- Zou, C.-Z. and J. Li, 2014: NOAA MSU Mean Layer Temperature. National Oceanic and Atmospheric Administration, Center for Satellite Applications and Research, 35 pp. http://www.star.nesdis.noaa.gov/smcd/emb/mscat/documents/MSU_TCDR_CATBD_Zou_Li.pdf
- Wahl, E.R. and J.E. Smerdon, 2012: Comparative performance of paleoclimate field and index reconstructions derived from climate proxies and noise-only predictors. *Geophysical Research Letters*, **39**, L06703. <http://dx.doi.org/10.1029/2012GL051086>
- Trouet, V., H.F. Diaz, E.R. Wahl, A.E. Viau, R. Graham, N. Graham, and E.R. Cook, 2013: A 1500-year reconstruction of annual mean temperature for temperate North America on decadal-to-multidecadal time scales. *Environmental Research Letters*, **8**, 024008. <http://dx.doi.org/10.1088/1748-9326/8/2/024008>
- Mears, C.A. and F.J. Wentz, 2009: Construction of the Remote Sensing Systems V3.2 atmospheric temperature records from the MSU and AMSU microwave sounders. *Journal of Atmospheric and Oceanic Technology*, **26**, 1040-1056. <http://dx.doi.org/10.1175/2008JTECHA1176.1>
- Zou, C.-Z., M. Gao, and M.D. Goldberg, 2009: Error structure and atmospheric temperature trends in observations from the microwave sounding unit. *Journal of Climate*, **22**, 1661-1681. <http://dx.doi.org/10.1175/2008JCLI2233.1>
- Christy, J.R., R.W. Spencer, W.B. Norris, W.D. Braswell, and D.E. Parker, 2003: Error estimates of version 5.0 of MSU-AMSU bulk atmospheric temperatures. *Journal of Atmospheric and Oceanic Technology*, **20**, 613-629. [http://dx.doi.org/10.1175/1520-0426\(2003\)20<613:EEOVOM>2.0.CO;2](http://dx.doi.org/10.1175/1520-0426(2003)20<613:EEOVOM>2.0.CO;2)
- Po-Chedley, S., T.J. Thorsen, and Q. Fu, 2015: Removing diurnal cycle contamination in satellite-derived tropospheric temperatures: Understanding tropical tropospheric trend discrepancies. *Journal of Climate*, **28**, 2274-2290. <http://dx.doi.org/10.1175/JCLI-D-13-00767.1>
- Fu, Q. and C.M. Johanson, 2005: Satellite-derived vertical dependence of tropical tropospheric temperature trends. *Geophysical Research Letters*, **32**, L10703. <http://dx.doi.org/10.1029/2004GL022266>





Appendix B

Model Weighting Strategy

Recommended Citation for Chapter

Sanderson, B.M. and M.F. Wehner, 2017: Model weighting strategy. In: *Climate Science Special Report: Fourth National Climate Assessment, Volume I* [Wuebbles, D.J., D.W. Fahey, K.A. Hibbard, D.J. Dokken, B.C. Stewart, and T.K. Maycock (eds.)]. U.S. Global Change Research Program, Washington, DC, USA, pp. 436-442, doi: 10.7930/J06T0JS3.

Introduction

This document briefly describes a weighting strategy for use with the Climate Model Inter-comparison Project, Phase 5 (CMIP5) multi-model archive in the Fourth National Climate Assessment (NCA4). This approach considers both skill in the climatological performance of models over North America and the interdependency of models arising from common parameterizations or tuning practices. The method exploits information relating to the climatological mean state of a number of projection-relevant variables as well as long-term metrics representing long-term statistics of weather extremes. The weights, once computed, can be used to simply compute weighted mean and significance information from an ensemble containing multiple initial condition members from co-dependent models of varying skill.

Our methodology is based on the concepts outlined in Sanderson et al. 2015,¹ and the specific application to the NCA4 is also described in that paper. The approach produces a single set of model weights that can be used to combine projections into a weighted mean result, with significance estimates which also treat the weighting appropriately.

The method, ideally, would seek to have two fundamental characteristics:

- If a duplicate of one ensemble member is added to the archive, the resulting mean and significance estimate for future change computed from the ensemble should not change.
- If a demonstrably unphysical model is added to the archive, the resulting mean and significance estimates should also not change.

Method

The analysis requires an assessment of both model skill and an estimate of intermodel relationships – for which intermodel root mean square difference is taken as a proxy. The model and observational data used here is for the contiguous United States (CONUS), and most of Canada, using high-resolution data where available. Intermodel distances are computed as simple root mean square differences. Data is derived from a number of mean state fields and a number of fields that represent extreme behavior – these are listed in Table B.1. All fields are masked to only include information from CONUS/Canada.



The root mean square error (RMSE) between observations and each model can be used to produce an overall ranking for model simu-

lations of the North American climate. Figure B.1 shows how this metric is influenced by different component variables.

Table B.1: Observational datasets used as observations.

Field	Description	Source	Reference	Years
TS	Surface Temperature (seasonal)	Livneh, Hutchinson	(Hopkinson et al. 2012; ³ Hutchinson et al. 2009; ⁴ Livneh et al. 2013 ⁵)	1950–2011
PR	Mean Precipitation (seasonal)	Livneh, Hutchinson	(Hopkinson et al. 2012; ³ Hutchinson et al. 2009; ⁴ Livneh et al. 2013 ⁵)	1950–2011
RSUT	TOA Shortwave Flux (seasonal)	CERES-EBAF	(Wielicki et al. 1996 ⁶)	2000–2005
RLUT	TOA Longwave Flux (seasonal)	CERES-EBAF	(Wielicki et al. 1996 ⁶)	2000–2005
T	Vertical Temperature Profile (seasonal)	AIRS*	(Aumann et al. 2003 ⁷)	2002–2010
RH	Vertical Humidity Profile (seasonal)	AIRS	(Aumann et al. 2003 ⁷)	2002–2010
PSL	Surface Pressure (seasonal)	ERA-40	(Uppala et al. 2005 ⁸)	1970–2000
Tnn	Coldest Night	Livneh, Hutchinson	(Hopkinson et al. 2012; ³ Hutchinson et al. 2009; ⁴ Livneh et al. 2013 ⁵)	1950–2011
Txn	Coldest Day	Livneh, Hutchinson	(Hopkinson et al. 2012; ³ Hutchinson et al. 2009; ⁴ Livneh et al. 2013 ⁵)	1950–2011
Tnx	Warmest Night	Livneh, Hutchinson	(Hopkinson et al. 2012; ³ Hutchinson et al. 2009; ⁴ Livneh et al. 2013 ⁵)	1950–2011
Txx	Warmest day	Livneh, Hutchinson	(Hopkinson et al. 2012; ³ Hutchinson et al. 2009; ⁴ Livneh et al. 2013 ⁵)	1950–2011
rx5day	seasonal max. 5-day total precip.	Livneh, Hutchinson	(Hopkinson et al. 2012; ³ Hutchinson et al. 2009; ⁴ Livneh et al. 2013 ⁵)	1950–2011



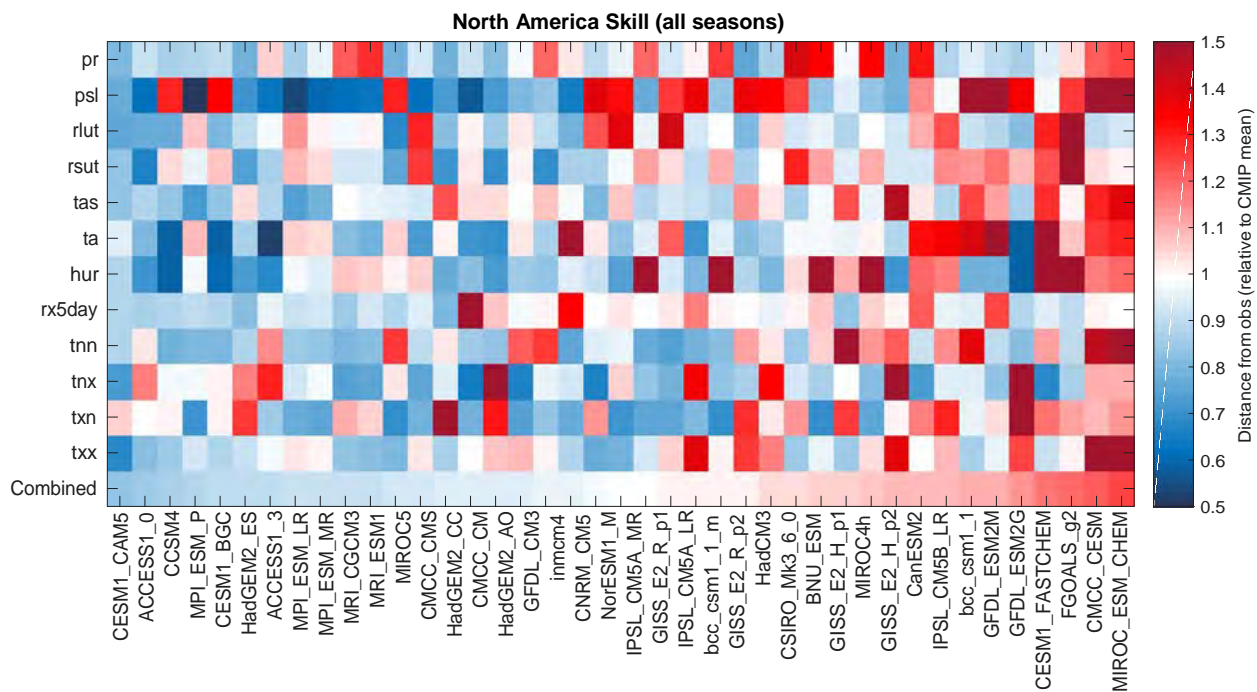


Figure B.1: A graphical representation of the intermodel distance matrix for CMIP5 and a set of observed values. Each row and column represents a single climate model (or observation). All scores are aggregated over seasons (individual seasons are not shown). Each box represents a pairwise distance, where warm (red) colors indicate a greater distance. Distances are measured as a fraction of the mean intermodel distance in the CMIP5 ensemble. (Figure source: Sanderson et al. 2017²).

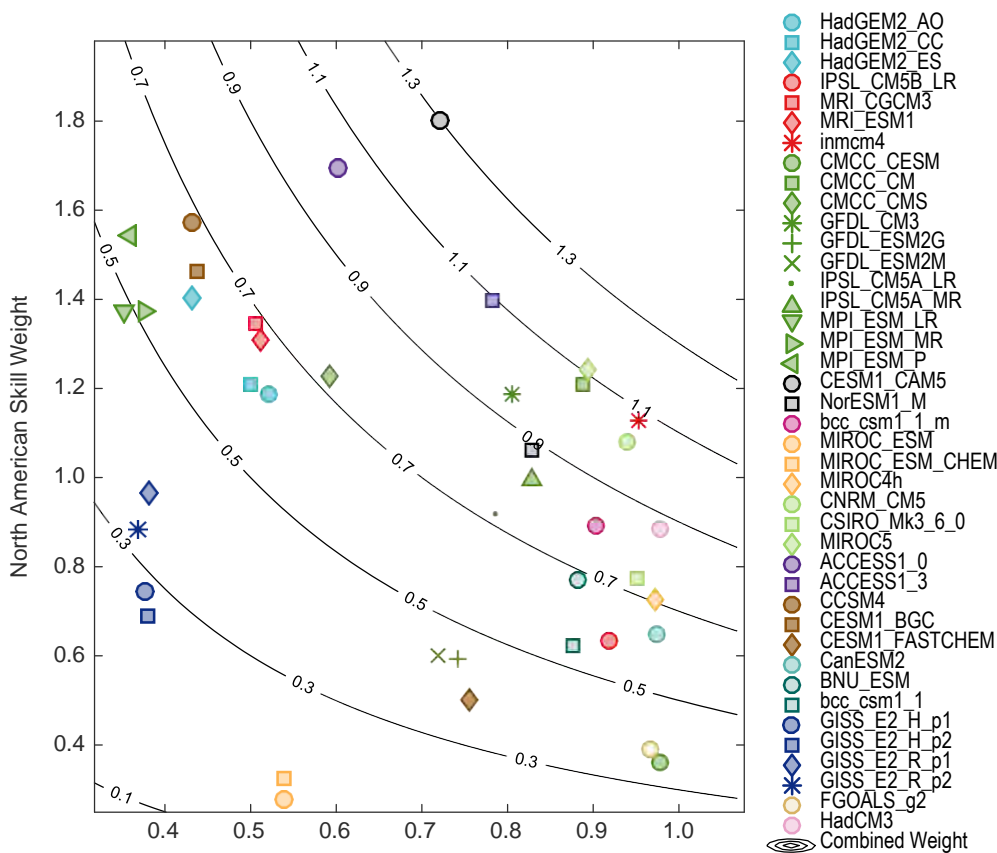


Figure B.2: Model skill and independence weights for the CMIP5 archive evaluated over the North American domain. Contours show the overall weighting, which is the product of the two individual weights. (Figure source: Sanderson et al. 2017²).

Models are downweighted for poor skill if their multivariate combined error is significantly greater than a “skill radius” term, which is a free parameter of the approach. The calibration of this parameter is determined through a perfect model study.² A pairwise distance matrix is computed to assess inter-model RMSE values for each model pair in the archive, and a model is downweighted for dependency if there exists another model with a pairwise distance to the original model significantly smaller than a “similarity radius.” This is the second parameter of the approach, which is calibrated by considering known relationships within the archive. The resulting skill and independence weights are multiplied to give an overall “combined” weight—illustrated in Figure B.2 for the CMIP5 ensemble and listed in Table B.2.

The weights are used in the Climate Science Special Report (CSSR) to produce weighted mean and significance maps of future change, where the following protocol is used:

- Stippling—large changes, where the weighted multimodel average change is greater than double the standard deviation of the 20-year mean from control simulations runs, and 90% of the weight corresponds to changes of the same sign.
- Hatching—No significant change, where the weighted multimodel average change is less than the standard deviation of the 20-year means from control simulations runs.
- Whited out—Inconclusive, where the weighted multimodel average change is greater than double the standard deviation of the 20-year mean from control runs and less than 90% of the weight corresponds to changes of the same sign.

We illustrate the application of this method to future projections of precipitation change under the higher scenario (RCP8.5) in Figure B.3. The weights used in the report are chosen to be conservative, minimizing the risk of overconfidence and maximizing out-of-sample predictive skill for future projections. This results (as in Figure B.3) in only modest differences in the weighted and unweighted maps. It is shown in Sanderson et al. 2017² that a more aggressive weighting strategy, or one focused on a particular variable, tends to exhibit a stronger constraint on future change relative to the unweighted case. It is also notable that tradeoffs exist between skill and replication in the archive (evident in Figure B.2), such that the weighting for both skill and uniqueness has a compensating effect. As such, mean projections using the CMIP5 ensemble are not strongly influenced by the weighting. However, the establishment of the weighting strategy used in the CSSR provides some insurance against a potential case in future assessments where there is a highly replicated, but poorly performing model.



Table B.2: Uniqueness, skill, and combined weights for CMIP5.

	Uniqueness Weight	Skill Weight	Combined
ACCESS1-0	0.60	1.69	1.02
ACCESS1-3	0.78	1.40	1.09
BNU-ESM	0.88	0.77	0.68
CCSM4	0.43	1.57	0.68
CESM1-BGC	0.44	1.46	0.64
CESM1-CAM5	0.72	1.80	1.30
CESM1-FASTCHEM	0.76	0.50	0.38
CMCC-CESM	0.98	0.36	0.35
CMCC-CM	0.89	1.21	1.07
CMCC-CMS	0.59	1.23	0.73
CNRM-CM5	0.94	1.08	1.01
CSIRO-Mk3-6-0	0.95	0.77	0.74
CanESM2	0.97	0.65	0.63
FGOALS-g2	0.97	0.39	0.38
GFDL-CM3	0.81	1.18	0.95
GFDL-ESM2G	0.74	0.59	0.44
GFDL-ESM2M	0.72	0.60	0.43
GISS-E2-H-p1	0.38	0.74	0.28
GISS-E2-H-p2	0.38	0.69	0.26
GISS-E2-R-p1	0.38	0.97	0.37
GISS-E2-R-p2	0.37	0.89	0.33
HadCM3	0.98	0.89	0.87
HadGEM2-AO	0.52	1.19	0.62
HadGEM2-CC	0.50	1.21	0.60
HadGEM2-ES	0.43	1.40	0.61
IPSL-CM5A-LR	0.79	0.92	0.72
IPSL-CM5A-MR	0.83	0.99	0.82
IPSL-CM5B-LR	0.92	0.63	0.58
MIROC-ESM	0.54	0.28	0.15
MIROC-ESM-CHEM	0.54	0.32	0.17
MIROC4h	0.97	0.73	0.71
MIROC5	0.89	1.24	1.11
MPI-ESM-LR	0.35	1.38	0.49
MPI-ESM-MR	0.38	1.37	0.52
MPI-ESM-P	0.36	1.54	0.56
MRI-CGCM3	0.51	1.35	0.68
MRI-ESM1	0.51	1.31	0.67
NorESM1-M	0.83	1.06	0.88
bcc-csm1-1	0.88	0.62	0.55
bcc-csm1-1-m	0.90	0.89	0.80
inmcm4	0.95	1.13	1.08



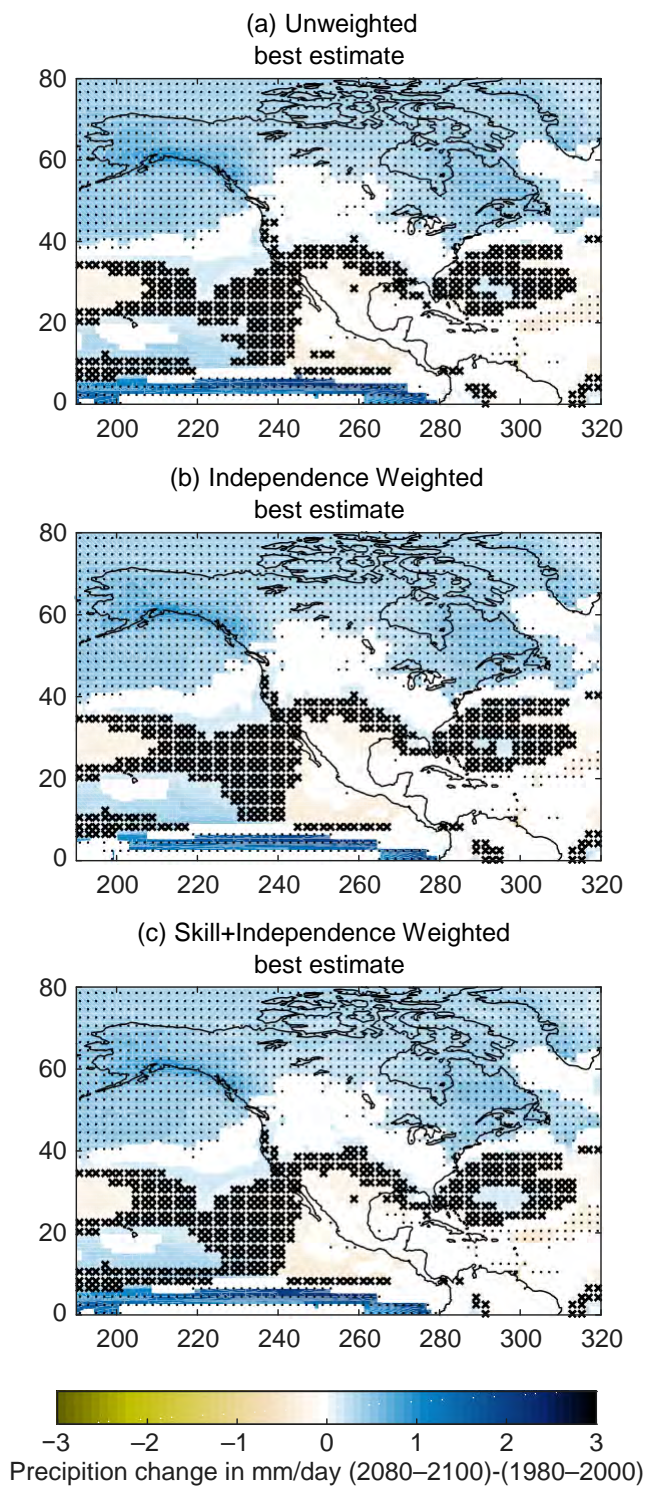


Figure B.3: Projections of precipitation change over North America in 2080–2100, relative to 1980–2000 under the higher scenario (RCP8.5). (a) Shows the simple unweighted CMIP5 multimodel average, using the significance methodology from IPCC⁹; (b) shows the weighted results as outlined in Section 3 for models weighted by uniqueness only; and (c) shows weighted results for models weighted by both uniqueness and skill. (Figure source: Sanderson et al. 2017²).



REFERENCES

1. Sanderson, B.M., R. Knutti, and P. Caldwell, 2015: A representative democracy to reduce interdependency in a multimodel ensemble. *Journal of Climate*, **28**, 5171-5194. <http://dx.doi.org/10.1175/jcli-d-14-00362.1>
2. Sanderson, B.M., M. Wehner, and R. Knutti, 2017: Skill and independence weighting for multi-model assessment. *Geoscientific Model Development*, **10**, 2379-2395. <http://dx.doi.org/10.5194/gmd-10-2379-2017>
3. Hopkinson, R.F., M.F. Hutchinson, D.W. McKenney, E.J. Milewska, and P. Papadopol, 2012: Optimizing input data for gridding climate normals for Canada. *Journal of Applied Meteorology and Climatology*, **51**, 1508-1518. <http://dx.doi.org/10.1175/jamc-d-12-018.1>
4. Hutchinson, M.F., D.W. McKenney, K. Lawrence, J.H. Pedlar, R.F. Hopkinson, E. Milewska, and P. Papadopol, 2009: Development and testing of Canada-wide interpolated spatial models of daily minimum-maximum temperature and precipitation for 1961-2003. *Journal of Applied Meteorology and Climatology*, **48**, 725-741. <http://dx.doi.org/10.1175/2008jamc1979.1>
5. Livneh, B., E.A. Rosenberg, C. Lin, B. Nijssen, V. Mishra, K.M. Andreadis, E.P. Maurer, and D.P. Lettenmaier, 2013: A long-term hydrologically based dataset of land surface fluxes and states for the conterminous United States: Update and extensions. *Journal of Climate*, **26**, 9384-9392. <http://dx.doi.org/10.1175/jcli-d-12-00508.1>
6. Wielicki, B.A., B.R. Barkstrom, E.F. Harrison, R.B. Lee III, G.L. Smith, and J.E. Cooper, 1996: Clouds and the Earth's Radiant Energy System (CERES): An Earth observing system experiment. *Bulletin of the American Meteorological Society*, **77**, 853-868. [http://dx.doi.org/10.1175/1520-0477\(1996\)077<0853:catere>2.0.co;2](http://dx.doi.org/10.1175/1520-0477(1996)077<0853:catere>2.0.co;2)
7. Aumann, H.H., M.T. Chahine, C. Gautier, M.D. Goldberg, E. Kalnay, L.M. McMillin, H. Revercomb, P.W. Rosenkranz, W.L. Smith, D.H. Staelin, L.L. Strow, and J. Susskind, 2003: AIRS/AMSU/HSB on the Aqua mission: Design, science objectives, data products, and processing systems. *IEEE Transactions on Geoscience and Remote Sensing*, **41**, 253-264. <http://dx.doi.org/10.1109/tgrs.2002.808356>
8. Uppala, S.M., P.W. Kållberg, A.J. Simmons, U. Andrae, V.D.C. Bechtold, M. Fiorino, J.K. Gibson, J. Haseler, A. Hernandez, G.A. Kelly, X. Li, K. Onogi, S. Saarinen, N. Sokka, R.P. Allan, E. Andersson, K. Arpe, M.A. Balmaseda, A.C.M. Beljaars, L.V.D. Berg, J. Bidlot, N. Bormann, S. Caires, F. Chevallier, A. Dethof, M. Dragosavac, M. Fisher, M. Fuentes, S. Hagemann, E. Hólm, B.J. Hoskins, L. Isaksen, P.A.E.M. Janssen, R. Jenne, A.P. McNally, J.F. Mahfouf, J.J. Morcrette, N.A. Rayner, R.W. Saunders, P. Simon, A. Sterl, K.E. Trenberth, A. Untch, D. Vasiljevic, P. Vit-erbo, and J. Woollen, 2005: The ERA-40 re-analysis. *Quarterly Journal of the Royal Meteorological Society*, **131**, 2961-3012. <http://dx.doi.org/10.1256/qj.04.176>
9. IPCC, 2013: *Climate Change 2013: The Physical Science Basis. Contribution of Working Group I to the Fifth Assessment Report of the Intergovernmental Panel on Climate Change*. Cambridge University Press, Cambridge, UK and New York, NY, 1535 pp. <http://www.climatechange2013.org/report/>





Appendix C

Detection and Attribution Methodologies Overview

Recommended Citation for Chapter

Knutson, T., 2017: Detection and attribution methodologies overview. In: *Climate Science Special Report: Fourth National Climate Assessment, Volume I* [Wuebbles, D.J., D.W. Fahey, K.A. Hibbard, D.J. Dokken, B.C. Stewart, and T.K. Maycock (eds.)]. U.S. Global Change Research Program, Washington, DC, USA, pp. 443-451, doi: 10.7930/J0319T2J.

C.1 Introduction and Conceptual Framework

In this appendix, we present a brief overview of the methodologies and methodological issues for detection and attribution of climate change. Attributing an observed change or an event partly to a causal factor (such as anthropogenic climate forcing) normally requires that the change first be detectable.¹ A *detectable* observed change is one which is determined to be highly unlikely to occur (less than about a 10% chance) due to internal variability alone, without necessarily being ascribed to a causal factor. An *attributable* change refers to a change in which the relative contribution of causal factors has been evaluated along with an assignment of statistical confidence (e.g., Bindoff et al. 2013;² Hegerl et al. 2010¹).

As outlined in Bindoff et al.,² the conceptual framework for most detection and attribution studies consists of four elements: 1) relevant observations; 2) the estimated time history of relevant climate forcings (such as greenhouse gas concentrations or volcanic activity); 3) a modeled estimate of the impact of the climate forcings on the climate variables of interest; and 4) an estimate of the internal (unforced) variability of the climate variables of inter-

est—that is, the changes that can occur due to natural unforced variations of the ocean, atmosphere, land, cryosphere, and other elements of the climate system in the absence of external forcings. The four elements above can be used together with a detection and attribution framework to assess possible causes of observed changes.

C.2 Fingerprint-Based Methods

A key methodological approach for detection and attribution is the regression-based “fingerprint” method (e.g., Hasselmann 1997;³ Allen and Stott 2003;⁴ Hegerl et al. 2007;⁵ Hegerl and Zwiers 2011;⁶ Bindoff et al. 2013²), where observed changes are regressed onto a model-generated response pattern to a particular forcing (or set of forcings), and regression scaling factors are obtained. When a scaling factor for a forcing pattern is determined to be significantly different from zero, a detectable change has been identified. If the uncertainty bars on the scaling factor encompass unity, the observed change is consistent with the modeled response, and the observed change can be attributed, at least in part, to the associated forcing agent, according to this methodology. Zwiers et al.⁷ showed how detection and attribution methods could be applied



to the problem of changes in daily temperature extremes at the regional scale by using a generalized extreme value (GEV) approach. In their approach, a time-evolving pattern of GEV location parameters (i.e., “fingerprint”) from models is fit to the observed extremes as a means of detecting and attributing changes in the extremes to certain forcing sets (for example, anthropogenic forcings).

A recent development in detection/attribution methodology⁸ uses hypothesis testing and an additive decomposition approach rather than linear regression of patterns. The new approach makes use of the magnitudes of responses from the models rather than using the model patterns and deriving the scaling factors (magnitudes of responses) from regression. The new method, in a first application, gives very similar attributable anthropogenic warming estimates to the earlier methods as reported in Bindoff et al.² and shown in Figure 3.2. Some further methodological developments for performing optimal fingerprint detection and attribution studies are proposed in Hannart,⁹ who, for example, focuses on the possible use of raw data in analyses without the use of dimensional reductions, such as projecting the data onto a limited number of basis functions, such as spherical harmonics, before analysis.

C.3 Non-Fingerprint Based Methods

A simpler detection/attribution/consistency calculation, which does not involve regression and pattern scaling, compares observed and simulated time series to assess whether observations are consistent with natural variability simulations or with simulations forced by both natural and anthropogenic forcing agents.^{10, 11} Cases where observations are inconsistent with model simulations using natural forcing only (a detectable change), while also being consistent with models that incorporate both anthropogenic and natural

forcings, are interpreted as having an attributable anthropogenic contribution, subject to caveats regarding uncertainties in observations, climate forcings, modeled responses, and simulated internal climate variability. This simpler method is useful for assessing trends over smaller regions such as sub-regions of the United States (see the example given in Figure 6.5 for regional surface temperature trends).

Delsole et al.¹² introduced a method of identifying internal (unforced) variability in climate data by decomposing variables by time scale, using a measure of their predictability. They found that while such internal variability could contribute to surface temperature trends of 30-years’ duration or less, and could be responsible for the accelerated global warming during 1977–2008 compared to earlier decades, the strong (approximately 0.8°C, or 1.4°F) warming trend seen in observations over the past century was not explainable by such internal variability. Constructed circulation analogs^{13, 14} is a method used to identify the part of observed surface temperature changes that is due to atmospheric circulation changes alone.

The time scale by which climate change signals will become detectable in various regions is a question of interest in detection and attribution studies, and methods of estimating this have been developed and applied (e.g., Mahlstein et al. 2011;¹⁵ Deser et al. 2012¹⁶). These studies illustrate how natural variability can obscure forced climate signals for decades, particularly for smaller (less than continental) space scales.

Other examples of detection and attribution methods include the use of multiple linear regression with energy balance models (e.g., Canty et al. 2013¹⁷) and Granger causality tests (e.g., Stern and Kaufmann 2014¹⁸). These are typically attempting to relate forcing time



series, such as the historical record of atmospheric CO₂ since 1860, to a climate response measure, such as global mean temperature or ocean heat content, but without using a full coupled climate model to explicitly estimate the response of the climate system to forcing (or the spatial pattern of the response to forcing). Granger causality, for example, explores the lead-lag relationships between different variables to infer causal relationships between them and attempts to control for any influence of a third variable that may be linked to the other two variables in question.

C.4 Multistep Attribution and Attribution without Detection

A growing number of climate change and extreme event attribution studies use a *multistep attribution* approach,¹ based on attribution of a change in climate conditions that are closely related to the variable or event of interest. In the multistep approach, an observed change in the variable of interest is attributed to a change in climate or other environmental conditions, and then the changes in the climate or environmental conditions are separately attributed to an external forcing, such as anthropogenic emissions of greenhouse gases. As an example, some attribution statements for phenomena such as droughts or hurricane activity—where there are not necessarily detectable trends in occurrence of the phenomenon itself—are based on models and on detected changes in related variables such as surface temperature, as well as an understanding of the relevant physical processes linking surface temperatures to hurricanes or drought. For example, some studies of the recent California drought (e.g., Mao et al. 2015;¹⁹ Williams et al. 2015²⁰) attribute a fraction of the event to anthropogenic warming or to long-term warming based on modeling or statistical analysis, although without claiming that there was a detectable change in the drought frequency or magnitude.

The multistep approach and model simulations are both methods that, in principle, can allow for attribution of a climate change or a change in the likelihood of occurrence of an event to a causal factor without necessarily detecting a significant change in the occurrence rate of the phenomenon or event itself (though in some cases, there may also be a detectable change in the variable of interest). For example, Murakami et al.²¹ used model simulations to conclude that the very active hurricane season observed near Hawai'i in 2014 was at least partially attributable to anthropogenic influence; they also show that there is no clear long-term detectable trend in historical hurricane occurrence near Hawai'i in available observations. If an attribution statement is made where there is not a detectable change in the phenomenon itself (for example, hurricane frequency or drought frequency) then this statement is an example of *attribution without detection*. Such an attribution without detection can be distinguished from a conventional single-step attribution (for example, global mean surface temperature) where in the latter case there is a detectable change in the variable of interest (or the scaling factor for a forcing pattern is significantly different from zero in observations) and attribution of the changes in that variable to specific external forcing agents. Regardless of whether a single-step or multistep attribution approach is used, or whether there is a detectable change in the variable of interest, attribution statements with relatively higher levels of confidence are underpinned by a thorough understanding of the physical processes involved.

There are reasons why attribution without detection statements can be appropriate, despite the lower confidence typically associated with such statements as compared to attribution statements that are supported by detection of a change in the phenomenon itself. For example, an event of interest may be



so rare that a trend analysis for similar events is not practical. Including attribution without detection events in the analysis of climate change impacts reduces the chances of a false negative, that is, incorrectly concluding that climate change had no influence on a given extreme events²² in a case where it did have an influence. However, avoiding this type of error through attribution without detection comes at the risk of increasing the rate of false positives, where one incorrectly concludes that anthropogenic climate change had a certain type of influence on an extreme event when in fact it did not have such an influence (see Box C.1).

C.5 Extreme Event Attribution Methodologies

Since the release of the Intergovernmental Panel on Climate Change's Fifth Assessment Report (IPCC AR5) and the Third National Climate Assessment (NCA3),²³ there have been further advances in the science of detection and attribution of climate change. An emerging area in the science of detection and attribution is the attribution of extreme weather and climate events.^{24, 25, 26} According to Hulme,²⁷ there are four general types of attribution methods that are applied in practice: physical reasoning, statistical analysis of time series, fraction of attributable risk (FAR) estimation, and the philosophical argument that there are no longer any purely natural weather events. As discussed in a recent National Academy of Sciences report,²⁴ possible anthropogenic influence on an extreme event can be assessed using a risk-based approach, which examines whether the odds of occurrence of a type of extreme event have changed, or through an ingredients-based or conditional attribution approach.

In the risk-based approach,^{24, 27, 28} one typically uses a model to estimate the probability (p) of occurrence of a weather or climate event with-

in two climate states: one state with anthropogenic influence (where the probability is p_1) and the other state without anthropogenic influence (where the probability is p_0). Then the ratio (p_1/p_0) describes how much more or less likely the event is in the modeled climate with anthropogenic influence compared to a modeled hypothetical climate without anthropogenic influences. Another common metric used with this approach is the fraction of attributable risk (FAR), defined as $FAR = 1 - (p_0/p_1)$. Further refinements on such an approach using causal theory are discussed in Hannart et al.²⁹

In the conditional or ingredients-based approach,^{24, 30, 31, 32} an investigator may look for changes in occurrence of atmospheric circulation and weather patterns relevant to the extreme event, or at the impact of certain environmental changes (for example, greater atmospheric moisture) on the character of an extreme event. Conditional or ingredients-based attribution can be applied to extreme events or to climate changes in general. An example of the ingredients-based approach and more discussion of this type of attribution method is given in Box C.2.

Hannart et al.²⁹ have discussed how causal theory can also be applied to attribution studies in order to distinguish between necessary and sufficient causation. Hannart et al.³³ further propose methodologies to use data assimilation systems, which are now used operationally to update short-term numerical weather prediction models, for detection and attribution. They envision how such systems could be used in the future to implement near-real time systematic causal attribution of weather and climate-related events.



Box C.1. On the Use of Significance Levels and Significance Tests in Attribution Studies

In detection/attribution studies, a detectable observed change is one which is determined to be highly unlikely to occur (less than about a 10% chance) due to internal variability alone. Some frequently asked questions concern the use of such a high statistical threshold (significance level) in attribution studies. In this box, we respond to several such questions received in the public review period.

Why is such a high degree of confidence (for example, statistical significance at p level of 0.05) typically required before concluding that an attributable anthropogenic component to a climate change or event has been detected? For example, could attribution studies be reframed to ask whether there is a 5% or more chance that anthropogenic climate change contributed to the event?

This question is partly related to the issue of risk avoidance. For example, if there is a particular climate change outcome that we wish to avoid (for example, global warming of 3°C, or 10°C, or a runaway greenhouse) then one can use the upper ranges of confidence intervals of climate model projections as guidance, based on available science, for avoiding such outcomes. Detection/attribution studies typically deal with smaller changes than climate projections over the next century or more. For detection/attribution studies, researchers are confronting models with historical data to explore whether or not observed climate change signals are emerging from the background of natural variability. Typically, the emergent signal is just a small fraction of what is predicted by the models for the coming century under continued strong greenhouse gas emission scenarios. Detecting that a change has emerged from natural variability is not the same as approaching a threshold to be avoided, unless the goal is to ensure no detectable anthropogenic influence on climate. Consequently, use of a relative strong confidence level (or p -value of 0.05) for determining climate change detection seems justified for the particular case of climate change detection, since one can also separately use risk-avoidance strategies or probability criteria to avoid reaching certain defined thresholds (for example, a 2°C global warming threshold).

A related question concerns ascribing blame for causing an extreme event. For example, if a damaging hurricane or typhoon strikes an area and causes much damage, affected residents may ask whether human-caused climate change was at least partially to blame for the event. In this case, climate scientists sometimes use the “Fraction of Attributable Risk” framework, where they examine whether the odds of some threshold event occurring have been increased due to anthropogenic climate change. This is typically a model-based calculation, where the probability distribution related to the event in question is modeled under preindustrial and present-day climate conditions, and the occurrence rates are compared for the two modeled distributions. Note that such an analysis can be done with or without the detection of a climate change signal for the occurrence of the event in question. In general, cases where there has been a detection and attribution of changes in the event in question to human causes, then the attribution of increased risk to anthropogenic forcing will be relatively more confident.

The question of whether it is more appropriate to use approaches that incorporate a high burden of statistical evidence before concluding that anthropogenic forcings contributed significantly (as in traditional detection/attribution studies) versus using models to estimate anthropogenic contributions when there may not even be a detectable signal present in the observations (as in some Fraction of Attributable Risk studies) may depend on what type of error or scenario one most wants to avoid. In the former case, one is attempting to avoid the error of concluding that anthropogenic forcing has contributed to some observed climate change, when in fact, it later turns out that anthropogenic forcing has not contributed to the change. In the second case, one is attempting to avoid the “error” of concluding that anthropogenic forcing has not contributed significantly to an observed



climate change or event when (as it later comes to be known) anthropogenic forcing had evidently contributed to the change, just not at a level that was detectable at the time compared to natural variability.

What is the tradeoff between false positives and false negatives in attribution statistical testing, and how is it decided which type of error one should focus on avoiding?

As discussed above, there are different types of errors or scenarios that we would ideally like to avoid. However, the decision of what type of analysis to do may involve a tradeoff where one decides that it is more important to avoid either falsely concluding that anthropogenic forcing *has* contributed, or to avoid falsely concluding that anthropogenic forcing had *not* made a detectable contribution to the event. Since there is no correct answer that can apply in all cases, it would be helpful if, in requesting scientific assessments, policymakers provide some guidance about which type of error or scenario they would most desire be avoided in the analyses and assessments in question.

Since substantial anthropogenic climate change (increased surface temperatures, increased atmospheric water vapor, etc.) has already occurred, aren't all extreme events affected to some degree by anthropogenic climate change?

Climate scientists are aware from modeling experiments that very tiny changes to initial conditions in model simulations lead to very different realizations of internal climate variability “noise” in the model simulations. Comparing large samples of this random background noise from models against observed changes is one way to test whether the observed changes are statistically distinguishable from internal climate variability. In any case, this experience also teaches us that any anthropogenic influence on climate, no matter how tiny, has some effect on the future trajectory of climate variability, and thus could affect the timing and occurrence of extreme events. More meaningful questions are: 1) Has anthropogenic forcing produced a statistically significant change in the probability of occurrence of some class of extreme event? 2) Can we determine with confidence the net sign of influence of anthropogenic climate change on the frequency, intensity, etc., of a type of extreme event? 3) Can climate scientists quantify (with credible confidence intervals) the effect of climate change on the occurrence frequency, the intensity, or some other aspect of an observed extreme event?



Box C.2 Illustration of Ingredients-based Event Attribution: The Case of Hurricane Sandy

To illustrate some aspects of the conditional or ingredients-based attribution approach, the case of Hurricane Sandy can be considered. If one considers Hurricane Sandy's surge event, there is strong evidence that sea level rise, at least partly anthropogenic in origin (see Ch. 12: Sea Level Rise), made Sandy's surge event worse, all other factors being equal.³⁴ The related question of whether anthropogenic climate change increased the risk of an event like Sandy involves not just the sea level ingredient to surge risk but also whether the frequency and/or intensity of Sandy-like storms has increased or decreased as a result of anthropogenic climate change. This latter question is more difficult and is briefly reviewed here.

A conditional or ingredients-based attribution approach, as applied to a hurricane event such as Sandy, may assume that the weather patterns in which the storm was embedded—and the storm itself—could have occurred in a preindustrial climate, and the event is re-simulated while changing only some aspects of the large-scale environment (for example, sea surface temperatures, atmospheric temperatures, and moisture) by an estimated anthropogenic climate change signal. Such an approach thus explores whether anthropogenic climate change to date has, for example, altered the intensity of a Hurricane Sandy-like storm, assuming the occurrence of a Sandy-like storm in both preindustrial and present-day climates. Modeling studies show, as expected, that the anomalously warm sea surface temperatures off the U.S. East Coast during Sandy led to a substantially more intense simulated storm than under present-day climatological conditions.³⁵ However, these anomalous sea surface temperatures and other environmental changes are a mixture of anthropogenic and natural influences, and so it is not generally possible to infer the anthropogenic component from such experiments. Another study³⁶ modeled the influence of just the anthropogenic changes to the thermodynamic environment (including sea surface temperatures, atmospheric temperatures, and moisture perturbations) and concluded that anthropogenic climate change to date had caused Hurricane Sandy to be about 5 hPa more intense, but that this modeled change was not statistically significant at the 95% confidence level. A third study used a statistical–dynamical model to compare simulated New York City-area tropical cyclones in pre-anthropogenic and anthropogenic time periods.³⁴ It concluded that there have been anthropogenically induced increases in the types of tropical cyclones that cause extreme surge events in the region, apart from the effects of sea level rise, such as increased radius of maximum winds in the anthropogenic era. However, the statistical–dynamical model used in the study simulates an unusually large increase in global tropical cyclone activity in 21st century projections³⁷ compared to other tropical cyclone modeling studies using dynamical models—a number of which simulate future decreases in late 21st century tropical storm frequency in the Atlantic basin (e.g., Christensen et al. 2013³⁸). This range of uncertainty among various model simulations of Atlantic tropical cyclone activity under climate change imply that there is low confidence in determining the net impact to date of anthropogenic climate change on the risk of Sandy-like events, though anthropogenic sea level rise, all other things equal, has increased the surge risk.

In summary, while there is agreement that sea level rise alone has caused greater storm surge risk in the New York City area, there is low confidence on whether a number of other important determinants of storm surge climate risk, such as the frequency, size, or intensity of Sandy-like storms in the New York region, have increased or decreased due to anthropogenic warming to date.



REFERENCES

1. Hegerl, G.C., O. Hoegh-Guldberg, G. Casassa, M.P. Hoerling, R.S. Kovats, C. Parmesan, D.W. Pierce, and P.A. Stott, 2010: Good practice guidance paper on detection and attribution related to anthropogenic climate change. *Meeting Report of the Intergovernmental Panel on Climate Change Expert Meeting on Detection and Attribution of Anthropogenic Climate Change*. Stocker, T.F., C.B. Field, D. Qin, V. Barros, G.-K. Plattner, M. Tignor, P.M. Midgley, and K.L. Ebi, Eds. IPCC Working Group I Technical Support Unit, University of Bern, Bern, Switzerland, 1-8. http://www.ipcc.ch/pdf/supporting-material/ipcc_good_practice_guidance_paper_anthropogenic.pdf
2. Bindoff, N.L., P.A. Stott, K.M. AchutaRao, M.R. Allen, N. Gillett, D. Gutzler, K. Hansingo, G. Hegerl, Y. Hu, S. Jain, I.I. Mokhov, J. Overland, J. Perlwitz, R. Sebbari, and X. Zhang, 2013: Detection and attribution of climate change: From global to regional. *Climate Change 2013: The Physical Science Basis. Contribution of Working Group I to the Fifth Assessment Report of the Intergovernmental Panel on Climate Change*. Stocker, T.F., D. Qin, G.-K. Plattner, M. Tignor, S.K. Allen, J. Boschung, A. Nauels, Y. Xia, V. Bex, and P.M. Midgley, Eds. Cambridge University Press, Cambridge, United Kingdom and New York, NY, USA, 867-952. <http://www.climatechange2013.org/report/full-report/>
3. Hasselmann, K., 1997: Multi-pattern fingerprint method for detection and attribution of climate change. *Climate Dynamics*, **13**, 601-611. <http://dx.doi.org/10.1007/s003820050185>
4. Allen, M.R. and P.A. Stott, 2003: Estimating signal amplitudes in optimal fingerprinting, Part I: Theory. *Climate Dynamics*, **21**, 477-491. <http://dx.doi.org/10.1007/s00382-003-0313-9>
5. Hegerl, G.C., F.W. Zwiers, P. Braconnot, N.P. Gillett, Y. Luo, J.A.M. Orsini, N. Nicholls, J.E. Penner, and P.A. Stott, 2007: Understanding and attributing climate change. *Climate Change 2007: The Physical Science Basis. Contribution of Working Group I to the Fourth Assessment Report of the Intergovernmental Panel on Climate Change*. Solomon, S., D. Qin, M. Manning, Z. Chen, M. Marquis, K.B. Averyt, M. Tignor, and H.L. Miller, Eds. Cambridge University Press, Cambridge, United Kingdom and New York, NY, USA, 663-745. http://www.ipcc.ch/publications_and_data/ar4/wg1/en/ch9.html
6. Hegerl, G. and F. Zwiers, 2011: Use of models in detection and attribution of climate change. *Wiley Interdisciplinary Reviews: Climate Change*, **2**, 570-591. <http://dx.doi.org/10.1002/wcc.121>
7. Zwiers, F.W., X.B. Zhang, and Y. Feng, 2011: Anthropogenic influence on long return period daily temperature extremes at regional scales. *Journal of Climate*, **24**, 881-892. <http://dx.doi.org/10.1175/2010jcli3908.1>
8. Ribes, A., F.W. Zwiers, J.-M. Azais, and P. Naveau, 2017: A new statistical approach to climate change detection and attribution. *Climate Dynamics*, **48**, 367-386. <http://dx.doi.org/10.1007/s00382-016-3079-6>
9. Hannart, A., 2016: Integrated optimal fingerprinting: Method description and illustration. *Journal of Climate*, **29**, 1977-1998. <http://dx.doi.org/10.1175/jcli-d-14-00124.1>
10. Knutson, T.R., F. Zeng, and A.T. Wittenberg, 2013: Multimodel assessment of regional surface temperature trends: CMIP3 and CMIP5 twentieth-century simulations. *Journal of Climate*, **26**, 8709-8743. <http://dx.doi.org/10.1175/JCLI-D-12-00567.1>
11. van Oldenborgh, G.J., F.J. Doblas Reyes, S.S. Drijfhout, and E. Hawkins, 2013: Reliability of regional climate model trends. *Environmental Research Letters*, **8**, 014055. <http://dx.doi.org/10.1088/1748-9326/8/1/014055>
12. DelSole, T., M.K. Tippett, and J. Shukla, 2011: A significant component of unforced multidecadal variability in the recent acceleration of global warming. *Journal of Climate*, **24**, 909-926. <http://dx.doi.org/10.1175/2010jcli3659.1>
13. van den Dool, H., J. Huang, and Y. Fan, 2003: Performance and analysis of the constructed analogue method applied to U.S. soil moisture over 1981-2001. *Journal of Geophysical Research*, **108**, 8617. <http://dx.doi.org/10.1029/2002JD003114>
14. Deser, C., L. Terray, and A.S. Phillips, 2016: Forced and internal components of winter air temperature trends over North America during the past 50 years: Mechanisms and implications. *Journal of Climate*, **29**, 2237-2258. <http://dx.doi.org/10.1175/JCLI-D-15-0304.1>
15. Mahlstein, I., R. Knutti, S. Solomon, and R.W. Portmann, 2011: Early onset of significant local warming in low latitude countries. *Environmental Research Letters*, **6**, 034009. <http://dx.doi.org/10.1088/1748-9326/6/3/034009>
16. Deser, C., R. Knutti, S. Solomon, and A.S. Phillips, 2012: Communication of the role of natural variability in future North American climate. *Nature Climate Change*, **2**, 775-779. <http://dx.doi.org/10.1038/nclimate1562>
17. Canty, T., N.R. Mascioli, M.D. Smarte, and R.J. Salawitch, 2013: An empirical model of global climate - Part 1: A critical evaluation of volcanic cooling. *Atmospheric Chemistry and Physics*, **13**, 3997-4031. <http://dx.doi.org/10.5194/acp-13-3997-2013>
18. Stern, D.I. and R.K. Kaufmann, 2014: Anthropogenic and natural causes of climate change. *Climatic Change*, **122**, 257-269. <http://dx.doi.org/10.1007/s10584-013-1007-x>



19. Mao, Y., B. Nijssen, and D.P. Lettenmaier, 2015: Is climate change implicated in the 2013–2014 California drought? A hydrologic perspective. *Geophysical Research Letters*, **42**, 2805–2813. <http://dx.doi.org/10.1002/2015GL063456>
20. Williams, A.P., R. Seager, J.T. Abatzoglou, B.I. Cook, J.E. Smerdon, and E.R. Cook, 2015: Contribution of anthropogenic warming to California drought during 2012–2014. *Geophysical Research Letters*, **42**, 6819–6828. <http://dx.doi.org/10.1002/2015GL064924>
21. Murakami, H., G.A. Vecchi, T.L. Delworth, K. Paffendorf, L. Jia, R. Gudgel, and F. Zeng, 2015: Investigating the influence of anthropogenic forcing and natural variability on the 2014 Hawaiian hurricane season [in “Explaining Extreme Events of 2014 from a Climate Perspective”]. *Bulletin of the American Meteorological Society*, **96** (12), S115–S119. <http://dx.doi.org/10.1175/BAMS-D-15-00119.1>
22. Anderegg, W.R.L., E.S. Callaway, M.T. Boykoff, G. Yohe, and T.y.L. Root, 2014: Awareness of both type 1 and 2 errors in climate science and assessment. *Bulletin of the American Meteorological Society*, **95**, 1445–1451. <http://dx.doi.org/10.1175/BAMS-D-13-00115.1>
23. Melillo, J.M., T.C. Richmond, and G.W. Yohe, eds., 2014: *Climate Change Impacts in the United States: The Third National Climate Assessment*. U.S. Global Change Research Program: Washington, D.C., 841 pp. <http://dx.doi.org/10.7930/J0Z31WJ2>
24. NAS, 2016: *Attribution of Extreme Weather Events in the Context of Climate Change*. The National Academies Press, Washington, DC, 186 pp. <http://dx.doi.org/10.17226/21852>
25. Stott, P., 2016: How climate change affects extreme weather events. *Science*, **352**, 1517–1518. <http://dx.doi.org/10.1126/science.aaf7271>
26. Easterling, D.R., K.E. Kunkel, M.F. Wehner, and L. Sun, 2016: Detection and attribution of climate extremes in the observed record. *Weather and Climate Extremes*, **11**, 17–27. <http://dx.doi.org/10.1016/j.wace.2016.01.001>
27. Hulme, M., 2014: Attributing weather extremes to ‘climate change’. *Progress in Physical Geography*, **38**, 499–511. <http://dx.doi.org/10.1177/0309133314538644>
28. Stott, P.A., D.A. Stone, and M.R. Allen, 2004: Human contribution to the European heatwave of 2003. *Nature*, **432**, 610–614. <http://dx.doi.org/10.1038/nature03089>
29. Hannart, A., J. Pearl, F.E.L. Otto, P. Naveau, and M. Ghil, 2016: Causal counterfactual theory for the attribution of weather and climate-related events. *Bulletin of the American Meteorological Society*, **97**, 99–110. <http://dx.doi.org/10.1175/bams-d-14-00034.1>
30. Horton, R.M., J.S. Mankin, C. Lesk, E. Coffel, and C. Raymond, 2016: A review of recent advances in research on extreme heat events. *Current Climate Change Reports*, **2**, 242–259. <http://dx.doi.org/10.1007/s40641-016-0042-x>
31. Shepherd, T.G., 2016: A common framework for approaches to extreme event attribution. *Current Climate Change Reports*, **2**, 28–38. <http://dx.doi.org/10.1007/s40641-016-0033-y>
32. Trenberth, K.E., J.T. Fasullo, and T.G. Shepherd, 2015: Attribution of climate extreme events. *Nature Climate Change*, **5**, 725–730. <http://dx.doi.org/10.1038/nclimate2657>
33. Hannart, A., A. Carrassi, M. Bocquet, M. Ghil, P. Naveau, M. Pulido, J. Ruiz, and P. Tandeo, 2016: DADA: Data assimilation for the detection and attribution of weather and climate-related events. *Climate Change*, **136**, 155–174. <http://dx.doi.org/10.1007/s10584-016-1595-3>
34. Reed, A.J., M.E. Mann, K.A. Emanuel, N. Lin, B.P. Horton, A.C. Kemp, and J.P. Donnelly, 2015: Increased threat of tropical cyclones and coastal flooding to New York City during the anthropogenic era. *Proceedings of the National Academy of Sciences*, **112**, 12610–12615. <http://dx.doi.org/10.1073/pnas.1513127112>
35. Magnusson, L., J.-R. Bidlot, S.T.K. Lang, A. Thorpe, N. Wedi, and M. Yamaguchi, 2014: Evaluation of medium-range forecasts for Hurricane Sandy. *Monthly Weather Review*, **142**, 1962–1981. <http://dx.doi.org/10.1175/mwr-d-13-00228.1>
36. Lackmann, G.M., 2015: Hurricane Sandy before 1900 and after 2100. *Bulletin of the American Meteorological Society*, **96** (12), 547–560. <http://dx.doi.org/10.1175/BAMS-D-14-00123.1>
37. Emanuel, K.A., 2013: Downscaling CMIP5 climate models shows increased tropical cyclone activity over the 21st century. *Proceedings of the National Academy of Sciences*, **110**, 12219–12224. <http://dx.doi.org/10.1073/pnas.1301293110>
38. Christensen, J.H., K. Krishna Kumar, E. Aldrian, S.-I. An, I.F.A. Cavalcanti, M. de Castro, W. Dong, P. Goswami, A. Hall, J.K. Kanyanga, A. Kitoh, J. Kosin, N.-C. Lau, J. Renwick, D.B. Stephenson, S.-P. Xie, and T. Zhou, 2013: Climate phenomena and their relevance for future regional climate change. *Climate Change 2013: The Physical Science Basis. Contribution of Working Group I to the Fifth Assessment Report of the Intergovernmental Panel on Climate Change*. Stocker, T.F., D. Qin, G.-K. Plattner, M. Tignor, S.K. Allen, J. Boschung, A. Nauels, Y. Xia, V. Bex, and P.M. Midgley, Eds. Cambridge University Press, Cambridge, United Kingdom and New York, NY, USA, 1217–1308. <http://www.climatechange2013.org/report/full-report/>





Appendix D

Acronyms and Units

doi: 10.7930/J0ZC811D

AGCM	atmospheric general circulation model
AIS	Antarctic Ice Sheet
AMO	Atlantic Multidecadal Oscillation
AMOC	Atlantic meridional overturning circulation
AMSU	Advanced Microwave Sounding Unit
AO	Arctic Oscillation
AOD	aerosol optical depth
AR	atmospheric river
AW	Atlantic Water
BAMS	Bulletin of the American Meteorological Society
BC	black carbon
BCE	Before Common Era
CAM5	Community Atmospheric Model, Version 5
CAPE	convective available potential energy
CCN	cloud condensation nuclei
CCSM3	Community Climate System Model, Version 3
CDR	carbon dioxide removal
CE	Common Era
CENRS	Committee on Environment, Natural Resources, and Sustainability (National Science and Technology Council, White House)



CESM-LE	Community Earth System Model Large Ensemble Project
CFCs	chlorofluorocarbons
CI	climate intervention
CMIP5	Coupled Model Intercomparison Project, Fifth Phase (also CMIP3 and CMIP6)
CONUS	contiguous United States
CP	Central Pacific
CSSR	Climate Science Special Report
DIC	dissolved inorganic carbon
DJF	December-January-February
DoD SERDP	U.S. Department of Defense, Strategic Environmental Research and Development Program
DOE	U.S. Department of Energy
EAIS	East Antarctic Ice Sheet
ECS	equilibrium climate sensitivity
ENSO	El Niño–Southern Oscillation
EOF analysis	empirical orthogonal function analysis
EP	Eastern Pacific
ERF	effective radiative forcing
ESD	empirical statistical downscaling
ESDM	empirical statistical downscaling model
ESM	Earth System Model
ESS	Earth system sensitivity
ETC	extratropical cyclone
ETCCDI	Expert Team on Climate Change Detection Indices
GBI	Greenland Blocking Index



GCIS	Global Change Information System
GCM	global climate model
GeoMIP	Geoengineering Model Intercomparison Project
GFDL HiRAM	Geophysical Fluid Dynamics Laboratory, global High Resolution Atmospheric Model (NOAA)
GHCN	Global Historical Climatology Network (National Centers for Environmental Information, NOAA)
GHG	greenhouse gas
GMSL	global mean sea level
GMT	global mean temperature
GPS	global positioning system
GRACE	Gravity Recovery and Climate Experiment
GrIS	Greenland Ice Sheet
GWP	global warming potential
HadCM3	Hadley Centre Coupled Model, Version 3
HadCRUT4	Hadley Centre Climatic Research Unit Gridded Surface Temperature Dataset 4
HCFCs	hydrochlorofluorocarbons
HFCs	hydrofluorocarbons
HOT	Hawai'i Ocean Time-series
HOT-DOGS	Hawai'i Ocean Time-series Data Organization & Graphical System
HURDAT2	revised Atlantic Hurricane Database (National Hurricane Center, NOAA)
IAM	integrated assessment model
IAV	impacts, adaptation, and vulnerability
INMCM	Institute for Numerical Mathematics Climate Model
IPCC	Intergovernmental Panel on Climate Change



IPCC AR5	Fifth Assessment Report of the IPCC; also SPM – Summary for Policymakers, and WG1, WG2, WG3 – Working Groups 1–3
IPO	Interdecadal Pacific Oscillation
IVT	integrated vapor transport
JGOFS	U.S. Joint Global Ocean Flux Study
JJA	June-July-August
JTWC	Joint Typhoon Warning Center
LCC	land-cover changes
LULCC	land-use and land-cover change
MAM	March-April-May
MSU	Microwave Sounding Unit
NAM	Northern Annular Mode
NAO	North Atlantic Oscillation
NARCCAP	North American Regional Climate Change Assessment Program (World Meteorological Organization)
NAS	National Academy of Sciences
NASA	National Aeronautics and Space Administration
NCA	National Climate Assessment
NCA3	Third National Climate Assessment
NCA4	Fourth National Climate Assessment
NCEI	National Centers for Environmental Information (NOAA)
NDC	nationally determined contribution
NOAA	National Oceanic and Atmospheric Administration
NPI	North Pacific Index
NPO	North Pacific oscillation



NPP	net primary production
OMZs	oxygen minimum zones
OSTP	Office of Science and Technology Policy (White House)
PCA	principle component analysis
PDO	Pacific Decadal Oscillation
PDSI	Palmer Drought Severity Index
PETM	Paleo-Eocene Thermal Maximum
PFCs	perfluorocarbons
PGW	pseudo-global warming
PNA	Pacific North American Pattern
RCM	regional climate models
RCP	Representative Concentration Pathway
RF	radiative forcing
RF_{aci}	aerosol–cloud interaction (effect on RF)
RF_{ari}	aerosol–radiation interaction (effect on RF)
RMSE	root mean square error
RSL	relative sea level
RSS	remote sensing systems
S06	surface-to-6 km layer
SCE	snow cover extent
SGCR	Subcommittee on Global Change Research (National Science and Technology Council, White House)
SLCF	short-lived climate forcer
SLCP	short-lived climate pollutant
SLR	sea level rise



SOC	soil organic carbon
SRES	IPCC Special Report on Emissions Scenarios
SREX	IPCC Special Report on Managing the Risks of Extreme Events and Disasters to Advance Climate Change Adaptation
SRM	solar radiation management
SSC	Science Steering Committee
SSI	solar spectral irradiance
SSP	Shared Socioeconomic Pathway
SST	sea surface temperature
STAR	Center for Satellite Applications and Research (NOAA)
SWCRE	shortwave cloud radiative effect (on radiative fluxes)
LWCRE	longwave cloud radiative effect (on radiative fluxes)
TA	total alkalinity
TC	tropical cyclone
TCR	transient climate response
TCRE	transient climate response to cumulative carbon emissions
TOPEX/JASON1,2	Topography Experiment/Joint Altimetry Satellite Oceanography Network satellites (NASA)
TSI	total solar irradiance
TTT	temperature total troposphere
UAH	University of Alabama, Huntsville
UHI	urban heat island (effect)
UNFCCC	United Nations Framework Convention on Climate Change
USGCRP	U.S. Global Change Research Program
USGS	U.S. Geological Survey



UV	ultraviolet
VOCs	volatile organic compounds
WAIS	West Antarctic Ice Sheet
WCRP	World Climate Research Programme
WMGHG	well-mixed greenhouse gas
WOCE	World Ocean Circulation Experiment (JGOFS)

Abbreviations and Units

C	carbon
CO	carbon monoxide
CH₄	methane
cm	centimeters
CO₂	carbon dioxide
°C	degrees Celsius
°F	degrees Fahrenheit
GtC	gigatonnes of carbon
hPA	hectopascal
H₂S	hydrogen sulfide
H₂SO₄	sulfuric acid
km	kilometers
m	meters
mm	millimeters
Mt	megaton
µatm	microatmosphere
N	nitrogen



N₂O	nitrous oxide
NO_x	nitrogen oxides
O₂	molecular oxygen
O₃	ozone
OH	hydroxyl radical
PgC	petagrams of carbon
ppb	parts per billion
ppm	parts per million
SF₆	sulfur hexafluoride
SO₂	sulfur dioxide
TgC	teragrams of carbon
W/m²	Watts per meter squared





Appendix E

Glossary Terms

doi: 10.7930/J0TM789P

Abrupt climate change

Change in the climate system on a timescale shorter than the timescale of the responsible forcing. In the case of anthropogenic forcing over the past century, abrupt change occurs over decades or less. Abrupt change need not be externally forced. (*CSSR, Ch. 15*)

Aerosol–cloud interaction

A process by which a perturbation to aerosol affects the microphysical properties and evolution of clouds through the aerosol role as cloud condensation nuclei or ice nuclei, particularly in ways that affect radiation or precipitation; such processes can also include the effect of clouds and precipitation on aerosol. The aerosol perturbation can be anthropogenic or come from some natural source. The radiative forcing from such interactions has traditionally been attributed to numerous indirect aerosol effects, but in this report, only two levels of radiative forcing (or effect) are distinguished:

The radiative forcing (or effect) due to aerosol–cloud interactions (**RF_{aci}**) is the radiative forcing (or radiative effect, if the perturbation is internally generated) due to the change in number or size distribution of cloud droplets or ice crystals that is the proximate result of an aerosol perturbation, with other variables (in particular total cloud water content) remaining equal. In liquid clouds, an increase in cloud droplet concentration and surface area would increase the cloud albedo. This effect is also known as the cloud albedo effect, first indirect effect, or Twomey effect. It is a largely theoretical concept that cannot readily be isolated in observations or comprehensive process models due to the rapidity and ubiquity of rapid adjustments. This is contrasted with the effective radiative forcing (or effect) due to aerosol–cloud interactions (**ERF_{aci}**)

The total effective radiative forcing due to both aerosol–cloud and aerosol–radiation interactions is denoted aerosol effective radiative forcing (**ERF_{aci+ari}**). See also **aerosol–radiation interaction**. (condensed from IPCC AR5 WGI Annex III: Glossary)

Aerosol–radiation interaction (RF_{ari})

The radiative forcing (or radiative effect, if the perturbation is internally generated) of an aerosol perturbation due directly to aerosol–radiation interactions, with all environmental variables remaining unaffected. It is traditionally known in the literature as the *direct aerosol forcing* (or *effect*).

The total effective radiative forcing due to both aerosol–cloud and aerosol–radiation interactions is denoted aerosol effective radiative forcing (**ERF_{aci+ari}**). See also **aerosol–cloud interaction**. (condensed from IPCC AR5 WGI Annex III: Glossary)

Agricultural drought

See **drought**.

Albedo

The fraction of solar radiation reflected by a surface or object, often expressed as a percentage. Snow-covered surfaces have a high albedo, the albedo of soils ranges from high to low, and vegetation-covered surfaces and oceans have a low albedo. The Earth’s planetary albedo varies mainly through varying cloudiness, snow, ice, leaf area, and land-cover changes. (IPCC AR5 WGI Annex III: Glossary)

Altimetry

A technique for measuring the height of the Earth’s surface with respect to the geocenter of the Earth within a defined terrestrial reference



frame (geocentric sea level). (IPCC AR5 WGI Annex III: Glossary)

Anticyclonic circulation

Fluid motion having a sense of rotation about the local vertical opposite to that of the earth's rotation; that is, clockwise in the Northern Hemisphere, counterclockwise in the Southern Hemisphere, and undefined at the equator. It is the opposite of **cyclonic circulation**. (AMS glossary).

Atlantic meridional overturning circulation (AMOC)

See **Meridional overturning circulation (MOC)**.

Atmospheric blocking

See **Blocking**.

Atmospheric river

A long, narrow, and transient corridor of strong horizontal water vapor transport that is typically associated with a low-level jet stream ahead of the cold front of an extratropical cyclone. The water vapor in atmospheric rivers is supplied by tropical and/or extratropical moisture sources. Atmospheric rivers frequently lead to heavy precipitation where they are forced upward—for example, by mountains or by ascent in the warm conveyor belt. Horizontal water vapor transport in the midlatitudes occurs primarily in atmospheric rivers and is focused in the lower troposphere. (AMS glossary).

Baroclinicity

The state of stratification in a fluid in which surfaces of constant pressure (isobaric) intersect surfaces of constant density (isosteric). (AMS glossary).

Bias correction method

One of two main statistical approaches used to alleviate the limitations of global and regional climate models, in which the statistics of the simulated model outputs are adjusted to those of the observation data. (The other approach is **empirical/stochastic downscaling**, described under **downscaling**). The rescaled variables can remove the effects of systematic errors in climate model outputs. (derived from Kim et al., 2015)

Biological pump

The suite of biologically mediated processes responsible for transporting carbon against a concentration gradient from the upper ocean to the deep ocean. (Passow and Carlson, 2012)

Blocking

Associated with persistent, slow-moving high pressure systems that obstruct the prevailing westerly winds in the middle and high latitudes and the normal eastward progress of extratropical transient storm systems. It is an important component of the intraseasonal climate variability in the extratropics and can cause long-lived weather conditions such as cold spells in winter and heat waves in summer. (IPCC AR5 WGI Annex III: Glossary)

Carbon dioxide fertilization

The enhancement of the growth of plants as a result of increased atmospheric CO₂ concentration. (IPCC AR5 WGI Annex III: Glossary)

Carbon dioxide removal

A set of techniques that aim to remove CO₂ directly from the atmosphere by either (1) increasing natural sinks for carbon or (2) using chemical engineering to remove the CO₂, with the intent of reducing the atmospheric CO₂ concentration. CDR methods involve the ocean, land and technical systems, including such methods as iron fertilization, large-scale afforestation and direct capture of CO₂ from the atmosphere using engineered chemical means. (truncated version from IPCC AR5 WGI Annex III: Glossary)

Climate engineering

See **geoengineering**.

Climate intervention

See **geoengineering**.

Climate sensitivity

In Intergovernmental Panel on Climate Change (IPCC) reports, **equilibrium climate sensitivity** (units: °C) refers to the equilibrium (steady state) change in the annual global mean surface temperature following a doubling of the atmospheric equivalent carbon dioxide concentration. The **effective climate sensitivity** (units: °C) is an estimate of the global mean surface temperature re-



sponse to doubled carbon dioxide concentration that is evaluated from model output or observations for evolving non-equilibrium conditions. It is a measure of the strengths of the climate feedbacks at a particular time and may vary with forcing history and climate state, and therefore may differ from equilibrium climate sensitivity. The **transient climate response** (units: °C) is the change in the global mean surface temperature, averaged over a 20-year period centered at the time of atmospheric carbon dioxide doubling, in a climate model simulation in which CO₂ increases at 1% per year. It is a measure of the strength and rapidity of the surface temperature response to greenhouse gas forcing. (IPCC AR5 WGI Annex III: Glossary)

Cloud radiative effect

The radiative effect of clouds relative to the identical situation without clouds (previously called cloud radiative forcing). (drawn from IPCC AR5 WGI Annex III: Glossary)

Clouds can act as a greenhouse ingredient to warm the Earth by trapping outgoing long-wave infrared radiative flux at the top of the atmosphere (the **longwave cloud radiative effect [LWCRE]**). Clouds can also enhance the planetary albedo by reflecting shortwave solar radiative flux back to space to cool the Earth (the **shortwave cloud radiative effect [SWCRE]**). The net effect of the two competing processes depends on the height, type, and the optical properties of the clouds. (edited from NOAA, Geophysical Fluid Dynamics Laboratory)

CMIP

The Coupled Model Intercomparison Project is a standard experimental protocol for studying the output of coupled atmosphere–ocean general circulation models (AOGCMs). Phases three and five (CMIP3 and CMIP5, respectively) coordinated and archived climate model simulations based on shared model inputs by modeling groups from around the world. The CMIP3 multi-model data set includes projections using the SRES scenarios drawn from the Intergovernmental Panel on Climate Change’s Special Report on Emissions Scenarios. The CMIP5 dataset includes projections using the **Representative**

Concentration Pathways. (edited from IPCC AR5 WGII Annex II: Glossary).

Compound event

An event that consists of 1) two or more extreme events occurring simultaneously or successively, 2) combinations of extreme events with underlying conditions that amplify the impact of the events, or 3) combinations of events that are not themselves extremes but lead to an extreme event or impact when combined. The contributing events can be of similar or different types. (CSSR, Ch. 15, drawing upon SREX 3.1.3)

Critical threshold

A threshold that arises within a system as a result of the amplifying effects of positive **feedbacks**. The crossing of a critical threshold commits the system to a change in state. (CSSR, Ch. 15)

Cryosphere

All regions on and beneath the surface of the Earth and ocean where water is in solid form, including sea ice, lake ice, river ice, snow cover, glaciers and ice sheets, and frozen ground (which includes permafrost). (IPCC AR5 WGI Annex III: Glossary)

Cyclonic circulation

Fluid motion in the same sense as that of the earth, that is, counterclockwise in the Northern Hemisphere, clockwise in the Southern Hemisphere, undefined at the equator. (AMS glossary).

Denitrification

As used in this report, refers to the loss of fixed nitrogen in the ocean through biogeochemical processes. (CSSR, Ch. 13).

Deoxygenation

See **hypoxia**.

Downscaling

A method that derives local- to regional-scale (10–100 km) information from larger-scale models or data analyses. Two main methods exist. **Dynamical downscaling** uses the output of regional climate models, global models with variable spatial resolution, or high-resolution global models. **Empirical/statistical downscaling**



ing methods develop statistical relationships that link the large-scale atmospheric variables with local/regional climate variables. In all cases, the quality of the driving model remains an important limitation on the quality of the downscaled information. (IPCC AR5 WGI Annex III: Glossary)

Drought

A period of abnormally dry weather long enough to cause a serious hydrological imbalance. Drought is a relative term; therefore, any discussion in terms of precipitation deficit must refer to the particular precipitation-related activity that is under discussion. For example, shortage of precipitation during the growing season impinges on crop production or ecosystem function in general (due to soil moisture drought, also termed **agricultural drought**), and during the runoff and percolation season primarily affects water supplies (**hydrological drought**). Storage changes in soil moisture and groundwater are also affected by increases in actual evapotranspiration in addition to reductions in precipitation. A period with an abnormal precipitation deficit is defined as a **meteorological drought**. (IPCC AR5 WGI Annex III: Glossary)

Dynamical downscaling

See **downscaling**.

Earth System Model

A coupled atmosphere–ocean general circulation model in which a representation of the carbon cycle is included, allowing for interactive calculation of atmospheric CO₂ or compatible emissions. Additional components (for example, atmospheric chemistry, ice sheets, dynamic vegetation, nitrogen cycle, but also urban or crop models) may be included. (IPCC AR5 WGI Annex III: Glossary)

Effective radiative forcing

See **radiative forcing**.

El Niño–Southern Oscillation

A natural variability in ocean water surface pressure that causes periodic changes in ocean surface temperatures in the tropical Pacific Ocean. El Niño–Southern Oscillation (ENSO)

has two phases: the warm oceanic phase, El Niño, accompanies high air surface pressure in the western Pacific, while the cold phase, La Niña, accompanies low air surface pressure in the western Pacific. Each phase generally lasts for 6 to 18 months. ENSO events occur irregularly, roughly every 3 to 7 years. The extremes of this climate pattern’s oscillations cause extreme weather (such as floods and droughts) in many regions of the world. (USGCRP)

Empirical/statistical downscaling

See **downscaling**.

Equivalent carbon dioxide concentration

The concentration of carbon dioxide that would cause the same radiative forcing as a given mixture of carbon dioxide and other forcing components. Those values may consider only greenhouse gases, or a combination of greenhouse gases and aerosols. Equivalent carbon dioxide concentration is a metric for comparing radiative forcing of a mix of different greenhouse gases at a particular time but does not imply equivalence of the corresponding climate change responses nor future forcing. There is generally no connection between equivalent carbon dioxide emissions and resulting equivalent carbon dioxide concentrations. (IPCC AR5 WGI Annex III: Glossary)

Eutrophication

Over-enrichment of water by nutrients such as nitrogen and phosphorus. It is one of the leading causes of water quality impairment. The two most acute symptoms of eutrophication are **hypoxia** (a state of oxygen depletion) and harmful algal blooms. (IPCC AR5 WGII Annex II: Glossary).

Extratropical cyclone

A large-scale (of order 1,000 km) storm in the middle or high latitudes having low central pressure and fronts with strong horizontal gradients in temperature and humidity. A major cause of extreme wind speeds and heavy precipitation especially in wintertime. (IPCC AR5 WGI Annex III: Glossary)



Feedbacks

An interaction between processes in the climate system, in which the result of an initial process triggers changes in a second process that in turn influences the initial one. A **positive feedback** magnifies the original process, while a **negative feedback** attenuates or diminishes it. Positive feedbacks are sometimes referred to as “vicious” or “virtuous” cycles, depending on whether their effects are viewed as harmful or beneficial. (CSSR, Ch. 15)

Geoengineering

A broad set of methods and technologies that aim to deliberately alter the climate system in order to alleviate the impacts of climate change (also known as **climate intervention** (National Academy of Sciences) or climate engineering). Most, but not all, methods seek to either 1) reduce the amount of absorbed solar energy in the climate system (**Solar Radiation Management**) or 2) increase net carbon sinks from the atmosphere at a scale sufficiently large to alter climate (**Carbon Dioxide Removal**). Scale and intent are of central importance. Two key characteristics of geoengineering methods of particular concern are that they use or affect the climate system (e.g., atmosphere, land, or ocean) globally or regionally and/or could have substantive unintended effects that cross national boundaries. (adapted from IPCC AR5 WGI Annex III: Glossary)

Glacial isostatic adjustment (GIA)

The deformation of the Earth and its gravity field due to the response of the earth–ocean system to changes in ice and associated water loads. It includes vertical and horizontal deformations of the Earth’s surface and changes in geoid due to the redistribution of mass during the ice–ocean mass exchange. GIA is currently contributing to relative sea level rise in much of the continental United States. (IPCC AR5 WGI Annex III: Glossary)

Glacier

A perennial mass of land ice that originates from compressed snow, shows evidence of past or present flow (through internal deformation and/or sliding at the base), and is constrained by internal stress and friction at the base and

sides. A glacier is maintained by accumulation of snow at high altitudes, balanced by melting at low altitudes and/or discharge into the sea.

An ice mass of the same origin as glaciers, but of continental size, is an **ice sheet**, defined further below. (IPCC AR5 WGI Annex III: Glossary)

Global mean sea level

The average of relative sea level or of sea surface height across the ocean.

Global warming potential (GWP)

An index, based on radiative properties of greenhouse gases, measuring the radiative forcing following a pulse emission of a unit mass of a given greenhouse gas in the present-day atmosphere integrated over a chosen time horizon, relative to that of carbon dioxide. The GWP represents the combined effect of the differing times these gases remain in the atmosphere and their relative effectiveness in causing radiative forcing. (truncated from IPCC AR5 WGI Annex III: Glossary)

Gravimetry

Measurement of the Earth’s gravitational field. Using satellite data from the Gravity Recovery and Climate Experiment (GRACE), measurements of the mean gravity field help scientists better understand the structure of the solid Earth and learn about ocean circulation. Monthly measurements of time-variable gravity can be used to study ground water fluctuations, sea ice, sea level rise, deep ocean currents, ocean bottom pressure, and ocean heat flux. (modified from *NASA Earth Observatory on the GRACE project*)

Greenhouse gas (GHG)

Greenhouse gases are those gaseous constituents of the atmosphere, both natural and anthropogenic, that absorb and emit radiation at specific wavelengths within the spectrum of terrestrial radiation emitted by the Earth’s surface, the atmosphere itself, and by clouds. This property causes the greenhouse effect. Water vapor (H₂O), carbon dioxide (CO₂), nitrous oxide (N₂O), methane (CH₄), and ozone (O₃) are the primary greenhouse gases in the Earth’s atmosphere. Moreover, there are a number of entirely human-made greenhouse gases in the atmosphere, such as the halocarbons and other chlorine- and



bromine-containing substances, dealt with under the Montreal Protocol. Beside CO₂, N₂O, and CH₄, the Kyoto Protocol dealt with the greenhouse gases sulfur hexafluoride (SF₆), hydrofluorocarbons (HFCs), and perfluorocarbons (PFCs). (adapted from IPCC AR5 WGI Annex III: Glossary)

Hydrological drought

See **drought**.

Hypoxia

Deficiency of oxygen in water bodies, which can be a symptom of **eutrophication** (nutrient overloading). **Deoxygenation** (the process of removing oxygen) leads to hypoxia, and the expansion of **oxygen minimum zones** (IPCC AR5 WGII Annex II: Glossary supplemented with other sources).

Ice sheet

A mass of land ice of continental size that is sufficiently thick to cover most of the underlying bed, so that its shape is mainly determined by its dynamics (the flow of the ice as it deforms internally and/or slides at its base). An ice sheet flows outward from a high central ice plateau with a small average surface slope. The margins usually slope more steeply, and most ice is discharged through fast flowing ice streams or outlet glaciers, in some cases into the sea or into ice shelves floating on the sea. There are only two ice sheets in the modern world, one on Greenland and one on Antarctica. During glacial periods there were others, including the Laurentide Ice Sheet in North America, whose loss is the primary driver of **glacial isostatic adjustment** in the United States today. (adapted from IPCC AR5 WGI Annex III: Glossary)

Ice wedge

Common features of the subsurface in permafrost regions, ice wedges develop by repeated frost cracking and ice vein growth over hundreds to thousands of years. Ice wedge formation causes the archetypal polygonal patterns seen in tundra across the Arctic landscape. (adapted from Liljedal et al., 2016)

Instantaneous radiative forcing

See **radiative forcing**.

Irreversible

Changes in components of the climate system that either cannot be reversed, or can only be reversed on timescales much longer than the timescale over which the original forcing occurred. (*CSSR, Ch. 15*)

Longwave cloud radiative effect (LWCRE)

See **cloud radiative effect**.

Meridional overturning circulation (MOC)

Meridional (north-south) overturning circulation in the ocean quantified by zonal (east-west) sums of mass transports in depth or density layers. In the North Atlantic, away from the subpolar regions, the Atlantic MOC (AMOC, which is in principle an observable quantity) is often identified with the thermohaline circulation (THC), which is a conceptual and incomplete interpretation. It must be borne in mind that the AMOC is also driven by wind, and can also include shallower overturning cells such as occur in the upper ocean in the tropics and subtropics, in which warm (light) waters moving poleward are transformed to slightly denser waters and subducted equatorward at deeper levels. (adapted from IPCC AR5 WGI Annex III: Glossary)

Meridional temperature gradient

North-South temperature variation

Meteorological drought

See **drought**.

Mode water

Water of exceptionally uniform properties over an extensive depth range, caused in most instances by convection. Mode waters represent regions of water mass formation; they are not necessarily water masses in their own right but contribute significant volumes of water to other water masses. Because they represent regions of deep sinking of surface water, mode water formation regions are atmospheric heat sources. Subantarctic Mode Water is formed during winter in the subantarctic zone just north of the subantarctic front and contributes to the lower temperature range of central water; only in the extreme eastern Pacific Ocean does it obtain a temperature low enough to contribute to Antarctic Intermediate Water. Subtropical



Mode Water is mostly formed through enhanced subduction at selected locations of the subtropics and contributes to the upper temperature range of central water. Examples of Subtropical Mode Water are the 18°C water formed in the Sargasso Sea, Madeira Mode Water formed at the same temperature but in the vicinity of Madeira, and 13°C water formed not by surface processes but through mixing in Agulhas Current eddies as they enter the Benguela Current. (AMS glossary).

Model ability/model skill

Representativeness of the ability of a climate model to reproduce historical climate observational data.

Model bias

Systematic error in model output that over- or under-emphasizes particular model mechanism or results.

Model ensemble

Also known as a multimodel ensemble (MME), a group of several different global climate models (GCMs) used to create a large number of climate simulations. An MME is designed to address **structural model uncertainty** between different climate models, rather than **parametric uncertainty** within any one particular model. (UK Met Office, *Climate Projections*, Glossary)

Model independence

An analysis of the degree to which models are different from one another. Also is used as an interpretation of an ensemble as constituting independent samples of a distribution which represents our collective understanding of the climate system. (summarized based on Annan and Hargreaves, 2017)

Nationally determined contributions (NDCs)

See **Paris Agreement**.

Negative feedbacks

See **feedbacks**.

Nitrogen mineralization

Mineralization/remineralization is the conversion of an element from its organic form to an inorganic form as a result of microbial decom-

position. In nitrogen mineralization, organic nitrogen from decaying plant and animal residues (proteins, nucleic acids, amino sugars and urea) is converted to ammonia (NH₃) and ammonium (NH₄⁺) by biological activity. (IPCC AR5 WGI Annex III: Glossary)

Ocean acidification

The process by which ocean waters have become more acidic due to the absorption of human-produced carbon dioxide, which interacts with ocean water to form carbonic acid and lower the ocean's pH. Acidity reduces the capacity of key plankton species and shelled animals to form and maintain shells. (USGCRP)

Ocean stratification

The existence or formation of distinct layers or laminae in the ocean identified by differences in thermal or salinity characteristics (e.g., densities) or by oxygen or nutrient content. (adapted from AMS glossary).

Oxygen minimum zones (OMZs)

The midwater layer (200–1,000 m) in the open ocean in which oxygen saturation is the lowest in the ocean. The degree of oxygen depletion depends on the largely bacterial consumption of organic matter, and the distribution of the OMZs is influenced by large-scale ocean circulation. In coastal oceans, OMZs extend to the shelves and may also affect benthic ecosystems. OMZs can expand through a process of **deoxygenation**. (supplemented version of IPCC AR5 WGII Annex II: Glossary).

Pacific Decadal Oscillation

The pattern and time series of the first empirical orthogonal function of sea surface temperature over the North Pacific north of 20°N. The PDO broadened to cover the whole Pacific Basin is known as the Interdecadal Pacific Oscillation. The PDO and IPO exhibit similar temporal evolution. (IPCC AR5 WGI Annex III: Glossary)

Parameterization

In climate models, this term refers to the technique of representing processes that cannot be explicitly resolved at the spatial or temporal resolution of the model (sub-grid scale processes) by relationships between model-resolved



larger-scale variables and the area- or time-averaged effect of such subgrid scale processes. (IPCC AR5 WGI Annex III: Glossary)

Parametric uncertainty

See **uncertainty**.

Paris Agreement

An international climate agreement with the central aim to hold global temperature rise this century well below 2°C above preindustrial levels and to pursue efforts to limit the temperature increase even further to 1.5°C. For the first time, all parties are required to put forward emissions reductions targets, and to strengthen those efforts in the years ahead as the Agreement is assessed every five years. Each country's proposed mitigation target (the intended nationally determined contribution [INDC]) becomes an official **nationally determined contribution (NDC)** when the country ratifies the agreement. The Paris Agreement was finalized on December 12, 2015, at the 21st Conference of Parties (COP 21) of the United Nations Framework Convention on Climate Change (UNFCCC). "Paris" entered into force on November 4, 2016, after ratification by 55 countries that account for at least 55% of global emissions). The agreement had a total of 125 national parties by early 2017. (summarized/edited from UNFCCC)

Pattern scaling

A simple and computationally cheap method to produce climate projections beyond the scenarios run with expensive global climate models (GCMs). The simplest technique has known limitations and assumes that a spatial climate anomaly pattern obtained from a GCM can be scaled by the global mean temperature anomaly. (Hegerl et al., 2015)

Permafrost

Ground that remains at or below freezing for at least two consecutive years. (*USGCRP*)

Permafrost active layer

The layer of ground that is subject to annual thawing and freezing in areas underlain by permafrost. (IPCC AR5 WGI Annex III: Glossary)

Petagram

One petagram (Pg) = 10^{15} grams or 10^{12} kilograms. A petagram is the same as a gigaton, which is a billion metric tons, where 1 metric ton is 1,000 kg. Estimated 2014 global fossil fuel emissions were 9.855 Pg = 9.855 Gt = 9,855 million metric tons of carbon. (CDIAC – Carbon Dioxide Information Center: Boden et al., 2017)

Positive feedbacks

See **feedbacks**.

Proxy

A way to indirectly measure aspects of climate. Biological or physical records from ice cores, tree rings, and soil boreholes are good examples of proxy data. (*USGCRP*)

Radiative forcing

The change in the net (downward minus upward) radiative flux (expressed in W/m^2) at the tropopause or top of atmosphere due to a change in an external driver of climate change, such as a change in the concentration of carbon dioxide or in the output of the Sun. Sometimes internal drivers are still treated as forcings even though they result from the alteration in climate, for example aerosol or greenhouse gas changes in paleoclimates. The traditional radiative forcing is computed with all tropospheric properties held fixed at their unperturbed values, and after allowing for stratospheric temperatures, if perturbed, to readjust to radiative-dynamical equilibrium. Radiative forcing is **instantaneous** if no change in stratospheric temperature is accounted for. The radiative forcing once rapid adjustments are accounted for is the **effective radiative forcing**. Radiative forcing is not to be confused with cloud radiative forcing, which describes an unrelated measure of the impact of clouds on the radiative flux at the top of the atmosphere. (truncated from IPCC AR5 WGI Annex III: Glossary)

Relative sea level

The height of the sea surface, measured with respect to the height of the underlying land. Relative sea level changes in response to both changes in the height of the sea surface and changes in the height of the underlying land.



Representative Concentration Pathways

Scenarios that include time series of emissions and concentrations of the full suite of greenhouse gases and aerosols and chemically active gases, as well as land use/land cover. The word “representative” signifies that each RCP provides only one of many possible scenarios that would lead to the specific radiative forcing characteristics. The term “pathway” emphasizes that not only the long-term concentration levels are of interest, but also the trajectory taken over time to reach that outcome. RCPs usually refer to the portion of the concentration pathway extending up to 2100. Four RCPs produced from Integrated Assessment Models were selected from the published literature for use in the Intergovernmental Panel on Climate Change’s Fifth Assessment Report: **RCP2.6**, a pathway where radiative forcing peaks at approximately 3 W/m² before 2100 and then declines; **RCP4.5** and **RCP6.0**, two intermediate stabilization pathways in which radiative forcing is stabilized at approximately 4.5 W/m² and 6.0 W/m², respectively, after 2100; and **RCP8.5**, a high pathway for which radiative forcing reaches greater than 8.5 W/m² by 2100 and continues to rise for some amount of time (truncated and adapted from IPCC AR5 WGI Annex III: Glossary, excluding discussion of extended concentration pathways)

Rossby waves

Rossby waves, also known as planetary waves, naturally occur in rotating fluids. Within the Earth’s ocean and atmosphere, these waves form as a result of the rotation of the planet. These waves affect the planet’s weather and climate. Oceanic Rossby waves are huge, undulating movements of the ocean that stretch horizontally across the planet for hundreds of kilometers in a westward direction. Atmospheric Rossby waves form primarily as a result of the Earth’s geography. Rossby waves help transfer heat from the tropics toward the poles and cold air toward the tropics in an attempt to return the atmosphere to balance. They also help locate the jet stream and mark out the track of surface low pressure systems. The slow motion of these waves often results in fairly long, persistent weather patterns. (adapted from NOAA National Ocean Service)

Saffir-Simpson hurricane scale

A classification scheme for hurricane intensity based on the maximum surface wind speed and the type and extent of damage done by the storm. The wind speed categories are as follows: 1) 33–42 m/s (65–82 knots or 74–95 mph); 2) 43–49 m/s (83–95 knots or 96–110 mph); 3) 50–58 m/s (96–113 knots or 111–129 mph); 4) 59–69 m/s (114–134 knots or 130–156 mph); and 5) 70 m/s (135 knots or 156 mph) and higher. These categories are used routinely by weather forecasters in North America to characterize the intensity of hurricanes for the public. (adapted from AMS glossary).

Saturation

The condition in which vapor pressure is equal to the equilibrium vapor pressure over a plane surface of pure liquid water, or sometimes ice. (AMS glossary).

Scenarios

Plausible descriptions of how the future may develop based on a coherent and internally consistent set of assumptions about key driving forces (e.g., rate of technological change, prices) and relationships. Note that scenarios are neither predictions nor forecasts, but are useful to provide a view of the implications of developments and actions. (IPCC AR5 WGI Annex III: Glossary)

Sea level pressure

The atmospheric pressure at mean sea level, either directly measured or, most commonly, empirically determined from the observed station pressure. In regions where the Earth’s surface is above sea level, it is standard observational practice to reduce the observed surface pressure to the value that would exist at a point at sea level directly below if air of a temperature corresponding to that actually present at the surface were present all the way down to sea level. In actual practice, the mean temperature for the preceding 12 hours is employed, rather than the current temperature. This “reduction of pressure to sea level” is responsible for many anomalies in the pressure field in mountainous areas on the surface synoptic chart. (AMS glossary).



Shared Socioeconomic Pathways

A basis for emissions and socioeconomic scenarios, an SSP is one of a collection of pathways that describe alternative futures of socioeconomic development in the absence of climate policy intervention. The combination of SSP-based socioeconomic scenarios and **Representative Concentration Pathway (RCP)**-based climate projections can provide a useful integrative frame for climate impact and policy analysis. (updated from IPCC AR5 WGIII Annex I: Glossary).

Shortwave cloud radiative effect (SWCRE)

See **cloud radiative effect**.

Snow water equivalent

The depth of liquid water that would result if a mass of snow melted completely. (IPCC AR5 WGI Annex III: Glossary)

Solar radiation management (SRM)

The intentional modification of the Earth's shortwave radiative budget with the aim to reduce climate change according to a given metric (for example, surface temperature, precipitation, regional impacts, etc). Artificial injection of stratospheric aerosols and cloud brightening are two examples of SRM techniques. Methods to modify some fast-responding elements of the longwave radiative budget (such as cirrus clouds), although not strictly speaking SRM, can be related to SRM. See also **geoengineering**. (edited from IPCC AR5 WGI Annex III: Glossary)

Static-equilibrium (sea level change) fingerprint

The near-instantaneous pattern of **relative sea level** change associated with changes in the distribution of mass at the surface of the Earth, for example due to the melting of ice on land. Near a shrinking ice sheet (within ~2,000 km of the margin), sea level will fall due to both crustal uplift and the reduction of the gravitational pull on the ocean from the ice sheet. Close to the ice sheet, this fall can be an order of magnitude greater than the equivalent rise in global mean sea level associated with the meltwater addition to the ocean. Far from the ice sheet, sea level will generally rise with greater amplitude as the distance from the ice sheet increases, and this rise

can exceed the global mean value by up to about 30%. (draws on Hay et al., 2012)

Structural model uncertainty

See **uncertainty**.

Teleconnection

A statistical association between climate variables at widely separated, geographically fixed spatial locations. Teleconnections are caused by large spatial structures such as basin-wide coupled modes of ocean-atmosphere variability, Rossby wave-trains, midlatitude jets and storm tracks, etc. (IPCC AR5 WGI Annex III: Glossary)

Thermohaline circulation (THC)

Large-scale circulation in the ocean that transforms low-density upper ocean waters to higher-density intermediate and deep waters and returns those waters back to the upper ocean. The circulation is asymmetric, with conversion to dense waters in restricted regions at high latitudes and the return to the surface involving slow upwelling and diffusive processes over much larger geographic regions. The THC is driven by high densities at or near the surface, caused by cold temperatures and/or high salinities, but despite its suggestive though common name, is also driven by mechanical forces such as wind and tides. Frequently, the name THC has been used synonymously with the **Meridional Overturning Circulation**. (IPCC AR5 WGI Annex III: Glossary)

Thermokarst

The process by which characteristic landforms result from the thawing of ice-rich permafrost or the melting of massive ground ice. (IPCC AR5 WGI Annex III: Glossary)

Threshold

The value of a parameter summarizing a system, or a process affecting a system, at which qualitatively different system behavior emerges. Beyond this value, the system may not conform to statistical relationships that described it previously. For example, beyond a threshold level of ocean acidification, wide-scale collapse of coral ecosystems may occur. (CSSR, Ch. 15)



Tipping elements

Systems with critical thresholds, beyond which small perturbations in forcing can – as a result of positive feedbacks – lead to large, nonlinear, and irreversible shifts in state. In the climate system, a tipping element is a subcomponent of the climate system (typically at a spatial scale of approximately 1,000 km or larger). (*CSSR, Ch. 15*)

Tipping point

The critical **threshold** of a tipping element. Some limit its use to critical thresholds in which both the commitment to change and the change itself occur without a significant lag, while others also apply it to situations where a commitment occurs rapidly, but the committed change may play out over centuries and even millennia. (*CSSR, Ch. 15*)

Transient climate response

See **climate sensitivity**.

Tropopause

The boundary between the troposphere and the stratosphere. (IPCC AR5 WGI Annex III: Glossary)

Uncertainty

A state of incomplete knowledge that can result from a lack of information or from disagreement about what is known or even knowable. It may have many types of sources, from imprecision in the data to ambiguously defined concepts or terminology, or uncertain projections of human behavior. Uncertainty can therefore be represented by quantitative measures (for example, a probability density function) or by qualitative

statements (for example, reflecting the judgment of a team of experts) (cut from IPCC AR5 WGII Annex II: Glossary).

Given that no model can represent the world with complete accuracy, **structural model uncertainty** refers to how well the physical processes of the real world are represented in the structure of a model. Different modeling research groups will represent the climate system in different ways, and to some extent this decision is a subjective judgement. The use of climate **model ensembles** can address the uncertainty of differently structured models. (adapted from *UK Met Office, Climate Projections, Glossary*)

In contrast, **parametric uncertainty** refers to incomplete knowledge about real world processes in a climate model. A parameter is well-specified in that it has a true value, even if this value is unknown. Such empirical quantities can be measured, and the level of uncertainty about them can be represented in probabilistic terms. (adapted from *Morgan and Henrion, 1990, pp 50-52*)

Urban heat island effect

The relative warmth of a city compared with surrounding rural areas, associated with changes in runoff, effects on heat retention, and changes in surface albedo. (IPCC AR5 WGI Annex III: Glossary)

Zonal mean

Data average along a latitudinal circle on the globe.





U.S. Global Change Research Program
1800 G Street, NW | Suite 9100 | Washington, DC 20006 USA
science2017.globalchange.gov